



THERMO.2014

14th International Conference on Thermochronology
Chamonix-Mont Blanc 8-14 September 2014

ABSTRACT PROGRAM

OSUG 2020



asi Australian Scientific Instruments Pty Ltd



TOTAL
COMMITTED TO BETTER ENERGY



Thermo
SCIENTIFIC



Laslett lecture and Dodson lecture

Thermochronology of the future

Andrew Gleadow

Melbourne Thermochronology Group, School of Earth Sciences, University of Melbourne, Australia

Geoff Laslett began a highly productive association with the Melbourne Thermochronology Group at the start of the 1980s, around the time of the first International Conference on Fission Track Dating in Pisa, at a time when an understanding of fission track annealing in various geological environments was just beginning to emerge. His close, day to day, association with the research group led to the recognition of a host of new problems that needed statistical resolution to which he became a major contributor. That early work, and his remarkable long-term collaboration with Rex Galbraith that began shortly afterwards, has constrained the entire field of fission track thermochronology within a theoretical statistical framework and provided an analytical rigour that was previously lacking. The influence of the resulting statistical approaches has spread more widely into other fields also, including U-Pb ion microprobe analysis and optically stimulated luminescence dating.

Ernest Rutherford and his collaborators laid the earliest foundations for what we now call thermochronology, 110 years ago this year, but thermochronology as a recognised discipline really emerged during the 1980s especially through developments in fission track analysis, $^{40}\text{Ar}/^{39}\text{Ar}$ step heating experiments, and the recognition that the early recognised problem of 'helium leakage' was a diffusional process that could be understood and quantified. Today we see a trend towards convergence of at least some aspects of these methods, and increasingly their joint use in multi-system applications, especially when it comes to thermal history modelling. There are also some areas where the different systems are interconnected with each other such as through the role of accumulated radiation damage, including fission tracks, in the helium retention properties of uranium bearing minerals. There is a great opportunity to increase the combined application of the constituent methods of thermochronology through developing a much deeper understanding of the fundamental processes involved.

We have made enormous advances and enjoyed many successes in the field of fission track thermochronology over the last 30 years, but still there remains much that we do not understand about the behaviour of fission tracks in minerals. The remarkable achievement of a widely agreed and reasonably uniform approach to data collection, interpretation and modelling, has perhaps left us in danger of forgetting, or overlooking, some of the fundamental issues that we do not understand at all well. I believe we need to recognise that our current largely pragmatic and empirical approach has little direct relationship to the fundamental atomic processes occurring at the nano-scale. For example our current methods take almost no account of what is currently known in solid state physics about latent track structure, nor of how this changes during thermal annealing, nor even how these changes translate into etched track behaviour. There is a challenge for the fission track thermochronology community to utilise this information in what we do and ideally to develop some predictive capability for fission track annealing behaviour.

There are many other basic questions about the behaviour of fission tracks in minerals that have been largely ignored for years, but would repay much closer attention. For example the broad relationship observed many years ago by Udo Haack (1972) between lattice energy and annealing properties in various minerals has remained dormant ever since, despite its potential for predicting annealing properties. Alternatively, might it be possible to develop a diffusion-

based model of track annealing that would explain the observed differences in annealing properties between minerals and with known compositional variation within a mineral group, such as apatite? Despite years of research, we still have almost no knowledge of the effect of compositional variation on track annealing in zircon or titanite. And in zircon there is growing empirical evidence that accumulating radiation damage from alpha decay affects both fission track annealing and the retention of helium, but we have only a vague idea of how this occurs. In apatite by contrast fission track annealing does not appear to vary with normally encountered levels of radiation damage, although effects are again observed on the helium retentivity. Could this contrast in behaviour be related to the apparent differences in latent tracks structure recently observed between apatite and zircon by Li et al. (2011 EPSL). The time is ripe for many of these fundamental questions to re-emerge as important questions for concerted study, making use of the remarkable range of technologies now at our disposal for this purpose, many of which did not exist 30 years ago.

In a different direction, current developments in fission track analytical procedures are changing the way data are collected and have the potential to significantly improve both the quantity and the quality of data that are available for interpretation and modelling. These include the development of autonomous digital microscopy and automated image analysis methods for track counting and measurement, as well as the increasing adoption of laser-ablation ICP-MS techniques for direct measurement of ^{238}U , rather than via ^{235}U as a proxy. Unlike neutron irradiation methods, laser-ablation is semi-destructive on a microscopic grain scale so there are particular advantages in combining this method with an image-based approach that provides a permanent record of the fission track information. Adoption of new analytical procedures also raises the question of whether it is timely to revisit an absolute age calibration via known (or in principle knowable) constants as compared to the current relative dating using an empirical calibration against a set of agreed age standards.

Much richer sets of measurements are also made possible by image analysis procedures that would be unthinkable with manual methods including different modes of track length and diameter measurements that can be related to annealing properties. Of course the classic fission track annealing experiments upon which our thermal history models are based will need to be remeasured using these new tools, but with the important advantage that the captured image sets could be made available to all workers in the field. Our present practice of utilising annealing measurements made in one laboratory to model differently collected data in another is fraught with problems, that at present are largely uncontrolled.

The current state of fission track thermochronology is the result of a relatively stable approach to procedures and interpretive strategies that have been widely adopted over the past few decades. New approaches now emerging, however, as well as ongoing developments in fundamental track structure, and opportunities for new research to achieve a deeper understanding of fission tracks and their behaviour, mean that we may be entering a new period of rapid advances not seen for several decades. These developments towards an improved theoretical as well as practical framework will lead to a more comprehensive system of fission track analysis in the future that can be more closely integrated with other systems to provide a much more powerful thermochronology than we have today.

References

1. Haack, U. Systematics in the fission track annealing of minerals. *Contributions to Mineralogy and Petrology* 35, 303-312 (1972).
2. Li, Weixing, Lang, M., Gleadow A.J.W., Zdorovets M.V. & Ewing R.C. Thermal annealing of unetched fission tracks in apatite. *Earth and Planetary Science Letters* 321-322, 121-127 (2012).

MDDI: A Thermochronometric Odyssey

Oscar M Lovera

University of California, Los Angeles, USA

Fifty years ago, geochronologists recognized that most mineral dates did not reflect rock forming ages due to the mobilization of the daughter product at high temperatures. What at first was viewed as a shortcoming to some geo-chronological methods, became a great advantage in revealing terrestrial thermal histories with the advent of the Dodson's closure theory (1973), setting the foundation of isotope-based thermochronology. Application of the closure theory requires however an empirical diffusion model, thus the geo-chronologic $^{40}\text{Ar}/^{39}\text{Ar}$ step heating method appears ideal yielding in a single experiment both diffusion and age information. Early studies just plotted closure temperatures vs total ages of coexisting K-feldspar samples having quite different diffusion properties to linearly extrapolating an estimation of the cooling history.

By 1987, Frank Richter and I got first involved after recognizing that the information contained in the age spectrum could provide a self-consistent test of the $^{40}\text{Ar}/^{39}\text{Ar}$ thermochronologic method. Although the test failed to validate the method, one more time as many years ago, this apparent shortcoming led to the transcendental breakthrough that was the Multi-Diffusion Domain Idea (MDDI). The MDD theory would simultaneously exploit the full thermochronological signal available within intracrystalline variations and provide samplespecific kinetic parameters. A self-consistent test of the MDD approach arises from the observed correlations between age and Arrhenius spectra showing that Ar diffusion occurs by the same mechanisms in nature as in the laboratory. Under certain conditions, these data permit the recovery of a unique cooling history. I will summarize the fundamental steps that led to the development and consolidation of the $^{40}\text{Ar}/^{39}\text{Ar}$ K-feldspar MDD thermochronology method, mainly as a recognition to all the people that contributed and supported me along this quest.

Session 1:

New analytical developments in thermochronology

Ultraviolet Laser (U-Th)/He Research

K.V. Hodges¹, M.V. van Soest¹, A. Tripathy-Lang², J.W. Boyce³, J.K. Hourigan⁴,
B.D. Monteleone⁵, A.M. Horne¹, and C.M. Mercer¹

1 School of Earth and Space Exploration, Arizona State University, Tempe, AZ, USA

2 Berkeley Geochronology Center, Berkeley, CA, USA

*3 Department of Earth, Planetary, and Space Sciences, UCLA, Los Angeles, CA
USA*

4 Earth & Planetary Sciences Program, UC-Santa Cruz, Santa Cruz, CA USA

5 Woods Hole Oceanographic Institution, Woods Hole, MA, USA

Ultraviolet lasers permit high spatial-resolution analysis of helium in subgrain domains within accessory minerals for a variety of geologic applications ranging from diffusion experiments to detrital mineral dating. While this technique has tremendous promise to reduce or retire some of the more vexing problems associated with bulk noble gas diffusion studies and bulk, single-crystal (U-Th)/He dating studies, it remains very much a work in progress and has its own fair share of analytical challenges. Here we present a progress report on past and current efforts to develop and mature these techniques.

Laser ablation depth profiling using an ArF excimer (193 nm-wavelength) enables the measurement of laboratory-induced diffusion profiles. Our first work in this realm was prompted by nuclear reaction analysis experiments on ³He diffusion in Durango fluorapatite apatite¹ that seemed to be at odds with earlier volumetric ('bulk') diffusion measurements². Large crystals of Durango fluorapatite were sectioned with specific crystallographic orientations and the sections were heated in vacuo for different time-temperature combinations. The laser was then used to raster a pit of a certain depth into each section (typically a few microns) and ⁴He was measured in the liberated gas using a magnetic sector noble gas mass spectrometer. This process was repeated multiple times to resolve the geometry of the induced diffusion profile and diffusivity for the specific experimental temperature. The array of data produced for all crystallographic orientations were collinear on an Arrhenius plot (confirming diffusional isotropy) and the calculated diffusion coefficients were in excellent agreement with those from volumetric diffusion results³. We are now applying the method to zircon standards and are finding in preliminary results that ⁴He diffusion in this mineral is decidedly anisotropic in accordance with the findings of Cherniak et al.¹.

The first proof-of-concept studies for laser microprobe (U-Th)/He dating were done on monazite because its sufficiently high U and Th concentrations enabled the use of an electron microprobe for their measurement. The method involved: 1) preparation of polished grain mounts; 2) characterization of mineral zoning in these mounts using backscattered electron imaging; 3) in vacuo ablation of pits in the polished grains and quadrupole mass spectrometric analysis of ⁴He abundance in the ablated material; 4) interferometric measurement of the ablation pits to enable the conversion of measured quantities of ⁴He to concentrations; 5) x-ray dispersive electron microprobe measurements of U and Th concentrations; and 6) apparent age determinations from the resulting data. Boyce et al. 4 demonstrated the basic technique first using large, gem quality Brazilian monazites, obtaining (U-Th)/He dates (455.3 ± 3.7 Ma) comparable to bulk sample results (449.6 ± 9.8 Ma). (All uncertainties are reported here as 2σ analytical imprecision.) In a subsequent study, Boyce et al. ⁵ published laser microprobe (U-Th)/He data for a Pleistocene granite from Nanga Parbat

in the Pakistan Himalaya showing how the technique could be used to date small, extremely young, high-(U+Th) crystals of monazite.

Current work by our group and others aims to modify the technique to include other, more familiar (U-Th)/He thermochronometers. We have maintained the concentration based approach but we have switched to the use of a magnetic sector instrument for helium isotopic measurements, and have tried both secondary ionization mass spectrometry (SIMS) and laser ablation inductively coupled mass spectrometry (LA-ICPMS) for parent element measurements. Tripathy-Lang et al. 6 demonstrated how the magnetic sector mass spectrometric measurements of ^4He and SIMS measurements of U and Th could be used to characterize (U-Th)/He apparent age distributions in detrital zircon suites. We now make parent element measurements by LA-ICPMS with a quadrupole mass spectrometer. Some of our most exciting work involves simultaneous measurement of Pb with U, Th, and Sm, thereby enabling U-Pb and (U-Th)/He double dating of zircons. Preliminary work on Fish Canyon tuff zircons samples has yielded ZrnHe dates of 28.34 ± 0.85 Ma (comparable to single-crystal ages of 28.3 ± 3.1 Ma; 7) and $\text{Zrn}(^{206}\text{Pb}/^{238}\text{U})$ dates of 28.15 ± 0.37 Ma (comparable to thermal ionization mass spectrometric ages ranging from 28.642 ± 0.025 to 28.196 ± 0.038 Ma; 8). We are currently experimenting with applications of the laser microprobe double-dating technique to detrital titanite and rutile. The high spatial resolution of the laser microprobe makes this technique potentially valuable for (U-Th)/He thermal history studies of accessory minerals in rare specimens ranging from meteorites to samples returned from missions to the Moon, Mars, and near-earth asteroids. Work on samples from the Apollo archive is currently in progress.

References

1. Cherniak, D. J., Watson, E. B. & Thomas, J. B. Diffusion of helium in zircon and apatite. *Chemical Geology* **268**, 155-166 (2009).
2. Farley, K. A. Helium diffusion from apatite: General behavior as illustrated by Durango fluorapatite. *Journal of Geophysical Research* **105**, 2903-2914 (2000).
3. van Soest, M. C., Monteleone, B. D., Hodges, K. V. & Boyce, J. W. Laser depth profiling studies of helium diffusion in Durango fluorapatite. *Geochimica et Cosmochimica Acta* **75**, 2409-2419 (2011).
4. Boyce, J. W. et al. Laser microprobe (U-Th)/He geochronology. *Geochimica et Cosmochimica Acta* **70**, 3031-3039, doi:10.1016/j.gca.2006.03.019 (2006).
5. Boyce, J. W. et al. Improved precision in (U-Th)/He thermochronology using the laser microprobe: An example from a Pleistocene leucogranite, Nanga Parbat, Pakistan. *Geochemistry Geophysics Geosystems* **10**, doi:10.1029/2009GC002497 (2009).
6. Tripathy-Lang, A., Hodges, K. V., Monteleone, B. D. & van Soest, M. C. Laser (U-Th)/He thermochronology of detrital zircons as a tool for studying surface processes in modern catchments. *Journal of Geophysical Research-Earth Surface* **118**, 1333-1341, doi:10.1002/jgrf.20091 (2013).
7. Dobson, K. J., Stuart, F. M. & Dempster, T. J. U and Th zonation in Fish Canyon Tuff zircons: Implications for a zircon (U-Th)/He standard. *Geochimica et Cosmochimica Acta* **72**, 4745-4755, doi:10.1016/j.gca.2008.07.015 (2008).
8. Wotzlaw, J. F. et al. Tracking the evolution of large-volume silicic magma reservoirs from assembly to supereruption. *Geology* **41**, 867-870, doi:10.1130/g34366.1 (2013).

U-Pb apatite dating by LA-ICPMS

David Chew¹, Joe Petrus², Balz Kamber¹, Nathan Cogné¹, Richard Spikings³, Ryan Cochrane³, Raymond A. Donelick⁴

1 Department of Geology, School of Natural Sciences, Trinity College Dublin, Ireland

2 Department of Earth Sciences, Laurentian University, Sudbury, Canada

3 Section of Earth and Environmental Sciences, University of Geneva, Switzerland

4 Apatite to Zircon, Inc., 1075 Matson Road, Viola, Idaho 83872-9709, U.S.A.

U-Pb dating of accessory minerals has been revolutionised in the last decade by substantial improvements in the LA-ICPMS technique that have facilitated progressively smaller spot sizes and shorter analysis times with a precision approaching that of SIMS analysis. This presentation investigates the application of LA-ICPMS U-Pb geochronology to U-bearing accessory minerals that contain common Pb, with particular focus on apatite.

Petrus and Kamber (2012) developed VizualAge¹ as a tool for reducing and visualising, in real time, U-Pb geochronology data obtained by LA-ICP-MS as an add-on for the freely available U-Pb geochronology data reduction scheme² of Paton et al. (2010) in Lolite. The most important feature of VizualAge is its ability to display a live concordia diagram, allowing users to inspect the data of a signal on a concordia diagram as the integration area it is being adjusted, thus providing immediate visual feedback regarding discordance, uncertainty, and common lead for different regions of the signal. It can also be used to construct histograms and probability distributions, standard and Tera-Wasserburg style concordia diagrams, as well as 3D U-Th-Pb and total U-Pb concordia diagrams.

More recently, Chew et al. (2014) presented a new data reduction scheme (VizualAge_UcomPbine)³ with much improved common Pb correction functionality. Common Pb is a problem for many U-bearing accessory minerals and an under-appreciated difficulty is the potential presence of (possibly unevenly distributed) common Pb in calibration standards, introducing systematic inaccuracy into entire datasets. One key feature of the new method is that it can correct for variable amounts of common Pb in any U-Pb accessory mineral standard as long as the standard is concordant in the U/Pb (and Th/Pb) systems after common Pb correction. Common Pb correction can be undertaken using either the ²⁰⁴Pb, ²⁰⁷Pb or ²⁰⁸Pb(no Th) methods. After common Pb correction to the user-selected age standard integrations, the scheme fits session-wide model U-Pb fractionation curves to the time-resolved U-Pb standard data. This down hole fractionation model is next applied to the unknowns and sample-standard bracketing (using a user specified interpolation method) is used to calculate final isotopic ratios and ages. ²⁰⁴Pb- and ²⁰⁸Pb(no Th)-corrected concordia diagrams and ²⁰⁴Pb-, ²⁰⁷Pb- and ²⁰⁸Pb(no Th)-corrected age channels can be calculated for user-specified initial Pb ratio(s). All other conventional common Pb correction methods (e.g. intercept or isochron methods on co-genetic analyses) can be performed offline.

Example applications of U-Pb dating of apatite by LA-ICPMS will be presented. These include i) integrated apatite fission track and U-Pb dating⁴ combined with trace element measurements (including chlorine⁵), ii) U-Pb apatite detrital geochronology and iii) *in situ* LA-ICPMS age profiles for U-Pb apatite thermochronology⁶.

The use of LA-ICP-MS to calculate U concentrations in fission track dating dramatically increases the speed of analysis and sample throughput compared to the conventional external detector method, as well as avoiding the need for neutron irradiation. A zeta-based approach is presented here⁴. Simultaneous Cl concentration measurements⁵ can be integrated with apatite fission track

dating, U-Pb age information and trace element concentration measurements to yield a very powerful LA-ICP-MS analytical protocol that combines high and low temperature cooling age data with information on apatite annealing kinetics.

Detrital U-Pb apatite dating offers some advantages compared to zircon in sedimentary provenance studies as it is more likely to represent first-cycle detritus and is also a nearly ubiquitous accessory phase in igneous rocks of both felsic and mafic composition (compared to zircon which is generally restricted to igneous rocks of felsic composition). A common Pb correction can be made in detrital samples using Pb evolution models using a starting estimate for the age of the apatite and adopting an iterative approach^{7,8}. Additionally, unlike zircon, the trace-element chemistry of detrital apatite also yields information on the parent igneous-rock type⁹.

U-Pb dating of apatite is employed in high-temperature thermochronology studies, with empirical and experimental closure temperatures of ca. 425–550 °C calculated for apatite¹⁰. We present here intra-grain apatite U-Pb dates from Akilia Island, SW Greenland. These apatites host ¹³C-depleted graphite inclusions that were interpreted as biogenic in origin and proposed to represent the oldest indications of life on Earth¹¹. Intra-grain U-Pb LA-ICPMS apatite age profiles yield ages as old as c. 2050 Ma in the cores and as young as c. 1650 Ma on the rims, which are characteristic of a sample that has undergone thermally activated diffusive loss of a radiogenic isotope during slow exhumation through its respective closure temperature window. Similar Fickian diffusion profiles have been documented for Pb in apatite based on a combination of U-Pb apatite TIMS and *in situ* LA-CIPMS age profiles⁶. The scatter and poor precision of the earlier U-Pb age determinations of Akilia Island apatite¹² can be attributed to combining spot analyses from multiple grains of variable size and hence variable closure ages (mixtures of analyses of variable grain size and/or variable positions within individual grains).

References

1. Petrus, J.A. & Kamber, B.S. VizualAge: a novel approach to laser ablation ICP-MS U-Pb geochronology data reduction. *Geostandards and Geoanalytical Research* **36**, 247-270 (2012).
2. Paton C., Woodhead J.D., Hellstrom J.C., Hergt J.M., Greig A. & Maas R. Improved laser ablation U-Pb zircon geochronology through robust downhole fractionation correction. *Geochemistry Geophysics, Geosystems* **11**, 1-36 (2010).
3. Chew, D.M., Petrus, J.A., & Kamber, B.S. U-Pb LA-ICPMS dating using accessory mineral standards with variable common Pb. *Chemical Geology* **363**, 185-199 (2014).
4. Chew, D.M., Donelick, R.A. in Combined apatite fission track and U-Pb dating by LA-ICPMS and its application in apatite provenance analysis (ed. Sylvester, P.) 42, 219-247 (Quantitative Mineralogy and Microanalysis of Sediments and Sedimentary Rocks, Mineralogical Association of Canada Short Course, 2012).
5. Chew, D.M., Donelick, R.A., Donelick, M.B., Kamber, B.S. & Stock, M. Apatite chlorine concentration measurements by LA-ICP-MS. *Geostandards and Geoanalytical Research* **38**, 23-35 (2014).
6. Cochrane, R., Spikings, R.A., Chew, D., Wotzlav, J.-F., Chiaradia, M., Tyrrell, S., Schaltegger, U. and Van der Lelij, R. High temperature (> 350 °C) thermochronology and mechanisms of Pb loss in apatite. *Geochimica et Cosmochimica Acta* **127**, 39–56 (2014).
7. Chew, D.M., Sylvester, P.J., Tubrett, M.N. U-Pb and Th-Pb dating of apatite by LA-ICPMS. *Chemical Geology* **280**, 200-216 (2011).
8. Thomson, S.N., Gehrels, G.E., Ruiz, J., Buchwaldt, R., Routine low-damage apatite U-Pb dating using laser ablation-multicollector-ICPMS. *Geochemistry Geophysics, Geosystems* **13** (2012).
9. Jennings, E.S., Marschall, H.R., Hawkesworth C.J. & Storey, C.D. Characterization of magma from inclusions in zircon: Apatite and biotite work well, feldspar less so. *Geology* **39**, 863-866 (2011).
10. Chamberlain, K.R. & Bowring, S.A. Apatite-feldspar U-Pb thermochronometer: A reliable, mid-range (450°C), diffusion-controlled system. *Chemical Geology* **172**, 173-200 (2000).
11. Mojzsis, S.J., Arrhenius, G., McKeegan, K.D., Harrison, T.M., Nutman, A.P., Friend, C.R.L. Evidence for life on Earth before 3800 million years ago. *Nature* **384** (6604), 55–59 (1996).
12. Sano, Y., Terada, K., Takahashi, Y., Nutman, A.P., 1999. Origin of life from apatite dating? *Nature* **400** (6740), 127 (1999).

Apatite fission track analysis by LA-ICP-MS: An evaluation of the absolute dating approach

Christian Seiler¹, Barry Kohn¹, Andrew Gleadow¹

1 School of Earth Sciences, The University of Melbourne, Victoria 3010, Australia

Analysis of trace element compositions by laser ablation ICP-MS has become a widely used tool in in-situ geochronology. Although primarily used for U-Pb dating, LA-ICP-MS has been successfully adapted to other techniques such as apatite fission track¹ or (U-Th)/He², making it an ideal tool for multi-system thermochronological studies.

For fission track dating, LA-ICP-MS has several important advantages over the conventional external detector method (EDM), particularly in terms of sample turn-around time and the fact that neutron irradiations (and the handling of radioactive materials) are no longer necessary, while providing a similar level of in-situ information. Another key benefit of LA-ICP-MS fission track dating is that it could potentially be used as an absolute dating technique, instead of the indirect “Zeta” approach that relies on calibration against independently dated age standards. However, beyond the pioneering studies of Hasebe et al.^{1,3}, little work has been reported to validate this new approach and address potential calibration and standardisation issues. Amongst the key unresolved questions are: What standards should be used and are there any matrix effects that need to be considered? Are there any limitations when applying LA-ICP-MS analysis to low-U minerals such as apatite? Are the parameters of the fission track equation sufficiently well-known? Are the results reproducible and how do they compare with the existing data?

To address some of the above questions, we present an extensive dataset of >500 fission track single grain ages from 15 samples that were analysed using both the LA-ICP-MS and EDM techniques. Both methods were applied on the same grains using identical spontaneous track densities, thereby eliminating uncertainties associated with natural variability in the fission decay. LA-ICP-MS experiments were conducted using single spot analyses on a New Wave Nd:YAG laser ($\lambda=213\text{nm}$; spot size= $25\text{-}40\mu\text{m}$; laser output= $\sim 3\text{J}/\text{cm}^2$; laser frequency= 5Hz) connected to an Agilent 7700x ICP-MS with NIST 612 as a calibration standard (^{238}U concentration of $37.38\pm 0.08\text{ppm}^4$). Samples were selected to represent a variety of fission track ages ($\sim 0\text{-}2\text{Ga}$), ^{238}U concentrations ($< 0.5\text{-}400\text{ppm}$) and mean track lengths ($< 12\mu\text{m}\text{-}15\mu\text{m}$). The latter are important because they relate the spontaneous fission track density – counted microscopically on an internal mineral surface – to the 3D distribution of ^{238}U fission events, which are then compared to the ^{238}U concentration measured by LA-ICP-MS to calculate the fission track age.

Results show that, with the exception of a few outliers, single grain fission track ages from LA-ICP-MS and EDM are concordant within analytical uncertainties and scatter symmetrically around the 1:1 correlation line, irrespective of the sample age (Fig. 1). Although the relative difference in single grain ages varies significantly in either direction, there are no systematic variations between the two methods, suggesting that this variation is simply due to random sampling effects. A similarly well-behaved and symmetrical correlation emerges if we compare the ^{238}U concentration as determined by the two techniques, which demonstrates that reliable measurements can be obtained across the range of ^{238}U concentrations normally found in apatite using just a single calibration standard. This is consistent with independent experiments, performed on a series of standard glasses with variable ^{238}U concentrations, which confirm that the LA-ICP-MS detection response is linear across several orders of magnitude.

Repeat ^{238}U measurements of apatite reference materials that are assumed to be largely homogenous at the grain scale (Durango and Mud Tank) show that ^{238}U analyses by LA-ICP-MS are reproducible within errors, both during analyses as well as across separate experiments. Sample

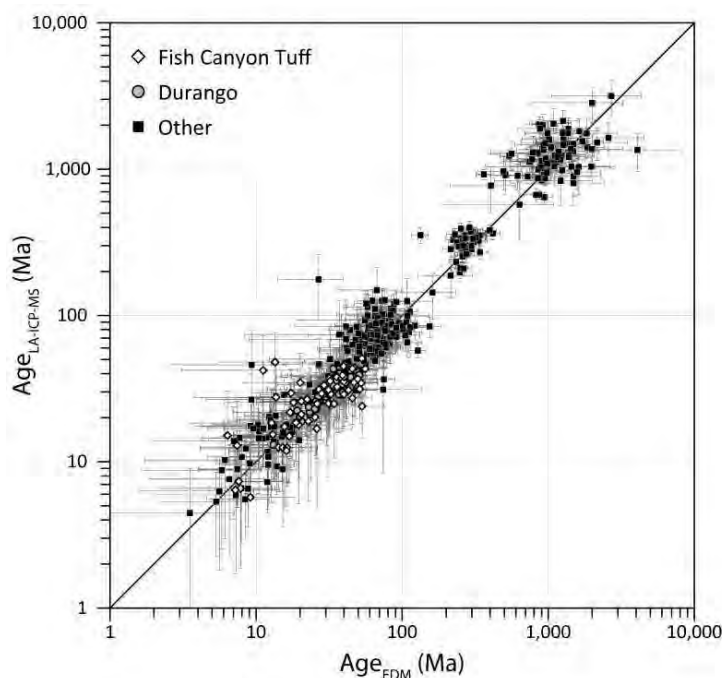


Figure 1. Comparison between apatite single grain ages ($N=517$) obtained by the LA-ICP-MS and EDM methods.

between central ages determined by LA-ICP-MS and those from EDM (the latter being consistently younger). Although less dramatic, a similar discrepancy is also apparent in the pooled ages. The observed age difference appears to be broadly correlated with the mean track length: For samples with long mean track lengths ($>13\mu\text{m}$), the differences between LA-ICP-MS and EDM ages are statistically insignificant and the corresponding pooled/central ages overlap within error. By comparison, samples with lower mean track lengths ($<12\text{--}13\mu\text{m}$) yield LA-ICP-MS pooled and central ages that are consistently older than those obtained by the EDM method, by a degree that seems to reflect the amount of track annealing (shortening) experienced by a sample.

Our data indicate that while absolute fission track dating using LA-ICP-MS works very well for samples with relatively simple and fast cooling histories (longer mean track lengths), systematic differences can occur between the EDM and LA-ICP-MS methods for samples that underwent slow, protracted or complex cooling histories (moderate to shorter mean track lengths). These results invite further examination of the possible factors that may cause the apparent discordance between LA-ICP-MS and EDM ages with enhanced track annealing.

References

1. Hasebe, N., Barbarand, J., Jarvis, K., Carter, A. & Hurford, A. J. Apatite fission-track chronometry using laser ablation ICP-MS. *Chemical Geology* **207**, 135-145 (2004).
2. Boyce, J. W., Hodges, K. V., Olszewski, W. J., Jercinovic, M. J., Carpenter, B. D. & Reiners, P. W. Laser microprobe (U-Th)/He geochronology. *Geochimica et Cosmochimica Acta* **70**, 3031-3039 (2006).
3. Hasebe, N., Carter, A., Hurford, A. J. & Arai, S. The effect of chemical etching on LA-ICP-MS analysis in determining uranium concentration for fission-track chronometry. *Geological Society, London, Special Publications* **324**, 37-46 (2009).
4. Jochum, K. P., Weis, U., Stoll, B., Kuzmin, D., Yang, Q., Raczek, I., Jacob, D. E., Stracke, A., Birbaum, K., Frick, D. A., Günther, D. & Enzweiler, J. Determination of Reference Values for NIST SRM 610–617 Glasses Following ISO Guidelines. *Geostandards and Geoanalytical Research* **35**, 397-429 (2011).

means for both apatites are indistinguishable from the corresponding isotope dilution ICP-MS values, suggesting that matrix effects are not a major problem for LA-ICP-MS analysis of apatite. Intra-grain variability of ^{238}U can be significantly larger for natural samples however, which may explain the somewhat larger dispersion of LA-ICP-MS single grain ages compared to those obtained by EDM.

Despite the strong correlation seen in the single grain data, pooled and central ages of the LA-ICP-MS and EDM methods do not always overlap within error. For age standards such as Durango or Fish Canyon, both pooled and central ages are statistically indistinguishable between the two methods, just as one would expect. In other samples, however, there is a significant deficit of up to 25%

Standardizing Isotopic Composition and Fission Track Parameters in the Apatite U-FT-Pb System

Ray Donelick¹, Margaret Donelick¹, Paul O'Sullivan¹, Rich Ketcham², Ann Blythe³

1 Apatite to Zircon, Inc., Viola, Idaho, U.S.A.

2 University of Texas at Austin, Austin, Texas, U.S.A.

3 Occidental College, Los Angeles, California, U.S.A.

Quadrupole mass spectrometry allows rapid data collection over a wide range of ion masses. Combined with laser ablation, the following parameters may be measured for a depth profile of an apatite crystal: a) relative uranium, thorium, and samarium concentrations, b) $^{206}\text{Pb}/^{238}\text{U}$, $^{207}\text{Pb}/^{235}\text{U}$, $^{207}\text{Pb}/^{206}\text{Pb}$, and c) relative concentrations of many other elements of interest (1-5 for relevant background).

We have long observed that accumulated alpha-damage in zircon correlates with LA-ICP-MS-derived Pb/U calibration factors for the U-Pb system⁶ (Pb/U calibration factors vary with laser-ablation pit depth; the ablation rate is higher for zircon containing greater alpha damage). Extending this experience to apatite, we prefer isotopic composition standards that are closely matrix-matched to the apatite crystals we are studying.

For zeta calibration of the apatite U-FT system, we have manufactured and are testing several matrix-matched U-FT standards: a) ApFCTN: Fish Canyon Tuff (Naeser locality), South Fork, Colorado, U.S.A.; ~28 Ma U-Pb age; narrow range of Dpar values; moderate range of relative uranium concentrations; Cl concentration assumed 0.82 weight percent in each crystal, and b) ApMTr: Triassic-aged Moenkopi Formation from Castle Valley, Utah, U.S.A.; Mesozoic to Precambrian U-Pb ages; Dpar = 1.5-3.2 μm ; uranium concentration = 0->100 ppm; Cl concentration = 0->1.5 weight percent. Unlike ApFCTN, ApMTr allows zeta to be calibrated as a function of Dpar and uranium concentration. Different combinations of Dpar and uranium concentration present to the laser beam different effective target matrices: an ApMTr crystal with large Dpar and high uranium concentration will have more of its target volume removed due to fission track etching than an ApMTr crystal with smaller Dpar (same uranium concentration), lesser uranium concentration (same Dpar), or both smaller Dpar and lesser uranium concentration.

Mean confined length of unannealed fission tracks (initial fission track length) parallel to the crystallographic c-axis is strongly correlated with Dpar; initial fission track length perpendicular to the c-axis is strongly correlated with Dper. U-FT standard ApMTr exhibits a wide range of Dpar, Dper, and Dpar/Dper values among its apatite crystals. As such, we are testing ApFCTN as an initial fission track length standard.

We have prepared a pair of standards containing only natural fission tracks: a) ApMTr-natural: the natural equivalent of U-FT standard ApMTr, and b) ApLaSal-natural: ~28Ma U-Pb age; narrow range of Dpar values; moderate range of relative uranium concentrations. Our unpublished data indicate the following general geological histories of these samples: a) ApMTr-natural was deposited at ~245 Ma; fast annealing small Dpar apatite grains were totally reset and slow annealing large Dpar grains were partially reset by the ~28 Ma shallow intrusive event that formed ApLaSal; removal of >1 km cover occurred since 10 Ma due to Colorado River canyon formation, and b) ApLaSal was intruded at ~28 Ma and has remained cool and near the surface since 28 Ma above the nearest Colorado River canyon rim. This combination of standards offers the analyst the ability to test: a) Dpar, Dper, chemical composition, U-Pb, and fission track parameter calibrations, and b) the geological history interpretation/modeling scheme used by the analyst.

Data collection for the U-FT system includes the visual study of images of various features including etch figures, fission semi-tracks, confined fission tracks (CFTs), and mineral and other inclusions (especially if a grain is to be dated by (U-Th-Sm)/He). In theory, the visual study of any of these features may be aided by computer analysis of digital images of these features. Computer analysis that includes machine learning is possible but requires Big Data sets of these features. Pattern matching may be applied in the machine learning algorithms. As such, we are building a public repository of digital images of these various features and software tools to process, view, and analyze the images. For example, the CFT digital image library may ultimately contain reflected light+transmitted light pairs of three-dimensional image stacks of >100,000 CFTs; this vetted set of standard images may be used to extract patterns for pattern matching and for training a machine learning algorithm to better aid the analyst in finding and characterizing new CFTs.

References

1. Chew, D.M., Donelick, R.A., Donelick, M.B., Kamber, B.S. & Stock, M.J., Apatite chlorine concentration measurements by LA-ICP-MS. *Geostandards and Geoanalytical Research*, **38**, 23-35 (2014).
2. Chew, D.M., Sylvester, P.J. & Tubrett, M.N., U-Pb and Th-Pb dating of apatite by LA-ICP-MS, *Chemical Geology*, **280**, 200-216 (2011).
3. Donelick, R.A., O'Sullivan, P.B. & Donelick, M.B., A Discordia-Based Method of Zircon U-Pb Dating from LA-ICP-MS Analysis of Single Spots. *Smart Science for Exploration and Mining*, **1-2**, 276-278 (2010).
4. Gehrels, G.E., Valencia, V.A. & Ruiz, J., Enhanced precision, accuracy, efficiency, and spatial resolution of U-Pb ages by laser ablation-multicollector-inductively coupled plasma-mass spectrometry. *Geochemistry Geophysics Geosystems*, American Geophysical Union, **9**, 13 p. (2008).
5. Hasebe, N., Barbarand, J., Jarvis, K., Carter, A. & Hurford, A.J., Apatite fission-track chronometry using laser ablation ICP-MS. *Chemical Geology*, **207**, 135-145 (2004).
6. Kylander-Clark, A.R.C., Hacker, B.R. & Cottle, J.M., Laser-ablation split-stream ICP petrochronology. *Chemical Geology*, **345**, 99-112 (2013).

Zircon $^4\text{He}/^3\text{He}$ thermochronometry: A proof-of-concept study using Fish Canyon Tuff

Alka Tripathy-Lang^{1,2}, David Shuster^{1,2}

¹ Berkeley Geochronology Center, Berkeley, CA 94709, USA

² University of California, Berkeley, CA 94720, USA

Studies focused on scientific questions related to tectonics and/or topographic development at Earth's surface often use thermochronometry to provide valuable information on low-temperature exhumation at fixed points in space. For example, $^{40}\text{Ar}/^{39}\text{Ar}$ thermochronometry of individual K-feldspars via multi-diffusion domain modeling¹ can constrain continuous cooling paths between $\sim 200\text{--}350^\circ\text{C}$, whereas $^4\text{He}/^3\text{He}$ thermochronometry of a single apatite crystal can resolve thermal paths² between $\sim 30\text{--}90^\circ\text{C}$. Such information can then be related to the geologic processes(s) that brought a given rock to the surface. However, an obvious gap exists between these two methods; here we propose $^4\text{He}/^3\text{He}$ thermochronometry of zircon as a new method to fill this gap in continuous tT space. We assess the temperature sensitivity of zircon $^4\text{He}/^3\text{He}$ thermochronometry and present $^4\text{He}/^3\text{He}$ data and an associated (U-Th) concentration map from Fish Canyon Tuff zircon as proof-of-concept. We also discuss assumptions and limitations as well as ongoing refinements of this technique.

To determine the temperature sensitivity of the $^4\text{He}/^3\text{He}$ thermochronometer in zircon, we calculate the opening and resetting temperatures (T_o and T_r)³. For a radius of $60\ \mu\text{m}$, a cooling rate of $10^\circ\text{C}/\text{Ma}$, and zircon diffusivity parameters from Reiners et al.⁴, T_o is 118°C and T_r is 215°C . A zircon $^4\text{He}/^3\text{He}$ step-wise degassing experiment will thus yield data that are sensitive to temperatures bounded by both T_o and T_r . The temperature sensitivity for different cooling rates and grain radii ranges from slightly less than 100°C to slightly greater than 250°C , with a typical grain providing information over a ~ 100 degree span within that range. Outside T_o and T_r , ^4He in zircon will either be quantitatively retained or completely lost by diffusion, and therefore constrains neither hotter nor cooler parts of a tT path.

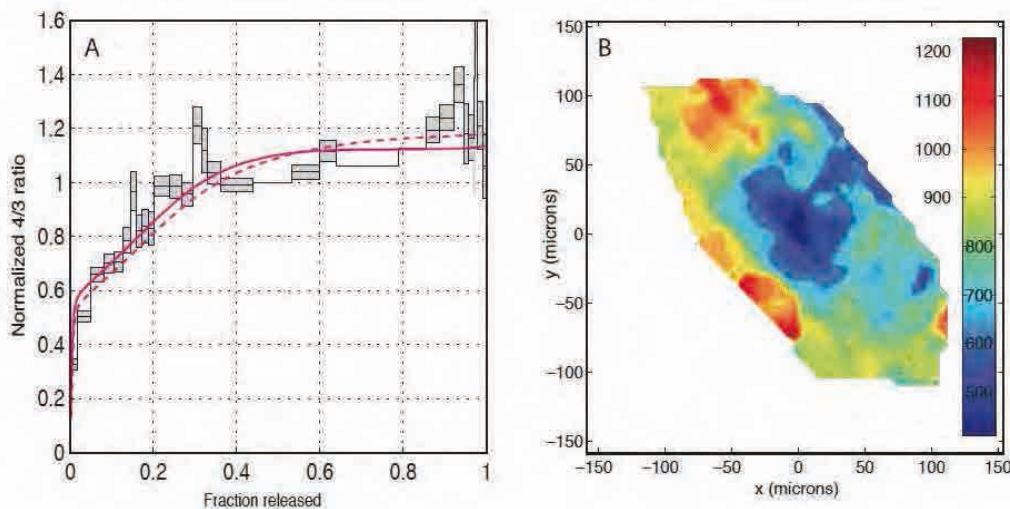


Figure 1. A. $^4\text{He}/^3\text{He}$ step-wise degassing experiment of a single Fish Canyon Tuff zircon crystal (grey boxes). Dashed curve is a model spectrum generated using the known tT path of FCT, but assuming a uniform spatial distribution of U and Th in the crystal. Solid curve is calculated using the same parameters and the eU zonation profile obtained from the eU concentration map. B. eU concentration map of the same crystal, which demonstrates a relatively low eU core and higher eU rim. In this case, the integrated complexity in eU zonation appears to have little effect on ^4He accumulation and diffusion. Color bar is eU concentration in ppm; $eU = [U] + 0.235[Th]$, defined by Flowers et al.⁷

We initially focus on Fish Canyon Tuff (FCT) zircon for several reasons. First, FCT is a commonly used standard for other thermochronometers, including the bulk zircon (U-Th)/He method. Furthermore, it has a known thermal history; its eruptive age is $28.305 \pm 0.03 \text{ Ma}^5$. In Figure 1a, we present the results of a $^4\text{He}/^3\text{He}$ stepwise degassing experiment of a single FCT zircon. Qualitatively, the profile appears to be consistent with an alpha-ejection dominated profile with some diffusive rounding. The slight concave down pattern between release fractions 0.4-0.85 implies that the rim is higher in U and/or Th concentration relative to the core, based on forward modeling of theoretical zoned zircons. The spatial distribution of U and Th measured in the same crystal using laser ablation ICPMS⁶ [Figure 1b; presented as effective Uranium (eU)⁷] corroborates this prediction.

Superimposed on the laboratory-derived spectrum in Figure 1a are two model spectra calculated by forward modeling of the known cooling history of FCT; one assumes no eU zonation, the other, the zonation shown in Figure 1b. Although the differences between these models are small, the model spectrum that incorporates zonation more closely resembles the measured ratio evolution diagram, particularly in the first half of the spectrum. Both models are unable to reproduce some complexity in the final tenth of the laboratory-derived spectrum. This may be due to additional complexity in the zoning profile that is not resolved by the LA-ICPMS method for (U-Th) concentration measurement. Alternatively, this might indicate that collapsing the 2D LA-ICPMS-derived U-Th concentration maps onto a single radial coordinate⁶ is not appropriate for this zircon. Further, these initial calculations assume ^4He diffusion kinetics of Reiners et al.⁴ and do not yet incorporate the possible effects of spatially variable ^4He diffusivity that may be related to radiation damage accumulation⁸.

To further develop this technique, we seek to better understand the complexity in profiles such as Figure 1a. We have generated combined $^4\text{He}/^3\text{He}$ degassing data and U and Th concentration maps from zircons with very different thermal histories than FCT. Our preliminary data indicate that despite complexity in U and Th zonation, zircon appears amenable to $^4\text{He}/^3\text{He}$ thermochronometry. This method should provide insight into the continuous cooling paths of rocks in a temperature range previously inaccessible from individual crystals.

References

1. Lovera, O. M., Grove, M., Harrison, T. M. & Mahon, K. I. Systematic analysis of K-feldspar $^{40}\text{Ar}/^{39}\text{Ar}$ step-heating experiments I: Significance of activation energy determinations. *Geochimica et Cosmochimica Acta* **61**, 3171-3192 (1997).
2. Shuster, D. L. & Farley, K. A. $^4\text{He}/^3\text{He}$ thermochronometry. *Earth and Planetary Science Letters* **217**, 1-17 (2004).
3. Gardes, E. & Montel, J.-M. Opening and resetting temperatures in heating geochronological systems. *Contributions to Mineralogy and Petrology* **158**, 185-195 (2009).
4. Reiners, P. W., Spell, T. L., Nicolescu, S. & Zanetti, K. A. Zircon (U-Th)/He thermochronometry: He diffusion and comparisons with $^{40}\text{Ar}/^{39}\text{Ar}$ dating. *Geochimica et Cosmochimica Acta* **68**, 1857-1887 (2004).
5. Renne, P. R. et al. Joint determination of ^{40}K decay constants and $^{40}\text{Ar}^*/^{40}\text{K}$ for the Fish Canyon sanidine standard, and improved accuracy for $^{40}\text{Ar}/^{39}\text{Ar}$ geochronology. *Geochimica et Cosmochimica Acta* **74**, 5349-5367 (2010).
6. Farley, K. A., Shuster, D. L. & Ketcham, R. A. U and Th zonation in apatite observed by laser ablation ICPMS, and implications for the (U-Th)/He system. *Geochimica et Cosmochimica Acta* **75**, 4515-4530 (2011).
7. Flowers, R. M., Ketcham, R. A., Shuster, D. L. & Farley, K. A. Apatite (U-Th)/He thermochronometry using a radiation damage accumulation and annealing model. *Geochimica et Cosmochimica Acta* **73**, 2347-2365 (2009).
8. Guenther, W. R. et al. Helium diffusion in natural zircon: radiation damage, anisotropy, and the interpretation of zircon (U-Th)/He thermochronology. *American Journal of Science* **313**, 145-198 (2013).

A quantitative assessment of the causes of dispersion of single grain apatite (U-Th)/He ages and a new inversion approach to deriving thermal histories from ‘over-dispersed’ data

Roderick Brown¹, Romain Beucher², Steven Roper³, Kerry Gallagher⁴, Cristina Persano¹ and Fin Stuart³

1 School of Geographical and Earth Sciences, University of Glasgow, United Kingdom

2 Department of Earth Science, University of Bergen, Bergen, Norway

3 School of Mathematics and Statistics, University of Glasgow, United Kingdom

4 Géosciences Rennes, Université de Rennes 1, Campus de Beaulieu, France

5 Scottish Universities Environmental Research Centre, East Kilbride, United Kingdom

The (U-Th)/He thermochronometry technique has revolutionised our ability to investigate low temperature processes within the shallow crust¹. It is now standard practice to analyse single grains rather than multigrain aliquots for a variety of reasons, and in most natural samples the vast majority of apatite grains are fragments of initially larger crystals. The grains have typically been broken along the distinct basal cleavage in apatite during the mineral separation process. In many instances the single grain ages from a given sample are severely dispersed, and often poorly or uncorrelated with either grain size (typically expressed as spherical equivalent radius) or U or Th content. This suggests that there must be another common cause of dispersion other than absolute grain size or differences in ⁴He diffusivity caused by radiation damage accumulation.

Using a numerical model and a finite cylinder geometry to approximate ⁴He diffusion in apatite we show that much of the range of this ‘over dispersion’ is explained when broken grains are treated explicitly as fragments of larger grains²⁻³. This situation is clearly indicated by the common occurrence of only 1 or no clear crystal terminations present on separated apatite grains and cleanly broken surfaces as indicated in SEM images of these grains.

The modelling also demonstrates that the shape of the ⁴He distribution within an individual crystal is indeed inherent in the pattern of dispersion of individual fragment ages for a given sample. We describe and demonstrate a new inversion approach that exploits this information by modelling the single grain ages explicitly as fragments of larger grains to obtain robust constraints on a sample’s thermal history. Our new approach yields similar thermal history constraints to those obtained from the single ⁴He/³He technique⁴, with the added advantage that it does not require the analysis to be performed on whole crystals. The practicality of the approach is demonstrated using a series of hypothetical thermal history styles representing a range of geologically plausible and variable thermal histories and using a real example from the Bushveld Igneous Complex in South Africa.

The advantage this new approach is that it can explicitly accommodate the effects of temporally variable diffusivity (e.g. radiation damage accumulation and annealing models), zonation of U and Th and arbitrary grain size variations, and it will work equally effectively for whole or broken crystals, or indeed the more likely situation where there is a mixture of both. Our experiments also indicate that when broken crystals with 1 and no terminations are analysed it is unreasonable to expect these analyses to replicate and to produce a single, discrete sample age. If broken grains with no terminations are analysed then these crystal ages may replicate, but would produce an erroneously ‘old’ sample age. We suggest that for routine single grain (U-Th)/He analyses on samples where whole grains are rare, or unavailable, then 15-20 single grain analyses are required to fully characterise the range and pattern of dispersion that is likely, and that a single ‘sample age’ has little physical meaning or use in these cases. The experiments also suggest that picking very short crystal fragments as well as long fragments, or even deliberately breaking long crystals to maximise the age dispersion arising from this cause, would ensure the best constraints on the thermal history models.

References

1. Farley, K.A., (U-Th)/He dating: techniques, calibrations and applications, *Reviews in Mineralogy and Geochemistry* **47**, 819-844 (2002).
2. Brown, R. W., Beucher, R., Roper, S., Persano, C., Stuart, F., & Fitzgerald, P., Natural age dispersion arising from the analysis of broken crystals, Part I. Theoretical basis and implications for the apatite (U-Th)/He thermochronometer, *Geochimica et Cosmochimica Acta* **122**, 478-497 (2013).
3. Beucher, R., Brown, R. W., Roper, S., Stuart, F., & Persano, C., 2013, Natural age dispersion arising from the analysis of broken crystals, Part II. Practical application to apatite (U-Th)/He thermochronometry, *Geochimica et Cosmochimica Acta* **120**, 395-416 (2013).
4. Shuster, D.L. and Farley, K.A., $^4\text{He}/^3\text{He}$ thermochronometry: theory, practice and potential applications, *Reviews in Mineralogy and Geochemistry* **58**, 181-203 (2005).

AFM observation of natural zircon: Is alpha recoil dating possible?

Noriko Hasebe¹, Kentaro Ito¹, Atsushi Matsuki¹, Takeshi Fukuma²

¹ Institute of Nature and Environmental Technology, Kanazawa University, Japan

² College of Science and Engineering, Kanazawa University, Japan

The number of fission tracks is counted under an optical microscope after etching. However, as fission track density per unit area rises, it becomes difficult to count the number of tracks because tracks overlap one another and are unable to be readily distinguished. The atomic force microscope (AFM) has a potential to observe fission tracks with high density after a short time etching^{1,2}. This research reports the several findings in observation of natural zircons by the AFM.

When zircon with high track density (e.g., > 30 tracks/ 10^{-6} cm²) was observed, many small pits with the depth less than 20 nm were found together with fission tracks (Figure 1). Fission tracks show deeper depths of ~50nm when the sample was readily etched and can be reasonably distinguished from other topographic lows. However, when etching time is too short (e.g., 1 hours at 230°C), depth difference is not perfectly obvious and the number of counted tracks were more than those expected based on U-Pb age, probably due to difficulties in recognising the fission tracks among structures other than fission tracks.

In the observation of young zircons collected from modern volcanic product, dynamic range of surface topography is less than 5 nm after the etching of 10 hrs (Figure 1). Many surface shallow etch pits with the depth of ~20 nm found in old zircons do not exit. Occasionally a hole with the depth of ca. 10 nm was found on the smooth surface. Because these zircons are from modern volcano and existence of a fission track is less plausible, these countable holes may be alpha recoil tracks. The depth of these holes is concordant with the shallow pits found in old zircon. Therefore, these shallow pits may also be alpha recoil tracks.

To see the behavior of shallow pits in old zircon, zircon was annealed at 600°C or 1000°C and observed. The surface topography have not changed much and 10~15nm pits were still preserved in the sample after 600°C annealing. After 1000°C annealing, the surface topography become a little flat, and as smooth as modern zircon. Fission tracks were not recognised after 1000°C annealing and this observation fits the previous annealing experiment to measure track length and density under the optical microscope. If shallow pits are assumed to be alpha recoil tracks, they are as resistant as fission tracks against heating.

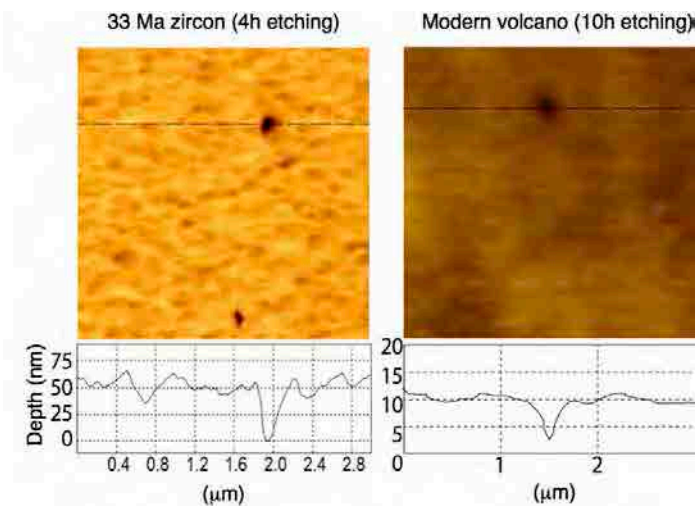


Figure 1. AFM images of zircons and depth profile along the dotted line.

References

1. Ohishi, S. & Hasebe, N. Observations of Fission-tracks in Zircons by Atomic Force Microscope, Radiation Measurements, 48, 554-556, 2012 Radiation Measurement **48**, 554-556 (2012).
2. Kohlmann, F., Kohn, B. P., Gleadow, A. J. W. & Siegele, R. Scanning force microscopy of ¹²⁹Iodine surface impact structures in muscovite, zircon and apatite as proxies for damage of simulated fission fragments in solids, Radiation Measurement **51-52**, 83-91 (2013).

Natural and artificial radiation damage effect on confined track lengths

Murat T. Tamer^{1,2}, Raymond Jonckheere², Richard A. Ketcham¹

1 Jackson School of Geosciences, The University of Texas at Austin, Austin TX, USA

2 Institut fuer Geologie, Technische Universitaet Bergakademie Freiberg, Germany

The common assumption that the annealing and etching behaviours of fission tracks induced to form in pre-annealed apatites and spontaneous fission tracks that form in non-pre-annealed apatites are equivalent has led to neglect of the possible influences of the background radiation damage that accumulates over geological time. From step-etched prismatic sections of a Durango apatite it was reported that the rate of increase of the mean induced track length in a pre-annealed section is low ($0.008 \pm 0.003 \mu\text{m/s}$) whereas the rate for the mean spontaneous track length is significantly higher ($0.025 \pm 0.003 \mu\text{m/s}$) under the same etching conditions (4.0 M HNO_3 at 25 °C) [1].

This investigation looks into the possible effects of natural radiation damage on spontaneous and induced confined track lengths in three different prismatic step-etched Durango apatite sections: 1- non-pre-annealed neutron irradiated; 2- natural; and 3- pre-annealed neutron irradiated. For this study step-etch experiments were performed from 20s to 60s at 10s intervals using more widely-used etching conditions (5.5 M HNO_3 at 21 °C). Using the assumption that the induced and spontaneous confined track length populations are normal distributions, the induced track data in the first Durango section were deconvoluted by fitting a pair of Gaussian curves, where the spontaneous track length distribution is adopted from the second section. We also observe that the fossil tracks become more anisotropic with etching time, whereas the induced tracks become more isotropic.

It has been reported that the mean track length can decrease in a step etch experiment [2] if the track length measurements are performed on different tracks for each etching step and recently-appeared tracks in the late etching steps are considered together with early-appearing tracks which had longer track etching times. In this work, in order to eliminate the difference between the track etching time and bulk crystal etching time, the track length data of recently-appeared confined tracks after 20s etching step were migrated to the 20s crystal etching time since their effective track etching time was lower than 20s.

In our and most other similar experiments to date, the rates of increase of the mean track length of fossil and induced tracks in natural apatite during step etching are indistinguishable from each other but faster than that of induced tracks in pre-annealed apatite. We infer that this difference is caused by radiation damage, principally from alpha recoil, accumulated over geological time in natural apatite. Further experiments planned to be completed by the meeting will elucidate whether the few observations that do not corroborate this trend may be due to poorly thermalized neutrons being used for irradiation. Clarifying the effect of background radiation damage on track etching will improve our ability to derive meaningful information from and concerning etch figures and initial track length, and ultimately address its role in annealing.

References

1. Jonckheere, R., Enkelmann, E., Min, M., Trautmann, C., Ratschbacher, L., 2007. Confined fission tracks in ion-irradiated and step-etched prismatic sections of Durango apatite. *Chemical Geology* **242**, 202-217.
2. Green, P.F., Duddy, I.R., Gleadow, A.J.W., Tingate, P.R., Laslett, G.M., 1986. Thermal annealing on fission tracks in apatite 1. A qualitative description. *Chemical Geology* **59**, 237-253.

Apatite fission-track dating of Fish Canyon tuff and Durango apatite using the automated counting-LA-ICP-MS methodology and a comparison with the External Detector Method

Raúl Lugo-Zazueta¹, Himansu Sahu², Andrew Gleadow², Barry Kohn²

1 Estación Regional del Noroeste, Instituto de Geología, Universidad Nacional Autónoma de México, Blvd. L.D. Colosio S/N y Madrid, 83240, Hermosillo, Sonora, México

2 School of Earth Sciences, University of Melbourne, Victoria 3010, Australia

Laser ablation mass spectrometry (LA-ICP-MS) in combination with recent developments in digital microscopy, image analysis and computer software has allowed the implementation of a new automated counting approach for apatite fission-track (AFT) analysis¹. We refer to this approach as the ‘automated counting-LA-ICP-MS’ method (ACLA). A major advantage of this methodology over conventional external detector method^{2,3} (EDM) is that since the uranium content of the apatite grains is determined by LA-ICP-MS neutron irradiation is not required and that a permanent digital imaging record for the analyzed grains is preserved. Two major components comprise the ACLA method; a) the ‘automated counting’ of spontaneous tracks performed on high-resolution images captured from apatite grains, and; b) the measurement of ²³⁸U content in apatite by LA-ICP-MS, which has been tested previously as a viable approach⁴. More details on the ACLA method using a calibration employing the zeta approach^{3,4} can be found in Lugo-Zazueta (2013)⁵.

In order to define the viability of the ACLA method and the reliability of results, we carried out a detailed study on apatite standards as well as on non-standard samples. This study involved data generation and analyses from 165 Fish Canyon Tuff apatite crystals and 40 Durango apatite crystals. Additionally, a comparative study between the EDM and the ACLA methods was performed on a set of thirteen granitoid samples from northwestern Mexico⁵ and four granitic samples from the eastern Dharwar craton (EDC), India⁶. For comparison at least 20 grains were analyzed per sample. Laser ablation of apatites was carried out using 25 µm laser beam diameter, with laser output energy of 70 mJ (5Hz) creating an ablation pit of ~9µm depth. For each apatite grain, single laser ablation measurements were carried out. Analyses on Fish Canyon Tuff crystals yielded an AFT age of 28.1±0.6 Ma (1σ), and 28.8±1.1 (1σ) Ma for Durango Apatite. These pooled-U AFT ages are in good agreement with the ages reported using other geochronology techniques³. Calculated AFT pooled-U ages from northwestern Mexico ranged from 13.4±0.9 Ma to 42.0±3.6 Ma, while AFT ages from the EDC ranged from 140±3.1 Ma to 218.4±12.1 Ma. The AFT ages determined by the ACLA method for these samples were in good agreement with the AFT ages previously determined by the conventional EDM method on the same samples^{5,6}.

Overall the results from the apatite standards and the comparative study were found to be very encouraging. We recommend further studies and assessments for development of a robust protocol for LA-ICP-MS to determine the uranium content, as well as assessing the viability of implementing a calibration factor for the ACLA method.

References

1. Gleadow, A. J. W., Gleadow, S. J., Belton, D. X., Kohn, B. P., Krochmal, M. S., & Brown, R. W. Coincidence mapping-a key strategy for the automatic counting of fission tracks in natural minerals: Geological Society, London, Special Publications **324**, p. 25-36 (2009).
2. Gleadow, A. J. W. Fission-track dating methods: What are the real alternatives?: Nuclear Tracks **5**, 3-14 (1981).
3. Hurford, A. J., and Green, P. F. The zeta age calibration of fission-track dating. Isotope Geoscience **1**, 285-317 (1983).
4. Hasebe, N., Barbarand, J., Jarvis, K., Carter, A., & Hurford, A. J., Apatite fission-track chronometry using laser ablation ICP-MS: Chemical Geology **207**, 135-145(2004).
5. Lugo-Zazueta, R., Thermochronology of the Basin and Range and Gulf of California extensional provinces, Sonora, Mexico: Ph.D. Thesis, School of Earth Sciences, University of Melbourne, Victoria, Australia, 286 p. (2013).
6. Sahu, H.S., Raab, M.J., Kohn, B.P. & Gleadow, A.J.W. Denudation history of crystalline Eastern Indian Peninsula from apatite fission track analysis: linking plume-related uplift and the sedimentary record, Tectonophysics **608**, 1413-1428 (2013).

Automated Fission Track and Etch Figure Characterization in Apatite Crystals

Lena Reed¹, Kevin Vigue¹, Ravi Kumar¹, Azubuike Ndefo-Dahl¹, Zachary Dodds¹,
Ray Donelick²

1 Harvey Mudd College, USA

2 Apatite to Zircon, Inc., USA

The purpose of this project is to implement automated feature detection in microscope images of apatite crystals. One of our goals is to automatically detect etch figures within apatite crystal images captured at different focal depths. Previously, we performed automated etch figure detection using algorithms designed to identify specific features of etch figures within an image. We are now taking a new approach to etch figure detection based on template matching techniques. Our method consists of finding locations in the image that closely match our etch figure template images from a large library of etch figure samples. Our algorithm searches not only within a single image but also within a stack of images at different focal depths, effectively searching for etch figures in three dimensions. Furthermore, our software uses a library of multi-layer template images that contain 3D data about etch figures.

In addition to detecting etch figures, another goal of our project is to automatically detect fission tracks in apatite crystal images. Our approach involves detecting tracks based on contrast differences between the center and edges of each potential track. For every position at each angle between 0 and 180 degrees, all potential tracks along the corresponding line are scored based on a combination of length and how closely they conformed to the expected traits of a fission track. The best track from each line is stored, and this library of tracks is periodically culled, removing tracks that are similar enough to be considered duplicates and then keeping only the best of the remaining tracks. The final track library is exported as a CSV file, which is read by our LabVIEW interface and presented for the user's judgment.

Finally, we also created a user interface to these command line analysis tools. For this, we use LabVIEW as it supports an easily customizable, module-based workflow. Since our feature analysis system is not perfect, it needs human input as well as the systems input. We are using LabVIEW so that the user can verify the output of the system as well as add any potential tracks that the system misses. We use the IMAQ functionality of LabVIEW, an image function that allows overlays to be added to the image. The system takes in a folder of images and uses the track finding module to calculate a rough estimate of track positions. The LabVIEW system draws lines based on these positions, at which point the user is able to categorize each line as accurate or inaccurate. If the track finding module missed any tracks, the user can also draw new track lines in LabVIEW.

Applications for ApUFT (apatite uranium fission track): combined apatite fission track + UPb dating by LA-ICP-MS

Paul O'Sullivan¹, Raymond Donelick¹, Jarson Barnes², Margaret Donelick¹
1 Apatite To Zircon, Inc. 1075 Matson Road Viola, ID 83872, USA
2 Department of Geosciences, University of Tuebingen, Germany

Recent advances in the use of LA-ICP-MS for fission track dating allow a new approach to apatite fission track analysis that obtains and utilizes LA-ICP-MS-derived UPb ages and chemical composition data for both age and length grains¹. ApUFT (apatite uranium fission track) provides additional information during the analysis to facilitate a better understanding and interpretation of apatite fission track data. We present two examples that highlight how these additional data were useful when interpreting results.

Example 1 – recognizing and removing contaminant grains. We received a sample with the following constraints: 1. subsurface cuttings, 2. stratigraphic age ~120 Ma, 3. present-day temperature ~60°C, 4. required uplift and erosion of ~1-1.5 km within last 5 m.y.). ApUFT data from this sample (age ~107 Ma, M.L. ~14 µm) were inconsistent with the geologic history of the region, which required that ~1-1.5 km of section had been removed from the surface since 5 Ma. All attempts to model the original data set failed due to the presence of abnormally old fission track grains that should not have been present in the sample, since it had recently cooled from significantly higher temperatures. After verification that contamination during processing was not an issue, it was ultimately determined that caving during the drilling process was the likely cause for the presence of the old fission track grains. Subsequently, by using the ApUFT results from the sample (Fig. 1A and 1B), which showed that the abnormally old fission track grains also had significantly older UPb ages, we were able to remove all fission track age and length data contributed by the older grains and successfully model the fission track results collected from only the younger fission track grain population.

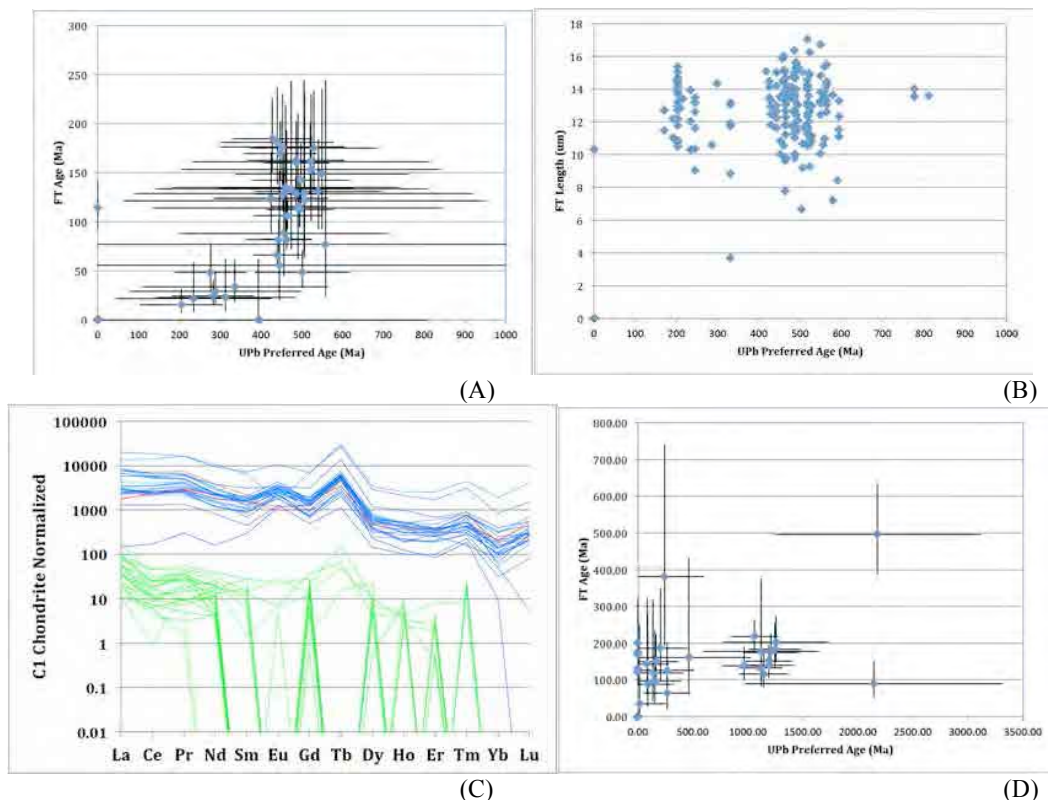


Figure 1. Example plots from the two samples discussed. 1A and 1B present the ApUFT age and track length data for Example 1 plotted against each grain's UPb age. Using this information, one can easily separate out both age and track length data from any of the different populations shown. 1C presents the REE (chemical composition) data for the ApUFT age grains discussed in Example 2. 1D presents ApUFT age data for Example 2 plotted against each grain's ApUPb age. The young ApUPb age population shown in 1D is the same population shown in green in 1C, with lower normalized C1 chondrite values.

Example 2 – recognizing and modeling individual detrital populations within a mixture. We received a sample with the following constraints: 1. subsurface cuttings, 2. stratigraphic age ~150 Ma, 3. present-day temperature ~75°C, 4.

geologic history that required significant burial within the last 5 m.y.). ApUFT data from this sample (age ~165 Ma, M.L. ~13.5 μm) were consistent with an interpretation that the sample had not yet equilibrated to prevailing present-day temperatures and, therefore, provided provenance information only. By using both the REE and UPb results from the sample (Fig. 1C and 1D), which showed there were at least two distinct populations of grains represented within the sample, we were able to split out the ApUFT age and length data contributed by each of the apparent grain populations and model their ApUFT results separately. A similar approach would also be applicable to detrital fission track studies, and could potentially greatly expand the amount of information gained from such studies.

References

1. Chew, D.M. & Donelick, R.A. Combined apatite fission track and U-Pb dating by LA-ICP-MS and its application in apatite provenance analysis in *Quantitative Mineralogy and Microanalysis of Sediments and Sedimentary Rocks* (ed. Sylvester, P.) 219-247 (Mineralogical Association of Canada Short Course 42, St. John's, Newfoundland and Labrador, 2012).

Visualization of neutron induced fission tracks in calcite

Sebastian Dederer¹, Ulrich A. Glasmacher¹, Michael Burchard¹
¹ Institute of Earth Sciences, University of Heidelberg, Germany

An etching technique was developed to visualize ion tracks in calcite that are induced by irradiation with swift heavy U-ions of a total high energy of about 2.1 GeV [1-2] at the UNILAC, GSI Darmstadt. The next step was to develop an etching technique able to visualize fission tracks induced by ions of about 160 MeV energy, which is more similar to natural processes but about 13 times less than the total particle energy used at the UNILAC.

Therefore, in two experiments calcite crystals have been covered with (a) CN-5 uranium glass to check the areal density of fission tracks displayed on the calcite crystal (Fig.1), and (b) with a polished epoxy mount bearing zircon single crystals. These packages were irradiated with thermal neutrons (1×10^{15} neutrons/cm²) at the FRM II in Munich to induce ²³⁵U-based fission tracks with energies of about 160 MeV in the calcite crystal.

To reveal the induced fission tracks the calcite crystals have been etched with the established etching procedures. The etching revealed clear defined etch pits of about 5 μ m length and 4 μ m width which are visible under an optical microscope. These etch pits are similar in shape than the etch pits caused by swift heavy ion irradiation (Fig 2).

The experiments proof that it is possible to visualize fission tracks in calcite. This technique might open a new branch of thermochronologic dating that provides a whole new archive: the U-bearing carbonate minerals and, therefore, carbonate rocks.

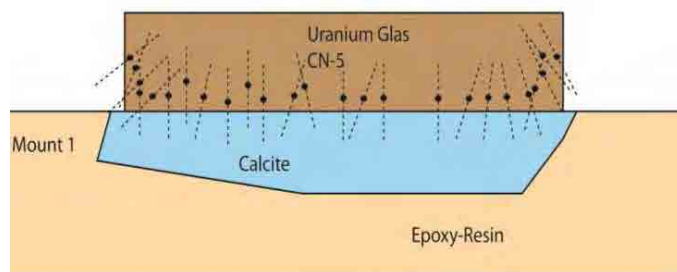


Figure 1: Sketch of the uranium glass – calcite experiment. The uranium glass is positioned directly on the polished calcite crystal and, therefore, provides a direct supply of fission tracks into the calcite.

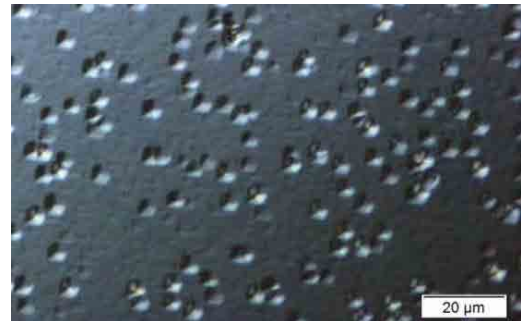


Figure 2: Etch pits on the calcite crystal surface. They have a pseudo-pentagonal shape and a size of about 5 μ m in length and 4 μ m in width.

References

1. Dederer, S., Glasmacher, U.A., Burchard, M. & Trautmann, C. Preparation of Carbonate Rocks for Irradiation with Swift Heavy Ions. (In Preparation)
2. Dederer, S., Glasmacher, U.A., Burchard, M. & Trautmann, C. Visualization of Heavy Ion Tracks in Calcite by EDTA etching techniques. (In Preparation)

Advances in Ar mass spectrometry – removing the H³⁵Cl interference

John Saxton

Nu Instruments Ltd, 74 Clywedog Road South, Wrexham, LL13 9XS, UK

Recent development of the Nu Instruments Noblesse noble gas mass spectrometer has resulted in increased mass resolving power (MRP), and much improved ability to deal with isobaric interferences. The source design also allows the MRP to be adjusted without the complexity of a movable source slit. We demonstrate this improved performance by considering the HCl and C₃ interferences at mass 36. These are particularly important in Ar-Ar dating as ³⁶Ar is used for correction of the trapped atmospheric component.

Data were obtained on an instrument which was – intentionally – only lightly baked and therefore had high levels of interferences.

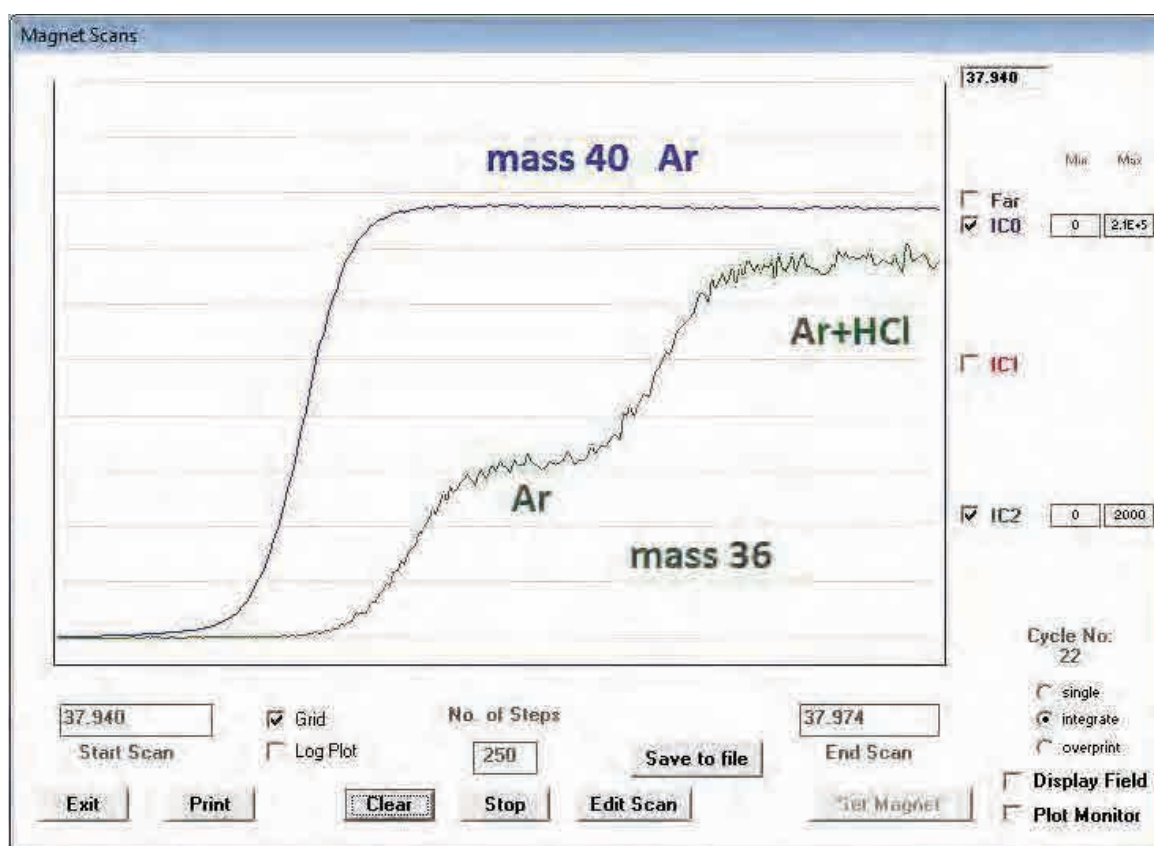


Figure 1. peak shapes at masses 40 and 36.

Instrument performance was assessed by admitting different sized air samples, and measuring the ³⁶Ar/⁴⁰Ar ratio. This was done for both larger samples (⁴⁰Ar measured on the Faraday, ³⁶Ar from 11 to 90 kcps) and smaller samples (⁴⁰Ar measured on an ion counter, ³⁶Ar from 300 to 2400 cps).

Data were plotted in the format ³⁶Ar/⁴⁰Ar vs. 1/⁴⁰Ar. This is suitable for a mixture of fixed blank and variable amounts of sample (=air), and is very useful for assessing instrument performance: the data should lie on straight line (assuming linear response); the slope gives the amount of interference; the intercept gives the ratio in the absence of interference; and dispersion can be assessed.

Several datasets have now been obtained. These indicate that up to 99% of the HCl is removed, depending on the exact ^{36}Ar mass setting. Furthermore, the reproducibility of the data is not significantly worsened by measuring ^{36}Ar alone in comparison to $^{36}\text{Ar}+\text{HCl}$ combined. In one example, one of the small sample datasets (comprising 54 measurements of $^{36}\text{Ar}/^{40}\text{Ar}$, 300 – 2400 cps of ^{36}Ar in the presence of 600 cps of HCl and 6000 cps of C_3) gave dispersions follows: ^{36}Ar alone, rms from mean 1.1%; ^{36}Ar alone, rms from line 0.7%; $^{36}\text{Ar}+\text{HCl}$ combined, rms from line 1.5%. The data will be described more fully at the conference.

Rapid characterization of noble-gas kinetics using continuous heating and gas accumulation

Bruce D. Idleman¹ and Peter K. Zeitler¹

¹*Dept. Earth and Environmental Sciences, Lehigh University, Bethlehem, PA 18015, USA*

Current understanding of the diffusion of noble gases in anhydrous minerals has come largely from step-heating experiments undertaken to provide kinetic constraints for U-Th/He, $^4\text{He}/^3\text{He}$, and $^{40}\text{Ar}/^{39}\text{Ar}$ thermochronology. However, despite its widespread use in noble gas studies, step heating is a time consuming and inefficient technique. For typical extraction steps involving heating, cooling, gas purification, analysis, and pumping, the time a sample is heated at the temperature of interest may represent only a small fraction of the total duration of an analysis. Consequently, detailed diffusion studies (e.g., dating of K-feldspar by the $^{40}\text{Ar}/^{39}\text{Ar}$ MDD method) commonly require several days or more to complete. Such studies are costly and tie up instrumentation for long periods, significantly impacting laboratory workflow and productivity.

We are investigating an alternative experimental approach to characterizing noble-gas diffusion that couples continuous sample heating with continuous accumulation and measurement of the evolved sample gas. An important advantage of this technique is that an entire diffusion experiment can be carried out in the time needed to complete only a few conventional heating steps, thereby raising the possibility of using it as a tool for rapid screening and characterization of samples, for example in routine U-Th/He thermochronology.

Our initial work has examined ^4He diffusion kinetics in apatite. In our experiments we subjected apatite samples to a ramped, rate-controlled heating schedule in a double-vacuum furnace under static vacuum conditions. The evolved gas was allowed to accumulate in the extraction line, and ^4He abundances were determined manometrically at 20-second intervals using a quadrupole mass spectrometer left continuously open to the extraction line. The furnace temperature was ramped from ~ 200 to 1150°C at rates of $10\text{-}20^\circ\text{C}/\text{minute}$, and about 225 measurements were made over a period of about 75 minutes for each experiment. Individual ^4He measurements were treated mathematically as square-pulse heating steps, using the net gas accumulated per step and the mean crucible temperature during the integration interval. Recovery of kinetic parameters then followed the standard methodology used for traditional step-heating experiments.

Continuous heating/accumulation experiments performed on aliquots of Durango apatite yielded simple, sigmoidal gas evolution curves and broadly linear and coincident arrays on Arrhenius diagrams. The Arrhenius results appear to be insensitive to variations in heating rate, and the activation energies defined by the low-temperature segments of the Arrhenius curves are consistent with those reported previously by Farley¹ for conventional step-heating experiments. We have also applied this technique to two Himalayan apatites that yielded anomalously old and unreproducible U-Th/He ages by conventional analytical techniques (see also abstract by Zeitler,

this volume). In marked contrast to the Durango results, the Arrhenius curves for these samples contain significant non-linear segments and sharp kinks at both low and high extraction temperatures that cannot be explained by simple models of diffusive loss and/or alpha ejection of ^4He . The continuous heating/accumulation results for the Himalayan apatites correspond closely with those obtained from conventional step-heating experiments (14 steps each), but they also reveal subtle details in behavior not evident in the step-heating data.

The continuous heating/accumulation method places unique and potentially challenging demands on instrumentation and methodology. To achieve the best results, mass spectrometers need to have wide dynamic range, good linearity, and the ability to maintain high analytical precision across their entire measurement range. Additionally, many of the experimental phenomena that influence isotopic abundances and ratios during noble gas analysis (e.g., gas consumption and fractionation, evolution of line blank and instrument background, etc.) are difficult to quantify and control in continuous heating/accumulation experiments. Given the substantial rates of gas consumption and isotopic fractionation exhibited by modern magnetic-sector noble-gas mass spectrometers during static analysis, application of the method to argon diffusion studies using these instruments will likely prove challenging, particularly if the goal is also to measure isotope ratios. However, the method's technical demands are less of an issue for routine ^4He measurements, since small quadrupole mass spectrometers commonly used to measure helium for thermochronology are capable of achieving good dynamic range and linearity while maintaining very low rates of gas consumption and fractionation.

References

1. Farley, K. A., Helium diffusion from apatite: General behavior as illustrated by Durango fluorapatite. *Journal of Geophysical Research: Solid Earth*, **105**, 2903-2914 (2000).

In-situ U-Th-Sm-He Thermochronology

Noreen Evans¹, Brent McInnes¹, Michael Shelley², Bradley McDonald¹, David Gibbs³, Ashley Norris⁴, Mike Hamel⁴, Cliff Gabay⁴ and Desmond Patterson⁵

1 John de Laeter Centre, Applied Geology/Applied Physics, Curtin University, Perth, Australia

2 Laurin Technic Pty Ltd, Canberra, ACT, Australia

3 Australian Scientific Instruments Pty Ltd, Canberra, ACT, Australia

4 Resonetics Ltd, Nashua NH, USA

5 Patterson Instruments Ltd, Austin TX, USA

The AuScope AGOS GeoHistory Facility at Curtin University houses the prototype RESOchron instrument suite designed to conduct rapid, automated *in-situ* U-Th-Sm-Pb-He (and trace element) analysis of multiple mineral grains. This novel capability permits a detailed interrogation of the time-temperature history of rock types containing apatite, zircon, rutile, titanite and other accessory phases. In addition to providing a conventional zircon U-Pb geochronology capability, the system provides thermochronometry data via in situ (U-Th-Sm)-He dating. The benefits of in-situ (U-Th-Sm)-He thermochronology relative to conventional standard single crystal analysis include:

- Increased research productivity (10-20 fold);
- Eliminate the need to use hazardous HF;
- Eliminate the need for Ft corrections;
- The ability to avoid mineral/gas inclusions and other sources of contamination;
- A new capability for He mapping and depth profiling.

The analytical system integrates three commercially available components:

- (1) A 193 nm excimer laser based on the Resonetics RESolution™ M-50-LR design,
- (2) A helium mass spectrometry module based on the Australian Scientific Instruments ALPHAchron™ design,
- (3) Two swappable analytical chambers built by Laurin Technic:
 - M50 flow-through cell for trace element analysis, and
 - An ultra-high vacuum (UHV) cell for helium analysis.

An ICP-MS instrument is required for analysis of parent isotopes, Pb and trace elements. Development work has begun with polished zircon grains, helium extracted in the UHV cell using the following optimised excimer laser ablation settings; 30s ablation, 33µm beam width, 3Hz frequency, 12% attenuation, 80-100mJ energy and 2.3J/cm² fluence. Pits are typically <8 µm deep and pit volumes are measured using confocal laser microscopy. U, Th and Sm are subsequently analysed in a laser pit ablated over the original helium pit using traditional ELA-ICP-MS methods¹. (U-Th)/He ages are calculated using standard radiometric decay equations.

Using the RESOchron instrument, ⁴He can be reliably measured in pits as small as 10 µm x 10 µm (diameter x depth) with a precision ±1.2% on larger volumes. The ⁴He extraction process has no discernable impact on the U and Th content of the residual sample material indicating an apparent preservation of parent-daughter relationships. Sri Lanka zircons B188 and RB140 are prospective *in-situ* double dating standards with RESOchron in-situ ages

falling within 5% of known (U-Th)/He ages (Table 1). A zircon from Cambodia with homogeneous U, Th and He distribution is another potential standard candidate.

Table 1. *Traditional and In situ (U-Th)/He ages of potential zircon standards*

Potential in situ (U-Th)/He Zircon Standard	U (ppm)*	Th (ppm)	In situ (U-Th)/He Age (Ma)	Traditional ² (U-Th)/He age (Ma)
B188	578 ± 18	58 ± 2	420 ± 13	435 ± 15
RB 140	318 ± 12	126 ± 5	415 ± 15	433 ± 20
Cambodia	102 ± 3	41 ± 1	319 ± 9	In progress

*Determined using ELA-ICP-MS; NIST 610 as primary standard and ²⁸Si as internal standard element

Continued technique development will focus on improving the accuracy and precision of age determinations, including:

- Optimizing instrument and sample preparation protocols for laser extraction and microanalysis of U, Th, Pb, Sm and He from a variety of minerals;
- Development of synthetic and natural mineral standards for in-situ U-Th-Pb-He dating;
- Optimise techniques for quantitative He measurement by testing various methods of laser pit volume measurement (and/or proxy isotope analysis).

References

1. Vermeesch, P., Sherlock S. C., Roberts, N. M. W. & Carter A. A simple method for in-situ U-Th-He dating, *Geochim. Cosmochim. Acta* **79**, 140–147 (2012).
2. Evans, N.J., Byrne, J.P., Keegan, J.T. & Dotter, L.E. Determination of uranium and thorium in zircon, apatite and fluorite: Application to laser (U-Th)/He Thermochronology *Journal of Analytical Chemistry* **60/12**, 1159-1165 (2005).

Optimizing (U-Th)/He thermochronology by full chemical characterization in apatites

Rosella Pinna-Jamme¹, Cécile Gautheron¹, Andy Carter², Maurice Pagel¹

¹*Geosciences Paris Sud (GEOPS, UMR 8148), Université Paris Sud XI- Orsay, France*

²*Departments of Earth and Planetary Sciences, Birkbeck University of London, UK*

Interpretation of the low-temperature thermochronometer apatite (U-Th)/He (AHe) data is based on our ability to describe the entire processes influencing the He system. Recent studies¹⁻² show that He retention in the apatite crystal lattice is not constant but is a function of the level of α -recoil damage created by U-Th decay. Models³⁻⁴ have been developed to explain He retentivity behavior in relation to alpha damage but not compositional effects. A recent study⁵ proposed that the recoil damage annealing is strongly dependent on the grain chemistry similar to what has been observed on apatite fission tracks⁶. A quantum investigation of the He diffusion also defined the influence of the chemistry on the He diffusion process⁷ and therefore we stress the importance of taking apatite composition into account when determining U-Th ages. To make this practical we have developed new analytical protocols in order to have: (i) an easy-to-use and straightforward chemistry protocol for sample preparation and full elemental analysis by ICP-MS; (ii) the use of La-ICP-MS and electronic microprobe complementary techniques for element cross-calibration and data validation. We also applied the protocol to a geological case study for validation.

The protocol was applied to samples of the Durango and Limberg tuff apatite standards and detrital apatite grains from Triassic sandstone, Paris Basin⁵. After grain picking and He degassing, associated apatites were dissolved and the major elements (including F, Cl), minor and trace elements were analysed by solution ICP-MS. Analytically, the protocol proved a promising tool for a complete chemistry investigation in terms of sensitivity (negligible background contribution for all elements), accuracy (13 to 15 repeated analysis runs for one sample), precision (relative precision < 4%) and time-consuming efficiency (high analysis rates). Preliminary *in situ* analyses on larger apatite grains by La-ICP-MS and electronic microprobe techniques also proved helpful for consistent U-Th content cross-calibration and achieving good reproducibility of the AHe ages.

References

1. Shuster D., Flowers, R., Farley, K.A. The influence of natural radiation damage on helium diffusion kinetics in apatite. *Earth Planet. Sci. Lett.*, 249: 148-161 (2006).
2. Green, P.F., Duddy, I.R. Interpretation of apatite (U-Th)/He ages and fission track ages from cratons. *Earth and Planetary Science Letters* **244**, 541-547 (2006).
1. Flowers R., Ketcham, R.A., Shuster, D., Farley, K.A., Apatite (U-Th)/He thermochronology using a radiation damage accumulation and annealing model. *Geochim. Cosmochim. Acta*, **73**: 2347-2365 (2009).
2. Gautheron C., Tassan-got, L., Barbarand, J., Pagel, M., 2009. Effect of alpha-damage annealing on apatite (U-Th)/He thermochronology. *Chemical Geology*, **266**: 166-179.
3. Gautheron C., Barbarand J., Ketcham R.A., Tassan-Got L., van der Beek P., Pagel M., Pinna-jamme R., Couffignal F., Fialin M., Chemical influence on α -recoil damage annealing in apatite: Implication for (U-Th)/He dating. *Chemical Geology*, **351**: 257-261 (2013).
4. Barbarand J., Carter, A., Wood, I., Hurford, T. Compositional and structural control of fission-track annealing in apatite. *Chem. Geol.*, **198**: 107-137 (2003).
5. Mbongo Djimbi, D. Gautheron C., Roques J., Tassan-Got L., Gerin C., Simoni E., Apatite composition on (U-Th)/He thermochronometer: a quantum point of view. Submitted to *Geochim. Cosmochim. Acta*.

An empirical test of the fragmentation effect and age dispersion in single grain apatite (U-Th)/He ages: a case study from the Ballachulish complex, Scotland

David Webster¹, Roderick Brown¹, Romain Beucher², Cristina Persano¹, Fin Stuart³ and Kerry Gallagher⁴

1 School of Geographical and Earth Sciences, University of Glasgow, UK

2 Department of Earth Science, University of Bergen, Bergen, Norway

3 Scottish Universities Environmental Research Centre, East Kilbride, UK

4 Géosciences Rennes, Université de Rennes 1, France

Over the last decade or so major progress has been made in developing both the theoretical and practical aspects of apatite (U-Th)/He thermochronology^{1,2}. However, a persistent problem of excessive age dispersion, especially from samples from slowly cooled terranes such as cratons, has not yet been satisfactorily explained³. This often undermines the routine application of the methodology.

The aim of this study was to carry out an empirical test of a novel new approach to (U-Th)/He thermochronology^{4,5} that recognises that a significant component of the natural dispersion commonly seen for single crystal (U-Th)/He (AHe) age measurements (i.e. the dispersion that exceeds that expected statistically from the analytical precision of measurements alone) arises because single grains are often fragments of larger grains. The individual prismatic crystals of apatite that are routinely analysed are often broken parallel to the weak cleavage direction perpendicular to the prismatic c-axis during rock crushing and mineral separation. This is indicated by the common occurrence of only 1 or no crystal terminations in separated apatite grains^{1,6}.

The experiment was conducted using a vertical sequence of 12 samples from the Ballachulish Complex in Scotland. The samples are from elevations between sea level and 1001m and yield excellent quality euhedral apatite crystals. Persano et al.⁷ report AHe ages on a sub-set of these samples (using multi-grain aliquots) of 77 ± 8 to 265 ± 26 Ma ($\pm 2\sigma$) and AFT of 186 ± 6 to 257 ± 12 Ma (elevation range 195 – 1001m).

In this study we aim to use the spectrum of ages as a function of elevation to examine the actual pattern of age dispersion with the theoretical pattern expected from populations of grain fragments⁴. We will report new single grain AHe age data from the Ballachulish profile to document the range and pattern of single grain age dispersion, both within samples and between samples, coupled with thermal history modeling tests performed using the Helfrag approach described by Beucher et al.⁵.

References

1. Farley, K. A. (U-Th)/He dating: techniques, calibrations and applications. *Rev. Min. Geochem.* **47**, 819-844 (2002)
2. Shuster, D. L. & Farley, K. A., 4He/3He thermochronometry: theory, practice and potential applications. *Rev. Min. Geochem.* **58**, 181-203 (2005)
3. Fitzgerald P. G. *et al.* Interpretation of (U-Th)/He single grain ages from slowly cooled crustal terranes: A case study from the Transantarctic Mountains of southern Victoria Land. *Chem. Geol.* **225**, 91-120 (2006)
4. Brown, W. R. *et al.* Natural age dispersion arising from the analysis of broken crystals. Part I: Theoretical basis and implications for the apatite (U-Th)/He thermochronometer. *Geochem. Cosmo. Acta.* **122**, 478-497 (2013)

5. Beucher, R. *et al.* Natural age dispersion arising from the analysis of broken crystals. Part II: Practical application to apatite (U-Th)/He thermochronometry. *Geochem. Cosmo. Acta.* **102**, 395-416 (2013)
6. Farley, K. A. *et al.* Numerical investigations of apatite 4He/3He thermochronometry, *Geochem. Geophys. Geosys.* **11**, **10**, 18 pp., (2010)
7. Persano, C. *et al.* Constraints on early Cenozoic underplating-driven uplift and denudation of western Scotland from low temperature thermochronometry. *Earth. Planet. Sci. Lett.* **263**, 404-419 (2007)

(U+Th)/Ne dating of secondary Pb mineralization from Leadhills-Wanlockhead, southwest Scotland, supports an origin during the onset of northern hemisphere glaciation.

Finlay M. Stuart

Isotope Geosciences Unit, Scottish Universities Environmental Research Centre, East Kilbride G75 0QF, UK

The weathering of base metal deposits gives rise to the development of assemblages of exotic low temperature mineral species that provide a record of the interaction between primary mineralization, groundwater and atmosphere. As well as tracing subtle changes in hydrology, these processes are often responsible for the enrichment of rare metals to economic grades. The timing of secondary mineral formation is, consequently, of importance for palaeo-environmental reconstruction and mineral exploration.

The secondary mineralization at Leadhills-Wanlockhead in SW Scotland is a globally-exceptional mineral assemblage that includes over 100 mineral species¹ that reflects unusual conditions of formation and/or circumstances of subsequent preservation. They are certainly pre-glacial - oxidised assemblages are scarcely developed on glacially exposed Pb deposits elsewhere in northern Europe, but are widely developed in less glaciated and unglaciated areas e.g. Cornwall. Belgian calamine deposits are known to be pre-late Cretaceous, and it seems likely that other oxidised ore bodies also retain Mesozoic atmospheric and water table information. The Leadhills-Wanlockhead secondary mineral assemblages contain a high-resolution record of protracted weathering. In an effort to develop a genetic model of secondary Pb mineralization we are determining the paragenetic sequence and the fluid compositions and physical conditions of the secondary mineralization.

The age of the secondary mineralization is difficult to measure. There are no Pb-free or K-bearing minerals that would allow conventional U/Pb or Ar/Ar age determinations. We have identified that several mineral species contain significant U levels (10-20 ppm), and sub-ppm Th. We have initiated a programme of (U+Th)/He and (U+Th)/Ne dating of vanadinite ($\text{Pb}_4(\text{VO}_4)_3\text{Cl}$) in an effort to constrain the timing and duration of secondary mineralization. Despite relatively high U concentrations, the extremely low He concentrations are indicative of complete diffusional loss. However, significant concentrations of ^{21}Ne in excess of atmosphere have been measured in all samples (n=6). Using the average U (and Th) content measured in multiple aliquots of vanadinite from the same sample, yields (U+Th)/Ne ages of 3-4 Ma for all samples. This coincides with the onset of northern hemisphere glaciation, and it is tempting to draw conclusions regarding the environmental conditions necessary to precipitate and preserve such an exceptional secondary mineral assemblage. Ongoing work is aimed at assessing the extent of diffusional loss of ^{21}Ne from vanadinite, and improving the precision of Ne isotope determinations.

References

1. Temple, AK The Leadhills-Wanlockhead lead and zinc deposits. *Transactions of the Royal Society of Edinburgh* **63**, 85-115 (1956).

ASL1: the first well-calibrated zircon standard for in-situ U-Th-He dating

Yuntao Tian¹, Pieter Vermeesch¹

¹ Department of Earth Sciences, University College London, United Kingdom

Zircon is an extremely durable mineral, which is commonly found in siliciclastic rocks and is rich in U and Th. These properties make zircon uniquely well suited for sedimentary provenance studies. Using micro-analytical methods such as LA-ICP-MS or SIMS, it has become routine practice to determine the probability distribution of ~100 detrital zircons (DZ) as a characteristic fingerprint to trace the flow of sand through modern and ancient sediment routing systems. Literally dozens of papers employing this method are published each year. The power of such provenance studies would greatly increase if it were possible to routinely double-date DZs with the U-Pb and U-Th-He methods. Several research groups around the world are currently pursuing this goal using a variety of approaches. Boyce et al.¹ and Tripathy-Lang et al.² use a 'first principles' approach, in which the absolute concentrations (e.g., in units of fmol/μm³) of U, Th and He are measured by laser ablation. Vermeesch et al.³ proposed an alternative approach, in which the raw mass spectrometric measurements are normalised to a standard of known ²⁰⁸Pb/²⁰⁶Pb and U-Th-He ages. The advantage of the latter approach is that it greatly reduces the influence of matrix effects and differences in ablation rate. We here present the compositional analysis of a commercially sourced megacrystic Sri Lanka zircon suitable as an in-situ U-Th-He dating age standard.

'SL-1' is of uniform pale-yellowish color. This large grain (1.2×0.8×0.8 cm) is rounded, with no original crystalline facets preserved, suggesting it has probably experienced long-distance fluvial transport. Cathodoluminescence (CL) imaging analyses of about 50 shards of SL-1 shows no visible internal texture variations, even though fine-tunings of signal intensity and brightness were implemented. This suggests that the zircon SL-1 is texturally homogeneous. The spatial uniform distributions of U and/or Th are demonstrated by two methods: spontaneous fission-track mapping by optical microscopy and elemental mapping by scanning electron microscopy (SEM) with energy dispersive X-ray spectrometry (EDS). Quantitative U and Th measurements were performed by Laser Ablation Inductively Coupled Plasma Mass Spectrometer (LA-ICP-MS). A general survey of 20 randomly selected shards and transect analyses along six profiles by LA-ICP-MS reveals no U and Th zoning, and determines the ²³⁸U and ²³²Th concentrations, at 358 ± 10 ppm and 736 ± 18 ppm respectively. Preliminary conventional U-Th-He age analyses on small fragments yield consistent ages of ~475 Ma. Since the parent nuclides are uniform in SL1, the consistent U-Th-He ages imply He is uniform within SL-1 as well. These primary results will be refined by more on-going analyses.

References

1. Boyce, J. W. et al. Laser microprobe (U-Th)/He geochronology. *Geochim. Cosmochim. Acta* **70**, 3031-3039 (2006).
2. Tripathy-Lang, A., Hodges, K. V., Monteleone, B. D. & van Soest, M. C. Laser (U-Th)/He thermochronology of detrital zircons as a tool for studying surface processes in modern catchments. *J. Geophys. Res.* **118**, 1333-1341 (2013).
3. Vermeesch, P., Sherlock, S. C., Roberts, N. M. W. & Carter, A. A simple method for in-situ U-Th-He dating. *Geochim. Cosmochim. Acta* **79**, 140-147 (2012).

Fluorite (U-Th)/He thermochronology: what do we really date?

Reinhard Wolff, István Dunkl, Hilmar von Eynatten
Geoscience Center, University of Goettingen, Germany, rwolf@gwdg.de

The (U-Th)/He thermochronology of accessory minerals like apatite and zircon provides excellent constraints on low temperature thermal histories. The majority of low-T thermochronological studies, however, is limited to the occurrence of these two minerals. Veins and hydrothermal deposits are major archives of localized fluid flow and short-lived thermal anomalies of the uppermost crust but in these deposits these usually dated minerals are typically lacking. Thermochronology beyond apatite and zircon is a key for understanding the age and the timing of such processes. The importance of fluorite as possible geo-thermometer is due to its common occurrence in ore deposits and carbonate host rocks and its sensitivity to thermal overprints below 200 °C^{1,2}.

The need to constrain the age of ore deposits led to the development of isotopic techniques for fluorite geochronology using Sm/Nd^{3,4} and U-Th-Pb⁵ techniques. Furthermore, fluorite low-temperature (U-Th)/He thermochronology (FHe) was introduced by Evans *et al.*¹ and applied by Pi *et al.*² and Siebel *et al.*⁶.

Fluorite commonly occurs in high- to low-temperature hydrothermal veins, as accessory mineral in granite, pegmatite, alkaline intrusives, carbonatite, and stratabound deposits, and as cement in sandstones. The diffusion parameters of helium in fluorite are still under debate and estimated closure temperature range from 90°C to 200°C^{1,2}. These estimates, however, are based on very few diffusion experiments only, not taking into account the huge chemical variability of fluorite.

To further evaluate fluorite (U-Th)/He methodology we followed a twofold strategy. First, the method is applied in a regional case study and the results are integrated in a multi-method thermochronological history together with already established thermochronological methods like AFT and AHe. The Erzgebirge is well suited for a field study because (i) it is well known for its various fluorite occurrences, and (ii) the possibility to apply additional low temperature thermochronometers. Once the exhumation and thermal history of the Erzgebirge is well constrained by other methods, the obtained fluorite (U-Th)/He ages can be included in the time-temperature path and information on the closure temperature range can be extracted (Fig. 1).

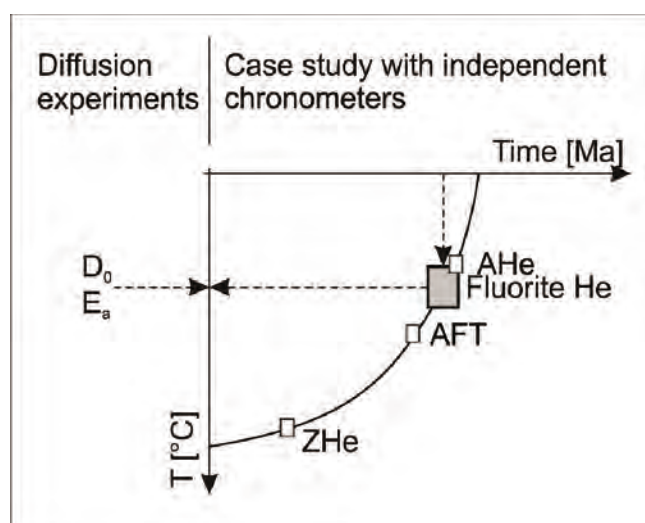


Figure 1. Time-temperature plot illustrating our twofold approach to determine the closure temperature for He diffusion in fluorite based on (i) diffusion experiments (left side) and (ii) a regional case study (right side).

Second, the resulting closure temperature of FHe is compared to the theoretical diffusion behavior of helium in fluorite. Bulk diffusion experiments on natural fluorite are performed to infer the activation energy E_a and the diffusivity D_0/a^2 . Variations in crystal chemistry and structure due to substitution for Ca by rare earth elements and Yttrium (REE+Y), and other cation are monitored by ICP-MS measurements.

The analysis of 180 fluorites has yield concentrations between zero and 74 ppm U, zero and 245 ppm Th, and zero and 165 ppm Sm. Mean concentrations are approx. 0.9 ppm U, 4.4 ppm Th, and 8.7 ppm Sm. The apparent fluorite (U-Th)/He ages are all Cretaceous in the entire Erzgebirge.

In a mining district of the German-Czech Ore Mountains (Horní Krupka) a fluorite sample of 300 ± 12 Ma (U-Th)/He age yields a closure temperature of ~ 170 °C, while the minerals with considerably younger Late Cretaceous cooling ages yield considerably lower closure temperature (~ 60 °C). This variation in closure temperature is correlated to the REE content. The high closure temperature variety of fluorite could keep quantitatively the helium since the formation of the fluorite-bearing ores in Carboniferous time⁷ in spite of the Mesozoic burial and hydrothermal heating of the area. On the contrary the low closure temperature variety of fluorite yields ages close to AFT cooling ages benchmarking the Late Cretaceous exhumation period in the region⁸.

Our study on fluorite (U-Th)/He thermochronology demonstrates the feasibility of dating the thermal history of hydrothermal deposits by fluorite chronometry, however, the highly variable closure temperature calls for detailed mineralogical and chemical characterisation of the dated fluorites.

References

1. Evans, N. J. Wilson, N. Cline, J. McInnes, B. I. A. & Byrne, J. Fluorite (U–Th)/He thermochronology: Constraints on the low temperature history of Yucca Mountain, Nevada, *Applied Geochemistry* **20**, 1099–1105 (2005).
2. Pi, T. Solé, J. & Taran, Y. (U-Th)/He dating of fluorite: application to the La Azul fluorspar deposit in the Taxco mining district, Mexico, *Mineralium Deposita* **39**, 976–982 (2005).
3. Chesley, J. Halliday, A. N. & Scrivener, R. C. Samarium-Neodymium Direct Dating of Fluorite Mineralization, *Science* **252**, 949–951 (1991).
4. Chesley, J. Halliday, A. N. Kyser, T. K. & Spry, P. G. Direct dating of mississippi valley-type mineralization; use of Sm-Nd in fluorite, *Economic Geology* **89**, 1192–1199 (1994).
5. Hofstra, A. H. Premo, W. R. Emsbo, P. Cline, J. S. & Aleinikoff, J. N. in *Geology and Ore Deposits 2000: The Great Basin and Beyond*. edited by J. K. Cluer, J. G. Price, E. M. Struhsacker, R. F. Hardyman & C. L. Morris (2000), pp. 61–65.
6. Siebel, W. *et al.* Age constraints on faulting and fault reactivation: a multi-chronological approach, *Int J Earth Sci (Geol Rundsch)* **99**, 1187–1197 (2009).
7. Romer, R. L. Thomas, R. Stein, H. & Rhede, D. Dating multiply overprinted Sn-mineralized granites - examples from the Erzgebirge, Germany, *Mineralium Deposita* **42**, 337–359 (2007).
8. Lange, J.-M. Tonk, C. & Wagner, G. A. Apatite fission track data for the Postvariscan thermotectonic evolution of the Saxon basement first results, *Zeitschrift der Deutschen Gesellschaft für Geowissenschaften* **159**, 123–132 (2008).

Garnet (U-Th)/He thermochronometry and its application to exhumed high-pressure low-temperature metamorphic rocks

Spencer Seman¹, Daniel F. Stockli¹, Andrew Smye¹, and Emily Hernandez-Goldstein¹
1 Department of Geological Sciences, University of Texas at Austin, USA

The timing of cooling and exhumation of HP-LT metamorphic terranes has traditionally been constrained by a combination of white-mica $^{40}\text{Ar}/^{39}\text{Ar}$ and lower temperature (U-Th)/He techniques (e.g. apatite and zircon). However, the interpretation of $^{40}\text{Ar}/^{39}\text{Ar}$ data from phengite is often clouded by complex multi-stage growth histories and extraneous Ar contamination¹. This leaves a significant ‘gap’ between 200-400°C for which there are no well-characterized thermochronometers. In the depressed geothermal gradient which characterizes subduction zone settings, cooling through this thermal window should be coincident with exhumation from mantle depths. Several newly developed (U-Th)/He thermochronometers, magnetite, rutile, and specifically garnet are sensitive to cooling through this temperature interval.

Garnet is a common, rock-forming phase in HP-LT assemblages across a variety of bulk compositions, making it a particularly attractive thermochronometric tool. Furthermore, previous diffusion experiments have suggested closure temperatures in excess of 250°C for pyrope-almandine compositions². However, the effect of compositional variance on He diffusion in garnet has not been thoroughly explored. We present new age determinations and diffusion data from natural, end-member composition garnets from a variety of geologic settings. Grossular-andradite compositions sourced from skarns are particularly tractable to the (U-Th)/He method due to their relatively high U concentrations (> 1 ppm). A diffusion experiment conducted on gem-quality grossular-andradite garnet from Mali yields a closure temperature of $312 \pm 35^\circ\text{C}$ for $10^\circ\text{C}/\text{m.y.}$ cooling rates (Fig. 1). Unlike skarn derived garnet, the concentrations of alpha producing ^{238}U , ^{235}U , ^{232}Th , and ^{147}Sm in HP-LT garnet are inherently low ($\ll 1$ ppm). Therefore, aliquot sizes approaching 1 mg are necessary for this method and raises the likely of introducing inclusions. Due to its high closure temperature, however, radiogenic He derived from more U and Th rich phases (e.g. zircon, apatite, epidote, etc.) may be retained by the host garnet once it has passed through its closure window, making it, effectively, a He ‘bottle’.

In order to test the viability of garnet (U-Th)/He in a HP-LT setting, we conducted age determinations and diffusion experiments for garnets from eclogite and blueschist facies assemblages from the Cycladic Blueschist Unit (CBU) of northern Syros Island, Greece. Previous garnet Lu-Hf dating constrains the timing of peak P-T conditions at $50 \pm 2 \text{ Ma}^3$. Zr-in-rutile thermometry data suggests that packages of HP-LT metamorphic rocks across Syros did not undergo markedly different P-T evolutions after reaching peak temperatures and pressures of 500-550°C and $\sim 1.6 \text{ GPa}^3$. Cooling below zircon and apatite (U-Th)/He closure temperatures occurred in the middle Miocene, concurrent with slab rollback and back-arc extension in the region. This 25 m.y. gap between peak P-T and exhumation from upper crustal levels together with the recent nature of metamorphism make the CBU the perfect testing ground for the ability of garnet to resolve cooling through the 300° to 200°C window. Blueschist facies garnet was sampled from > 1 cm diameter porphyroblasts. In thin section, garnets are fractured and inclusion rich, containing a variety of HP-LT minerals as well as U and Th-bearing zircon, apatite, rutile and titanite. Despite this, samples yield reproducible middle Miocene ages, consistent with magnetite, zircon, and apatite (U-Th)/He data. A diffusion experiment conducted on this garnet displays multi-domain behavior and yields temperatures within error of zircon closure temperatures (Fig. 1). Thus, both step-heating experiment and age data confirm a lower closure temperature than expected. We argue that fracturing and inclusions, particularly zircon, are controlling He diffusion in these garnet, rather than it acting as a He ‘bottle’. Cleaner and more intact HP-LT garnet could retain He at higher temperatures, and may shed light on the earlier exhumation history of the CBU on Syros.

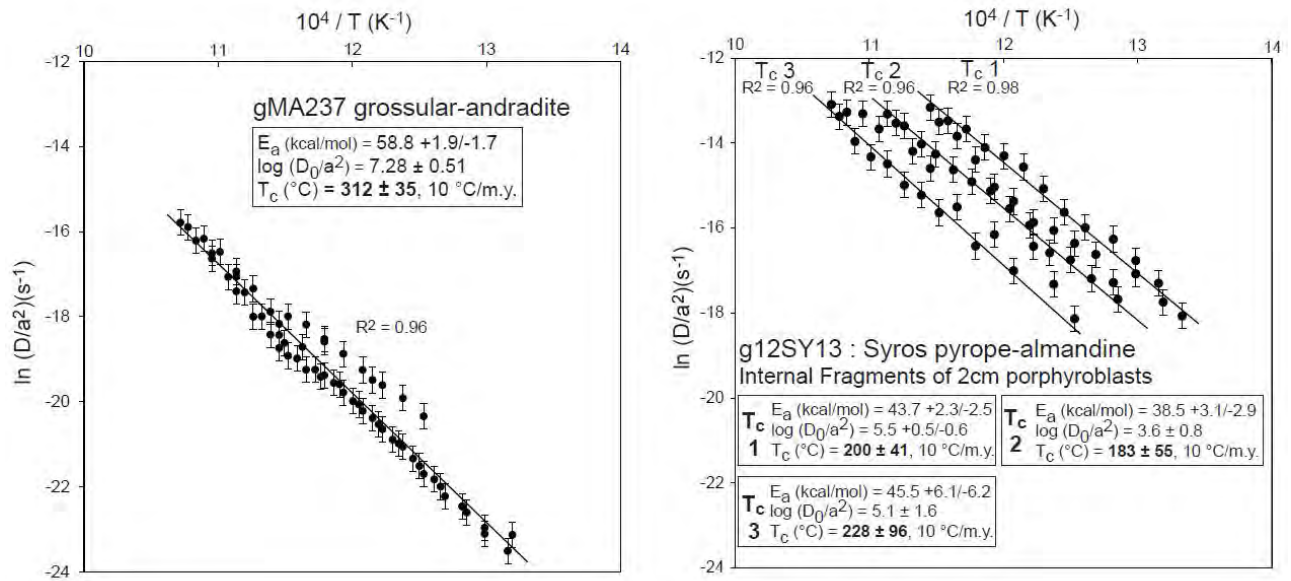


Figure 1. Results of step-heating experiments on two samples of garnet. MA237 is a sample of skarn derived grossular-andradite garnet from Mali. 12SY13 are internal fragments of garnet porphyroblasts from a blueschist-facies metasediment from Syros Island, Greece. Errors were calculated from least-squares regression at a 95% confidence level.

References

1. Kelley, S. Excess argon in K-Ar and Ar-Ar geochronology. *Chemical Geology* **188**, 1-22. (2002).
2. Blackburn, T. Development of new applications in volcanic (U-Th)/He geochronology. M.S. Thesis: University of Kansas. (2006)
3. Lagos M., Scherer E., Tomaschek F., Munker C., Keiter M., Berndt J., and Ballhaus C. High precision Lu-Hf geochronology of Eocene eclogite facies rocks from Syros, Cyclades, Greece. *Chemical Geology*. **243**. 16-35. (2007).

Spectroscopic study on ion irradiated carbonate minerals

Nicole Schöppner^{1#}, Sebastian Deder¹, Ulrich A. Glasmacher¹, Michael Burchard¹, Maxim Zdorovets^{2,3}, Christina Trautmann⁴

¹*Institute of Earth Sciences, University of Heidelberg, Heidelberg, Germany;* ²*Institute of Nuclear Physics, Almaty, Kazakhstan,* ³*Gumilyov Eurasian National University, Astana, Kazakhstan,* ⁴*Technische Universität Darmstadt and GSI Helmholtzzentrum Darmstadt, Germany*

Within geosciences, the use of fission tracks in various minerals as a thermochronological analytical technique is of high importance. The visualization of spontaneous and induced fission tracks uses the well established etching technique. Carbonate minerals have been tested in the past with differentiated results. The latest research clearly indicated that fission tracks develop in carbonate minerals and that specific etching conditions reveal fission tracks in carbonate minerals^{1,2}. As carbonate minerals are excellent minerals for spectroscopic analytical techniques the use of those techniques to non-destructively visualize fission tracks was tested.

Various carbonate minerals were irradiated within two different orders of ion energy. One energy in the order of GeV the other in the order of MeV, close to the normal fissioning energy. Mono crystalline samples of carbonate used in these experiment are: trigonal calcite (CaCO₃), rhomboedric aragonite (CaCO₃), monocline malachite (Cu₂[(OH)₂/CO₃]), trigonal rhodochrosite (MnCO₃), and trigonal dolomite (MgCO₃) were irradiated at the GSI, Darmstadt and the RGP Institute Yadernoi Fiziki, Astana, Kazakhstan.

At GSI carbonate minerals were irradiated by the UNILAC accelerator with, 11.1 MeV/u ¹⁹⁷Au ions, and 11.1 MeV/u ²⁰⁹Bi applying fluences of 1×10⁶, 5×10⁶, 1×10⁷, 5×10⁷, 1×10⁸, 1×10¹¹, and 1×10¹² ions/cm . At the RGP Institute carbonate minerals were irradiated by the Astana accelerator with 1.7 MeV/u ⁸⁴Kr ions applying fluences between 1×10¹⁰ and 1×10¹² ions/cm . The lower mass and energy of these Kr ions is closer to the conditions provided by the natural fissioning process of ²³⁸U.

All crystals were analyzed by Raman and UV spectroscopy. The results indicate the possible use of spectroscopic techniques for non-destructive quantifying the volume density of fission tracks in carbonate minerals.

References

1. Deder, S., Glasmacher, U.A., Burchard, M. & Trautmann, C. Preparation of Carbonate Rocks for Irradiation with Swift Heavy Ions. (In Preparation)
2. Deder, S., Glasmacher, U.A., Burchard, M. & Trautmann, C. Visualization of Heavy Ion Tracks in Calcite by EDTA etching techniques. (In Preparation)

(U-Th)/He geochronology of speleothems

Haviv Itai¹, Vaks Anton², Mason Andrew², Bar-Matthews Mira³, Frumkin Amos⁴

1 Department of Geology and Environmental Sciences, Ben Gurion University of the Negev, Israel

2 Department of Earth Sciences, University of Oxford, England

3 Geological Survey of Israel, Israel

4 Department of Geography, The Hebrew University of Jerusalem, Israel

Speleothems provide one of the best terrestrial archives for paleoclimate and its long-term variability, a record which is predominantly based on U-Th disequilibrium dating. We propose a new avenue to date speleothems utilizing (U-Th)/He in calcite and aragonite - a geochronometric system with no upper age limitation which could potentially extend speleothems-based paleoclimatic records beyond ~500 ka. The method can also complement and help cross-check the recently-matured U-Pb carbonate dating methodology and could potentially be easier to apply.

Our initial results indicate that radiogenic helium accumulates to measurable quantities in speleothems with common uranium content. In order to characterize and quantify the long-term helium retentivity of speleothem-derived carbonates we utilize speleothems from 7 caves with average annual temperatures which vary from 0°C to >20°C, stretching from Siberia at the north, to the northern margin of the Saharan-Arabian desert at the south, with independent age control provided by U-Th disequilibrium and U-Pb ages. Promising initial results delineate identical (U-Th)/He and U-Th disequilibrium ages and no helium loss for two samples from Siberia (~10C) vs. significant (~60-80%) but predictable loss for speleothems from a setting of 20°C.

Initial step-heating diffusion experiments for speleothem-derived calcite delineate activation energy of 29.2-31.4 kcal/mol and a multi diffusion domain (MDD) behavior. Such experimental data can be used to predict the fractional loss of helium under given long-term temperature conditions and could also constrain near-surface paleo-temperatures where independent speleothem ages are available.

Constraining thermal histories in carbonates and marine shales: exploring the conodont AHe thermochronometer

Rachel Landman¹, Rebecca Flowers¹, Nicholas Rosenau², James Metcalf¹, Jeremy Powell³

1 Department of Geological Sciences, University of Colorado, USA

2 Dolan Integration Group, Colorado, USA

3 Department of Earth Sciences, University of Ottawa, Canada

Apatite (U-Th)/He (AHe) thermochronology is one of the major tools used to decipher the thermal histories of rocks in the upper kilometers of the earth's crust. The method is sensitive to temperatures from ~30-90 °C depending on apatite chemistry, and AHe has been extensively applied in active orogens and basinal settings around the world to constrain thermal histories and associated episodes of burial and unroofing. However, AHe thermochronometry is currently limited to rocks in which crystalline apatites of sufficient quality occur. Although this mineral is common in granitoid, metamorphic, and coarse clastic sedimentary rocks, carbonates and shales generally contain neither apatites nor any other established thermochronometer. For this reason, the thermal histories of carbonates and shales cannot be constrained using current methods. Here we explore the potential of conodont AHe thermochronometry to solve this problem.

Conodonts are biomineralized structures composed of microcrystalline hydroxyapatite. They are thought to represent the feeding apparatus of a soft-bodied marine chordate that existed from Cambrian through Triassic time¹. Conodonts are often used as semi-quantitative indicators of peak temperature because remnant organic matter within the conodont irreversibly changes color as it progresses from ~50 to 600 °C²⁻³. This color progression is well-documented as the Conodont Alteration Index (CAI) but imposes no temporal constraints.

A pilot study by Peppe and Reiners⁴ suggested that conodont apatite retains helium across the same temperature range as crystalline apatite, and that conodont AHe data could therefore potentially be interpreted in the same manner as conventional AHe. These authors conducted two diffusion experiments on conodont apatite which yielded closure temperatures of 60 °C and 67 °C for a cooling rate of 10 °C/Myr and suggested that the diffusion domain is the entire conodont. These authors also dated conodonts from seven different locations, four of which displayed reproducible results corresponding to the local cooling histories indicated by other geologic and thermochronologic constraints. Three samples either displayed significant dispersion or yielded dates that did not correspond to the local thermal history.

Here we further explore the conodont AHe thermochronometer via three distinct approaches. First, we test the applicability of conodont AHe thermochronometry to core samples from the Illinois Basin of the midcontinent United States. Second, we will conduct calibration studies on outcrop samples from the southern Rocky Mountains of the western United States. Third, we will perform diffusion experiments on conodonts from both locations.

Our initial dataset consists of seven Pennsylvanian samples from two cores in the central Illinois Basin. Samples come from depths of 25 - 262 m and represent limestone, calcareous shale, and black shale lithologies. From these samples we obtained 47 individual conodont AHe dates representing a range of conodont sizes, morphologies, and chemical compositions. We developed simplified geometries and associated alpha-ejection corrections for five

morphology classes: cones, broken cones, blades, bars, and platform elements. Nearly all AHe dates are significantly younger than the Pennsylvanian depositional ages. All conodonts have CAI values of 1 to 1.5, indicating a maximum burial temperature of ≤ 90 °C, and therefore implying that the closure temperature for the conodont AHe system is no higher than that of the conventional AHe system. Sample reproducibility ranges from 30-45%, with a cluster of 6 conodonts from one sample displaying reproducibility as good as 15%. Analyzed conodonts display a wide range of eU values and Th/U ratios, from 5 to 260 ppm and from 0.1 to 140, respectively. Samples with the largest ranges in eU and Th/U ratios are the least reproducible, suggesting that mobility of U and Th during either diagenesis or sample processing is a factor affecting the conodont AHe system.

Future work will focus on calibration studies in the southern Rocky Mountains of the United States. The calibration studies will compare AFT and conventional AHe dates from crystalline basement or clastic sedimentary rocks with conodont AHe dates from nearby carbonates that have experienced identical thermal histories. Our 18 sample pairs collected in southern Colorado and northern New Mexico represent various well-understood thermal histories that range from rapid cooling in Miocene, Oligocene, and Paleocene time, to slower cooling during the Paleocene and Eocene, to complex histories involving shallow reburial and extended residence in the helium partial retention zone. CAI in these settings is expected to vary from 1 to 5. This range of thermal histories will allow us to evaluate results in a variety of geologic settings, with both simple and complex thermal histories, and test factors that could lead to dispersion including conodont size, morphology, CAI, and U-Th content. Additionally, FT corrections obtained via the simplified geometries described above will be compared to more accurate FT corrections obtained through detailed geometric characterization using X-ray computed microtomography.

Diffusion experiments are also underway to more fully characterize conodont He diffusivity. Experiments on whole conodonts of various morphologies and fragments that isolate tissue types will allow us to better understand the natural variability in conodont He diffusion systematics.

References

1. Sweet, W.C., and Donoghue, P.C.J., Conodonts: *Past, Present, Future: Journal of Paleontology*, v. **75**, no. 6, p.1174–1184 (2001).
2. Epstein, A.G., Epstein, J.B., and Harris, L.D., Conodont color alteration - an index to organic metamorphism: *USGS Professional Paper*, v. **995**, p. 1–27 (1977)
3. Rejebian, V.A., Harris, A.G., and Huebner, J.S., Conodont color and textural alteration: An index to regional metamorphism, contact metamorphism, and hydrothermal alteration: *Geological Society of America Bulletin*, v. **99**, p. 471–479. (1987)
4. Peppe, D.J., and Reiners, P.W., Conodont (U–Th)/He thermochronology: Initial results, potential, and problems: *Earth and Planetary Science Letters*, v. **258**, no. 3–4, p. 569–580 (2007).

Thermal evolution of the Anticosti Basin, Eastern Canada: an empirical calibration of the conodont (U-Th)/He thermochronometer

Jeremy Powell¹, David Schneider¹, Rebecca Flowers², James Metcalf², Daniel Stockli³

1 Department of Earth Sciences, University of Ottawa, Canada

2 Department of Geological Sciences, University of Colorado, USA

3 Jackson School of Geosciences, University of Texas at Austin, USA

Advances in our understanding of the systematics of thermally controlled diffusion of radiogenic helium in apatite and zircon have resulted in the increased application of the (U-Th)/He thermochronometer in sedimentary basin analysis. When integrated with apatite fission-track analysis (AFTA) these data provide critical temperature-time constraints on the thermal evolution of sedimentary basins. Unfortunately, these methods are of limited use in regions dominated by carbonate sedimentary rocks, as the accessory minerals required for the analyses are not common in the strata. Conodonts, phosphatic microfossils that are abundant in Cambrian through Triassic strata, may represent a solution to this problem. An initial investigation into the application of (U-Th)/He analysis on conodonts¹ showed that the method behaves similarly to magmatic apatite. However, more work is required to resolve the relationship between reproducible ages and morphology, microstructural complexity and thermal history.

Our study resolves to do a first-of-its-kind empirical investigation into the effects of temperature on conodont (U-Th)/He age, sampling from the subsurface of the Lower Paleozoic Anticosti Basin, Eastern Canada. Situated in the Gulf of St. Lawrence, the basin comprises a thick succession of Lower Ordovician through Silurian strata dominated by calcareous shales and carbonate rocks. These units thicken substantially as they dip into the subsurface in the SE, and structurally, the island is crosscut by a series of syn-sedimentary normal faults². Several potential hydrocarbon plays have resulted in extensive exploration drilling across the island. Many of these wells have close to two kilometers of continuous stratigraphic core and detailed organic thermal maturity profiles. As a result, our study is well constrained with regards to both modern and paleotemperatures, offering the unique potential to assess the behaviour of the conodont (U-Th)/He system with increasing depth and temperature in a single borehole.

In this study, ten samples were collected from two different boreholes. While sampling primarily targeted conodont-rich lithologies, material for apatite and zircon (U-Th)/He thermochronology (AHe, ZHe) was also collected where available. In the first well, six samples were taken at 300 m intervals to assess the effect of increasing temperature on the conodont (U-Th)/He system. In the second well, samples were collected from the metamorphic basement as well as the unconformable carbonate strata to compare the ages of conodont and apatite (U-Th)/He systems at the same temperature. In both wells, an Early Ordovician sandstone was sampled for AHe to provide an additional temperature-time constraint.

(U-Th)/He analysis of the basement (1700 m depth) yield mean AHe and ZHe ages of 29 ± 2 Ma and 617 ± 57 Ma respectively. Previous AFTA thermal modeling from the basement suggests two thermal events: a 120°C thermal maximum at c. 280 Ma, and a secondary heating episode between 100-60 Ma³. Our dataset of basement ZHe and AHe ages allows us to expand on this model, recording cooling through the ZHe closure temperature in the Cryogenian-Ediacaran, and refining our understanding of the Late Cretaceous to recent thermal history. Ultimately, these data provide a framework to aid in interpreting our conodont (U-Th)/He ages.

In addition to independent thermal constraints, it is imperative that the conodonts used in this study are well characterized to assess whether morphology or microstructure affect cooling age. X-ray computed microtomography is a potentially powerful tool to address these variables. In particular,

this method allows for 3D mapping and therefore a calculation of volume and an appropriate F_t correction for individual conodont elements. This is particularly important in very ornate morphologies, where a simplified correction may not fully account for the complex geometries. The microstructural variation between conodont tissue types, and potential variation in helium diffusion kinetics, may result in significant intrasample age scatter. X-ray microtomography is able to image the density contrast between several conodont tissue types and quantify their volume within the element⁴. In doing so, we are able to weigh whether or not anomalous ages are a function of the abundance, or lack of, certain tissue types in individual conodont elements.

The Anticosti Basin is an excellent natural laboratory to study and develop the conodont (U-Th)/He thermochronometer. Exploratory drilling has resulted in a subsurface that is well constrained with regards to modern and paleotemperatures, and thermal modeling of the basement provides an excellent framework to interpret our results. X-ray computed microtomography allows comparison of conodont-specific variables to measured age. Experiments to assess these relationships are ongoing. Ultimately, we believe that a well-constrained study with a well-characterized dataset is imperative to understanding this complex system and developing a powerful thermochronometer for carbonate strata.

References

1. Pepe, D. & Reiners, P. Conodont (U-Th)/He thermochronology: initial results, potential, and problems. *Earth and Planetary Science Letters* **258**, 569-580 (2007).
2. Bordet, E., Malo, M. & Kirkwood, D. A structural study of western Anticosti Island, St. Lawrence Platform, Québec: a fracture analysis that integrates surface and subsurface data. *Bulletin of Canadian Petroleum Geology* **58**, 36-55 (2010).
3. Lynch, G. & Grist, A. Thermal modelling of the Laurentian margin beneath Anticosti Island using AFTA, 1D well profiles and bulk fluid inclusions. *Canadian Society of Petroleum Geologists, Diamond Jubilee Convention, Calgary. Program with abstracts*, 210 (2002).
4. Murdock, D., Dong, X., Repetski, J., Marone, F., Stampanoni, M. & Donoghue, P. The origin of conodonts and of vertebrate mineralized skeletons. *Letters to Nature* **502**, 546-553 (2013).

Improved Methodology for Magnetite (U-Th)/He Dating of Serpentinites

Emily Hernandez Goldstein¹, Daniel Stockli¹, Richard Ketcham¹, Spencer Seman¹
1 Department of Geological Sciences, University of Texas at Austin, USA

Magnetite geochronology has the potential to transform our understanding of serpentinization as a widespread and fundamental process that has important influences on rheological strength, water geochemistry, the carbon cycle, and potentially the origin of life. While numerous studies exist on the petrology, structure and geochemistry of serpentinites, the timing of serpentinization has been restricted to relative chronologic constraints (e.g. dating of intrusions or overlying sediments) due to a lack of accessory minerals with well-established dating techniques. With technological advances in radiogenic isotope analysis in the past decade, it is now possible address the geochronology of serpentinization with (U-Th)/He dating of magnetites that form ubiquitously as a direct result of the breakdown of olivine and pyroxene in the presence of water. The ability to date serpentinization will allow investigation of important geologic issues, including, but not limited to: mantle exhumation during lithospheric break-up, carbon sequestration, and low temperature hydrothermal systems. This study presents a (U-Th)/He-based method that is tailored to analyzing magnetite formation in serpentinites.

Magnetite (U-Th)/He dating is an attractive approach to analyze crystallization and cooling ages in a variety of mafic to ultramafic systems that are not easily addressed by current dating techniques. While magnetite is proven as a viable geochronometer in basaltic to intermediate volcanic rocks¹ and ore deposits², refinement of the technique is necessary for widespread applicability due to complex mineral growth and low parent nuclide concentration. This study outlines the importance of sample screening and measuring the parent nuclide distribution for proper age determination.

In order to make magnetite He dating reliable, advanced sample screening is necessary to ensure suitability for dating in light of the commonality of skeletal or complexly intergrown magnetite in samples of interest. Routine application of High Resolution X-Ray Computed Tomography (CT) provides a non-destructive method to visualize the internal structure of a sample in 3D and directly improves multiple sample processing steps: First, whole-rock CT scanning is an effective way to assess the size, morphology, association and distribution of grains of interest in a specimen before crushing it for He analysis (Figure 1). This is particularly useful for precious samples, such as ODP cores. Second, CT scanning of individual grains provides internal visualization of opaque minerals to screen for inclusions or intergrowths that can affect parent and daughter nuclide distribution, diffusion domain size and possible F_T correction, which may be extensible to complex geometries. Finally, CT scanning grain populations before and after abrasion allows for potentially more accurate monitoring of volume loss from each grain. Furthermore, CT data from individual grains and whole-rock specimens are coupled with thin section and SEM and EDS analyses in order to fully characterize the petrologic context of magnetite in 3D and assess their suitability for (U-Th)/He dating.

In addition to proper grain screening, it is necessary to determine the parent nuclide concentration of the matrix compared to the magnetite to correct for either alpha ejection or implantation. It remains to be determined for serpentine-magnetite systems whether it is necessary to physically abrade a grain due to alpha implantation, or if an F_T correction³ can be applied in the case that implantation from the matrix is negligible. Magnetite He dating of basalts demonstrates an order of magnitude higher concentration of effective uranium (eU) in the matrix (ppm) compared to the magnetite (ppb), causing a He implantation halo around the grain boundary⁴. Physical abrasion is used to remove the outer 20 μm of the grain before analysis to correct for the effects of long alpha stopping distances, but this method may not be a viable option for small (<80 μm) and/or irregular grains common in serpentinites. Currently, this study incorporates whole rock eU measurements for

each magnetite sample analyzed. Preliminary results suggest that enrichment of eU in serpentine matrix vs. magnetite varies by sample and must be monitored.

The method described in this abstract is piloted with a case study using magnetite crystals from serpentinites in an exhumed high-pressure, low-temperature metamorphic terrane on Syros Island, Greece. Magnetites from this unit reveal reproducible middle Miocene ages in agreement with zircon (U-Th)/He cooling ages from related units. The ability to temporally constrain serpentinitization with magnetite (U-Th)/He has the potential to not only provide an additional t-T constraint on the exhumation of HP-LT terranes, but a viable option for dating ultramafic alteration in a variety of tectonic settings.

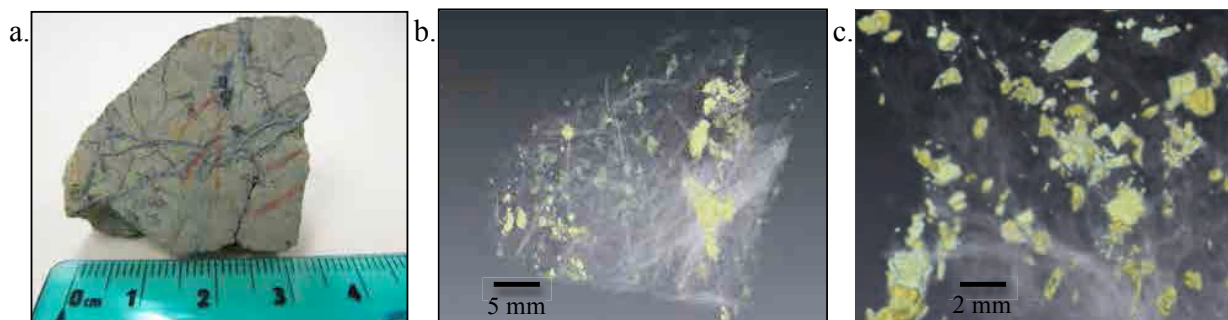


Figure 1. a) Photo of serpentinite hand sample from ODP Leg 209. b) Volume rendering of a CT scan of the whole rock specimen. Certain minerals are highlighted (white = serpentine veins with magnetite, yellow = chromite/magnetite grains). c) Zoomed in box from photo b shows euhedral crystals that are probable magnetite or chrome spinel.

References

- 1 Blackburn, T. J., Stockli, D. F. & Walker, J. D. Magnetite (U-Th)/He dating and its application to the geochronology of intermediate to mafic volcanic rocks. *Earth and Planetary Science Letters* **259**, 360-371, doi:10.1016/j.epsl.2007.04.044 (2007).
- 2 Fanale, F. & Kulp, J. L. The helium method and the age of the Cornwall, Pennsylvania magnetite ore. *Economic Geology* **57**, 735-746 (1962).
- 3 Farley, K., Wolf, R. & Silver, L. The effects of long alpha-stopping distances on (U-Th)/He ages. *Geochimica Et Cosmochimica Acta* **60**, 4223-4229 (1996).
- 4 Taylor, J. L. Practical Guide to Improved Magnetite (U-Th)/He Geochronometry - A case study from the Columbia River Basalt. *Masters Thesis, University of Kansas* (2012).

OSL-thermochronology of Mattertal (Swiss Alps)

Pierre G. Valla¹, Benny Guralnik², Georgina King¹, Jean-Daniel Champagnac², Frédéric Herman¹,
Kerry Leith³, Edward Rhodes⁴

1 Institute of Earth Surface Dynamics - University of Lausanne, Switzerland

2 Department of Earth Sciences - ETH Zurich, Switzerland

3 Chair of Landslide Research, Technical University of Munich, Germany

4 Department of Geography, University of Manchester, UK.

The initial calibration and testing of OSL-thermochronometry has focused on bedrock feldspar¹, due to the fact that its luminescence characteristics resemble those of sedimentary feldspar and thus allow a straightforward shift from traditional sediment geo- to bedrock thermo-chronology. Although feldspar luminescence can yield valuable constraints on the subsurface thermal structure on unprecedented (<100 ka) timescales, this system is often found in field steady-state at the Earth's surface, thus motivating a further search for alternative luminescence proxies (more sensitive to typical cooling rates). One such system is quartz blue light stimulated luminescence, initially assumed to have a closure temperature of ~30-35 °C². While the former estimate was based on well-established Arrhenius parameters of the relevant electron trap in sedimentary quartz (the 'fast component' of Wintle and Murray, 1999³), there is an increasing body of laboratory evidence suggesting that in bedrock quartz (rather than sedimentary quartz), (i) the 'fast component' is unsensitized (i.e. apparently non-present) and (ii) the actual component dominating the OSL has a significantly lower thermal stability⁵, implying potential closure within ~10 °C of the final cooling temperature (cf. Guralnik et al., 2013). To explore this hypothesis further, we present provisional data for a ~1.8 km high age-elevation profile from Mattertal (Switzerland), where the OSL ages range between ~20 ka (valley floor) and ~200 ka (high elevations). These preliminary ages are analyzed and compared to the valley development history since ~1 Ma, as inferred from a finite difference model combining the effects of tectonics, glacial erosion, and long-term bedrock strength⁶.

References

1. Guralnik, B., Valla, P. G. & Herman, F. OSL-Thermochronometry: observations, theory, and applications (this volume).
2. Herman, F., Rhodes, E.J., Braun, J. & Heiniger, L. Uniform erosion rates and relief amplitude during glacial cycles in the Southern Alps of New Zealand, as revealed from OSL-thermochronology. *Earth and Planetary Science Letters*, **297**, 183-189 (2010).
3. Murray, A. S., & Wintle, A. G. Isothermal decay of optically stimulated luminescence in quartz. *Radiation Measurements*, **30**, 119-125 (1999).
4. Guralnik, B., Jain, M., Herman, F., Paris, R.B., Harrison, T.M., Murray, A.S., Valla, P.G. & Rhodes, E.J. Effective closure temperature in leaky and/or saturating thermochronometers. *Earth and Planetary Science Letters*, **384**, 209-218 (2013).
5. Chen, R., Lawless, J. L. & Pagonis, V. Two-stage thermal stimulation of thermoluminescence. *Proceedings of the 13th International Conference on Luminescence and Electron Spin Resonance Dating*, p. 42 (2011).
6. Leith, K., Moore, J. R., Amann, F., & Loew, S. Subglacial extensional fracture development and implications for Alpine Valley evolution. *Journal of Geophysical Research: Earth Surface* **119**, 62–81 (2014).

OSL-thermochronology of Na- and K-feldspar from Namche Barwa, Tibet

G.E. King¹, F. Herman¹, P.G. Valla¹, B. Guralnik²

¹*Institute of Earth Surface Dynamics – University of Lausanne, Lausanne, Vaud, Switzerland*

²*Department of Earth Sciences – ETH-Zurich, Zurich, Switzerland*

OSL-thermochronology offers the potential to constrain changes in exhumation rates over Quaternary timescales. However application of the technique has proven challenging, with measured luminescence signals of Na- and K-feldspar samples from Alaska and Norway exhibiting field saturation due to a combination of early signal saturation, high environmental dose rates and high fading rates¹. Namche Barwa (eastern Himalaya) is thought to have experienced rapid exhumation throughout the Quaternary period, and therefore provides a useful test-site for the application of OSL-thermochronology. Six bedrock samples were hand crushed before using conventional methods to extract the 180-212 μm Na-feldspar ($\rho=2.62\text{-}2.65$) and K-feldspar ($\rho<2.58$) fractions.

The major challenge for OSL-thermochronology using feldspar is distinguishing between the respective depletion of trapped charges by athermal (fading) and thermal processes. Through measuring the Na- and K-feldspar extracts using a multiple elevated temperature (MET)-protocol comprising infra-red stimulated luminescence (IRSL) measurements at 50°C, 100°C, 150°C and 225 °C, signals with increasing athermal stability could be investigated. Fading measurements were made for all aliquots analysed and values are generally lower (<7%/decade) than reported in previous OSL-thermochronology studies (e.g. 1). The measured IRSL₅₀ fading rates varied from $g_{2\text{days}}$ of 3-5%/decade for K-feldspar extracts to 4-7%/decade for Na-feldspar extracts. Fading rates varied between samples but all samples exhibited lower fading rates at higher IRSL measurement temperatures.

To isolate the role of athermal charge detrapping the model proposed by Kars et al² was applied. Results show that the IRSL₅₀ signals of both the Na- and K-feldspar extracts of sample NB140, and the K-feldspar extract of sample NB19 exhibit thermal signatures, implying cooling rates >200-300 °C for this region, consistent with previous thermochronometric studies (e.g. 3). In contrast, both the K- and Na-feldspar extracts of samples NB109 and NB124 are in field saturation, which may partly be attributed to their relatively low saturation doses.

The 100°C and 150°C MET signals have lower signal intensities than the other emissions measured, and have greater scatter, however it appears that for the K- and Na- feldspar extracts of sample NB140, that these signals may also exhibit thermal signatures. In contrast, for sample NB109 these signals are in field saturation. These results imply that the different IRSL signals of both Na- and K-feldspar measured during a MET-protocol have different effective closure temperatures, and therefore may provide further insights into the thermal and exhumation histories of bedrock.

References

1. Guralnik, B. Unpublished PhD Thesis, ETH-Zurich (2014).
2. Kars, R.H., Wallinga, J., Cohen, K.M. *Radiation Measurements* **43**, 786-790 (2008).
3. Seward, D. and Burg, J.-P. *Tectonophysics* **451**, 282-289 (2008).

Combined $^{238}\text{U}/^{230}\text{Th}$ disequilibrium and (U-Th)/He dating of zircon - a 'new' dating tool for Quaternary science and archaeology

Martin Danišič¹, Axel K. Schmitt², Phil Shane³, Sonja Storm³,
Noreen J. Evans⁴, Jan M. Lindsay³, Erkan Aydar⁵, Erdal Şen⁶, İnan Ulusoy⁶, Oscar M.
Lovera²

1 Department of Earth and Ocean Sciences, Faculty of Science and Engineering, The University of Waikato, Hamilton, New Zealand

2 Department of Earth and Space Sciences, University of California Los Angeles, Los Angeles, California, USA

3 School of Environment, University of Auckland, Auckland, New Zealand

4 John de Laeter Centre for Isotope Research, Department of Applied Geology, Curtin University of Technology, Perth, Australia

5 ATERRA R&D, Kizilay, Ankara

6 Department of Geological Engineering, Hacettepe University, Ankara, Turkey

Accurate dating of Quaternary geological events is essential for addressing a range of key research questions related to paleoclimate and paleoenvironmental changes, volcanic activity, hominid evolution, assessments of geological hazards, and many others. Traditional dating tools such as radiocarbon, argon, cosmogenic nuclides or luminescence methods are sound and feasible, however their application is often limited by the lack of datable materials, meaning that there is a critical need for new dating methods appropriate to late Quaternary timescales. (U-Th)/He dating of zircon, when combined with $^{238}\text{U}/^{230}\text{Th}$ disequilibrium dating¹, is a novel approach for dating young (<1 Ma) volcanic rocks that helps overcome these limitations. In particular, this method is probably the only tool for dating silicic volcanic rocks as they are rich in zircon, but lack K-rich minerals and therefore cannot be dated by conventional argon methods. The ZDD method has enormous potential for Quaternary Earth Science²⁻⁵ and, as recently demonstrated by^{6,7}, the method has been successfully applied even in archaeology.

The approach, hereafter referred to as ZDD (zircon double-dating), is based on 'dependent' determination of crystallization and eruption ages for single zircon crystals by $^{238}\text{U}/^{230}\text{Th}$ disequilibrium and (U-Th)/He methods by using secondary ion mass spectrometry (SIMS) and conventional noble gas mass spectrometry, respectively. It is essential that both methods are applied in tandem in order to correct the (U-Th)/He based eruption ages for disequilibrium in the U and Th decay chains that is to be expected in grains younger than ~1 Ma⁸.

In our presentation we will first describe the analytical protocols for the ZDD methodology. Then we present a case study where the accuracy and precision of the ZDD is method is tested against high-precision radiocarbon dating by using Quaternary record of New Zealand's tephras as a natural testing site⁵. We will demonstrate that (i) the ZDD method is accurate and reasonably precise for geological applications, and (ii) that the age of the targeted deposits of coeval Rotoiti and Earthquake Flat eruptions (Taupo Volcanic Zone) are ~45 ka old, which makes them ~16 kyr younger than the long accepted age. Finally, we present results of a study where the ZDD method was successfully applied to date a historic eruption of Hasan Dağı volcano (Central Anatolia, Turkey). The measured age of 6960±640 BCE overlaps (within error) with the age of an archeologically important mural excavated at the Neolithic Çatalhöyük site. These results contribute to the ongoing discussion whether the mural could depict the World's oldest map⁷.

References

- 1 Schmitt, A. K., Stockli, D. F. & Hausback, B. P. Eruption and magma crystallization ages of Las Tres Virgenes (Baja California) constrained by combined $^{230}\text{Th}/^{238}\text{U}$ and (U–Th)/He dating of zircon. *J. Volcanol. Geotherm. Res.* **158**, 281-295 (2006).
- 2 Schmitt, A. K., Stockli, D. F., Niedermann, S., Lovera, O. M. & Hausback, B. P. Eruption ages of Las Tres Virgenes volcano (Baja California): a tale of two helium isotopes. *Quat. Geochronol.* **5**, 503-511 (2010).
- 3 Schmitt, A. K. *et al.* Episodic growth and homogenization of plutonic roots in arc volcanoes from combined U–Th and (U–Th)/He zircon dating. *Earth Planet. Sci. Lett.* **295**, 91-103 (2010).
- 4 Schmitt, A. K. *et al.* Acigöl rhyolite field, Central Anatolia (part 1): high-resolution dating of eruption episodes and zircon growth rates. *Contrib. Mineral. Petrol.* **162**, 1215-1231 (2011).
- 5 Danišik, M. *et al.* Re-anchoring the late Pleistocene tephrochronology of New Zealand based on concordant radiocarbon ages and combined $^{238}\text{U}/^{230}\text{Th}$ disequilibrium and (U–Th)/He zircon ages. *Earth Planet. Sci. Lett.* **349**, 240-250 (2012).
- 6 Schmitt, A. K., Martín, A., Stockli, D. F., Farley, K. A. & Lovera, O. M. (U–Th)/He zircon and archaeological ages for a late prehistoric eruption in the Salton Trough (California, USA). *Geology* **41**, 7-10 (2013).
- 7 Schmitt, A. K. *et al.* Identifying the Volcanic Eruption Depicted in a Neolithic Painting at Çatalhöyük, Central Anatolia, Turkey. *PLoS ONE* **9**, e84711, doi:10.1371/journal.pone.0084711 (2014).
- 8 Farley, K., Kohn, B. & Pillans, B. The effects of secular disequilibrium on (U–Th)/He systematics and dating of Quaternary volcanic zircon and apatite. *Earth Planet. Sci. Lett.* **201**, 117-125 (2002).

High temperature (> 350 °C) thermochronology and mechanisms of Pb loss in apatite

Richard Spikings¹, Ryan Cochrane¹, David Chew², Joern Wotzlaw¹, Andre Paul¹, Maria Ovtcharova¹

1 Department of Earth Sciences and the Environment, University of Geneva, Switzerland

2 School of Natural Sciences, Trinity College, Dublin, Ireland

Thermochronological methods rely on the assumption that the radiogenic isotopes produced are redistributed within minerals and ultimately lost to an infinite reservoir by thermally activated, volume diffusion¹. Previous studies support this assumption over laboratory time-scales, under controlled conditions². However, several authors have suggested that the mechanisms that control isotope transport through crystal lattices over geological time-scales are dominated by aqueous fluid flow along distinct pathways, and that thermally activated diffusion is of secondary importance³.

We present U-Pb isotopic data from natural apatites of variable grain sizes that are used to test the hypothesis that thermally activated volume diffusion over geological timescales controlled the loss of Pb. Confirmation of the hypothesis will establish the apatite U-Pb system as a reliable thermochronometer. The U-Pb system in most accessory phases is sensitive to temperatures >350°C², and therefore can provide Earth scientists with a unique tool to understand i) the tectonic stability of the lower crust and cratons, and iii) the tectonic history of active margins over long time periods (e.g. 500 Ma). Negation of the hypothesis would suggest that age variations may reflect interaction with aqueous fluids during retrogression or growth during prograde metamorphism.

A secondary aim of this study is to investigate any advantages gained by combining independent U-Pb data sets obtained using Isotope Dilution-Thermal Ionization Mass Spectrometry (ID-TIMS) and Multi Collector-Laser Ablation-Inductively Coupled Plasma Mass Spectrometry (MC-LA-ICP-MS) when extracting thermal history information from U-Pb dates. Both data sets can be used to reconstruct statistically likely thermal histories, and the histories obtained from each method should be indistinguishable. Re-heating gradual cooling and isothermal holding results in different core-rim intra-grain patterns of U-Pb dates, and this study measures apatite in-situ dates in an attempt to resolve between re-heating and slow-cooling paths.

Concordant ²⁰⁶Pb/²³⁸U (apatite; TIMS) dates from 14 grain size fractions extracted from a Triassic leucosome (S. Ecuador; LA-ICP-MS U-Pb zircon 247±4.3 Ma) range between 81.52 ± 2.61 and 137.46 ± 2.62 Ma (common Pb measured on alkali feldspar)⁴. Eleven of these grain sizes, which have Th/U<0.18, yield a positive correlation between U-Pb date, suggesting that Pb was lost by thermally activated diffusion. Three size aliquots yield anomalously high Th/U ratios (0.35 – 1.9), diverge from the grain size vs. date correlation and yield relatively young ²⁰⁶Pb/²³⁸U dates. Time-Temperature paths (Figure 1) have been obtained from the six grain size aliquots using HeFTy V1.7.0⁵, a spherical geometry, and established Pb-in-apatite diffusion parameters². Core-rim diffusion calculations yield a PbPRZ for these aliquots that ranges between 375 – 569°C. Input parameters include ²⁰⁶Pb/²³⁸U, grain radii and core-rim U concentration for each aliquot. Calculation of a theoretical ²⁰⁶Pb/²³⁸U date for any particular t-T path is performed by the net summation of the in-growth and diffusive loss of ²⁰⁶Pb over the entire time span of the simulation.

Theoretical core-to-rim U-Pb date profiles have been generated from the best-fit t-T solutions presented in Figure 1, and are compared with measured intra-grain ²⁰⁶Pb/²³⁸U LA-MC-ICP-MS dates to test the accuracy of the assumption that Pb has been lost by thermally activated, volume diffusion. Theoretical core-rim date profiles were made assuming both a homogeneous uranium concentration, and a heterogeneous concentration (determined from the in-situ U isotopic measurements, where the cores of the grains are enriched relative to the rims).

The close fit of the core-rim $^{206}\text{Pb}/^{238}\text{U}$ date profiles predicted by the best-fit t-T model, and the measured intra-grain dates strongly supports the hypothesis that Pb has been lost from the apatite by thermally activated, volume diffusion. Pb loss mechanisms advocating an interaction with aqueous fluids³ are not required to explain the single crystal and intra-grain U-Pb apatite dates. This conclusion is supported by i) small grains show no discernible variation in age from core to rim, and ii) BSE and CL imaging of the apatites reveal no intra-grain discontinuities, which could be interpreted as discrete growth domains or pathways for fluid infiltration.

Two main advantages arise when combining single crystal U-Pb dates (TIMS) and in-situ dates (LA-ICP-MS). First, in this study, these different techniques were applied to different apatite crystals extracted from the same leucosome, and therefore both datasets are mainly independent of each other. Concordance between the t-T solutions implies that they are accurate, whereas distinguishable differences would raise doubts about their usefulness. Discrepancies in the t-T models may arise due to non-thermally activated, core-to-rim diffusion profiles, which could have formed by Pb loss during fluid interaction with the crystals. The in-situ dates may provide information about the cause of the discrepancy, by revealing a multi-domain structure. The second advantage is the ability of this combination to distinguish between isothermal t-T paths, and reheating. In this example, inversion modeling of TIMS dates strongly favours reheating, although some isothermal paths are statistically permitted. However, isothermal holding is inconsistent with the in-situ U-Pb dates, leaving reheating as the only viable t-T solution.

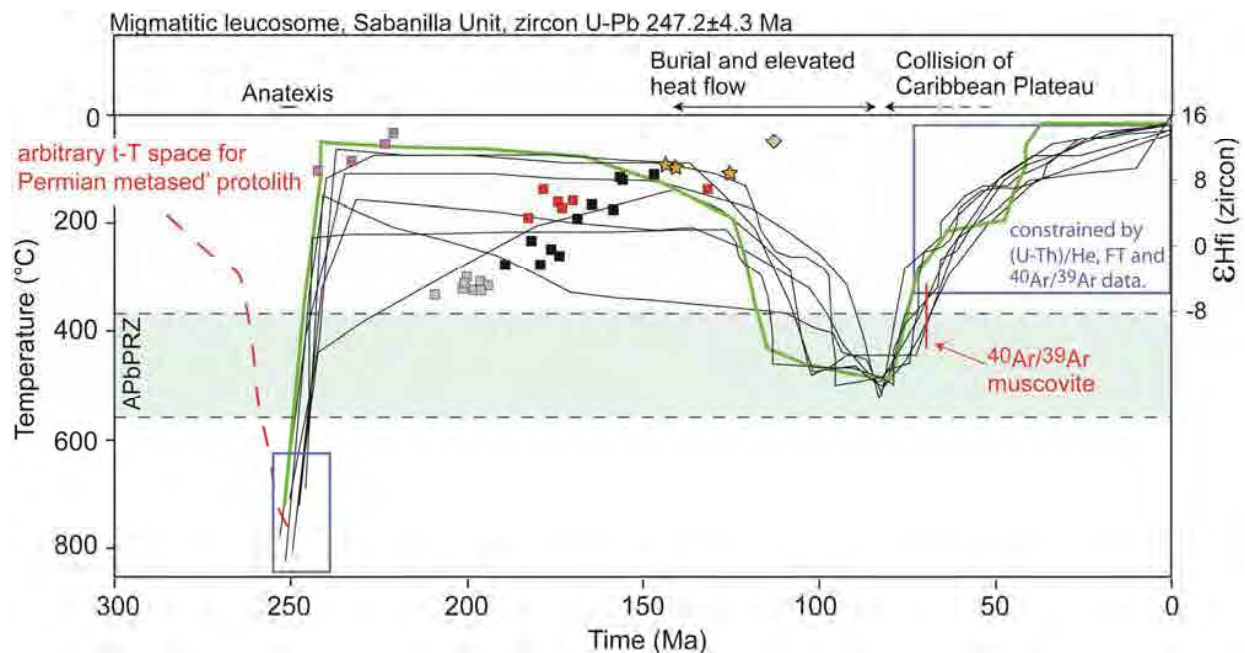


Figure 1. t-T paths obtained from bulk apatite $^{206}\text{Pb}/^{238}\text{U}$ dates (TIMS) using HeFTy V1.7.0⁵. ϵHf_i (zircon) are shown for magmatic rocks, corroborating the geological interpretations of the t-T.

References

1. Lovera, O.M., Grove, M., Mark Harrison, T. & Mahon, K.I. Systematic analysis of K-feldspar $^{40}\text{Ar}/^{39}\text{Ar}$ step heating results: I. Significance of activation energy determinations. *Geochimica et Cosmochimica Acta* **61**, 3171-3192 (1997).
2. Cherniak, D.J., Lanford, W.A. & Ryerson, F.J. Lead diffusion in apatite and zircon using ion implantation and Rutherford Backscattering techniques. *Geochimica et Cosmochimica Acta* **55**, 1663-1673 (1991).
3. Lee, J.K.W. Multipath diffusion in geochronology. *Contributions to Mineralogy and Petrology* **120**, 60-82 (1995).
4. Cochrane, R., Spikings, R.A., Chew, D., Wotzlaw, J-F., Chiaradia, M., Tyrell, S., Schaltegger, U. & Van der Lelij, R. High temperature (>350°C) thermochronology and mechanisms of Pb loss in apatite. *Geochimica et Cosmochimica Acta* **127**, 39-56 (2014).
5. Ketchum, R.A. Forward and Inverse Modeling of Low-Temperature Thermochronometry Data. *Reviews in Mineralogy and Geochemistry* **58**, 275-314 (2005).

Session 2:

Noble-gas diffusion (He, Ne, Ar) applied to thermochronology

Physical aspects of noble gas diffusion in crystals and their implication for thermochronology

Laurent Tassan-Got¹, Cécile Gautheron², Duval Mbongo¹, Jérôme Roques¹, Eric Simoni¹, Chloé Gerin²

1 Institut de Physique Nucléaire Orsay, France

2 UMR GEOPS, Université Paris-Sud, France

Diffusion of rare gases (helium, neon, argon) is a powerful tool in thermochronology for dating thermal events and re-build or test thermal histories. However the diffusion process is still under study nowadays, experimentally and theoretically as well, because it's not fully understood and an accurate description of the phenomenon is required for a safe use in thermochronology.

Firstly, the diffusion process occurring at the atomic level will be described as a hopping motion between interstitial sites of a damage-free crystal lattice. As an illustration for the apatite case I will show how the energies, barriers, hopping frequencies involved in this process can be computed quantum-mechanically within the framework of the Density Functional Theory (DFT). Beyond this static calculation the diffusion rate is extracted by a statistical approach called Transition State Theory (TST). The combination of DFT and TST allows extracting diffusion coefficients in damage-free crystals. In the case of helium diffusing in fluoroapatites, I will show that this leads to values, which compare satisfactorily with measurements¹.

When the chemical composition of apatites varies with the incorporation of chlorine atoms, the barriers are affected and due to the coexistence of different paths with possible workaround trips a larger scale approach is needed carried out by a Boltzmann kinetic Monte Carlo random walk over the lattice¹. For illustration I will show how this approach helps understand the effect of composition on the diffusivity, in particular the anisotropy.

Computing closure temperatures and ages for finite grains requires to solve the diffusion equation which mimics diffusion at the macroscopic level²⁻³. This can be done using measured or computed diffusivities. I will illustrate how the Monte Carlo method acting at the macroscopic level allows solving diffusion in any 3D configuration with anisotropy, zonation, implantation, abrasion.

The impact of damage and defects of the crystal on diffusion has been well recognized in the case of helium in apatites and zircon⁴. However the action of defects on diffusion is still unclear. At the microscopic level they may act as trapping volumes or surfaces, as implemented in the recent models. They may also scale down the diffusivity by blocking the favored diffusion channels. In addition the amount of damage is controlled by their annealing which is up to now copied from fission track annealing in the recent models. But alpha recoil damage are very different in shape compared to fission tracks and this could induce very different rates of annealing. I will discuss those open questions about the impact of defects on diffusion in crystals.

References

1. Mbongo Djimbi, D. Gautheron C., Roques J., Tassan-Got L., Gerin C., Simoni E., Apatite composition on (U-Th)/He thermochronometer: a quantum point of view. Submitted *Geochimica et Cosmochimica Acta*.
2. Gautheron C. et Tassan-Got. A Monte Carlo approach of diffusion applied to noble gas/helium thermochronology. *Chemical Geology*, **273**:212-224 (2010).

3. Gautheron C., Tassan-Got, L., Ketcham, R.A., Dobson, K.J. Accounting for long alpha-particle stopping distances in (U-Th-Sm)/He geochronology: 3D modeling of diffusion, zoning, implantation, and abrasion. *Geochimica et Cosmochimica Acta*, **96**: 44-56 (2012)
4. Gautheron C., Tassan-got, L., Barbarand, J., Pagel, M., Effect of alpha-damage annealing on apatite (U-Th)/He thermochronology. *Chemical Geology*, **266**: 166-179 (2009).

Interpreting zircon (U-Th)/He date-eU correlations with a new damage-based model for He diffusion in zircon

William Guenther¹, Peter Reiners², Richard Ketcham³, Lutz Nasdala⁴, Gerald Giester⁴

¹*Dept. of Geology, University of Illinois, Champaign, IL, USA*

²*Dept. of Geosciences, University of Arizona, Tucson, AZ, USA*

³*Jackson School of Geosciences, University of Texas, Austin, TX, USA*

⁴*Institute of Mineralogy and Crystallography, University of Vienna, Austria*

Despite the prevalent use of zircon (U-Th)/He dating as a low-temperature thermochronometer, our understanding of the fundamental kinetics of He diffusion in zircon remains limited. Various studies have shown that crystallographic anisotropy¹⁻³, heterogeneous distribution of parent nuclides⁴, and radiation damage⁵ are amongst some of the factors that influence a given zircon grain's He diffusivity. Of these factors, a grain's degree of radiation damage can have the most dramatic effect on intergranular variability in He diffusivity. This effect often manifests as positive or negative correlations between single-grain zircon He dates and effective uranium (eU, a proxy for radiation damage). Previously established universal kinetics⁶ are insufficient for explaining this systematic dispersion and more complex, grain-specific approaches need to be considered. Here, we demonstrate one such approach and use a new damage-based model to constrain thermal histories from date-eU correlations in samples from diverse geologic settings.

First, we present the model's salient details, including the kinetics constrained from cycled step-heating experiments on zircons with different degrees of damage and the functional form of the damage-diffusivity relationship. We examined c-axis oriented (parallel and orthogonal) slabs of grains that span nearly the full natural range of alpha dose (from $\sim 1 \times 10^{16}$ to $\sim 8 \times 10^{18}$ α/g), which we interpret to correlate with the amount of accumulated damage in a given grain. Between 1.2×10^{16} and 1.4×10^{18} α/g the frequency factor (D_0) measured in the c-axis parallel direction decreases by four orders of magnitude, whereas activation energy (E_a) remains roughly constant (~ 165 kJ/mol) over the same span in dose. Between $\sim 2 \times 10^{18}$ α/g and $\sim 8 \times 10^{18}$ α/g , E_a decreases by more than a factor of 2 (to ~ 70 kJ/mol). These kinetics translate into an increase in closure temperature from ~ 140 to ~ 220 °C between alpha doses of $\sim 1 \times 10^{16}$ and $\sim 1 \times 10^{18}$ α/g . Above $\sim 2 \times 10^{18}$ α/g , closure temperature drops dramatically. The relationship between damage and diffusivity can be parameterized and combined with a damage annealing model (based on zircon fission track annealing) to describe the co-evolution of damage, diffusivity, and He date within a given grain.

Several suites of igneous zircons from the Longmen Shan, China and ranges in the Laramide province of Wyoming highlight the ability of this coupled model to constrain time-temperature histories from negative date-eU correlations. For the Longmen Shan, the new damage-based model for diffusivity explains dispersion in He date results from published datasets that were previously considered to be spurious. Moreover, a damage-based approach can constrain the magnitude and timing of exhumation at specific locations and determine the spatial extent of two separate pulses of exhumation within the Longmen Shan at 35-20 Ma and 15-0 Ma.

A suite of detrital zircons from the Sevier belt of central Utah show both positive and negative date-eU correlations, which can be used to constrain the timing and magnitude of burial and exhumation in this portion of the U.S. Cordillera. These results are complex, however, as many of the grains are only partially reset and require a further consideration of pre-depositional damage and He inheritance. One approach for understanding these partially reset datasets is to combine the damage-diffusivity model with “inheritance envelopes.” We demonstrate this concept with one particular example from the Oquirrh Mountains near Provo, Utah. Inheritance envelopes for this sample constrain maximum burial temperatures of ~170 °C and several kilometers of exhumation beginning at 110 Ma.

References

1. Farley, K.A. He diffusion systematics in minerals: Evidence from synthetic monazite and zircon structure phosphates *Geochimica et Cosmochimica Acta* **71**, 4015-4024 (2007).
2. Reich, M., Ewing, R.C., Ehlers, T.A., Becker, U. Low-temperature anisotropic diffusion of helium in zircon: Implications for zircon (U-Th)/He thermochronometry *Geochimica et Cosmochimica Acta* **71**, 3119-3130 (2007).
3. Cherniak, D.J., Watson, E.B., Thomas, J.B. Diffusion of helium in zircon and apatite *Chemical Geology* **268**, 155-166 (2009).
4. Hourigan, J.K., Reiners, P.W., Brandon, M.T. U-Th zonation-dependent alpha-ejection in (U-Th)/He chronometry *Geochimica et Cosmochimica Acta* **69**, 3349-3365 (2005).
5. Guenther, W.R., Reiners, P.W., Ketcham, R.A., Nasdala, L., Giester, G. Helium diffusion in natural zircon: Radiation damage, anisotropy, and the interpretation of zircon (U-Th)/He thermochronology *American Journal of Science* **313**, 145-198 (2013).
6. Reiners, P.W., Spell, T.L., Nicolescu, S., Zanetti, K.A. Zircon (U-Th)/He thermochronometry: He diffusion and comparisons with Ar/Ar dating *Geochimica et Cosmochimica Acta* **68**, 1857-1887 (2004).

Crystallisation, cooling or contamination: interpreting dispersion in metamorphic $^{40}\text{Ar}/^{39}\text{Ar}$ ages

Clare J. Warren¹, Christopher S. McDonald¹, Catherine M. Mottram¹, Simon P. Kelley¹

1 Department of Environment, Earth and Ecosystems, CEPSAR, the Open University, Walton Hall, MK7 6AA, UK

Mica $^{40}\text{Ar}/^{39}\text{Ar}$ data, most generally determined by multi- or single-grain step-heating experiments, are commonly used to constrain the timing of cooling in high-temperature metamorphic terranes in conjunction with the Dodson (1973) closure temperature formulation¹. The pitfalls of this approach are well documented: blind associations between a mineral $^{40}\text{Ar}/^{39}\text{Ar}$ 'date' and a single temperature have previously led to many spurious tectonic interpretations. Experiments investigating the differences in $^{40}\text{Ar}/^{39}\text{Ar}$ ages, and age spreads, between step-heating, single grain fusion and intra-grain laser ablation methods from samples collected from different metamorphic terranes show that step heating may mask inter- and intra-grain age variability. This variability provides critical spatial information about where and how Ar is hosted, mobilised and removed during a metamorphic cycle.

Age dispersions far in excess of the range expected from variations in grain size in a fully open system have been observed in single grain fusion data from different metamorphic settings. This spread may be caused by differences in timing of crystallisation, variable amounts of contamination or variably inefficient diffusion. A robust interpretation requires a combination of detailed petrology, PT-path modelling, geochemical data and insights from diffusion modelling. The assumptions inherent in the Dodson closure temperature formulation - thermally activated volume diffusion, no initial Ar in the grain and an open grain boundary network that can efficiently remove Ar from the local rock volume¹ - can be tested using a combination of in-situ laser ablation spot profiling and single grain fusion methods. These highlight the spatial distribution of Ar both within and between different K-bearing and K-free minerals. Our data suggest that there is no simple lithologic or metamorphic grade pattern in the way that Ar is produced, stored, (re)cycled and removed during a metamorphic cycle. Each sample need careful investigation in order to most robustly link $^{40}\text{Ar}/^{39}\text{Ar}$ age to metamorphic stage.

References

1. Dodson, M.H., Closure temperature in cooling geochronological and petrological systems. *Contributions to Mineralogy and Petrology* **40**, 259-274 (1973)

Significance of micropores and low noble-gas solubilities for thermochronology

Peter K. Zeitler¹

1 Dept. Earth and Environmental Sciences, Lehigh University, USA

Noble-gas solubilities in minerals are known to be low; simple outgassing experiments conducted in atmosphere confirm this. This low solubility supports the assumption used in calculating U-Th/He ages that no initial helium is present in the lattice. It is also widely known that many mineral grains contain pores of various sizes, often originating as fluid inclusions.¹ Geochronology labs routinely screen samples for such inclusions because of the relatively high solubility of noble gases in fluids compared to radiogenic production in the host grain.²

Helium-solubility experiments using clear shards of Durango apatite standard verify that solubility is indeed low ($< 5 \times 10^{-7}$ cm³ STP/g-atm), but these experiments also reveal a very large scatter in helium contents in aliquots subjected to high partial pressures of helium. While most laboratories include “gem-quality” crystals of Durango as a standard, many crystals of Durango apatite have abundant inclusions, which is not surprising given this apatite’s origin.³ Declaration that an entire crystal is high-quality or selection of specific internal shards for dating usually involves optical characterization, but what is not known is the general size distribution of inclusions in Durango at the lower end. The best explanation for the observed scatter in the helium-uptake data is that helium diffusing into the crystal has become trapped in small pores acting as sinks, of which fluid inclusions might be a significant proportion.

Vacuum-crushing experiments confirm that samples of Durango standard treated at high pHe release significant quantities of “mechanical” helium (20 to 60%) that is therefore not derived from lattice sites. The helium partial pressures used in the solubility experiments were very high (up to 100 bars), so only a small volume of inclusions would be required to yield high helium values on measurement. These experiments suggest that even optically “clean” aliquots of apatite could contain some small volume of tiny pores or fluid inclusions.

This observation in itself would not cause concern because it is hard to imagine any geological environments addressed in thermochronology where noble-gas partial pressures would approach even a small fraction of the values used in laboratory solubility experiments. But crushing experiments on several natural untreated samples showed that some of them also released significant mechanical helium. Further, the degree of helium released mechanically correlated with the nature of the sample. Well-behaved, younger, more quickly cooled samples that replicate well (including natural Durango apatite), yielded very small helium release on crushing (1 to 3%), consistent with release from a few lattice sites exposed to surfaces by breakage. In contrast, a “bad actor” sample that replicated terribly released amounts of helium on crushing (50%) that are consistent with the anomalously older ages of the worst replicates. It seems plausible that for the latter, excess helium in fluid inclusions could be the source of this extraneous helium.

Slowly cooled samples were the other type of sample that released some helium on crushing (at least 5-10%). As noted by Watson and Cherniak,¹ small pores are often thought to enhance diffusion to the degree that they are interconnected and can provide short circuits, but if isolated, pores could impede diffusion. In a rough analogy to the RDAAM model for

radiation-damage modification of diffusion kinetics, pores could become traps for diffusing helium or argon. Unlike radiation traps, the behavior of helium or argon trapping and then release from small pores would not be likely to vary all that systematically with temperature, since the size-related stability of the pores or fluid inclusions and the poorly known temperature-dependence of solubility will all come into play. The number, size and thus total volume of such pores will depend on the nature of the particular sample and its origin, as well as its deformation history if other sorts of microstructures are also involved.

Slow cooling or isothermal residence would represent conditions most likely to lead to problems. Certainly in apatite U-Th/He dating, it is widely accepted that older, more slowly cooled samples tend to yield greater age dispersion, and there are many reasons that this can happen, mostly related to subtle difference in grain properties. But during slow cooling in the presence of pores, an additional effect could be “self-pollution” with radiogenic noble gases that would normally be expected to diffuse away from the crystal as part of the accumulation-diffusion process. An immediate objection to this model might be that such an effect would be trivial if the volume of inclusions or pores is so small as to be optically indistinguishable. But it is important to remember that the actual diffusive random walk within a typical grain is meters in length, compared to the net rms distance that defines the diffusion radius.⁴ In the immense number of diffusion jumps required to exit a crystal, the chances become very high if not 100% that a diffusing atom will encounter even a small-volume artifact. If a diffusing noble-gas atom enters a pore, it will in effect become trapped in the void because of low noble-gas lattice solubility, making it difficult for the attempt to return to the lattice, thus retarding its loss from the crystal.

If this model is correct for some samples, than it could be tested by examining borehole samples that have resided near or just above the higher-temperature parts of their partial retention zone: any such samples that contain isolated pores should show non-zero ages and mechanical release on crushing of most of their helium content. The phenomenon should also show up in laboratory kinetic studies, since the same diffusive random walk within a crystal will occur during outgassing. The pore-trapping effect would manifest itself as a delayed release of gas with respect to a simple volume-diffusion relationship. Using a new analytical approach involving continuous ramped heating and gas accumulation (see Idleman and Zeitler abstract, this volume), our preliminary data show that bad-actor samples that release helium on crushing also show significantly non-linear Arrhenius plots that stem from delayed release of helium.

References

1. Watson, E. B., Cherniak, D. J., Lattice diffusion of Ar in quartz, with constraints on Ar solubility and evidence for nanopores. *Geochimica et Cosmochimica Acta*. 67(11), 2043-2062 (2003).
2. Ozima, M., Podosek, F.A., Noble Gas Geochemistry. (Cambridge University Press, 1983).
3. Young, E., Myers, A., Munson, E., Conklin, N., Mineralogy and geochemistry of fluorapatite from Cerro de Mercado, Durango, Mexico. U.S. Geological Survey Professional Paper, 650-D, D84-D93.
4. Glicksman, M. E., Diffusion in Solids. (Wiley Interscience, 2000).Text in times new roman size 12. 1 page maximum with the references

$^4\text{He}/^3\text{He}$ and $(\text{U-Th})/^{21}\text{Ne}$ thermochronometry of polycrystalline minerals as illustrated by hematite

Ken Farley, Ryan McKeon, Stephen Cox

Division of Geological and Planetary Sciences, Caltech, Pasadena, CA 91125 USA

Compared with the apatite and zircon He systems, little is known about other phases potentially datable by the (U-Th)/He method, and even less is known about the behavior and potential utility of other isotopes produced by actinide decay, including Ne, Kr, and Xe isotopes. Here we discuss evidence suggesting that combination of the $^4\text{He}/^3\text{He}$ and $(\text{U-Th})/^{21}\text{Ne}$ techniques in polycrystalline mineral specimens, notably hematite, can reveal a wealth of cooling history information.

Noble gas thermochronometry requires knowledge of daughter product diffusion kinetics as a function of temperature. The necessary kinetic parameters are usually obtained from experiments undertaken at temperatures at which diffusion is measurable on a laboratory timescale linked to a physical model for how diffusivities can be extrapolated downward to temperatures relevant to the geologic timescale. This is most commonly done using an Arrhenius model ($D_0/a^2 = D/a^2 e^{-E_a/RT}$; **EQ 1**), from which the diffusion activation energy (E_a) and frequency factor (D_0/a^2 , diffusivity at infinite temperature divided by diffusion domain radius squared) are obtained. Provided a system obeys simple thermally activated volume diffusion, these two parameters are sufficient for thermochronometric applications. However, in many systems, daughter product diffusion does not conform to this model. If such a system is to be used for thermochronometry, a more sophisticated model is required. Perhaps the simplest case of greater complexity arises in minerals that occur as polycrystalline aggregates, including hematite¹ and goethite. He diffusion from these minerals defines a “declining lightning bolt” pattern on an Arrhenius plot, as illustrated by a supergene hematite associated with a BIF in Michigan (Fig.1A). This pattern is very similar to those seen in ^{39}Ar diffusion from some K-feldspars, an observation interpreted as diffusion from multiple noninteracting diffusion domains². In the case of hematite and goethite, these individual domains are readily attributed to crystallites of varying sizes (Fig.1B), and thus the bulk diffusivity is just the sum of multiple individual crystallites, each following **EQ 1** and with domain radius, likely corresponding to physical dimension, a . Because the smaller domains have higher diffusivity at a given temperature, they become depleted early in the experiment, causing the bulk diffusivity to decline following the lightning bolt pattern. The specific pattern depends on the domain size distribution and on the heating schedule used to interrogate the sample. We infer about a factor of 103 in domain size from the diffusion data in Fig.1A, which is reasonable given the range of crystallite sizes actually observed (Fig.1B). Each domain size has a characteristic He closure temperature; in the Michigan hematite, closure temperatures range from about 0 to 170°C. Using the $^4\text{He}/^3\text{He}$ method, polycrystalline specimens can be characterized for domain size distribution, diffusion activation energy, and age spectrum³ (Fig 1A,B). These parameters inform a forward model like HeFTy to identify allowable time-temperature paths experienced by the specimen. This methodology demands a) all domains have the same E_a , b) the domains have not changed in size, in nature or in the laboratory, c) the domains are not nested, and d) the parent elements are uniformly distributed through the crystallites, such that ^3He provides a proxy for computation of step He ages. Numerical “recovery experiments” show that a specimen with the domain size distribution found in the Michigan sample has the potential to accurately reveal thermal histories across the entire temperature range from 170°C to Earth surface conditions when analyzed as described above.

We have applied this methodology to high purity, coarse hematite specimens from multiple locations and environments. These and many other hematites we have investigated

have U and Th concentrations in the 0.1 to 10 ppm range, easily sufficient for analysis. All show highly reproducible He diffusion and age spectrum behavior, and crushing experiments confirm that, until a critical size is achieved, size reduction does not modify diffusivity. However, below that critical size, the largest domains inferred from He diffusivity begin to disappear. We will present model time-temperature paths for two proximal Michigan hematites showing how the method works. (U-Th)/²¹Ne dating provides a useful complement to this methodology because it may constrain formation age. This method is based on the production of nucleogenic ²¹Ne by α particle capture on ¹⁸O. Our recent direct determinations of ²¹Ne production rates confirm values previously proposed based on a compilation of neutron yield data and stopping power models⁴, suggesting ²¹Ne/⁴He ratios in the vicinity of 5×10^{-8} , depending on age and composition. Production rates are sufficiently well known that they contribute only a few percent to ²¹Ne age uncertainties. ²¹Ne yields are so low that fairly large amounts of sample (mgs) and fairly old ages (many Myr) are required. In addition, the presence of atmospheric Ne must not mask the nucleogenic ²¹Ne. These are restrictive requirements, but the method can be usefully applied to actinide rich trace minerals as well as to specimens with lower actinide contents but larger sample sizes, and may be especially applicable to minerals not presently dateable by alternative techniques. Hematite is an excellent candidate because it tends to carry remarkably low amounts of atmospheric Ne. For example, the Michigan specimen in Fig. 1 yielded a (U-Th)/²¹Ne age of 756 ± 18 Ma, with > 95% of ²¹Ne nucleogenic. As shown Fig.1B, the ²¹Ne age is in agreement with the oldest He step ages (“He age plateau”). This agreement is most easily attributed to formation of the specimen at ~ 760 Ma, with simultaneous closure of the entire system for ²¹Ne and of the coarsest domains for ⁴He at that time.

A key unresolved question that would greatly strengthen this interpretation is knowledge of the Ne diffusivity in hematite. This is a challenging measurement given the comparatively low abundance of ²¹Ne in our specimens, and the inability to create synthetic uniformly distributed neon by irradiation. Furthermore, work in progress on other phases suggests that Ne diffusion may in general be more complicated than He diffusion, for reasons unknown.

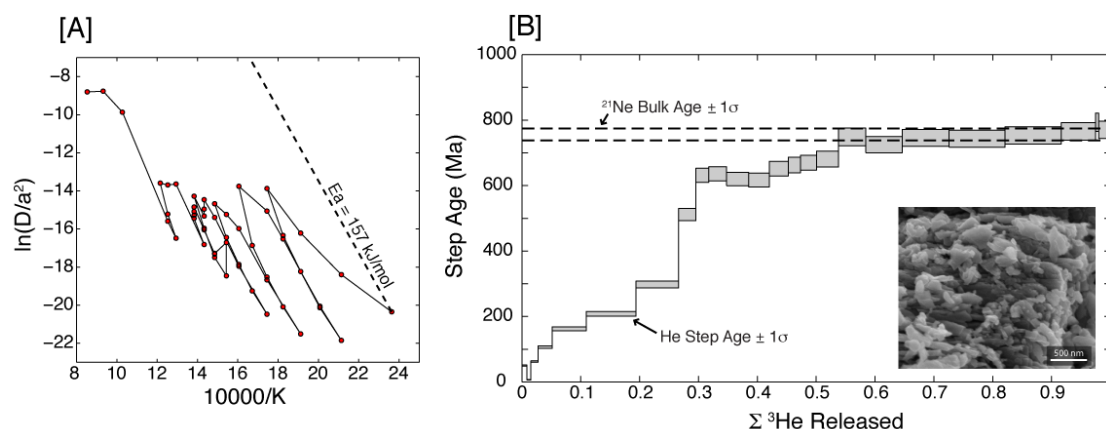


Figure 1: A) ³He-based diffusion data, with best-fit activation energy indicated by dashed line, and B) ⁴He/³He age spectrum and ²¹Ne bulk age of hematite specimen MI-43. Inset in B shows SEM image of this sample, revealing hematite crystallites spanning a range of sizes around 1 μm .

References

1. Bahr, R., Lippolt, H.J., Wernicke, R.S., JGR **99**, 695-617(1994).
2. Lovera, O., Richter, F., Harrison, T., JGR **96**, 2057-2069 (1993).
3. Farley K.A., Flowers, R.M., EPSL **359**, 131-140 (2012).
4. Gautheron, C.E., Tassan-Got, L., Farley, K.A., EPSL **243**, 520-535 (2006).

What really controls He migration in, and loss from, minerals?

Peter W. Reiners¹, Richard M. Thompson¹

¹ Department of Geosciences, University of Arizona, Tucson, AZ 85721, USA

Most thermochronologic interpretations rely on the assumption that noble gas behavior in minerals follows thermally activated volume diffusion. Practical calibrations are based on experiments interpreted in the context of the fundamental kinetic parameters (frequency factor D_0 , activation energy E_a , and diffusion domain lengthscale a), and computational models assume that noble gas atoms are interstitial impurities migrating through ideal crystal lattices. Some experimental evidence corroborates this, including anisotropic migration rates, grain-size correlations with bulk loss, and concentration profiles consistent with diffusion. In detail, however, many observations are inconsistent with simple volume diffusion, large discrepancies exist between molecular dynamics predictions and observed kinetics¹, and increasing evidence suggests that other phenomena may play critical roles in kinetics of noble gas migration and loss. Evidence from both Ar² and He³⁻⁶ kinetics suggest that crystallographic defects play a critical role, possibly through partitioning^{7,8} or kinetics fundamentally distinct from diffusion. For example, material science studies of He in metals and other substances consider diffusion unimportant relative to first-order single-jump mechanisms. This may also be important for minerals of thermochronologic interest⁹⁻¹¹.

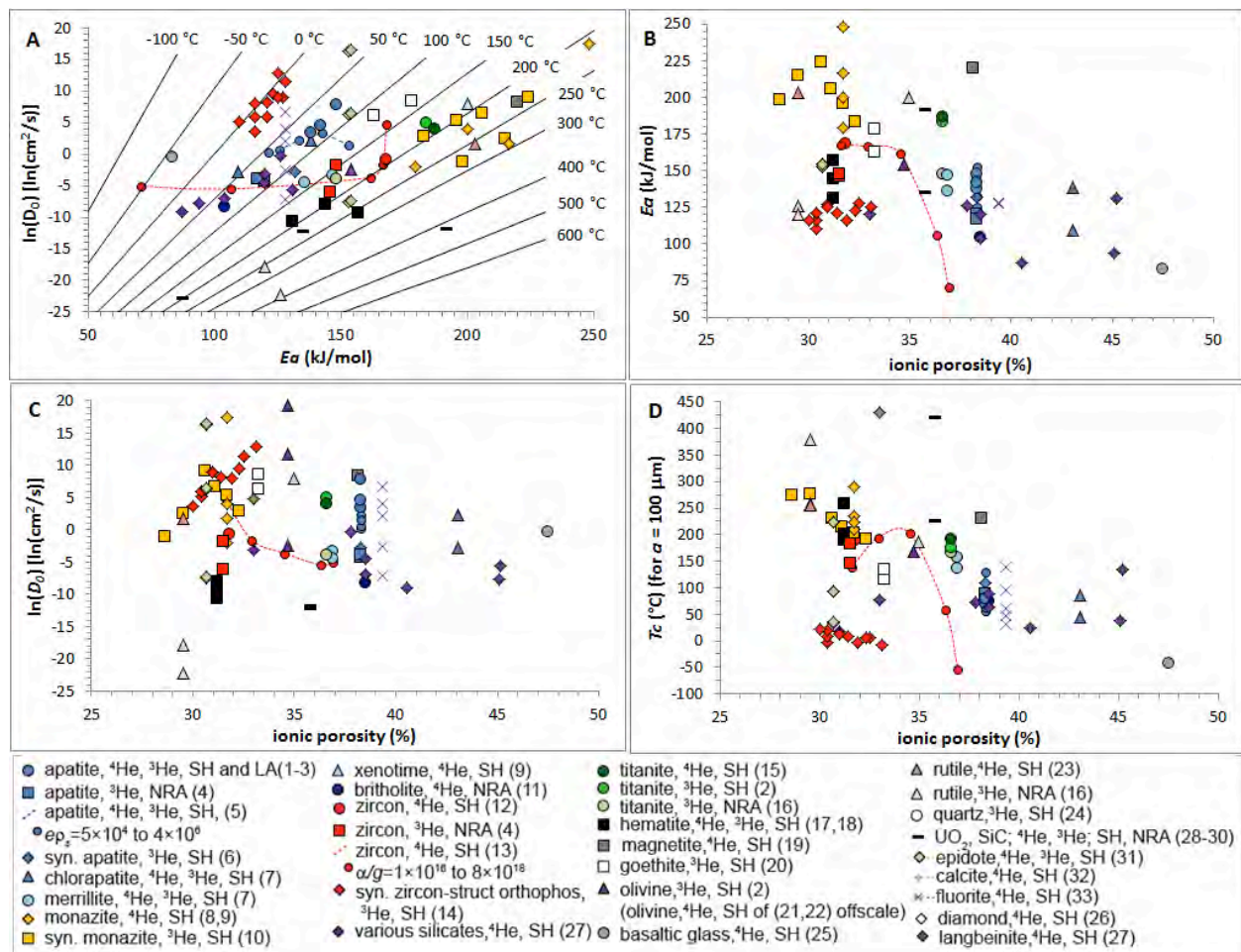


Figure 1. Compiled kinetic parameters and closure temperatures ($a=100 \mu\text{m}$ and $dT/dt=10 \text{ }^\circ\text{C}/\text{Ma}$) for He in minerals inferred from step-heating (SH), laser ablation (LA), and implantation-heating-in-situ analysis (NRA). Dashed red (blue) lines join zircon (apatite) with radiation dosages from 10^{16} to $10^{19} \alpha/g$ (e_p s from 5×10^4 to 4×10^6 track/cm²). Contours in A are closure temperature.

If volume diffusion of interstitial impurities through ideal crystal lattices is really the most

appropriate mechanistic description for thermochronology, then the fundamental kinetic parameters of volume diffusion interpreted from experiments should correlate with crystallographic properties of crystal lattices such as ionic porosity, or width and density of interstitial apertures¹² or planar porosity. If such properties do not scale with experimental kinetics, other mechanisms and other kinetic models need to be considered.

To test this hypothesis for He, we compiled kinetic parameters inferred from experiments on both ⁴He and ³He using step-heating, laser-ablation, and implantation/annealing/NRA on a variety of minerals (Fig. 1). E_a shows a broad inverse correlation with ionic porosity, as qualitatively expected, but large differences in E_a exist between different specimens, isomorphs, and in some cases among measurement techniques. Interestingly, available data suggest that hematite and magnetite have E_a lying far below and above, respectively, the broad correlation of other minerals. D_0 shows little correlation aside from a possible broad inverse correlation, contrary to qualitative expectations, although synthetic monazite specimens show the expected positive correlation¹³.

In general poor correlations between kinetic parameters and ionic porosity suggest that ionic porosity alone is not as good a predictor of He migration in minerals as it is for Pb¹⁴. Consideration of anisotropic or planar porosities may yield better correlations, thereby supporting volume diffusion as a dominant control. But this is not a simple proposition to evaluate, because the widest and lowest density apertures and planes may lie in non-orthogonal crystallographic orientations. Nonetheless, some support for this hypothesis comes from the fact that hematite, which has anomalously low E_a for its bulk ionic porosity (~32%), has at least two different relatively wide (~70-80 pm) low ionic-porosity (~50%) crystallographic planes. In contrast, magnetite, which has anomalously high E_a for its ionic porosity (~38%), has relatively narrow (~50-60 pm) planes with lower maximum porosity (<40%). Similar planar porosity differences for other minerals could explain other deviations from simple bulk ionic porosity expectations for volume diffusion kinetics.

References

1. Bengtson, A., Ewing, R. C., & Becker, U. He diffusion and closure temperatures in apatite and zircon: A density functional theory investigation. *GCA* **86**, 228-238 (2012).
2. Watson, E. B., & Cherniak, D. J. Lattice diffusion of Ar in quartz, with constraints on Ar solubility and evidence of nanopores. *GCA* **67**, 2043-2062 (2003).
3. Shuster, D.L., Flowers, R.A., and Farley, K.A. The influence of natural radiation damage on helium diffusion kinetics in apatite, *EPSL* **249**, 148-161 (2006).
4. Gautheron, C., Tassan-Got, L., Barbarand, J., & Pagel, M. Effect of alpha-damage annealing on apatite (U-Th)/He thermochronology. *Chemical Geology* **266**, 157-170 (2009).
5. Flowers, R.M., Ketcham, R.A., Shuster, D.L., and Farley, K.A. Apatite (U-Th)/He thermochronometry using a radiation damage accumulation and annealing model, *GCA* **73**, 2347-2365 (2009).
6. Guenther, W.R., Reiners, P.W., Ketcham, R.A., Nasdala, L., and Geister, G., Helium diffusion in natural zircon: Radiation damage, anisotropy, and the interpretation of zircon (U-Th)/He thermochronology, *AJS* **313**, 145-198 (2013).
7. Trull, T. W., Kurz, M. D., & Jenkins, W. J. Diffusion of cosmogenic ³He in olivine and quartz: implications for surface exposure dating. *EPSL* **103**, 241-256 (2001).
8. Farley, K. A. Helium diffusion from apatite: General behavior as illustrated by Durango fluorapatite. *Journal of Geophysical Research: Solid Earth* **105**, 2903-2914 (2000).
9. Hanson, G. N., & Gast, P. W. Kinetic studies in contact metamorphic zones. *GCA* **31**, 1119-1153 (1967).
10. Dodson, M. H. Closure temperature in cooling geochronological and petrological systems. *CMP* **40**, 259-274 (1973).
11. Yakubovich, O.V., Shukolyukova, Y.A., Kotova, A.B., Yakovlevaa, S.Z, and Sal'nikovaa, E.G. Geothermochronology Based on Noble Gases: II. Stability of the (U-Th)/He Isotope System in Zircon. *Petrology* **18**. 555-570 (2010).
12. Cherniak, D. J., & Watson, E. B. Helium diffusion in rutile and titanite, and consideration of the origin and implications of diffusional anisotropy. *Chemical Geology* **288**. 149-161 (2011).
13. Farley, K.A. He Diffusion Systematics in Minerals: Evidence from Synthetic Monazite and Zircon Structure Phosphates, *GCA* **71**. 4015-4024 (2007).
14. Dahl, P.S. A crystal-chemical basis for Pb retention and fission-track annealing systematics in U-bearing minerals, with implications for geochronology. *EPSL* **150**. 277-290 (1997).

Thermochronologic Investigation of Extraterrestrial Impact Events

Patrick Boehnke¹, Matt T. Heizler², T. Mark Harrison¹, Oscar M. Lovera¹, Paul H. Warren¹
1 University of California, Los Angeles, USA
2 New Mexico Bureau of Geology, USA

Although the $^{40}\text{Ar}/^{39}\text{Ar}$ step-heating method was devised as a tool to examine thermal disturbances in meteoritic and lunar samples [1,2], the sophistication of its application in this role has long lagged behind its terrestrial counterpart. This is surprising in that extraterrestrial impacts surely had a profound influence on development of the inner planets. For example, one of the most significant concepts to have emerged from Apollo-era lunar exploration is the hypothesis that an intense, discrete bombardment occurred in the inner solar system at ~ 3.9 Ga, possibly triggered by a sudden massive delivery of planetesimals from the outer solar system. The nature of this late heavy bombardment (LHB) has profound implications for the emergence of life on Earth ('impact frustration') [3], the role of giant planet migration in contributing to this inhospitable environment [4], and the calibration of 'crater counting' chronologies [5]. The original evidence for this hypothesis comes from Tera et al. [6] who interpreted isotopic resetting in lunar highlands samples as due to a terminal cataclysm at ~ 3.9 Ga. Subsequently, an apparent sharp cut-off of lunar $^{40}\text{Ar}/^{39}\text{Ar}$ ages at 3.9 Ga is viewed as supporting evidence of this short period of enhanced bombardment. This interpretation is problematic because the $^{40}\text{Ar}/^{39}\text{Ar}$ data from these complex lunar materials have for the most part not been rigorously interpreted in terms of diffusion and/or recoil effects. Indeed, arbitrarily assigned 'plateau ages' ca. 3.9 Ga [7] belie the fact that the vast majority of samples have bulk ages much younger or older than the assigned 'plateau age'. Unfortunately, this limitation is not simply ameliorated by using a more refined interpretive model; virtually all the analytical data to date [cf. 8] were obtained under conditions that effectively precludes recovery of sample-specific Arrhenius parameters from which thermal history information can be reliably determined.

We are addressing these deficiencies in analytical and interpretive procedures by performing thermochronologic investigations on both meteoritic and lunar samples. To gain an improved understanding of the thermal events in Apollo 16 samples, we have irradiated 27 specimens of various highland components from North Ray Crater and are using cycled step-heating to optimize data processing using the MDD model [9]. In order to model the diffusive loss experienced by our samples, we utilize a global optimization algorithm to simultaneously invert the Arrhenius plot and age spectra in terms of E , (D_0/r_0^2) , ρ , ϕ , and the intensity and timing of the reheating event. While the timing of the episodic loss is indicated by the initial degassing steps in well behaved samples, atmospheric Ar contamination in the initial steps requires modeling of both the last complete degassing event and the recent reheating in the majority of analyzed samples.

As shown in Fig. 1, the Arrhenius plot, shown in red triangles, for Apollo 16 sample 67704,11 exhibits complex multi-activation energy, multi-domain behavior. This data was gathered using a heating schedule with downcycles beginning at 600°C, 800°C, and 1100°C to optimize the extraction of kinetic information. From fitting the Arrhenius plot as well as the information revealed by temperature cycling, we conclude that the apparent linear behavior at low temperatures is not a reliable indicator of E and is instead an artifact of continually exhausting small domains in these fine grained samples. In addition to the visual evidence of the presence of multi- E 's in the temperature cycling portions, a single E yields a ~ 20 x worse goodness of fit relative to allowing two different E 's (and up to ten domain sizes per E). Note that for the constrained region (up to 1150°C) the model produces an excellent fit, shown in blue circles, to the measured data.

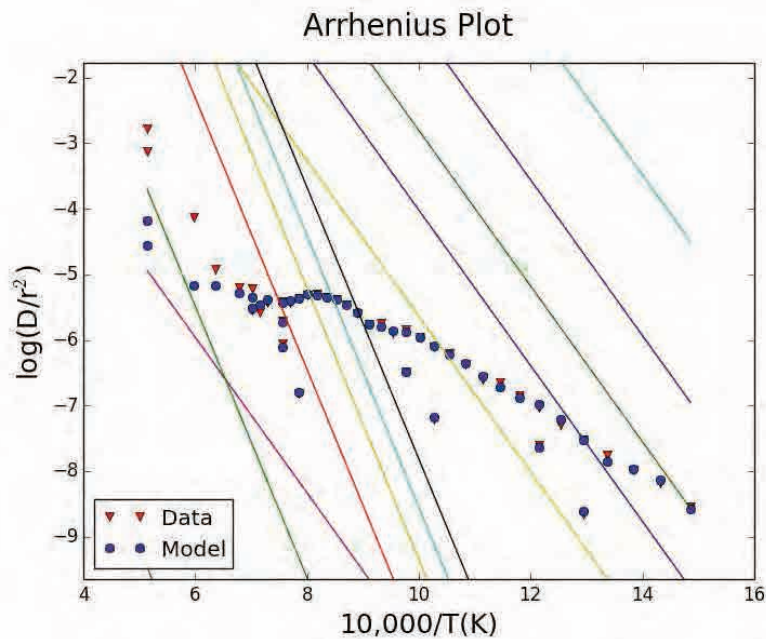


Figure 1. The Arrhenius plot for sample 67704,11 is shown in red triangles and the model fit in blue circles. The colored lines are fitted domains with $E \sim 54$ and 95 kcal/mol. Note the last 5 data points are not modeled because they were taken above the melting temperature.

In contrast to single phase (e.g., K-feldspar), multi-phase, multi- E samples do not yield unique fits to Arrhenius data. Thus, optimization of fit requires the additional constraints available from the age spectrum. This combined approach has allowed us to extract thermal history information from the majority of our analyzed Apollo 16 rocks. For the samples that exhibit recoil loss, our model allows for the calculation of one or more zero age domains in order to attempt recovery of accurate thermal information from otherwise pathologic specimen.

Our preliminary results show diverse behavior ranging from simple diffusive to complex diffusive and recoil loss spectra with a few samples exhibiting flat age spectra. Our data demonstrate that most, although not all, lunar samples are amenable to MDD modeling for reheating events. We further note that our preliminary data, though limited in number, do not support a spike in impact ages at ~ 3.9 Ga [cf. 7,10].

References

1. Merrihue, C. and Turner, G. (1966) *JGR*, 71, 2852-2857.
2. Turner, G. (1970) *Science*, 167, 466-468.
3. Sleep, N.H. et al. (1989) *Nature*, 342, 139-142.
4. Gomes, F. et al. (2005) *Nature*, 435, 466-469.
5. Head, J.W. (1976) *Rev. Geophys.*, 14, 265-300.
6. Tera, F. et al. (1974) *EPSL*, 22, 1-21.
7. Dalrymple, G. B. et al. (2001) *LPS 32*, Abstract #1225.
8. Shuster, D.L. et al. (2010) *EPSL*, 155-165.
9. Lovera, O.M. et al. (1991). *JGR*, 96, 2057-2069.
10. Norman, M.D. et al. (2006) *GCA* 70, 6032-6049.

Deconvolving Ar Diffusion Properties on Multi-domain, Multi-phase samples: Pitfalls and Die Hard Misconceptions

Oscar M. Lovera, T. Mark Harrison, Patrick Boehnke
University of California, Los Angeles, USA

Extracting meaningful diffusion information from samples comprising multi-domain and/or multi-phase aggregates via standard $^{40}\text{Ar}/^{39}\text{Ar}$ step-heating requires both innovative heating schedules that yield more diagnostic data and advanced numerical procedures that help to constrain the phase space (E, D_o, ϕ, ρ) of equivalent solutions.

The conventional monotonically increasing temperature step-heating approach is problematic in that it not only produces misleading, but seemingly well-correlated linear arrays, but also fails to reveal otherwise available diagnostic information with which to retrieve the sample diffusion properties.

High resolution $^{40}\text{Ar}/^{39}\text{Ar}$ step-heating schedules involving duplicate isothermal steps, temperature cycling, or initiating heating at high temperature, help not only to dramatically improve the likelihood of correctly inverting for the diffusion properties, but also avoid commonly encountered interpretive traps, such as viewing kinks in Arrhenius plots as due to thermo-structural modification of the sample, or that the initial linear array reflects an intrinsic diffusion property of the sample (or portion of it) rather than the apparent average diffusion of the multi-domain/phase sample. It has been shown that a sample comprising multi-diffusion domains having the same activation energy would show this diffusion characteristic in the linear array of the first few step-heating of degassing provided the smallest domains are not degassed beyond ~80%. However, the ordinate $\log(D_o / \rho_o^2)$ of this initial linear array does not represent a true domain size but rather an effective size depending on the size and concentration of all the domains in the sample. A common misconception in interpreting diffusion results from fragments of varying sizes is assuming that the position of the array does not change since the size of the smallest domains would not be affected by the crushing. Thus a correlation between the shift of this line with the actual size of the aggregates would unambiguously indicates that the sample comprise a single diffusion domain. However, the definition of the effective diffusion size of a MDD sample (i.e. a two domain sample, $\rho_o = (\frac{\phi_1}{\rho_1} + \frac{\phi_2}{\rho_2})^{-1}$) predicts a shift of the initial

linear array proportional to the actual size of the aggregate in uniform samples (e.g., Benson Mines or Madagascar orthoclases) where the proportion of the smallest domains is only a few percent and the largest domain size is close to the actual size of the aggregate.

Multi-phase samples having different activation energies introduce a highly-nonlinear convolution which, in some cases, require prior knowledge of the diffusion properties of at least some of the phases in order to separate them. Even in cases where the diffusion properties of these phases are well separated, large differences in activation energies among the phases could result in interpreting a misleading activation energy for the initial steps not correlated to the actual value of the less retentive phase. Thus, an accurate partition of the gas released from each phase and subsequent renormalization of the total gas to calculate individual Arrhenius plot is

necessary to avoid past interpretative mistakes. Lastly, we note that age spectra of samples containing multi-activation energies can yield different forms depending on laboratory heating schedule.

Finite element 2-D modeling of intracrystalline $^{40}\text{Ar}/^{39}\text{Ar}$ age gradients in natural muscovite crystals of arbitrary shape

Willis E. Hames¹, Dmitry V. Glotov², Amnon J. Meir², and B. Sedar Ngoma²

1. Department of Geology and Geography, 201 Petrie Hall, Auburn University, Auburn, Alabama 36849 USA (hameswe@auburn.edu)

2. Department of Mathematics and Statistics, Parker Hall, Auburn University, Auburn, Alabama 36849 Institutional address, Country

The distribution of ^{40}Ar in minerals has been established well to constrain thermal and crystallization histories for temperatures ranging from ca. 500-200°C. The most commonly utilized approach to evaluate a geologic thermal history and constrain a temperature-time path is to date minerals with differing diffusivity (e.g., hornblende, Hbl; muscovite, Mus; biotite, Bio; Figure 1A), and to use estimates of the integrated ‘closure temperatures’ that correspond to the time recorded by their apparent $^{40}\text{Ar}/^{39}\text{Ar}$ ages^{1,2}. The formalism of the closure temperature concept as provided in these classic papers by Dodson requires assumption of a brief transition from open to closed system behavior, and that the cooling history is linear within a T-t interval of partial isotopic retention. These conditions are met for the differing phases along path I and crystals of small effective diffusion dimension, but not for path II in Figure 1A and not for crystals with relatively large diffusion dimensions. Crystals of relatively large ^{40}Ar diffusion dimension, for which grain size controls the diffusion dimension on a millimeter-scale, tend to not conform well to Dodson’s earlier models^{1,2} because they tend to develop substantial core-to-rim patterns of age discordance over a large segment of the sample history (as in Figure 1B, calculated for a cylindrical geometry of 1.0 mm radius after Dodson³ and Wheeler⁴, with muscovite diffusion parameters from Hames and Bowring⁵). The recovery and interpretation of diffusion gradients in single grains can be more powerful than the approach of utilizing different minerals with differing closure temperatures as portrayed for contrasting T-t paths (Figure 1) that pass through temperatures of ca. 550, 350, and 300°C at similar times. Consider hornblende, muscovite, and biotite $^{40}\text{Ar}/^{39}\text{Ar}$ ages of rocks with cooling histories I and II. The discrete ages as obtained through bulk-sample $^{40}\text{Ar}/^{39}\text{Ar}$ methods, interpreted using Dodson’s^{1,2} closure temperature concept, and indicated with circles in Figure 1A would appear to be similar. However, the intracrystalline, apparent age profiles in muscovite crystals 1 mm in diameter (Figure 1B) are predicted to differ considerably for the two paths indicated

by solid curves, to a degree that could be easily measured with the resolution of current laser ablation methods for in situ $^{40}\text{Ar}/^{39}\text{Ar}$ analysis.

(An interpretation using the closure temperature concept would also be incorrect for path II, at least for the muscovite, as Dodson’s earlier

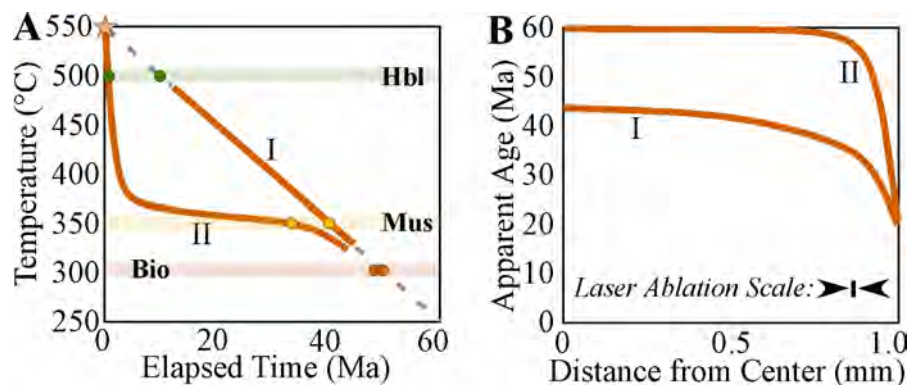


Figure 1: Contrasting, hypothetical thermal histories (A), with resulting apparent age profiles (B) predicted for muscovite crystals of 1 mm radius for cylindrical diffusion of ^{40}Ar (with diffusion parameters of Hames and Bowring, 1994). The closure profiles in B develop over the portions of the paths represented by the heavy line in A.

formalism requires rapid, linear cooling through mineral closure, as in path I.) Note for each path and the diffusion parameters chosen, muscovite with a millimeterscale diffusion dimension is predicted to partially retain radiogenic ^{40}Ar over a wide range of temperature (about 525 to 325°C for path II, and 475 to 325°C Ma for path I) and would lead to development of core-rim age variations of tens of millions of years.

Many studies over the past 25 years have documented apparent age gradients in micas that vary in complexity, but appear dominated by cylindrical diffusion at the grain scale, with ^{40}Ar loss along edges to (001) cleavage planes. We have developed 2-D models to describe argon diffusion in micas, that are dominated by cylindrical path diffusion but that allow the user to specify the size and shape of the actual mica. The new model utilizes the finite element method and the Matlab PDE toolbox, through which an arbitrary, user-defined 2-D shape is discretized into tens of thousands of triangles or elements, and the model can simulate argon accumulation, mobility and loss during complex cooling or thermal overprint histories. The model we have derived also permits investigation of the effects of fast diffusion pathways, that may be defects that form during growth of a crystal (as inclusions or other boundaries for composite grains) or through lattice deformation superimposed at some point in the sample's thermal history. Modeling of previously published in situ laser $^{40}\text{Ar}/^{39}\text{Ar}$ apparent age gradients in actual micas (e.g., grain-scale gradients reported in Paleozoic, Appalachian muscovite⁶, or Caledonian muscovite with grain-scale, core-to-rim age gradients⁷) with the new model yield satisfactory results, and are a better fit for describing the actual, natural system than previous models because the entire age distribution within a 2-D cleavage sheet can be evaluated.

The present focus of our model development is for forward modeling to predict the scale and form of $^{40}\text{Ar}/^{39}\text{Ar}$ age gradients in micas, but we anticipate future development of inverse approaches to derive thermal histories from observed age gradients. Dodson realized the petrological significance to applying Fick's laws of diffusion to the closure temperature concept beyond radiogenic isotopes to petrological systems and the study of elemental diffusion gradients. In a similar way, we feel that 2-D models as we are working to develop can be expanded to permit more generalized isotopic or elemental diffusion patterns at the scale of individual grains, and with shapes that are appropriate to their actual morphology. These integrated tools will be useful, for example, in evaluating P-T-t histories based on diffusion profiles in coexisting micas (with $^{40}\text{Ar}/^{39}\text{Ar}$ age gradients formed by loss of ^{40}Ar) and garnets (with growth zoning profiles modified by the diffusion of Fe-Mg-Mn-Ca).ext in Times New Roman size 12; single line spacing. Maximum length of the abstract: 2 pages including references. Use Nature reference style¹⁻³.

References

1. Dodson, M.H., Closure temperature in cooling geochronological and petrological systems. *Contributions to Mineralogy and Petrology*, 40:259 – 274 (1973).
2. Dodson, M.H., Kinetic processes and thermal history of slowly cooling solids. *Nature*, 259: 551 – 553 (1976).
3. Dodson, M.H., Closure profiles in cooling systems. *Materials Sci. Forum*, 7:145–154 (1986).
4. Wheeler, J., Diffarg: a program for simulating argon diffusion profiles in minerals. *Computers & Geosciences*, 22(8):919 – 929 (1996).
5. Hames, W.E., and Bowring, S.A., An empirical evaluation of the argon diffusion geometry in muscovite. *Earth and Planetary Science Letters*, 124:161 – 167 (1994).
6. Hames, W.E., and Hodges, K.V., Laser $^{40}\text{Ar}/^{39}\text{Ar}$ evaluation of slow cooling and episodic loss of ^{40}Ar from a sample of polymetamorphic muscovite. *Science*, 261:1721 – 1723 (1993).
7. Hames, W.E., and Andresen, A., Timing of Paleozoic orogeny and extension in the continental shelf of north-central Norway as indicated by laser $^{40}\text{Ar}/^{39}\text{Ar}$ muscovite dating. *Geology*, 24:1005 – 1008 (1996).

This material is based upon work supported by the National Science Foundation. Any opinion, findings, and conclusions or recommendations expressed in this material are those of the author(s) and do not necessarily reflect the views of the National Science Foundation.

The effects of rheology and strain localisation on white mica $^{40}\text{Ar}/^{39}\text{Ar}$ ages during retrograde metamorphism on Syros, Greece

Bertram Uunk^{1*}, Jan Wijbrans¹, Fraukje Brouwer¹

¹ Deep Earth and Planetary Science cluster, De Boelelaan 1085, 1081HV
Amsterdam, The Netherlands

*correspondence: bertr@muunk.nl

White mica $^{40}\text{Ar}/^{39}\text{Ar}$ dating is a proven powerful tool for constraining timing of metamorphism, deformation and exhumation. However, in high-pressure metamorphic rocks, wide age ranges can be found that do not agree with constraints from different isotopic systems, indicating that geological and chemical processes complicate straightforward dating. In this research project, white mica ages from rocks of the Cycladic Blueschist Unit on Syros, Greece with contrasting rheology and strain mechanisms are compared, in order to better understand the role of deformation, recrystallization and fluid flow on $^{40}\text{Ar}/^{39}\text{Ar}$ ages of white mica.

Resulting ages vary along different sections on the island, inconsistent with other isotopic constraints on eclogite-blueschist metamorphism (55-50 Ma) and greenschist overprinting (41-30 Ma). Two end-member models are possible: 1) Results represent continuous crystallization of white mica while moving from blueschist to greenschist conditions in the metamorphic P-T loop, or 2) white mica equilibrated in eclogite-blueschist conditions and their diffusion systematics were perturbed during greenschist overprinting. The single grain analyses yielded age ranges of different shapes, indicating differences in argon systematics. Step wise heating of larger grain populations resulted in flat plateau shapes, providing no evidence for partial resetting. Electron microprobe measurements of Si per formula unit, as a proxy for pressure during crystallisation, correlates well with age differences between samples with contrasting rheology and deformation mechanisms within a domain, but do not explain age variation on the island scale.

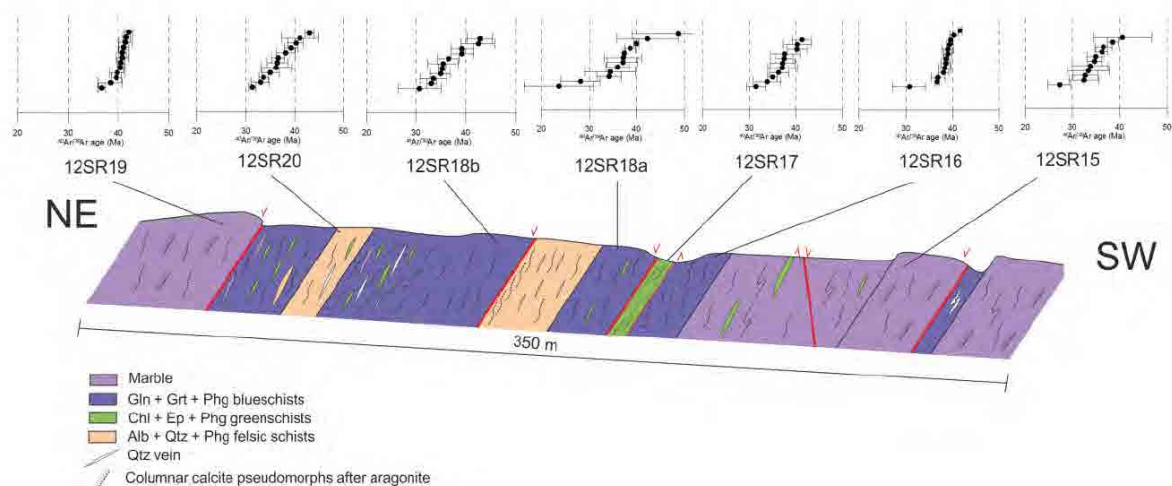


Figure 1. Shapes of multiple single grain age ranges along a road section with contrasting lithologies near Myttakas, central Syros. Varying shapes of age ranges show differences between normal and 'perturbed' argon systematics.

The previously unreported north-south age trend and age ranges per sample, as shown only in the $^{40}\text{Ar}/^{39}\text{Ar}$ system of the metapelitic and marble lithologies, contains key information that will allow us to test between different scenarios for age formation. Excess

argon infiltration at this stage seems to have been of minor importance. Our new approach should lead to a better understanding of the roles of these processes during and after HP metamorphism.

ERDA technique to study the He diffusion for the (U-Th)/He on apatite

Chloé Gerin¹, Laurent Tassan-Got², Cécile Gautheron¹, Erwan Oliviero³, Cyril Bachelet³,
Duval Mbongo², Jérôme Roques², Eric Simoni²

1 UMR GEOPS, CNRS/Université Paris-Sud, France

2 Institut de Physique Nucléaire, Orsay, France

3 CSNSM, CNRS/Université Paris-Sud, France

The knowledge of the helium diffusion behavior in minerals is a key issue to interpret thermochronological (U-Th)/He ages. Indeed, He age results from alpha particle accumulation produced during radioactive decay in a crystal and its diffusional loss by thermally activated diffusion. In apatite, recoil damage accumulation during alpha-decay is function of their production via the effective U content and their annealing^{1,2,3}, which depends on the temperature.

The damages have been recognized as playing an important role in helium diffusion in apatite. To study their effect we set up a series of experiments aiming at measuring the diffusion coefficient by the widening of a ⁴He implanted profile. For this purpose, dedicated experiments are conducted by using microbeam ERDA (Elastic Recoil Detection Analysis) on macro-apatite crystals. The ERDA is a method which uses the recoiled atoms to get information about the depth distribution of a target element. It is based on the elastic collision between a heavy incoming atom (here a carbon atom) and a lighter one present in the sample (an implanted ⁴He). Firstly a depth profile of helium is produced by implantation of ⁴He ions on a polished planar surface of apatite. Then the carbon beam is sent to the surface at a grazing angle of 15° and with an initial energy of 8.50 MeV and atoms slow down inside the sample. Most of them stop when they have lost the whole initial energy. But some of them collide with a light atom (helium or hydrogen) and transfer a fraction of their kinetic energy to the collided atom which is ejected and can be detected at some angle. The recoil energy is representative of the collision depth due to the slowing down of the incoming carbon and of the ejected atom. For a given ejected atom the lower the energy, the deeper the collision, and the energy spectrum is representative of the depth spectrum of the profile. The carbon beam fluences vary between 10¹⁷ and 10¹⁵ He/cm². The ERDA technique has already been used for apatite¹.

The He front is plumbed after He implantation, and after different annealing temperature heating steps. ERDA experiments are conducted on the same grain to characterize the possible effects of natural damages, irradiation-induced damages and amorphization due to the irradiation fluence.

The He implantation damages are calculated by TRIM⁵ simulations and compared to the natural damages, and we show that the implantation has an important impact on diffusion. Although diffusion has occurred, as demonstrated by the global decrease of the He quantity in the crystal, the heated He profile does not spread as expected. It indicates that a significant damaging has been produced by the implantation, and that the damages are not uniformly distributed, but rather peaked around the maximum of the concentration profile.

References

1. Gautheron C., Tassan-got, L., Barbarand, J. & Pagel, M. Effect of alpha-damage annealing on apatite (U-Th)/He thermochronology. *Chem. Geol.* **266**, 166-170 (2009).
2. Shuster, D.L. & Farley, K.A. The influence of artificial radiation damage and thermal annealing on helium diffusion kinetics in apatite. *Geochim. Cosmochim. Acta* **73**, 183-196 (2009).
3. Gautheron *et al.* Direct dating of thick- and thin-skin thrusts in the Peruvian Subandean zone through apatite (U-Th)/He and fission track thermochronometry. *Basin Research* **25**, 419-435 (2013).
4. Ouchani, S., Dran, J.-C. & Chaumont J. Exfoliation and diffusion following helium ion implantation in fluorapatite: implications for radiochronology and radioactive waste disposal. *Applied Geochem* **13**(6), 707-714 (1998).
5. Ziegler, J. F., & Biersack, J. P. The stopping and range of ions in matter. *Treatise on Heavy-Ion Science* 93-129. (Springer US, 1985).

Apatite composition effect on (U-Th)/He thermochronometer: a quantum point of view

Duval Mbongo-Dimbi¹, Cécile Gautheron², Jérôme Roques¹, Laurent Tassan-Got¹,
Chloé Gerin², Eric Simoni¹

1 Institut de Physique Nucléaire, Université Paris Sud, 91405 Orsay, France

2 UMR GEOPS, Université Paris Sud, 91405 Orsay, France

Periodic Density Functional Theory (DFT) calculations on apatite lattice have been performed to investigate the chemical composition effect on He diffusion and its impact on the (U-Th)/He thermochronometer. We determine the helium diffusion for a pure F-apatite lattice and for a lattice where a fluorine atom is substituted by a chlorine one. Two preferential diffusion directions in both structures have been identified, one along the fluorine atoms and the other one in the plane orthogonal to the later direction. A Nudged Elastic Band method (NEB) has been used to determine the activation energies between two He insertion sites, which range from 95,500 to 106,100 kJ/mol for the F-apatite and from 79,118 to 166,920 kJ/mol for the Cl_{0.25}-apatite. According to the energy barriers a small anisotropy is noticed in the case of the pure F-apatite and a more pronounced anisotropy in Cl_{0.25}-apatite. Consequently He diffuses preferentially in the plane in case of Cl_{0.25}-apatite while a 3 dimension (3D) diffusion process is observed in the pure F-apatite at low temperature.

In a second part, Kinetic Monte Carlo calculations have been performed to simulate the He 3D diffusion in the two-apatite lattices composition. From these calculations the Arrhenius law gives us access to the diffusion coefficient for infinite crystal such as:

$D \text{ (cm}^2\text{/s)} = 2.810^{-4} \text{ (cm}^2\text{/s)} \exp(-98.94 \text{ (kJ/mol)} / RT) \rightarrow \text{pure F-apatite}$

$D \text{ (cm}^2\text{/s)} = 3.010^{-4} \text{ (cm}^2\text{/s)} \exp(-108.00 \text{ (kJ/mol)} / RT) \rightarrow \text{Cl}_{0.25}\text{-apatite}$

He diffusion in F-apatite is significantly different that for the Cl_{0.25}-apatite, with calculated closure temperature of 41 to 71°C, for a 50 micron grain size and a cooling rate of 10°C/Ma. Then the closure temperature calculated from our DFT results is significantly different from the single existing DFT calculation¹, but is in good agreement with experimental results²⁻³ in the case of F-apatite for non-damaged apatite³. One can conclude that (1) the apatite grain shape and size are important parameters, as even the slight anisotropic He behavior of the Fapatite has some impact on the He age. The use of the active radius⁴ allows taking account of this behavior and will reduce the age dispersion. And (2) for high chlorine content ($\geq 25\%$), He diffusion behavior is significantly different compared to F-apatite and can explain some not understood He age variations.

References

1. Bengtson, A., Ewing, R.C. & Becker, U. He diffusion and closure temperatures in apatite and zircon: A density functional theory investigation GCA 86, 228-238 (2012).
2. Farley, K.A. Helium diffusion from apatite: general behavior as illustrated by Durango fluorapatite J. Geophys. Res 105, 2903-2914 (2000).
3. Shuster, D. & Farley, K.A. The influence of artificial radiation damage and thermal annealing on helium diffusion kinetics in apatite GCA 73, 183-196 (2009).
4. Gautheron, C. & Tassan-Got, L. A Monte Carlo approach of diffusion applied to noble gas/helium thermochronology Chem. Geol. 273, 212-224 (2010).

Migration of helium in natural semiconductors-semimetals

Olga Yakubovich^{1,2} & Alexander Kotov²

¹ Saint-Petersburg State University, Saint-Petersburg, Russia

² Institute of Precambrian Geology and Geochronology RAS, Saint-Petersburg, Russia

Retention of radiogenic ⁴He in crystal structures of most minerals is very low. Helium can escape easily from them in a course of geological history. However, in a group of minerals, namely native metals, the retention of radiogenic helium is anomalously high¹. Very low solubility of helium in metals leads to formation of atomic clusters, which manifest themselves as nanometer-scale helium "bubbles". Migration of such "bubbles" in the crystal structure requires relatively high temperature close to the metal melting temperature. Finding has already led to the creation of novel ¹⁹⁰Pt-⁴He method of isotope geochronology for the direct dating of platinum mineralization². Since the first main source of ⁴He in native minerals of platinum is α -decay of ¹⁹⁰Pt.

On practice the idea of anomalously high retention of radiogenic helium in crystal structures of native metals is confirmed by the results of ¹⁹⁰Pt-⁴He dating of isoferroplatinum from well-studied alkaline-ultramafic and dunite-clinopyroxenite complexes³. Comparison of obtained ¹⁹⁰Pt-⁴He ages with independent geochronological measurements is presented in table 1. Also the anomalously high retention of radiogenic helium was shown on the example of native gold. Thus for native gold from Witwatersrand deposit was obtained U-Th-He ages ~2300-3200 Ma⁴.

Table 1. Comparison of obtained ¹⁹⁰Pt-⁴He ages with independent geochronological measurements

deposit	¹⁹⁰ Pt- ⁴ He	⁴⁰ Ar/ ³⁹ Ar	Rb-Sr	Sm-Nd	U-Pb	K-Ar	U-Th-He	paleomagnetic age
Kondyor, Russia	125±6	120±1	126±1	131±35	125±2 baddeleyite	50-160	~10 apatite	modern - Paleozoic
Inagli, Russia	127±6	-	-	-	-	116±6; 141±7	-	-
Galmoenan, Russia	65±3	71-75	65-84	75-101	-	65-89	-	-
Fifield, Australia	450±23	-	-	-	445±6 zircon	397±16	-	-

Comment: data given by Ronkin et al., 2013; Elliot, Martin, 1991; Cabri et al., 1998; Karetnikov, 2005; et al.

Do not use headers or sub-headers in the abstract.

Separate different paragraphs of the abstract by single-line space.

References

1. Molnar, P. & England, P. Late Cenozoic uplift of mountain ranges and global climate change: chicken or egg? *Nature* **346**, 29-34 (1990).
2. Wagner, G. A. & Van den haute, P. *Fission Track Dating* (Elsevier, Amsterdam, 1992).
3. Ehlers, T. A. in *Low-temperature Thermochronology: Techniques, Interpretations, and Applications* (eds. Reiners, P. W. & Ehlers, T. A.) 315-350 (Mineralogical Society of America/Geochemical Society Reviews in Mineralogy and Geochemistry, Chantilly, Virginia, 2005).

Session 3:

Data, Models and Interpretation

Zircon (U-Th)/He radiation damage thermochronology: Some empirical observations

Barry Kohn¹, Andrew Gleadow¹, Ling Chung¹, Christian Seiler¹, Shimon Feinstein²

1 School of Earth Sciences, University of Melbourne, Victoria 3010, Australia

2 Geological & Environmental Sciences, Ben-Gurion University, Beer Sheva, 84105, Israel

The possibility that changes in physical properties accompanying the accumulation of radiation damage in zircon could be used as a tool to measure geological ages was first proposed more than 60 years ago¹. Later studies however, revealed that radiation damage could be thermally annealed² as well as enhance He diffusion³. These complexities soon led to abandonment of zircon radiation damage ages for application in geochronology. The later successful application of zircon fission track dating⁴ however demonstrated that a specific type of radiation damage age could form a viable geochronology technique. Subsequent laboratory and field studies elucidated the kinetics of fission track annealing and to date this exemplifies the most comprehensive understanding of the annealing of radiation damage in zircon (and other minerals) over geological timescales. With the development of SHRIMP zircon U/Pb spot analysis and the ability to carry out Raman analysis on the same spots to measure the degree of radiation damage in crystal structure⁵, as well as recent studies employing laser technology for obtaining spot zircon (U-Th)/He (ZHe) thermochronology data^{6,7}, it is timely to reassess the viability of zircon radiation damage ages, particularly for constraining low temperature thermal events.

Since the advent of modern (U-Th)/He thermochronology, several ZHe studies have demonstrated their potential for broad application in geochronology⁸⁻¹⁰. Although thermally activated volume diffusion is thought to be central in controlling He migration, crystal defects and radiation damage, are also considered important, but their precise role is not well understood. A first-order proxy for estimating the degree of accumulated radiation damage in grains is derived by calculating an estimate of the α -dosage ($D\alpha$) from its effective uranium concentration [eU]. This system works particularly well in quickly cooled volcanic or sub-volcanic rocks with low radiation damage. This is perhaps best illustrated by zircon from reference standards such as the Fish Canyon Tuff (FCT) and Mt Dromedary monzonite (MTD), whose ZHe ages tend to be concordant within analytical uncertainties with their well-established emplacement ages. The effective uranium concentration [eU] for these zircons, typically ranges between ~200-600 ppm corresponding to $D\alpha = \sim 0.02-0.05 \times 10^{18} \text{ } \alpha/\text{g}$ (FCT) and $0.1-0.2 \times 10^{18} \text{ } \alpha/\text{g}$ (MTD). These dosages are relatively low and in a range where zircon step-heating experiments indicate a pronounced decrease in He diffusivity¹¹, which, explains the well-behaved response of the ZHe system for these standards. Plots of ZHe age versus [eU] may be positive or negative depending on degree of radiation damage and thermal history¹¹. Here, we present case studies demonstrating how ZHe data and consideration of their radiation damage may yield unexpected relationships when used in combination with other thermochronological data.

Tasmania, southeastern Australia, hosts a large volume of Early Jurassic (~180 Ma) tholeiitic intrusives. Cropping out as dolerite intrusions over an area of ~30,000 km², it forms part of one of the world's major continental flood basalt provinces (Tasmania-Ferrar-Karoo Igneous Province) and is regarded as a precursor to the break-up and dispersal of Gondwana. Apart from two anomalously old ages exceeding the age of intrusion, ZHe data from dolerites yield either the age of dolerite emplacement for grains with relatively low radiation damage ($D\alpha = \sim 0.2-0.3 \times 10^{18} \text{ } \alpha/\text{g}$), or mid Cretaceous ages for grains with increased α dosage ($D\alpha = \sim 0.4-1.0 \times 10^{18} \text{ } \alpha/\text{g}$). The mid Cretaceous ZHe ages are concordant with apatite fission track (AFT) ages (~95 Ma) for dolerites in central and eastern Tasmania and consistent with their slightly younger apatite (U-Th-Sm)/He ages, and represent a cooling episode associated with continental extension prior to opening of the Tasman Sea. In western Tasmania, AFT ages are somewhat younger

(Late Cretaceous to Early Tertiary) than the corresponding mid Cretaceous ZHe ages, and are interpreted as a local cooling event related to transform margin formation in that area. Zircons from Tasmanian dolerites recording higher α -dosage therefore appear to record the distinctive, widespread mid Cretaceous cooling episode. Vitrinite reflectance data from Lower Permian sediments underlying the dolerites (but not in close contact) suggest they have experienced maximum post-depositional temperatures of $\sim 140^{\circ}$ - 160° C. This was achieved in the mid Cretaceous during maximum burial under the now largely eroded Mesozoic Victoria Basin¹².

Zircon fission track (ZFT) ages from Neoproterozoic rocks (deep boreholes and outcrops) in southern Israel and Sinai indicate a regional Late Devonian-Early Carboniferous cooling event ($\sim 360 \pm 30$ Ma) following earlier burial to temperatures $\sim 225^{\circ} \pm 50^{\circ}$ C, which totally resetting zircon FT clocks but only partially reset the titanite FT system¹³. The cooling episode involved removal of a lower Paleozoic section, probably exceeding the ~ 2.5 - 3 km currently preserved in southern Jordan and Saudi Arabia, adjacent to the study area. Regional stratigraphic evidence indicates that the Late Devonian-Early Carboniferous event was confined to a belt extending from the Gulf of Suez area to the vicinity of NE Syria and SE Turkey. ZHe data from similar Neoproterozoic lithologies in the same region, as well as from SW Jordan however, generally yield older ages (typically ~ 400 - 500 Ma) than those obtained from ZFT dating, but are similar to titanite FT ages ~ 400 - 450 Ma. In this data set a threshold of $D\alpha = \geq 1.0 \times 10^{18}$ α /g marks the effective radiation dosage where ZHe age decreases markedly, broadly consistent with existing He diffusivity experiments¹¹.

In another example from the Gulf Extensional Province (GEP) in southern Baja California, Mexico, the relationship between ZFT and ZHe ages in Cretaceous plutonic rocks varies according to sample post-intrusion exhumation history, despite all displaying a similar range of α -dosage ($D\alpha = \sim 0.1$ - 0.7×10^{18} α /g). ZHe > ZFT ages occur in samples where exhumation has been relatively subdued, but the relationship is reversed in samples that experienced marked exhumation related to GEP Miocene-Recent tectonics. These findings strongly suggest that factors controlling annealing of α - damage in relation to FT damage are not well understood and underscore the complexity of the radiation damage-He diffusion relationship.

References

1. Holland, H. L. & Kulp, J. L. Geologic age from metamict minerals. *Science* **111**, 312 (1950).
2. Holland, H. L. & Gottfried, D. The effect of nuclear radiation on the structure of zircon. *Acta Crystallogr.* **8**, 291-300 (1955).
3. Hurley, P. M. in *Nuclear Geology* (ed. Faul, H.) 301-329 (New York, Wiley, 1954).
4. Fleischer, R. L. Price, P. B. & Walker, R. M. Fission-track ages of zircons. *J. Geophys. Res.* **69**, 4885-4888 (1964).
5. Pidgeon, R. T. Zircon radiation damage ages. *Chemical Geology* **367**, 13-22 (2014).
6. Vermeesch, P. Sherlock, S. C., Roberts, N. M. W. & Carter, A. A simple method for in-situ U-Th-He dating. *Geochimica et Cosmochimica Acta* **79**, 140-147 (2012).
7. Tripathy-Lang, A. Hodges, K. V. Monteleone, B. D. & van Soest, M. C. Laser (U-Th)/He thermochronology of detrital zircons as a tool for studying surface processes in modern catchments. *J. Geophys. Res.: Earth Surface* **118**, 1333-1341 (2013).
8. Reiners, P. W. Spell, T. L. Nicolescu, S. & Zanetti, K. A. Zircon (U-Th)/He thermochronometry: He diffusion and comparisons with $^{40}\text{Ar}/^{39}\text{Ar}$ dating. *Geochimica et Cosmochimica Acta* **68**, 1857-1887 (2004).
9. Reiners, P. W. in *Low-temperature Thermochronology: Techniques, Interpretations, and Applications* (eds. Reiners, P. W. & Ehlers, T. A.) 151-179 (Mineralogical Society of America/Geochemical Society Reviews in Mineralogy and Geochemistry **58**, Chantilly, Virginia, 2005).
10. Wolfe, M. R. & Stockli, D. F. Zircon (U-Th)/He thermochronometry in the KTB drill hole, Germany, and its implication for bulk He diffusion kinetics in zircon. *Earth and Planetary Science Letters* **295**, 69-82 (2010).
11. Guenther, W. R. Reiners, P. W. Ketcham, R. A. Nasdala, L. & Giester, G. Helium diffusion in natural zircon: Radiation damage, anisotropy, and the interpretation of zircon (U-Th)/He thermochronology. *American Journal of Science* **313**, 145-198 (2013).
12. Lisker, F. & Läufer, A. L. The Mesozoic Victoria Basin: Vanished link between Antarctica and Australia. *Geology* **41**, 1043-1046 (2013).
13. Kohn, B. P. Eyal, M. & Feinstein, S. A major late Devonian-Early Carboniferous (Hercynian) thermotectonic event at the NW margin of the Arabian-Nubian shield: Evidence from zircon fission track dating. *Tectonics* **11**, 1018- 1027 (1992).

Thermal History Modeling using Multiple Thermochronometric Systems: A Progress Report

Richard A. Ketcham¹

1 Jackson School of Geosciences, University of Texas, Austin, TX, USA

Modeling has become a focal point through which most thermochronological data now pass. This is an outgrowth of the fact that the community has, in a sense, outgrown the original Dodson framework of closure temperature¹. Whereas ages were once (and in some cases still are) hoped to correspond to discrete geologic “events”, we continue to absorb the full impact of the early lessons demonstrated by Naeser² and others that, due to partial resetting and retention, ages frequently occupy a continuum. Thermochronometric age is not so much a function of cooling rate as the entire time-temperature path, and the particular kinetics of each instance of each system.

At the same time, one of the great and continuing contributions of the closure temperature framework has been to bring order to the influence of temperature on radiometric ages, allowing the temperature sensitivity of different systems to be organized and arranged to help clarify their respective contributions to our understanding of different segments of thermal histories. Given the increasing number of studies that employ multiple thermochronometric systems, not to mention the interconnectivity among systems such as posited by radiation-damage-influenced models of helium diffusivity, there is a need for similar organization in the context of modeling.

Currently, the lens through which we quantitatively consider multiple systems together is statistics, for which there are a number of approaches. HeFTy³ attempts to use the simplifying concept of expected value: given a particular t-T path, set of kinetics, and analytical precision, there is an expected range of outcomes that can be compared with a set of measurements. The success of this approach hinges on the fidelity with which disparate systems can be fit into this framework. However, each of the commonly employed thermochronometric systems has its own idiosyncrasies. Tellingly, the more-used and more-studied a system is, the more complex it has turned out to be.

The apatite fission-track (AFT) system has the unusual luxury of large analytical uncertainties that tend to swamp errors, oversimplifications and incompletely-understood and thus poorly quantified physical processes of formation, annealing, and etching that are nevertheless present. However, these shortcomings can become evident as data quantities rise, which promises to occur with increasing frequency given the continuing progress of semi-automated data acquisition systems. Excess variation is often attributed to either kinetics or provenance, or a mixture of the two; however, the statistical tools we use for this separation contain no kinetic information, and our ability to estimate kinetics accurately via composition or solubility remains limited. The zircon fission-track system (ZFT) is understood through only a limited set of experimental data sets. Although it has been asserted that radiation damage influences ZFT annealing rates⁴, there are not yet sufficient laboratory data to quantify this effect.

Apatite is also the most-studied mineral for the (U-Th)/He system, and in some ways the depth of our understanding of the apatite helium (AHe) system exceeds that for fission tracks. However, the scatter among AHe data regularly exceeds the limits implied by analytical precision and analysis of standards, both in the occurrence of outliers and smaller-scale dispersion. In many cases this dispersion can be interpreted as a result of kinetic effects from grain size and/or radiation damage^{5,6}, but there is also danger in this approach for modeling if other factors, such as inclusions, zoning⁷, bad neighbors⁸, fragmentation⁹, or composition¹⁰, are responsible for the scatter. As with fission tracks, the zircon system is less-studied; some kinetic influences such as radiation damage and zoning¹¹ are more severe and complex, while some others are probably less important.

Appropriate calculation and scaling of uncertainties is complicated because of the presence of errors that are to varying extents stationary or non-stationary with respect to thermal history. Stationary factors are generally responsible for symmetrical or modestly biased dispersion of limited magnitude, such as counting and etching efficiency for fission-track dating and alpha ejection calculation for (U-Th)/He. Conversely, kinetic factors are non-stationary because their influence is linked to thermal history, and can be of arbitrarily large magnitude. Our ability to quantitatively interpret systems affected by kinetic variation hinges on both our understanding of the kinetics and the reliability with which we can and do estimate them. In the (U-Th)/He system, factors such as fragmentation and zoning are hybrids: the magnitudes of their effects are influenced by thermal history, but remain limited.

Stationary and semi-stationary factors, and their effects on the expected dispersion among measurements, can and should be included in consideration of how best to estimate and report uncertainties. For semi-stationary factors it may be warranted to consider an increment of estimated uncertainty that is linked to thermal history. A quantitative accounting would also facilitate cost-benefit analysis of analytical measures that can be taken to address them.

To the extent that measurements are affected by departures caused by unquantified kinetics or other sources of variation, failure can be a desirable result; modeling is a test of a hypothesis, and a failure of that test is informative. However, this is not always the case in practice – modeling can in many cases converge on an “answer” even when it should not, with a meaningless or misleading result. We thus don’t want to ignore dispersion, or arbitrarily over-estimate uncertainties simply to make modeling easier.

Ultimately, statistics are an admission of ignorance. It is worth considering how to better include this ignorance in the statistics underlying our data interpretation and especially our modeling, quantifying our “known unknowns” as possible and respecting the presence of “unknown unknowns” without being paralyzed by them.

References

1. Dodson, M. H. Closure temperature in cool geochronological and petrological systems. *Contrib. Mineral. Petrol.* **40**, 259-274 (1973).
2. Naeser, C. W. & Faul, H. Fission track annealing in apatite and sphene. *J. Geophys. Res.* **74**, 705-710 (1969).
3. Ketcham, R. A. in *Rev. Mineral. Geochem.* Vol. 58 (eds. P.W. Reiners & T.A. Ehlers) 275-314 (2005).
4. Rahn, M. K., Brandon, M. T., Batt, G. E. & Garver, J. I. A zero-damage model for fission-track annealing in zircon. *Am. Mineral.* **89**, 473-484 (2004).
5. Flowers, R. M., Ketcham, R. A., Shuster, D. L. & Farley, K. A. Apatite (U-Th)/He thermochronometry using a radiation damage accumulation and annealing model. *Geochim. Cosmochim. Acta* **73**, 2347-2365 (2009).
6. Gautheron, C., Tassan-Got, L., Barbarand, J. & Pagel, M. Effect of alpha-damage annealing on apatite (U-Th)/He thermochronology. *Chem. Geol.* **266**, 157-170 (2009).
7. Ault, A. K. & Flowers, R. M. Is apatite U-Th zonation information necessary for accurate interpretation of apatite (U-Th)/He thermochronometry data? *Geochim. Cosmochim. Acta* **79**, 60-78 (2012).
8. Spiegel, C., Kohn, B. L., Belton, D. X., Berner, Z. & Gleadow, A. J. W. Apatite (U-Th-Sm)/He thermochronology of rapidly cooled samples: The effect of He implantation. *Earth Planet. Sci. Lett.* **285**, 105-114 (2009).
9. Brown, R. W. et al. Natural age dispersion arising from the analysis of broken crystals. Part I: Theoretical basis and implications for the apatite (U-Th)/He thermochronometer. *Geochim. Cosmochim. Acta* **122**, 478-497 (2013).
10. Gautheron, C. et al. Chemical influence on α -recoil damage annealing in apatite: Implications for (U-Th)/He dating. *Chem. Geol.* **351**, 257-267 (2013).
11. Guenther, W. R., Reiners, P. W., Ketcham, R. A., Nasdala, L. & Giester, G. Helium diffusion in natural zircon: radiation damage, anisotropy, and the interpretation of zircon (U-Th)/He thermochronology. *Am. J. Sci.* **313**, 145-198 (2013).

Inverted apatite (U-Th)/He and fission-track dates from the Southern Canadian Shield: Evaluating the internal consistency of apatite (U-Th)/He and fission-track thermochronology datasets

James R. Metcalf¹, Barry P. Kohn², Rebecca M. Flowers¹, Kirk G. Osadetz³, Andrew J.W. Gleadow²

1 Department of Geological Sciences, University of Colorado - Boulder, USA

2 School of Earth Sciences, University of Melbourne, Australia

3 Geological Survey of Canada, Calgary, Alberta, Canada

The well-documented dependence of He diffusivity in apatite on the amount of accumulated radiation damage in a crystal has, to first-order, helped explain a variety of common observations in apatite (U-Th)/He (AHe) datasets, including large spreads in AHe dates from the same sample and “inverted” datasets where reproducible and reliable AHe dates are older than corresponding apatite fission-track (AFT) dates. Models for He diffusivity indicate that changes in He diffusive behavior are most apparent in samples that have experienced long residence at moderate to low-temperatures, such as samples from the relatively stable interiors of cratons. In this study we use new, paired AHe and AFT thermochronology on basement samples from the Canadian Shield in southern Ontario to both constrain the thermal history of the region and to evaluate the internal consistency of AHe and AFT data that record long (100’s of Ma) timescales using the most recent apatite He diffusion kinetic and FT annealing models.

New AHe and AFT thermochronology data from the southern Canadian Shield record complex and spatially variable thermal histories, consistent with differing amounts of sedimentary burial and reheating during the Paleozoic and Mesozoic. AFT dates range from ~360 – 530 Ma and are generally younger towards the southeast. AHe dates on single-grains from the same sample exhibit more complex behavior. He dates range from ~240 – 730 Ma with effective Uranium (eU) values between 3-60 ppm. AHe dates are either older or younger than corresponding AFT dates, depending on the individual sample, its geographic location, and the range of eU values of the analyzed apatites. Samples with only low eU grains yield AHe dates younger than or equivalent to AFT dates. In samples with significant variation in eU, some show uniform dates regardless of eU while others display positive date-eU correlations, together reflecting the geographic variability in thermal histories recorded by the AFT data. For the latter data pattern, higher-eU grains are significantly older than corresponding AFT dates, and lower-eU grains equivalent or younger than corresponding AFT dates. For example, sample 01-OE-23 (Figure 1) has an AFT central age of 381 ± 20 Ma, yet yields AHe dates ranging from 357 ± 34 Ma (eU = 15) to 637 ± 48 Ma (eU = 35). The AHe and AFT results from these samples are qualitatively consistent with models that predict lower He diffusivities, and consequently older He dates, for grains with substantial accumulated radiation damage, and provide an excellent test case for our current understanding of AFT and AHe behavior. Samples from the southern Canadian shield combine high-quality apatite, variable apatite eU concentrations, an extensive fission-track thermochronology data set, and protracted and spatially variable thermal histories, and as such provide an excellent natural laboratory in which to investigate the behavior of low-temperature thermochronometers over long time scales.

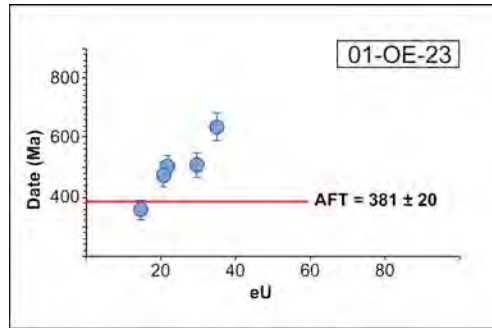


Figure 1. Apatite (U-Th)/He (blue circles) and fission-track (red line) data from 01-OE-23, a sample from the northwest shore of Lake Superior in southern Ontario. Note that the low-eU AHe date is younger than the corresponding AFT date, but higher-eU grains yield systematically older dates.

The influence of slow cooling and zonation on apatite $^4\text{He}/^3\text{He}$ thermochronometry

Ryan McKeon¹, David Shuster²

1 Division of Geological and Planetary Sciences, Caltech, Pasadena, CA 91125 USA

2 Department of Earth and Planetary Science, University of California, Berkeley, California 94720-4767, USA, and Berkeley Geochronology Center, 2455 Ridge Road, Berkeley, California 94709, USA

It is now well established that the kinetics of helium diffusion in apatite is an evolving function of grain-specific characteristics and the thermal history that a sample experienced^{1,2,3}. As we push to utilize the low temperature sensitivity of apatite U-Th/He (AHe) and $^4\text{He}/^3\text{He}$ thermochronometry into different lithologies and less dynamic topography, these variables can influence the cooling ages and ^4He concentration profiles we measure, making meaningful interpretation of the thermal history difficult without careful sample characterization⁴. Here we present new $^4\text{He}/^3\text{He}$ data coupled with U and Th zonation maps from the same grains for samples from a complex AHe data set from the southern Appalachian Mountains in eastern North America⁵. We illustrate how these techniques elucidate the causes of poor AHe age reproducibility between individual apatites from the same rock and we explore how such complexity and grain-specific differences provide additional leverage on the thermal history.

Previous work to quantify the timing and rate of bedrock exhumation in the southern Appalachians produced a complex data set with poor AHe age reproducibility both between adjacent samples and within individual samples⁵. An extreme example is sample SY-2 that was derived from Proterozoic gneiss on a high ridge in the rugged mountains of western North Carolina, U.S.A. Replicate AHe analyses of this sample produced a range cooling ages from 66 to 219 Ma with no correlation with eU concentration. However, after physical abrasion, grains from the same sample produced ages from 48 to 195 Ma that were strongly correlated with eU concentration. Inverse modeling of the age-eU relationship of the abraded grains suggests steady slow cooling corresponding to an erosion rate of 20 m/Ma over the last 180 Ma. Following proton irradiation to produce a uniform distribution of ^3He through spallation reactions⁶ $^4\text{He}/^3\text{He}$ ratio evolution diagrams of three individual apatite grains from SY-2 were measured. Two of these spectra are convex and suggest variable degrees of core-enriched zonation of U and Th (Figure 1). These apatite grains were recovered, mounted, and polished for LA-ICPMS mapping of the distribution of U and Th; the data confirm the presence of strong core-enriched zonation in two of the grains (Figure 1).

U and Th zonation has been investigated for its impact on the alpha-loss correction used for AHe dating^{4,7}. However, the impact of spatially heterogeneous radiation damage, which is a by-product of U and Th zonation, has not been fully explored. Forward modeling using the inferred slow-cooling thermal history from the abraded data set illustrates the impact of heterogeneous radiation damage on $^4\text{He}/^3\text{He}$ results (Figure 1). When spatial variability in radiation damage is considered using the zonation map data, predicted $^4\text{He}/^3\text{He}$ ratio evolutions display a convex shape similar to the strongly zoned grains from SY-2. A homogenous eU distribution generates a concave shape that is a poor fit to the strongly zoned grains because it misses the enrichment of ^4He during the high temperature steps. The reason for the disparity between the two models is partly because more ^4He is produced in the enriched core relative to the rim. This effect is compounded during slow cooling since the highly enriched (and thus more damaged) cores more rapidly evolve towards lower ^4He diffusivity at a higher temperature than the low eU rims; in this case, the rims remain open to diffusive loss down to very low temperatures. When incorporating these sample-specific complexities, a single thermal path can explain much of the observed data for all three samples. Therefore, differences in the spatial distributions of production and diffusion between individual crystals from the same rock provide additional leverages on constraining a thermal path.

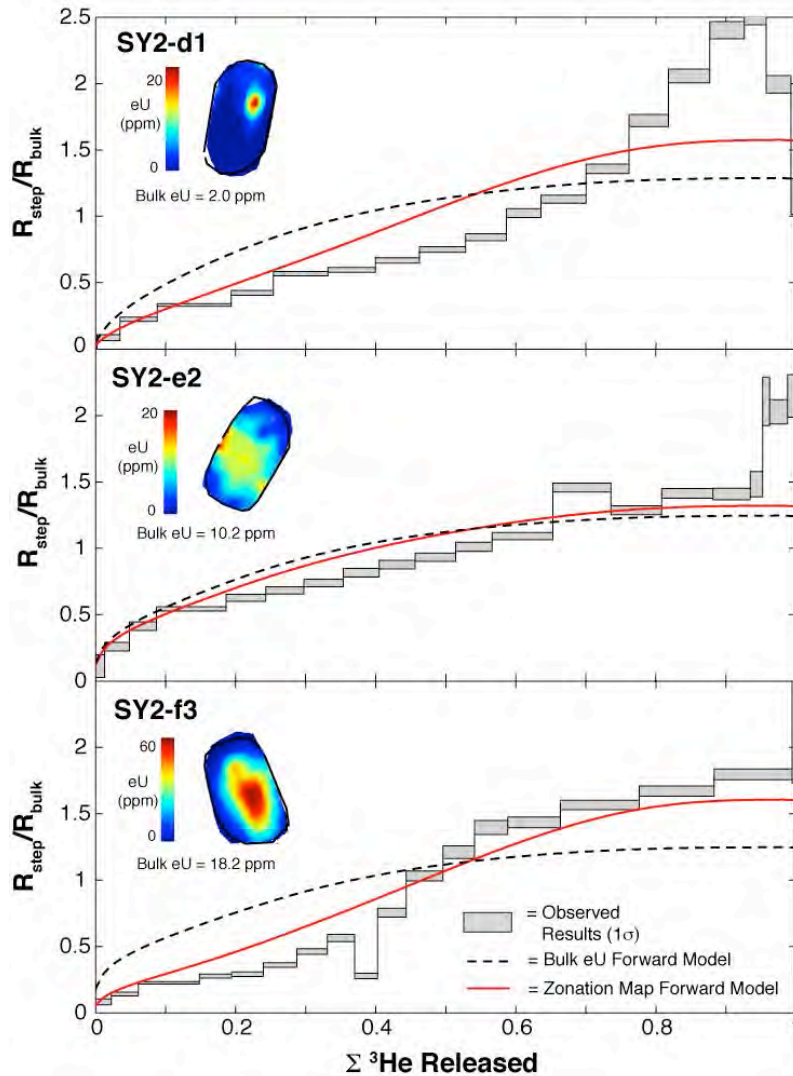


Figure 1. ${}^4\text{He}/{}^3\text{He}$ thermochronometric and [eU] mapping results for three apatite grains from sample SY-2 from the southern Appalachians, U.S.A. Inset contour plots illustrate the U and Th zonation characteristics for each grain. The ratio evolution diagrams show the normalized results of ${}^4\text{He}/{}^3\text{He}$ step-heating experiments (gray boxes) compared to forward model predictions. The forward model results share a common time-Temperature history and show the impact of the observed zonation modeled as radially symmetric 1D distribution of eU (red lines) relative to an assumed homogenous distribution eU (dashed black lines).

References

1. Shuster, D., Flowers, R. & Farley, K. The influence of natural radiation damage on helium diffusion kinetics in apatite. *Earth and Planetary Science Letters* **249**, 148–161 (2006).
2. Flowers, R. M., Ketcham, R. A., Shuster, D. L. & Farley, K. A. Apatite (U-Th)/He thermochronometry using radiation damage accumulation and annealing model. *Geochimica et Cosmochimica Acta* **73**, 2347–2365 (2009).
3. Farley, K. A., Shuster, D. L., Watson, E. B., Wanser, K. H. & Balco, G. Numerical investigations of apatite $4\text{He}/3\text{He}$ thermochronometry. *Geochem. Geophys. Geosyst.* **11**, Q10001 (2010).
4. Farley, K. A., Shuster, D. L. & Ketcham, R. A. U and Th zonation in apatite observed by laser ablation ICPMS, and implications for the (U-Th)/He system. *Geochimica et Cosmochimica Acta* **75**, 4515–4530 (2011).
5. McKeon, R. E., Zeitler, P. K., Pazzaglia, F. J., Idleman, B. D. & Enkelmann, E. Decay of an old orogen: Inferences about Appalachian landscape evolution from low-temperature thermochronology. *Geol Soc America Bull* **126**, 31–46 (2014).
6. Shuster, D., Farley, K., Sisterson, J. & Burnett, D. Quantifying the diffusion kinetics and spatial distributions of radiogenic ${}^4\text{He}$ in minerals. *Earth and Planetary Science Letters* **217**, 19–32 (2004).
7. Ault, A. K. & Flowers, R. M. Is apatite U-Th zonation information necessary for accurate interpretation of apatite (U-Th)/He thermochronometry data? *Geochimica et Cosmochimica Acta* **79**, 60–78 (2012).

High temperature thermochronology and the relationship between Pb diffusion and apatite composition

André Paul¹, Richard Spikings¹, Maria Ovtcharova¹, Alexey Ulianov²

1 Section of Earth and Environmental Sciences, University of Geneva, Switzerland

2 Institute of Earth Sciences, University of Lausanne, Switzerland

High temperature (>350°C) thermochronometry can be achieved by exploiting the loss of Pb from accessory minerals such as apatite, titanite and rutile, assuming that lead is lost by a thermally activated process. Studies within man-made¹ and natural² laboratories support this assumption. Some studies have proposed that interaction with aqueous fluids dominates daughter isotope loss from crystal lattices³, although Cochrane et al. (2014)² recently showed that Pb loss from apatite is a function of temperature, and aqueous interaction is not required. Cochrane et al. (2014)² also showed that meaningful t-T paths can be obtained from modeling volume diffusion of Pb through apatite by combining diffusion parameters¹, U-Pb dates, grain sizes and the distribution of U within the apatite. The aims of this study are i) to generate t-T paths from apatites using HeFTy V1.8.0, ii) to investigate the relationship between Pb diffusion in apatite, titanite and rutile, and composition, and iii) to examine the nature of Pb loss by comparing in-situ (MC-LA-ICPMS) and bulk (ID- TIMS) dates.

Accessory phases have been extracted from Triassic S-type granites and migmatitic leucosomes from the Andes of Ecuador and Colombia. U-Pb dates have been obtained from the apatites using Thermal Ionization Mass Spectrometry, and these are compared with grain size (50 – 200 µm). Thermal history paths have been obtained from apatites that lie on well-defined trends, which are predicted from volume diffusion. The t-T paths have been obtained using HeFTy V1.8.0⁴, and the activation energy for diffusion and diffusivity for Pb in apatite¹. The thermal history of the region has been previously constrained at temperatures <350°C⁵, which were experienced after 75 Ma, providing a constraint for the t-T models.

The trace element composition of the apatites has been determined using TIMS-TEA⁶, which utilizes solution nebulization ICPMS of the same apatite that was dated. Previous work showed that outliers on date vs. grain size trends have elevated Th/U ratios, which may be a proxy for other compositional variations. This study will accumulate a database of apatite compositions, which will be used to seek relationships between apatite composition, activation energy for diffusion and absolute diffusivity.

In-situ dates will be obtained using MC-LA-ICPMS, combined with element mapping using a quadrupole. The in-situ dates will be compared with the core-rim date profiles that are predicted from the t-T models constructed using the bulk (TIMS) dates. A statistical match between predicted and measured in-situ dates would validate the assumption that Pb has been lost from the apatites by thermally activated diffusion. Discrepancies would suggest that either i) Pb was lost by mechanisms other than volume diffusion, ii) volume diffusion has operated although the intrinsic diffusion parameters used¹ are not applicable (e.g. due to compositional variations), or iii) the grain has a multi-domain structure with respect to diffusion. This study will investigate these discrepancies.

The study is in a preliminary phase, and the apatite U-Pb dates acquired so far range between 210 – 75 Ma for apatites with radii varying between 100 and 175µm. Concordant zircon U-Pb dates (LA- ICPMS) show that the leucosomes are Triassic indicating that Pb has been lost from these apatites.

References

1. Cherniak, D. J., Langford, W. A. & Ryerson, F. J. Lead diffusion in apatite and zircon using ion implantation and Rutherford Backscattering techniques. *Geochimica et Cosmochimica Acta* **55**, 1663-1673 (1991).
2. Cochrane, R., Spikings, R. A., Chew, D., Wotzlaw, J. F., Chiaradia, M., Tyrell, S., Schaltegger, U. & Van der Lelij, R. High temperature (>350°C) thermochronology and mechanisms of Pb loss in apatite. *Geochimica et Cosmochimica Acta* **127**, 39-56 (2014).
3. Lee, J. K. W. Multipath diffusion in geochronology. *Contributions to Mineralogy and Petrology* **120**, 60-82 (1982).
4. Ketchum, R. A. Forward and inverse modeling of low-temperature thermochronometry data. *Reviews in Mineralogy and Geochemistry* **58**, 275-314 (2005).
5. Spikings, R., Crowhurst, P. V., Winkler, W. & Villagomez, D. Syn- and post accretionary cooling history of the Ecuadorian Andes constrained by their in-situ and detrital thermochronometric record. *Journal of South American Earth Sciences* **30**, 121 – 133 (2010).
6. Schoene, B., Latkoczy, C., Schaltegger, U. & Günther, D. A new method integrating high-precision U–Pb geochronology with zircon trace element analysis (U–Pb TIMS-TEA). *Geochimica et Cosmochimica Acta* **74**, 7144- 7159 (2010).

Rigorous data reduction and error propagation of high precision $^{40}\text{Ar}/^{39}\text{Ar}$ data

James Schwanethal¹, Pieter Vermeesch¹

1 London Geochronology Centre, University College London, London WC1E 6BT, United Kingdom

Recent advances in noble gas mass spectrometry, notably the development of high sensitivity multicollector instruments such as the Thermo Finnigan ARGUS and Nu Instruments Noblesse have greatly improved the precision of $^{40}\text{Ar}/^{39}\text{Ar}$ geochronology¹. As a consequence, certain commonly made simplifying assumptions for data reduction and error propagation are no longer valid. Similar technological advances in U-Pb geochronology have prompted that community to re-evaluate the error propagation routines for TIMS and LA-ICP-MS². These new insights were implemented in a computer program called ‘U-Pb_Redux’³. We have developed a similar program (‘Ar-Ar_Redux’) to put $^{40}\text{Ar}/^{39}\text{Ar}$ geochronology on an equally firm statistical footing as the U-Pb method. Specific improvements over previous data handling approaches are:

1. The program performs error propagation using the common linear Taylor Series approximation, but explicitly takes into account all the previously neglected covariance terms, resulting in more accurate (and tighter) error bounds.
2. Isotopic ratios of multicollector data are calculated by regressing the (logarithmically transformed) ratio measurements, rather than by extrapolating each mass independently and taking the ratios of the y-intercepts.
3. Isochron regression takes into account correlated errors between the X- and Y-variables.
4. Weighted mean plateau ages take into account systematic errors by using a maximum likelihood approach including full covariance terms.

Both U-Pb_Redux and Ar-Ar_Redux are written in Java and, hence, platform independent.

References

1. Mark, D. F., Barfod D., Stuart, F. M. & Imlach, J. The ARGUS multicollector noble gas mass spectrometer: Performance for $^{40}\text{Ar}/^{39}\text{Ar}$ geochronology. *Geochemistry, Geophysics, Geosystems* **10**, 10 (2009).
2. McLean, N. M., Bowring, J. F., & Bowring, S. A. An algorithm for U-Pb isotope dilution data reduction and uncertainty propagation. *Geochemistry, Geophysics, Geosystems* **12**, 6 (2011).
3. Bowring, J. F., McLean, N. M., & Bowring, S. A. Engineering cyber infrastructure for U-Pb geochronology: Tripoli and U-Pb_Redux. *Geochemistry, Geophysics, Geosystems* **12**, 6 (2011).

Zircon (U-Th)/He ages from the Pyrenees and damage dependent sensitivity to thermal processes

Raphaël Pik¹, Arnaud Vacherat², Nicolas Bellahsen², Frédéric Mouthereau², Matthias Bernet³, Yoann Denèle⁴

1 CRPG, UMR 7358 - CNRS & Univ. Lorraine, Vandoeuvre-Lès-nancy, France, rpik@crpg.cnrs-nancy.fr

2 IStEP, UMR 7193 - CNRS & UPMC, Paris, France

3 ISterre, UMR 5275, CNRS - Univ. Joseph Fourier, Grenoble, France

4 GET, UMR 5563 - CNRS & Univ. Paul Sabatier, Toulouse, France

During the last decade (U-Th)/He thermochronology experienced important developments and improvements based on the combined use of extensive age documentation on various contexts and numerous experimental data. The main advance has been achieved when it has been shown that He diffusion in apatites, and consequently specific individual closure temperature, are partly controlled by the amount of radiation damages accumulated in the grains¹. Concerning zircons, although the amount of available measured data is less important, it has been noticed² that Z-He ages could positively or negatively correlate with the amount of effective uranium (eU) of the grains (a parameter proportional to the accumulated damages). This has been recently investigated and modeled^{3,4} using new diffusion experiments performed on grains affected by a large range of alpha-dose. It has been shown that the alpha-dose is correlated to the amount of accumulated radiation damages and controls the diffusivity of helium by first inhibiting helium migration at low damage, before a threshold (2×10^{18} alpha/g), after which interconnection of damage zones drastically drives higher diffusivity at high damage. This complex behavior controlled by the production/preservation of radiation damages implies that various zircons from a single sample can be characterized by a large range of closure temperatures from about 200 °C to less than 100 °C. Because it is less common to measure Z-He than A-He ages, the amount of available data to test and validate this new model is still rather limited.

In this study we provide new Zircon Fission Track ages (ZFT) and single grain Zircon (U-Th)/He ages (Z-He) for the Bielsa and Néouvielle granites in the Pyrenees (see other data from Vacherat et al. and Boutoux et al. this volume). The time-temperature history of exhumation for the western part of the Axial Zone in the Pyrenees is particularly well suited for such an investigation given that (1) the age of granite bodies is very well known (~ 305 Ma), and (2) they have spent a large part of their Mesozoic history close to the surface favoring accumulation of radiation damages before Paleocene sedimentary and tectonic burial⁵. Up to 10 single Z-He ages per samples have been measured in order to document the larger eU range. Data exhibit a wide range of ages (Fig. 1), which is larger for the Bielsa samples than for the Néouvielle samples. For both, the maximum of age variation is mainly recorded for a narrow eU concentration window from 200 to 500 ppm, with a first steep positive gradient, and a subsequent more gentle negative one up to the youngest ages recorded for the highest eU. The total age variation for both granites range from published AFT dates for the lower bound to ages in good agreement with individual ZFT for the upper bound, indicating that Néouvielle granite has been buried deeper (or suffered higher thermal gradient) than the Bielsa one before Oligo-Miocene exhumation. Such pattern is qualitatively in pretty good agreement with the model of Guenther et al.⁴, yet it is not possible to fit the Bielsa and Néouvielle data with a t-T history constrained by independent parameters (age of granites, old exhumation period followed by Cretaceous sediment burial). Even considering the maximum alpha-dose experienced by the samples (i.e. produced by the grains since granites emplaced without any annealing), the inversion of positive to negative trends in Bielsa and Neouvielle samples is centered at about $2 - 3 \times 10^{17}$ alpha/g, significantly lower than the value used in the models^{3,4}. Preliminary Raman Spectroscopy data indicate that the total amount of damages experienced by these samples is

well correlated with this double-trend pattern, and in the range of values used for quantification of the model with experimental diffusion data.

These data from Pyrenean granites represent a good and independently constrained dataset to test the new complex models of age simulation and to optimize their calibration. They suggest in particular that the quantification, nature and preservation of damages acting for the modulation of He diffusion in zircons should be investigated and documented more extensively in the future.

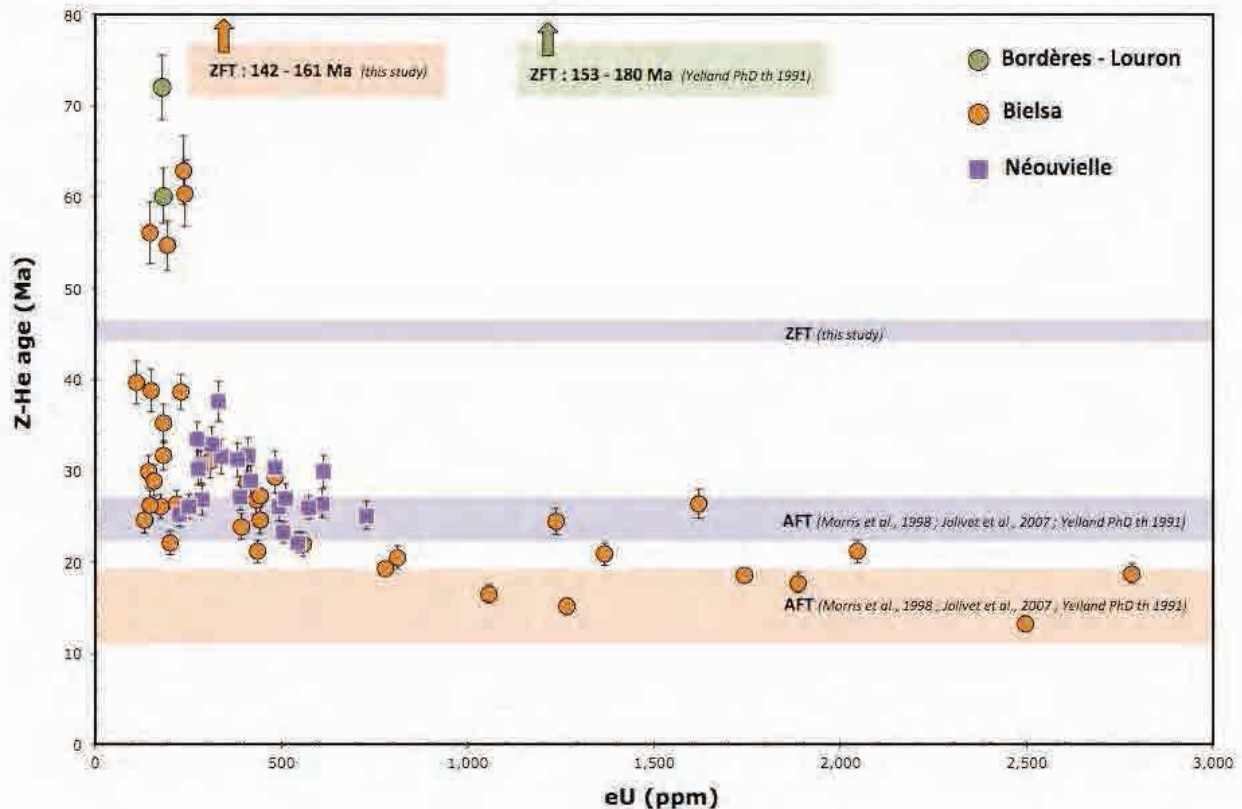


Figure 1. Correlation between single grain (U-Th)/He ages and the eU concentration for samples from the Bielsa and Néouvielle granites (Pyrenees). Fission Track ages are from this study for Bielsa and Néouvielles zircons and from literature^{5, 6, 7} for Bordere-Louron zircons and Bielsa and Neouvielle apatites.

References

1. Shuster, D. L., Flowers, R. M. & Farley, K. A. The influence of natural radiation damage on helium diffusion kinetics in apatite. *Earth Planet. Sci. Lett.* **249**, 148–161 (2006).
2. Reiners, P. W. in *Low-temperature Thermochronology: Techniques, interpretations, and applications* (eds. Reiners P. W. & Ehlers, T. A.) 151–179 (Mineralogical Society of America/Geochemical Society Reviews in Mineralogy and Geochemistry, Chantilly, Virginia, 2005).
3. Ketcham, R. A., Guenther, W. R. & Reiners, P. W. Geometric analysis of radiation damage connectivity in zircon and its implications for helium diffusion. *American Mineralogist* **98**, 350–360 (2013).
4. Guenther, W. R., Reiners, P. W., Ketcham, R. A., Nasdala, L. & Giester, G. Helium diffusion in natural zircon: radiation damage, anisotropy, and the interpretation of zircon (U-Th)/He thermochronology. *American Journal of Science* **313**, 145–198 (2013).
5. Jolivet, M., Labaume, P., Monié, P., Brunet, M., Arnaud, N. & Campani, M. Thermochronology constraints for the propagation sequence of the south Pyrenean basement thrust system (France-Spain). *Tectonics* **26** (2007).
6. Morris, R. G., Sinclair, H. D. & Yelland, A. J. Exhumation of the Pyrenean orogen: Implications for sediment discharge. *Basin Res.* **10**, 69 – 85 (1998).
7. Yelland, A. J. Thermo-tectonics of the Pyrenees and Provence from Fission Track studies. PhD thesis, University of London (1991).

Recovery of dynamic thermal histories recorded by highly damaged zircon with (U-Th)/He

Adam S. Goldsmith¹, Daniel F. Stockli¹, Richard A. Ketcham¹
¹ The University of Texas at Austin, Austin, TX, USA

Zircon (U-Th)/He (ZHe) thermochronometry is an increasingly popular technique for the interpretation of low-temperature thermal histories in a variety of geologic settings. As has also proved the case for apatite¹, however, accounting for the effect of radiation damage on helium diffusion kinetics is crucial for quantitative interpretation of ZHe data. Over geologic time, the crystal lattice of zircon becomes increasingly disordered due to energy released from the α -decay of U and Th, and the spontaneous fission of ²³⁸U. With the growing number of ZHe analyses performed worldwide, many researchers have noted negative correlations between apparent ZHe age and effective uranium concentration ($eU = [U] + 0.23[Th]$, in this context as a proxy for radiation dose) in the form of variations of up to hundreds of millions of years from different zircons separated from the same rock. Furthermore, in some cases these correlations appear to be systematic and to record actual thermal histories, in a similar but opposite fashion to the positive date-eU correlations observed for apatite (U-Th)/He thermochronometry¹. These data demonstrate that, in settings in which zircon populations have accumulated relatively high and/or highly variable radiation doses, ZHe thermochronometry is capable of recording thermal histories continuously over a range of temperatures and/or multiple thermal events. Unless the relationship between radiation dose and diffusion kinetics is quantitatively known, however, it is impossible to extract thermal history information from these data. It has long been recognized that radiation doses exceeding $\sim 2 - 4 \times 10^{18}$ α -decays/g cause sufficient damage to the crystalline structure to increase He diffusivity beyond the point at which the system is a reliable thermochronometer^{2,3}, however a fully quantitative understanding of the potential effects of lower radiation doses has remained elusive.

The model by Guenther *et al.*³ was intended to address this issue and others; these results, however, have only been tested in a limited number of settings. This study seeks to examine more closely the onset and progression of the increase in helium diffusivity associated with high radiation doses, by the characterization of a large number of zircons from different settings which display negative date-eU correlations with a multitude of techniques. To estimate α -radiation dose, we use Raman spectroscopy, which is a well-demonstrated non-destructive technique of measuring disorder in the crystal lattice⁴. To detect and account for heterogeneous U and Th distributions, we use laser ablation ICP-MS pit profiling over the outer ~ 20 μm of each grain. Finally, to determine diffusion kinetics we perform step-heated, fractional loss diffusion experiments on grains selected based on size and relative consistency of parent nuclide distribution down the laser ablation pit. Analyses are performed on zircons from assorted crystalline basement rocks of the Sinai Peninsula, Egypt and from intrusive rocks along a transect from the Hall Peninsula of Baffin Island, Nunavut, Canada. Analyses from both settings yield differences in apparent ZHe age over hundreds of millions of years from single rock samples, and with a clear negative log-linear relationship to eU. Results from diffusion experiments so far have shown a positive correlation between diffusivity and Raman-estimated radiation dose, with doses at least one order of magnitude lower than previously associated with significant diffusivity increases (Fig 1)³. Furthermore we observe closure temperatures as low as 116 °C ($dT/dt = 10$ °C/m.y.), as well as significant changes in diffusive behavior occurring at temperatures 540 - 560 °C including decreases in D_0/a^2 over two orders of magnitude. We believe that the results from these and future experiments will be instrumental in quantitatively understanding the relationship between radiation damage and helium diffusion kinetics in zircon, and in improving our capability to extract complex thermal histories from the zircon (U-Th)/He thermochronometer at high radiation doses.

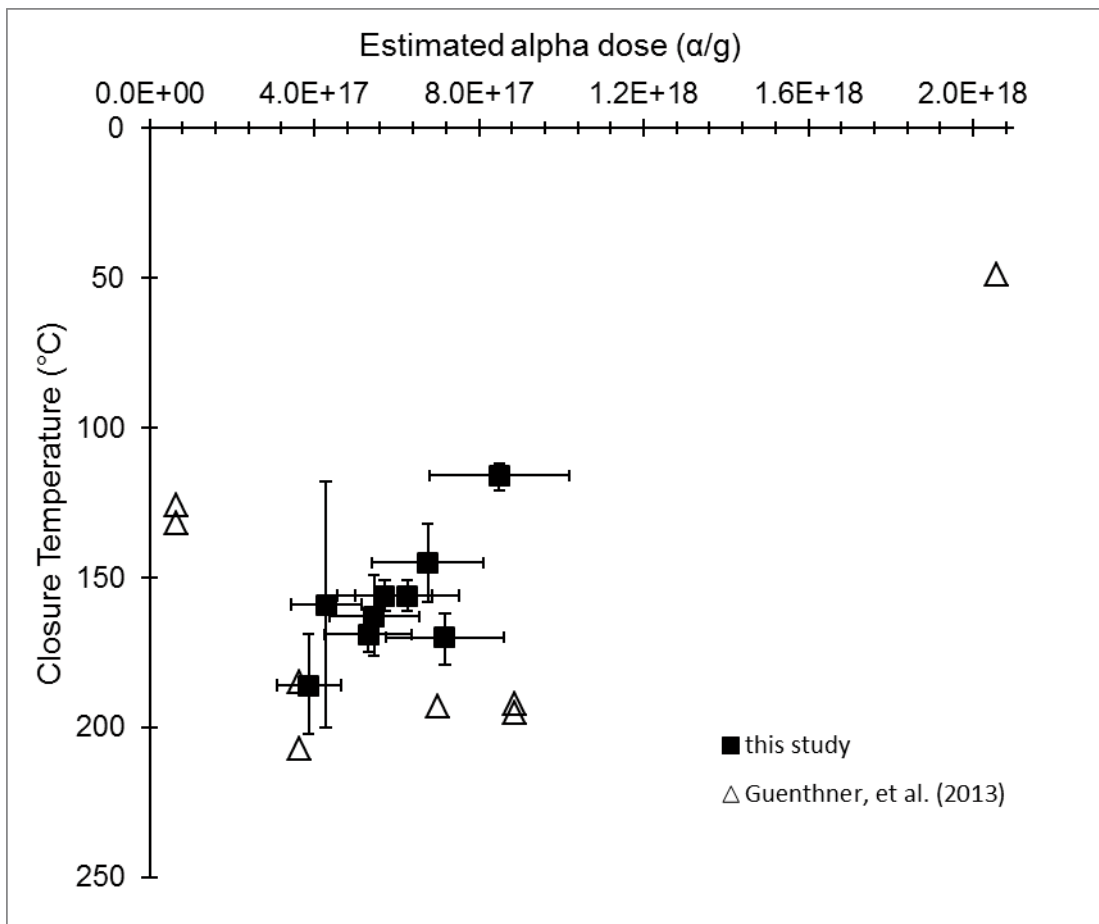


Figure 1. Contrasting results of diffusion experiments from this study, and those of Guenthner et al³. Radiation dose estimates are calculated from Raman spectroscopy, and closure temperatures are calculated for $dT/dt = 10$ °C/m.y.

References

1. Flowers, R. M., Ketcham, R. A., Shuster, D. L. & Farley, K. A. Apatite (U-Th)/He thermochronometry using a radiation damage accumulation and annealing model. *Geochimica et Cosmochimica Acta* **73**, 2347-2365 (2009).
2. Reiners, P. W. in *Low-temperature Thermochronology: Techniques, Interpretations, and Applications* (eds. Reiners, P. W. & Ehlers, T. A.) 151-179 (Mineralogical Society of America/Geochemical Society Reviews in Mineralogy and Geochemistry, Chantilly, Virginia, 2005).
3. Guenther, W. R., Reiners, P. W., Ketcham, R.A., Nasdala, L. & Geister, G. Helium diffusion in natural zircon: radiation damage, anisotropy, and the interpretation of zircon (U-Th)/He thermochronology. *American Journal of Science* **313**, 145-198 (2013).
3. Nasdala, L., Reiners, P. W., Garver, J. I., Kennedy, A. K., Stern, R. A., Balan, E. & Wirth, R. Incomplete retention of radiation damage in zircon from Sri Lanka. *American Mineralogist* **89**, 219-231 (2004).

Effect of U-Th-rich coating on apatite (U-Th)/He dating: an example from the thermochronology of the Carpathian foreland in Ukraine

Benedetta Andreucci^{1*}, Massimiliano Zattin¹, Peter Reiners², Fabrizio Nestola¹

1 Department of Geosciences, University of Padua, Via Gradenigo, 6, Padova 35131 Italy

2 Department of Geosciences, University of Arizona, Tucson, AZ 85721, USA

** Corresponding author: benedetta.andreucci@unipd.it; +39 339 4051435*

Helium implantation from U and Th rich phases bounding apatite grains is a proven source of imprecision in the (U-Th)/He dating, and can be an important cause of data dispersion. Chemical or mechanical abrasion of apatite grains before analysis has been demonstrated to significantly decrease the impact of He implantation from external sources on AHe dates (e.g.¹⁻³). Nonetheless in most cases apatite grains are not big enough to allow this procedure to be undertaken and routinely used in laboratories. In fact, data dispersion induced by He implantation from external sources cannot generally be avoided and a method to identify and approach datasets affected by this problem is necessary.

We present a case study from the Podolia region of the Carpathian foreland in Ukraine. This region underwent a major uplift phase between the Devonian and the Middle Jurassic, represented by a regional unconformity in the stratigraphic record.

Coupled AFT and AHe analyses were performed on good quality grains from four samples of Silurian bentonites. Considering that previous work on these deposits reports post-depositional burial temperatures well higher than the AHe PRZ, unreasonably dispersed AHe dates were obtained (500-170 Ma), with some dates even older than the stratigraphic (i.e. volcanic) dates of the samples (ca. 420 Ma). On the other hand, AFT dates are reproducible (dispersion within the 20% of the mean), younger than most of the AHe dates and compatible with the inferred age of the regional uplift (central ages: 215-170 Ma).

Anomalously old AHe data generally occur in crystals with low Th concentrations (and possibly with low eU, [U] and Th/U), and in two of four cases a good negative correlation between age and crystal size is observed.

A secondary, opaque brown phase is commonly observed on many of the apatite grains from these samples. We hypothesize that the observed AHe age dispersion was mostly induced by He implantation from external U- and Th-bearing phases bounding or coating the apatite grains. Implantation would generally produce larger dispersion for smaller and lower-eU grains, which could explain the inverse age-eU and age-size correlations observed.

To test this hypothesis we performed mineralogical and chemical analyses (RAMAN spectroscopy, SEM microanalysis, single crystal XRD) on the opaque phases and alteration material present on the mineral separates, with a particular focus on the material coating the apatite grains. The results of these analyses indicate that the secondary phases pervading the sample mainly consist of a mixture of goethite and quartz, with minor rutile and hematite.

As goethite and hematite can contain significant amounts of U and Th, we consider He implantation as a likely cause for data dispersion in this dataset.

Thus, assuming a major effect of He implantation, we used for geological interpretation the young AHe dates, belonging to Th-U rich and large grains. These AHe dates are systematically a few Ma younger than the AFT central dates on the same samples, this supporting the guess of these being actual cooling ages and confirming the worthwhileness of this approach. Coupled AFT and selected AHe dates were used to describe cooling histories, being compatible with relatively slow cooling (1-5°C/Myr) occurred between the Triassic and the Middle Jurassic.

The contribution of this work on the He implantation issue can be summarized as follows:

- the effect of He implantation rapidly decreases with the increase of U and Th contents and crystal size; this implies that (i) grain size becomes the most important feature for crystal selection for AHe analyses of altered rocks; (ii) in sedimentary rocks, where U and Th contents can significantly vary from grain to grain, their relationship with age is a valuable test of He implantation impact on dates; (iii) negative correlation between age and the listed parameters, in presence of altered rocks, can arise from an He implantation effect and (iv) once the effectiveness of He implantation has been demonstrated for a given sample/dataset, the biggest, youngest and U-Th richest grains may be considered the most reliable and suitable for geological interpretation;
- coupling AFT/AHe analyses is strongly advised to cross check the data: inverted AFT-AHe dates, in presence of altered rocks and provided reliable AFT data (good samples, robust statistics), very likely depend on anomalously old AHe dates due to He implantation;
- if hypothesized on the basis of alteration, high data dispersion, AFT-AHe inversion, correlation between age and $R_s/Th/U$, the presence of U-Th-rich material coating the apatite grains is generally easy to verify (if pervading the whole sample) with SEM microanalysis and/or FT density, provided some of the coating remains on the grains after mineral separation.

Thus the approach we used to deal with the He implantation effect that could not be avoided was: i) check the data dispersion and its dependency on grain size, [U], [Th]; (ii) verify the actual presence of material rich in U and/or Th (iii) use for geologic interpretation the youngest, biggest, U-Th richer grains.

We suggest that the same approach may be used for other datasets, and that, provided good description of shape and mineralogy of the opaque phases, He dating may be attempted to better quantify their U and Th content and possibly their formation age.

References

1. Orme, D. A. & Reiners, P. W. Effects of External Parent Nuclides on Apatite Helium Dates: Sources and Solutions. Proceedings of the Thermo 2010 Congress. Glasgow, p.140 (2010).
2. Reiners, P. W. Fe-oxides as (U-Th)/He dating friend and foe. Proceedings of the Thermo 2010 Congress. Glasgow, p. 54 (2010).
3. Spiegel, C., Kohn, B., Belton, D., Berner, Z. & Gleadow, A. Apatite (U-Th-Sm)/He thermochronology of rapidly cooled samples: the effect of He implantation. *Earth and Planetary Science Letters* **285**, 105-114 (2009).

Investigating the influence of pore water and sedimentary transport on apatite (U-Th)/He thermochronology

Examples from Tethyan Himalaya

Mohammad S. Sohi¹, Ruben Rosenkranz¹, Cornelia Spiegel¹

1 Universität Bremen, FB5 – Geowissenschaften, 28344 Bremen, Germany

In the field of the Apatite (U-Th)/He thermochronology, there are still some methodological uncertainties. As a routine, apatite (U-Th)/He data are corrected according to grain size and morphology to adjust for He loss from alpha ejection at the grain margins (i.e. alpha correction)¹. Sometimes, however, He implantation from the surrounding may lead to erroneous dates, and attention should be paid applying the alpha correction². While previous study focused on the implantation resulting from U-Th-rich minerals in the vicinity of apatite, this study focuses on a potential effect resulting from He-rich pore water.

Another problem, especially for detrital AHe thermochronology, when applying the alpha correction, is that the He depleted outer part of the grain may be mechanically abraded during sediment transport. In this case, alpha-ejection correction would lead to overcorrection and thus to He dates which are too old. There is no laboratory data and sufficient age data to evaluate the significance of these phenomena³.

To quantify and probably overcome these issues, several areas around the Himalaya have been selected as natural laboratories. A sampling design has been developed specifically on our needs. We identified different lithological units, in order to evaluate whether the expected differences in AHe ages may be correlated to the composition of the pore waters. In addition various sedimentary basins will be considered, to observe how the pore water composition is influenced by the source rock on one hand, and on the other hand if the long term residence in a sedimentary basin influences the AHe age.

Furthermore, we address the question whether abrasion and sediment transport affects the (U-Th)/He system. To do so, we will date river sands from Himalayan source area with relatively well- defined and suitable age patterns. The general idea is to trace the signal of the apatites along the upper Kali Gandaki valley, to see if, and then how, the natural abrasion would lead to an age bias of the apatites we analyze. In a second step, we will mechanically abrade apatites of the same samples using a Krogh-type cell in the laboratory. For grains which are unzoned and rapidly cooled, laboratory abrasion should do away with the need of applying alpha correction. This approach would help circumnavigating the uncertainties on how much alpha correction is appropriate for grains partially or fully abraded during sediment transport.

In addition to the methodological aspects, the study will also provide constraints on the past exhumation of the Tethyan Himalaya. Sampling the upper Kali Gandaki valley through the stratigraphic section can give us information on differences of source rock exhumation through time. The erosion rate of that area is now pretty slow, due to the arid climate. We know, however, due to palynological studies that the climate was more humid in the past, potentially leading to faster erosion⁴. Within these Tethyan strata in fact, rates appear somewhat slower than along the High Himalaya likely due to tectonic causes (slip on the South Tibetan Detachment or a less

steep Main Himalayan Thrust beneath southern Tibet) or in response to the drier climate⁵. A better understanding of changes in rates will likely emerge from applying low-temperature thermochronometers to sediments as well as to age-elevation profiles from the source areas, leading to new insights into the exhumation history of the Tethyan Himalaya.

References

1. Farley, K., Wolf, R. & Silver, L. The effects of long alpha-stopping distances on (U-Th)/He ages. *Geochimica et Cosmochimica Acta* **60**, 4223–4229 (1996).
2. Spiegel, C., Kohn, B., Belton, D., Berner, Z. & Gleadow, A. Apatite (U–Th–Sm)/He thermochronology of rapidly cooled samples: the effect of He implantation. *Earth and Planetary Science Letters* **285**, 105–114 (2009).
3. Farley, K. A. (U-Th)/He dating: Techniques, calibrations, and applications. *Reviews in Mineralogy and Geochemistry* **47**, 819–844 (2002).
4. Garzione, C. N., DeCelles, P. G., Hodkinson, D. G., Ojha, T. P. & Upreti, B. N. East-west extension and Miocene environmental change in the southern Tibetan plateau: Thakkhola graben, central Nepal. *Geological Society of America Bulletin* **115**, 3–20 (2003).
5. Blythe, A., Burbank, D., Carter, A., Schmidt, K. & Putkonen, J. Plio-Quaternary exhumation history of the central Nepalese Himalaya: 1. Apatite and zircon fission track and apatite [U-Th]/He analyses. *Tectonics* **26**, (2007).

Little Devil's Postpile Revisited: Behavior of Multiple Thermochronometers in a Contact Aureole

Jennifer L. Schmidt¹, Peter K. Zeitler¹, Richard A. Ketcham², Peter W. Reiners³, David L. Shuster^{4,5}, Leif Karlstrom⁶

1 Dept. Earth and Environmental Science, Lehigh University, USA

2 Jackson School of Earth Sciences, University of Texas, Austin, USA

3 Dept. Geosciences, University of Arizona, USA

4 Dept. Earth and Planetary Science, UC Berkeley, USA

5 Berkeley Geochronology Center, USA

6 Dept. Geophysics, Stanford University, USA

The Little Devil's Postpile intrusion in Yosemite National Park is an ideal location for testing validity in extrapolation of laboratory-derived kinetic parameters to a natural setting and the comparative response of multiple thermochronometers to a sharp thermal pulse. This ~100 m diameter basalt body intruded at ~8 Ma into Sierran granite with a crystallization age of ~89 Ma. The intrusion was the subject of Calk and Naeser's classic study demonstrating that fission-track mineral ages display a quantifiable sensitivity to temperature¹. We report our efforts to replicate and expand this study by exploring the behavior of numerous key thermochronometers in the intrusion's thermal aureole. We collected two transects orthogonal to the intrusion contact. The granitic country-rock contains multiple phases amenable to thermochronology, and we present data for the apatite, zircon, and magnetite (U-Th)/He, apatite and zircon ⁴He/³He, K-feldspar, plagioclase, and biotite ⁴⁰Ar/³⁹Ar, and apatite and zircon fission-track systems.

The apatite and zircon (U-Th)/He and apatite fission-track systems display expected age-distance relationships predicted for a short-duration thermal pulse due to the intrusion. Zircon (U-Th)/He ages are completely reset within 2.6 m of the intrusion and are partially reset out to 16 m from the intrusion. At distal locations > 30 m, zircon ages average ~76 Ma. Apatite (U-Th)/He ages are completely reset to within 6 m of the contact, partially reset out to 16 m, and reach background values of 55-60 Ma at greater distances. At expected locations, apatite ⁴He/³He spectra have forms consistent with diffusive loss of previously-accumulated ⁴He during reheating; the initial step ages of these partially-reset samples constrain the timing of the intrusion. In contrast, both the proximal and distal samples have ⁴He/³He spectra consistent with complete and zero diffusive loss of ⁴He, respectively, due to the intrusion. Apatite fission-track age results are broadly consistent with the AHe data, and are completely reset within 9 m of the contact and at distal locations approach ~70 Ma. However, AFT age+length data do not produce thermal histories during HeFTy inversion modeling that are also consistent with the AHe ages, indicating potential disagreement among their respective kinetic models or calibrations.

Biotite ⁴⁰Ar/³⁹Ar ages as close as 4.5 m from the contact are unaffected by the intrusion and have an average age of 85.4 Ma; these results are consistent with previously reported Ar diffusion kinetics. K-feldspar and plagioclase ⁴⁰Ar/³⁹Ar samples from more proximal locations have age spectra indicative of small degrees of diffusive loss. Maximum ages of analyzed K-feldspars are ~80 Ma. Mineral-age and feldspar MDD data from distal locations indicate rapid post-crystallization cooling of the granitic country-rock, followed by more gradual cooling to low temperature until emplacement of the basalt intrusion. This gradual cooling is consistent with the AHe ages observed in distal samples.

The data also have second-order features that we are still examining. We find a correlation between eU (effective uranium) and (U-Th)/He age only in partially reset apatites, which is consistent with the predicted effects of radiation damage on ⁴He retentivity in apatite^{2,3}. Several single-grain anomalies in these correlations are consistent with the additional influence of grain size. Samples immediately adjacent to the intrusion have a range of ages between 8 and 9 Ma. AHe and AFT ages at one point along one

transect are anomalously young where stable-isotope data suggest an anomaly that may indicate the presence of fluid flow, although field observations show no obvious evidence of this.

To constrain the subsurface shape of the intrusion, we collected a NW-SE oriented magnetometer transect across the intrusion. There is a negative total-field anomaly associated with the intrusion, and two-dimensional modeling of the anomaly suggests that the intrusion amounts to a ~30 m sheet that is dipping towards the northwest. Simple thermal models using an analytical 3D code confirms that the observed ages are best fit if the vertical extent of the intrusion is limited to 30 meters, consistent with the magnetometer survey. The modeling constrains the thermal pulse of the intrusion to a duration of ~20 years, with temperatures reaching close to background by ~150 years. The dipping intrusion geometry revealed by field and magnetic observations preclude a fully accurate 3D model. We will discuss a radially-symmetrical 2.5D model that incorporates latent heat and temperature-dependent heat capacity and conductivity⁴. Using an emplacement temperature constrained by basalt analyses, we will use this model to provide a framework for comparing thermochronological results.

Despite these complexities, data from Little Devil's Postpile confirm the expected relative behavior of the thermochronometric systems in most common use and to at least first order, shows that their kinetic calibrations are accurate with respect to the heat input associated with the intrusion.

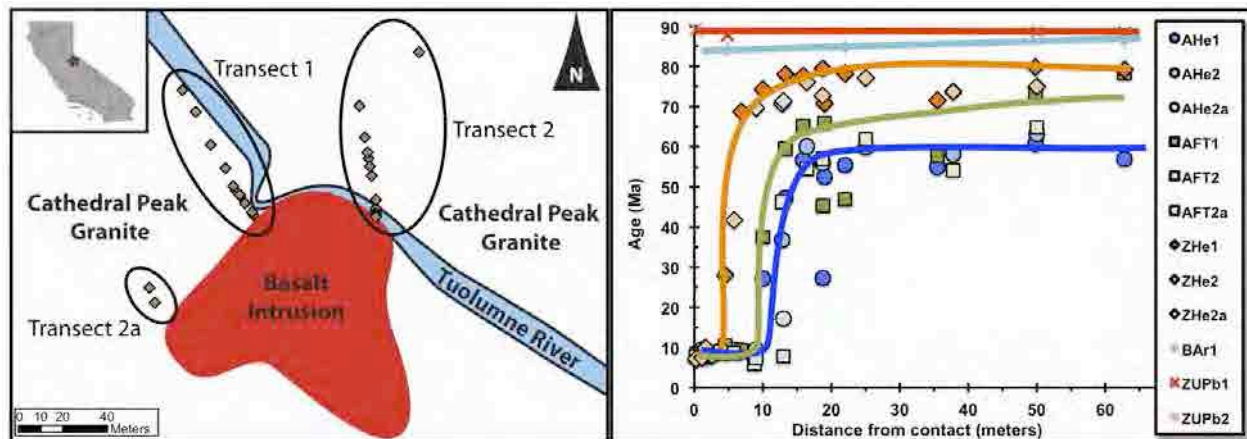


Figure 1. Transect locations (left panel) and ages for apatite and zircon (U-Th)/He, biotite $^{40}\text{Ar}/^{39}\text{Ar}$, apatite fission-track, and zircon U-Pb systems displaying expected age-distance relationship (right panel). Overall trends through the data are drawn as solid lines. Legend indicates thermochronometer system and transect number.

References

1. Calk, L. C. & Naeser, C. W. The Thermal Effect of a Basalt Intrusion on Fission Tracks in Quartz Monzonite. *Journal of Geology* **81**, 189-198 (1973).
2. Shuster, D. L., Flowers, R. M. & Farley, K. A. The Influence of Natural Radiation Damage on Helium Diffusion Kinetics in Apatite. *Earth and Planetary Science Letters* **249**, 148-161 (2006).
3. Flowers, R. M., Ketcham, R. A., Shuster, D. L. & Farley, K. A. Apatite (U-Th)/He Thermochronometry Using a Radiation Damage Accumulation and Annealing Model. *Geochimica et Cosmochimica Acta* **73**, 2347-2365 (2009).
4. Nabelek, P.I., Hofmeister, A. M. & Whittington, A. G. The influence of temperature-dependent thermal diffusivity on the conductive cooling rates of plutons and temperature-time paths in contact aureoles. *Earth and Planetary Science Letters* **318-318**, 157-164 (2012).

The 61Ma Tardree Rhyolite (Northern Ireland) as a new neutron monitor standard, a discussion

Morgan Ganerød¹, Camilla Maya Wilkinson¹

1 Geological Survey of Norway, Leiv Eirikssonsvei 39, 7040 Trondheim, Norway

The Geological Time Scale (GTS) lies at the very core of Earth Sciences. Accurate and precise age determinations are crucial to unraveling past causes and effects, and help us to understand the driving forces that cause dramatic events such as volcanic eruptions climate changes, continental rifting episodes, Large Igneous Provinces, mass extinctions, and development of oil and gas. Other scientific disciplines, such as evolutionary biology and climate science, strongly depend on accurate timing of geological processes to provide a baseline for their investigations. Dating geological events and structures represent the core of our understanding of how our planet was formed and evolved. In the last decades, a grand leap forward has been acquired by perfecting geochronological tools. However, high resolution geochronology has been hampered partly by the current precision, and inconsistencies between different geochronometers.

The $^{40}\text{Ar}/^{39}\text{Ar}$ method is a relative geochronometer whose accuracy depends on accurate and precise knowledge of the age of the monitors used. It is based on the conventional $^{40}\text{K}/^{40}\text{Ar}$ method where the ^{40}K is measured indirectly through ^{39}Ar , which is derived from ^{39}K (bombardment of fast neutrons in a nuclear reactor). To circumvent determining the absolute dose of fast neutrons the sample has received, the unknowns are irradiated together with a natural standard sample of accurately and precisely known age. There are several fluence monitors in use (e.g. Fish Canyon sanidine, Taylor Creek sanidine, and Adler Creek sanidine). Ideally, the standard should be of similar age and have a K/Ca ratio to that of the unknown, reducing the ratios to be compared. Most sanidine standards are so-called intercalibrated secondary standards (or higher order), whose ages are calibrated against another standard, preferably a primary standard with an age obtained by the K/Ar method or from an independent method. However, by using $^{40}\text{Ar}/^{39}\text{Ar}$ geochronology, accurate and precise age determinations have been hampered by the lack of consensus in what the real age of monitors are and reducing systematic errors. Reducing the systematic errors in $^{40}\text{Ar}/^{39}\text{Ar}$ geochronology, includes revision of the ^{40}K decay constant, and especially, the age of the widely used Fish Canyon sanidine (FCs), which has been of a symbolic issue. Even though the FCs has proven to have exceptionally high intra-laboratory reproducibility¹, inter-laboratory results, using many approaches, give ages of FCs that vary by several percent¹⁻⁶.

To ultimately bridge different geochronometers together (e.g. $^{40}\text{Ar}/^{39}\text{Ar}$ and U/Pb), there is a need for a database of accurate and precisely dated units with a very simple thermal history and giving the same age. This study aims to contribute by adding a much-needed knowledge on an Early Paleocene tie point from the Tardree Rhyolite Complex (TRC) in Northern Ireland. Initial ^{238}U - ^{206}Pb and $^{40}\text{Ar}/^{39}\text{Ar}$ data from the TRC⁴ indicate simultaneously closure for both systems and a simple thermal history. Hence, TRC will serve as an optimal U/Pb- $^{40}\text{Ar}/^{39}\text{Ar}$ pair, which will be used to 1) calibrate radioisotopic clocks (U-Pb, $^{40}\text{Ar}/^{39}\text{Ar}$ methods), and 2) function as a new 61 Ma standard $^{40}\text{Ar}/^{39}\text{Ar}$ fluence monitor for the community in general.

References

1. Renne, P. R., Swisher, C. C., Deino, A. L., Karner, D. B., Owens, T. L. & DePaolo, D. J. Intercalibration of standards, absolute ages and uncertainties in $^{40}\text{Ar}/^{39}\text{Ar}$ dating. *Chem. Geol.* **145**, 117 (1998).
2. Daze, A., Lee, J. K. W. & Villeneuve, M. An intercalibration study of the Fish Canyon sanidine and biotite Ar-40/Ar-39 standards and some comments on the age of the Fish Canyon Tuff. *Chem. Geol.* **199**, 111-127 (2003).
3. Renne, P. R., Mundil, R., Balco, G., Min, K. W. & Ludwig, K. R. Joint determination of K-40 decay constants and Ar-40*/K-40 for the Fish Canyon sanidine standard, and improved accuracy for Ar-40/Ar-39 geochronology. *Geochimica Cosmochimica Acta* **74**, 5349-5367 (2010).
4. Ganerød, M., Chew, D. M., Smethurst, M. A., Troll, V. R., Corfu, F., Maede, F. & Prestvik, T. Geochronology of the Tardree Rhyolite Complex, Northern Ireland: Implications for zircon fission track studies, the North Atlantic Igneous Province and the age of the Fish Canyon sanidine standard. *Chem. Geol.* **286**, 222-228 (2011).
5. Kuiper, K. F., Demo, A., Hilgen, F. J., Krijgsman, W., Renne, P. R. & Wijbrans, J. R. Synchronizing rock clocks of Earth history. *Science* **320**, 500-504 (2008).
6. Channell, J. E. T., Hodell, D. A., Singer, B. S. & Xuan, C. Reconciling astrochronological and (40)Ar/(39)Ar ages for the Matuyama-Brunhes boundary and late Matuyama Chron. *Geochem Geophys Geosy.* **11** (2010).

Can I calculate an average at all? - a method for bimodality test of age distributions with low numbers of observations

István Dunkl¹, Raimon Tolosana-Delgado², Hilmar von Eynatten¹
1 Geoscience Center, University of Göttingen, Germany
2 Helmholtz Institute Freiberg for Resource Technology, Germany

The statistical treatment of individual single-grain ages is a key issue in detrital geochronology. Calculating an average and expressing the usual statistical parameters assuming unimodal distribution can be done only for a part of detrital samples. The identification of two or more subpopulations (=age components) and description of the entire data set by the parameters of each subpopulation is necessary in case of complex distributions. But which distribution is complex? This question is crucial at the interpretation of the results and especially complicated, because of the number of data is typically much lower than it is usually required to obtain sufficient statistical significance. The geochronologists got frequently critics from statisticians that the number of observations should be higher. However, fulfilling this theoretically correct request has practical limits (available material, analytical costs, time, manpower) that call for pragmatic solutions.

There are several algorithms and computer programs available for the identification of age components from complex distributions, e.g., (1) to (5). In this contribution we concentrate on the decision of unimodal vs. bimodal distribution, and offer a computer program that presents graphically the probability of bimodality under different conditions.

In case of low number of data the observed clustering may be the result of random grouping, thus we should use statistical criteria that considers (i) the number of data, (ii) the distance between the means of the assumed/identified subpopulations, relative to one of the standard deviations of the subpopulations considered, (iii) the relative spread of each subpopulation (i.e., the ratio of the two standard deviations), and (iv) the weight ratio of the subpopulations (i.e. the ratio of the sizes of the two subpopulations). We performed a systematic modeling to identify the probability of detecting bimodality when the above mentioned four conditions are varied. The results are plotted on different projection plains; Figure 1 presents two examples.

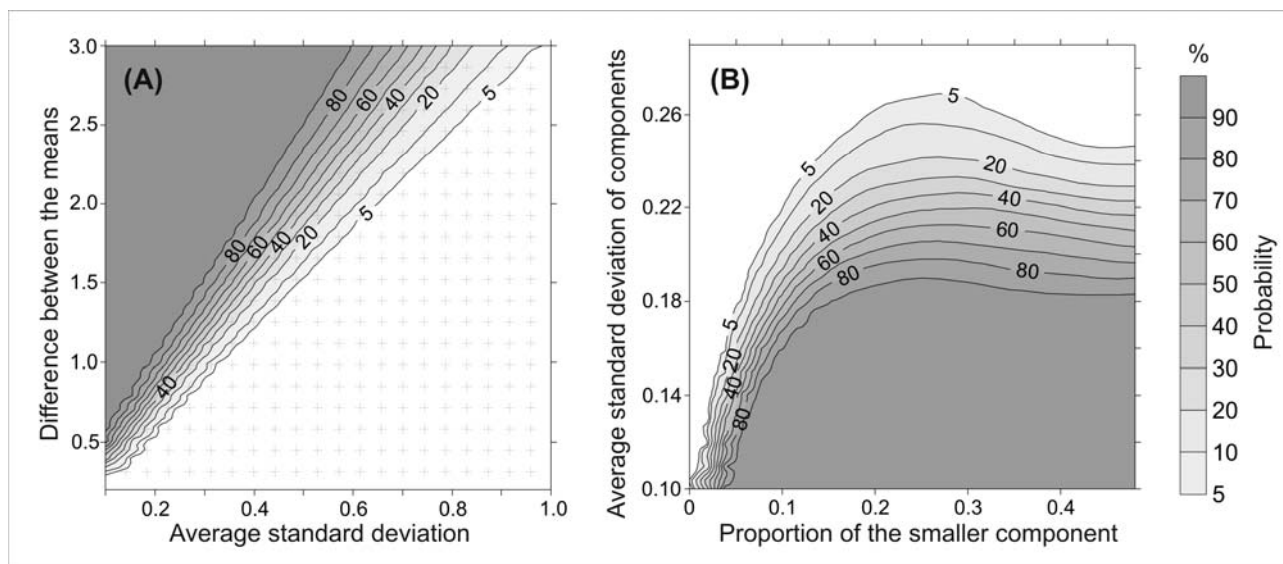


Figure 1. Probability of detecting bimodality calculated for some of the conditions (darker gray indicates higher probabilities), as estimated by the bimodality coefficient method. The contour lines are computed by interpolating a rough data grid of 20x20 elements (included in (A)). Each element

of the grid expresses the probability of bimodality and is based on 10,000 randomly generated data that is composed of two Gaussian distributions according to the variables and the fixed conditions.
(A) Fix: number of observations = 50, proportion of the two components = 1:1; Variables: standard deviation, difference between the means.
(B) Fix: number of observations = 100, difference between the means = 0.8; Variables: proportion of the two components, standard deviation.

References

1. Sambridge, M.S. and Compston, W. Mixture modeling of multi-component data sets with application to ion-probe zircon ages. *Earth Planet. Sci. Lett.* **128**, 373-390 (1994).
2. Ludwig, K.R. Isoplot - A Geochronological Toolkit for Microsoft Excel. *Berkeley Geochronology Center Special Publication No. 4* (2003).
3. Brandon, M.T. Decomposition of fission-track grain-age distribution. *Am. J. Sci.* **292**, 535-564 (1992).
4. Dunkl, I. & Székely, B. Component analysis with visualization of fitting - PopShare, a Windows program for data analysis. Goldschmidt conference abstracts. *Geochim. Cosmochim. Acta* **66**(15A), 201 (2002).
5. Vermeesch, P. On the visualisation of detrital age distributions. *Chemical Geology* **312-313**, 190-194 (2012).

Thermal history modeling: HeFTy vs. QTQt

Pieter Vermeesch¹, Yuntao Tian¹

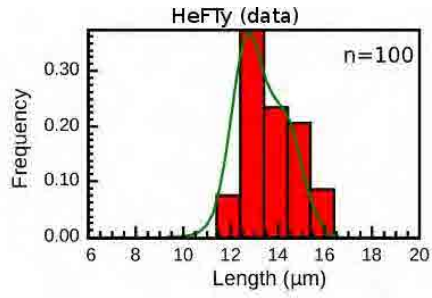
¹ London Geochronology Centre, University College London, United Kingdom

HeFTy is a popular thermal history modeling program which is named after a brand of thrash bags as a reminder of the ‘garbage in, garbage out’ principle. QTQt is an alternative program whose name refers to its ability to extract visually appealing (‘cute’) time-temperature paths from complex thermochronological datasets. Both codes consist of ‘forward’ and ‘inverse’ modeling functionalities. The ‘forward model’ allows the user to predict the expected data distribution for any given thermal history. The ‘inverse model’ finds the thermal history that best matches some input data. HeFTy and QTQt are based on the same physical principles and their forward modeling functionalities are therefore nearly identical. In contrast, their inverse modeling algorithms are fundamentally different, with important consequences. HeFTy uses a heuristic ‘Frequentist’ approach, in which formalised statistical hypothesis tests assess the goodness-of-fit between the input data and the thermal model predictions. QTQt uses a Bayesian ‘Markov Chain Monte Carlo’ (MCMC) algorithm, in which a random walk through model space results in an assemblage of ‘most likely’ thermal histories. In principle, the main advantage of the Frequentist approach is that it contains a built-in quality control mechanism which detects bad data (‘garbage’) and protects the novice user against applying inappropriate models. In practice, however, this quality-control mechanism does not work for small or imprecise datasets due to an undesirable sensitivity of the Frequentist algorithm to sample size, which causes HeFTy to ‘break’ when datasets are sufficiently large or precise [Figure 1(i-ii)]. QTQt does not suffer from this problem, as its performance improves with increasing sample size in the form of tighter credibility intervals [Figure 1(iii)]. However, the robustness of the MCMC approach also carries a risk, as QTQt will accept physically impossible datasets and come up with ‘best fitting’ thermal histories for them [Figure 1(iv)]. This can be dangerous in the hands of novice users. In conclusion, the name ‘HeFTy’ would have been more appropriate for QTQt, and vice versa.

Figure 1 (next page). (i)-(ii) – data (left column) and inverse model solutions (right column) produced by HeFTy¹ (v1.8.2) for Tibetan granite sample KL29 (GPS: 33.87N, 95.33E). ‘Bounding boxes’ (blue) were used to reduce the model space and speed up the inverse modeling. (i) – red and green time-temperature paths mark ‘good’ and ‘acceptable’ fits to the data, corresponding to *p*-values of 0.5 and 0.05, respectively. (ii) – as the number of track length measurements (*n*) increases, *p*-values decrease and HeFTy struggles to find acceptable solutions; eventually, when *n*=821, the program ‘breaks’. (iii) – in contrast, QTQt² (v4.5) has no trouble fitting the large dataset; BUT (iv) – neither does QTQt complain when a physically impossible dataset with short fission tracks and identical AFT and AHe ages is fed into it.

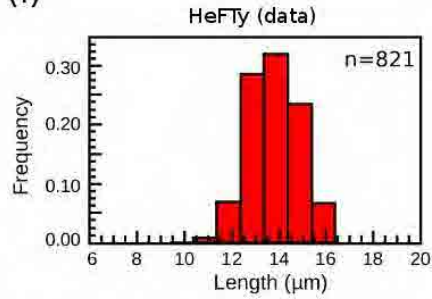
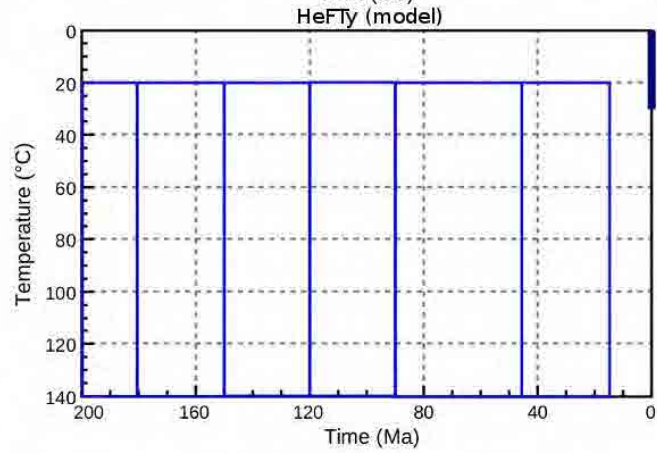
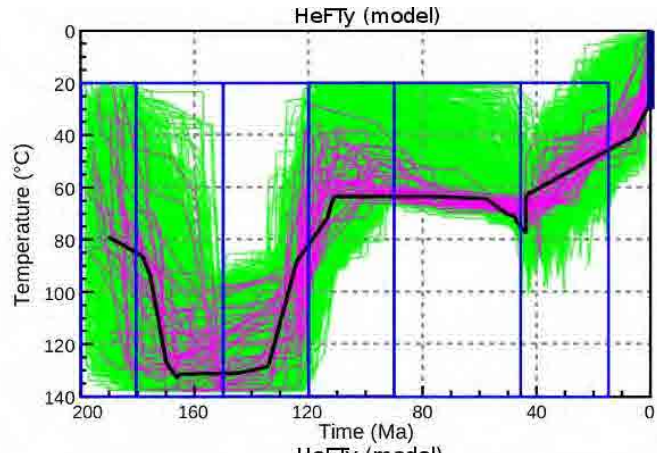
References

1. Ketcham, R.A. Forward and inverse modeling of low-temperature thermochronometry data. *Reviews in Mineralogy and Geochemistry*, **58**, 275–314 (2005).
2. Gallagher, K. Transdimensional inverse thermal history modeling for quantitative thermochronology. *Journal of Geophysical Research: Solid Earth* (1978–2012), **117** (2012).



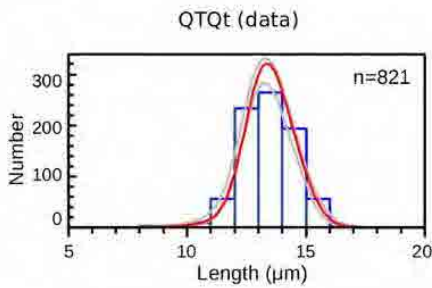
	MTL	AFT age	AHe age
Measured	13.4 ± 1.0	102 ± 7	55 ± 5
Modelled	13.3 ± 1.1	102	59

(i)



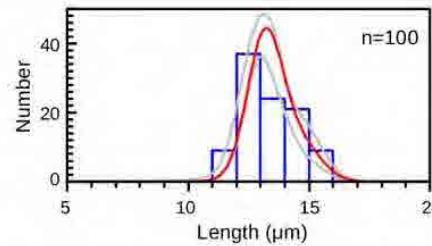
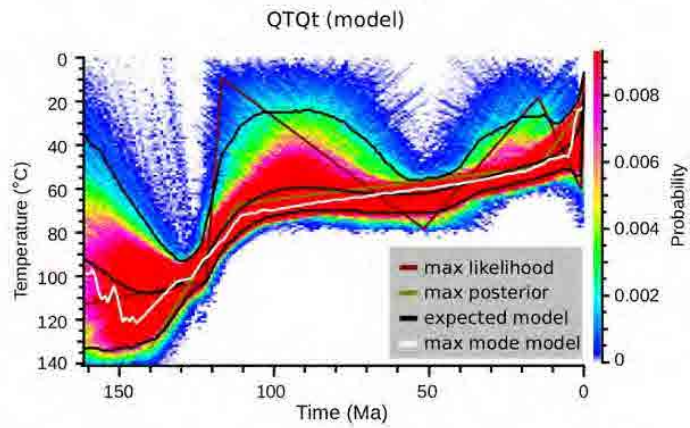
	MTL	AFT age	AHe age
Measured	13.4 ± 1.0	102 ± 7	55 ± 5
Modelled	-	-	-

(ii)



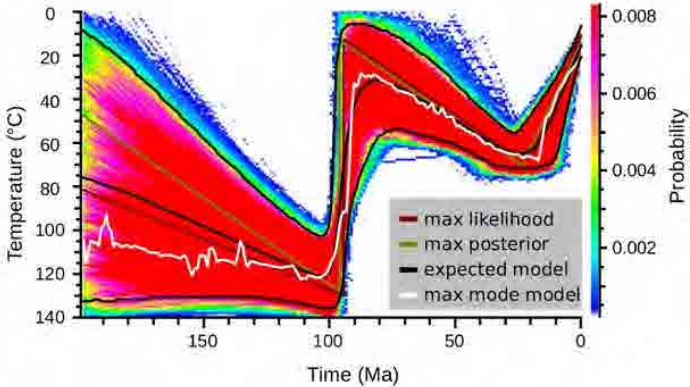
	MTL	AFT age	AHe age
Measured	13.4 ± 1.2	102 ± 7	55 ± 5
Modelled	13.9 ± 0.9	102 ± 5	59 ± 4

(iii)



	MTL	AFT age	AHe age
Measured	13.3 ± 1.2	102 ± 7	102 ± 7
Modelled	13.6 ± 0.9	81 ± 5	78 ± 6

(iv)



Monotonic cooling vs episodic heating and cooling for interpreting low temperature thermochronology data from basement terrains

Paul Green¹, Ian Duddy¹

1 Geotrack International, 37 Melville Road, Brunswick West, VIC 3055, AUSTRALIA

A variety of methods have been developed for extracting thermal history information from low temperature thermochronology (LTT) data (see Green et al. 2013¹ for a review). Applications to basement terrains are routinely presented within a paradigm of monotonic cooling, reflecting the assumption that such terrains are continuously denuded and samples continuously cool, with measured ages from various thermochronological systems defining the time at which samples cooled through a “closure temperature”².

In cratonic regions devoid of sedimentary cover this approach is compatible with geological evidence, but is it the most appropriate general strategy? In a number of published studies, monotonic cooling scenarios have been applied to basement terrains where the presence of sedimentary remnants shows that monotonic cooling to the present day is not a viable scenario. The conclusions of such studies, presented within a monotonic cooling scenario, conflict with geological evidence and are clearly incorrect. This problem becomes even more pronounced when thermal history indicators such as vitrinite reflectance or other organic maturity data from the sedimentary remnants shows that these have been buried and subsequently exhumed.

Thermochronology data alone can only record times at which samples were hotter than they are today. This results from the way in which fission tracks in apatite respond to heating and cooling¹⁻³. The same is probably true of all methods of low temperature thermochronology. The only way that periods of cooling and re-heating can be defined from such data is to impose independent constraints on times at which the sample was at the surface, based on geological evidence.

Where sedimentary outliers are present, the underlying rocks were clearly exhumed and cooled to surface temperature prior to the onset of deposition. LTT data from such situations commonly show that the sedimentary outliers, together with the underlying basement, were heated after deposition, with results implying km-scale re-burial by younger section, often in multiple episodes. Such behavior was demonstrated dramatically by Flowers and Kelly (2011)⁴ who studied core samples from basement in a shallow borehole located in Kansas, overlain by Cambrian, Permian and Cretaceous sedimentary units, each separated by a major regional unconformity. Flowers and Kelly⁴ showed that their AFT and apatite (U-Th)/He (AHe) data from the basement cores required episodes of heating and cooling in each of the intervals represented by these unconformities, resulting in a thermal history demonstrating multiple cycles of cooling-heating-cooling of decreasing magnitude through time. Similar histories have been reported in a wide variety of similar settings where the presence of sedimentary outliers on basement reveals exhumation to the surface followed by reburial, including Greenland, Namibia and southeastern Australia, as reviewed by Green et al. (2013)¹. Holford et al. (2010)⁵ reported a similar history for the Scottish Highlands based on the presence of Triassic and younger sedimentary remnants, while Weber et al. (2005)⁶ reported a similar style of history for samples from the Yilgarn Shield in Western Australia, where remnant Permian glacial deposits show that basement rocks now at outcrop were close to the surface in Permian time and were subsequently reheated and cooled to the present-day.

Histories involving episodic heating and cooling are therefore surprisingly common, but can only be defined with confidence where sedimentary outliers are present. In adjacent regions, where no sedimentary cover is preserved, while the geological evidence would allow a monotonic cooling scenario this makes no sense when combined with the presence of the nearby sedimentary outliers, without invoking either a major fault offset or folding. In regions devoid of sedimentary cover, we suggest that a

history involving episodic heating and cooling which has resulted in total erosion of the cover is at least equally likely as one involving monotonic cooling, and in fact is much more likely. We see no reason why sediment free regions should behave any differently to those where sedimentary remnants are preserved.

Any thermal history extracted from LTT data can only capture the broad features of the history, and the accuracy of the results depends critically on that of the framework within which the thermal history is specified. In this context, results presented within a framework of monotonic cooling will always represent a very poor approximation to the real history. In particular, long-term denudation rates derived over 100s of millions of years cannot be regarded as having any geological meaning.

More importantly, perhaps, we suggest that the type of history defined by Flowers and Kelly (2011)⁴ and others referenced above is characteristic of the response of the crust to stresses resulting from plate tectonic forces. The nature of the underlying processes is not understood at present, and a concerted effort is required to study and understand the mechanisms responsible for the multiple episodes of burial and exhumation which result in the episodic heating and cooling histories described above. Insisting on extracting thermal histories within a framework of monotonic cooling provides no insight into the real nature of the underlying processes, and will produce only misleading results.

We suggest that in order to fully understand the nature of the processes involved in denudation of continents and exhumation of basement terrains, studies should be focused in regions where sedimentary cover is preserved above basement. Study of “naked basement terrains”, where no sedimentary cover is preserved, can only provide the most limited of insights into the real history. More generally, we suggest that thermal histories involving episodic heating and cooling are at least as likely as monotonic cooling, and the use of the latter should be recognized as an assumption with little foundation, and an unrealistic framework for extracting thermal history information from low temperature thermochronology in general.

References

1. Green, P. F., Lidmar-Bergström, K., Japsen, P. J., Bonow, J. M. & Chalmers, J. A. Stratigraphic landscape analysis, thermochronology and the episodic development of elevated, passive continental margins. *Geological Survey of Denmark and Greenland Bulletin* **30**, 150pp (2013).
2. Dodson M.H. Closure temperature in cooling geochronological and petrological systems. *Contrib Mineral Petrol* **40**, 259-274 (1973).
3. Green, P. F. & Duddy, I. R. in *Analyzing the Thermal History of Sedimentary Basins: Methods and Case Histories* (eds. Harris, N. D. & Peters, K.) 65-104 (*SEPM Special Publication* **11**, 2012).
4. Flowers, R. M. & Kelly, S. A. Interpreting data dispersion and “inverted” dates in apatite (U–Th)/He and fission-track datasets: An example from the US Midcontinent. *Geochimica et Cosmochimica Acta* **75**, 5169–5186 (2011).
5. Holford, S. P., Green, P. F., Hillis, R. R., Underhill, J. R., Stoker, M. S. & Duddy, I. R. Multiple post-Caledonian exhumation episodes across NW Scotland revealed by apatite fission-track analysis. *Journal of the Geological Society (London)* **167**, 675–694 (2010).
6. Weber, U. D., Kohn, B. P., Gleadow, A. J. W. & Nelson, D. R. Low temperature Phanerozoic history of the Northern Yilgarn Craton, Western Australia. *Tectonophysics* **400**, 127–151 (2005).

Towards more robust interpretation of low-temperature thermochronologic ages in magmatic terranes

Kendra E. Murray¹, Peter W. Reiners¹, Jean Braun², Thibaud Simon-Labric^{2,3}

1 Dept. of Geosciences, University of Arizona, 1040 E 4th St., Tucson, Az, USA

2 ISTerre, Université Grenoble-Alpes, CNRS, BP 53, Grenoble cedex 9, France

3 IDYST, Université de Lausanne, Lausanne, Switzerland

Because they can reliably yield abundant apatite and zircon, igneous rocks in active and ancient orogens are often targeted for low-temperature thermochronologic dating to constrain the timing, rates, and patterns of erosion. However, interpreting the thermal histories of regions currently or formerly magmatically active is complicated by (1) transient heating and cooling within and adjacent to plutons, (2) changes in regional geothermal gradients, (3) interaction between advective and conductive cooling, and (4) the potential for coupled magmatic and erosional exhumation. In these settings, when is it actually appropriate to interpret low-temperature cooling ages as reflecting the timing or rate of purely erosional exhumation? We explore this question using examples of cooling-age patterns predicted by a modified version of the 3D finite-element code Pecube.

Within a pluton, all low-temperature chronometers will be the same age or younger than the crystallization age. In a vertical transect the transition between rapid cooling from local thermal relaxation of the pluton and subsequent slower (exhumational) cooling is located near a chronometer's paleo-closure depth (Z_C , Fig. 1A-C). The thickness of the transition zone from magmatic to exhumational cooling ages—as well as its shape—depends on the thermal structure of the crust during and immediately after intrusion. In rapidly exhuming terranes, where advective heat transport dominates cooling (i.e. the Péclet number is high), there is less distinction between magmatic and exhumational cooling rates and their convolution results in overestimates of erosional exhumation rates, in some cases by an order of magnitude or more (Fig. 1D-F). In these settings the age-elevation relationship doesn't reflect exhumational cooling rates until >1 km deeper than the regional closure depth (Fig. 1F).

Outside a pluton in the country rocks, cooling ages in rocks shallower than Z_C at the time of intrusion (1) reflect the pre-intrusion cooling history where far enough away from the pluton to not be heated, (2) are younger than the pluton crystallization age where close enough to be completely reset, or (3) are partially reset and fall between these two end members (Fig. 1A-C,G). Where ages are partially reset the age-elevation relationships along each transect resemble a partial retention zone. As a result, the slope of an age-elevation relationship in the “resetting aureole” for a particular system—an thereby the exhumation rate one would interpret—is close to the regional exhumation rate near the surface, shallows significantly through deeper partially reset rocks, oversteepens at depths approaching Z_C , and converges with the regional exhumation rates at depths greater than Z_C (Fig. 1D-F). The further away from the pluton a vertical transect is, the deeper and closer to Z_C rocks have to be at the time of intrusion to see the effects of resetting because the horizontal width of the resetting aureole increases at depths approaching Z_C (Fig. 1G). Fundamentally, the 3D extent of each low-temperature system's resetting aureole will reflect not only the size and temperature of the pluton, but also the regional geothermal gradient. Our ongoing work compares these model-derived trends to observed age patterns. In Miocene

plutons from the Cascades and Patagonia, there are steep apatite He age-elevation relationships in which the cooling ages are several million years younger than the crystallization ages of the plutons. This lag time between crystallization and cooling appears to be greater than can be attributed purely to local magmatic cooling if the exhumation rate before, during, and after intrusion is constant. Therefore, it is likely this cooling is related to exhumation, though it is possible that regional thermal relaxation played a role. In a completely different setting—the Colorado Plateau—apatites in sedimentary rocks reset during shallow Oligocene pluton emplacement preserve a clear record of post-Oligocene erosional history of a region where Cenozoic erosion has, in general, not been sufficient to otherwise exhume this signal.

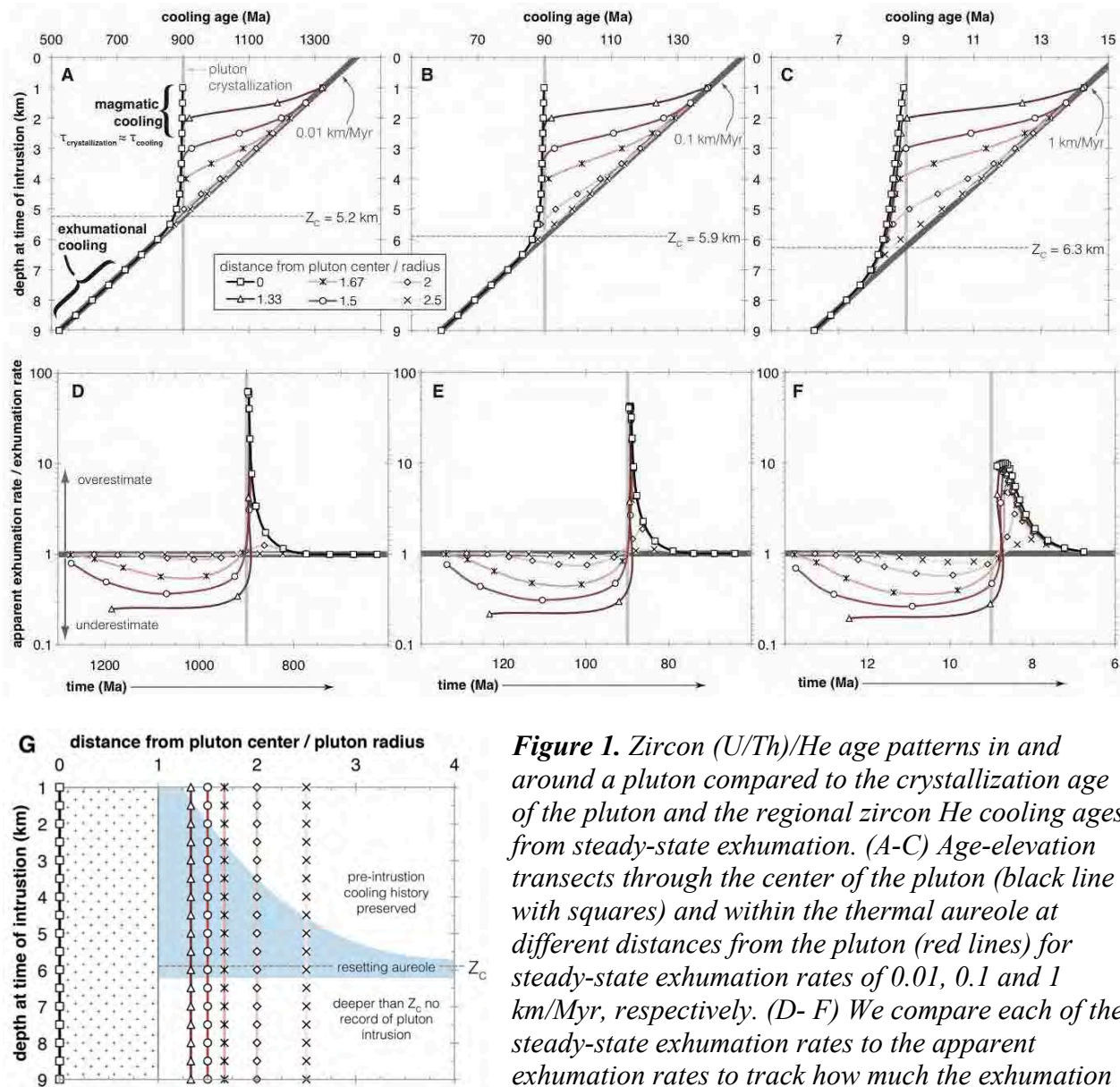


Figure 1. Zircon (U/Th)/He age patterns in and around a pluton compared to the crystallization age of the pluton and the regional zircon He cooling ages from steady-state exhumation. (A-C) Age-elevation transects through the center of the pluton (black line with squares) and within the thermal aureole at different distances from the pluton (red lines) for steady-state exhumation rates of 0.01, 0.1 and 1 km/Myr, respectively. (D-F) We compare each of the steady-state exhumation rates to the apparent exhumation rates to track how much the exhumation rate would be underestimated and overestimated within the resetting zone. (G) Schematic cross section of vertical transect locations relative to pluton (patterned field) and extent of the resetting aureole (blue field).

within the resetting zone. (G) Schematic cross section of vertical transect locations relative to pluton (patterned field) and extent of the resetting aureole (blue field).

Distinguishing thermal rift-related inheritance from subsequent orogenic exhumation in the Pyrenees

Arnaud Vacherat^{1,2,3}, Frédéric Mouthereau^{1,2}, Raphaël Pik³, Cécile Gautheron⁴, Matthias Bernet⁵, Nicolas Bellahsen^{1,2}

1 Sorbonne Universités. UPMC Univ Paris 06, UMR 7193, Institut des Sciences de la Terre Paris (iSTeP), 4 Place Jussieu, F-75005 Paris, France (arnaud.vacherat@upmc.fr)

2 CNRS, UMR 7193, Institut des Sciences de la Terre Paris (iSTeP), 4 Place Jussieu, F-75005 Paris, France

3 CRPG-CNRS, 15 rue Notre-Dame des Pauvres, 54500 Vandoeuvre-lès-Nancy, France

4 UMR Interactions et Dynamique des Environnements de Surface-CNRS 8148, Univ Paris Sud, Bâtiment 504, Rue du Belvédère, 91405 Orsay, France

5 Institut des Sciences de la Terre (ISTerre), Univ Joseph Fourier, 1381 rue de la piscine, Grenoble 38041, France

Collisional orogenic belts result from the shortening of previously thinned continental margins. If the last episode of collision-related cooling is generally well recorded from low-temperature thermochronology, the earliest cooling stages related to incipient continental accretion are generally much more difficult to resolve. There are however keys for dating the onset of cooling and therefore to better evaluate shortening and plate reconstructions. Here, we constrain the long-term cooling history of the Pyrenees by distinguishing the onset of collision thermal conditions from rift-related processes from subsequent orogenic evolution.

Kinematic reconstructions of the Iberian and European plates motions indicate that during Lower Cretaceous, extension in the Pyrenees resulted in a wider domain of extremely thinned crust between the central and western parts of the belt. Here, we first focus on the Mauléon basin (north-western Pyrenees) using detrital zircons (U-Th-Sm)/He and fission track analyses. To capture the role of rift-related processes in collision we inverse modeled our thermochronological data using relationships between zircon (U-Th-Sm)/He ages and Uranium content combined with thermo-kinematic models from rifting to collision. We show that the basin recorded a significant rift-related heating event at about 100 Ma characterized by high geothermal gradients (~80°C/km). After inversion started ca. 84 Ma, these high temperatures lasted 30 Myr until collision occurred in relation with onset of orogenic exhumation at ca. 50 Ma.

In the Central Pyrenees, we performed in-situ apatite and zircon fission track and (U-Th-Sm)/He analyses on granitic bedrock samples of the Ariège massifs (Trois-Seigneurs and Arize). Our data show cooling from mid-crustal level in Late Cretaceous and fast cooling at ca. 50 Ma. Although, these data show remarkably consistent cooling event between the Western and Central Pyrenees at 50 Ma indicating coeval exhumation in the Ariège and Mauléon region, detailed analyses of the earlier stages show some significant differences.

Thermal constraints from the Ariège region are compared with RSCM temperatures obtained from the surrounding folded Mesozoic units. A significant gap is found between maximum temperatures reached in the massifs and the adjacent sedimentary cover. This suggests a distinctive tectonic history between the crystalline basement and the basins, providing clues on how plate convergence was accommodated within the northern Pyrenean domain.

New thermochronological constraints for the exhumation of the Aiguilles Rouges massif, Western Alps

Alexandre Boutoux^{1,2}, Nicolas Bellahsen^{1,2}, Raphaël Pik³, Yann Rolland⁴, Anne Verlaquet^{1,2}, Olivier Lacombe^{1,2}

1 Sorbonne Université. UPMC Univ Paris 06, UMR 7193, ISTE_P, F-75005 Paris, France.

2 CNRS, UMR 7193, ISTE_P, F-75005 Paris, France.

3 CRPG, UMR 7358, Université de Lorraine - CNRS, BP20, 54501 Vandœuvre-Lès-Nancy Cedex, France.

4 Géoazur, Université de Nice Sophia-Antipolis, CNRS, UMR 7329, Observatoire de la Côte d'Azur, 250 av Einstein 06560 Valbonne, France.

During Oligo-Miocene times, the proximal part of the European passive margin underwent collisional shortening. In the outermost part of the Alpine arc, this shortening occurred in the fold-and-thrust belts (Bornes, Bauges, Chartreuse and Vercors massifs) with no significant tectonic burial. In the External Crystalline Massifs (ECM: Mont Blanc, Aiguilles Rouges, Belledonne, Oisans massifs), the crust was buried at mid-crustal depths below the internal units.

Along the ECORS profile, the timing of the Mont Blanc massif deformation and exhumation is now well constrained. However, the exhumation of the Aiguilles Rouges massif is much less constrained and this led to various and contrasting interpretations in terms of structural style and sequence of shortening.

In this contribution, we present a new thermochronological dataset documenting the cooling of the southwestern part of the Aiguilles Rouges massif. (U-Th-Sm)/He ages on single grain zircons were obtained on three different elevation profiles. The results (Fig. 1A) exhibit a narrow age distribution, from 5.3 Ma to 8.5 Ma. There is no significant difference between profiles, except maybe the fact that one has slightly younger ages (Prarion, Fig. 1A). The eU concentrations range between 100 to 1100 ppm, negatively correlated to the age. In the southwestern part of the massif, the ZHe ages are older than the AFT ages² (Fig. 1A, B). In the northeastern part, the AHe ages⁶ are as young as AFT ages³ (Fig. 1A, B).

Eventually those new results will allow us to better constrain the timing of the Aiguilles Rouges massifs exhumation relative to the Mont Blanc massif and decipher whether these massifs are deformed and/or exhumed in the forward sequence¹ or not, if there were some out-of-sequence major shear zones/thrusts⁵, or if these massifs were deformed sub-coevally. This has major implications in terms of both Alpine collisional wedge kinematics and crustal rheology of the European margin during the Tertiary collision.

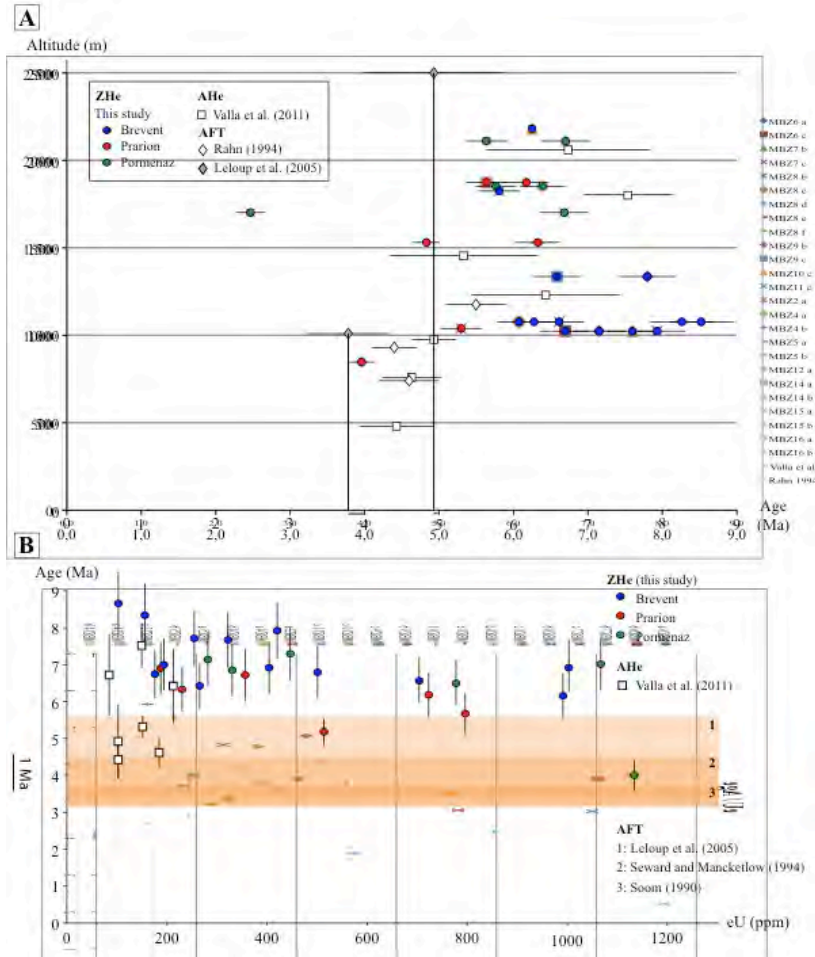


Figure 1. (A) Age/elevation distribution of the Aiguilles Rouges massif samples ZHe data (this study), AHe data⁶, and AFT data^{2,3}. (B) Age/eU distribution of the Aiguilles Rouges massif from ZHe data (this study) and AHe data⁶. Orange areas represent AFT ages^{2,4,5}.

References

- Burkhard, M. & Sommaruga, A. in Cenozoic Foreland Basins of Western Europe (eds. Mascle A., Puigdefabregas, C., Luterbacher, H. P. & Fernandez, M.) **134**, 279-298 (*Geological Society, London Special Publication*, 1998).
- Leloup, P. H., Arnaud, N., Sobel, E. R. & Lacassin, R. Alpine thermal and structural evolution of the highest external crystalline massif: the Mont Blanc. *Tectonics* **24** (2005).
- Rahn, M. K. Incipient metamorphism of the Glarus Alps: Petrology of the Tavéyanne Greywacke and fission track dating, Ph.D. thesis, 209 pp., Univ. of Basel, Basel, Switzerland (1994).
- Seward, D. & Mancktelow, N. S. Neogene kinematics of the central and western Alps: Evidence from fission-track dating, *Geology* **22**, 803–806 (1994).
- Soom, M. A. Abkühlungs- und Hebungsgeschichte der Externmassive und der penninischen Decken beidseits der Simplon-Rhoneinie seit dem Oligozän: Spaltspurdaterungen an Apatit/Zirkon und K-Ar- Datierungen an Biotit/Muskowit. PhD thesis, Bern (1990).
- Valla, P. G., Van der Beek, P., Shuster, D. L., Braun, J., Herman, F., Tassan-Got, L. & Gautheron, C. Late Neogene exhumation and relief development of the Aar and Aiguilles Rouges massifs (Swiss Alps) from low-temperature thermochronology modeling and ⁴He/³He thermochronometry. *Journal of Geophysical Research: Earth Surface* **117** (2012).

Late Cenozoic enhanced exhumation along the eastern Periadriatic fault and its linkage to the Tauern window, Eastern Alps

Bianca Heberer¹, Franz Neubauer¹, István Dunkl², Johann Genser¹

1 Dept. Geography & Geology, Univ. of Salzburg, Hellbrunner Str. 34, A-5020 Salzburg, Austria

2 Geoscience Center, Univ. of Göttingen, Goldschmidtstrasse 3, D-37077 Göttingen, Germany

Indentation of rigid blocks into rheologically weak orogens is generally associated with lateral and vertical extrusion of rocks. In this study, we report an example from the Eastern European Alps, in which subvertical extrusion of crustal blocks associated with exhumation in distant areas is connected by a transfer fault, which likely corresponds to a block boundary in the deeper crust or even lithosphere.

We applied apatite (U-Th)/He (AHe) dating to Triassic granites and Oligocene tonalites from the Karawanken plutonic belts located in the immediate vicinity of the eastern Periadriatic fault near the Austrian-Slovenian border. The Periadriatic fault forms the largest and most important discontinuity in the European Alps. Exhumation along the fault and the adjacent blocks was studied in detail in its western and central parts, but only little is known on late-stage exhumation for the eastern fault segments. This is surprising when considering that the Eastern Alps are tectonically more active than the western and central parts of Alps. The eastern part of the Periadriatic fault is segmented into three portions: a straight segment west of the Hochstuhl-Möll Valley (HVM) fault system, a central segment between the NW-trending HVM and Lavant Valley faults with a Neogene positive flower structure separating the north-vergent North Karawanken from the south-vergent South Karawanken unit, and an eastern segment largely buried underneath Neogene Pannonian basin sediments. In the central segment, the Periadriatic fault is dextrally displaced by the HVM and Lavant Valley faults and the North Karawanken unit is thrust over the Neogene flexural, intra- orogenic Klagenfurt basin, which contains sediments ranging from Sarmatian (ca. 11 Ma) to Pliocene or possibly even Quaternary.

In the central segment, we find AHe ages mostly ranging from 6 to 9 Ma. This is in contrast to older ages west of the HVM directly at the PAF, where an age of 20 ± 1 Ma has been found. The basement north of the Klagenfurt basin yields also older AHe and apatite fission track ages ranging from ca. 25 to 30 Ma. This age pattern confirms and constrains the positive flower structure as an area of young exhumation and argues for a late Miocene exhumation pulse along the eastern segment of the Periadriatic fault. This pulse was associated with surface uplift and topography building during the formation of the positive Karawanken flower structure, as indicated by the clastic record of the Klagenfurt basin, i.e. the progradation of latest Miocene to (?) Pliocene fluvial deposits (Bärental Conglomerate), interbedded with large carbonate slide blocks^{1,2}. Exhumation was not locally restricted to the flower structure but a more widespread phenomenon during NW-SE compression: Young AHe ages similar to the central segment of the eastern Periadriatic fault were reported from basement domes of the southeastern Tauern window^{3,4}. These domal structures are transected by the HVM. We therefore suggest that the HVM fault system acts as a transfer fault and connects shortening of an apparent positive flower structure and associated exhumation with coeval updoming in the eastern Tauern window, particularly within the strongly shortened Sonnblick dome³. Interestingly, the HVM fault

corresponds roughly with the western boundary of the lower crustal Pannonian fragment⁵.

Our new findings indicate a hitherto undetected late Miocene deformation event within the Eastern Alpine system, possibly triggered by revived indentation of the Adriatic indenter. Further evidence for such a shortening phase comes from the widespread inversion in the entire Alpine-Carpathian- Pannonian system as well as the ca. coeval development of the Sava folds in Slovenia.

References

1. Polinski, R. K. & Eisbacher, G. H. Deformation Partitioning during Polyphase Oblique Convergence in the Karawanken Mountains, Southeastern Alps. *J. Struct. Geol.* **14**, 1203-1213 (1992).
2. van Husen, D. Synsedimentäre Gleitschollen grossen Ausmasses im terrestrischen Jungtertiär der Karawanken. *Geol. Rundsch.* **73**, 433-445 (1984).
3. Wolfler, A., Stuwe, K., Danisik, M. & Evans, N. J. Low temperature thermochronology in the Eastern Alps: Implications for structural and topographic evolution. *Tectonophysics* **541**, 1-18 (2012).
4. Foeken, J. P. T., Persano, C., Stuart, F. M. & ter Voorde, M. Role of topography in isotherm perturbation: Apatite (U-Th)/He and fission track results from the Malta tunnel, Tauern Window, Austria. *Tectonics* **26** (2007).
5. Bruckl, E., Behm, M., Decker, K., Grad, M., Guterch, A., Keller, G. R. & Thybo, H. Crustal structure and active tectonics in the Eastern Alps. *Tectonics* **29** (2010).

Thermal history of western Ireland

Nathan Cogné¹, David Chew¹, Fin M. Stuart²

1 Geology Department, Trinity College Dublin, College Green, Dublin 2, Ireland

2 SUERC, Scottish Enterprise Technology Park, East Kilbride G750QF, United Kingdom

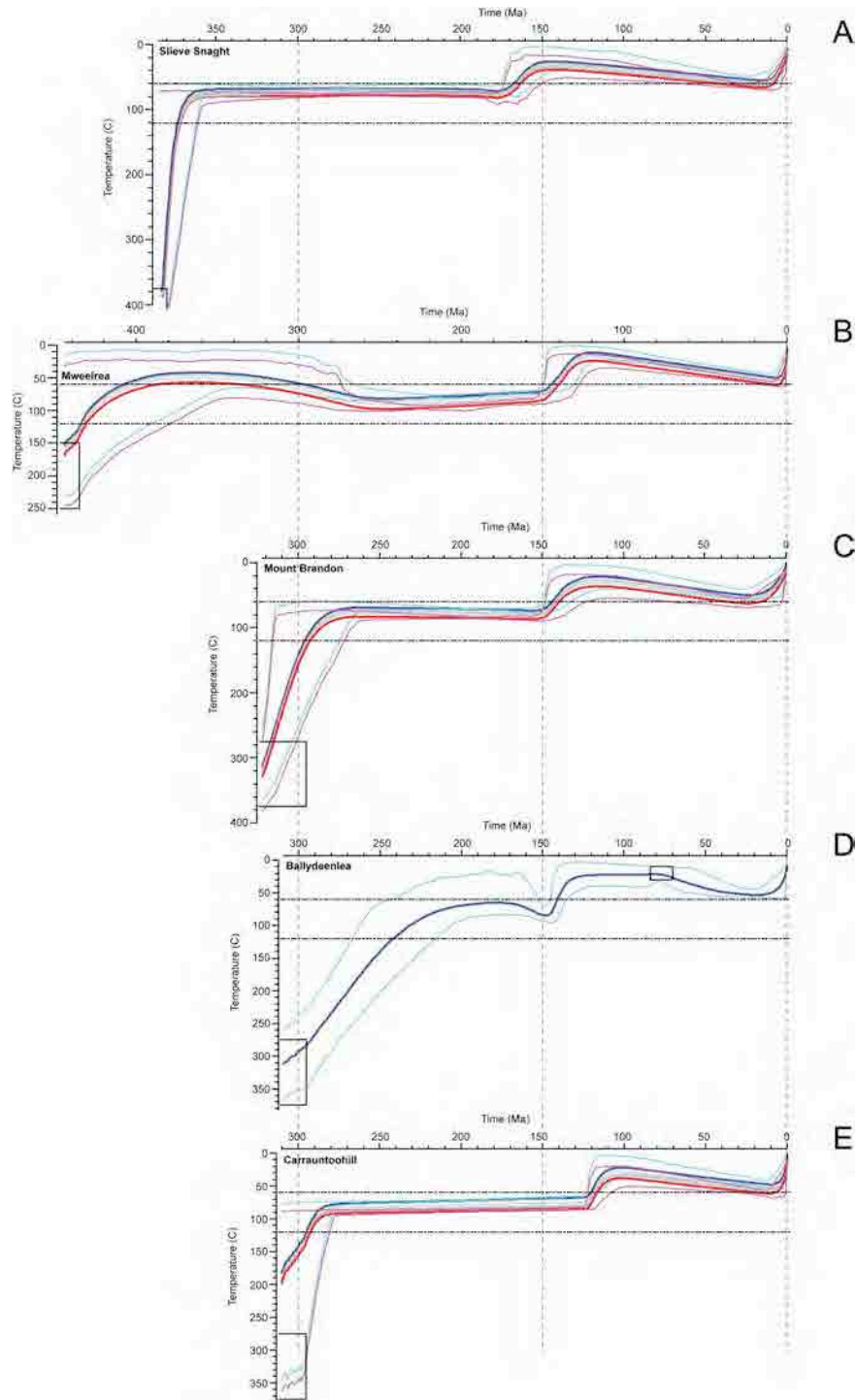
The thermal history of a passive margin yields key information on its tectonic evolution, as phases of tectonic activity (e.g. exhumation or burial) can be inferred from periods of enhanced cooling or heating. We present here the results of a thermochronological study (apatite fission track and U- Th/He dating) on selected targets along the western coast of Ireland (four vertical thermochronology profiles in Counties Kerry, Mayo and Donegal). The combined use of U- Th/He and vertical profiles for the first time in Ireland should allow us to constrain better phases of cooling / heating.

The fission track and U-Th/He ages range from the Late Jurassic to Early Cretaceous and show relatively little inter-sample variation. Inverse modelling of the age and track length data shows that during post-orogenic exhumation the samples cooled to temperatures of around 80°C. A rapid cooling event (down to temperatures as low as 20°C) occurred during the Late Jurassic to Early Cretaceous and is slightly diachronous from North to South. We attribute this cooling event to rift- shoulder related exhumation and erosion, which can be temporally linked to the main stage of rifting in the western Irish offshore (the Porcupine, Slyne and Erris basins).

During the Cretaceous and Early Tertiary slow reheating is inferred to temperatures of about 50-60°C, and is probably linked to a small pulse of sedimentation onshore. Finally a rapid cooling event during the Neogene is observed. This late cooling phase could be linked to a reactivation of the margin under compressive forces (i.e. due to Alpine collision and/or mid oceanic ridge-push). Our inverse modelling does not therefore require an Early Cenozoic cooling / exhumation phase as proposed by many author¹⁻². However constrained tests shows that introducing an Early Cenozoic phase of cooling does not change significantly the model predictions nor the presence of Mesozoic and Late Cenozoic cooling phases and thus the it is possible that an Early Cenozoic exhumation event accounts for part of the total Cenozoic cooling.

This onshore study is now being complimented by a new thermochronological study on the Porcupine High and on the wells of the western offshore basins. The first results from the Porcupine High show a remarkable similarity in the timing of rift-related exhumation with the onshore part of the margin.

Figure 1. *Graphs of the thermal histories inferred from the inverse modelling of the different profiles. For each thermal history model, the thick dark blue line is the coolest (highest elevation sample) of the profile, with its credible interval denoted by thin blue lines. The thick red line is the hottest (lowest elevation sample) of the profile, with its credible interval denoted by thin purple lines. The grey lines are the intermediate samples and the dashed horizontal lines are the temperature limits of the PAZ. The black boxes are user-specified temperature-time constraints. (a) Slieve Snaght profile; (b) Mweelrea profile; (c) Mount Brandon profile; (d) Ballydeenlea sample and (e) Carrauntoohill profile.*



References

1. Allen, P.A., Bennett, S.D., Cunningham, M.J.M., Carter, A., Gallagher, K., Lazzaretti, E., Galewsky, J., Densmore, A.L., Phillips, W.E.A., Naylor, D. & Hach, C.S. The post-Variscan thermal and denudational history of Ireland. *Geological Society, London, Special Publications* **196**, 371-399 (2002).
2. Green, P.F., Duddy, I.R., Hegarty, K.A., Bray, R.J., Sevastopulo, G., Clayton, G. & Johnston, D. The post-Carboniferous evolution of Ireland: evidence from Thermal History Reconstruction. *Proceedings of the Geologists' Association* **111**, 307-320 (2000).

Modelling the thermal structure of onshore Ireland and its offshore basins

Daniel Döpke¹, David M. Chew¹, Finlay M. Stuart²

1 Department of Geology, School of Natural Science, Trinity College Dublin, Dublin 2, Ireland

2 Isotope Geosciences Unit, Scottish Universities Environmental Research Centre, Scottish Enterprise Technology Park, East Kilbride, UK

Ireland and Britain make a superb natural laboratory in which to evaluate the various techniques for estimating the timing and magnitude of exhumation because of the wealth of data provided by the hydrocarbon industry (Corcoran & Doré, 2005) as well as previous regional scale low temperature thermochronology studies (e.g. Allen et al., 2002). This database includes vitrinite reflectance, shale compaction and a large amount of apatite fission track (AFT) data. However, the Cenozoic exhumation history of Ireland and Britain remains contentious as it is hindered by the lack of Mesozoic/Cenozoic onshore outcrops. Constraining the timing and magnitude of Cenozoic exhumation is very important as it controls the geological outcrop pattern, physiography and distribution of hydrocarbon resources of this sector of the NW European margin.

This project seeks to characterize the timing and mechanisms of exhumation of onshore Ireland and Britain and their offshore basins to address the Cenozoic exhumation history. This includes modelling the thermal evolution, evaluating regions of high heat flow (onshore) as targets for geothermal purposes and the timing of basin inversion (offshore) for the hydrocarbon industry. We collected samples from mainland Ireland (focussing mainly on the eastern Irish coast), Isle of Man and the Isle of Arran and also incorporated samples from previous projects from Ireland (TULIP) and Scotland (SUERC: Scottish Universities Environmental Research Centre).

Sampling was undertaken on both a regional scale around the Irish Sea and on a pseudo-vertical profile on the Isle of Arran (Scotland) (Fig.1). Regional scale sampling serves to detect regional exhumation pattern such as the postulated dome-like structure for Cenozoic denudation around the Irish Sea (Jones et al., 2002), whereas vertical profile yield highly constrained temperature-time models which can help determine the timing of Cenozoic denudation.

Thermal history analysis of these samples is being undertaken using low temperature thermochronometers such as the AFT and (U-Th-Sm)/He on apatite (AHe) methods. The AFT research is being undertaken in the fission track lab at Trinity College Dublin (TCD) and the AHe studies in East Kilbride are being undertaken in conjunction with Dr. Finlay Stuart (SUERC). The results from the AFT and AHe analysis will then be modelled to produce 2D and 3D thermal models of Ireland and Britain. Combined, the AFT and AHe techniques provide thermal history information between 120°C to 40°C which corresponds to crustal depths of 1 – 5km for typical geothermal gradients. Therefore these methods are well suited for determining the moderate amounts (~1–2 km) of denudation postulated for Ireland and Britain during Cenozoic times (Jones et al., 2002; Holford et al., 2005). The combination of the AFT and AHe methods is also well suited to investigate the thermal history of sedimentary basins (including characterizing the timing of inversion episodes) which is important for hydrocarbon exploration companies while the oil maturation window lies within the temperature range of AFT and AHe (between 120°C and 40°C).

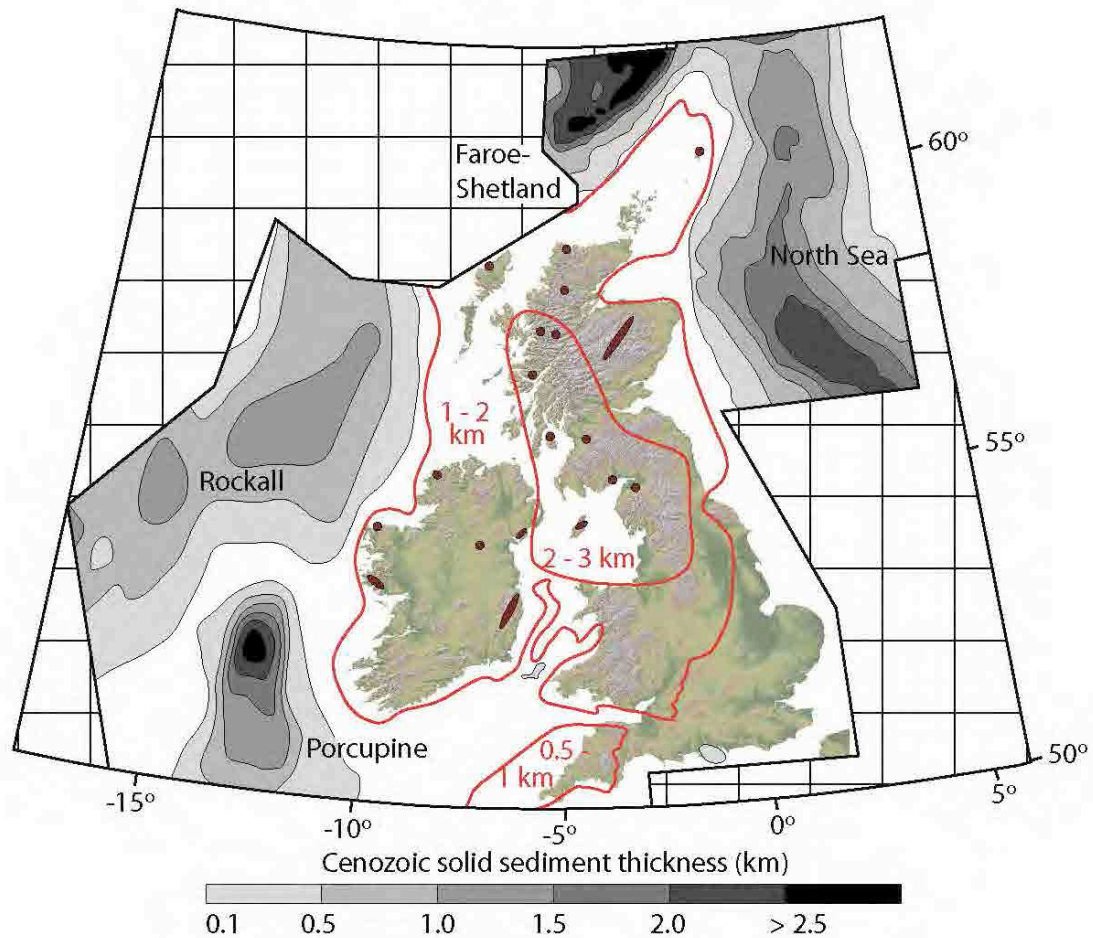


Figure 1. NW European shelf with: grey scale: isopachs of Cenozoic solid sediments (Jones et al., 2002); red line: estimate of Cenozoic denudation (Jones et al., 2002); red dots: sampling sites and provided samples.

References

1. Allen, P.A. et al. in Exhumation of the North Atlantic Margin: Timing, Mechanisms and Implications for Petroleum Exploration (eds. Doré, A.G., Cartwright, J.A., Stoker, M.S., Turner, J.P. & White, N.) 371-399 (*Geological Society Special Publications* **196**, London, 2002).
2. Corcoran, D.V. & Doré, A.G. A review of techniques for the estimation of magnitude and timing of exhumation in offshore basins. *Earth-Science Reviews* **72**, 129 – 168 (2005).
3. Holford, S.P., Turner, J.P. & Green, P.F. in Petroleum Geology: North-West Europe and Global Perspective- Proceedings (eds. Doré, A.G. & Vining, B.) 1-13 (*the 6th Petroleum Geology Conference*, Article I.D **18**, 2005).
4. Jones, S.M., White, N.J., Clarke, B.J., Rowley, E. & Gallagher, K. in Exhumation of the North Atlantic Margin: Timing, Mechanisms and Implications for Petroleum Exploration (eds. : Doré, A.G., Cartwright, J.A., Stoker, M.S., Turner, J.P. & White, N.) 13-25 (*Geological Society Special Publications* **196**, London, 2002).

Unraveling deformation events associated with the Svecofennian Orogeny on Ringvassøy, Northern Norway: New $^{40}\text{Ar}/^{39}\text{Ar}$ ages and discussion

Camilla Maya Wilkinson¹, Iain Henderson¹, Morgan Ganerød¹
1 Norges geologiske undersøkelse (NGU), Norway

The Baltic Shield is composed of Archaean and Palaeoproterozoic terranes, the tectonic architecture of which, is becoming apparent through recent advances. These terranes are juxtaposed by crustal scale ductile shear zones during the Svecofennian Orogeny at approximately 1.9 - 1.7 Ga¹. Svecofennian deformation affected the tonalitic gneisses and supracrustal units of the West-Troms Basement Complex (WTBC) by producing firstly, regional, NE-directed thrusts, NW-SE trending inclined to upright macro-folds followed by NW-SE striking, steep anastomosing strike-slip ductile shear zone networks¹. Mineralisation is often concentrated in these shear zones and therefore a knowledge of their development is crucial to prospectivity. However, despite a wealth of general age dating carried out on magmatic rocks across the Baltic Shield, very few contributions have dated directly the timing of deformation and mineralisation. We attempt to place the multi-stage Svecofennian deformation events occurring along such structures into a solid chronological framework, as well as refining the method for dating complex structures. This combined structural and $^{40}\text{Ar}/^{39}\text{Ar}$ dating study of crustal scale shear zones and the intervening tectonic domains will help develop a crustal scale tectonic model for the Palaeoproterozoic in northern Norway. $^{40}\text{Ar}/^{39}\text{Ar}$ dating has been carried out on samples collected from the island of Ringvassøy in the West Troms Basement Complex (WTBC) on the western margin of the Baltic Shield, where a robust tectonic framework provided by Bergh *et al.*, (2010), represents the basis for the direct dating of specific deformational events.

Preliminary $^{40}\text{Ar}/^{39}\text{Ar}$ laser step-heating data obtained so far, from multiple mineral phases, has revealed a range of ages (~1800 to ~460 Ma). Biotite from two samples, tentatively related to the latest phase of thrusting yield slightly younger ages of ~1680 Ma. However, the oldest age, obtained from amphibole within a post thrusting diabase dyke falls within the range of U-Pb ages obtained from the region (ca. 1.7 – 1.9 Ga). In addition, muscovite ages within the most intense thrust structures are considerably younger than both biotite and amphibole, recording ages of ~880 Ma and ~460 Ma, suggesting that the thrust structures may have been partially reactivated during the Caledonian Event at ca. 400 Ma.

Isotopic analyses of several generations of micas, which record different stages of deformation can be carried out more easily on a single-grain level, and avoid obtaining ‘mixing ages’². Is muscovite recording the actual age of crystallization or recrystallization as a result of later reactivation along the shear zone due to the Caledonian Orogeny? Or do the ages represent relic muscovite which has experienced significant argon diffusion following initial crystallization, in response to a re-heating episode? It may be possible to extract more useful age information from such samples using a high spatial resolution laser ablation technique (i.e., UV *in situ* spot analysis³⁻¹⁰). The use of such a method permits a direct link between the measured $^{40}\text{Ar}/^{39}\text{Ar}$ ratio and spatial information within the grain, and can provide a way to distinguish between partially reset grains and those recording a crystallization age and therefore dating a deformation event. Further work and the analysis of additional samples and use of a range of different $^{40}\text{Ar}/^{39}\text{Ar}$ techniques will provide a more complete picture of the Ringvassøy Greenstone belt’s thermal history and the complex history of the West Troms Basement Complex.

References

1. Bergh, S. G., Kullerud, K., Armitage, P. E. B., Zwaan, K. B., Corfu, F., Ravna, E. J. K. & Myhre, P. I. Neoproterozoic to Svecofennian tectono-magmatic evolution of the West Troms Basement Complex, North Norway. *Norwegian Journal of Geology* **90**, 21-48 (2010).
2. Beltrando, M., Lister, G. S., Forster, M., Dunlap, W. J., Fraser, G. & Hermann, J. Dating microstructures by the $^{40}\text{Ar}/^{39}\text{Ar}$ step-heating technique: Deformation pressure temperature time history of the Penninic Units of the Western Alps. *Lithos* **113**, 801–819 (2009).
3. Hames, W. E. & Cheney, J. T. On the loss of $^{40}\text{Ar}^*$ from muscovite during polymetamorphism. *Geochimica et Cosmochimica Acta* **61**, 3863–3872 (1997).
4. Di Vincenzo, G., Carosi, R. & Palmeri, R. The relationship between tectono-metamorphic evolution and Ar isotope records in white mica: constraints from *in situ* ^{40}Ar – ^{39}Ar laser analysis of the Variscan basement of Sardinia (Italy). *Journal of Petrology* **45**, 1013-1043 (2004).
5. Mulch, A., Cosca, M. A. & Handy, M. R. In-situ UV-laser $^{40}\text{Ar}/^{39}\text{Ar}$ geochronology of a micaceous mylonite: an example of defect-enhanced argon loss. *Contrib. Mineral Petrol.* **142**, 738-752 (2002).
6. Mulch, A., Cosca, M. A., Andresen, A. & Fiebig, J. Timescales of deformation and Exhumation in extensional detachment systems determined by high-spatial resolution *in situ* UV-laser $^{40}\text{Ar}/^{39}\text{Ar}$ dating. *Earth Planet. Sci. Lett.* **233**, 275–390 (2005).
7. Arnaud, N. O. & Kelley, S. Evidence for excess Ar during high pressure metamorphism in the Dora-Maira (western Alps, Italy), using a Ultra-Violet Laser Ablation Microprobe $^{40}\text{Ar}/^{39}\text{Ar}$ technique. *Contrib. Mineral. Petrol.* **121**, 1–11 (1995).
8. Scaillet, S. Excess ^{40}Ar transport scale and mechanism in high-pressure phengites: A case study from an eclogitized metabasite of the Dora-Maira nappe, western Alps. *Geology* **6**, 1075-1090 (1996).
9. Sherlock, S., Kelley, S., Inger, S., Harris, N. & Okay, A. ^{40}Ar - ^{39}Ar and Rb-Sr geochronology of high-pressure metamorphism and exhumation history of the Tavsanli Zone, NW Turkey. *Contrib. Mineral Petrol.* **137**, 46-58 (1999).
10. Warren, C. J., Hanke, F. & Kelley, S. P. When can muscovite $^{40}\text{Ar}/^{39}\text{Ar}$ dating constrain the timing of metamorphic exhumation? *Chemical Geology* **291**, 79-86 (2012).

Vertical profile AFT dating in East Greenland

C. Johnson¹, K. Gallagher², A. Carter³, T.C. Kinnaird^{1,4*}, A.G. Whitham¹, A.G. Szulc^{1#}

1 CASP, University of Cambridge, 181A Huntingdon Road, Cambridge, CB30DH, UK

2 Géosciences Rennes, UMR 6118, Université de Rennes 1, 35042 Rennes, France

3 Department of Earth and Planetary Sciences, Birkbeck College, London, WC17HX, UK

4 SUERC, Rankine Avenue, Scottish Enterprise Technology Park, East Kilbride, G75 0QF, UK

* current address, # presenting author (adam.szulc@casp.cam.ac.uk)

Following the break-up of the Caledonian orogeny, East Greenland experienced protracted rifting from the Devonian until the separation of the Jan Mayen microcontinent in the Late Eocene-Early Oligocene. The present-day continent-ocean boundary is proximal to the coast of East Greenland¹. Therefore, a large volume of East Greenland-derived sediment is likely to now reside in basins of hydrocarbon importance on the Norwegian conjugate margin. The Caledonian basement in East Greenland is locally cut by planation surfaces that are of uncertain age. Post-Caledonian stratigraphy includes several biostratigraphically dated unconformities. Apatite fission track dating constrains the timing of the denudation events that resulted in these surfaces and contributed abundant sediment to Mid Norway. A suite of 69 samples from 14 vertical profiles (up to 1 km thick) was taken from Devonian and Carboniferous strata and Caledonian basement across East Greenland (70-75°N). Following the method of Johnson and Gallagher (2000), data from multiple samples along individual profiles were modelled together to better constrain the cooling history of the rock columns represented by the profiles. Palaeotemperature gradients were combined with thermal conductivity data on individual samples to estimate palaeoheatflow and thereby the thickness of the missing sections. Central AFT ages range from 274 ± 13 Ma to 32 ± 3 Ma. AFT age peaks define four distinct periods of denudation at 205-176 Ma, 156- 148 Ma, 107-86 Ma, and 50-20 Ma. The age peaks are spatially correlated with major Caledonian structures, implying reactivation until at least the Neogene. The results highlight the importance of a Mid-Late Permian angular unconformity that is overlain by minimal syn- rift sediment, and a Mid Jurassic unconformity that is overlain by abundant syn-rift sediment. AFT ages from two planation surfaces that cut the Caledonian basement indicate rapid denudation during the Mid Permian-Early Triassic and a second phase during the Late Cretaceous-Mid Palaeogene, which may account for the limited Cretaceous strata on Jameson Land. It is likely that other planation surfaces located variously beneath Palaeogene, Triassic, and Mid Jurassic strata also originated during the Mid-Late Permian. The most recent period of denudation followed the emplacement of flood basalts at ~58-56 Ma. The results indicate that the basalts were once widely distributed between the Bløseville Kyst and Hold with Hope. Denuded sediment volume estimates exceed the present-day accommodation space of the East Greenland margin. This provides additional evidence that much East Greenland- derived sediment now resides on the Mid Norway continental margin.

References

1. Scott, R.A. Mesozoic-Cenozoic evolution of East Greenland: implications of a reinterpreted continent- ocean boundary location. *Polarforschung*, **68**, 83-91 (2000).
2. Johnson, C. & Gallagher, K. A preliminary Mesozoic and Cenozoic denudation history of the NE Greenland onshore margin. *Global and Planetary Change*, **24**, 261-274 (2000).

Apatite Fission Track Thermal History Analysis of the Beaufort-Mackenzie Basin, Arctic Canada: A Natural Laboratory for Testing Multi-Kinetic Thermal Annealing Models

Dale R. Issler¹, Alexander M. Grist²

1 Geological Survey of Canada, 3303-33rd St. NW, Calgary, AB, Canada T2L 2A7

2 Department of Earth Sciences, Dalhousie University, Halifax, NS, Canada B3H 4J1

The Arctic Beaufort-Mackenzie basin (BMB) is a natural laboratory for testing composition-based apatite fission track (AFT) annealing models because it comprises compositionally homogeneous Upper Cretaceous-Cenozoic deltaic successions with highly variable heating/cooling histories and long residence times in the AFT partial annealing zone. Sixty AFT (mainly core) samples from 25 wells are available from Paleogene post-rift (Aklak, Taglu, Richards and Kugmallit sequences), Upper Jurassic-Lower Cretaceous syn-rift (Husky, Martin Creek and Kamik formations), and Devonian pre-rift (Imperial Formation) successions (Figure 1). All major tectonic elements are sampled, including the western Tertiary fold belt, Tertiary growth faults of the Tarsiut-Amauligak and Taglu fault zones, the Kugmallit Trough (formed by Jurassic-Early Cretaceous rifting), and intact continental crust of the Anderson Basin to the southeast. Multi-parameter well data (*e.g.*, temperature^{1, 2, 3}, stratigraphy, thermal maturity⁴ and porosity) were compiled for integrated thermal history analysis as part of a major government-industry funded study of BMB petroleum systems.

Samples collected during the initial phase of the study (generally at low thermal maturity; < 0.5 %Ro) yielded mainly single grain ages that passed the chi-squared test, giving an initial impression of compositionally uniform AFT age populations. Subsequent sampling from successions with higher thermal maturity (> 0.5 %Ro) yielded many samples with single grain ages that failed the chi-squared test, indicating mixed AFT age populations within samples. Further analysis of single grain ages using the binomial peak-fitting program (Binomfit) of Mark Brandon (Yale University) suggests that most of the samples have two statistically significant age populations. This interpretation is supported by elemental data and microscopic observations that show significant variability in elemental abundances and etch figure sizes (Dpar) among apatite grains. The r_{mr0} parameter⁶ (based on elemental data) is more successful at defining separate statistical AFT populations with distinct annealing kinetics than widely used kinetic parameters based on chlorine content or Dpar. Elemental data indicate that most samples have two statistical kinetic populations with different annealing properties that behave as separate thermochronometers: a fluorine-rich apatite (lower track retentivity) and an iron-rich apatite (higher track retentivity).

Low uranium concentrations of apatite grains, rapid exhumation of sediment source areas, and variable degrees of post-depositional annealing present challenges to defining statistical kinetic populations. However, insight into multi-kinetic annealing is gained by examining the spatial variation in AFT data within a regional thermal maturity framework⁴, leading to successful multi-kinetic thermal models that satisfy available geological constraints. Apatite composition is similar for all Paleogene samples with approximately equal abundances of fluorine-rich and iron-rich apatite. The apparent uniform AFT age of low maturity samples can be attributed to rapid cooling of apatite source areas and this eliminates variation in detrital provenance age as a factor in modeling. The different kinetic populations within a sample can be modeled using the same thermal history, indicating that compositionally-related differential annealing is the main factor causing grain age dispersion at higher thermal maturity. The fluorine-rich apatite is more sensitive to the post-depositional thermal history whereas the iron-rich apatite retains information on the pre-depositional rapid cooling history of detrital apatite source areas. AFT data from other areas of western and northern Canada suggest that compositional variation in detrital apatite is common and needs to be considered when undertaking thermochronology studies.

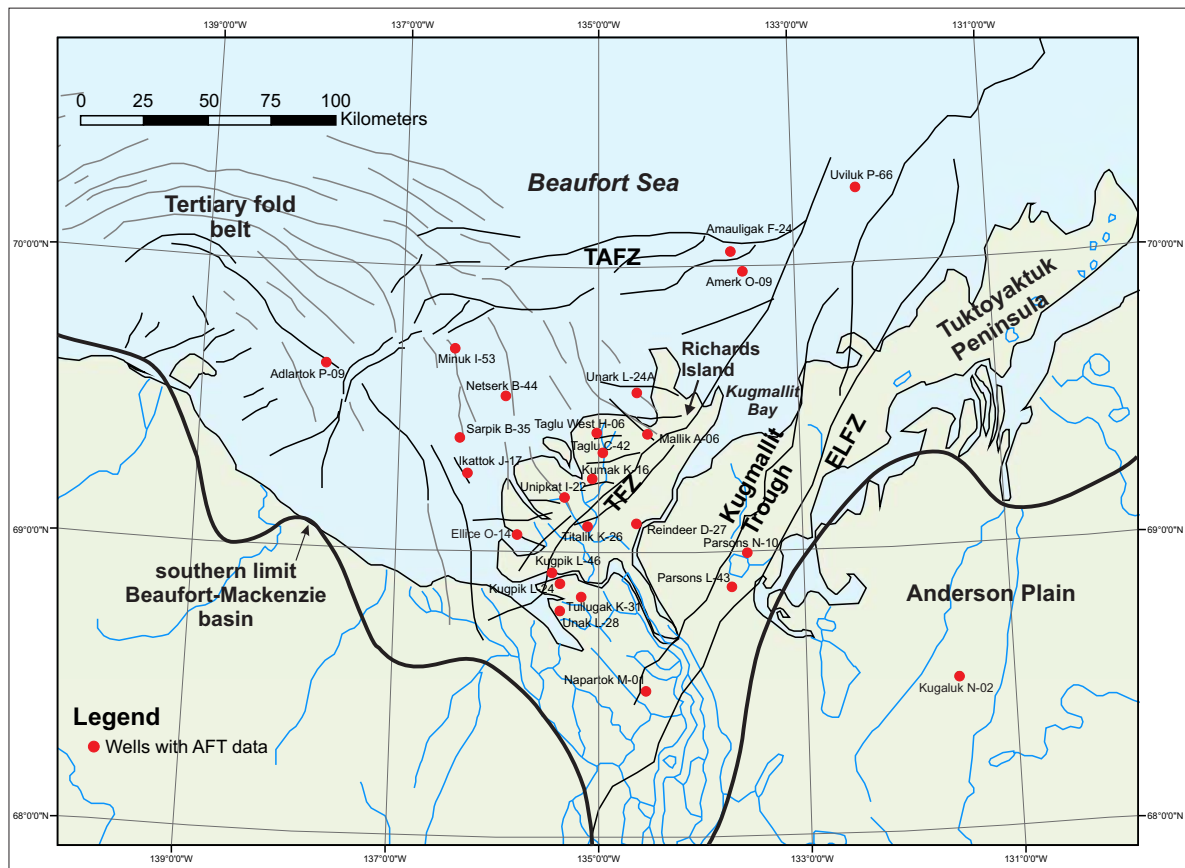


Figure 1. Location of 25 wells with AFT and standardized percent vitrinite reflectance⁴ (%Ro) data. %Ro is a cumulative paleotemperature indicator that is sensitive to heating whereas AFT parameters are most sensitive to cooling. The exhumation history of the basin margin and the rapid heating of offshore sedimentary successions are constrained using an updated version of an in-house inverse AFT thermal model⁵ that includes multi-kinetic AFT annealing⁶ and a temperature-dependent kinetic model for %Ro⁷. Our modeling approach incorporates geological constraints on deposition, burial heating rates, and temperatures to generate statistically acceptable thermal histories. ELFZ: Eskimo Lakes Fault Zone; TFZ: Taglu Fault Zone; TAFZ: Tarsiut-Amauligak Fault Zone.

References

1. Chen, Z., Osadetz, K. G., Issler, D. R. & Grasby, S. E. Hydrocarbon migration detected by regional temperature field variations, Beaufort-Mackenzie Basin, Canada. *AAPG Bulletin* **92**, 1639-1653 (2008).
2. Hu, K., Issler, D. R. & Jessop, A. Well temperature data compilation, correction and quality assessment for the Beaufort-Mackenzie Basin. *Geological Survey of Canada, Open File* **6057**, 17p. (2010).
3. Issler, D. R., Hu, K., Lane, L. S. & Dietrich, J. R. GIS compilations of overpressure, permafrost distribution, geothermal gradient, and geology, Beaufort-Mackenzie region, northern Canada. *Geological Survey of Canada, Open File* **5689** (2011).
4. Issler, D. R., Reyes, J., Chen, Z., Hu, K., Negulic, E., Grist, A., Stasiuk, L. & Goodarzi, F. in *New Understandings of the Petroleum Systems of Continental Margins of the World* **32**, 609-641 (Papers Presented at the 32nd Annual GCSSEPM Foundation Bob F. Perkins Research Conference, Houston, Texas, DVD, 2012).
5. Issler, D. R., Grist, A. M. & Stasiuk, L. D. Post-Early Devonian thermal constraints on hydrocarbon source rock maturation in the Keele Tectonic Zone, Tulita area, NWT, Canada, from multi-kinetic apatite fission track thermochronology, vitrinite reflectance and shale compaction. *Bull. Can. Petr. Geol.* **53**, 405-431 (2005).
6. Ketcham, R. A., Donelick, R. A. & Carlson, W. D. Variability of apatite fission-track annealing kinetics: III. Extrapolation to geological time scales. *American Mineralogist* **84**, 1235-1255 (1999).
7. Sweeney, J. J. & Burnham, A. K. Evaluation of a simple model of vitrinite reflectance based on chemical kinetics. *AAPG Bulletin* **74**, 1559-1570 (1990).

Cenozoic exhumation patterns in an Arctic region : new low-T thermochronology and RSCM data from the Brooks Range, Alaska

Bigot-Buschendorf Maélianna^{1,2}, Fillon Charlotte^{1,3}, Mouthereau Frédéric^{1,2}, Labrousse Loïc^{1,2}

1 UPMC University Paris 06, UMR 7193, IStEP, F-75005 Paris, France

2 CNRS, UMR 7193, IStEP, F-75005, Paris, France

3 Instituto de Ciencias de la Tierra "Jaume Almera" CSIC, Barcelona, Espana

The Alaskan Brooks Range and its canadian counterpart, the British Mountains result from the Meso-Cenozoic collision of the Arctic continental margin with accreted volcanic arcs and adjacent continental Terranes.

Because of its location and known potential for oil industries, more attention is brought to this area since a few years. But while the timing of collisional events is roughly understood, duration and rates of exhumation associated with mountain building are essentially unconstrained.

Here we aim at reconstructing the time-temperature evolution of the Brooks Range and the British Mountains by combining new (U-Th)/He and fission-tracks ages on zircon and apatite with RSCM thermometry on Carbonaceous Material. We pay a particular attention to the sequence of activation of thrust sheet units, as well as identifying erosional signal.

The timing of fault activity and exhumation across the Brooks Range is explored using thermo-kinematic modeling (Pecube^{1,2}) by inverting the already existing AFT dataset³⁻⁵ together with new AFT, AHe and ZHe data (Figure 1). Rocks were sampled along a 400 km long profile across the range. We obtained 7 AFT ages, 8 AHe ages, 15 ZHe and 11 RSCM temperatures.

RSCM data reflect the maximum temperatures reached by the rocks and reveals that, on our profile, temperatures did not exceed 325 °C. Temperatures show a decrease from this value to 192 °C at the topographic front.

Both published data and our new age constraints are consistent with a progressive cooling from 105 to 25 Ma. Our modeling approach shows that rates of exhumation were kept constant across the range until 35 Ma. From 35 Ma onwards, exhumation likely reduced and was associated with underplating/duplexing in the inner part of the belt (Doonerak window) and activation of the northernmost thrust.

We show that some of the fault activity periods and amplitude are still unresolved consistently, due to the lack of data and probably also to the very slow exhumation experienced by the area since Eocene times. Model resolution however increases for the latest event at 35 Ma, allowing us to resolve an average exhumation rate of 0.21 km/Ma.

Our results support the view that the exhumation of thrust sheets was continuous, rather than punctuated from 105 to 35 Ma and occurred in a dominant north-propagating sequence.

The earliest stage of cooling marks the start of the Brookian orogeny and is coincident with onset

of the coarsening upward sequence observed in the foreland basin. The late- orogenic stage of Miocene cooling appears to be linked to a reorganization of shortening within the orogenic wedge, possibly related to the larger scale effect of plate tectonics and/or climate changes.

We finally discuss the results of the modeling with more regional geological constraints, including seismic reflection data north and north-eastward of the Brooks Range, to discuss the relationships, during the Cenozoic, between the growth of the Brooks Range, the geodynamics of the Pacific subduction system and the climate of this arctic region.

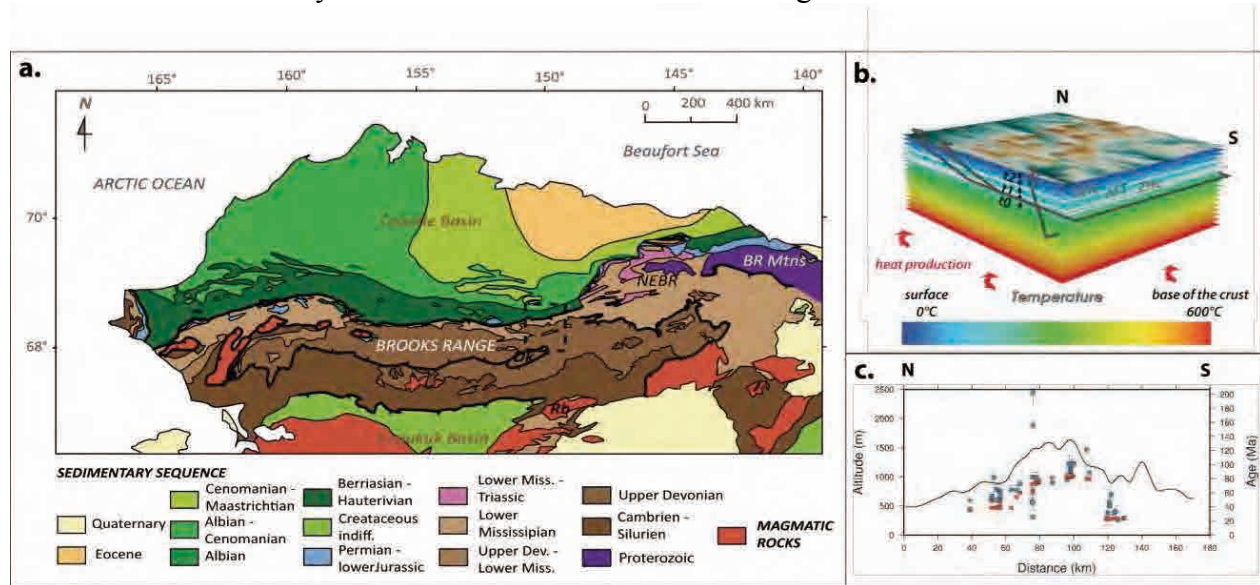


Figure 1. a. Geological map of the Brooks Range. b. Model set-up, including the faults geometry. c. Graph showing comparison between observed (blue) and calculated (red) ages as function of the distance, along N-S profile, across the Brooks Range.

References

1. Braun, J. Pecube: a new finite-element code to solve the 3D heat transport equation including the effect of a time-varying finite amplitude surface topography. *Comput. Geosci.* **29**, 787-794 (2003).
2. Braun, J., van der Beek, P., Valla, P., Robert, X., Herman, F., Glotzbach, C., Pedersen, V., Perry, C., Simon-Labric, T. & Prigent, C. Quantifying rates of landscape evolution and tectonic processes by thermochronology and numerical modeling of crustal heat transport using PECUBE. *Tectonics* **524-525**, 1-28 (2012).
3. O'Sullivan, P. B., Murphy, J. M., Moore, T. E. & Howell, D. G. Results of 110 apatite fission-track analyses from the Brooks Range and North Slope of Northern Alaska, completed in cooperation with the Trans-Alaska Crustal Transect (TACT), U.S. Department of the Interior – U.S. Geological Survey, Open-File Report 93-545 (1993).
4. O'Sullivan, P. B. in Thermal evolution of sedimentary basins in Alaska (eds. Johnsson, M. J. & Howell, D. G.) Bulletin 2142 (U.S. Geological Survey, 1996).
5. O'Sullivan, P. B., Murphy, J. M. & Blythe, A. E. Late Mesozoic and Cenozoic thermotectonic evolution of the central Brooks Range and adjacent North Slope foreland basin, Alaska: including fission track results from the Trans-Alaska Crustal Transect (TACT). *Journal of Geophysical Research* **102**, 20,821-20,845 (1997).

Exhumation of the Idaho Batholith and the western Idaho shear zone

Annia K. Fayon¹, Richard Gaschnig², Maureen J. Kahn³, Basil Tikoff⁴

¹ Department of Earth Sciences, University of Minnesota, 310 Pillsbury Dr SE, Minneapolis, MN 55455, USA

² Department of Geology, University of Maryland, College Park, MD 20742, USA

³ Geology, Carleton College, 300 North College St, Northfield, MN 55057, USA

⁴ Department of Geoscience, University of Wisconsin, 1215 W Dayton St, Madison, WI 53706, USA

Rocks exposed within the northern North American cordillera record a complex history of deformation, magmatism, accretion, and exhumation. This region roughly coincides with the Cretaceous-age margin of western North America that is in part defined by the 0.706 Sr isopleth¹ (Figure 1). Rocks exposed to the west of the 0.706 isopleth are oceanic terranes that accreted to the North American craton, whereas rocks to the east retain a continental affinity. In western Idaho, the Cretaceous to Early Tertiary Idaho batholith is exposed east of the deformed Cretaceous rocks of the western Idaho shear zone (WISZ). The WISZ is generally characterized by intense deformational fabrics and steep isotopic (Sr, Nd, O) gradients. Recent investigations document reactivation and deformation of the WISZ following accretion². (U-Th)/He zircon ages presented here focus on the cooling and exhumation of the WISZ and the adjacent Atlanta lobe of the Idaho batholith (Figure 1b). Results clearly indicate the WISZ records a different (older) cooling path than the Atlanta lobe and that the Atlanta lobe likely experienced internal deformation, potential resetting due to younger volcanic activity, and/or differential exhumation subsequent to deformation along the WISZ.

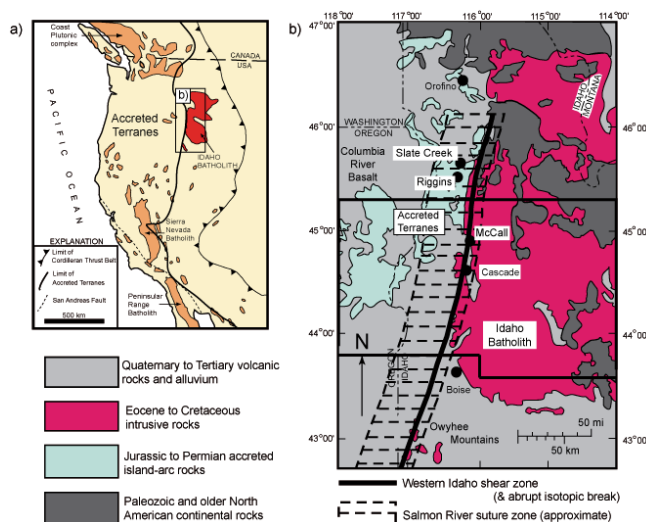


Figure 1. A. Map showing the location of the 0.706 Sr isopleth and the distribution of major intrusions in western North America. Idaho batholith is highlighted in red. B. Location map of the Salmon River suture zone, western Idaho shear zone (WISZ), and the Idaho batholith.

(U-Th)/He zircon ages are presented in Figure 2. Rocks within the WISZ (west of 116° W at ~ 44.5° N) yield the oldest (U-Th)/He zircon ages ranging from 75 to 65 Ma. U-Pb ages in this area range from 110 to 90 Ma³. Combined, these data are consistent with cooling rates of ~ 17 to 24 °C/m.y. Similar results were obtained in other exposures of the WISZ. To the north near McCall ⁴⁰Ar/³⁹Ar thermochronology studies indicate that cooling below 325 °C occurred at ~ 75 Ma (Ar/Ar on biotite) and 110 °C at ~40 Ma (apatite fission-track)². To the south the northern Owyhee Mountains of Idaho consist of granitic rocks locally affected by deformation associated

with the WISZ. As in other exposures of the WISZ, biotite $^{40}\text{Ar}/^{39}\text{Ar}$ analyses range from 71.5 ± 0.2 Ma in the east to 82.7 ± 0.2 Ma in the west. The consistency of the WISZ thermochronologic data support the through-going nature of the WISZ from the north southward across the western Snake River plain.

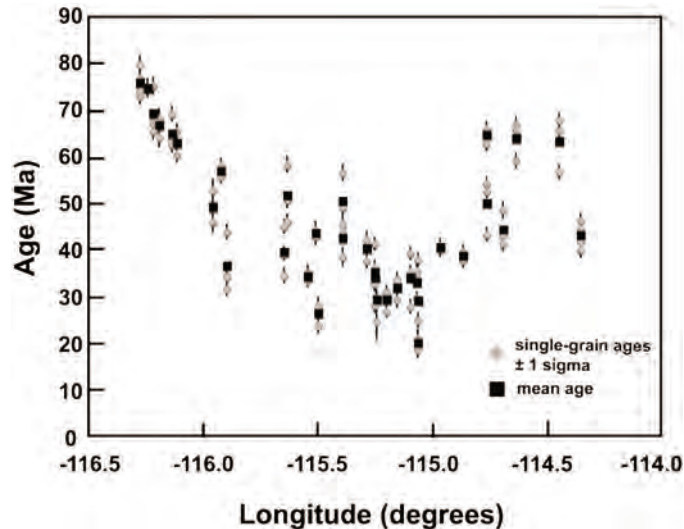


Figure 2. (U-Th)/He zircon single grain ages and mean ages for samples collected from the WISZ and Atlanta lobe of the Idaho batholith. Note the consistent cooling pattern west of 116° W, within the WISZ. East of 116° W, ages are more varied and inconsistent across the east- west transect.

East of the WISZ, the Atlanta lobe of the Idaho batholith is exposed³. (U-Th)/He zircon analyses from this phase yield more variations in ages ranging from 60 Ma to as young as 20 Ma. Combined with previous U-Pb ages, cooling rates vary significantly from as high as $40^\circ\text{C}/\text{m.y.}$ to less than $10^\circ\text{C}/\text{m.y.}$ The youngest ages obtained in this study are located in the normal fault bounded Sawtooth Mountains of central Idaho. Ages here range from 20.2 ± 0.3 to 34.2 ± 0.5 Ma. We interpret these young ages as recording the onset of cooling/normal faulting in Tertiary time.

In summary, the new (U-Th)/He zircon ages indicate a variable cooling history spanning ~ 50 m.y. for the igneous rocks of central Idaho. New ages obtained for rocks exposed within the WISZ near 44° N are consistent with results from other exposures of the shear zone and indicate the WISZ cooled below 200°C by 70 Ma. In contrast, the Atlanta lobe records a significantly different cooling history. Results clearly show the Atlanta lobe remained at temperatures greater than 200°C while the WISZ remained thermally stable.

References

1. Armstrong, R. L., Taubeneck, W. H. & Hales, P. O. Rb-Sr and K-Ar geochronometry of Mesozoic granitic rocks and their Sr isotopic composition, Oregon, Washington, and Idaho. *Geological Society of America Bulletin* **88**, 397-411 (1977).
2. Giorgis, S., McClelland, W., Fayon, A., Singer, B. S. & Tikoff, B. Timing of deformation and exhumation in the western Idaho shear zone, McCall, Idaho. *Geological Society of America Bulletin* **120**, 1119-1133 (2008).
3. Gaschnig, R. M., Vervoort, J. D., Lewis, R. S., & McClelland, W. C. Migrating magmatism in the northern US Cordillera: in situ U-Pb geochronology of the Idaho batholith. *Contributions to Mineralogy and Petrology* **159**, 863-883 (2010).

Thermochronology of the Santander Massif, Eastern Cordillera, Colombia, South America.

Sergio Amaya¹, Matthias Bernet², Carlos A Zuluaga³

1 National University of Colombia, building Manuel Ancizar 224, office 301 Bogota, Colombia

2 Université Joseph Fourier, 1381 Rue de la piscine, BP 53, 38041 Grenoble Cedex, France

3 National University of Colombia, building Manuel Ancizar 224, office 301, Bogota, Colombia

New data thermochronological, geochronological and petrological of different lithodemic units that constitute the metamorphic basement of the Santander massif, permit to establish a link between the metamorphic age and magmatic history of the Santander Massif with its most recent evolution (Cenozoic exhumation and surface elevation, since most of the previous works have focused on metamorphic petrology and not on the recent tectonic evolution). After all Santander Massif plays a key role in understanding the evolution of the Northern Andes.

This research allows identifying which are the ages of the different events that record the evolution tectono - metamorphic of Santander Massif; when and how the thermal history was, how much was the rate of exhumation, which factors controlled the exhumation and how is the relationship exhumation of Santander Massif regarding: the exhumation of the Sierra de Mérida in Venezuela, Sierra Nevada de Santa Marta and the Eastern Cordillera in Colombia in order to understand the regional tectonic setting of the Andean north in South America.

The basement of the Santander Massif consists of metamorphic rocks, Precambrian age to Paleozoic, cut by intrusive bodies of Triassic and Jurassic¹⁻². The metamorphic rocks of the basement has been divided into three units that of the lowest structural position toward up are Neis of Bucaramanga, Silgará Schists and Ortoneis. The basement Santander Massif is unconformably covered by rocks with low-grade metamorphism of the metasedimentary Guaca - Virgin (formerly Floresta Formation metamorphosed), by the Lower Devonian clastic sediments (Tibet Formation) and by calcareous and clastic sediments of the Carboniferous and Permian (Diamond Formación and Paleozoic of Snowy river) that unconformably cover it, due to pre - Cretaceous erosional events. See Figure 1 for location of the studied area.

References

1. Goldsmith, R., Marvin, R. & Mehnert, H Radiometric ages in the Santander Massif, Eastern Cordillera, Colombia Andes. U.S.A *Geological Survey Professional Paper*, **750-D**, 41-49 (1971).
2. Boinet, T., Bourgeois, J., Bellon, H. & Toussaint, J.F Age et répartition du magmatisme Prémésozoïque des Andes de Colombie. *Compte-rendu de l'Académie des Sciences de Paris*, **300**, 445-450 (1985).

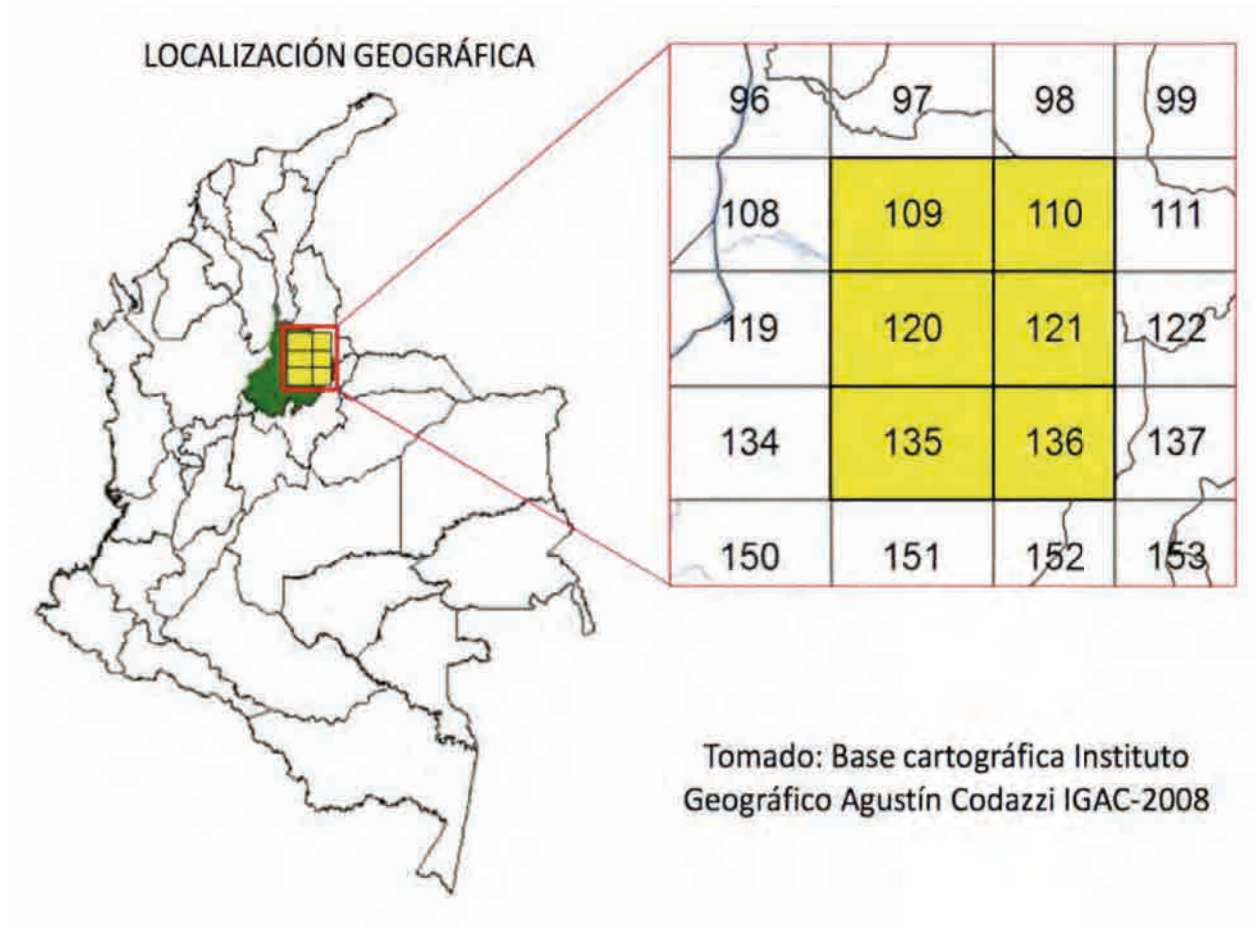


Figure 1. Geographical location of the work area, in the central and southern part of the Massif, in the Department of Santander, Colombia, South America.

Dating Apparent Erosion in the Northeast Brazilian Rifted Margin Using Quantitative Thermochronology

Gilvan P. Hamsi Jr.¹, Kerry Gallagher²
1 PETROBRAS, Brazil

2 Université de Rennes, Géosciences Rennes, France

The aim of this work was to date the apparent erosion displayed in four wells onshore the Northeast Brazilian Rifted Margin. Apparent erosion, the difference between maximum and present burial¹, of 200 to 700 m have been measured using sonic logs in two wells from the north compartment and two wells from the south compartment. A remarkable unconformity separates the Plio-Pleistocene cover from the sin-rift Early Cretaceous or post rift Late Cretaceous strata. The unconformity represents a wide hiatus from 70 to 100 M.y. High uncertainties in basin modelling are brought by wide erosion ages, as most of the processes are influenced by the time of maximum compaction. The four studied wells have been sampled for Apatite Fission Track with 5 to 7 samples each. The apatite sampled at each well crosses the apatite fission track annealing zone (60-120°C). Thermal histories consistent with each AFTA dataset have been determined by transdimensional inversion² in a Bayesian approach. Expected (average) thermal histories models have been selected from 100.000 to 1500.00 model runs, controlled by Markov-Chain Monte Carlo sampling, using as acceptance criteria mean apatite fission track lengths, mean apatite fission track ages and vitrinite reflectances². Prior information defined the model space for the Markov-Chain Monte Carlo sampling²: 1) temperature ranges, starting from the shallowest sample present temperature and encompassing the annealing zone; 2) wide range of time, encompassing the rift onset; 3) temperature gradient from the temperature difference between the shallowest and deepest samples, and 4) time-temperature number of points, which defines the complexity of the thermal history. The maximum likelihood models is the one that best fits the data, while the maximum posterior probability model tells what additional information there is in the data, relative to what was previously known². Expected models of each well, the average of accepted models, have been selected, as they bring more information about the uncertainty in the thermal histories. The expected models point to gradual cooling after 90 to 60 M.a., which suggests widespread deposition of the albo-turonian Marine Carbonatic megasequence³ and local deposition of the neo-cretaceous Silicicatic Transgressive megasequence³.

References

1. Corcoran, D. V. & Doré, A. G. A review of techniques for the estimation of magnitude and timing of exhumation in offshore basins. *Earth-Science Reviews* **72**, 129-168 (2005).
2. Gallagher, K. Transdimensional inverse thermal history modeling for quantitative thermochronology. *J. Geophys. Res.* **117**, B02408 (2012).
3. Chang, H. K., Kowsmann, R. O., Figueiredo, A. M. F. & Bender, A. A. Tectonics and stratigraphy of the East Brazil Rift system: an overview. *Tectonophysics* **213**, 97-138 (1992).

Reactivation of structural lineaments in northeastern Brazil and the influence of Equatorial Atlantic Opening: Apatite fission-track modelling enhanced by heavy ions irradiation.

Daniel Françoso de Godoy^{1*}, Peter C. Hackspacher¹, Ulrich A. Glasmacher²

1 Departamento de Petrologia e Metalogenia, Instituto de Geociências e Ciências Exatas, Universidade Estadual Paulista (Unesp), Brazil

2 Institute of Earth Sciences, University of Heidelberg, Germany

* Corresponding author: dfgodoy@gmail.com

The opening of the Atlantic Ocean during the break-up of Gondwana had a critical influence on the reactivation of the South American Platform, resulting in reactivation of major lineaments, extensive volcanic activity, and substantial modification of topographic relief. Current knowledge of the tectonic evolution of northeastern Brazil suggests some influence by the Central Atlantic opening (Triassic–Jurassic) but a more significant influence by the Equatorial Atlantic opening (Early Cretaceous). To verify the influence of the break-up of Gondwana in northeastern Brazil, we focused on the Sobral-Dom Pedro II Shear Zone and the Senador Pompeu Shear Zone where they converge with the Parnaíba Basin, western Ceará State. These northwest–southeast trending shear zones surround two transtensional basins, the Jaibaras and Cococi Basins (Cambro-Ordovician) respectively, which evolved from troughs formed by brittle reactivation of the shear zones. Apatite fission track ages from the Sobral-Dom Pedro II Shear Zone area range from 86 ± 12 to 158 ± 25 Ma (± 1 sigma), indicating movement in the shear zone during the Upper Cretaceous. Ages from the Senador Pompeu Shear Zone area cluster in two groups around 320 and 235 Ma representing a nearly 100 Ma age difference between samples from the same elevation in an area with no mapped structures. The thermal history modelling enhanced by heavy ions irradiation of samples from both sites shows a faster cooling during Eocene. Therefore Senador Pompeu Shear Zone underwent cooling in the Late Carboniferous, Late Triassic, and Early Jurassic. The first and second cooling events are temporally equivalent to discordances in the Parnaíba Basin, indicating rock and surface uplift over a broader area. The third event was contemporaneous to the deposition of volcanic rocks in the Mosquito Formation (Parnaíba Basin), which is part of the Central Atlantic Magmatic Province. The results from Sobral-Dom Pedro II Shear Zone area indicate that it was reactivated at approximately 120 Ma, pointing to the influence of the opening of the Equatorial Atlantic. No such reactivation was detected in the Senador Pompeu Shear Zone.

Finally the thermal history modelling shows that both areas underwent to a reactivation during Eocene followed by erosion. Such reactivation may have contributed to volcanism in the Ceará and Potiguar Basins.

Acknowledgements: To Capes (Coordenadoria para o Aperfeiçoamento de Pessoal de Nível Superior) and CNPq (Conselho Nacional de Desenvolvimento Científico e Tecnológico) for financial support of this work; To GSI (Helmholtzzentrum für Schwerionenforschung GmbH) for heavy ion irradiations.

Post-Rift Reactivation in the Southeastern Brazilian Passive Continental Margin: Long-Term Landscape Evolution through AFT- and ZFT-data

Ana Olivia Barufi Franco-Magalhães¹, Matheus Augusto Alves Cuglieri¹, Peter Christian Hackspacher³, Antonio Roberto Saad⁴

¹ Universidade Federal de Alfenas – Campus Poços de Caldas, Brazil

² Petrobras, Brazil

³ Universidade Estadual Paulista – Unesp/Rio Claro, Brazil

⁴ Universidade Guarulhos, Brazil

Zircon and Apatite fission-track low-temperature thermochronology were applied at the Brazilian passive continental margin (Figure 1) in order to understand and reconstruct the post-rift evolution since the break-up of southwestern Gondwana. The thermochronological data obtained from samples of both the Precambrian basement and the Paleogene to Neogene sedimentary rocks from the Continental Rift of Southeastern Brazil provided ZFT-ages between 148 (15) Ma and 64 (6) Ma, and AFT- ages of 81 (8) to 29 (3) Ma. These data clearly indicate syn- and post-rift reactivations during the Early Cretaceous, with great emphasis in Paleogene to Neogene times. ZFT and AFT- ages yield spread values that become younger as samples are closer to the reactivated Neoproterozoic shear zones, parallel to the Taubaté Basin and might reflect source area exhumation. The analysis of ZFT- and AFT- data allowed interpretations regarding the main phases that occurred in the study area related to the thermotectonic and tectono-stratigraphic evolution from Early Cretaceous, which can be described in three main phases: (1) Late Jurassic to Early Cretaceous, (2) Late Cretaceous, and (3) Paleogene to Neogene.

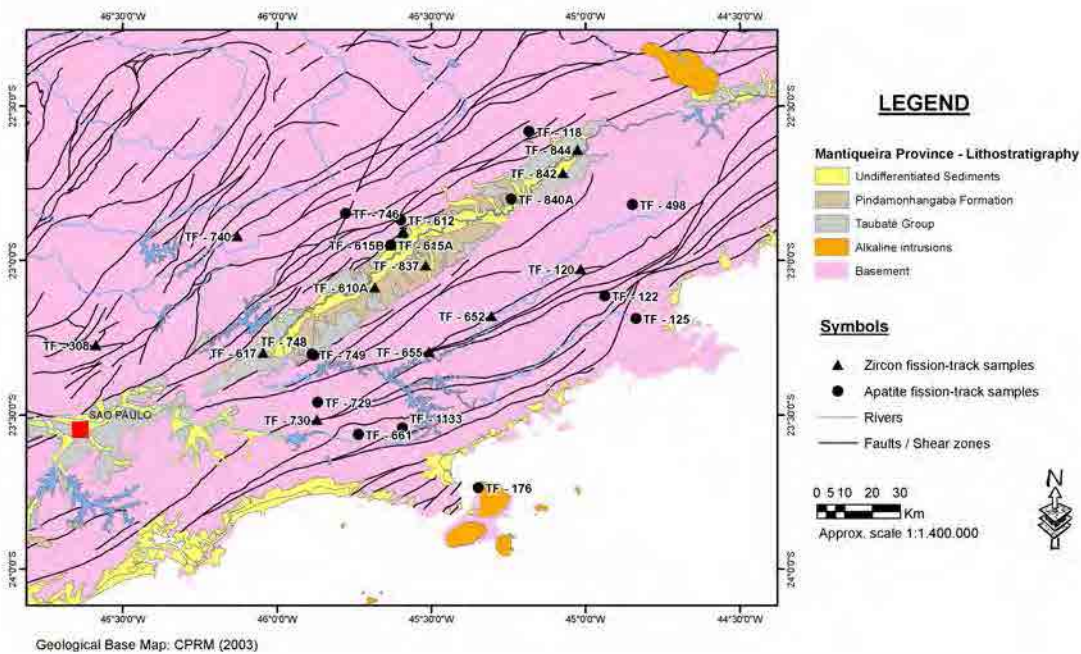


Figure 1. Geological map of the study-area with collected samples for AFT- and ZFT-analysis. Geological base from CPRM/Geological Survey of Brazil¹.

Acknowledgements for financial support from “State of Minas Gerais Research Foundation/FAPEMIG” and IPEN/CNEN Nuclear Reactor, Brazil, for the sample irradiations.

References

1. CPRM Companhia de Pesquisa de Recursos Minerais/ Geological Survey of Brazil. Geologia e Recursos Minerais do Estado de São Paulo: Sistemas de Informações Geográficas (SIG). Mapas Geológicos Estaduais escala 1:750 000. CD-ROM (2006).

Evolution of the Serra do Mar mountains implications interpreting apatite fission track and (U-Th)/He ages from passive continental margin

Marli C. Siqueira-Ribeiro¹, Everton T. Sulato¹, Danieli F. Canaver Marin¹, Peter C. Hackspacher¹, Finlay M. Stuart²

1 Department of Petrology and Metallogeny, São Paulo State University, Rio Claro (SP), Brazil

2 Scottish Universities Environmental Research Centre, East Kilbride G75 0QF, United Kingdom

The Serra do Mar mountains (SdM) along the southern part of the Brazilian passive continental margin is characterized by a low-lying coastal plateau separated from the elevated inland plateau by a steep escarpment. They are the result of complex tectono- magmatic evolution since the breakup of Western Gondwana and opening of the South Atlantic Ocean in Early Cretaceous¹. We are investigating the formation of the SdM by combined apatite fission track (AFT) and apatite (U-Th)/He (AHe) thermochronology in order to understand and reconstruct the post-rift evolution since the break-up of southern Gondwana and landscape evolution of different morphologies that comprise the SdM.

AFT data of samples of Precambrian crystalline basement indicate that the SdM underwent slow cooling from early Cretaceous to Paleocene¹⁻⁵ associated extensional reactivation processes correlated to the rift stage process in Atlantic margin and evolution of continental rift systems¹⁻⁵. Exhumation during the early Cretaceous was accommodated by normal faults along the Taxaquara and Cubatão shear zones. The mountain range and present day drainage network was likely established at this time. Late Cretaceous cooling ages are related to a regional tectonic reactivation and erosion to the uplift and denudation of the Serra do Mar coeval, with associated Cabo-Frio alkaline magmatism¹. A later phase of uplift and erosion in the Paleocene is associated with the formation of the graben-structures which generated Taubate basin (Figure 1).

Attempts to provide better constraints on the exhumation history of the SdM are hampered by AHe ages that are frequently older than corresponding AFT ages. The reason for this is currently not clear. Chemical and mechanical abrasion of selected apatite samples is being undertaken in order to quantify the effect of parent element zonation and/or implanted He.

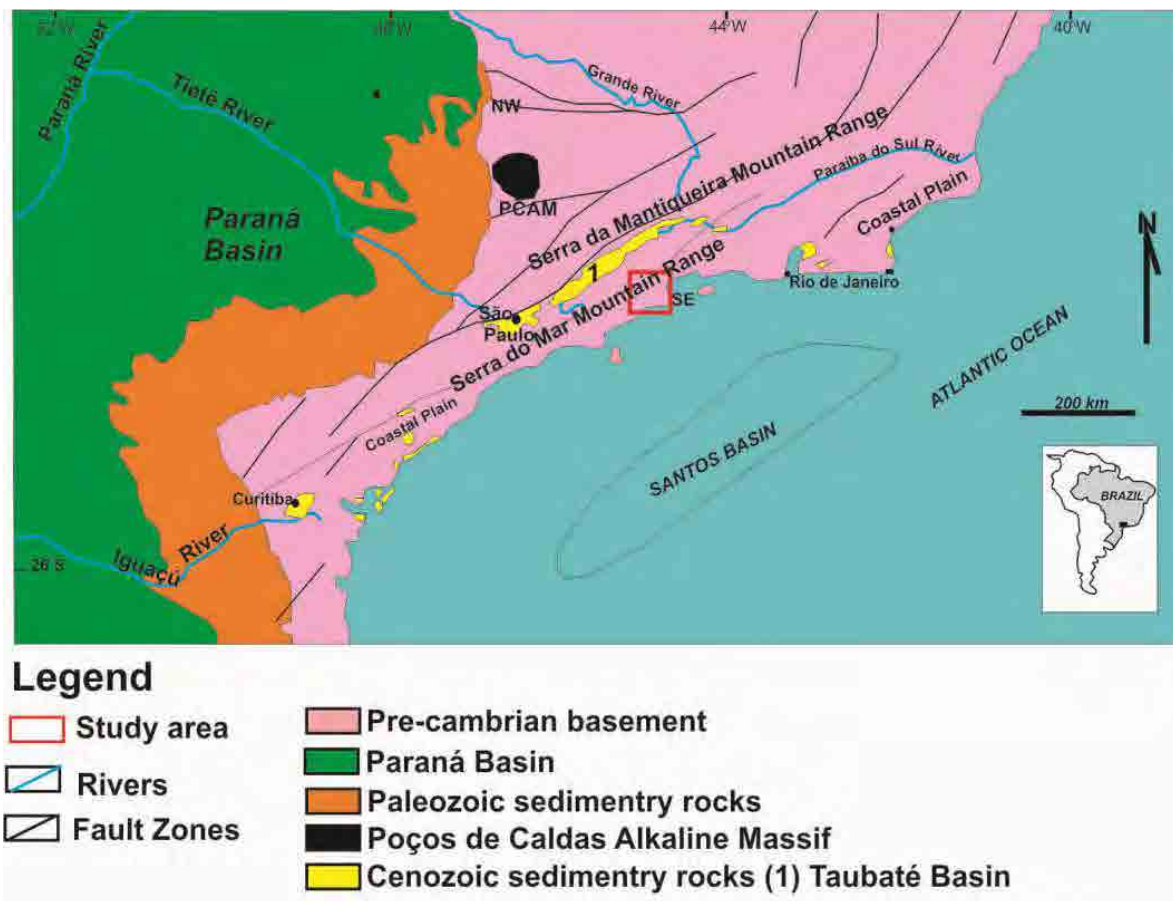


Figure 1. Geological map of the Serra do Mar. Modified from²

Acknowledgments: The authors are grateful to the São Paulo State Research Foundation (FAPESP) for scholarship of the Marli Carina Siqueira Ribeiro (Proc. 03/07574-0 and Capes (Ciência sem Fronteiras) (processo número: 081/2012).

References

1. Almeida, F. F. M. & Carneiro, C. Dal Ré. Origem e evolução da Serra do Mar. *R.B.G.* **28**, 135-150 (1998).
2. Riccomini, C., et al. in *Geologia do Continente Sul Americano Evolução geológica do Rift Continental do Sudeste do Brasil* 383-405 (2004).
3. Hackspacher, P. C., Ribeiro, L. F. B., Ribeiro, M. C. S., Fetter, A. H., Hadler Neto, J. C., Tello, C. E. S. & Dantas E.L. Consolidation and Break-up of the South American Platform in Southeastern Brazil: Tectonothermal and Denudation Histories. *Gondwana Research* **7**, 91-101(2004).
4. Hiruma, S.T., Riccomini, C., Modenesi-Gauttieri, M. C., Hackspacher, P., Hadler Neto, J. C. & Franco-Magalhães, A. O. B. Denudation history of the Bocaina Plateau, Serra do Mar, southeastern Brazil: Relationships Gondwana breakup and passive margin development. *Gondwana Research* **18**, 674-687 (2010).
5. Siqueira-Ribeiro, M. C., Hackspacher, P. C., Ribeiro, L. F. B. & Hadler Neto, J. C. Evolução Tectônica e denudacional da Serra do Mar (SE/Brasil) no limite entre o Cretáceo Superior e Paleoceno, utilizando análises de traços de fissão e U-Th/He em apatitas. *Revista Brasileira de Geomorfologia* **12**, 3-14 (2011).

The Paleocene and Eocene on the South Atlantic margins: low temperature thermochronology at southeast Brazil and south of Angola

Peter C. Hackspacher¹, Rosante Kaique², Antonio O. Gonçalves³, Ulrich A. Glasmacher⁴

1 IGCE/UNESP, Universidade Estadual Paulista, Brazil, phack@rc.unesp.br

2 Pos-Grad Regional Geology, Universidade Estadual Paulista, Brazil

3 Departamento de Geologia da Faculdade de Ciências da Universidade Agostinho Neto, Angola

4 Institute of Earth Sciences, University Heidelberg, Germany

The thermochronological evolution of the South Atlantic margins and its post-break-up history needs to be understood using different geological and geomorphologic knowledge in on- and offshore regions. The literature describes a complex history with: i) Early Cretaceous tectonic, magmatism and exhumation processes related to the Gondwana break-up, around 130 Ma; ii) Late Cretaceous basement uplift; iii) Early Paleocene extensional tectonic causing uplift and erosion; and iv) Oligocene to Miocene reactivation in NE-SW and NW-SE directions followed by exhumation and denudation. Related sedimentary basins are described in off- and onshore regions.

Thermochronological data on a NW-SE profile south of Rio de Janeiro (Brazil), and a E-W profile south of Luanda (Angola), shows some correlations in the counterparts, upside the complete spatial evolution. Considering only the Paleocen and Eocen, the southeast Brazilian margin present boths tectonic evolutions, in Angola the Eocen reactivation is missing. Evidences of paleothermal event at 20-10 Ma were related at the Kwanza basin.

The cause of the heterogeneous evolution on both side of the South Atlantic margins need to be discussed using crustal and mantle dynamics.

The tectonic-thermal history of the Southern Brazilian Shield and the relation to the depositional history of the Parana Basin

Andréa Ritter Jelinek¹, Ruy Paulo Philipp¹, Farid Chemale Jr.², Ubiratan Faccini³,
Adriano R. Viana⁴, Ernesto Lavina³

1 Instituto de Geociências, Universidade Federal do Rio Grande do Sul, Brazil

2 Instituto de Geociências, Universidade de Brasília, Brazil

*3 Programa de Pós-Graduação em Geociências, Universidade do Vale do Rio dos
Sinos, Brazil*

4 Petrobras, Brazil

Apatite fission track thermochronology studies are applied to unravel the tectonic history of the onshore southernmost Brazilian margin. Analyzed samples are collected in the Sul-rio-grandense Shield to address the Phanerozoic morphotectonic evolution of the margin, which included the intracratonic Paraná Basin and Mesocenoic rocks.

The Sul-rio-grandense southern shield, southern Brazil, is a major geotectonic feature of southernmost Brazil that includes Paleoproterozoic basement areas and Neoproterozoic fold belts linked to Brasiliano/Pan-African cycle. Crustal reworking and juvenile accretion events related to this cycle were positioned in the region between 900 and 500 Ma¹ and were responsible for the assembly of southwestern Gondwana in southeastern South America. This shield is surrounded by the Paleozoic to Triassic sedimentary rocks of the Paraná Basin, which is in turn covered by the Cretaceous magmatic rocks of the Serra Geral Fm., so-called Paraná basalts. The shield is divided into four terranes, namely, Taquerembó, São Gabriel, Tijucas, and Pelotas- Florianópolis ones. The first one is mostly composed by granulitic granitic-gneissic complex intruded by Brasiliano granites, whereas the other three are composed mainly by Neoproterozoic to Eopaleozoic bounded by major suture zones.

The intracratonic Paraná Basin, deposited on the Precambrian to Eopaleozoic basement rocks, is a NE–SW-elongated intracratonic basin in South America and covers a surface area of around 1,700,000 km². Six second-order stratigraphic megasequences are recognized in this basin, separated by regional discordances, as follow: Rio Ivaí (Caradocian-Llandoveryan), Paraná (Lochkovian-Frasnian), Gondwana I (Westphalian-Scythian), Gondwana II (Anisian-Norian), Gondwana III (Neojurassic-Berriasian) and Bauru (Aptian-Maastrichtian). Many authors^{2,3} have related the reactivation of basement structures with regional-scale tectonic events, recognizing its controls on basin structuration, sedimentary processes, subsidence rates, and position of depocenters throughout basin history.

Apatite fission track analyses were performed followed three approximately NW-SE and two NE- SW profiles in basement adjacent to the Paraná Basin. The apparent fission track ages vary from 383 ± 41 to 70 ± 5 Ma and can be divided into four groups, related with regional-scale tectonic events. The Devonian-Carboniferous ages (380-340 Ma) are exclusive to Paleoproterozoic Taquarembó terrane. This period may reflect tectonic activity of the Famatinian Event with the generation of the unconformity between the Rio Ivaí and the Rio Paraná megasequences. The Permian ages were recognized in samples collected in São Gabriel terrane, where we recognized two clusters, one from 293 to 275 Ma and other from 245 to 250 Ma. The

age close to 280 Ma marks the unconformity between Gondwana Ia and Gondwana Ib sequences in Paraná Basin, while the ages close to 250 Ma record the Gondwanides orogenic event (Pangea Formation). The samples collected in the Tijucas terrain registered Upper Triassic – Lower Jurassic ages, interpreted as late orogenic process of the Gondwanides Event. The easternmost terrane, Pelotas Batholith, contains fission tracks apparent ages of 277-200 Ma, in the NE sector, and younger ages of 190 to 150 Ma, mostly representing the late stages of the Gondwanides and early plate adjustment of pre-drifting of South America and Africa plates.

However along the major Brasiliano suture zones, as Caçapava do Sul and Canguçu Dorsal shear zone, ages of 130 to 70 Ma are determined. These Cretaceous ages can be correlated to the tectonic movements associated with NE-SW and NW-SE-trending strike-slip and normal faults³, which do they correspond to basement reactivated structures during the rift and post-rift phases of Atlantic ocean opening.

Based on thermal history modeling we recognized five cooling episodes which they can be associated with the following intervals: (1) 380-300 Ma (Devonian-Carboniferous) (2) 290-250 Ma (Permian), (3) 250-200 Ma (Triassic), (4) 150-100 Ma (Early Cretaceous), and (5) 60 Ma to the present (Cenozoic). The four first intervals correspond roughly to the depositional time of the Megasequences Paraná, Gondwana I, II, and III. The latter one is related to the Cenozoic adjustment and reorganization plate with denudation and consequently deposition of the Pelotas Basin sedimentation.

References

1. Chemale Jr., F. in *Geologia do Rio Grande do Sul* (eds. Holz, M. & De Ros, L. F.) 13-52 (CIGO/Universidade Federal do Rio Grande do Sul, Porto Alegre, 2000).
2. Milani, E. J. & Ramos, V. A. Orogenias Paleozóicas no domínio sul-ocidental do Gondwana e os ciclos de subsidência da Bacia do Paraná. *Revista Brasileira de Geociências* **28**, 473-484 (1998).
3. Zerfass, H., Chemale Jr., F. & Lavina, E. Tectonic Control of the Triassic Santa Maria Supersequence of the Paraná Basin, Southernmost Brazil, and its Correlation to the Waterberg Basin, Namibia. *Gondwana Research*, **2**, 163-176 (2005).

Mesozoic-Cenozoic evolution of the northern West African Craton

Rémi Leprêtre¹, Yves Missenard¹, Jocelyn Barbarand¹, Cécile Gautheron¹, Omar Saddiqi², Rosella Pinna-Jamme¹

¹ Université Paris Sud, GEOPS UMR CNRS 8148, Relief et bassin, Bât. 504, rue du Belvédère 91405 Orsay, France

² Université Hassan II Ain Chock, Laboratoire Géosciences, BP 5366 Maârif, Casablanca, Morocco

Cratonic areas are affected by vertical motions¹ (i.e. denudation or burial), the mechanisms of the latter being nonetheless still debated. Tempo and rhythms of these motions have been studied for few cases, but often based on stratigraphical recent formations² and limited to predictions for the Neogene, or Cenozoic information. The solo methodology that brings true new insights for longer timescales is the low-temperature thermochronology. We focused our study on the impact of the development of a passive margin, to explore its impact and the wavelength of this phenomenon deep in a cratonic continental interior. The dynamic of the craton itself has also been questioned with respect to the development of the margin to distinct “intrinsic” features, related to the craton itself and “extrinsic” ones.

These questions were handled with the study of the West African Craton (WAC), and especially the Reguibat Shield in its northern part. This craton has an intermediate size for a craton, and holds an key location in Africa (Figure 1). The Reguibat Shield is bounded north and south by two long-term subsiding cratonic basins, Tindouf and Taoudeni. Its eastern boundary reaches the Panafrican suture where evidences of reactivation exist throughout the Phanerozoic³. Moreover, it also represents a portion of the passive margin of the eastern Central Atlantic Ocean, subjected to rifting and extension during Early and Middle Jurassic⁴.

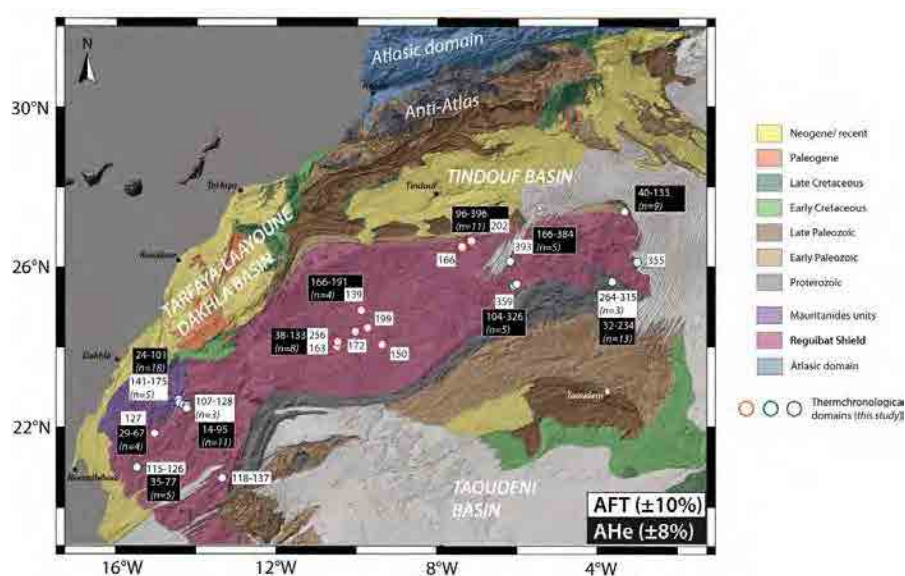


Figure 1. Geological map of the Northern WAC. AFT and AHe ages are presented in white and black boxes, respectively. Errors are 10% for AFT ages and 8% for AHe ages (corrected for α -ejection).

We present the first low-temperature thermochronology study that undertakes the evolution of the WAC. This craton represents a very interesting location as it experienced a complex array of geodynamic configurations through times: Africa underwent the rifting of Central Atlantic ocean from Trias to Early-Middle Jurassic⁵, then a wide so-called “quiescent” period from Middle-Late Jurassic to Late Cretaceous and the onset of Africa/Europe convergence from Late Cretaceous on. The data presented here show that this simple division is not accurate and thermochronology allows to further discuss the problem of supposed stability in cratonic areas.

We collected 29 samples of basement rocks from the Reguibat Shield following an East-West transect. The AFT ages range from 107 ± 8 Ma to 393 ± 36 Ma, with MTLs from 9.4 ± 0.27 μm to 12.5 ± 0.18 μm . The AHe ages, corrected from α -ejection, range from 14 ± 1 Ma to 396 ± 32 Ma. We observe a clearly younging trend in both AFT and AHe ages when going seaward. Thermal modelings have been processed for all samples with inverse and forward approaches.

The modelings strengthened some aspects of the evolution of the WAC. First, an important cooling event, together with spread denudation of the Reguibat Shield occurred throughout the region, from Late Jurassic to mid-Lower Cretaceous, though it was more important for the western and central part of the shield. This event is concomitant with the drowning of the whole North Africa under immense coarse, detrital deposits named “Continental Intercalaire”. Second, and previously unidentified, more or less developed reheating phases occurred until Late Cretaceous, where we reveal a spatialization of the patterns of exhumation from West to East. The margin is indeed more affected by local events than the interior of the craton.

References

1. Cogné, N., Gallagher, K., Cobbold, P. R., Riccomini, C. & Gautheron, C. Post-breakup tectonics in southeast Brazil from thermochronological data and combined inverse-forward thermal history modeling. *Journal of Geophysical Research* **117** (2012).
2. Japsen, P., Bonow, J. M., Green, P. F., Cobbold, P. R., Chiossi, D., Lilletveit, R., Magnavita, L. P. & Pedreira, A. Episodic burial and exhumation in NE Brazil after opening of the South Atlantic. *Geological Society of America Bulletin* **124**, 800-816 (2012).
3. Beauvais, A. & Chardon, D. Modes, tempo, and spatial variability of Cenozoic cratonic denudation: The West African example. *Geochemistry, Geophysics, Geosystems* **14** (2013).
4. Fabre, J., *Géologie du Sahara occidental et central* (Tervuren African Geoscience Collection, 108, Musée Royal de l'Afrique Central, 2005).
5. Labails, C., Olivet, J. L., Aslanian, D. & Roest, W. R. An alternative early opening scenario for the Central Atlantic Ocean. *EPSL* **297**, 355-368 (2010).

(U-Th)/He dating of apatite and zircon constrains erosion patterns and emplacement ages of kimberlites across the Kaapvaal Craton

Jessica R. Stanley¹, Rebecca M. Flowers¹, David R. Bell²

1 Department of Geological Sciences, University of Colorado, Boulder, CO, USA

2 School of Earth and Space Exploration and Department of Chemistry and Biochemistry, Arizona State University, Tempe, AZ, USA

Deciphering the patterns and causes of erosion and elevation change histories in continental interiors is commonly not straightforward. Many continental shield regions were repeatedly intruded by small volume kimberlite magmas, which commonly contain rich xenolith records of the state of the lithosphere and the sedimentary cover at the time of eruption. Here we show that zircon (U-Th)/He (ZHe) dating of kimberlites to determine eruption ages, combined with apatite (U-Th)/He (AHe) cooling dates, can be used to constrain detailed thermal histories associated with erosion through the upper 1-3 km of crust. Mantle xenoliths from kimberlites erupted at different times also record perturbations to the lithospheric mantle, indicators of changes to the mantle below. The coeval deep and shallow records of kimberlite pipes thus allow the potential to link deep earth processes with the surface response.

Here we present an example of this approach in the southern African Plateau. This region was elevated from sea level to >1000 m elevation in post-Paleozoic time while distal from convergent plate boundaries and with little surface deformation. The timing and mechanisms of surface uplift are debated. Our published AHe data for four kimberlites off the southwestern corner of the Kaapvaal Craton indicate a substantial Mesozoic unroofing episode that was largely completed by 90 Ma. This erosion phase is contemporaneous with significant warming, metasomatism, and thinning of the lithospheric mantle revealed in the peridotite xenoliths and garnet xenocrysts in these same pipes. We suggest that this surface signal is the erosional response to regional, mantle-induced surface uplift. These data also detect a lesser Cenozoic erosion signature in some pipes, focused around a proposed Tertiary paleo-tributary to the Orange River, suggesting that the Cenozoic signal is associated with drainage network evolution rather than long-wavelength surface uplift. Here we extend this method to a larger transect of kimberlites across the Kaapvaal Craton. AHe data indicate a similar mid-Cretaceous unroofing event with some spatio-temporal variability. We also show that ZHe can be used to determine the emplacement ages of these pipes, which are sometimes challenging to date by other methods. The combination of ZHe and AHe on kimberlites together with the wealth of other geologic information contained in these pipes provides a powerful tool for discerning detailed erosion histories of cratons and potential deep-seated causes.

The southern African plateau – the first empirical evidence for prolonged geomorphic stability of the cratonic interior

Vhairi Mackintosh^{1*}, Roderick Brown¹, Mark Wildman¹, Romain Beucher², Andrew Hutcheson¹, Fin Stuart³

1 School of Geographical & Earth Sciences, University of Glasgow, Glasgow, Scotland

2 Department of Earth Science, University of Bergen, Bergen, Norway

3 Scottish Universities Environmental Research Centre, East Kilbride, Scotland

**Now at: School of Earth Sciences, University of Melbourne, Melbourne, Victoria 3010, Australia*

The high elevation of the interior of southern Africa is anomalous for a region in which convergent plate boundary processes are absent¹. For this reason, the history of the southern African plateau has been the subject of much scientific interest to thermochronologists and geomorphologists attempting to constrain the timing, rate and underlying cause of uplift. Thermochronology provides a quantitative method for determining cooling and constraining denudation histories. The technique cannot measure uplift directly, however, when other geological or geomorphological evidence and reasoning suggest that cooling and denudation are linked to surface uplift then it can provide the basis for constraining uplift histories.

A large number of low-temperature thermochronology studies carried out in southern Africa propose that a rapid cooling event - mainly interpreted as the result of uplift and erosion - occurred in the mid-late Cretaceous¹⁻³. The majority of these studies utilised apatite fission track (AFT) thermochronometry. However, the reliability of these results are restricted largely to the temperature range, ~60-110 °C, and corresponding crustal depths over which this technique is applicable⁴. The apatite (U-Th)/He (AHe) dating method is sensitive over a lower temperature range, typically ~35- 75°C, and thus may provide greater certainty in constraining the more recent thermal history⁵. Additionally, combining data obtained using both techniques should ideally result in consistent thermal histories that have a greater reliability due to their overlapping temperature sensitivity ranges⁵. In slowly cooled cratonic settings, such as the interior of southern Africa, complicating factors often lead to apparent discrepancies between the expected apatite fission track and (U- Th)/He age relationship⁶. New insights into the range of controls on age dispersion and diffusivity of He within apatite now enable this dispersion to be harnessed constructively to constrain thermal histories and to resolve these apparent discrepancies⁷⁻⁹. Nevertheless, combined low-temperature thermochronology studies are distinctly lacking in the Kaapvaal craton due to the shortage of apatite (U-Th)/He data in comparison to the extent of previous apatite fission track work reported from southern Africa.

This study reports 25 new single grain apatite (U-Th)/He ages for three samples ranging in depth from 194 m to 430 m taken from the Kraaipan (DBT) borehole located within the north-west Kaapvaal craton, South Africa, as well as new apatite fission track analysis data from two of the samples. The mean (U-Th)/He date and standard deviation for the three samples analysed is 306.1±44.0 Ma. The two AFT ages obtained were 380±22 Ma (194 m) and 277±14 Ma (277 m) with both samples yielding unimodal, negatively skewed track length distributions with mean lengths of c. 13.4 µm. These dates suggest that the region has resided below the apatite (U-Th)/He closure temperature of approximately 70°C¹⁰ since at least the late Paleozoic. Joint thermal history modelling of the combined AHe and AFT data indicates significant cooling from elevated palaeotemperatures during the Devonian-Carboniferous (possibly related to the Pan African Orogeny) followed by a prolonged period of thermal stability since at least ~250 Ma.

These results indicate that this location within the interior of southern Africa did not experience the mid-late Cretaceous period of accelerated cooling documented elsewhere by low-temperature thermochronological studies¹⁻³. Hence, whilst the outer continental locations, and parts of the interior,

experienced significant cooling driven by erosion and associated with, for instance, the breakup of Gondwanaland¹¹, the north-west region of the Kaapvaal craton was undergoing gradual denudation with concomitant sedimentation into the Kalahari basin. This interpretation is supported by the preservation of early Cretaceous and younger fluvial gravels in the area¹². The considerable intra-sample variation in single grain AHe ages is also consistent with samples that have experienced slow cooling with long residence within the partial retention zone of the (U-Th)/He system⁸. Preliminary investigation of this dispersion within the data, that exceeds analytical error, suggests that radiation damage, the presence of U-Th rich micro-inclusions and grain fragmentation are the main factors affecting the single grain ages.

The low-temperature thermochronology results from the Kraaipan (DBT) borehole, including the new (U-Th)/He ages from this study, are the first borehole data confirming that the central craton of southern Africa has not experienced significant cooling or related erosion since the late Paleozoic. Consequently, this suggests that the southern African plateau has experienced significant differential erosion (and by inference uplift) during the Mesozoic - varying from negligible amounts to several kilometers depending on location. This study highlights the importance of obtaining more low- temperature thermochronology data from the interior of southern Africa, especially combined AHe and AFT analysis, to further constrain this pattern of differential cooling and erosion.

References

1. Tinker, J., de Wit, M. & Brown, R. Mesozoic exhumation of the southern Cape, South Africa, quantified using apatite fission track thermochronology. *Tectonophysics* **455**, 77–93 (2008).
2. Brown, R. W., Gleadow, A. J. W. & Summerfield, M. A. Denudational history along a transect across the Drakensberg Escarpment of southern Africa derived from apatite fission track thermochronology. *J. Geophys. Res.* **107**, ETG 10, 1–18 (2002).
3. Flowers, R. M. & Schoene, B. (U-Th)/He thermochronometry constraints on unroofing of the eastern Kaapvaal craton and significance for uplift of the southern African Plateau. *Geology* **38**, 827–830 (2010).
4. Gleadow, A. J. W., Belton, D. X., Kohn, B. P. & Brown, R. W. Fission Track Dating of Phosphate Minerals and the Thermochronology of Apatite. *Rev. Mineral. Geochemistry* **48**, 579–630 (2002).
5. Farley, K. A. & Stockli, D. F. (U-Th)/He Dating of Phosphates: Apatite, Monazite, and Xenotime. *Rev. Mineral. Geochemistry* **48**, 559–577 (2002).
6. Green, P. F. & Duddy, I. R. Interpretation of apatite (U-Th)/He ages and fission track ages from cratons. *Earth Planet. Sci. Lett.* **244**, 541–547 (2006).
7. Brown, R. W. *et al.* Natural age dispersion arising from the analysis of broken crystals. Part I: Theoretical basis and implications for the apatite (U-Th)/He thermochronometer. *Geochim. Cosmochim. Acta* **122**, 478–497 (2013).
8. Fitzgerald, P. G., Baldwin, S. L., Webb, L. E. & O’Sullivan, P. B. Interpretation of (U-Th)/He single grain ages from slowly cooled crustal terranes: A case study from the Transantarctic Mountains of southern Victoria Land. *Chem. Geol.* **225**, 91–120 (2006).
9. Flowers, R. M. & Kelley, S. A. Interpreting data dispersion and “inverted” dates in apatite (U-Th)/He and fission-track datasets: An example from the US midcontinent. *Geochim. Cosmochim. Acta* **75**, 5169–5186 (2011).
10. Ehlers, T. A. & Farley, K. A. Apatite (U-Th)/He thermochronometry : methods and applications to problems in tectonic and surface processes. *Earth Planet. Sci. Lett.* **206**, 1–14 (2003).
11. De Wit, M. The Kalahari Epeirogeny and climate change: differentiating cause and effect from core to space. *South African J. Geol.* **110**, 367–392 (2007).
12. De Wit, M. C. J., Ward, J. D., Bamford, M. K. & Roberts, M. J. The Significance of the Cretaceous Diamondiferous Gravel Deposit At Mahura Muthla, Northern Cape Province, South Africa. *South African J. Geol.* **112**, 89–108 (2009).

The enigmatic uplift of southern Africa: comparing predictions from coupled thermo-mechanical and surface processes models with thermochronological data and sediment thickness offshore

Romain Beucher¹, Ritske S. Huisman¹, Roderick Brown², Cécile Robin³

1 University of Bergen, Department of Mathematics and Earth Sciences, Bergen, Norway

2 University of Glasgow, School of Geography and Earth Sciences, Glasgow, United-Kingdom

3 Université de Rennes, Observatoire des Sciences de l'Univers de Rennes, Rennes, France

The topography of southern and eastern Africa (referred to as the African Superswell by Nyblade and Robinson, 1994) is anomalously high (> 900m) relative to central and west Africa, and also to other continents. The southern tip of Africa is surrounded by passive margins and mid ocean ridges as a result of continental rifting (early Jurassic in the east, late Jurassic in the west) and Gondwana break up. Recent studies have also identified the Earth's largest low seismic velocity anomaly in the mid-lower mantle beneath southern Africa and catalysed interest in the role the interactions between surface and deep processes play in generating large scale topography. Understanding how the relief evolved since rifting onset is fundamental to advancing knowledge about the coupling between deep tectonics and dynamic topography. Such a large scale topographic feature may also have important impact on atmosphere circulation and precipitation patterns.

To understand the complexity of such a system requires an integrated approach looking at interactions between tectonics and surface processes on a range of spatial and temporal scales. We use high-resolution numerical experiments coupling a 2D upper-mantle-scale thermo-mechanical model with a plan-form 2D surface processes model (SPM) to investigate the factors controlling the style of deformation. The experiments consist of simple extensional models involving lithosphere with variable thickness (normal lithosphere to thick, cratonic-like lithosphere) and explore the effects of rheological and compositional variability of the of the crustal and the lithosphere layers. Evidence from seismic tomography and geochemistry suggests a possible counterflow in the lower lithosphere in below parts of the western margins of Africa. We discuss the effect of a gravitationally driven lithospheric counterflow of depleted lower lithosphere (compositionally less dense than normal sublithospheric mantle) on the rift geometry, and the effect of the isostatic responses in terms of uplift or subsidence on the surrounding topography.

We explore a range of erosion, deposition and basin filling scenarios and compare the predictions to estimates derived from modelling of thermochronological data (Apatite Fission Track ages (AFT) and U-Th/He ages(AHe)) and sediment budgets offshore. Thermochnology enables constraints to be placed on the timing and amount of cooling, which in turn can be used to discuss the viscosity and the density structure of the underlying lithosphere / mantle.

We discuss the perspectives offered by joint analyses of thermochronological data and the utilization of thermo-mechanical and surface erosion models to provide new insights into south-African uplift and the role of mantle dynamics.

References

1. Nyblade, A. & Robinson, S. The African Superswell. *Geophys. Res. Lett.* **21**, 765-768 (1994).

Cenozoic exhumation history of Sulu terrane: implications from (U-Th)/He thermochronology

Lin Wu^{1,2}, Patrick Monié², Fei Wang¹, Wei Lin¹, Michael Bonno², Philippe Münch²

1 State Key Laboratory of Lithospheric Evolution, Institute of Geology and Geophysics, Chinese Academy of Sciences, Beijing 10029, China

2 Géosciences Montpellier, UMR-CNRS 5243, Université de Montpellier 2, Pl. E. – Bataillon, F-34095 Montpellier Cedex, France

The Sulu ultra-high pressure (UHP) orogenic belt, bounded by Tan-Lu fault to the west, Yantai-Qingdao-Wulian fault (YQWF) to the north and Jiashan-Xiangshui fault (JXF) to the southeast, is the eastern extension of giant Qinling-Dabie-Sulu orogen belt which resulted from continental collision between the North China and Yangtze cratons in Early Triassic¹. The discovery of UHP minerals in zircon inclusions suggested that the crust was subducted to deeper than 120 km in the mantle^{2,3} and then exhumed to the shallow crustal level⁴. At present, low-T thermochronology has been applied to constrain the final exhumation of Dabie Shan⁵⁻⁸, but there are few studies for the Cenozoic exhumation history of the Sulu UHP belt^{9,10}.

Here we report some (U-Th)/He single ages for various lithologies including granite, migmatite and mylonite from Sulu Orogenic belt and its northern Jiaobei terrane. The single grain He ages range between 18 Ma and 92 Ma and most of the samples have large inter grain age dispersion. Several reasons such as invisible U/Th-rich inclusions, grain size effect, chemical composition variation, slow cooling rate, zonation of parent nuclide or radiation damage effect¹¹ may account for the large intra-sample dispersion. However, the most possible factors are slow cooling and undetectable U/Th-rich inclusions.

The general distribution of the single grain age population exhibits a peak at 45 ± 5 Ma. Drill hole fission track age pattern in Hefei Basin to the southwest of Sulu area indicated an exhumed partial annealing zone at ~ 50 Ma¹². This age pattern combining with our (U-Th)/He age pattern of the Sulu area implied an enhanced exhumation/cooling (but still slow relative to the Early Cretaceous rapid cooling) in Early – Middle Eocene in the south part of Tan-Lu fault zone. Kinematic analysis of faults in the southern Tan-Lu Fault Zone suggested that a transpression event with NNE-SSW to NE-SW shortening occurred during Early to Middle Eocene^{13,14} ($\sim 52 - 46$ Ma). Soon after the above mentioned transpression event, the eastern China experienced widespread rifting ($\sim 46 - 30$ Ma) and many rifting basins initiated during this rifting stage^{14,15}. The convergence rate between Pacific Plate and Eurasia decreased substantially during early Tertiary time and reached a minimum in Eocene time of $\sim 30-40$ mm/yr while at the same time the collision between India and Asia was completed and the two continents contacted totally¹⁶. In conclusion, the Cenozoic exhumation history of the Sulu Orogenic Belt was a combined result of far-field effect of India-Asia collision and declined subduction rate of the Pacific Plate under Eurasia continent.

References

1. Hacker, B. R. et al. High-temperature geochronology constraints on the tectonic history and architecture of the ultra-high-pressure Dabie-Sulu orogen. *Tectonics* **25**, TC5006 (2006).
2. Xu, S. T. et al. Diamond from the Dabie Shan metamorphic rocks and its implication for tectonic setting. *Science* **256**, 80-82(1992).
3. Ye, K. et al. The possible subduction of continental material to depth greater than 200 km. *Nature* **407**, 734-737 (2000).
4. Liu, F. L. et al. Differential subduction and exhumation of crustal slices in the Sulu HP-UHP metamorphic terrane : insights from mineral inclusions, trace elements, U-Pb and Lu-Hf isotope analyses of zircon in orthogneiss. *Journal of Metamorphic Geology* **27**, 805-825 (2009a).
5. Reiners, P. W. et al. Post-orogenic evolution of the Dabie shan, Eastern China, From (U-Th)/He and fission-track thermochronology. *American Journal of Sciences* **303**, 489-518 (2003).
6. Wang, R. C. et al. Protolith age and exhumation history of metagranites from the Dabie UHP metamorphic belt in east-central China: A multi-chronological study. *Geochemical Journal* **38**, 345-362 (2004).
7. Xu, C. H. et al. Apatite-fission-track geochronology and its tectonic correlation in the Dabieshan orogen, central China. *Science in China Ser. D Earth Sciences* **48**, 506-520 (2005).
8. Hu, S. B. et al. Cretaceous and Cenozoic cooling history across ultrahigh pressure Tongbai-Dabie belt, central China, from apatite fission-track thermochronology. *Tectonophysics* **420**, 409-429 (2006).
9. Liu, S. S. et al. Fission track analysis and thermotectonic history of the main borehole of the Chinese Continental Scientific Drilling project. *Tectonophysics* **475**, 318-326 (2009b).
10. Siebel, W. et al. From emplacement to unroofing: thermal history of the Jiazishan gabbro, Sulu UHP terrane, China. *Mineral Petrology* **96**, 163-175 (2009).
11. Shuster, D. L. et al. The influence of natural radiation damage on helium diffusion kinetics in apatite. *Earth and Planetary Science Letters* **249**, 148-161 (2006).
12. Chen, G. et al. Fission Track evidence for the tectonic-thermal history of the Hefei Basin. *Chinese Journal of Geophysics* **48**, 1433-1442 (2005).
13. Ratchbacher, L. et al. Exhumation of the ultra-high pressure crust in eastern China: Cretaceous to Cenozoic unroofing and the Tan-Lu fault. *Journal of Geophysical Research* **105**, 13,303-13,338 (2000).
14. Mercier, J. L. et al. Structural records of the Late Cretaceous – Cenozoic extension in Eastern China and the kinematics of the Southern Tan-Lu and Qinling Fault Zone (Anhui and Shanxi Province, PR China). *Tectonophysics* **582**, 50-75 (2013).
15. Ren, J. Y. et al. Late Mesozoic and Cenozoic rifting and its dynamic setting in Eastern China and adjacent areas. *Tectonophysics* **344**, 175-205 (2002).
16. Rowley, D. B. Age of initiation of collision between India and Asia: A review of stratigraphic data. *Earth and Planetary Science Letters* **145**, 1-13 (1996).

The Cretaceous-Tertiary thermal evolution of the Gawler Craton, South Australia: Implications for the long-term stability of cratons

Samuel Boone¹, Christian Seiler¹, Andrew Gleadow¹, Barry Kohn¹
1 School of Earth Sciences, The University of Melbourne, Victoria, 3010, Australia

In a previous low-temperature thermochronology survey of the basement rocks of the central Archean-Proterozoic Gawler Craton, South Australia, Gleadow et al. ¹ reported a number of samples with anomalously young apatite fission track ages that appear to postdate the regional Paleozoic (~400 Ma) exhumation of the craton. These younger ages, if confirmed, would indicate that some areas of the Gawler Craton underwent localized reheating during a poorly defined interval in the Cretaceous or Paleogene, at some time between ~120-40 Ma. Such a scenario would challenge the concept of cratonic interiors as regions of long-term thermal, structural and erosional stability, indicating a more dynamic Phanerozoic surface evolution.

In order to take a more in-depth look at the Cretaceous-Tertiary thermal evolution of the Gawler Craton, additional basement samples from the region were collected. These samples were analysed using the LA-ICP-MS apatite fission track method to better constrain the timing of the apparent reheating event, understand its spatial and physical characteristics and investigate potential sources for reheating. For samples with limited numbers of confined fission tracks, the true (3D) lengths of surface-intersecting fission tracks, or semi-tracks, were measured as a qualitative indicator for the complexity of the cooling history experienced.

We report data from 21 newly analysed samples that yield fission track ages ranging from 330.2 ± 36.8 to 540.0 ± 86.1 Ma. These ages are similar to those obtained elsewhere on the Gawler Craton and do not appear, at first sight, to support the hypothesis of a Cretaceous reheating event. However, some samples exhibit relative short mean track lengths (MTL) (~11-11.5 μm), compared to the lengths of ~12.5 to 14 μm that are typical for samples of the Gawler Craton. Time-temperature modeling of these samples allows for, but do not require, a mild and short-lived reheating event (up to 80 °C) during the Cretaceous, before cooling to near-surface temperatures in the Paleogene.

A possible cause for Cretaceous-Paleogene reheating is the Jurassic-Paleogene Eromanga Basin, which has its modern margin approximately 400 km north of the study area. The widespread distribution of Eromanga outliers in the study area suggests a much more extensive cover in the past. Its present day maximum sedimentary thickness of ~1.5 km combined with a high geothermal gradient of up to 50 °C/km suggest that burial by the sediments of the Eromanga Basin could potentially have overprinted parts of the Gawler Craton.

References

1. Gleadow, A. J. W., Kohn, B., Brown, R., O'Sullivan, P. & Raza, A. Fission track thermotectonic imaging of the Australian continent. *Tectonophysics* **349**, 5-21 (2002).

Thermo-tectonic evolution of Tasmania and the South Tasman Rise

Ling Chung¹, Barry P. Kohn¹, Andrew J.W. Gleadow¹

1 School of Earth Sciences, University of Melbourne, Victoria 3010, Australia

The crustal architecture of previously adjacent basement terranes in SE Australia, Tasmania and northern Victoria Land (NVL), Antarctica is a legacy of late Neoproterozoic-Paleozoic subduction along the east Gondwana margin, highlighting the Cambro-Ordovician Delamerian-Ross Orogeny. Structures in this ancient crust were reactivated during late Mesozoic-Cenozoic Gondwana breakup¹. Tasmania and the offshore South Tasman Rise (STR) lie in a crucial location at the centre of Gondwana continental fragments and potentially contain clues related to the nature of its dispersal (Fig. 1). This study reports results of a systematic thermochronological study carried out on offshore STR dredge samples and onshore Tasmanian dolerites to uncover the history of the ancient subduction system and the post-break up thermal history recorded in their crust.

Offshore, a different thermo-tectonic evolution of the western and eastern terranes of the STR (W-STR and E-STR, respectively) was clearly revealed. Analytical results allow temporal comparisons to be made between existing age datasets obtained from S-SE Australia and NVL², and those reported here from the thermochronologically less studied offshore STR region. ⁴⁰Ar/³⁹Ar mica data from the W-STR (~495-460 Ma) aid in refining its paleo-position and support reconstructions, which indicate that W-STR was originally attached to Antarctica and was activated along with the Wilson Terrane, NVL during the Cambrian Delamerian Orogeny prior to Mesozoic breakup¹. For E-STR, ⁴⁰Ar/³⁹Ar mica ages (325-357 Ma) are synchronous with a major phase of Carboniferous granite emplacement and mineralization, which occurred in western Tasmania and these are correlated with post-Tabberabberan Orogeny deformation in Tasmania and Victoria.

This study also reports the first apatite (U-Th-Sm)/He (AHe) thermochronometry results from the Tasmanian region. The data not only provide further spatial and temporal constraints, but also allow evaluation of the quality of AHe ages obtained from mafic lithologies with lower U and Th content than felsic rocks and yielding less apparent age dispersion. Mid Jurassic (~180 Ma) dolerite³ is widely distributed across onshore Tasmania making such a study possible. The dolerite forms part of the Ferrar Group continental flood basalt (CFB) emplaced prior to eastern Gondwana breakup. Its spatial/temporal significance and chemical composition make it an ideal rock-type to aid in documenting the regional post-continental breakup history and to test the influence of different parameters such as a-radiation damage and U and Th zonation on AHe age dispersion from a relatively low eU perspective.

Low-temperature thermal modelling of AFT and AHe data from onshore and offshore Tasmania reveals several distinct cooling episodes. (1) Mid-Cretaceous cooling, which involved km-scale denudation (~3-4 km) onshore in response to continental extension prior to the onset of actual seafloor spreading in the Tasman Sea. (2) onset of opening of the Tasman Sea at ~80 Ma. (3) Late Cretaceous-early Tertiary cooling, restricted to the west margin of Tasmania in response to amalgamation of the W- and E-STR blocks and transform margin tectonism to the west, (4) a shift in the relative motion between Australia and Antarctica since the early Eocene, and (5) final clearance of continental breakup and onset of the opening of the Tasman Gateway. In addition,

no correlation could be found between AHe ages and some potential factors influencing age dispersion observed such as radiation damage, grain size or U-Th zonation.

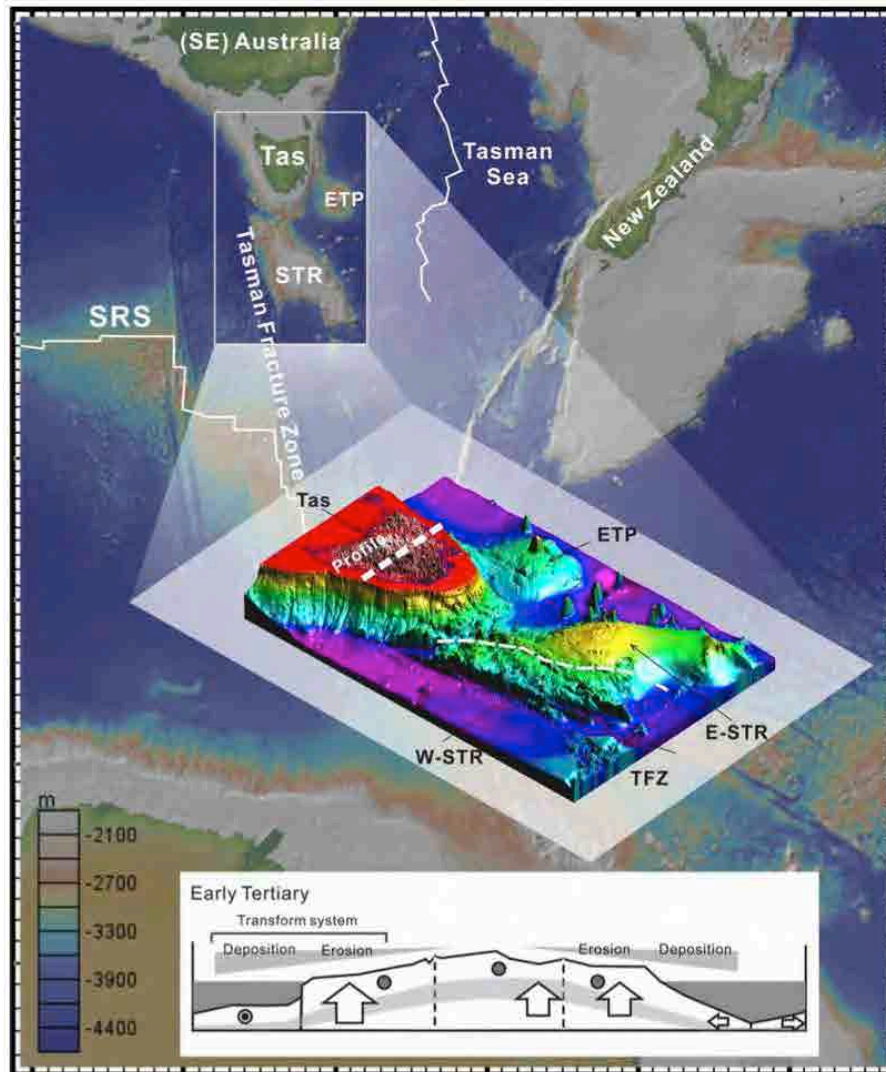


Figure 1. Global multi-resolution topography (GMRT) image of Tasmania and contiguous regions and 3-D view of the sea-floor off southern Tasmania. (Tas=Tasmania; NVL=Northern Victoria Land; STR=South Tasman Rise; E- and W-STR=east and west STR; ETP=East Tasman Plateau; SRS=Southern Rift System; TFZ=Tasman Fracture Zone). Proposed post-rift evolution (early Tertiary reconstruction) of onshore Tasmania is also shown by schematic cross section.

References

1. Gibson, G. M. Morse, M. P. Ireland, T. R. & Nayak, G. K. Arc-continent collision and orogenesis in western Tasmanides: Insights from reactivated basement structures and formation of an ocean-continent transform boundary off western Tasmania. *Gondwana Research* **19**, 608-627 (2011).
2. Adams, C. J. in Antarctica Contributions to Global Earth Sciences (eds. Fütterer, D. K., Damaske, D., Dleinschmidt, G., Miller, H. & Tessensohn, F.) 45-54 (Springer, Berlin, Heidelberg, New York, 2006).
3. Brauns, C. M., Hergt, J. M. & Woodhead, J. D. Os isotopes and the origin of the Tasmanian dolerites. *Journal of Petrology* **41**, 905-918 (2000).

Evolution of the Transantarctic Mountains, Antarctica: Collapse of a Mesozoic West Antarctic Plateau supported by apatite fission track and (U-Th)/He analyses from the Byrd Glacier outlet

Ann E. Blythe¹, Audrey D. Huerta²

¹ Occidental College, Los Angeles, CA, USA

² Central Washington University, Ellensburg, WA, USA

The structural and denudational evolution of the Transantarctic Mountains (TAM) along the Byrd Glacier outlet is evaluated using apatite fission track (AFT) and (U-Th)/He (He) analyses. These data are used to test the hypothesis that the TAM formed as the abandoned margin of a collapsed Mesozoic West Antarctic Plateau, which has been proposed based on geodynamic models as well as geomorphic evidence for drainage reversal^{1,2}. The hypothesized collapse of a Mesozoic Plateau should produce a diagnostic thermal evolution recording Cretaceous erosion of the East-Antarctica-facing flank of the plateau followed by cooling during unroofing of the West-Antarctica-facing flank of the TAM and subsequent incision by glaciers as they shape the landscape.

Samples were collected on three near-vertical transects (Horney Bluff, McClintock Ridge, and Quackenbush Ridge), as well as at low elevations near the surface of Byrd glacier, and at higher elevations farther from the glacier (Figure 1).

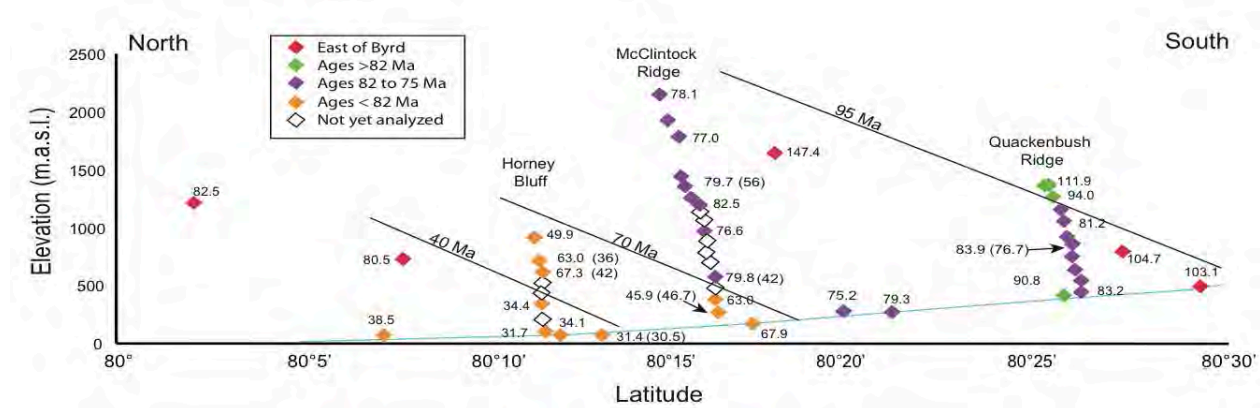


Figure 1. Plot of sample elevation and N-S location near Byrd Glacier. The light blue line is the surface elevation of Byrd Glacier, which flows towards the northeast. Sample symbols are color-coded for apatite fission track age (with representative ages included). (U-Th)/He ages are shown in parentheses.

The data indicate the following:

1. Along the level of the glacier surface, AFT and He ages become progressively younger towards West Antarctica (ranging from >80 Ma in the south to 31 Ma in the north).
2. Significant rapid cooling (and presumably exhumation) is indicated for both Quackenbush and McClintock Ridges at ~78 Ma. In the case of McClintock Ridge, samples spanning >2 km of elevation have AFT ages of ~78 Ma. This is a robust signal for a significant tectonic event occurring at this time.

3. Near the base of Horney Bluff, 4 samples yielded AFT ages of 34 to 31 Ma (with long mean track lengths), and a He age of 30.5 Ma. These analyses are consistent with a rapid cooling event at this time.
4. The overall pattern of ages from this study indicates that the TAM near Byrd Glacier have undergone a greater amount of total exhumation towards West Antarctica. On Figure 1, black lines bracketing the apatite fission track ages have been drawn to illustrate the relative tilting of the region that has occurred.

The spatial and temporal distribution of AFT and He ages is consistent with the plateau collapse model. The exhumation at ~80 Ma can be explained by the crustal response to plateau construction, whereas the general younging of thermochronologic ages to the north (towards West Antarctica) along the Byrd Glacier outlet is consistent with regional tilting, with the pulse of exhumation at ~30 Ma predicted by the plateau collapse model.

References

1. Huerta, A. D. & Harry, D. L. The transition from diffuse to focused extension: Modeled evolution of the West Antarctic Rift system. *EPSL* **255**, 133-147 (2007).
2. Bialis, R. W., Buck, W. R., Studinger, M. & Fitzgerald, P.G. Plateau collapse model for the Transantarctic Mountains–West Antarctic Rift System: insights from numerical experiments. *Geology* **35**, 687-690 (2007).

Re-interpretation of the thermal history of the Shackleton Range, Antarctica, based on Ferrar volcanoclastic rocks

Nicole Lucka¹, Frank Lisker¹, Andreas Läufer², Cornelia Spiegel¹

1 Department 5 Geosciences, University of Bremen, PF 330440, 28334 Bremen, Germany

2 Federal Institute for Geosciences and Natural Resources, Stilleweg 2, 30655 Hannover, Germany

The Shackleton Range is situated between 80°–81°S and 19°–31°W where it forms the topographic continuation of the Transantarctic Mountains in the Weddell Sea sector. The recent morphology is characterized by up to 1800 m elevated plateau surfaces with 300 m high cliffs along its margins. The geological architecture of the Shackleton Range consists of Precambrian igneous and (meta-) sedimentary rocks of an Early Paleozoic nappe stack and post-orogenic red beds. The exhumation of the region has been analyzed via fission track (FT) analysis¹. Zircon FT ages vary between ~160 and 210 Ma, while apatite FT ages range from 94±6 to 168±16 Ma are associated with mean track lengths of 12.7–14.1 μm (standard deviation 1.0–1.4 μm). These data have been interpreted qualitatively in terms of two cooling/ exhumation stages during Jurassic and mid-Cretaceous times.

However, the recognition of 180–186 Ma Ferrar volcanoclastic rocks in the vicinity of the sample locations challenges this exhumation concept². The superficial position of these sediments in Jurassic times and substantially younger fission track ages rigorously contradict a continuous cooling hypothesis and require a new interpretation. Hence, existing apatite FT age data were supplemented with D_{par} and new track length measurements, and new apatite FT and AHe age analyses performed to allowing thermal history modeling with HeFTy³. The apatite FT data set now comprises ages between 94±6 and 223±38 Ma, track lengths of 12.4–14.2 μm and associated standard deviations of 0.8–2.9 μm. AHe ages of 110±13–151±18 Ma are only little younger than FT ages of the same samples.

All samples show a similar age pattern, with a break in slope at different elevations, indicating vertical displacements subsequent to cooling. Thermal history modeling of the combined thermochronological data and geological and geomorphological constraints suggests early Mesozoic cooling followed by (post) Jurassic re-heating. Final cooling from temperatures up to 100°C to surface temperatures occurred since the Late Cretaceous. This scenario requires burial of the Shackleton Range region within a sedimentary basin. Subsequent basin inversion may then have triggered isostatic uplift and induced vertical displacement and escarpment formation. The now vanished sedimentary strata were 2 km in thickness. Post-Ferrar sediment basins of up to 3.5 km burial depth are also reported from the Transantarctic Mountains⁴, and may be indicative for a more general mechanism.

References

1. Lisker, F., Schäfer, T. & Olesch, M. The Uplift/Denudation History of the Shackleton Range (Antarctica) Based on Fission-Track Analyses. *Terra Antarctica* **6**, 345-352 (1999).
2. Buggisch, W., Kleinschmidt, G., Kreuzer, H. & Krumm, S. Metamorphic and structural evolution of the southern Shackleton Range during the Ross Orogeny. *Polarforschung* **63**, 33-56 (1994).

3. Ketcham, R. A. Forward and Inverse Modeling of Low-Temperature Thermochronometry Data. *Reviews in Mineralogy and Geochemistry* **58**, 275-314 (2005).
4. Prenzel, J., Lisker, F., Balestrieri, M. L., Läufer, A. & Spiegel, C. The Eisenhower Range, Transantarctic Mountains: Evaluation of qualitative interpretation concepts of thermochronological data. *Chemical Geology* **352**, 176-187 (2013).

Thermochronological data from the Dronning Maud Land Mountains, East Antarctica – a review

Hallgeir Sirevaag¹, Joachim Jacobs¹, Anna Ksienzyk¹, István Dunkl²
1 Department of Earth Science, University of Bergen, Allégaten 41, 5007 Bergen, Norway
2 Geoscience Center, University of Göttingen, Goldschmidtstrasse 3, D-37077 Göttingen, Germany

The paleo-topography of East Antarctica is highly relevant for the development of the East Antarctic ice-sheet. It is likely that the 1500 km long, coast-parallel Dronning Maud Land Mountains (Figure 1) have resulted in a significant amount of precipitation prior to the initiation of the 34 Ma glaciation history of East Antarctica. Due to this, the paleo-topography should be used as an important input parameter for the glaciation history.

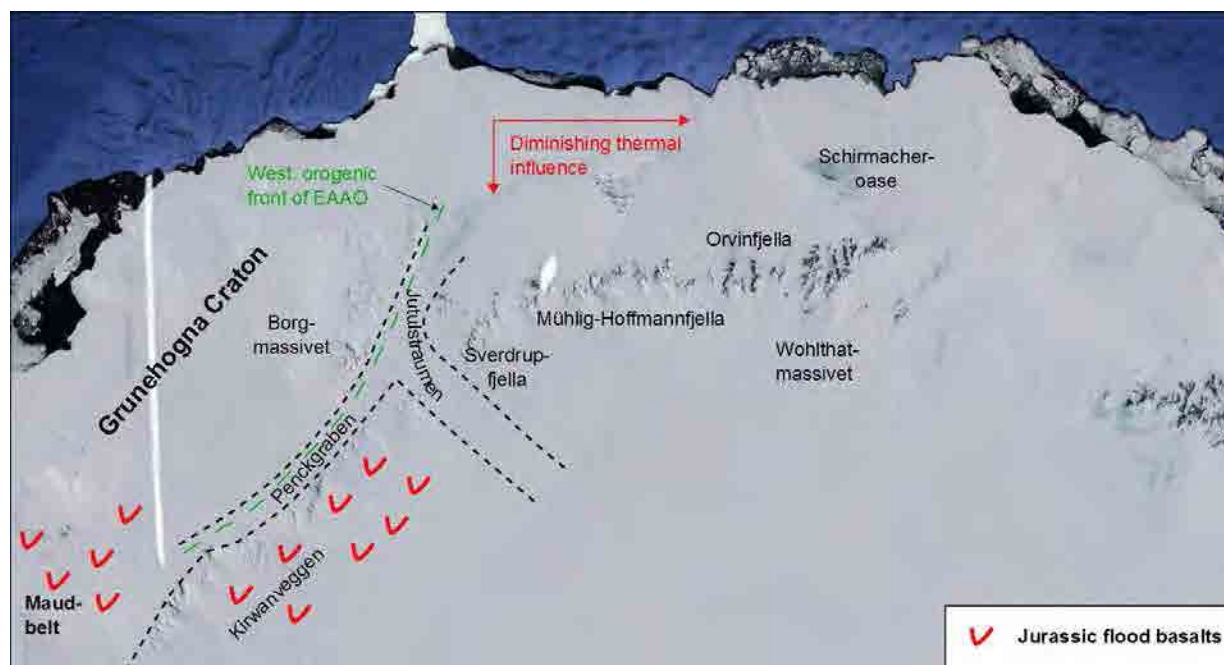


Figure 1. Satellite image of the Dronning Maud Land Mountains, East Antarctica. Note the direction of the diminishing thermal influence, observed as progressively older AFT ages towards east.

The amount of quantitative measurements for the exhumation history of Antarctica is very limited as 98% of the continent is covered by ice. However, since the onset of thermochronological studies in the Dronning Maud Land Mountains in 1992¹, the area has been a subject of several thermochronological studies¹⁻⁷.

The first thermochronological studies from Heimefrontfjella and Mannefjellknausane recorded a Jurassic thermal event associated with the Jurassic flood basalts related to the Karoo mantle plume and the rifting between East Antarctica and East Africa^{1,2}. Thermochronological data from Heimefrontfjella and Mannefjellknausane published by Jacobs and Lisker³ indicated that the

Mesoproterozoic basement and the Permian sandstones were covered by 2000 meters of Jurassic flood basalt. In the Mühlig-Hofmann Mountains and the Gjelsvikfjella to the E, no significant Jurassic thermal event have been recorded. However, a combined titanite and apatite study by Emmel, et al.⁷ did not record any significant Jurassic thermal event in the Gjelsvikfjella and Mühlig-Hofmann Mountains. This has been used as a constraint for the lateral extent of the flood basalts. Also, the thermochronological analyses presented in Jacobs and Lisker³ indicated that the AFT ages get progressively older towards the SE. Based on these analyses, paleo-isotherms dipping towards the SE were suggested.

In addition to the already published data, new, unpublished AHe data from a transect of the northern part of Jutulstraumen show relatively young ages at the rift flanks (~50 Ma) and progressively older ages further away from the rift flanks, indicating significant Cenozoic erosion (Ksienzyk et al., unpublished data). This is the basis for presently ongoing thermochronological studies.

References

1. Jacobs, J., Hejl, E., Wagner, G. A. & Weber, K. in Recent Progress in Antarctic Earth Science (eds. Yoshida, Y., Kaminuma, K. & Shiraishi, K.) 323-330 (1992).
2. Jacobs, J., Ahrendt, H., Kreutzer, H. & Weber, K. K-Ar, ⁴⁰Ar-³⁹Ar and apatite fission-track evidence for Neoproterozoic and Mesozoic basement rejuvenation events in the Heimefrontfjella and Mannefallknausane (East Antarctica). *Precambrian Research* **75**, 251-262 (1995).
3. Jacobs, J. & Lisker, F. Post Permian tectono-thermal evolution of western Dronning Maud Land, East Antarctica: an apatite fission-track approach. *Antarctic Science* **11**, 451-460 (1999).
4. Meier, S. Paleozoic and Mesozoic tectono-thermal history of central Dronning Maud Land, East Antarctica-evidence from fission-track thermochronology. *Berichte zur Polarforschung (Reports on Polar Research)* **337** (1999).
5. Meier, S., Jacobs, J. & Olesch, M. Tectono-thermal Evolution of Central Dronning Maud Land, East Antarctica, from Mid-Palaeozoic to Cenozoic Times: Zircon and Apatite Fission-Track Data from the Conradgebirge and Ostliche Petermannkette. *Geologisches Jahrbuch Reihe* **B96**, 423-448 (2004).
6. Emmel, B., Jacobs, J., Crowhurst, P. & Daszinnies, M. Combined apatite fission-track and single grain apatite (U-Th)/He ages from basement rocks of central Dronning Maud Land (East Antarctica) – Possible identification of thermally overprinted crustal segments? *Earth and Planetary Science Letters* **264**, 72-88 (2007).
7. Emmel, B., Jacobs, J. & Daszinnies, M. C. Combined titanite and apatite fission-track data from Gjelsvikfjella, East Antarctica – another piece of a concealed intracontinental Permo-Triassic Gondwana rift basin? *Geological Society, London, Special Publications* **324**, 317-330 (2009).

Session 4:

Thermochronology in active orogenic belts

Using structural thermochronology to resolve the evolution of the retroside of the Alpine wedge

Mark Brandon¹

1 Yale University, and Devin McPhillips, Syracuse University

We use thermochronology to measure Cenozoic tilting in the retro-side of the Alpine orogenic wedge in southern Switzerland and northern Italy. Argand (1916) was first to recognize that the structure of the southern part of the Alps was dominated by a large back fold, with a vergence to the south, which opposite that for the more frontal part of the Alps to the north. Modern concepts of wedge tectonics would ascribe this deformation to "back shearing" within the retroside of a doubly vergent wedge. Densely distributed cooling ages can be used to define isochrones, which are surfaces of equal cooling age. Stratigraphic markers within the frontal part of the Alps indicate that thermochronologic isochrones should have quite complex structure within the frontal part of mountain belts, where accretion and thrust imbrication dominate. The situation is simpler in the rear of the Alps, where the overall structure is more coherent and less dismembered by faults. When cooling ages are sparse, we tend to view each age as an estimate of the time and depth of exhumation. A denser vertical transect might be allow an interpretation using the correlation of age with elevation, but this approach requires that thermochronologic isochrones are horizontal. We consider here a more generalized used of thermochronology, as a kind of stratigraphic marker for structural geologic analysis.

Our analysis is based on some 50 fission-track zircon (FTZ) ages in the Ticino part of the Alps, which range from 250 to 12 Ma. The FTZ system has a nominal closure temperature of ~240 C and, in the Alps, a closure depth of ~8 km, which is deep enough to ensure that the FTZ isochrones are initiated as planar horizontal surfaces, much like bedding. But unlike bedding, the FTZ isochrones in the retroside of the Alps were formed as an "upside down" stratigraphy, with zero ages at the closure isotherm and getting older with increasing height from that surface.

We introduce a set of empirical least-squares models for analysis of these data. This approach shows that the FTZ data are well represented by a series of gently dipping isochrones, with average dip of ~4 degrees to the south. The southward dip of the isochrones is consistent with top-south shearing in the retro- side of the Alp wedge. Our analysis also shows a well defined "break-in-slope" at 15 Ma within these tilted isochrones, recording an increase in the vertical velocity of rock through the closure isotherm. We have developed a generic kinematic model for formation of thermochronologic isochrones within the retroside of an orogenic wedge. This model indicates that the trailing limit of the Alpine wedge has remained fixed during its evolution. We extend that model to account for thermal and thermochronologic evolution of the FTZ cooling ages. That work shows that the "break-in-slope" recorded at 15 Ma was caused by the onset of fast erosion at ~30 Ma, which roughly coincides with the subaerial emergence of the Alps. The lag simply reflects the response of the closure isotherm to a change in erosion rate. The Alps highlight the ability of thermochronology to "paint" in a kind of stratigraphy onto rock sequences that otherwise lack stratigraphic markers. We need to greatly increase the spatial density of our dating if we are going to take advantage of this opportunity.

Growth and exhumation of the Pamir orogen revealed by multi-dating of detrital minerals from Tajikistan and China

Barbara Carrapa¹, Fariq Shazanee Mustapha¹, Lindsay M. Schoenbohm², Michael Cosca³, Peter G. DeCelles¹, Edward R. Sobel⁴

1 University of Arizona, U.S.A.

2 University of Toronto Mississauga, Canada

3 USGS, U.S.A

4 University of Potsdam, Germany

The Pamir is the western continuation of Tibet and the site of some of the highest mountains on Earth, yet comparatively little is known about its crustal and tectonic evolution and exhumation history. Whereas shortening, crustal thickening and uplift of Tibet as a result of India-Asia collision has been underway since at least 50 Ma, timing and mechanisms of Pamir orogenesis are largely unknown.

Although both the Pamir and Tibet are composed of rocks with similar affinity, the exhumation history of the two regions appears significantly different. Multi-dating of modern rivers sand samples derived from the eastern (China) and western Pamir (Tajikistan) show a marked difference timing and magnitude of exhumation along strike. Detrital mica $^{40}\text{Ar}/^{39}\text{Ar}$ ages for the northeastern drainages are generally older than ages from the western drainages, indicating younger or lower magnitude exhumation of the northeastern Pamir with respect to the western Pamir. Apatite fission track data show strong Miocene-Pliocene signals for both the northeastern and western drainages indicating protracted regional short-term erosion. Deeper exhumation of the western Pamir is associated with tectonic exhumation of Central Pamir gneiss domes and coincides with higher precipitation today. We suggest that relatively intense precipitation on the windward side of the Pamir has been a major factor since at least the early Miocene in controlling bedrock exhumation and eastward retreat of the orogenic drainage divide. If this is correct this implies that an orographic barrier, and topography, similar to the modern one was established by the early Miocene. Hypsometric analysis supports differential exhumation and show a remarkably good fit between hypsometry curves of large and small catchments from the western Pamir and PDFs of thermochronological ages. This suggests regional and quasi-uniform exhumation across different catchments despite structural and lithological differences. Thermochronological ages from the Pamir record younger (mid-late Miocene), and in average faster, exhumation than that recorded in Tibet.

An outstanding question remains: was the Pamir mainly built in the Miocene or did mountain building start earlier? Data from Paleogene sedimentary rocks preserved in the adjacent basin (Tajik depression) show that a transition between marine to continental environment occurred at ~39 Ma and coincides with strong magmatic activity in the source region. This, combined with the record of tectonic subsidence, suggests that growth of the Pamir Mountains, initiation of a foreland basin deposition and exhumation and uplift of the Pamir may have started as early as late Eocene time.

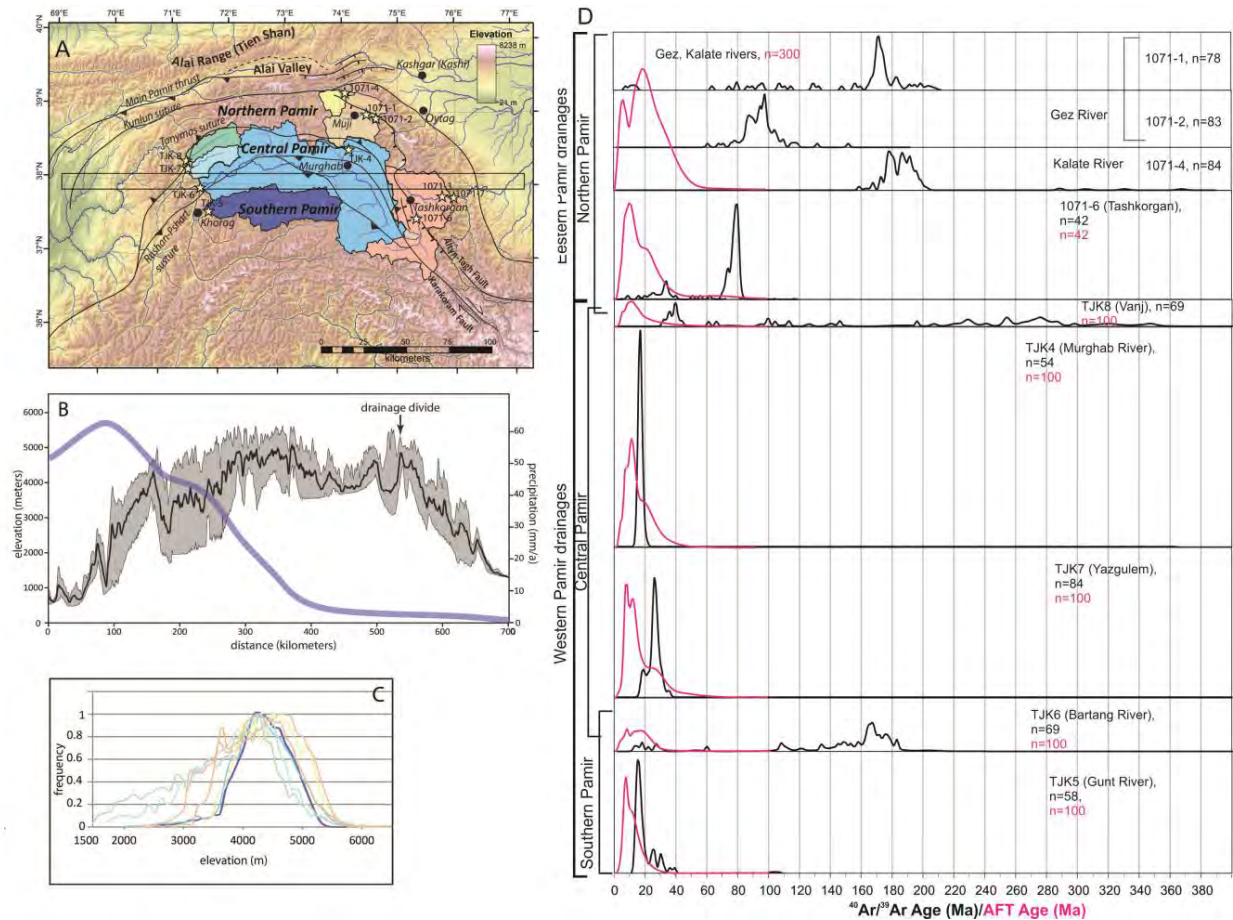


Figure 1. A. DEM and shaded relief map of the Pamir on SRTM base (<http://www2.jpl.nasa.gov/srtm/>). Sample locations and upstream drainage areas marked with stars and shaded regions, respectively. Major structures indicated with black lines and standard structural symbols. B. Swath profile and precipitation data. Gray shaded region indicates maximum and minimum elevation and black line indicates mean. Drainage divide, pushed far to the east, is indicated. Relief is higher on the western side of the Pamir. C. Hypsometric curves. D. Normalized probability density function curves of detrital $^{40}\text{Ar}/^{39}\text{Ar}$ and AFT (pink) ages. $^{40}\text{Ar}/^{39}\text{Ar}$ ages for the western Pamir drainages from¹.

References

1. Lukens, C. Carrapa, B. Singer, B. Gehrels G., Miocene exhumation revealed by detrital minerals of Tajik rivers: Implications for the tectonic evolution of the Pamir, *Tectonics* **31**, TC2014 (2012).

Integrative thermochronology, petrology and modelling reveal the 4-D evolution of active plate boundary zones

Suzanne L. Baldwin¹, Mauricio A. Bermúdez^{1,2}, Paul G. Fitzgerald¹, Laura E. Webb³

1 Department of Earth Sciences, Syracuse University, Syracuse, New York 13244, USA

2 Escuela de Geología, Minas y Geofísica, Universidad Central de Venezuela, Venezuela

3 Department of Geology, University of Vermont, Burlington, Vermont, 05405, USA

Plate boundary zones are dynamic regions where (re)crystallization of mineral assemblages, and chemical and isotopic disequilibrium occurs at all scales. In convergent plate boundaries mineral assemblages preserve the depth-temperature-time-deformation paths followed by rocks. In the case of ultrahigh pressure (UHP) terranes, this includes transport into the mantle and return to the surface. Extracting the details of this journey is challenging because the application of a broad range of isotopic methods on minerals from a variety of rock types is required in order to successfully “see through” overprinting thermal events that may have obliterated, or variably overprinted the rock record. Evidence for chemical and isotopic disequilibrium in rocks exhumed within plate boundaries is pervasive and results from non-steady state conditions. The closure temperature concept is only rarely applicable.

Using thermochronologic and petrologic data from the youngest known ultrahigh and high pressure (U)HP terrane on Earth (i.e., the Woodlark Rift of eastern Papua New Guinea), we illustrate the challenges and successes of using integrative thermochronology to extract records from heterogeneous lithologies exhumed in the rapidly evolving Australian-Pacific plate boundary zone. We found that only mafic coesite eclogite preserves chemical and isotopic variations that can be interpreted to record peak UHP metamorphic conditions. Lu-Hf garnet, U-Pb zircon and $^{40}\text{Ar}/^{39}\text{Ar}$ phengite data combined with thermobarometry indicate UHP metamorphism occurred at ~8 Ma at $T < 750^\circ\text{C}$ and depths of >90 km. These data imply low paleogeothermal gradients during UHP metamorphism and indicate rapid cm/yr exhumation rates. In contrast, the timing and conditions of (U)HP metamorphism are rarely preserved in felsic host gneisses where mineral compositions and their isotopic systematics are partially to completely reset. For example, micas in host gneisses were recrystallized during exhumation and their $^{40}\text{Ar}/^{39}\text{Ar}$ ages reflect complete resetting of Ar systematics since ~8 Ma. Furthermore, the record of rock exhumation is complicated by thermal overprinting due to rifting as the Woodlark sea-flooring spreading system propagated westwards into the UHP terrane. For example, $^{40}\text{Ar}/^{39}\text{Ar}$ step heat data on some feldspars preserve a record of ~8 Ma ages in their most retentive sites and yield complex spectra in the form of pronounced age gradients. In these cases, feldspars were neither 1) recrystallized and/or completely outgassed during exhumation, nor 2) reset by thermal overprinting associated with Plio-Pleistocene mantle upwelling.

$^{40}\text{Ar}/^{39}\text{Ar}$ ages (0.50-0.02 Ma) on rift-related basaltic andesites erupted ~10 km to the west of the UHP locality provide minimum ages to constrain the timing of mantle upwelling ahead of the propagating Woodlark seafloor spreading system. Based on thermobarometry of tephra, these magmas equilibrated prior to their extraction from the mantle at temperatures of 1150-1200°C, and pressures of 0.55-0.75 GPa¹. These temperatures are well above those necessary for preservation of UHP mineral assemblages and the retention of radiometric daughter products. This implies that (U)HP rocks were exhumed to shallow depths (and remained cool) prior to

rifting. Rifting led to an increase in geothermal gradients and was accompanied by mantle upwelling, Quaternary volcanism, and formation of hot springs. The inferred variation and changes in paleogeothermal gradients (from low to high) documented in the rock record is supported by geophysical data that indicate profound thermal gradients persist in the region. This includes intermediate depth earthquakes (70-110 km)² that occur ~100 km along strike to the west of the Late Miocene coesite eclogite locality. (U)HP rocks may occur at depth there, but have yet to be exhumed. In addition tomography indicates significant lateral velocity variations and by inference significant lateral thermal gradients³. Overall we infer dramatically changing geothermal gradients in the region over time, both laterally and vertically. Ongoing efforts to incorporate integrative thermochronologic data sets (⁴⁰Ar/³⁹Ar, AFT, ZFT, ZHe, and AHe) into forward and inverse thermokinematic models will also be discussed, as well as their application to assess the evolution of plate boundaries, including the role of reactivated inherited structures in (U)HP exhumation.

References

1. Ruprecht, P., Plank, T. A., Jin, G. & Abers, G. A. Rifting and UHP exhumation in Eastern Papua New Guinea: temperature and pressure constraints from primitive magmas, American Geophysical Union, Fall Meeting 2013, abstract #T21B-2559.
2. Dieck, C. M., Abers, G. A., Eilon, Z., Gaherty, J. B. & Verave, R. Seismicity in an active rift exposing ultra-high pressure metamorphic rocks: D'Entrecasteaux Islands, Papua New Guinea, American Geophysical Union, Fall Meeting 2013, abstract #T21A-2524.
3. Eilon, Z., Abers, G. A., Jin, G. & Gaherty, J. B. Anisotropy beneath a highly extended continental rift. *Geochemistry, Geophysics, Geosystems* (2014).

Coupling sequential restoration of balanced cross-sections and low-temperature thermochronometry: the case study of the Polish Carpathians.

Ada Castelluccio¹, Benedetta Andreucci¹, Richard A. Ketcham², Leszek Jankowski³,
Stefano Mazzoli⁴, Rafał Szaniawski⁵, Massimiliano Zattin¹

1 Department of Geosciences, University of Padua, Via G. Gradenigo, 6, Padova 35131
Italy

2 Jackson School of Geosciences, The University of Texas at Austin, 1 University
Station C1160 Austin, TX 78712

3 Polish Geological Institute-Carpathian Branch, ul. Skrzatów 1, Cracow, 31-560, Poland

4 Department of Earth Sciences, University of Naples "Federico II", Largo San
Marcellino 10, Napoli, 80138 Italy

5 Institute of Geophysics, Polish Academy of Science, Ks. Janusza 64, Warsaw, 01-452,
Poland

Thermochronometry can provide powerful constraints to sequential restoration of balanced cross-sections. Structural modeling can define style, relative timing of the tectonic events, and deformation rate. By integrating this kinematic model with thermal parameters, cooling ages can be calculated for different thermochronometers (such as apatite fission track and apatite (U-Th-Sm)/He data) along the present-day topographic profile of a given geological cross-section. For this purpose we use FETKIN¹, a software dedicated to low-temperature thermochronological age prediction, that couples 2D kinematic modeling with a Finite Element (FEM) computation of temperatures. This approach allows us to refine and validate our kinematic restoration, based on the agreement between the predicted thermochronometric data and the measured ones. In addition, we can evaluate also the influence of tectonic deformation and regional uplift on the modeled cooling ages. Where no syn-orogenic deposits are preserved and cooling is directly associated with deformation, modeled ages can provide also the absolute timing of the tectonic event.

Here we present an application of this approach to the Polish Carpathian thrust and fold belt, for which the tectonic and thermal evolution is still a matter of heated scientific discussion. According to the commonly accepted interpretation, the Carpathians result from the collision of the ALCAPA and Tisza-Dacia microplates with the southern margin of the East European Platform. The subsequent subduction of the Meliata-Maliac oceanic crust below the former microplates caused the formation of a narrow belt made of sheared and deformed successions, the so-called Pieniny Klippen Belt (PKB). It is located between the two main tectonic domains building the Carpathian chain: the Inner (IC) and Outer Carpathians (OC). The IC are formed by the Precambrian crystalline basement and Paleozoic and Mesozoic successions buried under the Paleogene deposits belonging to the Central Carpathian Paleogene Basin (CCPB). The OC thrust and fold belt consists of siliciclastic deposits from the Upper Jurassic to the Lower Miocene, and the PKB is made of Mesozoic olistolites and olistostromes surrounded by less competent Upper Cretaceous to Paleocene matrix. In the last decade some workers² have suggested an alternative interpretation for the origin of the PKB, doubting its role as oceanic suture. With this contribution we suggest a new scenario in which the PKB is the foreland basin of the IC range. In addition, we focused on the exhumation histories of the Carpathian belt, evaluating the role of the extensional tectonics, thrusting and regional uplift in its cooling history. Three balanced cross-sections have been constructed across the Polish Carpathians. Their sequential restoration has been integrated with thermal parameters³ in order to predict the cooling ages along the present-day profiles. According to our thermo-kinematic restoration, exhumation can be constrained to the last 20 Ma. Apatite fission track modeled age profiles (Fig.1a) show that some areas, including the most external part of the OC and some of the Oligocene deposits belonging to the CCPB, are non reset. Only the Podhale basin belonging to the IC domain is partially reset in its northern part and

completely reset to the south. The rest of the OC show cooling ages between 20 to 15 Ma in the Western Polish region with a pattern that is influenced by the magnitude of thrust sheet displacement. In the Eastern Polish Carpathians, cooling ages are younger (ranging between 10 and 6 Ma) and are associated with post-thrusting low-angle normal faults. Samples collected along the PKB show a partial or total reset of the AFT ages, revealing a non homogeneous burial along this belt. Thermal modeling performed for apatite (U-Th-Sm)/He ages (Fig.1b) show two completely non-reset areas: the outer part of the OC and part of the CCPB. The inner nappes of the OC, the PKB and the crystalline basement cropping out in the IC region are totally reset and show cooling ages ranging between 18 Ma and 4 Ma. Even in this case, cooling ages are influenced by thrusting in the Western Polish region and post-thrusting normal faulting in the Eastern Polish Carpathians.

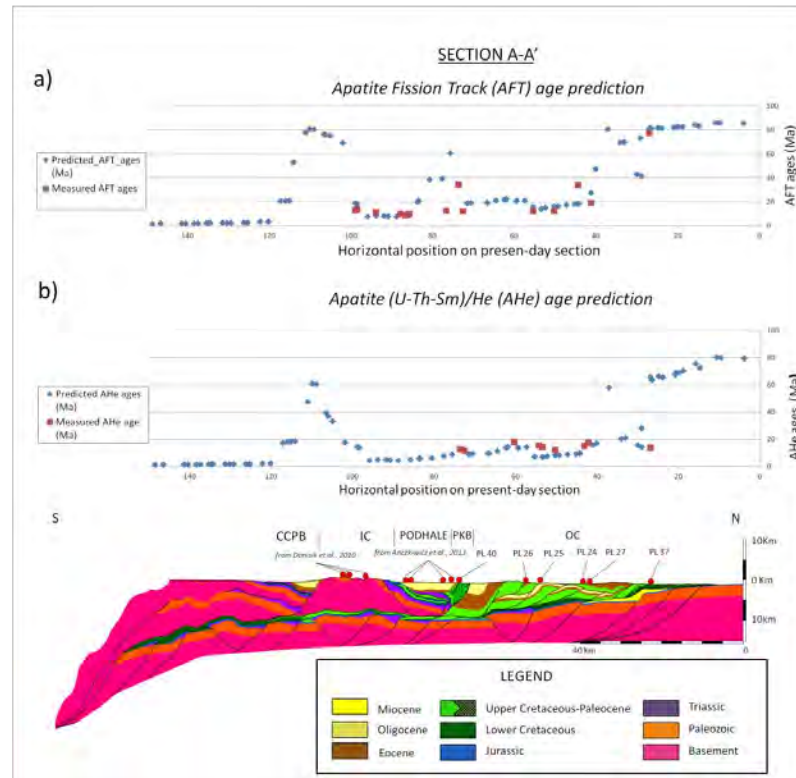


Figure 1. Balanced cross-section across the Western Polish Carpathians with location of analyzed sample. a) Comparison between forward modeled AFT ages from FETKIN and AFT ages measured on collected samples; b) comparison between forward modeled AHe ages from FETKIN and AHe ages measured on collected samples

References

1. Almendral, A., Robles, W., Parra, M., Mora, A. & Ketcham, R. A. FETKIN: Coupling kinematic restorations and temperature to predict exhumation histories. Submitted to AAPG Bulletin.
2. Roca, E., Bessereau, G., Jawor, E., Kotarba, M. & Roure, F. Pre-Neogene evolution of the Western Carpathians: Constraints from the Bochnia-Tatra Mountains section (Polish Western Carpathians). *Tectonics* **14**, 855-873 (1995).
3. Andreucci, B., Castelluccio A., Jankowski L., Mazzoli S., Szaniawski R. & Zattin M. Burial and exhumation history of the Polish Outer Carpathians: Discriminating the role of thrusting and post-thrusting extension. *Tectonophysics* **608**, 866-883 (2013).

Influence of structural complexities on low-angle normal fault slip rates

Michael G. Prior¹, Daniel F. Stockli¹

1 Department of Geological Sciences, University of Texas at Austin, USA

Calculating fault slip rates using thermochronometry is an often-applied method in both contractional and extensional tectonics. Within extensional settings the timing, magnitude and rates of extension can be determined using thermochronometry¹, but several structural processes can significantly complicate the interpretation of these data. Many fundamental ideas about continental extension and the structural evolution of low-angle normal faults were formulated in the Colorado River extensional corridor (CREC) of eastern California and western Arizona where continental crust is extended along regional low-angle normal fault systems that accommodated up to 40-50 km of displacement. The timing, magnitude, and rates of extension along low-angle normal faults are predominantly constrained with thermochronometry in the absence of unambiguous offset marker units; therefore understanding how low-angle normal fault systems evolve and accommodate exhumation of mid-crustal rocks relies on accurate thermochronometric measurements.

Previous authors have interpreted very rapid slip rates of up to ~30 km/Myr from apatite (U-Th)/He dating in the Harcuvar Mountains² core complex, but whether these estimates are reasonable or accurately measure fault slip rates is questionable. The Harquahala Mountains core complex is directly south of the Harcuvar Mountains and is the southernmost exposure of Tertiary mylonites exhumed along a regional low-angle normal fault system that connects the lower plate of the Chemehuevi, Whipple, Buckskin-Rawhide, and the Harcuvar Mountains. The regional setting of the Harquahala Mountains makes it a key location to test the validity of rapid slip estimates and understand the pattern of extension within the CREC as a coherent system. An ~45 km transect of samples for zircon and apatite (U-Th)/He dating (n=18) was collected from the Harquahala footwall along the regional extension direction of ~060° to determine the cooling history associated with core complex exhumation and slip along the Eagle Eye detachment (EED). Zircon (U-Th)/He ages (ZHe) plotted versus distance from the EED display three key characteristics: **1**) samples furthest from the EED record older, pre- extension cooling ages of ~40-50 Ma, **2**) a decrease in ZHe ages through a fossil partial retention zone (PRZ), and **3**) ten nearly invariant ages that decrease from 17.6 ± 0.3 to ~15-16 Ma over the last 22 km and record cooling due to slip on the EED (fig.1). The inflection point between the PRZ and ZHe ages recording fault slip indicates extension began at ~17-18 Ma in the Harquahala Mountains and that the Eagle Eye detachment accommodated ~22 km of displacement (fig. 1). An inflection point in cooling ages is rarely observed in core complexes and indicates extension starts later in the Harquahala Mountains and the EED accommodates less displacement than structurally lower core complexes (e.g. Buckskin-Rawhide Mountains)³.

Standard linear regression of the nearly invariant ZHe ages yields slip rates of up to ~50 km/Myr which are interpreted as geologically unreasonable, whereas rates of ~10-16 km/Myr are calculated by simply taking the 22 km distance over the ZHe age difference. Apatite (U-Th)/He ages along the same transect distance show one slope that yields a slip rates of $4.3 \pm 1.6, -1.0$ km/Myr. Several structural possibilities that could cause invariant age profiles in thermochronometric studies are investigated to better interpret scenarios where a simple

regression is not valid. The most probable scenarios include isostatic rebound, pervasive hanging wall thinning during fault slip, and repetition or perturbation of cooling profiles along high or low-angle faults. An inherent assumption when calculating slip rates is that the hanging wall behaves as a rigid block; therefore structural thinning of the hanging wall will cause an overestimation of slip rates⁴. Hanging wall extension can also cause isostatic rebound of the footwall and may contribute a significant component of vertical exhumation. Coeval or subsequent low and high-angle faulting can also alter otherwise linear age versus distance relationships and are most pronounced in under sampled transects that can overestimate slip rates. Combined geometric and thermal modeling will provide new constraints on the relative importance of the aforementioned processes and give new insights into the structural evolution of low-angle normal fault systems.

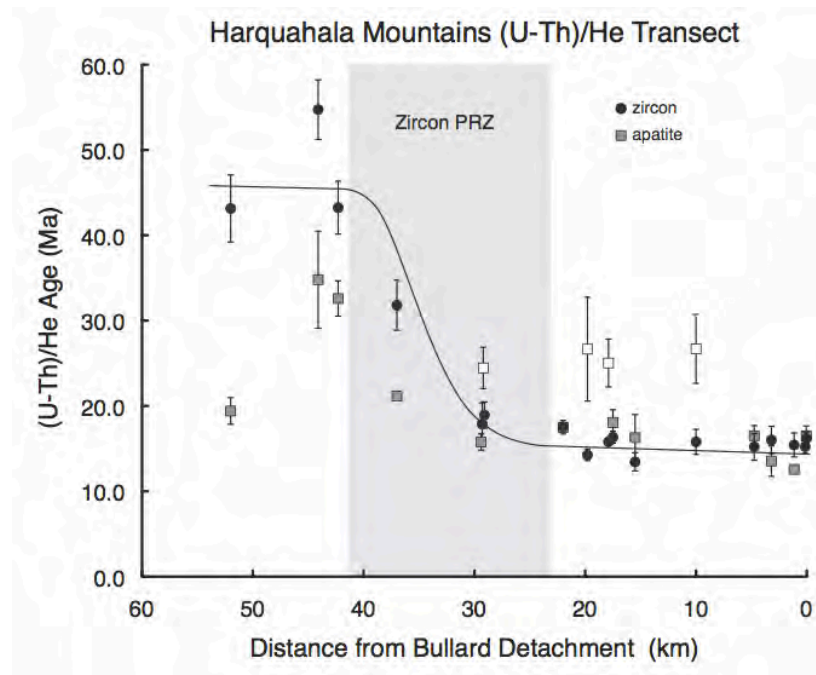


Figure 1. Transect of (U-Th)/He ages plotted as a function of distance from the Eagle Eye detachment. (U-Th)/He ages of zircons and apatites are shown in blue circles and black squares, respectively; open squares indicate analyses excluded based on age inversion most likely due to inclusions in apatites. Error bars shown at 1σ . See text for discussion of ages.

References

1. Stockli, D. F. in *Low-temperature Thermochronology: Techniques, Interpretations, and Applications* (eds. Reiners, P. W. & Ehlers, T. A.) 411-418 (Mineralogical Society of America/Geochemical Society Reviews in Mineralogy and Geochemistry, Chantilly, Virginia, 2005).
2. Carter, T. J., Kohn, B. P., Foster, D. A. & Gleadow, A. J. W. How the Harcuvar Mountains metamorphic core complex became cool: Evidence from (U-Th)/He thermochronometry. *Geology* **32**, 985-988 (2004).
3. Singleton, J. S., Stockli, D. F., Gans, P. & Prior, M. G. Timing, rate, and magnitude of slip on the Buckskin-Rawhide detachment fault, west-central Arizona. *Tectonics* (in review).
4. Wells, M. L., Snee, L. W. & Blythe, A. E. Dating of major normal fault systems using thermochronology: An example from the Raft River detachment, Basin and Range, western United States. *J. Geophys. Res.* **105**, 303-327 (2000).

Cenozoic (U-Th)/He ages in Lofoten - Vesterålen islands, Northern Norway

Sébastien Lénard¹, Cécile Gautheron¹, Bernard Bingen², Rosella Pinna-Jamme¹,
Bart W. H. Hendriks³

1 Geosciences Paris Sud GEOPS, Université Paris-sud, 91405, Orsay, France

2 Geological Survey of Norway, P.O. Box 6315 Sluppen, 7491, Trondheim, Norway

3 Statoil ASA, Arkitekt Ebbells veg 10, 7053, Trondheim, Norway

The old passive margins, especially in the North-East Atlantic above 60° North latitude, present peculiarly high topography, either in Eastern Greenland or in Northern Norway¹⁻². No agreement exists about the grounds of this phenomenon. Unquestionably tectonics has stood as the favorite root cause for more than a century. However, for the northern part of Norway, present topography should only result from erosion and isostasy, thus embodying climate into the real conductor of denudation.

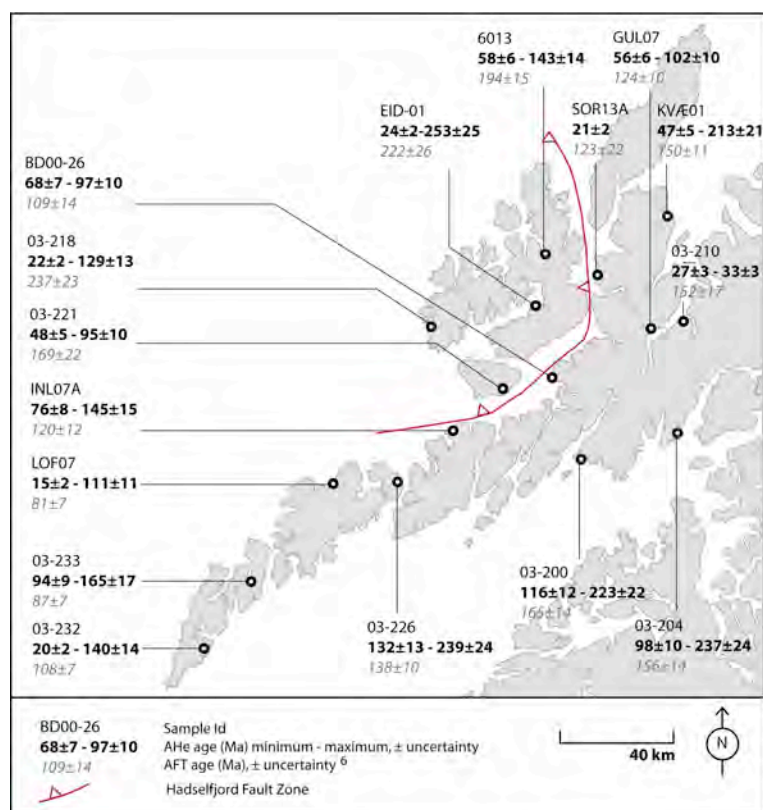
AHe, (U-Th)/He low temperature thermochronometer on apatite is a relevant tool to investigate these natural intriguing phenomena. The thermochronometer is ruled by He diffusion in apatite and this diffusion is sensitive in the 50°C to 120°C range. Uppermost crust denudation can thus be quantified and recent relief evolution be constrained. Concerning the North East Atlantic, few AHe data exist and are widely scattered or even much older than apatite fission track (AFT) ages. We assert today that major improvements were brought to the technique, as the influence on He diffusion of recoil damage fraction and grain chemistry³⁻⁴.

In this study, we focused on the Northern Norwegian margin. Our aim is to supply AHe ages and thus better constrain and understand the recent denudation in the region. We chose 16 samples from Lofoten - Vesterålen islands, already analyzed by AFT data⁵. Apatite AHe ages are within a range from 15±2 to 253±25 Ma (see *Figure 1*) and are characterized by a very low eU content ranging from 1 to 22 ppm plus one sample with higher eU content (up to 328 ppm). The low eU content induces a very low closure temperature for these samples in the 50-60°C range.

The revealed ages are younger than any published AHe age in the North East Atlantic. Paleogene or even Neogene ages do occur for 10 samples out of 16 (*Fig. 1*). Ages contrast widely with the AFT ages of the same samples, which may be up to 200 Ma older (*Fig. 1*). The contrast is even more striking if we consider recent AFT data farther to the north of the area⁶. The geographical distribution of ages differs completely from the distribution of AFT ages. The Hadsselfjord Fault Zone does not constitute a gap any more between ages in the north-west and the rest of the area. Older ages remain limited to a few samples in the south.

Our early data clearly indicate a late Cenozoic episode of denudation in Lofoten - Vesterålen. This episode follows the earlier episode previously detected by AFT ages. However, as for past regional studies we report a wide scattering of single grain ages by sample, commonly a difference of ~50-120 Ma between the younger grain and the older grain. This scattering stays as a great challenge to secure ages interpretation. We are therefore doing further analyses and our main line of research is detecting and evaluating the influence of zonation and chemistry on our samples. Thus we would be able to better interpret the AHe data and performed inverse simulation in order to reconstruct more finely the Cenozoic denudation. Nevertheless it is assumed that according to these results, the newly exposed episode stems from a different mechanism. Geographical distribution of AHe ages show no important impact of recent tectonic movements in the area and the present topography of the area should be explained simply by progressive and continuous denudation. In that case glacial and periglacial erosion combined with isostasy should control relief at this latitude.

Figure 1. Map of the apatite samples in Lofoten-Vesterålen islands. (U-Th)/He ages obtained in this study are displayed in bold. AFT ages of a former study are presented in italic for comparison⁶.



References

- Japsen, P., Green, P. F., Bonow, J. M., Nielsen, T. F. D. & Chalmers, J. A. From volcanic plains to glaciated peaks: Burial, uplift and exhumation history of southern East Greenland after opening of the NE Atlantic. *Global and Planetary Change* **116**, 91-114 (2014).
- Nielsen, S. B., Gallagher, K., Leighton, C., Balling, N., Svenningsen, L., Jacobsen, B. H., Thomsen, E., Nielsen, O. B., Heilmann-Clausen, C., Egholm D. L., Summerfield, M. A., Clause, n O. R., Piotrowski, J. A., Thorsen, M. R., Huuse, M., Abrahamsen, N., King, C. & Lykke-Andersen, H. The evolution of western Scandinavian topography: a review of Neogene uplift versus the ICE (isostasy-climate-erosion) hypothesis. *Journal of Geodynamics* **47**, 72-95 (2009).
- Gautheron, C., Tassan-Got, L., Barbarand, J. & Pagel, M. Effect of alpha-damage annealing on apatite (U-Th)/He thermochronology. *Chemical Geology* **266**, 166-179 (2009).
- Gautheron, C., Barbarand, J., Ketcham, R. A., Tassan-Got, L., van der Beek, P., Pagel M., Pinna-Jamme, R., Couffignal, F. & Fialin, M. Chemical influence on α -recoil damage annealing in apatite: Implications for (U-Th)/He dating. *Chemical Geology* **351**, 257-267 (2013).
- Hendriks, B. W. H., Osmundsen, P. T. & Redfield, T. F. Normal faulting and block tilting in Lofoten and Vesterålen constrained by Apatite Fission Track data. *Tectonophysics* **485**, 154-163 (2010).
- Davids, C., Wemmer, K., Zwingmann, H., Kohlmann, F., Jacobs, J. & Bergh, S. G. K-Ar illite and apatite fission track constraints on brittle faulting and the evolution of the northern Norwegian passive margin. *Tectonophysics* **608**, 196-211 (2013).

Describing orogenic wedges by a combination of numerical sandbox models and low-temperature thermochronology - Implications for the exhumation of the Central Alps

Simon Elfert¹, Linda Wenk², Katrin Huhn², Cornelia Spiegel¹

1 Department of Geosciences, University of Bremen, Germany

2 MARUM Center of Marine Environmental Science, University of Bremen, Germany

Orogenic growth is controlled by tectonics, erosion and climate. The influence of each of these processes and their potential interrelations are still debated. The Alps are probably the most intensively studied mountain belt in the world and thus provide an ideal setting for addressing this topic. For this study, we investigated the late stage exhumation history of the Lepontine Dome in the Central European Alps, and related it to potential climatic and tectonic steering factors. In addition, we tested the influence of lower crustal mechanic and kinematic properties on upper crustal exhumation and erosion. In a final step, we studied the influence of different valley incision scenarios on surface cooling patterns, testing valley incision at 31 Ma (i.e., constant over the entire post-collisional history), at 5 Ma (contemporaneously with enhanced foreland deposition rates) and at 1 Ma (contemporaneously with major Alpine glaciation).

For this we used apatite fission track and (U-Th-Sm)/He thermochronology combined with numerical sandbox experiments. The set up for the numerical sandbox models was based on two deep seismic reflection profiles crossing the Central Alps perpendicular to strike (NFP 20 east & west). Numerical sandbox modelling allows tracking the pathways of single particles. Assuming a geothermal gradient, these pathways were transferred into cooling histories. The cooling histories were in turn used as the basis for forward modelling of thermochronology data, yielding synthetic AFT data, which could be compared to the AFT data actually observed across the Lepontine Dome.

AFT ages observed range from 4 to 19 Ma and form a distinct U-shape pattern, with higher cooling rates in the center of the Lepontine Dome as compared to lower cooling rates at the northern and southern terminations of the profiles. Until the latest Miocene, exhumation is characterized by small scale differences, with both, episodic and continuous cooling occurring close to each other. Miocene exhumation is obviously related to the activity of prominent tectonic structures such as the northern and southern steep belts and is thus explained by ongoing compressional tectonic activity. By contrast, at around the Miocene-Pliocene boundary, cooling becomes more uniform and independent from tectonic structures, suggesting en-block exhumation of the Lepontine area. We explain this as indicating a shift from tectonically-dominated to climatically-dominated erosion. At the Plio-Pleistocene boundary, cooling accelerated, which we interpret as enhanced erosion due to the onset of Alpine glaciation, i.e., again climatically controlled.

Using the numerical sandbox model, we were able to reproduce the main structural entities and the major fault systems of the Central Alps (such as the Adriatic indenter, the Aar basal thrust, the northern steep belt and the Insubric Line), and also the U-shape AFT pattern. Numerical sandbox modelling also showed that the AFT age distribution and thus surface erosion patterns are strongly influenced by mechanic and kinematic properties of the lower crust, particularly by

the décollement strength. When comparing the synthetic AFT ages from the different valley incision scenarios with the AFT data observed across the Lepontine Dome, the best fit is achieved for valley incision at 5 Ma. This is in agreement with the change of the cooling style at the Miocene-Pliocene boundary as observed from thermal history modelling of the AFT data and underlines the assumption of a major change of the Alpine erosion regime at that time.

A coupled AHe and AFT study on the late-stage exhumation history of the Swiss Alps (Rhône valley): Deciphering tectonic, climatic-induced and hydrothermal signals

Pierre Valla¹, Meinert Rahn^{2,3}, David L. Shuster^{4,5}, Peter A. van der Beek⁶

¹ Institute of Earth Surface Dynamics, University of Lausanne, Switzerland

² Swiss Federal Nuclear Safety Inspectorate, Brugg, Switzerland

³ Department of Mineralogy and Geochemistry, University of Freiburg, Germany

⁴ Department of Earth & Planetary Science, University of California, Berkeley, USA

⁵ Berkeley Geochronology Center, Berkeley, USA

⁶ Institute of Earth Sciences, University of Grenoble, France

Neogene exhumation of the European Alps is understood as the interlude of tectonics and erosion¹. While the former has been influenced by a decrease in plate convergence, the latter has been suggested to be affected by climatic variation^{2,3}, leading to relief amplification⁴. However, even though geomorphologic and sedimentologic studies both suggest topographic relief change and transition from fluvial to oscillations between glacial/fluvial conditions^{5,6}, precise quantifications on both the timing and magnitude of this transition are yet sparse^{4,7}, and areas of sufficient time resolution are restricted to spots of very fast exhumation during the last few million years and thus very young thermochronologic data².

This study focuses on the upper Rhône valley (Swiss Central Alps) within the Visp-Brig area (Aar massif, Valais). This area encompasses some of the most spectacular reliefs within the Alps with several nearby summits around or above 4000 m crosscut by the glacially overdeepened Rhône valley. It also shows among the highest late Neogene exhumation rates within the Western-Central European Alps^{2,4}, influenced by tectonic activity along the major Simplon-Rhône extensional fault system⁸⁻¹⁰. Moreover, the upper Rhône valley has experienced enhanced glacial erosion associated with strong relief development during the Pliocene-Quaternary period^{4,6}. Finally, structural inheritance, late-stage tectonics and rapid exhumation may have promoted recent hydrothermal activity in this region¹¹, although timing of its onset and its precise causes remain poorly understood.

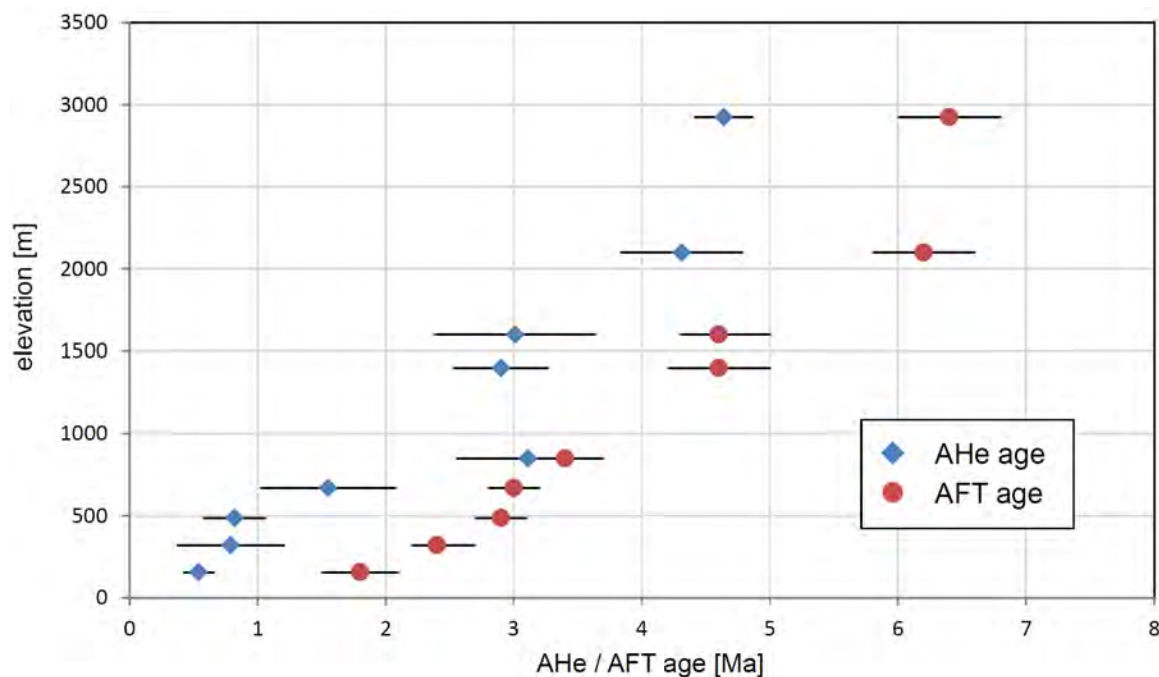


Figure 1. Apatite He (AHe) and fission track (AFT) ages from the Visp-Brig area.

The cooling history has been investigated by using different low-temperature thermochronometers along a pseudo-vertical bedrock profile (elevation between 600 and 2900 m) and additional samples from an on-site 500-m geothermal well, resulting in a total elevation difference of nearly 3 km (Fig. 1). Apatite fission-track (AFT) ages and track-length data have been added to previously published⁴ and new apatite (U-Th-Sm)/He (AHe) and ⁴He/³He data.

Results confirm high-exhumation rates (0.6 to 0.9 km/myr) within late-Cenozoic to Pliocene times. Combined with AFT data from the literature, our age pattern reveals no exhumation difference across the Simplon fault system during the last 6-8 Ma, suggesting only strike-slip detachment activity of the structure during that period. Thermal modelling using HeFTy confirms strong exhumation and evidences a late-stage cooling contrast between high-elevation and valley-bottom/geothermal well samples, in agreement with previous ⁴He/³He data⁴. This late-stage exhumation is associated to the onset of major Alpine glaciation triggering the Rhône valley carving at ~1 Ma. Apatite track length measurements suggest that the well samples may have been affected by recent hydrothermal activity. This agrees well with the present-day observation of high geothermal activity below the Rhône valley floor, whose origin has been primarily linked to structural inheritance (Simplon-Rhône extensional fault system). Our thermochronology data helps to put constrain on the onset timing of this geothermal activity, which we propose to be concordant with the onset of major alpine glaciations, glacial erosion and bedrock fracture development¹² promoting localized fluid circulation and hydrothermal activity below the Rhône valley floor.

References

1. Willett, S. D. Late Neogene Erosion of the Alps: A Climate Driver? *Annual Review of Earth and Planetary Sciences* **38**, 411-437 (2010).
2. Kuhlemann, J., Frisch, W., Szekely, B., Dunkl, I. & Kazmer, M. Post-collisional sediment budget history of the Alps: Tectonic versus climatic Control. *International Journal of Earth Sciences* **91**, 818-837 (2002).
3. Vernon, A. J., van der Beek, P. A., Sinclair, H. D. & Rahn, M. K. Increase in late Neogene denudation of the European Alps confirmed by analysis of a fission track thermochronology database. *Earth and Planetary Science Letters* **270**, 316-329 (2008).
4. Valla, P. G., Shuster, D. L. & van der Beek, P. A. Major increase in relief of the European Alps during mid-Pleistocene glaciations recorded by apatite ⁴He/³He thermochronometry. *Nature Geoscience* **4**, 688-692 (2011).
5. Muttoni, G., Carcano, C., Garzanti, E., Ghielmi, M., Piccin, A., Pini, R., Rogledi, S. & Sciunnach, D. Onset of major Pleistocene glaciations in the Alps. *Geology* **31**, 989-992 (2003).
6. Norton, K. P., Abbühl, L. M. & Schlunegger, F. Glacial conditioning as an erosional driving force in the central Alps. *Geology* **38**, 655-658 (2010).
7. Häuselmann, P., Granger, D.E., Jeannin, P. Y. & Lauritzen, S. E. Abrupt glacial valley incision at 0.8 Ma dated from cave deposits in Switzerland. *Geology* **35**, 143-146 (2007).
8. Mancktelow, N. The Simplon Line: A major displacement zone in the Western Lepontine Alps. *Eclogae Geologicae Helveticae* **78**, 73-96 (1985).
9. Campani, M., Herman, F. & Mancktelow, N. Two- and three-dimensional thermal modeling of a low-angle detachment: Exhumation history of the Simplon Fault Zone, central Alps. *Journal of Geophysical Research* **115**, B10420 (2010).
10. Baran, R., Friedrich, A. & Schlunegger, F. The late Miocene to Holocene erosion pattern of the Alpine foreland basin reflects Eurasian slab unloading beneath the western Alps rather than global climate change. *Lithosphere* **6**, 124-131 (2014).
11. Sonney, R. & Vuattaz, F. D. Properties of geothermal fluids in Switzerland: A new interactive database. *Geothermics* **37**, 496-509 (2008).
12. Leith, K., Moore, J. R., Amann, F. & Loew, S. Subglacial extensional fracture development and implications for Alpine Valley evolution, *Journal of Geophysical Research Earth Surface* **119**, 62-81 (2014).

Apatite fission track data from External Crystalline Massifs of the French Western Alps

M. Lidia Vignol-Lelarge¹, Gérard Poupeau²

1 Instituto de Geociências - Laboratório de Geologia Isotópica- Universidade Federal do Rio Grande do Sul, Av. Bento Gonçalves 9500 - 91501-970 Porto Alegre, RS, Brazil.

lidia.vignol@ufrgs.br

2 Institut de Recherche sur les Archéomatériaux, UMR 5060, CNRS-Université de Bordeaux, and UMR 7194, CNRS-Muséum National d'Histoire Naturelle, Département de Préhistoire, Place du Trocadéro, 75016 Paris, France, gpoupeau@mnhn.fr

Thirty-three samples from the Belledonne and Grand Chatelard External Crystalline Massifs (ECM) and the easternmost Internal Zone of the Dauphinois (French Alps) were dated by fission tracks (FT) on apatites¹. They were taken either on the ground surface or along a tunnel crossing through the Belledonne massif at an altitude varying from 450 to 500 m. It was determined by electron microprobe that all samples were fluorapatites, thus having similar thermal track retention characteristics. Given the low fossil track densities ($\pm 10 \times 10^4 \text{ t.cm}^{-2}$) and the small number of grains per sample, it was not possible to obtain enough induced track densities for an optimization of the data.

As in other ECM, all FT ages were found to be lower than 10^7 Ma. On the SW slope of the Belledonne massif, the FT ages vary with altitude between about 1 Ma at an altitude of 500 m to 7.5 Ma at 2750 m, corresponding to an apparent denudation rate of 0.4 km/Ma. The less well documented slope-dependent age variations in the eastern Flysh Zone and the southernmost Grand Chatelard suggest a slightly higher rate, of about 0.7 km/Ma, between 5 and 3 Ma. These rates are consistent with the rates found for other ECM (*inter alia*²⁻⁴). They are also consistent with the 0.7-3.5 Ma ages found for the Belledonne tunnel samples. The more complex age-altitude relationship on samples from the NE Belledonne was interpreted as the result of a local block tectonic movement, one hypothesis inferred from field evidences⁵.

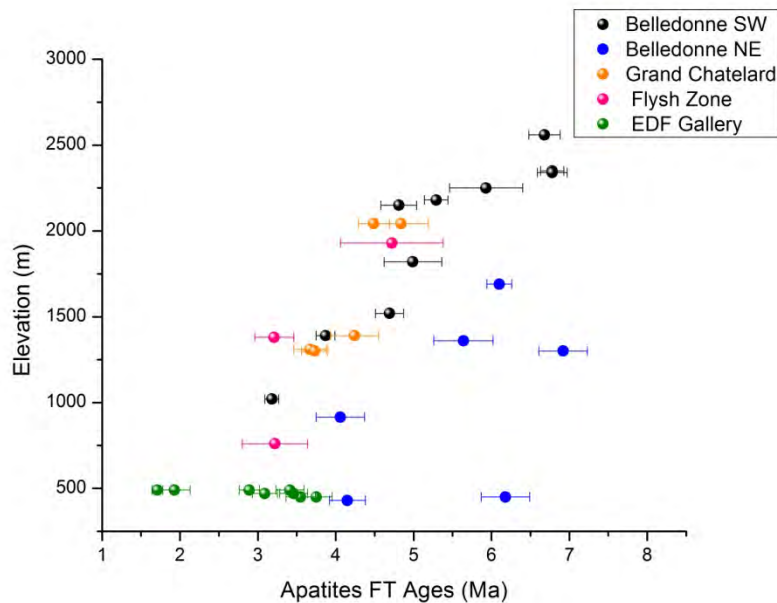


Figure 1. Age-elevation distribution for all samples.

References

1. Vignol-Lelarge, M. L. Thermochronologie par la méthode des traces de fission d'une marge passive (Dôme de Ponta Grossa, SE Brésil) et au sein d'une chaîne de collision (zone externe de l'Arc Alpin, France). Ph.D., Université Joseph Fourier, Grenoble (1993).
2. Van der Beek, P. A., Valla, G., Herman, F., Braun, J., Persano, C., Dobson, K. J. & Labrin, L. Inversion of thermochronological age–elevation profiles to extract independent estimates of denudation and relief history — II: Application to the French Western Alps. *Earth and Planet. Sci. Letters* **296**, 9-22 (2010).
3. Glotzbach, C., Reinecker, J., Danisik, M., Rahn, M., Frisch and W., Spiegel, C. Neogene exhumation history of the Mont Blanc massif, western Alps. *Tectonics* **27**, TC4011 (2008).
4. Bigot-Cormier, F., Sosson, M., Poupeau, G., Stephan, J.-F., Labrin, E. The denudation history of the Argentera Alpine External Crystalline Massif (Western Alps, France–Italy): an overview from the analysis of fission tracks in apatites and zircons. *Geodyn. Acta* **19**, 455–473 (2006).
5. Ménard, G. Structures et cinématiques d'une chaîne de collision : les Alpes occidentales et centrales. Ph.D., Université Joseph Fourier, Grenoble (1988).

Exhumation of the Barles half-window (southern western Alps, France) constrained by apatite (U-Th)/He thermochronology

Stéphane Schwartz¹, Cécile Gautheron², Thierry Dumont¹, Jérôme Nomade¹, Laurence Audin¹, Rosella Pinna-Jamme²

¹ ISTERre, Université Joseph-Fourier Grenoble, France

² UMR GEOPS, Université Paris sud, France

The frontal part of the southeastern Alpine belt is characterized by important compressional deformation marked by the emplacement of the Digne nappe thrust sheet (Figure 1). The final displacement of this nappe is dated Late Miocene thanks to continental molasses of the northeastern margin of the foreland basin, which are folded in its footwall and form the famous Vélodrome recumbent syncline^{1,2}. The stratigraphic series of the Digne nappe is made of more than 5000 m thick Liassic to Eocene deposits³, a part of which overthrust the vélodrome syncline. In order to quantify this overburden and the timing of the subsequent exhumation and erosion of the Barles half-window, we performed a low temperature apatite (U-Th)/He study on the Tertiary molasse sampled at different locations within it. Preliminary AHe ages obtained in Early Miocene marine molasse, range from 4 to 6 Ma, with effective Uranium content ranging from 30 to 80 ppm. The lack of correlation between the AHe ages and the eU content⁴ indicates an important reheating phase (up to 80°C), which has reset the He system before the final exhumation. More apatite (U-Th)/He data coupled with apatite fission-tracks will be done in the future in order to better characterize the timing and the burial maximal temperature.

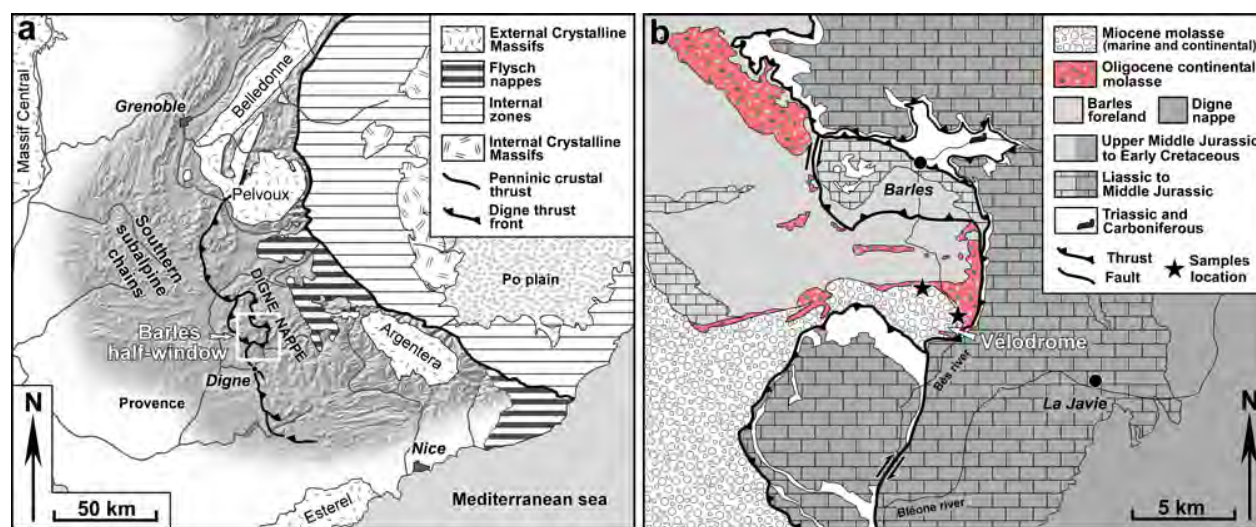


Figure 1. a-Structural sketch map of the western Alps and its foreland. The Barles half-window is located in the footwall of the Digne nappe thrust sheet. b-Geological map of the Barles half-window with the location of the Vélodrome study area.

These first thermochronological results obtained in the Barles half-window have important structural implications:

- The thermal conditions during burial associated with the Digne nappe thrusting were sufficient enough to reset the detrital apatites in Miocene sediments. This implies several kilometers of tectonic overload.
- Maximum burial occurred 6 to 4 Ma ago, which precludes the occurrence of any Messinian incision overlain by the nappe in the Barles half-window as recently proposed⁵.
- This localized exhumation and erosion is related to large-wavelength anticlinal bending of the Barles area, which is coeval with the ultimate SSW-directed motion of the main part of the nappe.

This thickening, which is compatible with outward propagation of deformation in the frontal part of the Alpine orogenic wedge, could be a consequence either of sedimentary cover stacking, or of deep-seated basement involved shortening.

References

1. Gidon, M. & Pairs, J. L. Relations entre le charriage de la nappe de Digne et la structure de son autochtone dans la vallée du Bès (Alpes de Haute-Provence, France). *Eclogae Geologicae Helvetiae* **85**, 327-359 (1992).
2. Fournier, M., Agard, P. & Petit, C. Micro-tectonic constraints on the evolution of the Barles half-window (Digne nappe, southern Alps). Implications for the timing of folding in the Valensole foreland basin. *Bulletin de la Société Géologique de France* **179**, 551-568 (2008).
3. Gidon, M. Les chaînons subalpins au Nord-Est de Sisteron et l'histoire tectonique de la nappe de Digne. *Géologie Alpine* **73**, 23-57 (1997).
4. Gautheron, C., Tassan-Got L., Barbarand J. & Pagel M. Effect of alpha-damage annealing on apatite (U- Th)/He thermochronology. *Chemical Geology* **266**, 166-179 (2009).
5. Hippolyte, J. C., Clauzon, G. & Suc, J. P. Messinian-Zanclean canyons in the Digne nappe (southwestern Alps): tectonic implications. *Bulletin de la Société Géologique de France* **182**, 111-132 (2011).

Two- and three-dimensional thermokinematic modeling of the Katschberg low-angle detachment (Eastern Alps)

Andreas Wöfler¹, Christoph Glotzbach¹, István Dunkl², Kurt Stüwe³

1 Institute of Geology, University of Hannover, Callinstrasse 30, D-30167 Hannover, Germany, woelfler@geowi.uni-hannover.de

2 Sedimentology & Environmental Geology, Geoscience Center, University of Göttingen, Goldschmidstrasse 3, D-37077 Göttingen, Germany

3 Institute of Earth Sciences, University of Graz, Heinrichstrasse 26, A-8010 Graz, Austria

In this study we investigate the Katschberg low-angle detachment that was mainly responsible for the exhumation of the eastern Tauern Window during Miocene lateral extrusion. This fault zone consists of an extensional ductile shear zone comprising a ~5 km thick belt of mylonites with brittle overprint and kinematic indicators document top-to-the east and southeast ductile shearing^{1,2}.

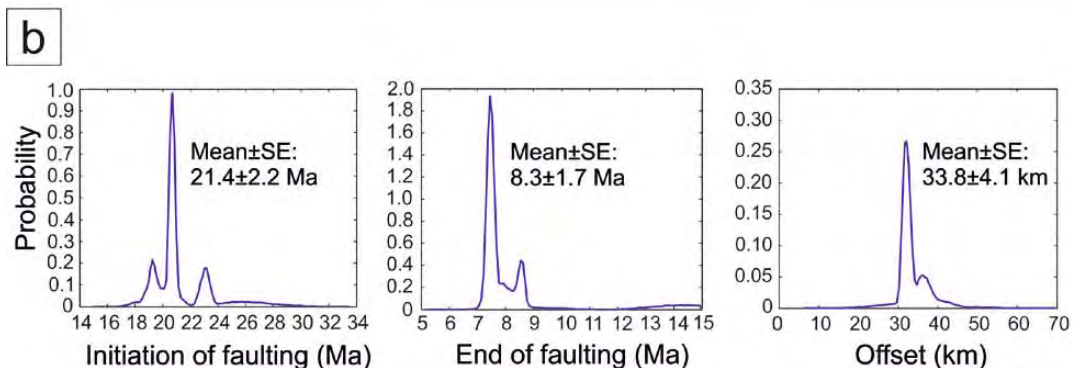
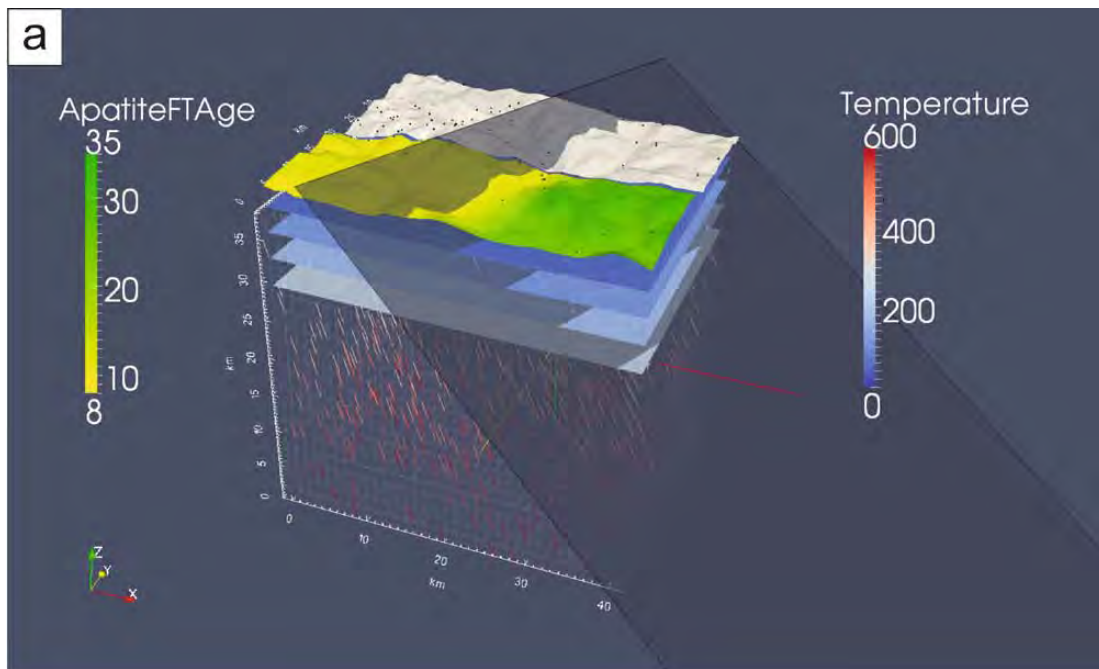


Figure 1. (a) Model setup of inverse thermal-kinematic modeling and **(b)** forward modeling results. Exhumation of rocks is controlled by the 30° ESE dipping Katschberg low-angle detachment.

We sampled two E-W profiles that extend 25 km in the footwall and 20 km into the hanging wall. The samples from these profiles display Middle to Late Miocene apatite fission track and Late Miocene to Pliocene apatite (U-Th)/He ages. A database of new and published thermochronological data provides the basis for two- and three- dimensional thermokinematic modeling using the Pecube v.3 modelling package^{3,4} (Fig 1a). The dataset comprises K/Ar, Ar/Ar, Rb/Sr, zircon and apatite fission track data, as well as apatite (U- Th)/He ages from the foot- and hanging wall, respectively. For thermal modeling we use a finite- element code to solve the heat equation in 3D and predict the thermal evolution of the Katschberg low-angle detachment under given spatially and temporally variable boundary conditions. An inversion routine is used to find the best-fitting parameter combination, which reduces the misfits between modeled and measured thermochronological ages.

According to our modeling results the fault zone is predicted to start at 21.4 ± 2.2 Ma with an offset of 33.8 ± 4.1 km and a vertical through between foot- and hanging wall of ~ 15 to 16 km. Fault activity ended at 8.3 ± 1.7 Ma (Fig. 1b). Our results are in agreement with previous studies that suggest that the Katschberg detachment was active between ~ 23 and ~ 12 Ma^{2,5}.

References

1. Genser, J. & Neubauer, F. Low angle normal faults at the eastern margin of the Tauern Window (Eastern Alps). *Mitteilungen der Österreichischen Geologischen Gesellschaft* **81**, 233-243 (1989).
2. Scharf, A. Handy, M. R. Favaro, S. Schmid, S. M. Bertrand, A. Modes of orogen-parallel stretching and extensional exhumation in response to microplate indentation and roll-back subduction (Tauern Window, Eastern Alps). *International Journal of Earth Sciences* **102**, 1627-1654 (2013).
3. Braun, J. Pecube: a new finite-element code to solve 3D heat transport equation including the effects of a time-varying, finite amplitude surface topography. *Computers & Geosciences* **29**, 787-794 (2003).
4. Braun, J. van der Beek, P. Valla, P. Robert, X. Herman, F. Glotzbach, C. Pedersen, V. Perry, P. Simon-Labric, T. Prigent, C. Quantifying rates of landscape evolution and tectonic processes by thermochronology and numerical modeling of crustal heat transport using PECUBE. *Tectonophysics* **524-525**, 1-28 (2012).
5. Wölfler, A. Dekant, C. Danišik, M. Kurz, W. Dunkl, I. Putiš, M. Frisch, W. Late stage differential exhumation of crustal blocks in the central Eastern Alps: evidence from fission track and (U-Th)/He thermochronology. *Terra Nova* **20**, 378-384 (2008).

Timing of shortening-extension pair migration and topographic evolution in the Catena Costiera and Sila Massif, southern Italy

Maria Laura Balestrieri¹, Valerio Olivetti², Finlay M. Stuart³, Stuart N. Thomson⁴

¹ CNR, Institute of Earth Sciences and Georesources, Florence, Italy

² Department of Sciences, Roma3 University, Italy

³ Scottish Universities Environmental Research Centre, East Kilbride, UK

⁴ Department of Geosciences, University of Arizona, USA

The Calabrian-Peloritani arc (Figure 1a, b) is a small emerged-above-sea-level portion of an orogenic wedge seated on top of a narrow and active subduction zone¹⁻². The Cenozoic evolution of the Calabrian wedge is marked by a multiphase history that started with oceanic subduction, evolved into continental subduction, and since the Oligocene has been dominated by southeastward slab retreat. Subduction trench roll-back led to spreading of back-arc basins (Liguro-Provencal and Tyrrhenian) and within the wedge, induced syn-orogenic extension nearly coeval with thrusting at the wedge front³⁻⁶.

During the last two decades, low temperature thermochronology has proven a powerful tool to investigate the processes of syn-orogenic exhumation and constrain the timing of shortening-extension pair migration.

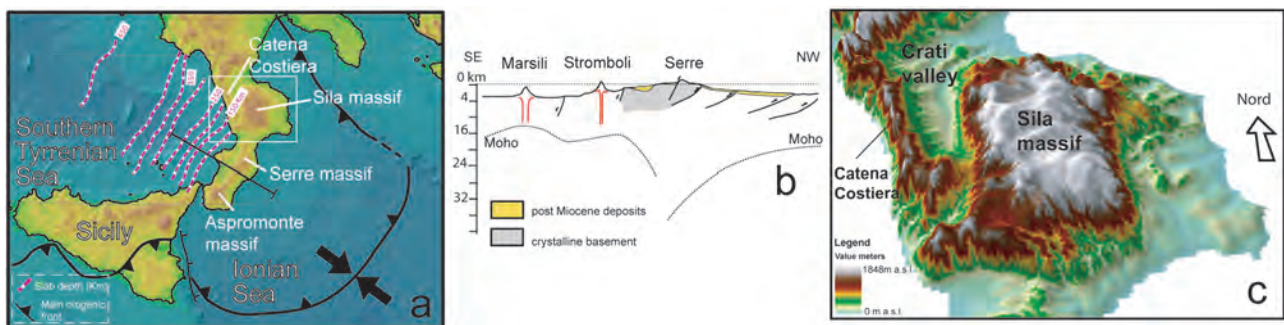


Figure 1. a - Topography, bathymetry and main tectonic features of southern Italy (square: study area). Purple dashed lines are depth contour lines of the Wadati-Benioff zone associated with the Calabria subduction zone. b - Crustal thickness along a NW-SE profile (indicated in 1a) across central Calabria. c - 3D view of the Catena Costiera and Sila Massif topography.

In this study we integrate apatite fission-track (AFT) literature data⁷⁻⁹ with new apatite (U-Th)/He (AHe) data along a transect from Tyrrhenian to Ionian sea through the Catena Costiera and Sila Massif (Figure 1c). The complex geodynamic evolution of the Calabrian wedge left a signature in the thermal history of the rocks of the Calabrian arc. In Eastern Sila, AFT data show that most of the different portions of the Sila basement cooled at 18-13 Ma. The inception of the main exhumation phase was detected through a break in slope in an age-elevation profile at 18-17 Ma. It was likely driven by erosion associated with top to the east thrust imbrication. AHe ages are younger but close to the AFT age values pointing to a rapid phase of exhumation followed by an abrupt decrease of the exhumation rate. An inverse AFT age-elevation relationship in a profile on top of the summit area of the eastern Sila implies a later phase of relief degradation, which is in agreement with the Sila massif upland topography showing a low-relief relict surface, covering 600 km² (Fig. 1c).

Exhumation in the Catena Costiera and western Sila started in the Oligocene through top-to-the-W ductile low-angle extensional faults which later transitioned to brittle extensional tectonics. Literature AFT data⁵⁻⁶ and new AHe show similar values between the Catena Costiera and western Sila despite the two areas being separated by the Crati Valley (Figure 1c). The ages are slightly younger than those on eastern side of the Sila. Our new data reveal that in early-middle Miocene the Catena Costiera and western Sila were exhuming as a single block. Only in the Tortonian with the opening of the Crati valley¹⁰ did the two areas become topographically separated.

Literature and new thermochronologic data are generally older than 10 Ma, and do not record any more recent tectonic event, conversely to what expected for a region with Recent high active seismicity, high relief, and high regional uplift rates. Geomorphic indicators, in fact indicate that the present day high topography was only established in the last few million years, with insufficient time for associated exhumation and incision to be recorded by low temperature thermochronometry

References

1. Faccenna, C., Becker, T. W., Lucente, F. P. & Rossetti, F. History of subduction and back-arc extension in the central Mediterranean. *Geophysical Journal International* **145**, 809–820 (2001).
2. Faccenna, C., Molin, P., Orecchio, B., Olivetti, V., Bellier, O., Funicello, F., Minelli, L., Piromallo, C. & Billi, A. Topography of the Calabria subduction zone (southern Italy): Clues for the origin of Mt. Etna. *Tectonics* **30**, (2011).
3. Jolivet, L., Faccenna, C., Goffé, B., Burov, E. & Agard, P. Subduction tectonics and exhumation of High-Pressure metamorphic rocks in the Mediterranean orogens. *American Journal of Science* **303**, 353–409 (2003).
4. Malinverno, A. & Ryan W. Extension in the Tyrrhenian sea and shortening in the Apennines as result of arc migration driven by sinking of the lithosphere. *Tectonics* **5**, 227-245 (1986).
5. Rosenbaum, G., Lister, G. S. & Duboz, C. The Mesozoic and Cenozoic motion of Adria (central Mediterranean): a review of constraints and limitations. *Geodinamica Acta* **17** (2), 125–139 (2004).
6. Rossetti, F., Goffé, B., Monié, P., Faccenna, C. & Vignaroli, G. Alpine orogenic PTt deformation history of the Catena Costiera area and surrounding regions (Calabrian Arc, southern Italy): the nappe edifice of Northern Calabria revised with insights on the Tyrrhenian–Apennine system formation. *Tectonics* **23**, 1–26 (2004).
7. Thomson, S.N. Fission track analysis of the crystalline basement rocks of the Calabrian Arc, southern Italy: evidence of Oligo-Miocene late orogenic extension and erosion. *Tectonophysics* **238**, 331–352 (1994).
8. Thomson, S. N. Assessing the nature of tectonic contacts using fission-track thermochronology: an example from the Calabrian Arc, southern Italy. *Terra Nova* **10**, 32–36 (1998).
9. Vignaroli, G., Minelli, L., Rossetti, F., Balestrieri, M. L. & Faccenna, C. Miocene thrusting in the eastern Sila Massif: Implication for the evolution of the Calabria-Peloritani orogenic wedge (southern Italy). *Tectonophysics* **538–540**, 105–119 (2012).
10. Spina, V., Tondi, E. & Mazzoli, S. Complex basin development in a wrench-dominated back-arc area: Tectonic evolution of the Crati Basin, Calabria, Italy. *Journal of Geodynamics* **51**, 90–109 (2011).

Intraplate deformation in North-West Africa: the northern front of the Atlas mountains in Morocco

Isabelle Jouvie¹, Cécile Gautheron¹, Yves Missenard¹, Rosella Pinna-Jamme¹, Omar Saddiqi²

1 UMR GEOPS, Université Paris Sud, 91405 Orsay, France

2 Faculté des Sciences Ain Chock, 20100 Casablanca, Morocco

The Atlas mountains form an intraplate mountain range of 2500 km long from Morocco to Tunisia. Our study focus on the Moroccan part of the Atlas, also named the High Atlas. It is the highest region of the whole belt (4167 m, jbel Toubkal) and of North Africa. Two components are advanced to explain the present topography in the Moroccan High Atlas: the first one is the crustal deformation caused by the convergence between Eurasia and Africa, which expresses itself by thrusts and décollements in the cover above Paleozoic or Precambrian basement¹. The second one is a lithospheric component (thin lithosphere and abnormally hot mantle), whose origin remains discussed².

The Atlas range has formed during Cenozoic, confining the compressive deformation along old normal faults inherited from the Mesozoic Atlantic and Tethyan riftings³. This rifting phase was itself driven by old inherited Variscan structures. Nowadays, Mesozoic sediments that have been uplifted during the Cenozoic are found high in the Atlas mountains, especially in the Eastern and Central High Atlas where Jurassic rocks have been well preserved and cover most of the belt. The coastal part of the Western High Atlas also shows a Triassic to Cretaceous cover. Between them, the Marrakech High Atlas and the rest of the Western High Atlas show a different geology: only few patches of Mesozoic cover remain, and most of the area consists of Proterozoic and Paleozoic basement.

The precise timing of the Cenozoic inversion is still a matter of debate. Over the years, several studies have been published concerning the uplift chronology in the High Atlas. To constrain the timing of exhumation, thermochronology data have been collected using mainly Fission Tracks (and more recently (U-Th)/He) methods on apatite and zircon. Exhumation ages that have been obtained range from Cenozoic to Neogene, with one or several phases according to the different authors. No consensus has emerged yet, and this is the reason why we choose to bring new data and try to correlate them with previous studies.

In order to better characterize the structural inversion timing inside the High Atlas, we performed a combined structural and low temperature apatite (U-Th)/He study. Our study area is located in the Amizmiz region (figure 1A), on the North front of the Western High Atlas (to the South-West of Marrakech). There, we find the Variscan Paleozoic outcrops and some Mesozoic plateaus above them, both being separated by an angular unconformity (figure 1B). The plateaus are mainly composed of Cretaceous rocks, and often lack Jurassic deposits. Patches of Eocene sediments are found on the southern limit of the Cretaceous plateaus. A field study showed that those cover units present a slightly monoclinical trend to the South and are minimally deformed (figure 1B). It seems that, despite the fact that the Jurassic and early Cretaceous rocks contain thick levels of evaporites, the compressive deformation has not spread through them. The uplift would have affected whole blocks of Paleozoic basement (with their Mesozoic cover on top) with thick-skin thrusts. Our study area is delimited by two of these E-W basement thrusts: the northern

one is the Amizmiz thrust, and the southern one is the southern border of the plateaus.

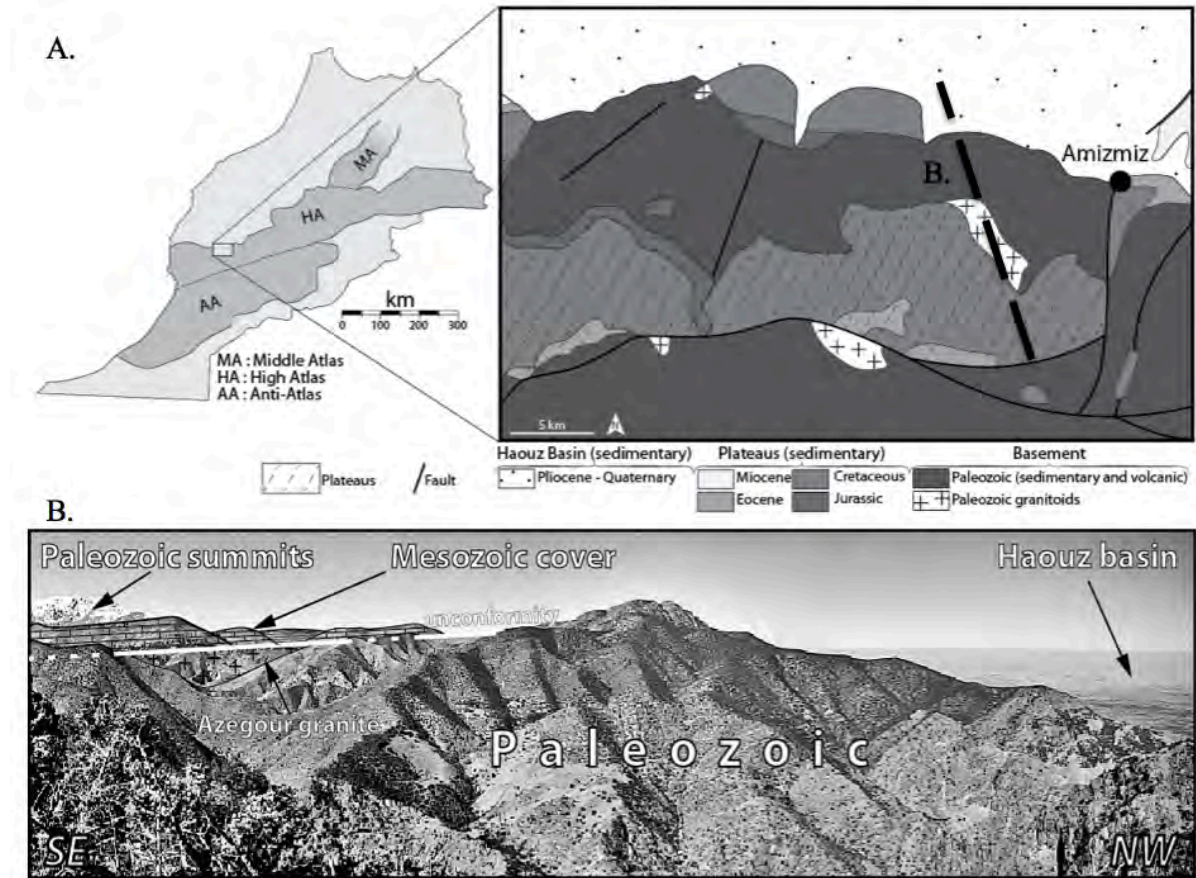


Figure 1. A. Map of the studied area drawn after the 1:1 million scale geological map of Morocco. B. Highlighting of the very straight trend of the unconformity between the Mesozoic (mainly Cretaceous) cover and the Paleozoic basement which contains igneous intrusions. A thermochronological apatite (U-Th)/He study of the granitoid units sampled in the Paleozoic basement, with altitudes range from 860 m to 2065 m, will be performed in the next months. It will provide a time constraint to the structural model. Ages will be discussed in the light of estimated thickness variations of the sedimentary cover that will determine if sediments may be considered as syn-rift deposits. Cross sections cutting through the granites, the cover and the basement, will allow to define the different structural contacts.

References

1. Missenard, Y., Taki, Z., Frizon de Lamotte, D., Benammi, M., Hafid, M., Leturmy, P. & Sébrier, M. Tectonic styles in the Marrakesh High Atlas (Morocco) : The role of heritage and mechanical stratigraphy. *Journal of African Earth Sciences* **48**, 247-266 (2007).
2. Missenard, Y. & Cadoux, A. Can Moroccan Atlas lithospheric thinning and volcanism be induced by Edge-Driven Convection? *Terra Nova* **24**, 27-33 (2012).
3. Frizon de Lamotte, D., Zizi, M., Missenard, Y., Hafid, M., El Azzouzi, M., Maury, R.C., Charrière, A., Taki, Z., Benammi, M. & Michard, A. in *Continental Evolution : The Geology of Morocco. Lecture Notes in Earth Sciences* (eds. Michard, A., Saddiqi, O., Chalouan, A. & Frizon de Lamotte, D.) 133-202 (Springer-Verlag Berlin Heidelberg, 2008).

Uplift history of the eastern Moroccan Atlas Mountains and influence of the Rif system assessed by low temperature thermochronology

Ludovic Lafforgue¹, Jocelyn Barbarand¹, Cécile Gautheron¹, Rosella Pinna-Jamme¹
¹ UMR UPS-CNRS GEOPS, Université Paris Sud, Orsay, France

The Moroccan Atlas Mountains are an intracontinental chain caused by the inversion of the Mesozoic Atlantic and Tethysian Basins during Eocene initially then Quaternary. It dominates the North African reliefs with more than 4000m high. Nevertheless, toward East and Northeast of Morocco, the relief of the chain decreases roughly to ~1000 m, following the eastern High Atlas and Middle Atlas. This study aims to decipher the erosion and uplift history of this domain.

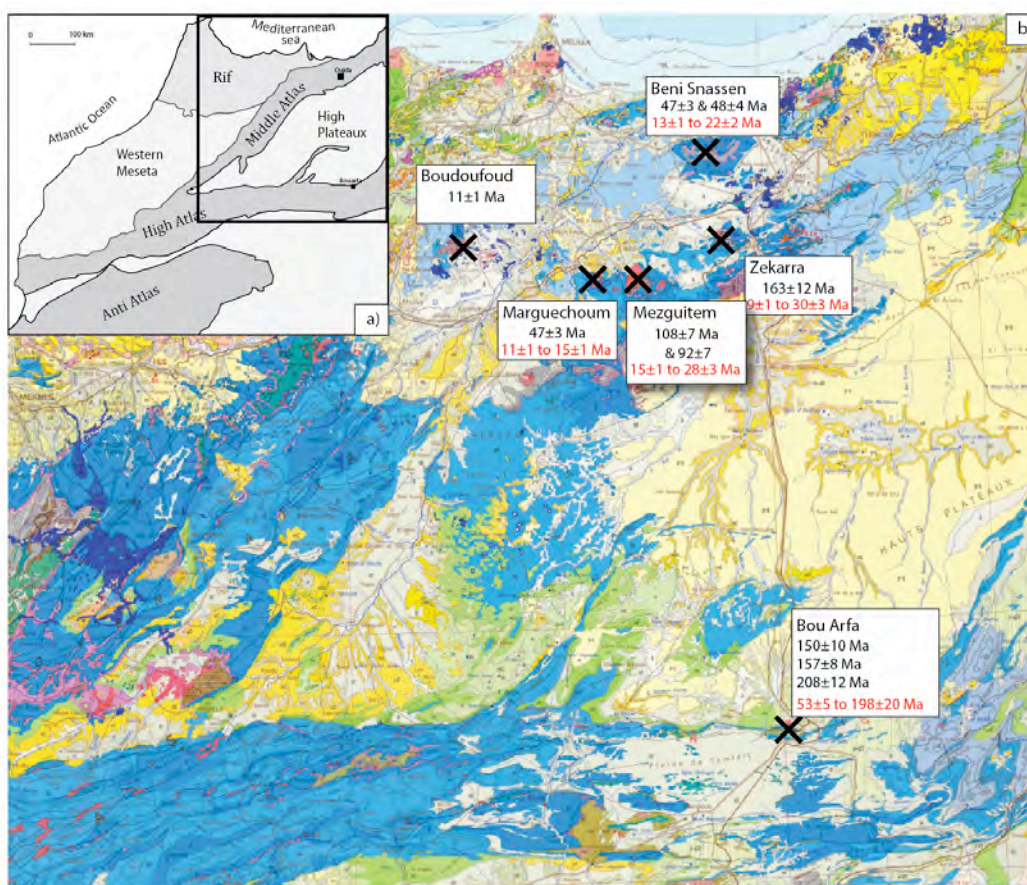


Figure 1: a) Map of geological units in Morocco. The localization of the studied area is in framed. b) Map of AFT (in black) and Helium (in red) ages.

In the core of the eastern High Atlas, at ~1000 m, 200 to 300 m of Jurassic poorly deformed sedimentary rocks are preserved in the Tamlelt plain composed of Paleozoic metamorphized basement. The deformation and reliefs are mainly located on the South Atlasic Front (SAF) and North Atlasic Front (NAF). On the North, close to the former mining town of Bouarfa, the Pliensbachian sand contains the remains of a granitic hercynian massif eroded, which are suitable to apatite fission tracks (AFT) and (U-Th)/He (AHe) analysis. The apatite fission-track central ages range between 150±10 Ma to 208±12 Ma and AHe ages range between 53±5 Ma to 198±20 Ma. These data, in association with fission-tracks lengths indicate a slow cooling during Mesozoic time with little effect of the Atlas convergence.

On the northeast part, in the “Pays des Horsts” chain, relief is formed by several Jurassic units like the Beni Snassen, Mezguitem and is separated from the Middle Atlas by the Cenozoic Guercif Basin. At the base of these relics are located the variscan basement composed of calc-alkaline granitoids. The AFT analysis carried on those granitoids give various ages: 163 ± 12 Ma (Horst chain) to 46 ± 3 Ma (Beni Snassen). Furthermore, AHe ages are very young: 13 ± 1 to 22 ± 2 Ma (Beni Snassen). Unlike previous results those suggest that in the thermal history Northeast of Morocco is characterized by several stages trough Meso-Cenozoic time. This region is adjacent to the Rif system, further west, which is linked to the closure of the south tethysian margin that has been initiated during late Eocene. Therefore this event could explain the youngest ages obtained by low temperature thermochronology, and the difference with the results of the eastern High Atlas.

Late Miocene to Present-day exhumation and uplift of the Internal Zone of the Rif chain : insights from low-temperature thermochronometry and basin analysis

Romagny A.¹, Münch P.², Cornée J. J.², Corsini M.¹, Azdimousa A.³, Melinte-Dobrinescu M. C.⁴, Drinia H.⁵, Bonno M.², Arnaud N.², Monié P.², Quillévéré F.⁶, Ben Moussa A.⁷

1 Laboratoire Géoazur, Université Nice-Sophia Antipolis, Nice, France

2 Géosciences Montpellier, Université Montpellier 2, Montpellier, France

3 Laboratoire de Géosciences Appliquées, Faculté des Sciences Université Mohammed 1, Oujda, Morocco

4 NIRD GeoEcoMar, Marine Geology and Sedimentology, Bucarest, Romania

5 National and Kapodistrian University of Athens, Faculty of Geology and Geoenvironment, Athens, Grece

6 Laboratoire de géologie de Lyon, Terre, Planètes et Environnement, UMR 5276, Université Lyon 1, Lyon, France

7 Département de Géologie, Université Abdelmalek Esaadi, 93003 Tetuán, Morocco

Located on the margin of the west Alboran basin, the Gibraltar Arc (Betic-Rif mountain belt) displays post-Pliocene vertical movements evidenced by uplifted marine sedimentary basins and marine terraces. Quantification of vertical movements is an important clue to understand the origin of present-day relief generation in the Betic-Rif mountain chain together with the causes of the Messinian Salinity Crisis. In this paper, we present the results of a pluridisciplinary study combining an analysis of low temperature thermochronology and Pliocene basins evolution to constrain the exhumation history and surface uplift of internal units of the Rif belt (Northern Morocco). The mean (U-Th)/He apatite ages obtained from 11 samples are comprised between 14.1 and 17.8 Ma and display a wide dispersion, which could be explained by a great variability of apatite chemistries in the analyzed samples. No correlations between altitude and age have been found along altitudinal profile suggesting a rapid exhumation during this period. Thermal modeling using our (U-Th)/He apatite ages and geochronological data previously obtained in the same area (⁴⁰Ar/³⁹Ar and K/Ar data on biotite, zircon and apatite fission track) allow us to propose a cooling history. The rocks suffered a rapid cooling at 60–100°C/Ma between 22.5 and 19 Ma, then cooled to temperatures around 40°C between 19 and 18 Ma. They were re-heated at around 110°C between 18 and 15 Ma then rapidly cooled and exhumed to reach the surface temperature at around 13 Ma. The re-heating could be related to a renewal in thrusting and burying of the inner zones. Between 15 and 13 Ma the cooling resumed at a rate of 50°C/%A indicating an exhumation rate of 0.8 mm/y considering an average 40 °C/km geothermal gradient. This exhumation may be linked to the extension in the Alboran Sea. Otherwise biostratigraphic and sedimentological analysis of Pliocene basins of the internal Rif provided informations on the more recent events and vertical movements. Pliocene deposits of the Rifian coast represent a passive infilling of palaeo-rias between 5.33 and 3.8 Ma. The whole coastal area was uplifted at slow average rates (0.01 to 0.03 mm/y) in relation with a northeastward tilting of 0.2 to 0.3° since the Lower-Pliocene. A Late Pliocene to Present extensional tectonics associated to uplift has been identified all along the coastal ranges of the Internal Zone of the Rif chain. This extension was coeval with the major Late Pliocene to Pleistocene extensional episode of the Alboran Sea and appears to be still active nowadays. No significant Late Messinian uplift was

evidenced, thus calling into question the geodynamic models relating to closure of the marine gateways and the MSC to slab roll back.

Low-temperature evolution of the Serbo-Macedonian massif (SE Serbia): evidence from Ap and Zr fission-track analysis

Milorad Antić¹, Alexandre Kounov¹, Branislav Trivić²

¹*Geologisch-Paläontologisches Institut, Universität Basel, Bernoullistrasse 32, 4056 Basel, Switzerland; m.antic@unibas.ch*

²*Faculty of Mining and Geology, University of Belgrade, Đušina 7, 11000 Belgrade, Serbia*

Serbo-Macedonian massif (SMM) is a crystalline terrane situated between the two diverging branches of the Eastern Mediterranean Alpine orogenic system, the northeast-vergent Carpatho-Balkanides and the southwest-vergent Dinarides and the Hellenides. It is outcropping from the Pannonian basin to the Aegean Sea along central and southeastern Serbia, southwestern Bulgaria, eastern Macedonia and central Greece. Its affiliation to European or African plate basement is still questionable due to the lack of reliable geochronological dating and detailed structural investigation along its boundaries. The massif is also a key area to understand the bipolarity of the Alpine orogenic system, as well as the interaction of the Pannonian and Aegean back-arc extension during the Cenozoic time.

SMM has been traditionally considered to comprise an Upper (low-grade) and a Lower (medium to high-grade) complex. The protoliths of both units have been reported as volcano-sedimentary successions, which have subsequently experienced several stages of deformation and metamorphism. Additionally, both units have been intruded by magmatic rocks during several distinct pulses.

We have applied fission-track analysis on apatites and zircons from the rocks of the SMM coupled with structural field observations in order to reveal its low-temperature evolution. Two distinct phases of cooling have been distinguished in the study area. The region west of Južna Morava River has experienced relatively fast cooling through zircon and apatite closure temperatures (300°-60°C) during the late Cretaceous (94-67 Ma). This event is interpreted as a post-orogenic cooling following the regional nappe-stacking event ("Austrian" phase). In the eastern part of the study area, same late Cretaceous cooling has been recorded by the zircon data, whereas the apatite has remained at temperatures higher than 120°C (but lower than ~200°C) prior to the late Eocene extension and post-magmatic cooling (39-35 Ma). The Crnook area is an exception since both zircon and apatite fission-track data have revealed a late Eocene (45-38 Ma) cooling event related to the extension and the exhumation of the apparent dome structure along low angle normal faults. Thus, the Crnook dome has been recognised as a continuation of the Osogovo-Lisets extensional complex in Serbia.

Low-temperature thermochronological evolution of the eastern Pontides, the eastern Anatolian plateau and the northwestern Lesser Caucasus (Turkey, Georgia, Armenia)

Irene Albino¹, William Cavazza², Massimiliano Zattin³, Aral I. Okay³, Shota Adamia⁴,
Nino Sadradze⁵, Raphael Melkonian⁶, Ghazar Galoyan⁶

1 Dept. of Biological, Geological and Environmental Sciences, University of Bologna, Italy

2 Dept. of Geosciences, University of Padua, Italy

3 Instabul Technical University, Eurasia Institute of Earth Sciences, Turkey

4 Institute of Geophysics Tbilisi, Georgia

5 Geological Institute Tbilisi, Georgia

6 Armenian Academy of Sciences, Yerevan, Armenia

The collision between Arabia and Eurasia led to the development of (i) the Bitlis Zagros suture and associated orogenic belt, (ii) the formation of the North and East Anatolian Fault systems, (iii) the structural inversion of the Caucasian basin(s), and (iv) a widespread deformation in what is now the Anatolian-Armenian-Iranian plateau. The latter effect has been the subject of much debate, with contrasting hypothesis linking the development of the plateau either to compressional stress transfer or to wholesome, mantle-driven uplift (i.e. an effect of dynamic topography). Widespread Plio- Quaternary volcanism across much of the plateau seems to underscore the importance of extensional tectonics during this time frame, as the ascent of such large quantities of magma would be hampered by compressional tectonics.

Despite the importance of the event, the timing of collision-related deformation is poorly known, with estimates ranging from Late Cretaceous¹⁻³, to Late Eocene-Oligocene (35-25 Ma)⁴⁻⁶; to Miocene⁷⁻¹⁰. The low-temperature thermochronological data available for the Bitlis-Pütürge massif point to an episode of fast exhumation in the Middle Miocene¹¹.

The application of the low-temperature thermochronological method based on apatite fission-track analysis, has produced significant constraints to geological evolution of Anatolia and Transcaucasia following Arabia-Eurasia collision. The AFT samples have a wide spatial distribution and include different type of rocks: Paleogene sandstone and magmatic rock with Jurassic to Eocene intrusion ages. Despite the disparate lithologies and large distance, AFT ages from the easternmost Pontides, the northwestern Lesser Caucasus, the eastern Anatolian Plateau, and the Bitlis collision zone show a distinct geographic pattern. Exhumation of the Cretaceous and Eocene granitoids along the Black Sea coast in the eastern Pontides region occurred in the Middle Miocene, mirroring the age of maximum tectonic coupling between the Eurasia and Arabia plates along the 2,400 km long Bitlis-Zagros suture zone, some 200 km to the south. In fact, exhumation ages along the easternmost Pontides are virtually identical to those obtained along the Bitlis segment of the suture¹¹. The mid-Miocene ages obtained along the easternmost Pontides are interpreted as a far-field tectonic effect of the Arabia-Eurasia collision. Such effects are concentrated along the Black Sea coast at the boundary between the polydeformed continental lithosphere and the rheologically stronger oceanic lithosphere of the Eastern Black Sea. Exhumation in the Anatolian Plateau occurred in the Paleogene (with a cluster of ages in the Middle-Late Eocene). Such exhumation ages were the results of the deformation related to the

closure of the Izmir-Ankara-Erzincan ocean and the corresponding collision between the Sakarya and Anatolide- Tauride terranes. The memory of this continental amalgamation has been retained by the AFT thermochronometer because limited exhumation during the creation of the Anatolian Plateau was insufficient to expose a new Apatite Parzial Annealing Zone (PAZ). Stress from the Bitlis collision zone was transmitted heterogeneously in the region of the Lesser Caucasus: the Adjara-Trialeti zone of western Georgia was structurally affected but exhumation was insufficient to expose a new apatite PAZ whereas exhumation in northern Armenia is instead coeval with the Arabia-Eurasia collision and focused along preexisting structural discontinuities like the Paleogene Sevan-Akera suture zone and was strong enough to expose the surface a new PAZ¹².

References

1. Hall, R. Ophiolite emplacement and the evolution of the Taurus suture zone, southeastern Turkey. *Geol. Soc. Am. Bull.* **87**, 1078-1088 (1976).
2. Berberian, M. & King, G. Toward a palaeogeography and tectonic evolution of Iran. *Can. J. of Earth Sci.* **18**, 210- 265 (1981).
3. Alavi, M. Tectonic of Zagros orogenic belt of Iran – new data and interpretation. *Tectonophysics* **229**, 221-228 (1994).
4. Jolivet, L. & Faccenna, C. Mediterranean extension and the Africa-Eurasia collision. *Tectonics* **19**, 095-1106 (2000).
5. Agard, P. Omrani, J. Jolivet, L. & Moutherau F. Convergence history across Zagros (Iran): constraints from collisional and earlier deformation. *Int. J. Earth Sci.* **94**, 401-409 (2005).
6. Allen, M. & Armstrong, H. A. Arabia-Eurasia collision and the forging of midCenozoic global cooling. *Palaeogeography, Palaeoclimatology, Palaeoecology* **265**, 52-58 (2008).
7. Şengör A. M. C., Görür N. & Şaroğlu F. in Strike-slip deformation basin formation and sedimentation: Strike-slip faulting and related basin deformation in zones of tectonic escape: Turkey as a case study (eds. Bibble, K. D. & Christie-Blick N.) **17**, 227-274 (SEPM Spec. Publ., 1985).
8. Dewey, J. F. Hempton, M. R. Kidd, W. S. F. Şaroğlu, F. & Şengör, A. M. C. in Collision Tectonics: Shortening of continental lithosphere: the neotectonics of Eastern Anatolia – a young collision zone (eds. Coward, M. P. & Ries A. C.) **97**, 3-36 (*Geol. Soc. London Spec. Publ.*, 1986).
9. Yılmaz Y. New evidence and model on the evolution of southeast Anatolian orogen. *Geol. Soc. Am. Bull.* **105**, 251- 271 (1993).
10. Robertson, A. H. F. Parlak, O. Rizaouğlu, T. Ünlügenç, Ü. Inan, N. Tasli, K. & Ustaömer, T. in Deformation of continental crust: Tectonic evolution of the South Tethyan ocean: evidence from the Eastern Taurus Mountains (eds. Ries, A. C., Butler, R.W.H. & Graham, R. H.) **272**, 231-270 (*Geol. Soc. London Spec. Publ.*, 2007).
11. Okay, A. I., Zattin, M. & Cavazza, W. Apatite fission-track data for the Miocene Arabia-Eurasia collision. *Geology* **38**, 35-38 (2010).
12. Albino, I., Cavazza, W., Zattin, M., Okay, A. I., Adamia, S. & Sadradze, N. Far-field tectonic effects of the Arabia- Eurasia collision and the inception of the North Anatolian Fault system. *Geological Magazine* **151**, 372-379 (2014).

Tectonics and surface processes interactions in exhumation history of South Alaska: insights from the thermochronological record

Pierre G. Valla^{1,2}, Jean-Daniel Champagnac², David L. Shuster^{3,4}, Frédéric Herman¹,
Maria Giuditta Fellin²

1 Institute of Earth Surface Dynamics, University of Lausanne, Switzerland

2 Department of Earth Sciences, ETH Zurich, Switzerland

3 Department of Earth and Planetary Science, UC Berkeley, United States

4 Berkeley Geochronology Center, United States

The southern Alaska Range (Figure 1) presents an ideal setting to study complex interactions between tectonics, climate and surface processes in landscape evolution¹. It exhibits active tectonics with the ongoing of subduction/collision between Pacific and North America, and major active seismogenic reverse and strike-slip faults². The alpine landscape, rugged topography and the important present-day ice coverage reveal a strong glacial imprint associated with high erosion and sediment transport rates. Therefore, the relative importance of glacial erosion and tectonics for the observed late-exhumation history appears to be quite complex to decipher. This problem partly arises from the fact that most studies have been focused on the southern coast of Alaska where both glacial erosion and tectonic processes are both very active and act together in driving high exhumation rates³.

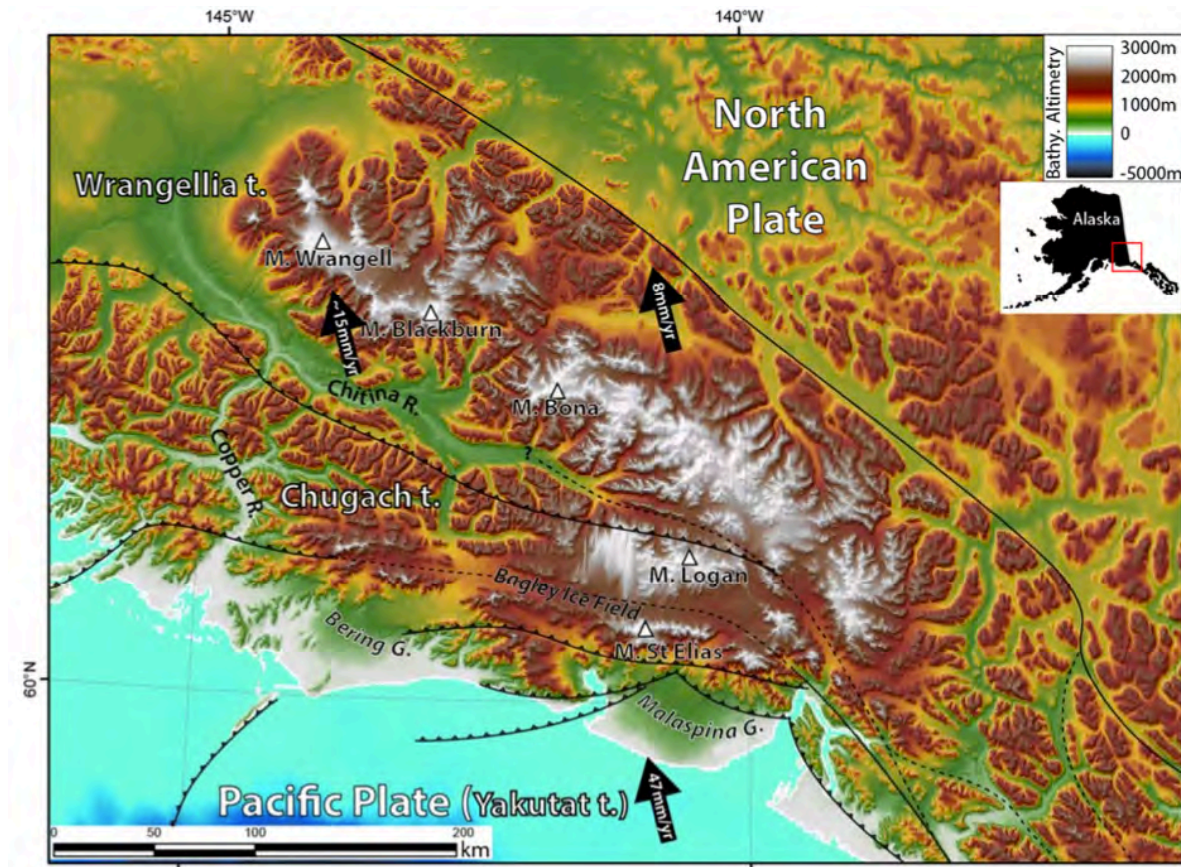


Figure 1. Digital Elevation Model of the Wrangell-St-Elias Range, Alaska.

Here, we first perform a formal inversion of an extensive bedrock thermochronological dataset collected in southern Alaska over the last decades to quantify the large-scale 20-Myr exhumation history. Our results confirm high exhumation rates in the St Elias “syntaxis” and frontal fold and thrust belts for the last 0-2 Myr, where major ice fields and high precipitation rates likely promoted high erosion rates. It also highlights localized exhumation in the last 4-6 Myr along major tectonic features such like the Fairweather and Border Ranges faults. Large-scale inverse modeling therefore suggests that the late-stage exhumation history of South Alaska has mainly been driven by tectonic processes; the impact of late Cenozoic glaciations impact being less visible there than in less active mountain ranges such as the European Alps, British Columbia or Patagonia⁴⁻⁶.

To overcome this potential bias in resolving the glacial impact on erosion history, we studied to the Granite Range (Wrangell-St Elias National Park, Alaska), an area presenting a strong glacial imprint but minor tectonic activity with only localized brittle deformation. We sampled four elevation profiles over an East-West transect for low-temperature thermochrometry. Apatite (U-Th-Sm)/He dating provides ages between ~10 and 30 Ma, in agreement with published data, and shows apparent low long-term exhumation rates (~0.05-0.1 km/Myr). ⁴He/³He thermochronometry on a subset of samples reveals a more complex exhumation history, with a significant increase in exhumation/erosion since ~6-5 Ma that we relate to the early onset of glaciations and glacial erosion processes. Our results thus confirm early glacial activity and associated topographic response in Alaska, well before the onset of Pliocene- Pleistocene Northern Hemisphere glaciations.

References

1. Champagnac, J. D., Molnar, P., Sue, C. & Herman, F. Tectonics, Climate, and Mountain Topography. *Journal of Geophysical Research B: Solid Earth* **117** (2012).
2. Meigs, A., Johnston, S., Garver, J. & Spotila, J. Crustal-scale structural architecture, shortening, and exhumation of an active, eroding orogenic wedge (Chugach/St Elias Range, southern Alaska). *Tectonics* **27** (2008).
3. Enkelmann, E., Zeitler, P. K., Pavlis, T. L., Garver, J. I. & Ridgway, K. D. Intense localized rock uplift and erosion in the StElias orogen of Alaska. *Nature Geoscience* **2**, 360-363 (2009).
4. Valla, P. G., Shuster, D. L. & Van Der Beek, P. A. Significant increase in relief of the European Alps during Mid-Pleistocene glaciations. *Nature Geoscience* **4**, 688-692 (2011).
5. Shuster, D. L., Ehlers, T. A., Rusmore, M. E. & Farley, K. A. Rapid glacial erosion at 1.8 Ma revealed by ⁴He/³He thermochronometry *Science* **310**, 1668-1670 (2005).
6. Thomson, S. N. *et al.* Glaciation as a destructive and constructive control on mountain building. *Nature* **467**, 313-317 (2010).

Cooling history and provenance of cobbles from the Seward-Malaspina Glacier, SE Alaska

Sarah Falkowski¹, Jörg A. Pfänder², Kerstin Drost¹, Eva Enkelmann³

¹ Universität Tübingen, Germany

² TU Bergakademie Freiberg, Germany

³ University of Cincinnati, OH, USA

Our study focuses on the eastern syntaxis of the convergent Chugach-St. Elias Mountains, the St. Elias syntaxis (Fig. 1), and the extent of the area of the most rapid and deep-seated exhumation that has been observed there¹. This is also the area of the orogen's thickest and most extensive ice fields (Seward Ice Field, Hubbard Glacier), of which the ~5000 km²-large Seward-Malaspina Glacier catchment is of particular interest as it comprises a large part of the syntaxis area (Fig. 1). Extensive glaciation of orogens poses a considerable challenge to sampling for thermochronologic and geochronologic studies. In the glaciated Chugach-St. Elias Mountains in southeast Alaska/ southwest Yukon the sampling strategy has often been to collect bedrock samples from the ice-free parts of the mountains, i.e., from relatively high elevations²⁻⁴. We demonstrate that our approach of petrographic analyses in combination with multiple dating (zircon U/Pb, hornblende and biotite ⁴⁰Ar/³⁹Ar, zircon and apatite (U-Th)/He,) of cobble-sized outwash material gives us information on rock exhumation and provenance within the catchment. Furthermore, we establish time-temperature paths for the rocks.

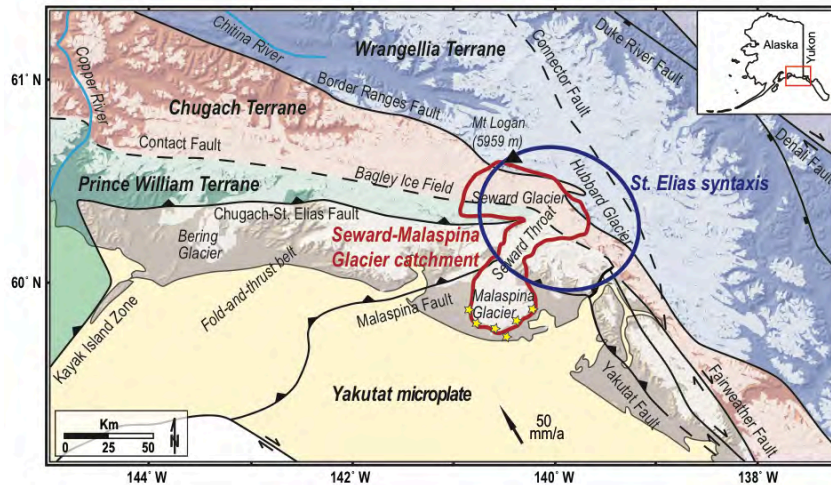


Figure 1. Overview of southeast Alaskan tectonics and terranes. Sample locations of cobble-sized glacial outwash are indicated by stars.

The Chugach-St. Elias Mountains are a result of the oblique subduction-collision of the Yakutat microplate with the North American Plate. In the St. Elias syntaxis area the dextral motion along the plate bounding Fairweather Fault transitions into convergence (Fig. 1). While flat-slab subduction has been going on since at least the Late Oligocene⁵, collision probably started in the Middle Miocene and became much more intense 6–5 Ma due to increasing resistance to subduction of the eastward thickening oceanic Yakutat lithosphere^{6,7}. Around the same time glaciation of the orogen began and climate and tectonic systems have been coevolving since then. Analyses of bedrock samples, mainly with apatite (U-Th)/He dating, give a general exhumation pattern of young cooling ages/recent rapid exhumation at the southern flanks of the mountains at the coast and the northern part of the Fairweather Fault²⁻⁴. The syntaxis area has

also been recognized as rapidly exhuming^{2,4}. However, only through a detrital sampling approach of collecting modern sand, which has been eroded from below the ice in the valleys, the rapidity and depth of exhumation could be appreciated¹. Strain localization in the St. Elias syntaxis area and the efficient glacial erosion of structurally stressed rocks in major fault zones might have become the driving forces to initiate the rapid and deep exhumation on the North American Plate⁷. Rapid exhumation observed in other parts of the mountains on the Yakutat microplate, such as the fold-and-thrust belt and the Yakutat foothills, occurs along shallower paths. The St. Elias syntaxis has been suggested to represent an early stage of the geodynamic processes that also act in the Himalayan syntaxes to cause very young cooling ages and expose high-grade metamorphic rocks⁴.

Despite the fact that analyses of modern sand can cover a wide sampling area and yield exhumation signals from below the ice, the drawback is that the spatial resolution is significantly decreased. Therefore, another detrital sampling approach has been undertaken that used cobble-sized material from the Seward-Malaspina Glacier catchment taken at the Malaspina Glacier terminus⁶ (Fig. 1). Grabowski *et al.*⁶ made sure to still target material derived from below the ice and that the lithologic information was not lost and could be used as first estimate for provenance. Zircon (U-Th)/He dating was applied to identify cobbles with young cooling signal, that must be derived from the area of rapid and deep exhumation within the catchment, and the lithology was then used to assign the rocks to one of the four, roughly east-west striking, different terranes constituting the catchment's geology (Fig. 1). However, lithology is not a sufficient provenance tool and, therefore, we complement the study by applying zircon U/Pb dating to the same samples used in that study to better distinguish between the terranes by characteristic crystallization ages.

We present zircon U/Pb ages of 22 cobbles, for which zircon (U-Th)/He ages as well as petro- graphic analyses are available. Additionally, we dated 8 of those cobbles by hornblende or biotite ⁴⁰Ar/³⁹Ar analyses and 5 cobbles by the apatite (U-Th)/He method. The U-Pb ages range from ~30 Ma to ~277 Ma and support the conclusion that a larger part of the catchment is affected by rapid and deep exhumation, as cobbles with young zircon (U-Th)/He cooling ages are certainly derived from the Wrangellia and Chugach Terranes and possibly from the Yakutat microplate (Fig. 1). However, Neogene exhumation has not been deep enough to produce young ⁴⁰Ar/³⁹Ar cooling ages like at the Himalayan syntaxes⁸. The ⁴⁰Ar/³⁹Ar cooling ages from the Seward-Malaspina Glacier catchment are in most cases just a few million years younger than the crystallization age. The detailed study of individual samples further bears conclusions on the regional tectonic history, e.g., by providing information on metamorphism and cooling after the Eocene development of the Chugach Metamorphic Complex of the Chugach Terrane.

References

1. Enkelmann, E., Zeitler, P. K., Pavlis, T. L., Garver, J. I. & Ridgway, K. D. Intense localized rock uplift and erosion in the St. Elias orogen of Alaska. *Nat. Geosci.* **2**, 360–363 (2009).
2. O'Sullivan, P. B. & Currie, L. D. Thermotectonic history of Mt. Logan, Yukon Territory, Canada: Implications of multiple episodes of Middle to Late Cenozoic denudation. *Earth Planet. Sci. Lett.* **144**, 251–261 (1996).
3. McAleer, R. J., Spotila J. A., Enkelmann, E. & Berger, A. L. Exhumation along the Fairweather Fault, southeastern Alaska, based on low-temperature thermochronometry. *Tectonics* **28**, TC1007 (2009).
4. Spotila, J. A. & Berger, A. L. Exhumation at orogenic indentor corners under long-term glacial conditions: Example of the St. Elias orogen, southern Alaska. *Tectonophysics* **490**, 241–256 (2010).
5. Finzel, E. S., Trop, J. M., Ridgway, K. D. & Enkelmann, E. Upper plate proxies for flat-slab subduction processes in southern Alaska. *Earth Planet. Sci. Lett.* **303**, 348–360 (2011).
6. Grabowski, D. M., Enkelmann, E. & Ehlers, T. A. Spatial extent of rapid denudation in the glaciated St. Elias syntaxis region, SE Alaska. *J. Geophys. Res. Earth Surf.* **118**, 1921–1938 (2013).
7. Falkowski, S., Enkelmann, E. & Ehlers, T. A. Constraining the area of rapid and deep-seated exhumation at the St. Elias syntaxis, Southeast Alaska, with detrital zircon fission-track analysis. *Tectonics* (2014).
8. Zeitler, P. K. *et al.* Crustal reworking at Nanga Parbat, Pakistan: Metamorphic consequences of thermal-mechanical coupling facilitated by erosion. *Tectonics* **20**, 712–728 (2001).

Spatial and temporal constraints of rapid exhumation in the St. Elias syntaxis, southeast Alaska and southwest Yukon

Adam Piestrzeniewicz¹, Eva Enkelmann¹, Sarah Falkowski²

1 University of Cincinnati, Cincinnati, OH, USA

2 Universität Tübingen, Tübingen, Germany

The conjunction of three prominent mountain ranges, the Chugach-St. Elias Range, Fairweather Range, and Wrangell Mountains, occurs at the border between southeast Alaska and southwest Yukon in what is known as the St. Elias syntaxis. This region contains some of the highest coastal mountain peaks in the world that amount to nearly 6,000 meters of local relief. The extreme relief coincides with thick and widespread glaciation in an area that receives an annual average precipitation of up to 7 m/yr. The St. Elias syntaxis is structurally situated in a unique location within a bend in the Yakutat and North American plate boundary where dextral motion along the Fairweather strike-slip fault shifts to subduction (Fig. 1). Syntaxial bends are often collocated with areas of intense deformation and focused strain accumulation that may be sensitive to climate and surface processes¹. Crustal collision at the indenter corner of the Yakutat microplate may stimulate strain accumulation, and, combined with effective removal of material accommodated by glacial erosion, might attribute to accelerated exhumation². Previous thermochronologic data from this region include apatite fission track (AFT) ages along a transect of Mt. Logan³, sparse apatite (U-Th)/He ages from the high ice fields within the St. Elias syntaxis¹, and detrital thermochronology of sediment derived from beneath the glaciers within the syntaxis^{2,4-7}. The detrital studies provide evidence for enhanced exhumation north of the Fairweather-Contact Fault transition in the core of the St. Elias syntaxis but the extent of rapid exhumation north and east of the syntaxis and the variation of exhumation rates across the Connector Fault are not known (Fig. 1).

Widespread glaciation makes direct bedrock sampling at low elevations impossible, however, detrital studies on modern glaciofluvial sand and cobble-sized glacial detritus show a strong signal for young ages beneath the Seward Glacier^{2,4-7}. Detrital thermochronology ages also show evidence for rapid exhumation farther north and east, beneath the Hubbard Glacier and in adjacent catchments within the syntaxis area. A similar young signal has not been observed in bedrock samples from the area possibly due to the fact that bedrock sampling in the area of the high ice fields is difficult given the remote region and rugged, glaciated terrain. We present 31 new AFT ages for bedrock samples collected above glacial valleys along north and east trending transects radiating away from the St. Elias syntaxis through the ice-free outboard mountain ridges and beyond the Denali Fault and Duke River Fault (Fig. 1). AFT ages are combined with new apatite and zircon (U-Th)/He ages to resolve the temporal variation in rock cooling for this region. Preliminary AFT ages range from 6.5 Ma in the core of the syntaxis to 107.6 Ma approximately 140 km east of the syntaxis. Ages become younger northeast of the Denali Fault and indicate a change in the cooling history across the fault. Young bedrock ages at the core of the syntaxis support previous data that suggest focused rapid exhumation within the Yakutat indenter corner and provide a better spatial resolution to complement published detrital data from the Alaska side of the syntaxis area⁵⁻⁷. The spatial distribution of ages help constrain the extent of rapid exhumation within the St. Elias syntaxis and quantify the role of the ice-covered Connector Fault (Fig. 1), which might accommodate differential vertical motion and facilitate rapid and deep exhumation. The new bedrock thermochronology data presented herein are compared with

the AFT age profile collected over ~5000 m elevation on Mt. Logan³ and results of the detrital thermochronology that reveals exhumation beneath the ice^{2,4-7}.

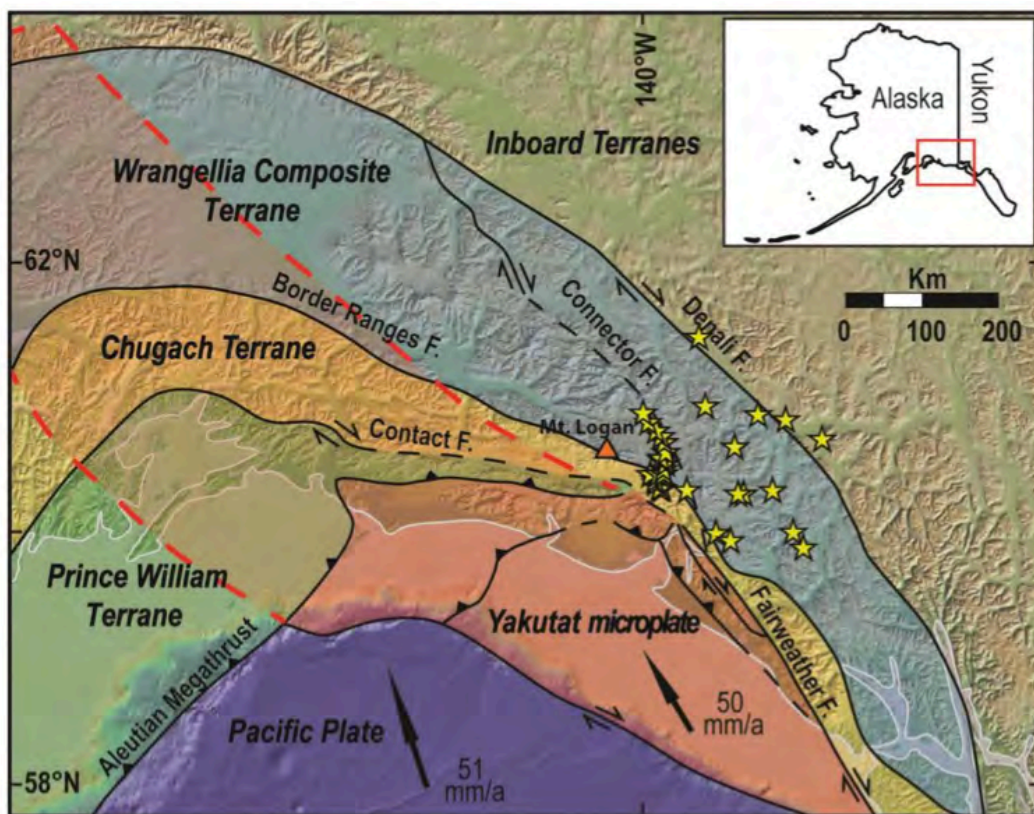


Figure 1. Regional structural map showing major terranes and faults. Yellow stars mark AFT sample locations. The red dashed outline represents the subducted portion of the Yakutat lithosphere.

References

1. Spotila, J. A. & Berger, A. L. Exhumation at orogenic indentor corners under long-term glacial conditions: Example of the St. Elias orogen, Southern Alaska. *Tectonophysics* **490**, 241-256 (2010).
2. O'Sullivan, P. B. & Currie, L. D. Thermotectonic history of Mt. Logan, Yukon Territory, Canada: Implications of multiple episodes of Middle to Late Cenozoic denudation. *Earth Planet. Sci. Lett.* **144**, 251-261 (1996).
3. Enkelmann, E., Zeitler, P. K., Pavlis, T. L., Garver, J. I. & Ridgway, K. D. Intense localized rock uplift and erosion in the St. Elias orogen of Alaska. *Nature Geoscience* **2**, 360-363 (2009).
4. Enkelmann, E., Garver, J. I. & Pavlis, T. L. Rapid exhumation of ice-covered rocks of the Chugach-St. Elias orogen, Southeast Alaska. *Geology* **36**, 915-918 (2008).
5. Enkelmann, E., Zeitler, P. K., Garver, J. I., Pavlis, T. L., & Hooks, B. P. The thermochronological record of tectonic and surface process interaction at the Yakutat-North American collision zone in Southeast Alaska. *American Journal of Science* **310**, 231-260 (2010).
6. Falkowski, S., Enkelmann, E. & Ehlers, T. A. Constraining the area of rapid and deep-seated exhumation at the Yakutat plate corner, southeast Alaska. *Tectonics* **33**, (2014).
7. Grabowski, D. M., Enkelmann, E. & Ehlers, T. A. Spatial extent of rapid denudation in the glaciated St. Elias syntaxis region, SE Alaska. *Journal of Geophysical Research: Earth Surface* **118**, 1-18 (2013).

Rapid Oligocene Exhumation of the Western Canadian Rocky Mountains

Annika Szameitat¹, Randall R Parrish^{1,2}, Finlay M Stuart³, Andrew Carter⁴, Stewart Fishwick¹

1 Department of Geology, University of Leicester, UK

2 NERC Isotope Geosciences Laboratory, Keyworth, UK

3 Scottish Universities Environmental Research Center, East Kilbride, UK

4 Birkbeck College, University of London, UK

As part of the North American Cordillera the Rocky Mountains of Canada play a significant role in influencing climate on a local and global scale. They impact deflection of weather systems and the jet stream^{1,2} and form a distinct barrier to Pacific moisture reaching the continental interior³. The extent to which this climatic pattern extended into the past is at present uncertain, so improving our understanding of the elevation history of the Rockies is critical to determining the controls on climate change within the Northern Hemisphere³.

We have undertaken a comprehensive apatite (U-Th-Sm)/He and fission track study of the southeastern Canadian Cordillera, i.e. the southern Canadian Rocky Mountains, in order to provide insight into the mid to late Cenozoic uplift and exhumation history of this region. In contrast to the northern Rockies the southern part has peaks reaching almost 4000 m and thus is most likely to have undergone recent uplift. Thermal history and exhumation models of widespread low elevation samples in combination with 6 vertical profiles covering elevations from 500 up to 3100 m a.s.l. show at least 1500 m of rapid exhumation of the Monashee and Sellkirk Ranges west of the Rocky Mountain Trench (RMT) during the Oligocene (Figure 1). In the ranges east of the RMT low elevation samples show Eocene ages throughout, indicating that the area does not share the same exhumation history. The presented data show a very different history of recent uplift of the Canadian Rockies compared to what is currently known from published work, which mostly infer that the eastern Canadian Cordillera has not experienced significant uplift since the Eocene⁴⁻⁶.

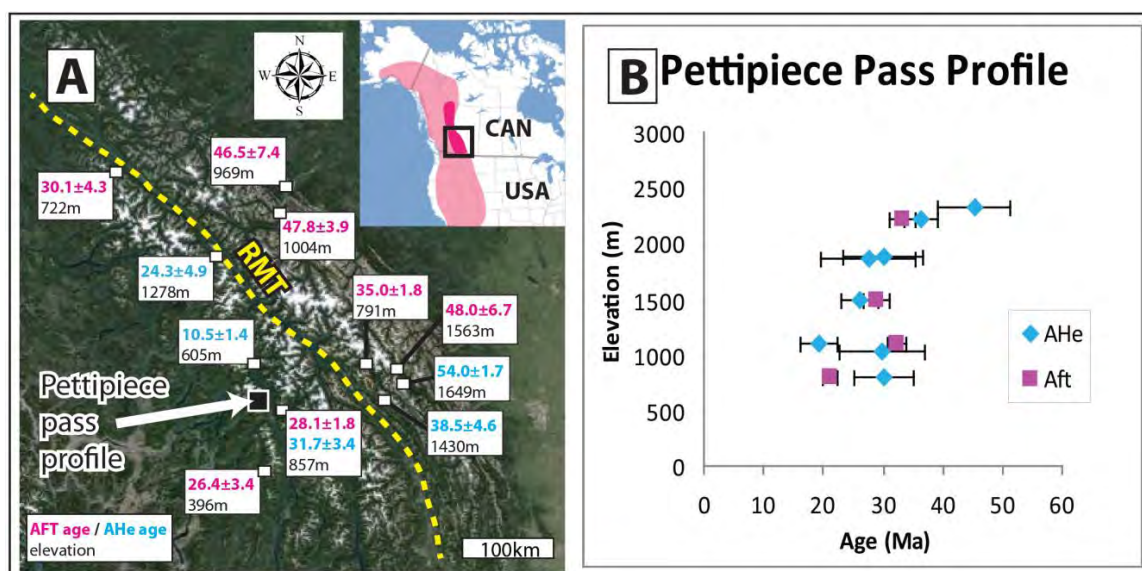


Figure 1. A: Study area and profile location map also showing a selection of the observed AFT (pink) and AHe (blue) ages. Inlet: Study area (black box) within the Canadian Rocky Mountains (dark pink) as part of the North American Cordillera (light pink). B: Age elevation plot of a vertical profile sampled on the western side of Pettipiece Pass, 55km north of Revelstoke, British Columbia. The data clearly show that both AHe and AFT ages of samples between elevations 800 to 2300 m a.s.l. overlap within error around an age of 30Ma, thus indicating rapid exhumation of this elevation range through both closure temperatures at that time.

We propose that the most likely cause of this rock uplift was upwelling of asthenosphere around the eastward subducting Farallon Plate⁷. This also led to the eruption of the nearby mainly Miocene Chilcotin Group flood basalts, the earliest members of which date back to the Oligocene^{8,9}, and could have caused underplating of the thin lithosphere west of the RMT, adding to the buoyancy of the plate and lifting the range. Because the Trench marks the edge of the normal thickness craton which was underthrust beneath the Rocky Mountains during the initial upper Cretaceous orogeny, the eastern Rockies have a normal lithospheric thickness. This would impede recent uplift and provides an explanation for the older ages found in the east. Furthermore the data appear to show that ages do not mimic present day topography, suggesting that current topographic relief, at least west of the Trench, is younger still, possibly late Neogene or Quaternary and thus potentially caused by increased erosion during glacial episodes.

While the most recent history of the Canadian Rockies will require further investigation, the data presented clearly show that our perception of the history of the Canadian Rocky Mountains will have to be revised in order to improve our understanding of their influence on the Northern Hemisphere Climate.

References

1. Ruddiman, W. F. & Kutzbach, J. E. Forcing of the Late Cenozoic Northern Hemisphere climate by plateau uplift in southern Asia and the America West. *J. Geophys. Res.* **94**, 18409–18427 (1989).
2. Seager, R., Battisti, D. S., Yin, J., Gordon, N., Naik, N., Clement, A. C. & Cane, M. A. Is the gulf stream responsible for europe’s mild winters. *Q. J. R. Meteorol. Soc.* **128**, 2563–2586 (2002).
3. Foster, G. L., Lunt, D. J. & Parrish, R. R. Mountain uplift and the glaciation of North America – a sensitivity study. *Clim. Past* **6**, 1–10 (2010).
4. Simony, P. S. & Carr, S. D. Cretaceous to Eocene evolution of the southeastern Canadian Cordillera: Continuity of Rocky Mountain thrust systems with zones of “in-sequence” mid-crustal flow. *Journal of Structural Geology* **33**, 1417-1434 (2011).
5. Mathews, W. H. in *Geology of the Cordilleran Orogen in Canada* (eds. Gabrielse, H. & Yorath C. J.) 403-418 (Geological Survey of Canada, *Geology of Canada* **4**, Chapter 11, 1991), also in Geological Society of America, *The Geology of North America*, **G-2**, 1991).
6. Osborn, G., Stockmahl, G. & Haspel, R. Emergence of the Canadian Rockies and adjacent plains: a comparison of physiography between end-of-Laramide time and present day. *Geomorphology* **75**, 450-477 (2006).
7. Hyndman, R. D., Currie, C. A. & Mazzotti, S. Subduction zone backarcs, continental mobile belts, and orogenic heat. *GSA Today* **15**, 4–10 (2005).
8. Mathews, W. H. Neogene Chilcotin basalts in southcentral British Columbia; geology, ages, and geomorphic history. *Canadian Journal of Earth Sciences* **26**, 969–982 (1989).
9. Bevier, M. L. Implications of Chemical and Isotopic Composition for Petrogenesis of Chilcotin Group Basalts, British Columbia. *Journal of Petrology* **24**, 207-226 (1983).

Late Cenozoic upper-crustal cooling history of the Shuswap Metamorphic Core Complex, southern Canadian Cordillera, British Columbia: new insights from low-temperature multi-thermochronometry and inverse thermal modeling

B. Louis¹, I. Coutand¹, H.D. Gibson² and L. Godin³

¹ Dalhousie University, Department of Earth Sciences, Halifax, NS, Canada

² Simon Fraser University, Department of Earth Sciences, Burnaby, BC, Canada

³ Queen's University, Department of Geological Sciences & Geological Engineering, Kingston, ON, Canada

The Shuswap Metamorphic Complex (SMC) is located in the southern Omineca belt of the Canadian Cordillera (Fig. 1). In the Early Jurassic, convergence between the westward drifting North American craton and the eastward subducting Farallon plate (later Pacific plate)^{1,2} caused crustal thickening in the southern Canadian Cordillera. By Early Eocene, post-orogenic collapse of the Canadian Cordillera caused a transition from contractional to extensional tectonics leading to widespread exhumation of the Shuswap Metamorphic Complex³⁻⁵ (Fig. 1).

The study area encompasses the SMC, which includes some of the most deeply exhumed rocks of the southern Canadian Cordillera, and the underlying Monashee complex, where North American basement gneisses are exposed⁶⁻⁹ (Fig. 1). The SMC is bound to the west by the Eocene WNW- dipping Okanagan-Eagle River extensional shear zone¹⁰⁻¹³. The east dipping Columbia River fault, a brittle-to-ductile Eocene extensional fault zone¹⁴, marks the eastern limit of the Monashee complex. Between these two faults, the high-grade gneisses and schists of the SMC that belong to the 'Middle Crustal Zone'¹⁵ are separated from the ortho- and paragneisses of the Monashee complex¹⁵ to the east by the shallow-dipping Monashee décollement, a northeast- directed, crustal-scale compressional shear zone¹⁶ (Fig. 1).

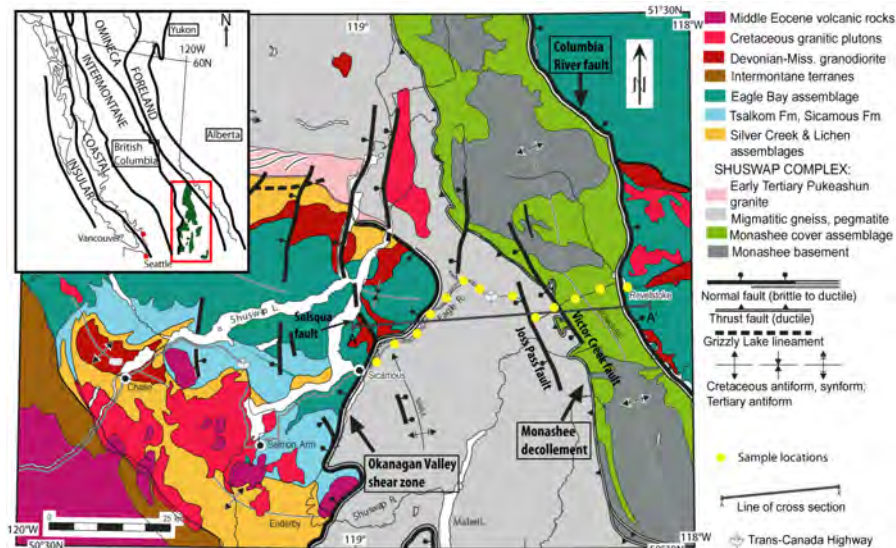


Figure 1. Location and geology of the study area (modified after¹⁹). Yellow dots indicate sample locations. The inset map shows the five morphogeological belts of the Canadian Cordillera and the location of the Shuswap Metamorphic Complex (in green) within the southern Omineca belt.

Published geochronologic data suggest that rapid cooling from metamorphic temperatures in excess of

500°C was associated with the early stages of Eocene extensional exhumation^{13,17}, with average cooling rates ranging from 15°C/Ma to more than 30°C/Ma in some areas¹⁷. However, the latest upper crustal stage of this extensional episode is only loosely constrained¹⁸. The goal of this study is to use low-temperature multi-thermochronology combined with inverse thermal modeling to characterize the late upper-crustal cooling history of the SMC. In particular, we aim to (1) constrain whether cooling rates changed through time, from deep to shallow structural levels during the SMC exhumation and (2) document and quantify the role played by a series of brittle normal faults documented along the transect (Fig. 1) during the late stage exhumation of the SMC.

We present a new dataset including 12 apatite and 19 zircon (U-Th)/He ages, respectively, and 15 apatite fission track (AFT) data distributed along a ~50 km-long transect across the SMC and Monashee complex from Sicamous to Revelstoke (Fig. 1), British Columbia. ZHe ages range from 122.5±11.22 Ma to 36±7.32 Ma and AFT ages from 88.14±8.85 Ma to 36.1±1.89 Ma, with the oldest ages located to the west, in the hanging wall of the Okanagan Valley shear zone (Fig. 1). The AHe ages are much younger, ranging from 32.1±1.5 Ma to 1.19±1.15 Ma. These preliminary results indicate that extensional cooling associated with the SMC 1) occurred in the late Eocene at a rapid rate, and 2) had stopped by the Late Eocene / Early Oligocene). The much younger AHe ages suggest that cooling significantly slowed down after this time period probably due to the absence of significant post-Eocene extensional deformation in the area.

References

1. Atwater, T. Implications of plate tectonics for the Cenozoic tectonic evolution of western North America. *Geological Society of America Bulletin* **81**, 3513–36 (1970).
2. Coney, P. J. Cordilleran tectonics and North America plate motion. *Am. J. Sci.* **272**, 603-628 (1972).
3. Ewing, T. E. Paleogene tectonic evolution of the Pacific northwest. *Journal of Geology* **88**, 619-638 (1980).
4. Parrish, R. R., Carr, S. D. & Parkinson, D. L. Eocene extensional tectonics and geochronology of the Southern Omineca belt, British Columbia and Washington. *Tectonics* **7**, 181–212 (1988).
5. Brown, R. L. & Journey, J. M. Tectonic denudation of the Shuswap metamorphic terrane of southeastern British Columbia. *Geology*, **15**: 142-146 (1987).
6. Brown, R. L. Metamorphic complex of southeastern Canadian Cordillera and relationship to foreland thrusting, thrust and nappe tectonics. *Geological Society of London*, 463-473 (1981).
7. Brown, R. L. & Read, P. B. Shuswap terrane of British Columbia: a Mesozoic 'core complex'. *Geology* **11**, 164-168 (1983).
8. Armstrong, R. L. et al. Early Proterozoic basement exposures in the southern Canadian Cordillera: core gneiss of Frenchman Cap, Unit I of the Grand Forks Gneiss, and the Vaseaux Formation. *Canadian Journal of Earth Sciences* **28**, 1169-1201 (1991).
9. Crowley, J. L. U-Pb geochronologic constraints on the cover sequence of the Monashee complex, Canadian Cordillera: Paleoproterozoic deposition on basement. *Can. J. Earth Sci.* **34**, 1008-1022 (1997).
10. Tempelman-Kluit, D. & Parkinson, D. Extension across the Eocene Okanagan crustal shear in southern British Columbia. *Geology* **14**, 318–321 (1986).
11. Johnson, B. J. & Brown, R. L. Crustal structure and early Tertiary extensional tectonics of Omineca belt, 51°N latitude, southern Canadian Cordillera. *Canadian Journal of Earth Sciences* **33**, 1596–1611 (1996).
12. Bardoux, M., and Mareschal, J.-C. Extension in south-central British Columbia; mechanical and thermal controls. *Tectonophysics*, **238**(1-4): 451-470 (1994).
13. Brown, S.R. et al. New constraints on Eocene extension within the Canadian Cordillera and identification of Phanerozoic protoliths for footwall gneisses of the Okanagan Valley shear zone. *Lithosphere*, **4**: 354 – 377 (2012).
14. Lane, L.S. Brittle deformation in the Columbia River fault zone near Revelstoke, southern British Columbia. *CAN Canadian Journal of Earth Sciences*, **21**: 584-598 (1984).
15. Carr, S.D. Three crustal zones in the Thor-Odin - Pinnacles area, southern Omineca Belt, British Columbia. *Canadian Journal of Earth Sciences*, **28**, 2003-2023 (1991).
16. Brown, R.L. et al. The Monashee decollement of the southern Canadian Cordillera: a crustal-scale shear zone linking the Rocky Mountain Foreland belt to the lower crust beneath accreted terranes. *Thrust Tectonics*, 357-364 (1992).
17. Johnson, B. Structure and tectonic setting of the Okanagan Valley fault system in the Shuswap Lake area, southern British Columbia [Ph.D. thesis]: 266 (Ottawa, Ontario, CA, Carleton University, 1994).
18. Lorencak, M., Seward, D., Vanderhaeghe, O., Teysier, C., and Burg, J.P. Low-temperature cooling history of the Shuswap metamorphic core complex, British Columbia; constraints from apatite and zircon fission-track ages. *Canadian Journal of Earth Sciences*, **38**: 1615–1625 (2001).
19. Johnson, B. Extensional shear zones, granitic melts, and linkage of overstepping, normal faults bounding the Shuswap metamorphic core complex, British Columbia. *GSA Bulletin*, **118** (3/4):366–382 (2006)

Middle Miocene-Pliocene Hotspot-Related Uplift, Exhumation, and Extension north of the Snake River Plain: Evidence from Apatite (U-Th)/He Thermochronology

David A. Foster¹, James J. Vogl¹, Kyoungwon Min¹, Alina L. Bricker¹ and Patrick W. Gelato¹

1 Department of Geological Sciences, University of Florida, Gainesville, FL 32611 USA

Passage of North America over the Yellowstone hotspot has had a profound influence on the topography of the northern Rocky Mountains. One of the most prominent topographic features is the Yellowstone crescent of high topography, which comprises two elevated shoulders bounding the eastern Snake River Plain (SRP) and converging at a topographic swell centered on the Yellowstone region (Figure 1). Kilometer-scale erosion has occurred locally within the topographic crescent, but it is unclear if rock exhumation is due to surface uplift surrounding the propagating hot spot, subsidence of the Snake River Plain after passage of the hot spot, or relief initiated by extension in the Northern Basin and Range Province.

We have applied (U-Th/He) apatite (AHe) thermochronology to the Pioneer-Boulder Mountains (PBM), and Boise Mountains (BM) on the northern flank of the SRP, and the southern Beartooth Mountains (BTM) directly north of the modern Yellowstone caldera, to constrain the timing, rates, and spatial distribution of exhumation. AHe ages from the PBM indicate that >2-3 km of exhumation occurred since ~11 Ma. Age-elevation relationships suggest an exhumation rate of ~0.3 mm/yr between ~11 and 8 Ma. Eocene Challis volcanic rocks are extensively preserved and Eocene topographic highs are locally preserved to the north and south of the topographic culmination in the PBM, indicating minimal erosion adjacent to the PBM culmination. Spatial patterns of both exhumation and topography indicate that faulting was not the primary control on uplift and exhumation. Results from the BM also indicate significant erosional exhumation between ~11 and 9 Ma. Regional exhumation at 11-8 Ma was synchronous with silicic eruptions from the ~10.3 Ma Picabo volcanic field located immediately to the south and with S-tilting of the southern flank of the PBM that is likely the result of loading of the ESRP by mid-crustal mafic intrusions. AHe data from Archean rocks in the Yellowstone Canyon of the southern BTM reveal Miocene-Pliocene cooling ages (~12-2 Ma). Discordant single grain ages in samples with Miocene mean ages suggest that exhumation is now reaching to depths of the Miocene He partial retention zone. Age/elevation relationships suggest that exhumation at rates >0.2 mm/yr is related to integration of the Yellowstone River drainage system and incision of the Yellowstone Canyon.

The thermochronologic data from these locations along the northern margin of the SRP shows that localized uplift, exhumation and incision occurred progressively as NA moved over the hot spot, but that exhumation is not uniform and not always controlled by Neogene basin-bounding faults. This suggests a causal relationship between hotspot processes and exhumation through potential contributions of flexure and mantle dynamics to uplift, and changes in drainage networks and base-level associate with uplift and/or extension.

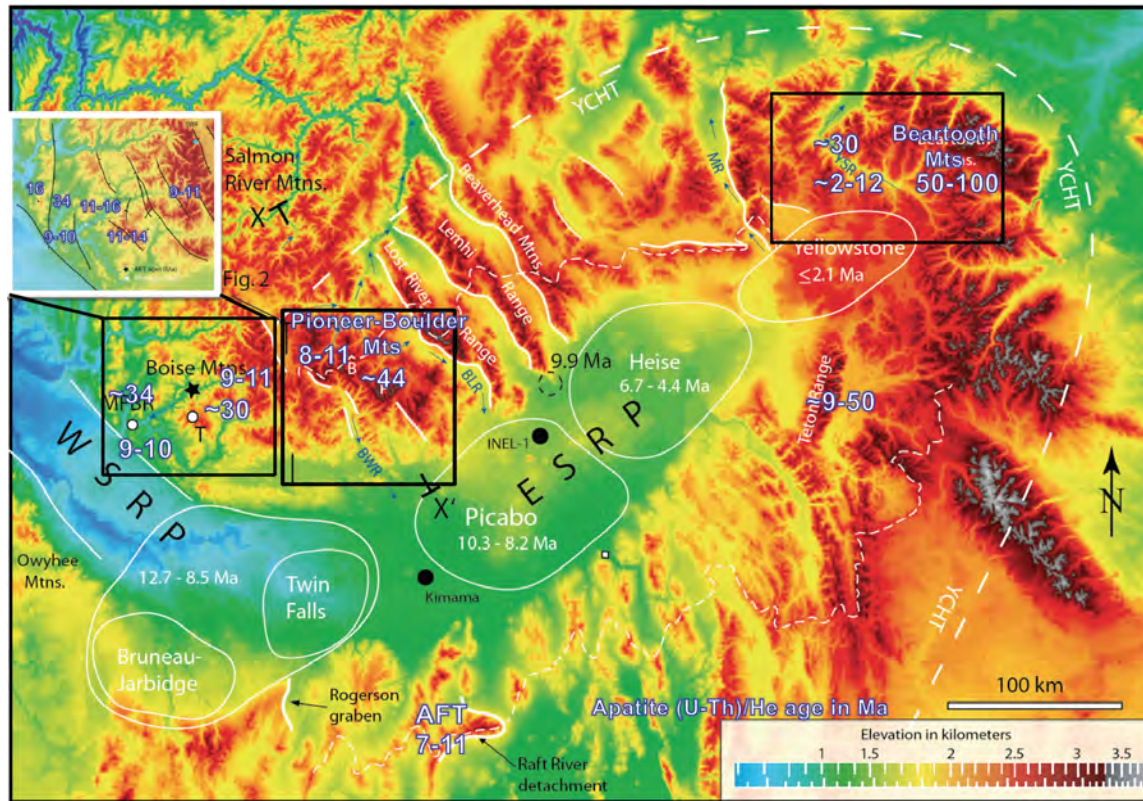


Figure 1. DEM of Snake River Plain and Yellowstone regions. Short dashed lines show position of drainage divides on flanks of Eastern Snake River Plain (ESRP). Long dashed lines define outer margin of Yellowstone crescent of high terrain (YCHT). Solid white lines are selected normal faults. Solid white outlines are silicic volcanic centers with ages. White circles in Boise Mts. are locations of Late Miocene AHe ages from Trinity Mtn. (T) and the Middle Fork Boise River (MFBR) areas.

Apatite fission-track studies in northwestern Mexico: cooling history in the Basin and Range and Gulf of California extensional provinces.

Thierry Calmus¹, Raúl Lugo Zazueta¹, Matthias Bernet²

*1 Estación Regional del Noroeste, Instituto de Geología,
Universidad Nacional Autónoma de México,*

Blvd. L.D. Colosio S/N y Madrid, 83240, Hermosillo, Sonora, Mexico

*2 Institut des Sciences de la Terre, Université Joseph Fourier, 1381, rue de la
Piscine, 38041 Grenoble, France*

Determining the thermal history of orogenic processes allows constraining the timing and rate of associated phenomena such as erosion and tectonic denudation. In the case of Basin and Range tectonics, fission-track analysis permits to date cooling of relatively deep sections of the crust, e.g. in the metamorphic core complex belt. In northwestern Mexico, as well as the whole Basin and Range, fission-track dating results can be used for modeling the progressive exhumation of the footwall rocks below a low-angle normal fault. In the case of exhumation of blocks limited by high-angle normal faults, in general no major apatite fission-track (AFT) age variation is depicted in the footwall in a direction perpendicular to the strike of the fault, which suggests a more homogeneous cooling history.

In order to distinguish the cooling history related only to the formation of the Basin and Range, and to the superimposed Gulf of California opening, we want to test the hypothesis that the eastern limit of the Gulf of California extensional province in Central Sonora is aligned with the graben of Empalme and the graben of Hermosillo¹. We analyzed samples of the Laramide plutons (90 to 50 Ma), which are widespread in NW Mexico and represent useful objects to constrain the geometry, timing and kinematics of Tertiary tectonics in the region. For the first case of only Basin and Range extension we present new AFT results for samples collected in the Sierra La Madera pluton, localized close to the western limit of the Sierra Madre Occidental, and in the Sierra Bachoco (southern part of the Hermosillo batholith) which is presumably along the eastern limit of the Gulf of California extensional province.

Eleven samples of the Sierra Bachoco provided AFT ages between 8.1 and 14.7 Ma. These AFT ages suggest that cooling within the AFT partial annealing zone for the Laramide igneous basement in central Sonora is coeval with the age of initial continental rifting at ~12 Ma, which preceded the Late Miocene-Pliocene opening of the Gulf of California. Furthermore, the length and the unimodal distribution of fission track lengths show that rapid cooling occurred through the partial annealing zone, and that there is no cooling history associated with Basin and Range extension in the Sierra Bachoco. In other words, the Basin and Range extension did not allow exhuming the present topographic surface of the Sierra Bachoco at depth shallower than the partial annealing zone. On the contrary, the granite of the Cerro Colorado, which is located 6 km west of Cerro Bachoco, is overlain by 12.5 Ma old ignimbrites², which suggests an exhumation before the Middle Miocene, directly related to Basin and Range tectonics. The region of Hermosillo is characterized today by a heat flow of 2.25 ± 0.02 $\mu\text{cal}/\text{cm}^2\text{sec}$ and a reduced heat flow of 1.94 $\mu\text{cal}/\text{cm}^2\text{sec}$ ³, which is similar to higher values of the Basin and Range province. The geothermal gradient near Hermosillo obtained from the heat flow data is $32.78 \pm 0.17^\circ\text{C}/\text{km}$. Assuming a similar paleo-

geothermal gradient during continental rifting and break-up of the Gulf of California, and a surface temperature of 20°C, we calculate a paleodepth of partial annealing zone comprised between ~1.2 and ~2.7 km.

The four samples of the Sierra La Madera provided AFT ages between 26.5 and 18.4 Ma along a NE-SW oriented cross section. We interpret these results as cooling ages related with the exhumation of the pluton La Madera related with Basin and Range extension coupled with the erosion of the thick overlying volcanic sequence of the Sierra Madre Occidental along its western limit. Nevertheless, more recent results obtained along the western flank of the Sierra La Madera show a good correlation between elevation and AFT ages, suggesting a progressive cooling within the footwall of the normal fault between 26 and 11 Ma⁴.

Based on these results, we conclude that the Bachoco granitoid cooled at low temperatures during the rifting of the Proto Gulf of California even if local geological data suggest that other Laramide plutons were completely exhumed at the same time. East of the Sierra La Madera, AFT ages are related to the Basin and Range extension, but tectonic denudation or erosion were active until Late Miocene. The overlap between Basin and Range and Gulf of California extensional provinces in western and central Sonora makes difficult the distinction between cooling effects due to Late Oligocene to Miocene Basin and Range extension and Late Miocene extension related to the Gulf of California opening.

References

1. Roldán-Quintana, J., Mora-Alvarez, G., Calmus, T., Valencia-Moreno, M., Lozano-Santacruz, R., El Graben de Empalme, Sonora, México: Magmatismo y tectónica extensional asociados a la rupturainicial del Golfo de California. *Revista Mexicana de Ciencias Geológicas* **21**, 320-334 (2004).
2. Vidal-Solano, J., Paz-Moreno, F. A., Iriondo, A., Demant, A. & Cochemé, J. J. Middle Miocene peralkaline ignimbrites in the Hermosillo region (Sonora, Mexico): Geodynamic implications. *C.R. Geoscience* **337**, 1421-1430 (2005).
3. Smith, D.L., Heat flow, radioactive heat generation, and theoretical tectonics for northwestern Mexico, *Earth and Planetary Science Letters* **23**, 43-52 (1974).
4. Lugo-Zazueta, L. Thermochronology of the Basin and Range and Gulf of California extensional provinces, Sonora, Mexico. Ph.D. Thesis, School of Earth Sciences, The University of Melbourne, Victoria, Australia, 286 pp. (2013).

Exhumation processes in the Western Cordillera of Colombia, interpretation on Andean Orogenic derived from cooling ages from plutons nested in a tectonic stacking zone.

Alejandro Piraquive¹, Matthias Bernet², Andreas Kammer¹, Juan Sebastian Diaz¹
Thomas Maurin³

1 Grupo de Investigación en Geología Estructural y Fracturas Universidad Nacional de Colombia. apartado Aéreo, 14490 Bogotá, Colombia

2 Institut des Sciences de la Terre Université Joseph Fourier 1381 Rue de la piscine BP 53 38041 Grenoble Cedex France

3 TOTAL SA, Courbevoie, France

The Western Cordillera of Colombia comprises a vast area of mountain thrustbelt, related to the Andean episode. This mountain range composed of uplifted Cretaceous sedimentary marine rocks, is bounded to the East by a suture regionally known as the Romeral Suture Zone, which is a major feature that separates the continental crust from accreted terrains mainly of oceanic affinity, evidences for such boundary are the large thrust faults separating tectonic sheets that expose different lithostratigraphy, tectonic styles and metamorphism. Several batholiths and stocks of Upper Cretaceous to Eocene ages intrude this margin, westward to the Pacific trench Eocene batholiths form the Baudó range, attributed to a late accretion of an island arc related to the convergence between North and South America.

In this work we show a structural reconstruction integrating recently acquired apatite fission-track (AFT) cooling ages from samples of the plutonic rocks of the continental crust (Antioquia Batholith), and plutons related to accreted and lately exhumed oceanic crust mostly Upper Cretaceous and Paleocene age (Santafé Batholith, Santa Cecilia la X Complex, Tonusco Intrusive) and a late Eocene plutonic episode (Mandé Batholith). Exhumation is probably related to large-scale lithospheric folding in response of the end of subduction at the Romeral Suture Zone. Several decompression stages, which forced a magmatic differentiation, giving origin to the most recent plutonic bodies may be related to an accelerated exhumation after plutons emplacement.

Thermochronology analysis allows establishing a time frame for cooling, pointing that uplift and exhumation of duplex stacking structure alongside west of Romeral Suture Zone is considerably older (52Ma) than Antioquia Batholith (46Ma) and Santa Cecilia la X (33.2Ma) ages. The AFT cooling ages indicate a younger exhumation towards the west in the Western Cordillera and Baudó Range, and also a rapid cooling related to exhumation processes at high speed rates from Lower Eocene to recent. Underthrusting was favored by a high erosive regime, which prevented propagation of thrust wedges and allowed the duplex formation.

The evolution of the Cretaceous sedimentary basin is linked to pluton emplacement and exhumation. Erosion is constant and high due to rapid exhumation. In this way we explain how ages are younger to the west in response to a Upper Cretaceous subduction stop, late collision, and the start of cooling in Upper Paleocene related to exhumation process driven by the very first pulse of Andean Orogeny. Further work focused on provenance analysis will provide information on source-sink relations and indicate when the uplift of the oceanic crust was enough for

interrupting deposition in the Cretaceous basin of sediment derived from the continental crust source areas to the east.

Key words: Andean Orogeny, Apatite Fission Tracks, Cooling ages, Eocene Plutonism Romeral Suture Zone, Upper Cretaceous Plutonism.

Metamorphic Evolution and Exhumation of the Santander Massif (Eastern Cordillera, Colombia)

Cindy Lizeth Urueña¹, Carlos Zuluaga², Matthias Bernet³

¹ Universidad Nacional de Colombia, Colombia. cluruenas@unal.edu.co

² Universidad Nacional de Colombia, Colombia. cazuluagacas@unal.edu.co

³ Institut des Sciences de la Terre (ISTerre) Université Joseph Fourier, France.

In this work we report new thermochronology data from Bucaramanga Gneiss, the oldest lithodemic unit of the crystalline basement in the Santander Massif. The interpretations here are drawn from a database that also includes previous reported thermochronological data.

The Santander Massif is located in the northeastern sector of the Eastern Cordillera of the Colombia Andes; it belongs to an uplifted block limited to the west by the Bucaramanga Fault¹, a mayor structural feature in the northern Andes (Fig. 1). The basement is composed by igneous and metamorphic rocks assembled in different tectonic events that affected Colombia since the Precambrian. The oldest and structurally deepest unit is the Bucaramanga Gneiss, this unit is composed of amphibolite to granulite facies rocks, originated during a regional metamorphism event that involved migmatization. The lithologies are mainly biotite and sillimanite quartz-feldspar gneiss, with minor hornblende gneiss, quartzite and amphibolite². Regional metamorphic microstructures and assemblages are overprinted locally by dynamic and thermal metamorphism; the thermal events are related to the numerous intrusive bodies in the massif. The metamorphic evolution of the massif, as represented in the Bucaramanga Gneiss, is summarized in three stages²: (I) A prograde stage indicated by the stable mineral assemblage garnet ± plagioclase ± quartz ± sillimanite ± biotite ± amphibol ± muscovite, with temperature and pressure conditions of around $675 \pm 68^\circ\text{C}$ and 6.5 to 7 Kbar. (II) An isobaric temperature increasing stage, temperatures increased up to 810°C reaching the transition to granulite facies; this stage caused garnet homogenization by diffusion processes, appearance of clinopyroxene in amphibolites, and migmatite development. (III) A retrograde stage related to exhumation indicated by Mn enrichment in garnets rims and development of symplectites and myrmekites as response to temperature falls.

The timing of the final cooling and exhumation event, as interpreted from the thermochronological database (new data reported here and compiled published information for apatite³⁻⁵ and zircon^{3,5}, likely began at Late Eocene (~35 - 30 M.a.) and continued until Oligocene - Miocene (~25 - 20 M.a.) in the northeast part of the area. The database also indicates partition of the exhumation in faulted blocks having variable exhumation rates.

Fission track data from the northeastern sector in the study area indicate a late thermal event at 11.3 ± 2.7 M.a., this is related to the youngest reported mineralization pulse in a magmatic-hydrothermal event.

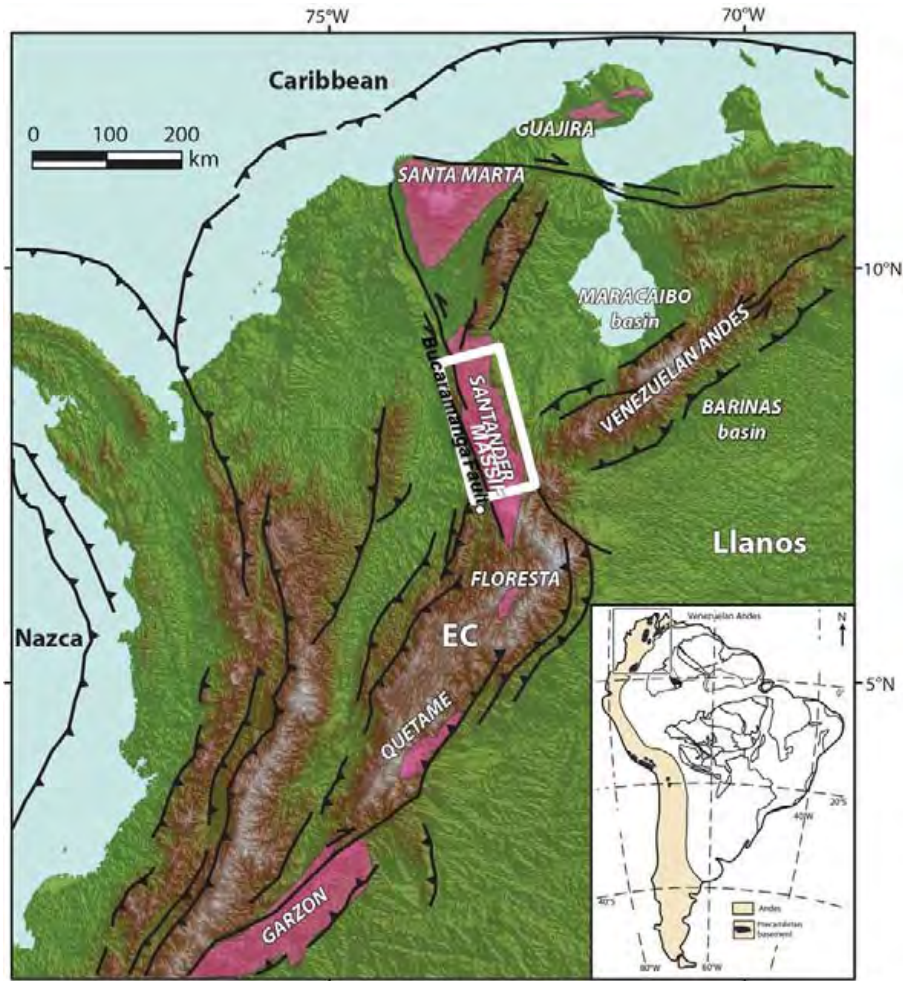


Figure 1. Colombian Northern Andes, the Santander Massif is located where the Eastern Cordillera branches in two ranges: northern Eastern Cordillera and Venezuelan Andes. White box indicates study area.

References

1. García, C., Ríos, C. & Castellanos, O. Medium-pressure metamorphism in the Central Santander Massif, Eastern Cordillera, Colombian Andes. *Boletín de Geología* **27**, 43-68 (2005).
2. Urueña, C. Metamorfismo, Exhumación y Termocronología del Neis de Bucaramanga (Macizo de Santander, Colombia). PhD Thesis, 191pp., Universidad Nacional de Colombia, Bogotá (2014).
3. van der Lelij, R. Reconstructing north-western Gondwana with implications for the evolution of the Iapetus and Rheic Oceans : a geochronological, thermochronological and geochemical study. PhD Thesis, 221pp., Universidad de Gêneva. Facultad de Ciencias, Gêneva, Suiza (2013).
4. Caballero, V., Mora, A., Quintero, I., Blanco, V., Parra, M., Rojas, L. E., López, C., Sánchez, N., Horton, B., Stockli, D. & Duddy, I. in Thick-Skin-Dominated Orogens: From Initial Inversion to Full Accretion (eds. Nemcok, M., Mora, A. & Cosgrove, J. W.) *Geological Society, London, Special Publications*, **377** (2013).
5. Shagam, R., Kohn, B. P., Banks, P. O., Dasch, L. E., Vargas, R., Rodriguez, G. I. & Pimentel, N. Tectonic implications of Cretaceous–Pliocene fission-track ages from rocks of the circum-Maracaibo Basin region of western Venezuela and eastern Colombia. *Geological Society of America Memoir* **162**, 385-412 (1994).

Tectonic inheritance control on exhumation and deformation of the Eastern Cordillera and Subandean zone in North Peru (5-8°S), using Thermochronology and Balanced Cross-Section

Adrien Eude¹, Stéphanie Brichau¹, Martin Roddaz¹, Stéphane Brusset¹, Ysabel Calderon^{1,2}, Patrice Baby^{1,2}

1 Géosciences Environnement Toulouse (GET), Université de Toulouse, Université Paul Sabatier – Toulouse III, UMR 5563, CNRS, IRD, UPS, 14 Avenue Edouard Belin, 31400 Toulouse, France

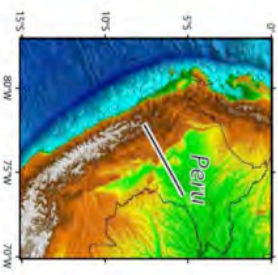
2 PERUPETRO S.A., Av. Luis Aldana No 320 San Borja, Lima 41, Peru

In the Andes, precise knowledge of deformation and exhumation timing in Eastern Cordillera (EC) and Subandean Zone (SAZ) is fundamental to decipher the respective role of tectonic activity and climate forcing in shaping topography and to understand mechanisms responsible for mountain growth^{1,2}. In this study, we report a 500 km balanced cross section (Figure 1) constructed according to surface and subsurface data, apatite fission-track (AFT) and (U-Th)/He (AHe) ages and vitrinite reflectance (Ro) values from northern Peruvian EC and SAZ. The balanced cross section (Figure 1) shows that the structural architecture is composed by thick skinned thrust related to the inversion of the Triassic rift normal faults and reactivation of Late Permian thrust faults. The SAZ is characterized by a combination of thick and thin skinned tectonics. The total amount of shortening calculated from the balanced cross-section is 142 km (i.e., ~28 %). AFT and AHe ages indicate that exhumation timing in EC and SAZ is coeval and occurred between ca 17 Ma and 8 Ma. Sequential restoration calibrated by AFT, AHe and Ro data reveals that shortening rates vary from 7.1 to 3.6 mm.yr⁻¹ between, respectively, 17-8 Ma and 8-0 Ma. Considering these results for the first ~49 km of horizontal shortening, we propose that the transfer of the Andean deformation into the EC and SAZ started at about ~30 or ~24 Ma. Active deformation recorded by seismic activity³ in the Marañón foredeep argues for a forward propagation of the Andean shortening. We suggest that tectonic deformation style is the main mechanism controlling Andean erosion and exhumation in relation with inherited basement structures. This tectonic inheritance control is still on going with reactivations of Permian faults in Marañón foredeep, promoting forward propagation and maintaining the Eastern Andean Peruvian wedge in a supercritical state.

Figure 1. (Next page) *Balanced cross section of the northern Central Andes eastern orogenic wedge, location on the top left corner digital elevation model of Peru. L-T, low temperature; AFT, apatite fission track; AHe, (U-Th-Sm)/He on apatite. Supposed present-day thick-skinned active faults are drawn in dotted line.*

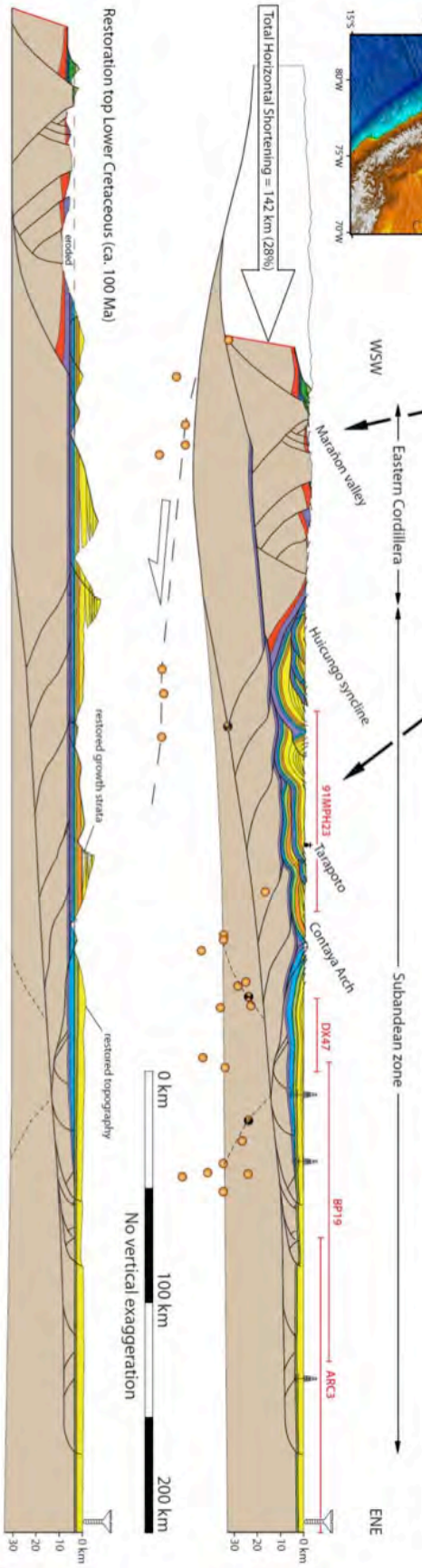
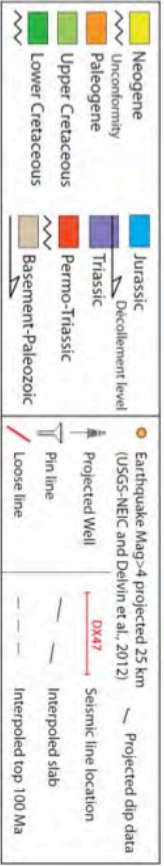
References

1. Barnes, J. B., Ehlers, T. A., Insel, N., McQuarrie, N. & Poulsen, C. J. Linking orography, climate, and exhumation across the central Andes. *Geology* 40, 1135-1138 (2012).
2. Gautheron, C. et al. Direct dating of thick- and thin-skin thrusts in the Peruvian Subandean zone through apatite (U-Th)/He and fission track thermochronometry. *Basin Res.* 25, 419-435 (2013).
3. Devlin, S., Isacks, B. L., Pritchard, M. E., Barnhart, W. D. & Lohman, R. B. Depths and focal mechanisms of crustal earthquakes in the central Andes determined from teleseismic waveform analysis and InSAR. *Tectonics* 31 (2012).



L-T Thermochronology (AFT-AHe ages)

Age-Elevation profile and Thrust activation dating



Restoration top Lower Cretaceous (ca. 100 Ma)

Recent (< 8 Ma) tectonics and exhumation processes in Cordilleras Blanca and Negra, Central Peru: Constraints from apatite (U-Th)/He and Fission-Track dating

Audrey Margirier^{1,2}, Xavier Robert^{1,2,3}, Cécile Gautheron⁴, Laurence Audin^{1,2,3}

1 Univ. Grenoble Alpes, ISTERre, F-38041 Grenoble, France

2 CNRS, ISTERre, F-38041 Grenoble, France

3 IRD, ISTERre, F-38041 Grenoble, France

4 UMR GEOPS, CNRS 8148, Université Paris Sud, 91405 Orsay, France

The Central Andes are a classical example of topography building in front of an oceanic subduction. However, many first order questions are still debated: How do subduction processes and observed tectonic uplift interact along the Andean margin? What is the impact of tectonic, magmatism and climate on exhumation?

Here we focus on one of the highest Andean relief, the Cordilleras Blanca (6768 m) and Negra (5181 m), located above the Peruvian flat-slab in north Central Peru, to investigate the link between slab flattening and uplift and to identify the impact of magmatism on crustal thickening. Both ranges trend parallel to the subduction zone and are separated by the NW-SE Rio Santa valley (Fig. 1). The Cordillera Blanca pluton formed in an active subduction crustal context at 8-5 Ma^{1,2} and renders an abnormal magmatic activity over a planar subduction. In contrast with the Cordillera Blanca, the Cordillera Negra is an older relief³, which evolution and exhumation history has never been studied. The Cordillera Blanca composed the footwall of a ~200 km-long normal fault (Fig. 1). This fault located on the western flank of the CB shows ~4500 m of vertical displacement since 5 Ma⁴. We perform a morphotectonic study on both Cordilleras coupled with low-temperature thermochronology apatite (U-Th)/He and fission-track dating to quantify the impact of magmatism and subduction processes on exhumation.

Geomorphic parameters and altitude contrasts between these two ranges indicate a differential uplift. The Cordillera Negra displays a smooth and asymmetric relief from the West to the East whereas the Cordillera Blanca shows higher and sharper relief with North/South and East/West contrasts. We obtain 35 new apatite fission-tracks ages and 20 (U-Th)/He ages for samples located along vertical and horizontal profiles at different latitudes of the Cordilleras Blanca and Negra (Fig. 1). The (U-Th)/He ages range from 5.6 ± 0.6 to 13.4 ± 1.3 Ma in the Cordillera Negra and range from 2.0 ± 0.2 to 11.8 ± 1.2 Ma in the Cordillera Blanca. The fission-track ages range from 23.6 ± 2.5 to 30 ± 3.0 Ma in the Cordillera Negra and range from 2.8 ± 2.2 to 8 ± 2.5 Ma in the Cordillera Blanca. We use these thermochronological data as inputs for QTQt tools for time-temperature reconstruction and thus to constrain the exhumation history.

Whole ages evidence a regional exhumation in both Cordilleras Blanca and Negra. Exhumation history inferred from low-temperature thermochronology ages coupled with geomorphologic characteristics suggests a regional component of uplift above the Peruvian flat-slab. Time-temperature reconstruction indicates a recent exhumation initiated ~4 Ma ago in the Cordillera Negra. Moreover, ages from the Cordillera Blanca indicate higher exhumation rates than in the neighbouring Cordillera Negra. Our set of thermochronological data brings new constraint on both Cordilleras thermal histories suggesting that the flattening of the Peruvian slab controls the regional exhumation as locally proposed for the Cordillera Blanca exhumation⁵. The Cordillera Blanca records additional exhumation controlled by plutonism and facilitated by structural inheritance. These processes occur as a response to the flattening of the Peruvian slab and confirm the role of the subducting plate geometry in topography building in Central Andes.

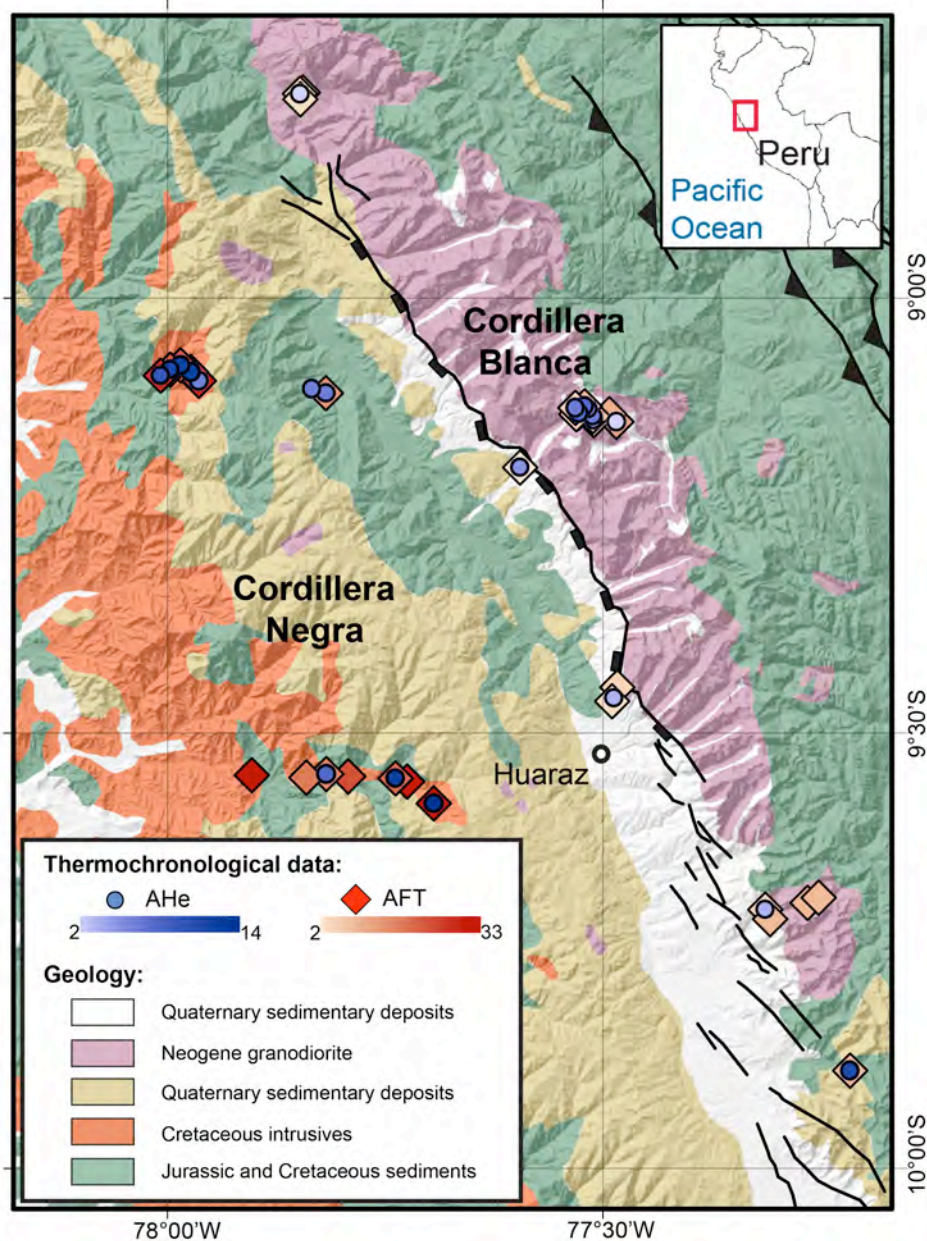


Figure 1. Geological map (modified from INGEMMET, 2012) draped on a digital elevation model (GDEM data, 30 m resolution) showing location of the Cordillera Blanca and the Cordillera Negra. The apatite (U-Th)/He ages and apatite fission-track ages are localized respectively by blue circles and red squares. Coordinates are given in WGS 84 longitude and latitude (degrees).

References

1. McNulty, B. A., Farber, D. L., Wallace, G. S., Lopez, R. & Palacios, O. Role of plate kinematics and plate-slip-vector partitioning in continental magmatic arcs: Evidence from the Cordillera Blanca, Peru. *Geology*, **26**, 827-830 (1998).
2. Giovanni, M. K. Tectonic and thermal evolution of the Cordillera Blanca Fault Zone, Peruvian Andes: Implications for normal faulting in contractional orogen. *Ph.D. Dissertation, Department of Earth Sciences, University of California, Los Angeles* (2007).
3. Noble, D. C., McKee, E. H., Mourier, T. & Mégard, F. Cenozoic stratigraphy, magmatic activity, compressive deformation, and uplift in northern Peru. *Geological Society of America Bulletin*, **102**, 1105-1113 (1990).
4. Bonnot, D. Néotectonique et tectonique active de la Cordillère Blanche et du Callejon de Huaylas (Andes nord-péruviennes). *Thèse de l'université de Paris sud, Centre d'Orsay* (1984).
5. McNulty, B. A. & Farber, D. L. Active detachment faulting above the Peruvian flat slab. *Geology*, **30**, 567-570 (2002).
6. INGEMMET, 2012. Mapa geológica del Departamento de Ancash (Escala 1:500,000). Instituto Geológico Minero y Metalúrgico, Lima.

Initiation and evolution of uplift along the western Andes (Peru) constrained by apatite (U-Th)/He thermochronology

Carlos Benavente^{1,3}, Laurence Audin¹, Cécile Gautheron², Peter van der Beek¹, Xavier Robert¹, Stéphane Schwartz¹, Fabrizio Delgado³

1 ISTERre, IRD, Université de Grenoble, France

2 UMR GEOPS, Université Paris sud, 91405 Orsay, France

3 INGEMMET, Peru

The Andes is the classic example of a mountain range formed during subduction of an oceanic plate under a continental plate. Recent studies suggest that the 80 km-thick crust related to the Altiplano plateau¹ is mainly due to crustal shortening focused at the eastern edge of the orogen during the Miocene^{2,3}. However, the timing of uplift remains poorly constrained at the western edge of the plateau with relatively few estimates ranging from ca. 60 to ca. 2 Ma.

In southwest Peru, neighboring the volcanic arc, uplift of the plateau has been approached through quantification of canyon incision^{4,6}, providing evidence for ~3 km of incision (and, by inference, uplift) between ~14 and 2 Ma. However, these studies all focused on the forearc region, where cooling histories recorded by thermochronologic data are complicated by occurrences of an abrupt heating event during the Middle Miocene⁵.

We present new structural and apatite (U-Th)/He (AHe) thermochronologic data from the Nazca region, away from the Neogene volcanic arc, aiming to provide insights into exhumation and topographic development of the western margin of the Andes. Our sampling strategy focused in particular on obtaining elevation profiles. AHe ages range from 3.0 ± 0.1 to 60 ± 6 Myr in the Nazca and Cañete canyons. In addition, systematic fieldwork along strike in the Western Cordillera complemented by DEM and aerial image analysis throws light on the crustal deformation processes active in the Western Andes of Southern Peru for the Neogene.

Using the different results, we characterize the upper-crustal cooling history from several sites north of the well-studied giant canyons of Ocoña and Colca^{4,6} and away from the Neogene volcanic arc. In conclusion and in contrast to the previous studies⁷, our preliminary results show a much older initiation of cooling and thus probable exhumation in the Western Cordillera.

References

1. Phillips, K. & Clayton, R. W. Structure of the subduction transition region from seismic array data in southern Peru. *Geophysical Journal International* **196**, 1889-1905 (2014).
2. Lamb, S. & Hoke, L. Origin of the high plateau in the Central Andes, Bolivia, South America. *Tectonics* **16**, 623-649 (1997).
3. Garzzone C., Auerbach, D., Jin-Sook, J., Rosario, J., Passey, B., Jordan, T. & Eiler, J. Clumped isotope evidence for diachronous surface cooling of the Altiplano and pulsed surface uplift of the Central Andes. *Earth Planet. Sc. Lett.* **393**, 173-181 (2014).
4. Schildgen, T. F., Ehlers, T. A., Whipp Jr., D. M., van Soest, M. C., Whipple, K. X. & Hodges, K. V. Quantifying canyon incision and Andean Plateau surface uplift, southwest Peru: a thermochronometer and numerical modeling approach. *J. Geophys. Res. Earth Surf.* **114**, F04014 (2009)
5. Gunnell, Y., Thouret, J. C., Bricchau, S., Carter, A. & Gallagher, K. Low-temperature thermochronology in the Peruvian Central Andes: implications for long-term continental denudation, timing of plateau uplift, canyon incision and lithosphere dynamics. *J. Geol. Soc. London* **167**, 803 – 815 (2010)

6. Thouret, J. C., Wörner, G., Gunnell, Y., Singer, B., Zhang, X. & Souriot, T. Geochronologic and stratigraphic constraints on canyon incision and Miocene uplift of the Central Andes in Peru. *Earth Planet. Sci. Lett.* **263**, 151-166 (2007).
7. Wipf, M., Zeilinger, G., Seward, D. & Schlunegger, F. Focused subaerial erosion during ridge subduction: impact on the geomorphology in south-central Peru. *Terra Nova* **20**, 1-10 (2008).

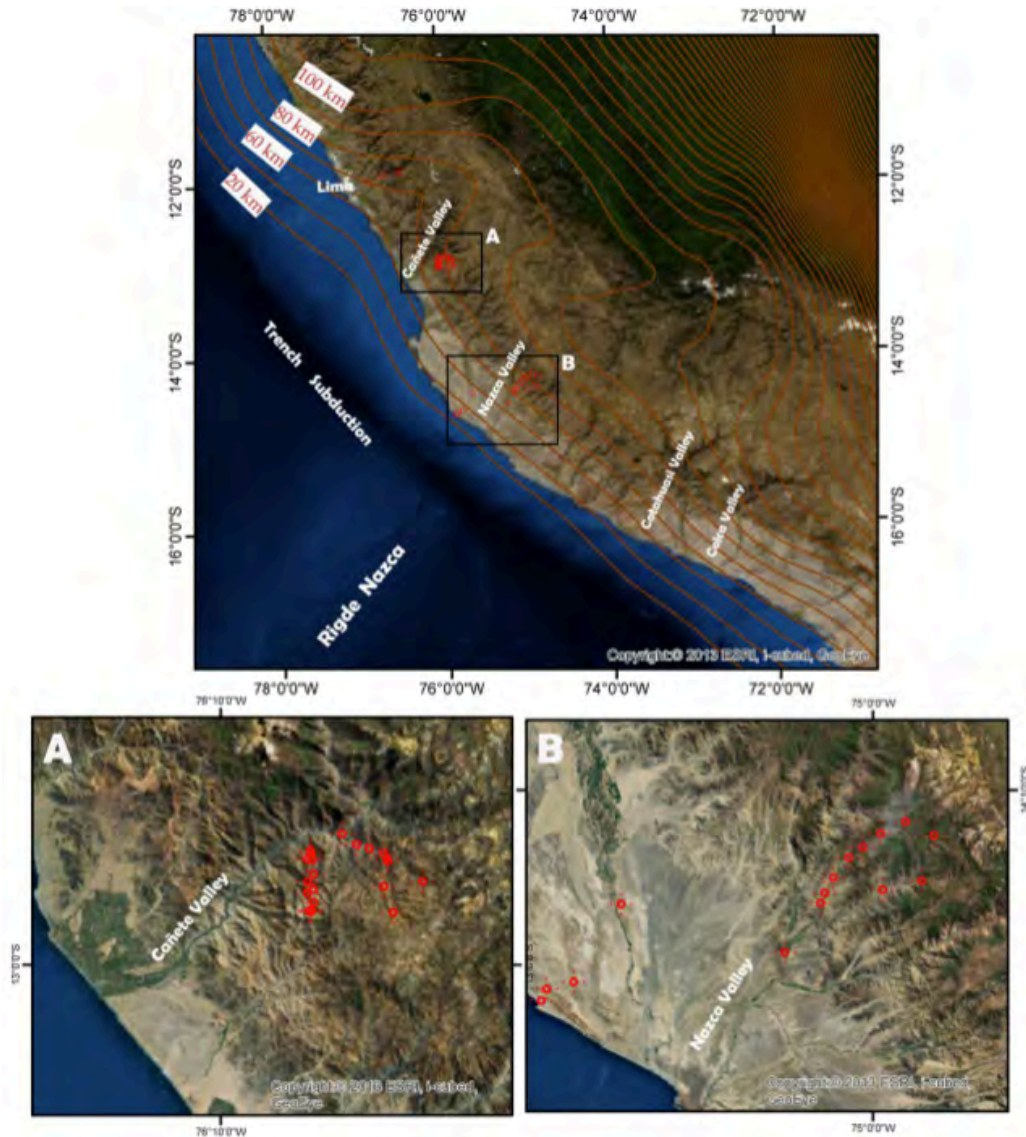


Figure 1. Top figure shows the western margin of the central Andes and the subduction zone. The main transverse valleys to the Andean chain, such as the Colca, Cotahuasi, Nazca, Cañete, and Lima valleys, are indicated. Red circles indicate sample locations, while the red lines show the depth-contours (10 km) of the oceanic slab. Squares A and B show in detail the sample locations and the relief of the study area.

Timing and modes of exhumation of basement and arc rocks in the forearc of southwesternmost Peru, Central Andes.

Mélanie Noury^{1,2}, Matthias Bernet^{1,2}, Thierry Sempéré^{1,2,3}

1 Univ. Grenoble Alpes, ISTERre, F-38041 Grenoble, France

2 CNRS, ISTERre, F-38041 Grenoble, France

3 IRD, ISTERre, F-38041 Grenoble, France.

The Central Andes are an outstanding orogen where crustal thickness reaches >70 km over a large area in the absence of continent-continent collision. This overthickness is commonly viewed as the result of crustal shortening. However, in the present day forearc of southwesternmost Peru, where crustal thickness increases from 30 km along the coastline to >60 km below the active arc, the upper crust exhibits little to no evidence of crustal shortening and in contrast many extensional features. How and when this crustal overthickness was acquired is poorly documented and thus understood.

We address this issue through a regional-scale study of exhumation using fission-tracks thermochronology. In southwestern Peru, the thermochronologic database is currently extremely limited and previous studies mainly focused on the Neogene history of Canyon incision. However, this relatively restricted area provides extensive outcrops of Precambrian to Ordovician basement as well as Early Jurassic to Late Cretaceous arc plutons and large volumes of forearc continental deposits. This configuration permits to compare the relationships and the history of exhumation of these different domains.

We based our sampling on a detailed knowledge of the geology of the forearc of southern Peru targeting key units in order to provide a maximum of information at a regional scale. We sampled rocks from exposed bedrock, arc related plutonic rocks of different ages as well as from the stratigraphic record of synorogenic basins and present-day river sediments. Structural mapping was carried out in order to identify the controls of tectonic exhumation on the Peruvian Andes. Finally, in order to verify the influence of the arc on the thermochronological ages, we sampled these units in the coastal area and closer to the present-day arc.

This study thus primarily aims at obtaining new thermochronologic data in order to advance a number of fundamental issues regarding the Cenozoic and Mesozoic evolution of mountain building in the Central Andes.

Tectonic uplift and topographic growth above oceanic ridge subduction - Northern Patagonian Icefield, southern Chile

Viktoria Georgieva¹, Daniel Melnick¹, Taylor Schildgen¹, Todd Ehlers², Manfred Strecker¹

1 Universität Potsdam, Institut für Erd- und Umweltwissenschaften, Karl-Liebknecht Str. 24- 25, 14476 Potsdam, Germany

2 Universität Tübingen, Geowissenschaften, Wilhelmstr. 56, 72076 Tübingen, Germany

Glacial processes throughout the Late Cenozoic have predominantly shaped the Patagonian Andes¹⁻³; however, the topographic signature shows distinct along-strike anomalies. In the Northern Patagonian Andes, maximum elevations exceed 2 km and relief is uniform, averaging 2 km. In the Southern Patagonian Andes, topography abruptly rises with peak summits between 3 and 4 km, and the local relief increases and becomes highly variable, locally exceeding 5 km where the highest peaks are adjacent to deep glacial fjords. The abrupt increase of both summit elevations and total relief coincides with the current position of the Nazca-Antarctic-South America Triple Junction (Chile Triple Junction, CTJ), where several ridge segments of the Chile Rise have been subducted since ~ 6 Ma⁴. A causal relationship between the closely spaced subduction of several successive ridge segments close to the present-day position of the triple junction and the location of the topographic anomaly has been proposed^{5,6}. Nevertheless, so far there is no direct structural field evidence for the mechanisms of such tectonic and surface uplift in that region.

Here we present geomorphic and structural evidence supported by thermochronometer data that indicate neotectonic activity along the flanks of the Northern Patagonian Icefield (NPI). The NPI is a poorly known region in terms of geology and neotectonics, located immediately east of the CTJ, which marks the major topographic anomaly at the transition between the Northern and Southern Patagonian Andes. We define two hitherto unrecognized fault systems, the Cachet and Exploradores Faults, which run along the eastern and northeastern foothills of the NPI, respectively. Based on the offset of deep glacial valleys and other morphologic parameters, as well as apatite (U-Th)/He data, we suggest that both faults have been active at least during the past 2-3 Ma.

We interpret margin-parallel strike-slip deformation along the eastern flank of the NPI to arise from localized, oblique collision of three segments of the Chile Rise at 6, 3, and 0 Ma at these latitudes⁴. This ridge subduction resulted in decoupling of the NPI from the Patagonian foreland along the Cachet Fault system. We suggest that northward motion of the NPI is accommodated by the Exploradores and other reverse fault systems along its northern and northeastern flanks, which act as a crustal ramp. This interpretation is further supported by the pronounced age shift between age- elevation relationships of apatite (U-Th)/He bedrock ages in vertical transects approaching the Exploradores Fault and the highest topography. The shift of about 2 Ma is interpreted to reflect deeper levels of exhumation closer to the Exploradores Fault Zone. We integrate the kinematics of these two fault systems with data from regional tectonic structures⁷, to propose a simple neotectonic model, which may help to explain the topographic anomalies in the Patagonian Andes.

References

1. Hein, A. S. *et al.* Middle Pleistocene glaciation in Patagonia dated by cosmogenic-nuclide measurements on outwash gravels. *Earth and Planetary Science Letters* **286**, 184-197 (2009).
2. Lagabrielle, Y., Scalabrino, B., Suarez, M. & Ritz, J. F. Mio-Pliocene glaciations of Central Patagonia: New evidence and tectonic implications. *Andean Geology* **37**, 276-299 (2010).
3. Rabassa, J., Coronato, A. M. & Salemme, M. Chronology of the Late Cenozoic Patagonian and their correlation with biostratigraphic glaciations units of the Pampean region (Argentina). *Journal of South American Earth Sciences* **20**, 81-103, doi:10.1016/j.jsames.2005.07.004 (2005).
4. Breitsprecher, K. & Thorkelson, D. J. Neogene kinematic history of Nazca-Antarctic-Phoenix slab windows beneath Patagonia and the Antarctic Peninsula. *Tectonophysics* **464**, 10--20 (2009).
5. Guillaume, B., Moroni, M., Funicello, F., Martinod, J. & Faccenna, C. Mantle flow and dynamic topography associated with slab window opening: Insights from laboratory models. *Tectonophysics* **496**, 83-98, doi:10.1016/j.tecto.2010.10.014 (2010).
6. Ramos, V. A. Seismic ridge subduction and topography: Foreland deformation in the Patagonian Andes. *Tectonophysics* **399**, 73-86, doi:10.1016/j.tecto.2004.12.016 (2005).
7. Rosenau, M., Melnick, D. & Echtler, H. Kinematic constraints on intra-arc shear and strain partitioning in the southern Andes between 38 degrees S and 42 degrees S latitude. *Tectonics* **25** (2006).

Impact of glaciations on the long-term erosion in Southern Patagonian Andes

Thibaud Simon-Labric¹, Frederic Herman¹, Lukas Baumgartner¹, David L. Shuster^{2,3},
Pete W. Reiners⁴, Jean Braun⁵, Pierre G. Valla¹, Julien Leuthold⁶

1 IDYST, University of Lausanne, CH-1015 Lausanne, Switzerland,

2 Berkeley Geochronology Center, 2455 Ridge Road, Berkeley, CA 94707,

3 Department of Earth and Planetary Science, University of California, Berkeley, CA 94720.

4 Geosciences, University of Arizona, Tucson, AZ, USA,

5 ISTERre, Université Joseph Fourier, BP53, 38041 Grenoble, France,

6 School of Earth Sciences, University of Bristol, Wills Memorial Building, Bristol BS8 1RJ, UK.

The Southern Patagonian Andes are an ideal setting to study the impact of Late-Cenozoic climate cooling and onset of glaciations impact on the erosional history of mountain belts. The lack of tectonic activity during the last ~12 Myr makes the denudation history mainly controlled by surface processes, not by tectonics. Moreover, the glaciations history of Patagonia shows the best-preserved records within the southern hemisphere (with the exception of Antarctica). Indeed, the dry climate on the leeward side of Patagonia and the presence of lava flows interbedded with glacial deposits has allowed an exceptional preservation of late Cenozoic moraines with precise dating using K-Ar analyses on lava flow. The chronology of moraines reveals a long history covering all the Quaternary, Pliocene, and up to the Upper Miocene. The early growth of large glaciers flowing on eastern foothills started at ~7-6 Myr, while the maximum ice-sheet extent dates from approximately 1.1 Myr.

In order to quantify the erosion history of the Southern Patagonian Andes and compare it to the glaciations sediment record, we collected samples along an age-elevation profile for low-temperature thermochronology in the eastern side of the mountain belt (Torres del Paine massif). The (U-Th)/He age-elevation relationship shows a clear convex shape providing an apparent long-term exhumation rate of ~0.2 km/Myr followed by an exhumation rate increase at ~6 Myr. Preliminary results of ⁴He/³He thermochronometry for a subset of samples complete the erosion history for the Plio-Pleistocene epoch. We used inverse procedure predicting ⁴He distributions within an apatite grain using a radiation-damage and annealing model to quantify He-diffusion kinetics in apatite. The model also allows quantifying the impact of potential U-Th zonation throughout each apatite crystal. Inversion results reveal a denudation history composed by a pulse of denudation at ~6 Ma, as suggested by the age-elevation relationship, followed by a decrease in denudation rate to very low value (<0.1 km/Myr) and late-stage exhumation phase at ~1 km/Myr for the last ~2 Myr.

Our (U-Th)/He and ⁴He/³He data demonstrate a tight connection between the glaciation history from moraines record and long-term erosion rates derived from low-temperature thermochronology. These results highlight the high sensitivity of the Southern Patagonian Andes to the progressive Late-Cenozoic climate cooling and the strong glacial imprint on erosion history and landscape evolution since the Late Miocene. Indeed, we interpret the observed increase in erosion at ~6 Myr as the landscape response to the onset of the Patagonian ice cap, while the inferred recent increase in erosion rates may reflect the intensification of the climate cooling since the Plio-Pleistocene.

Thermochronologic evidence of a Late Miocene-Pliocene change in Pamir deformation style

Edward R. Sobel¹, Alejandro Bande¹, Rasmus Thiede¹, Alexander Mikolaichuk², Euan Macaulay³, Chen Jie⁴

1 Universitaet Potsdam, Institut für Erd- und Umweltwissenschaften, 14476 Potsdam, Germany

2 Geological Institute National Academy of Sciences, Bishkek, 720040, Kyrgyzstan

3 Midland Valley Exploration Ltd., 144 West George Street, Glasgow, G2 2HG, Scotland

4 Institute of Geology, China Earthquake Administration, Beijing 100029, China

One of the major debates about the Cenozoic geodynamic evolution of the Pamir orogen concerns the style and timing of deformation along the boundary between the Eastern Pamir and the Tarim block. On the one hand, during the late Oligocene (?) - Early Miocene, the Pamir apparently began indenting northward along the Kashgar Yecheng Transfer System (KYTS)¹. On the other hand, basin-vergent deformation along the margin of Tarim began in the past ca. 10 Ma or even in the Pliocene^{2,3}. These two contrasting interpretations have not yet been reconciled in publications. We propose a novel interpretation that is compatible with both suites of observations.

Pamir indentation was accommodated by a south-dipping intracontinental subduction system coupled to major shear systems on both flanks. The Alai basin to the north constitutes the downgoing plate, with the bulk of the convergence accommodated by underthrusting. East of the Pamir lies the Tarim basin, which in turn overlies a rigid Precambrian block. The boundary between the Pamir and Tarim is a complex dextral shear zone, which includes the KYTS. Indentation of the Pamir was underway by ~20 Ma based on AFT ages along the KYTS. Our preferred interpretation is that this structure represents the surface expression of a STEP fault, which is a lithospheric tear that allows the south-dipping Pamir subduction zone to roll back to the north with respect to Tarim⁴. However, GPS shows that Tarim and Pamir are moving northward at same velocity today; therefore, indentation is no longer accommodated along the KYTS. River incision across the KYTS combined with thermochronologic modeling suggests that this fault system has been largely inactive for at least 3-5 Ma⁵.

The northward indentation of the Pamir salient was accommodated not only by the right-lateral KYTS but also by the Shache-Yangdaman Fault (SYF)⁶, which lies in the subsurface of the Western Tarim basin. Grounded by a thorough outcrop and subsurface data summary, these authors propose that a right stepover between these two faults formed the 6 km thick Yecheng pull-apart basin. Based on the map pattern and timing, we suggest that the dextral Talas-Fergana Fault (TFF) can be connected to the newly described SYF, which thereby represents the southernmost portion of a major right-lateral strike-slip system. AFT ages from restraining bends and coupled thrust faults at both the southern⁷ and northern ends of the TFF show that this system became active around 25 Ma⁸. This interpretation explains how the regional strike-slip system was able to transfer shortening driven by Pamir indentation to the NW Tien Shan. Magnetostratigraphy shows that shortening in the Kokshaal range propagated rapidly southward into the Tarim basin between 16.3 and 13.5 Ma⁹. Therefore, relatively rapid slip along the TFF persisted from ca. 25 Ma until at least 13.5 Ma. Subsequently, the slip rate apparently decreased. Late Oligocene (?) - Early Miocene slip along the TFF agrees well with the formation of the transtensional Yecheng depression in the SW Tarim basin, supporting our contention that the SYF and TFF are kinematically linked. Furthermore, this transtension implies that the relative motion of the Pamir with respect to Tarim was slightly divergent during the late Oligocene (?) - Early Miocene, which would have inhibited significant contractile exhumation along the eastern Pamir.

The above described deformation is also consistent with thermochronologic data from other margins of Tarim. Early Miocene cooling and 80-100 km of shortening is documented far to the south, in the Western Kunlun Shan^{10,11} and in isolated localities in the Tien Shan¹²⁻¹⁶. These widely distributed cooling ages are linked with roughly N-S shortening, pointing to a relatively weak regional contractile period both north and south of Tarim, roughly synchronous with Pamir indentation. This interval also coincides with rapid

sinistral slip along the Altyn Tagh Fault (ATF)¹⁷, which separates the southern margin of Tarim from Northern Tibet.

A significant change in regional deformation and exhumation patterns occurred in the Middle-Late Miocene. AFT samples from structures adjacent to western Tarim yield ages between 10-6 Ma³. Stratigraphic relationships in structures close to the margin of western and southwestern Tarim and in the subsurface suggest that basin vergent thrusting initiated or intensified in the Late Miocene or Pliocene (e.g., 2). Rapid cooling and accelerated sedimentation began at 12-10 Ma in the many parts of the Tien Shan^{15,16,18-21}. Motion along the ATF slowed significantly around this time¹⁷.

Comparing the style and magnitude of these two episodes of deformation suggests that a significant regional geodynamic change occurred in the mid-late Miocene. Tarim apparently began to move northward, such that Tarim and the Pamir are presently moving north with the same velocity; this led to significant crustal shortening within the Tien Shan⁵. In turn, this caused a significant decrease in slip rate along the KYTS. This interval corresponds to the onset of contractile deformation in western and southwest Tarim. As consequence, it is likely that much of the modern morphology was built in this period, obscuring earlier deformation.

References

1. Sobel, E. R. & Dumitru, T. A. Exhumation of the margins of the western Tarim basin during the Himalayan orogeny. *Journal of Geophysical Research* **102**, 5043-5064 (1997).
2. Zhang, W., Qi, J. & Li, Y. Structural styles in south-western margin of Tarim Basin and their dominate factors. *Chinese Journal of Geology* **46**, 723-732 (2011).
3. Cao, K. et al. Cenozoic thermo-tectonic evolution of the northeastern Pamir revealed by zircon and apatite fission-track thermochronology. *Tectonophysics* **589**, 17-32 (2013).
4. Sobel, E. R. et al. Oceanic-style subduction controls late Cenozoic deformation of the Northern Pamir Orogen. *Earth and Planetary Science Letters* **363**, 204-218 (2013).
5. Sobel, E. R. et al. Late Miocene-Pliocene deceleration of dextral slip between Pamir and Tarim: Implications for Pamir orogenesis. *Earth and Planetary Science Letters* **304**, 369-378 (2011).
6. Wei, H. H., Meng, Q. R., Ding, L. & Li, Z. Y. Tertiary evolution of the western Tarim basin, northwest China: A tectono-sedimentary response to northward indentation of the Pamir salient. *Tectonics* **32**, 558-575 (2013).
7. Sobel, E. R., Chen, J. & Heermance, R. V. Late Oligocene - Early Miocene initiation of shortening in the Southwestern Chinese Tian Shan: Implications for Neogene shortening rate variations. *Earth and Planetary Science Letters* **247**, 70-81 (2006).
8. Bande, A., Sobel, E. R., Mikolaichuk, A. & Torres, A. V. in *Geological evolution of Central Asian Basins and the Tien-Shan Range* (eds. Brunet, M. F., McCann, T. & Sobel, E. R.) (in review).
9. Heermance, R. V., Chen, J., Burbank, D. W. & Miao, J. Temporal constraints and pulsed Late Cenozoic deformation during the structural disruption of the active Kashi foreland, northwest China. *Tectonics* **27**, TC6012 (2008).
10. Li, D. P. et al. Fission track thermochronologic constraints on plateau surface and geomorphic relief formation in the northwestern margin of the Tibetan Plateau. *Acta Petrologica Sinica* **25**, 900-910 (2007).
11. Jiang, X. D., Li, Z. X. & Li, H. B. Uplift of the West Kunlun Range, northern Tibetan Plateau, dominated by brittle thickening of the upper crust. *Geology* **41**, 439-442 (2013).
12. Hendrix, M. S., Dumitru, T. A. & Graham, S. A. Late Oligocene-Early Miocene unroofing in the Chinese Tian Shan: An early effect of the India-Asia collision. *Geology* **22**, 487-490 (1994).
13. Glorie, S. et al. Tectonic history of the Kyrgyz South Tien Shan (Atbashi-Inylchek) suture zone: The role of inherited structures during deformation-propagation. *Tectonics* **30**, TC6016 (2011).
14. De Grave, J. et al. Thermo-tectonic history of the Issyk Kul basement (Kyrgyz Northern Tien Shan, Central Asia). *Gondwana Research* **23**, 998-1020 (2013).
15. Macaulay, E. A. et al. Thermochronologic insight into Late Cenozoic deformation in the basement-cored Terskey Range, Kyrgyz Tien Shan. *Tectonics* **32**, 487-500 (2013).
16. Macaulay, E. A. et al. Cenozoic deformation and exhumation history of the Central Kyrgyz Tien Shan. *Tectonics* **33**, 135-165 (2014).
17. Yue, Y. J. et al. Slowing extrusion tectonics: lowered estimate of post-Early Miocene slip rate for the Altyn Tagh fault. *Earth and Planetary Science Letters* **217**, 111-122 (2003).
18. Bullen, M. E., Burbank, D. W., Garver, J. I. & Abdrakhmatov, K. Y. Late Cenozoic tectonic evolution of the northwestern Tien Shan: New age estimates for the initiation of mountain building. *Geol. Soc. Am. Bull.* **113**, 1544-1559 (2001).
19. Abdrakhmatov, K. E. et al. Origin, direction, and rate of modern compression of the central Tien Shan (Kyrgyzstan). *Geol. Geofiz.* **42**, 1585-1609 (2001).
20. Charreau, J. et al. Magnetostratigraphy and rock magnetism of the Neogene Kuitun He section (northwest China): implications for Late Cenozoic uplift of the Tianshan mountains. *Earth Planet. Sci. Lett.* **230**, 177-192 (2005).
21. Shen, C. B. et al. Fission track evidence for the Mesozoic-Cenozoic tectonic uplift of Mt. Bogda, Xinjiang, Northwest China. *Chinese Journal of Geochemistry* **25**, 143-151 (2006).

Quantifying Tectonic Controls on Pamir Erosion with Thermochronology

Konstanze Stübner¹, Todd A. Ehlers¹, Elena Grin¹, István Dunkl², Lothar Ratschbacher³
1 Dept. of Geosciences, University Tübingen, Germany
2 Geoscience Center, University Göttingen, Germany
3 Institut für Geologie, TU Bergakademie Freiberg, Germany

High-relief mountain ranges correspond to tectonically active areas. Topographic relief created by tectonic uplift increases erosion rates; it is widely accepted that erosion rates scale with slope, local relief, and elevation either linearly¹ or through more complex relationships that take into account limits to hillslope gradients², or the effects of glaciation on topographic relief. A change of topography with time, or variable topography across a mountain range, may result from variations in tectonic uplift rates, but may also reflect temporal and spatial climate changes.

The Pamirs, Central Asia, are an excellent natural laboratory to test hypotheses of tectonic–climate–relief development interactions because this orogen is tectonically highly active, it is one of the few areas worldwide with a local relief > 2000 m, and a strong climatic contrast exists between the arid eastern and the more humid western Pamir (Figure 1). Correlating with the precipitation gradient, topographic relief and local slope are higher in the western than the eastern Pamir (Figure 1); thermochronological data indicate higher erosion rates in the west³. On the other hand, within the Shakh dara gneiss dome, southwest Pamir geological and geomorphological observations indicate that over the last ~5 Ma denudation was restricted to incision of rivers and canyons. The South Pamir detachment, a Miocene low-angle normal fault, is preserved as a weakly eroded subhorizontal surface at ~4000 m a.s.l., and remnants of Miocene sedimentary basins can be found on top of the detachment. This surface is visible, for example, in a local-slope map (Figure 1 center, blue shades within the Shakh dara dome).

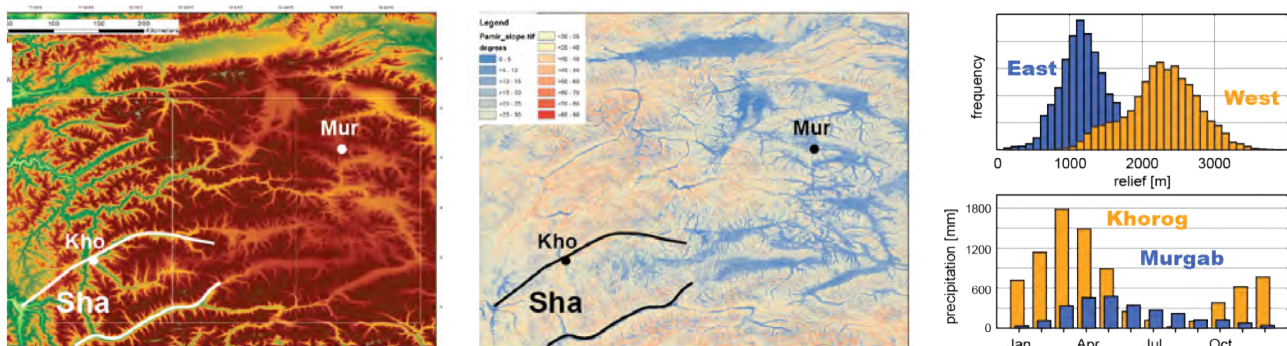


Figure 1. Topography (left) and local slope (center) of the Pamir. Diagrams on right side show frequency distribution of local relief (top) and monthly precipitation⁵ (bottom) for the western (orange) and eastern Pamir (blue). Outline of the Shakh dara gneiss dome (Sha), and weather stations Khorog (Kho) and Murgab (Mur) are indicated.

We use apatite fission track and (U-Th)/He thermochronology and cosmogenic isotopes in modern river sands to quantify the spatial and temporal distribution of erosion rates in the southwest Pamir. Our aim is to understand (1) why in this region of active shortening (e.g., 15 mm/yr across the Main Pamir thrust⁴) long-term erosion rates are apparently low (preservation of

Miocene paleosurface); (2) if, why, and when globally established relationships between erosion rates and relief fail in the southwest Pamir; (3) if and how glaciation affects these topography–erosion rate relationships.

Hitherto existing bedrock apatite fission-track³ (AFT) and apatite (U-Th)/He (AHe) ages quantify the long-term average erosion history. The youngest AFT ages (2–3 Ma) are obtained from bedrock samples near the southern dome margin and denote the end of tectonic exhumation ('doming'). In the central and northern dome, AFT ages range from ~4 to 10 Ma and correlate with AHe ages between ~1 and 7 Ma. Cooling ages of both chronometers vary systematically with elevation, but not with lateral position within the dome. This pattern suggests that cooling from >120 °C to surface temperatures was controlled mostly by erosion rather than tectonic processes, and that rivers have incised up to 4 km since the middle Miocene at long-term average incision rates of 0.3–0.5 mm/yr. Further data is needed to reveal spatial and temporal variations in the erosion history.

References

1. Ahnert, F. Functional relationship between denudation, relief, and uplift in large mid-latitude drainage basins. *Am. J. Sci.* **268**, 243-263 (1970).
2. Montgomery, D. R. & Brandon, M. T. Topographic controls on erosion rates in tectonically active mountain ranges. *Earth Planet. Sci. Lett.* **201**, 481-489 (2002).
3. Stübner, K., Ratschbacher, L., Weise, C. et al. The giant Shakh dara migmatitic gneiss dome, Pamir, India-Asia collision zone: 2. Timing of dome formation. *Tectonics* **32**, (2013).
4. Ischuk, A., Bendick, R., Rybin, A., et al. Kinematics of the Pamir and Hindu Kush regions from GPS geodesy. *J. Geophys. Res.* **118**, 2408-2416 (2013).
5. Kalnay, E., Kanamitsu, M., Kistler, R. et al. The NCEP/NCAR 40-year reanalysis project. *Bull. Amer. Meteor. Soc.* **77**, 437-470 (1996).

Uplift and River Incision of the western Pamir Plateau - New insights from river-profile analysis and thermochronology

Rasmus C. Thiede¹, Edward Sobel¹, Paolo Ballato¹, Mustafó Gadoev², Ilhomjon Oimahmadov², Todd Ehlers³, Manfred Strecker¹

1 Potsdam University, Inst. f. Erd- und Umweltwissenschaften, Potsdam-Golm, Germany (thiede@geo.uni-potsdam.de),

2 Acad o Science, Inst. o. Geology, Seismology, Dushanbe, Tajikistan

3 University of Tuebingen Inst. f. Geowissenschaften, Germany

The mechanisms responsible for driving the growth and destruction of orogenic plateaus are subject of ongoing controversial debate. In addition to thermo-mechanical and structural models, a third class of models emphasizes the pivotal role of surface processes in concert with tectonic processes. The Pamir forms a high elevation plateau representing the NW extension of the Tibetan Plateau. Crustal shortening and uplift throughout the Cenozoic formed the plateau and continues along its western and northern flanks until today. In contrast to the mostly internally drained Tibet at present the Pamir is mostly externally drained and internal drainage occurs only in a few inert plateau domains. Also in contrast to other plateaus the major climatic gradients across Pamir are oriented E-W, perpendicular to N-S oriented crustal shortening. Until now the tectonic growth, uplift and incision history of both marginal and interior parts of the Western Pamir are only poorly constrained.

To assess the impact of the surface-process systems on the geomorphic evolution of the plateau, we performed several standard morphometric analyses across entire Pamir, for now focusing along the western margin. In particular, we analyzed the local topographic relief, the overall character of the drainage network, and performed the novel integral approach to river profile analysis (CHI) of major drainage basins. Furthermore we have started measuring apatite He/U-Th data (AHe) to decipher the timing of deep seated valley incision. Combined, our new geomorphic observations and the preliminary thermochronology data provide proxies for the uplift history of the orogeny, which may ultimately provide insights into the nature of deep-seated processes that caused plateau growth and widespread valley incision.

Our analysis reveals three zones with different geomorphic characteristics of the fluvial network. First, along a 50-km-wide swath profile across the W-NW flank of the orogen, we find low-relief landscapes with gentle, concave river profiles. These are interrupted by major knick points, followed by steep segments in the downstream section, when draining towards the deeply incised trunk valley, the Panj. These low relief areas may reflect relict landscape and hence predate the most recent pulse of uplift, which led to the development of the present day morphology. Second, beyond this western to northwestern frontal zone of low-internal relief lies the Panj River, which is the trunk stream of five major watersheds, draining the internal parts of the western Pamir plateau margin. All of these tributaries are deeply incised (2-3 km of local relief), are U-shaped in the vicinity of the drainage mouth, and rise continuously until they reach the inner plateau realm. In turn, river profiles of tributary valleys of these watersheds are all steep in the lower parts and some cases, they have the typical morphology of glacial hanging valleys and are dominated by alpine glacial landscape at high elevation. Three preliminary AHe cooling ages between 5 and 3 Ma provide valuable estimates on the timing of valley incision, indicating that incision was ongoing during the latest Miocene onwards. Third, the central and eastern parts of the Pamir are predominantly characterized by wide, (Quaternary?) sediment filled basins at elevations >3km and gentle stream gradients from at present day remnants of the plateau.

Based on our preliminary observations we suggest that the topographic growth of the western flank is recorded by the deeply incised hydrologic system draining the plateau interior and its margins:

(1) the frontal segment of the western flank of the Pamir has been rapidly uplifted on the order of 2 to 3 km not earlier than during late Miocene; (2) the internal portion of the western Pamir constitutes an important orographic barrier for westerly moisture sources, which has facilitated deep glacial/fluvial incision during the late Cenozoic.

Structure and exhumation of the Tajik Depression (western foreland of the Pamir): towards an integrated kinematic model

Łukasz Gaḡała^{1,2}, Alexandra Kässner¹, Sanaa Abdulhameed¹, Adam Szulc^{1,4}, Lothar Ratschbacher¹, Jean-Claude Ringenbach³, Richard Gloaguen¹, Negmat Rajabov⁵, Rustam Mirkamalov⁶

1 Institut für Geologie, TU Bergakademie Freiberg, Germany

2 Georex Assistance Technique, France

3 TOTAL, France

4 Cambridge Arctic Shelf Programme (CASP), United Kingdom

5 Institute of Geology, Tajik Academy of Sciences, Tajikistan

6 State Committee of the Republic of Uzbekistan on Geology and Mineral Resources

The Tajik Depression is the westernmost and widest part of the Neogene-Recent foreland basin of the Pamir. It is confined between the Pamir, Tien Shan and Ghissar mountain belts. In the Neogene, the Cretaceous-Recent fill of the Tajik Depression was detached along Late Jurassic evaporites, folded and thrust towards the W–NW in front of the advancing Pamir. We propose a new kinematic model that integrates an updated structural interpretation with apatite fission-track and (U-Th)/He thermochronology constraints on the timing of exhumation.

The structural interpretation is based on a series of balanced cross-sections tied to field observations and new seismic data. The cross-sections show how thin-skinned folds and thrust sheets interact with thick-skinned structures in the basement. The western (foreland) part of the thin-skinned system features thrust sheets stacked along backthrusts that accommodated significant displacement. The eastern (hinterland) part accommodated less shortening and is characterized by thrust detachment folds. The thick-skinned belts surrounding the Tajik Depression originated from reactivation of pre-existing structures (Tien Shan) and recent thick-skinned thrusting (Ghissar).

Samples were collected for apatite from Early-Mid Jurassic and Early Cretaceous sandstones and from pre-Jurassic metamorphic/igneous basement. The thermochronology results are supported by vitrinite reflectance data. Ghissar AFT and (U-Th)/He ages show a similar range (12.7 ± 1.2 – 4.1 ± 1.2 Ma and 11.9 ± 3.8 – 4.3 ± 1.1 Ma, respectively), indicating rapid exhumation through the 110°C and 75°C isotherms. AFT and (U-Th)/He ages from the Tajik Depression range between 11.8 ± 0.8 – 3.5 ± 0.3 Ma and 10.6 ± 1.3 – 1.0 ± 0.8 Ma, respectively. These results suggest that exhumation was diachronous from west to east across the Tajik Depression. The central part of the Tajik Depression yielded the oldest AFT age (11.8 ± 0.8 Ma). This is a maximum age for the activation of the detachment along the Late Jurassic evaporites. Tien Shan AFT and (U-Th)/He ages range between 145.6 ± 12.0 – 1.6 ± 0.3 Ma. The wide range of the Tien Shan ages reflects a mix of fully reset, partially reset and un-reset age components. An offset between the youngest AFT ages (12.6 ± 0.9 – 3.3 ± 0.3 Ma) and (U-Th)/He ages (8.9 ± 1.8 – 1.9 ± 0.8 Ma) indicates that exhumation was slower in the Tien Shan compared to the Ghissar.

According to AFT and (U-Th)/He constraints the frontal homocline of the Pamir started to form at ~ 13 Ma (Figure 1), coevally with far-field uplift of the Ghissar and the Tien Shan. At ~ 12 Ma the slip was transferred from the Pamir to the Upper Jurassic detachment triggering thin-skinned

deformation in the Tajik Depression. Until ~6 Ma, thin-skinned shortening was restricted to the external (foreland) part of the Tajik Depression where long-displacement back thrusts built a hinterland-vergent imbricate stack. Increasingly internal zones of the Tajik Depression were then successively folded. Thin-skinned deformation was largely completed by ~4 Ma. The most recent folding of the internal part of the Tajik Depression was associated with reactivation of the pre-Jurassic basement.

This research was conducted under patronage of Total[®].

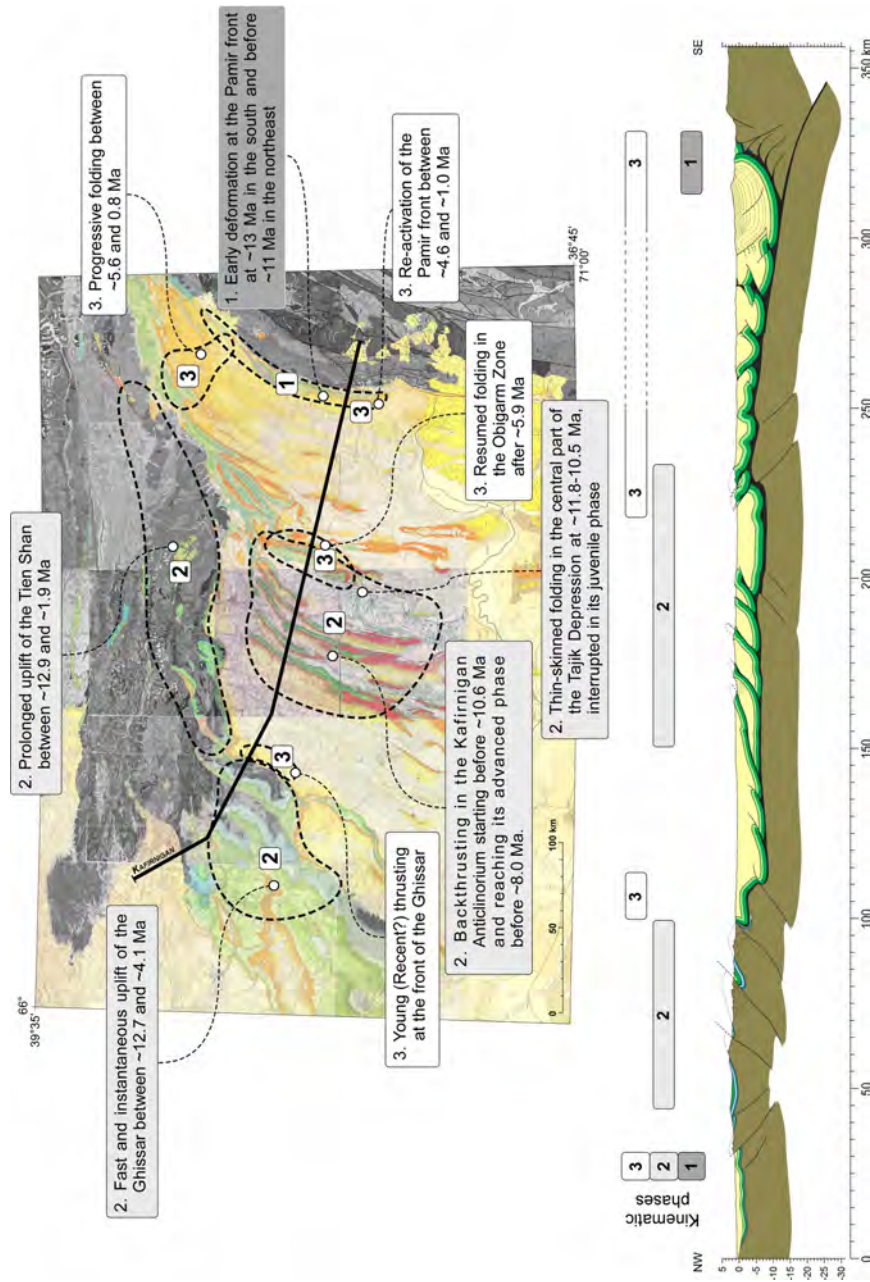


Figure 1. Timing of deformation in the Tajik Depression and the surrounding thick-skinned belts. Numbers 1-3 indicate a general succession of deformation constrained by the AFT and (U-Th)He data.

Neocene rapid uplift and deformation of the South Tianshan and Kuqa fold-and-thrust belt, NW China: constraints from apatite (U-Th)/He thermochronometer

Jian Chang^{1,2}, Qiu Nansheng^{1,2}

1 State Key Laboratory of Petroleum Resources and Prospecting, China University of Petroleum, Beijing 102249, China

2 Basin and Reservoir Research Centre, China University of Petroleum, Beijing 102249, China

Kuqa fold-and thrust belt (KFTB) is located between South Tianshan (a part of the Central Asia Tianshan) and Tarim Basin and its deformation is related to the reactivation of the Tianshan due to the progressive collision of India with Eurasia in the Cenozoic. The issues about the latest uplift time of the South Tianshan and the deformation initial time of the Kuqa fold-and-thrust belt are still controversial. The latest uplift time of the South Tianshan revealed by the AFT data was much older than that by the Magnetostratigraphic data, which could be caused by that AFT dating cannot record the uplift events in the lower temperature than 60 °C. Compared to AFT dating, the apatite (U-Th)/He dating can reveal the cooling histories at lower temperature which range from 40°C to 75°C¹.

In this study, we firstly present 42 apatite (U-Th)/He ages of 13 samples collected along the Kuqa River to study the latest uplift event of the South Tianshan and deformation time and process of the KFTB. The relationship between measured AHe ages and relative stratigraphic position shows that the AHe ages of samples KC1, KC2, KC5, KC8, KC11, KC13, KC14, KC17 and KC19 range from 5.9±0.4 Ma to 80.5±5.0Ma which were younger than their depositional age and could reveal the cooling events occurred in South Tianshan and KFTB (Fig. 1). For the samples KC22, KC26, KC27 and KC28, their AHe ages were older than their depositional ages which means that they did not experience He diffusion after deposition in KFTB and just reflect the provenance information (Fig. 1). The dispersion among replicates for each sample exists (Fig. 1), which results from eU (effective uranium concentration) or grain sizes. For better understanding uplift and deformation evolution of the South Tianshan and KFTB, the thermal histories of samples KC1, KC2, KC5, KC8, KC11, KC13, KC14, KC17 and KC19 have been simulated using the HeFty software implemented with radiation damage accumulation and annealing model (RDAAM) which takes eU and grain size into account²⁻³.

For the sample KC1 from the South Tianshan, its youngest grain AHe age with 18.2±0.8 Ma and its thermal modeling results indicated that the South Tianshan experienced a Miocene rapid uplift event which initiated at ~18 Ma and continued to ~6 Ma. The Samples KC2, KC5, KC8, KC13 and KC14 from the northern monocline belt in KFTB experienced total He diffusion and effectively recorded the deformation process of the KFTB (Fig. 1). The AHe ages of sample KC2 from the northern margin of the KFTB and its thermal modeling results revealed that the KFTB deformed initially at ~15 Ma, while AHe ages and thermal modeling results of other samples indicated that the centre and south of the northern monocline belt deformed initially at ~10 Ma and continued to ~4 Ma. For the Cretaceous samples KC17 and KC19 from the Kelasu-Yiqikelike thrust belt in KFTB, just two grains which AHe ages are 6.9±0.4 Ma and 8.3±0.4 Ma experienced total He diffusion and its thermal modeling results indicated that the southern of the Kelasu-Yiqikelike thrust belt deformed initially at ~6 Ma and continued to ~2 Ma. Finally, the Neocene tectonic-thermal evolution model of the KFTB were reconstructed based on the thermal modeling results, field observation and seismic interpretation and showed that the KFTB deformed gradually from north to south.

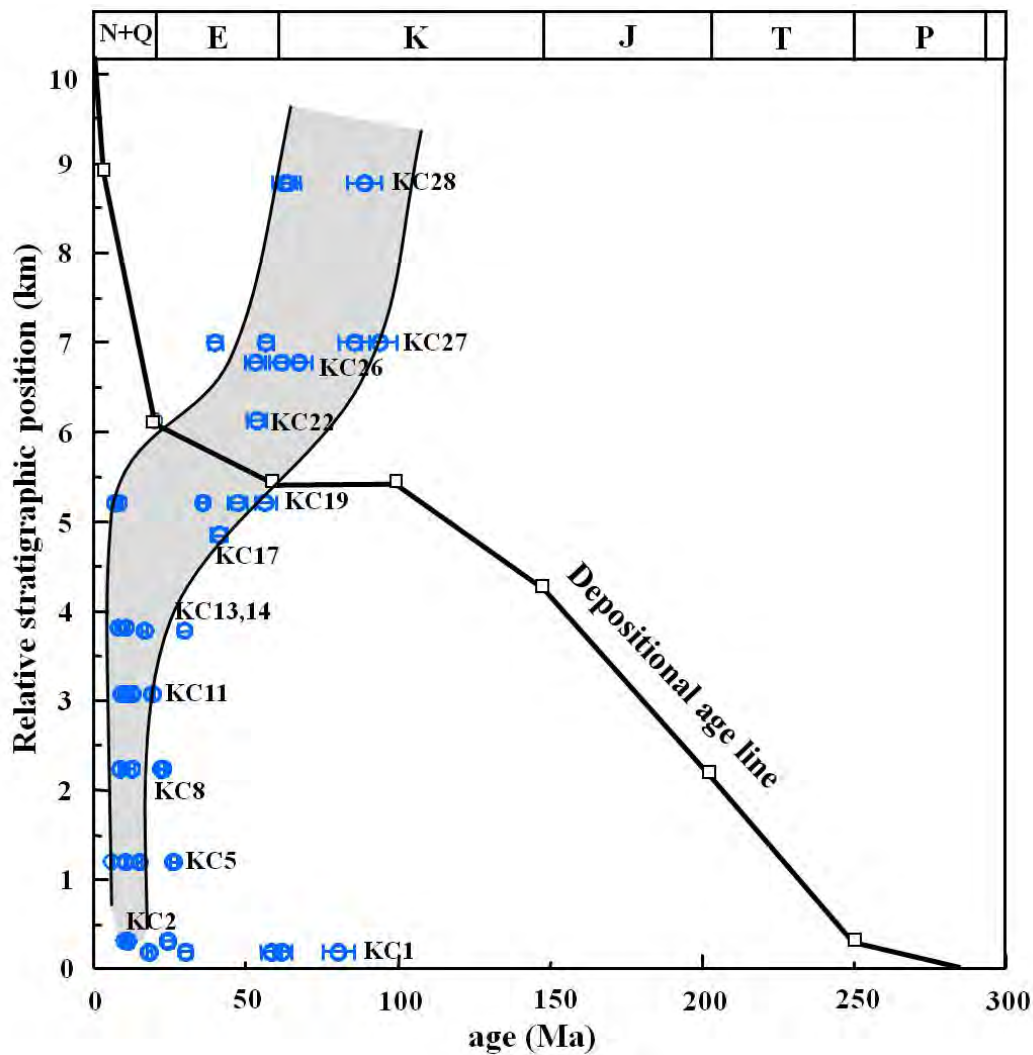


Figure 1. The measured AHe ages were plotted against the relative stratigraphic position.

References

1. Wolf, R. A., Farley, K. A. & Kass, D. M. Modeling of the temperature sensitivity of the apatite (U–Th)/He thermochronometer. *Chemical Geology* **148**, 105-114 (1998).
2. Ketcham, R. A. Forward and Inverse Modeling of Low-Temperature Thermochronometry Data. *Reviews in Mineralogy and Geochemistry* **58**, 275-314 (2005).
3. Flowers, R. M., Ketcham, R. A., Shuster, D. L. & Farley, K. A. Apatite (U–Th)/He thermochronometry using a radiation damage accumulation and annealing model. *Geochimica et Cosmochimica Acta* **73**, 2347-2365 (2009).

P-T history and $^{40}\text{Ar}/^{39}\text{Ar}$ dating of the Jinshuikou group, Eastern Kunlun Mountains, Qinghai, China

C.J.C. Bontje¹, F.M. Brouwer¹, H.W. Zhou², J.R. Wijbrans¹

1 Department of Earth Sciences, VU University, Amsterdam, The Netherlands

2 Department of Structural Geology, China University of Geosciences, Wuhan, China

The Kunlun Mountains, located along the northern margin of the Tibetan Plateau in Qinghai, Western China play an important role in the collision history between Eurasia and India. However, not much research has been done on both metamorphic P-T conditions and geochronology. From recent studies it appears that the convergence of the Kunlun mountains lasted at least from Early Palaeozoic up to Cenozoic¹. Liu et al.¹ and Arnaud et al.² identified four age groups of different tectonic events in the Kunlun mountains, of which at least two could be ascribed to distinct metamorphic events of granulite and amphibolite facies of Middle Silurian - Late Devonian and Triassic age. This was followed by magmatic intrusions and partial overprinting. Also a sinistral deformation regime of Middle Jurassic – Lower Cretaceous age can be found in these metamorphic rocks as strike-slip structures in mylonites. The last age group represents late-stage exhumation of Oligocene age.

This study will focus on the Jinshuikou group in the Kunlun Mountains. This group consists mainly of gneisses, schists and amphibolites. The aim of the study is to improve the understanding of the tectonic history of the Jinshuikou group in the Kunlun Mountains. This is done by investigating the internal variations in metamorphic grade and $^{40}\text{Ar}/^{39}\text{Ar}$ dating of selected samples from the Jinshuikou group. P-T conditions and timing of metamorphism in the Jinshuikou group will lead to a better understanding of the tectonic history of the Kunlun Mountains.

To establish the geochronology and metamorphic conditions, a fieldwork was executed and gneisses, amphibolites and granites (both syn- and post metamorphic) were sampled at five locations along a transect in the Jinshuikou group. The transect was orientated along the mountain belt over a distance of approximately 430 km. Field observations provided indications that the metamorphic grade decreases towards the east. Also extensive granitic intrusions in the Jinshuikou group are present and are interpreted as the result of a subducting slab beneath the group. The presence of mylonitic structures at the top of the group indicates that ductile deformation by shear strain has taken place. The presence of migmatites at the bottom of the group implies prograde metamorphism with high temperatures.

$^{40}\text{Ar}/^{39}\text{Ar}$ dating on microcline, biotite, hornblende and muscovite was executed on the samples collected during the fieldwork. In addition, mineral compositions are determined by electron microprobe measurements on thin sections in order to model the metamorphic P-T conditions in Perple_X.

Cooling ages of microcline and biotite from the granitic samples give respectively the following age ranges: 186.29 ± 15.10 Ma to 207.60 ± 14.12 Ma and 229.82 ± 2.98 Ma to 282.91 ± 3.46 Ma. The metamorphic samples show the following cooling ages: for microcline, 210.98 ± 3.05 Ma to 228.54 ± 19.57 Ma; for biotite, 307.60 ± 1.64 Ma; for muscovite, 418.15 ± 2.45 Ma and for hornblende, 337.34 ± 6.28 Ma to 406.76 ± 14.33 Ma. From these ages it emerges that the granitic

intrusions are younger than the metamorphic rocks as was previously stated by Arnaud et al.².

References

1. Liu, Y., Genser, J., Neubauer, F., Jin, W., Ge, X., Handler, R. & Takasu, A. $^{40}\text{Ar}/^{39}\text{Ar}$ mineral ages from basement rocks in the Eastern Kunlun Mountains, NW China, and their tectonic implications: *Tectonophysics*, v. **398**, 199-224 (2005).
2. Arnaud, N., Tapponnier, P., Roger, F., Brunel, M., Scharer, U., Wen, C. & Zhiqin, X. Evidence for Mesozoic shear along the western Kunlun and Altyn-Tagh fault, northern Tibet (China). *Journal of Geophysical Research: Solid Earth* **108**, B12053 (2003).

Fission Track Thermochronology: New Evidence on Tectonic Activities in Bayinguole Area, Eastern Kunlun Mountains

Chen Xiaoning¹, Yuan Wanming¹, Mo Xuanxue¹, Zhang Aikui², Duan Hongwei¹, Hao Nana¹, Feng Yunlei¹, Cao Jianhui¹

¹ Institute of Earth Sciences, China University of Geosciences, Beijing 100083, China

² Third Institute of Qinghai Geological Mineral Prospecting, Xining 810008, China

The Eastern Kunlun Mountain is located in the northern Qinghai-Tibetan plateau, and bounded to the north by the Qaidam Basin (Fig. 1). The Bayinguole research region belongs to the western Qimantage area in the north of Kunbei fault, western part of Eastern Kunlun Mountain. Although it experienced complex geological evolution and significant mineralization¹, a few research works have been done because of the bad nature condition and inaccessibility in the plateau. This work uses apatite and zircon fission-track method to probe tectonic activity, thermal history and uplifting around Bayinguole river in Qimantage belt.

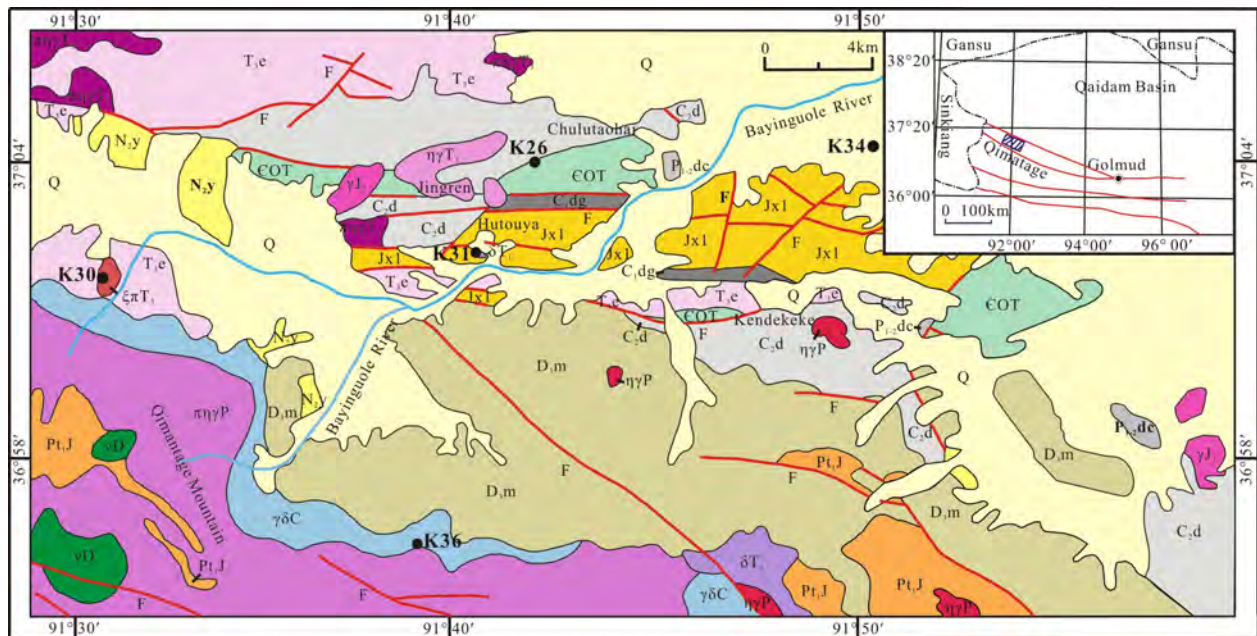


Figure 1. Geological map with the sample locations in Bayinguole area

There are some polymetallic ore deposits around Bayinguole river, such as Hutouya, Jingren and Kendekeke polymetallic ore deposits. The strike NE, NW, EW and NWW faults develop in Bayinguole area. The main strata include Pt1, ϵ O, D3, C1, C2, P1-2, T3 and Jx. It experienced multiple superimposed tectonism and magmatism. The neutral acid magmatic intrusion, mainly including diorite, granodiorite and monzonitic granite, developed in Variscan, Indo-sinian epoch and especially Triassic period.

Samples were collected from granitoid outcrops and drill-core in Bayinguole region. The fission track dating sample pieces were made according to typical experiment method. All samples were irradiated in a well-thermalized neutron flux in the 492 Swim Reactor at Beijing. Neutron fluence

was monitored using the CN2 and CN5 uranium dosimeter glasses for the zircon and apatite samples respectively. Then ages are calculated using the Zeta calibration method² with Zeta-value of 353 ± 18 and 85.4 ± 4 for apatite and zircon samples respectively.

This paper achieves 3 apatite and 6 zircon fission track dating results. All of the results are more than 20 datable grains. The most samples with χ^2 values higher than 5% and we use the central age. For the samples with χ^2 values less than 5%, we use the ages decomposed by BINOMFIT program³. The final ages can be divided into different groups that reveal multiphase tectonic-magmatic activities.

The zircon fission track ages range from 201 Ma to 109 Ma that might be divided into five groups: 201 Ma, 185 Ma, 164-163 Ma, 139-124 Ma and 109 Ma. The apatite fission track ages range from 120 Ma to 67 Ma that might be composed of three groups: 120-100 Ma, 67 Ma and 54-47 Ma. These ages indicate the complex geological thermal events in this area very well. The zircon fission track ages 201 Ma, 139-109 Ma, and the apatite fission track ages 120-100 Ma and 67 Ma represent northward subductions of Qiangtang terrane, Gangdese terrane and Himalayan terrane in Middle- Later Triassic, Late Jurassic and Early Cretaceous, Late Cretaceous respectively, resulting in collision-convergences with north-side terranes⁴. What's more, the 201 Ma extrusion event led to sharply rising in Eastern Kunlun mountain, coupled with widely magmatism and thickening of earth's crust, and sinistral slip took place in Kunbei fault. The 139-109 Ma and 120-100 Ma accord with the north part of Qinghai-Tibetan plateau and the periphery of Qaidam basin experienced uplifting-cooling events in Yanshanian. The age group of 67 Ma is also a remote response of Yarlung-Zangbo ocean closure and the collision between Indian plate and Eurasian plate. The zircon ages of 185 Ma, 164-163 Ma and the apatite ages of 54-47 Ma reflect post-orogenic stretching events in Early Jurassic, Late Jurassic and Eocene respectively. There are distribution of coal measure strata in early-middle Jurassic and existence of pyrite, which indicate at that time the tectonic environment is extensional, consisting with synchronous granite rock's geochemical characteristic and relevant evidence of geophysical data. Two kinds of represented fern, i.e. Cyatheaceae and Dicksoniaceae during the Toarcian and Bathonian-Callovian periods signify two higher temperature and aridity events occurred and led to climatic anomaly.

Three stages of thermal evolution history are revealed by apatite fission track modeling using the AFTSolve in this region. First stage from 180 Ma to 140 Ma was in the bottom temperature of apatite fission track anneal zone and reflects Gangdese terrane northward subduction during late Jurassic to early Cretaceous and the closure of Bangong-Nujiang oceanic. Second stage of 140-13 Ma records slow cooling. The last stage since 13 Ma indicates rapid cooling with temperature dropped 55°C . Some experts pointed the major uplift period for Qinghai-Tibetan plateau is from 13 Ma.

The erosion ranges during the three stages are 1.0 km, 0.6 km and 1.6 km respectively and the erosion rates are 0.025 mm/a, 0.005 mm/a, 0.11 mm/a respectively. The cumulative amount of erosion is about 3.2 km. The rock uplift values for the three apatite samples are calculated according to formula $U=D+\Delta H+\Delta s$ ⁵ and are 6270 m, 6120 m, 5830 m respectively, averaging 6070 m. Surface uplift is related to the rock uplift, that is $U=\text{Surface uplift}+\text{Erosion}$ ⁶. Thus the surface uplift extent are averaging 2870 m from Cretaceous in the research region.

This study was supported by the China Geological Survey (No. 2011-03-04-06), the National Natural Science Foundation of China (Nos. 41172088 and 40872141) and the Geology & Mineral Exploration Foundation of Qinghai Province (2013-103).

References

1. Yuan, W. M., Dong, J. Q., Wang, S. C. & Carter, A. Apatite fission track evidence for Neogene uplift in the eastern Kunlun Mountains, northern Qinghai–Tibet Plateau, China. *Journal of Asian Earth Sciences* **27**, 847–856 (2006).
2. Hurford, A. J. & Green, P. F. The Zeta age calibration of fission track dating. *Chemical Geology* **41**, 285-317 (1983).
3. Brandon, M. T. Decomposition of Fission-Track Grain-Age Distributions. *American Journal of Science* **292**, 535-564 (1992).
4. Cui, J. W., Zhang, X. W. & Tang, Z. M. Tectonic divisions of the Qinghai-Tibet Plateau and structural characteristics of deformation on their boundaries. *Geology in China* **33**, 556-567 (2006) (in Chinese with English abstract).
5. England P. & Molnar P. Surface uplift, uplift of rocks, and exhumation of rocks. *Geology* **18**, 1173-1177 (1990).
6. Brown R. W. Backstacking apatite fission-track “stratigraphy”: A method for resolving the erosional and isostatic rebound components of tectonic uplift histories. *Geology* **19**, 74-77 (1991).

The latest Oligocene rapid exhumation of the Elashan range, northeastern Tibet

Haijian Lu¹, Haibing Li¹, Dongliang Liu¹

1 Geology institute, Chinese Geological Academy of Sciences, China

A vertical transect of four samples (mainly diorite) for AFT analyses, were collected from the northern part of the Elashan range, northeastern Tibet to constrain its cooling history (Fig. 1). These samples are located within the hanging wall of the SSW-vergent North Qaidam thrust fault, spanning ~600 m of topographic relief down to the foot of the mountain. Apatite grains were extracted from rock samples following standard magnetic and heavy liquid density separations. Apatite ages were determined at the State Key Laboratory of Earthquake Dynamics, the Institute of Geology, China Earthquake Administration, using the external detector method¹ and a zeta calibration factor² for Durango age ($31.4 \pm 0.5\text{Ma}$) standard. Confined fission track-lengths measurements were measured on an OLYMPUS microscope using a magnification of 1000× under oil immersion objectives for apatite.

The ages of the four samples decrease from 22.2 Ma to 18.6 Ma (Fig. 2) down the transect and this ensures that such ages can be interpreted in terms of exhumation³. The fission track lengths, on the other hand, are relatively long ($\geq 13 \mu\text{m}$) and all corresponding track length histograms show a single mode (Fig. 2). Collectively, these data suggest that these samples may have experienced rapid cooling.

To try to obtain a more precise estimate on the onset of the rapid cooling, simple inverse Monte Carlo thermal modeling⁴ was run for the four samples with determined ages (Fig. 2), based on stratigraphic record in this region, fission track age and length distribution data. The best estimate from the simple model suggests that the onset of a rapid cooling from ~120 °C may be as early as 25 Ma.

Moreover, as an important part of basin-mountain coupling system, the basal age of basin sediments can be used to constrain the timing of surface uplift of adjoining mountains. Magnetostratigraphic studies suggest early Miocene initiation of sedimentation within the basins surrounding the Elashan range. As a subsequent response to rapid range uplift, the onset of sedimentation should more or less postdate the initiation of mountain growth. Hence, the onset age of mountain uplift should predate 22-21 Ma, which represents the oldest age of basal sediments as recorded within the Wulan basin and Gonghe basin (Fig. 1). Therefore, we prefer to consider the onset time of rapid uplift in relation to the widespread thrust motion be latest Oligocene.

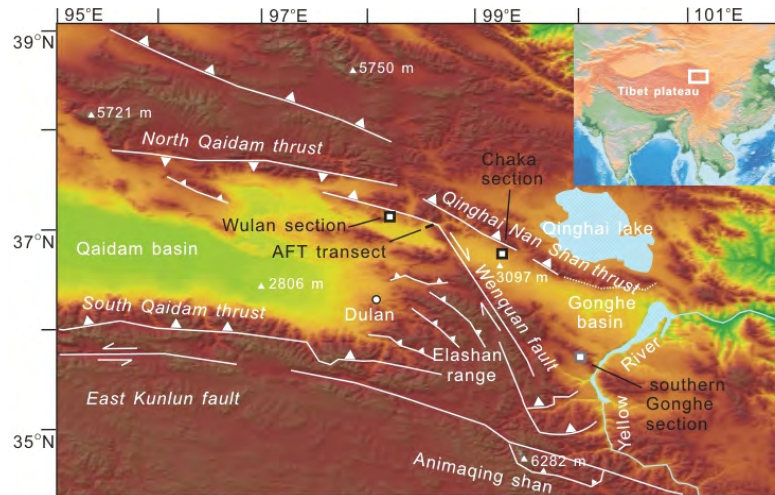


Figure 1. Regional shaded relief map of the northeast Tibet showing general structural feature and study area. The study area includes an AFT transect and two sections which are marked by two black square.

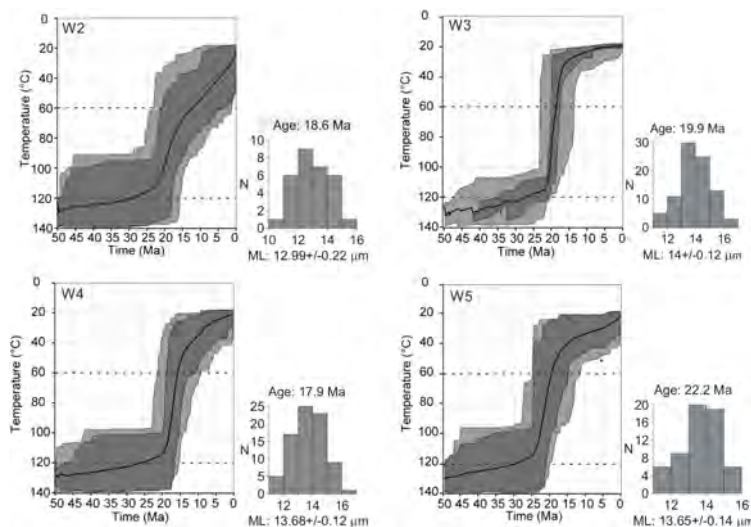


Figure 2. Track-length distributions and temperature-time paths within the PAZ modeled with HeFTy³. Envelopes of good and acceptable paths in dark grey and light grey, respectively. Dashed lines indicate the PAZ boundaries. N and ML indicate the number of confined track and mean track length, respectively.

References

1. Gleadow, A. J. W. & Duddy, I. R. A natural long-term annealing experiment for apatite. *Nuclear Tracks and Radiation Measurements* **5**, 169-174 (1981).
2. Hurford, A. J. & Green, P. F. The zeta age calibration of fission-track dating. *Isot. Geosci.* **1**, 285-317 (1983).
3. Ketchum, R. A. Forward and inverse modeling of low-temperature thermochronometry data. *Reviews in Mineralogy & Geochemistry* **58**, 275-314 (2005).
4. Malusà, M. G., Villa, I. M., Vezzoli, G. & Garzanti, E. Detrital geochronology of unroofing magmatic complexes and the slow erosion of Oligocene volcanoes in the Alps. *Earth and Planetary Science Letters* **301**, 324-336 (2011).

Recent southward migration of the Main Himalayan Thrust ramp in west Nepal?

Jonathan Harvey¹, Douglas Burbank¹, Jeremy Hourigan²

¹ University of California Santa Barbara, Santa Barbara, CA, 93106, USA

² University of California Santa Cruz, Santa Cruz, CA, 95064, USA

Slip along the Main Himalayan Thrust (MHT) accommodates ~20 mm/yr of Indo-Asian convergence across the Nepalese Himalaya. A mid-crustal ramp in the MHT is often implicated in driving uplift of the High Himalaya and supporting the steep topographic step between the lesser and higher Himalaya¹. In west Nepal, however, this topographic rise is split across two less dramatic steps. The spatial pattern of these steps is mimicked by the pattern of elevated geomorphic (Fig.1) metrics and earthquake hypocenters, suggesting that the topographic discontinuity reflects an along-strike change in tectonic forcing away from that predicted by the standard model of active tectonics in the central Himalaya. This apparent complexity has important implications for earthquake hazard in west Nepal, for the Cenozoic history of the range, and for kinematic models of orogenic growth.

Although multiple mechanisms may adequately explain the above geomorphic and seismic patterns, our preferred conceptual model holds that the MHT ramp in west Nepal has recently stepped southward to a position along strike with the ramp to the east and west². This model is supported by the presence of low-relief landscape remnants at ~2700-3500 m ASL between the two steps. It predicts a recent acceleration of rock uplift for the block between the former and current positions of the MHT ramp, and a steadier, higher uplift rate in the block to the north. In order to test this prediction, bedrock samples were collected along several relief transects in west Nepal to be analyzed via U-Th/He dating of Apatite and Zircon.

Three relief transects were collected: one north of the northern topographic step, expected to reflect cooling rates comparable to the High Himalaya in central Nepal and NW India; one in the center of the block between the topographic steps, expected to show cooling rates slower than the high Himalaya to the north; and one from near the southern topographic step, predicted to show slow- then-rapid cooling rates reflecting an increase in tectonic forcing due to southward migration of the MHT ramp in the Pliocene. The thermochronological analysis is in progress, and results are not available as of the abstract deadline. However, we fully expect a presentable dataset will be in hand in time for the conference.

References

1. Cattin, R. & Avouac, J. P. Modeling mountain building and the seismic cycle in the Himalaya of Nepal. *J. Geophys. Res.* **105**, 13389–13407 (2000).
2. Harvey, J. E. & Burbank, D. W. A tectonic and topographic discontinuity in the west Nepal Himalaya. In prep.
3. Ader, T. et al. Convergence rate across the Nepal Himalaya and interseismic coupling on the Main Himalayan Thrust: Implications for seismic hazard. *J. Geophys. Res.* **117**, B04403 (2012).

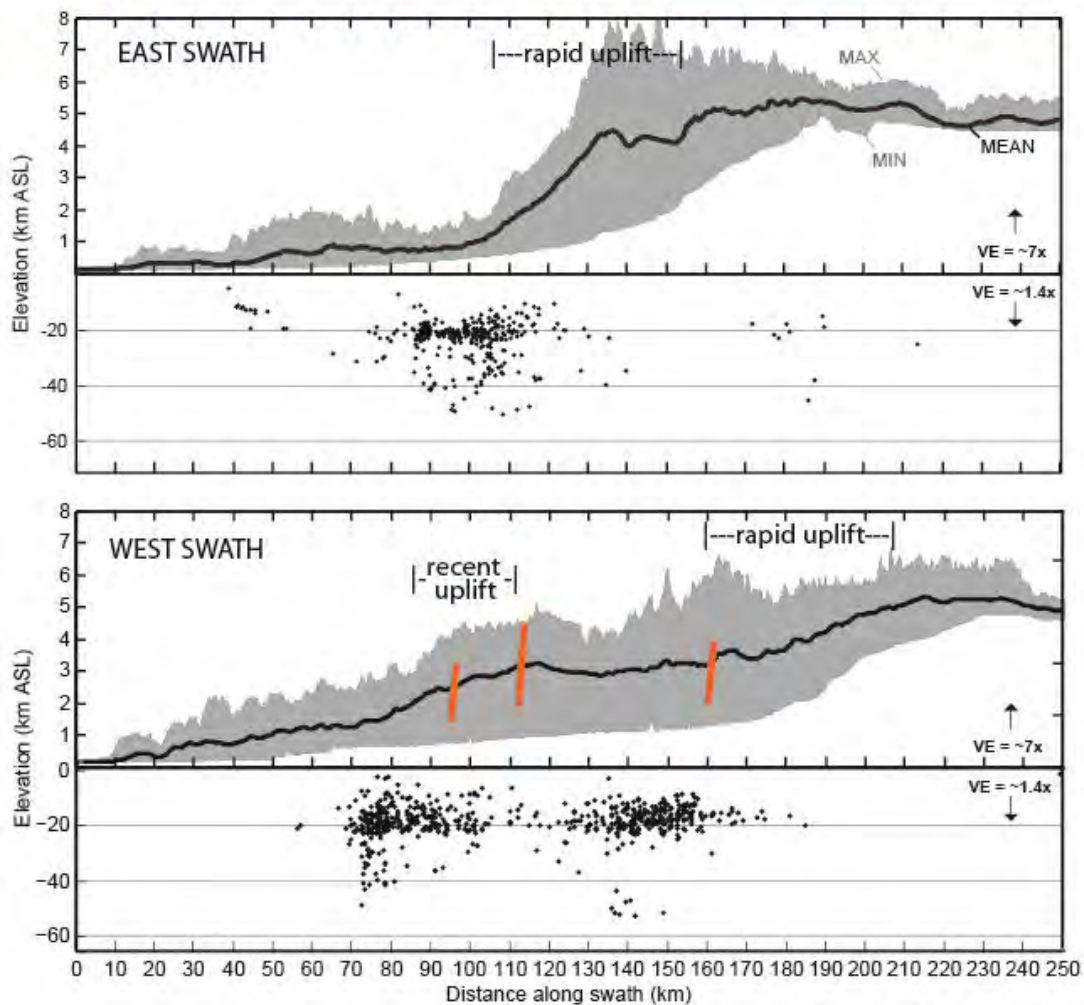
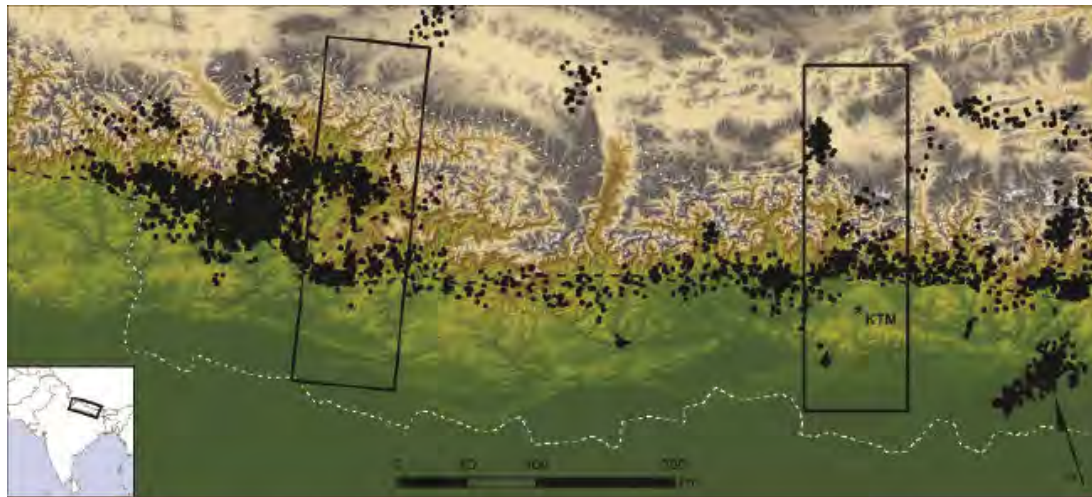


Figure 1. Shaded relief map of Nepal showing earthquake hypocenters (black dots) from 1995-2000³. Boxes show boundaries of swath profiles comparing the morphology of the Himalayan range front in central (middle) and west (bottom) Nepal. Note the two-step rise in topography in west Nepal and the parallel two-band seismicity. Relief transects were collected approximately along the orange lines.

Northward and lateral cooling history of Himalayan metamorphic nappe confirmed by fission-track thermochronometry

Harutaka Sakai¹, Hideki Iwano², Tohru Danhara², Yutaka Takigami³, Yuji Orihashi⁴, Takafumi Hirata¹, Rie Fujii¹, Santa Man Rai⁵, Bishal Nath Upreti⁵

1 Division of Earth and Planetary Science, Kyoto University, Japan

2 Kyoto Fission-Track Co., Ltd., Japan

3 Kanto Gakuen University, Japan

4 Earthquake Research Institute, the University of Tokyo, Japan

5 Department of Geology, Tri-Chandra Campus, Tribhuvan University, Nepal

For a long time, cooling rates in mountain ranges have been estimated by using the altitude difference and the age difference between the sampling sites in a rock sequence, on the assumption that the upper part of the geologic body has undergone cooling earlier along with the uplift of the mountain range. Following this assumption, Quaternary rapid uplift and erosion at nearly 10 mm /yr of the Nanga Parbat region in the northwestern Himalaya was first reported using fission-track (FT) data¹. Since then, thermochronologic investigations of the Himalaya mountain range as the world's greatest continental relief have long been conducted based mainly on rocks from the Higher Himalaya range²⁻⁵. We report here fission-track data of metamorphic nappe covering 120 km from the Higher Himalaya to the Lesser Himalayan front in eastern Nepal.

We divided the nappe in eastern Nepal into three zones and carried out thermochronologic investigation: 1) root zone in the Everest area, 2) central zone in the Taplejung area and 3) frontal zone in Tribeni area. In the root zone, new FT data using zircon and apatite along the Everest-Dudh Koshi transect from the Main Central Thrust (MCT) zone up to the Qomolangma detachment showed that the inner part of the metamorphic sequence has gradually cooled down at 240 centigrade degree (closure temperature of zircon FT) by 3.0 Ma and 100 centigrade degree (closure temperature of apatite FT) by 1.0 Ma, whereas the topmost Yellow Band under the summit of Mt. Everest rapidly cooled down at 14.5 Ma⁶. It is noteworthy that FT ages from the lower part of ~10 km in thick showed similar ages of 4.7 to 3.0 Ma for zircon and 1.5 to 0.8 Ma for apatite, respectively. A series of zircon and apatite FT age means that the inner part of the metamorphic rocks had kept high temperature around 240 centigrade degree for ~10 myr, and then cooled down below 100 centigrade degree after middle Pleistocene. Of course, the constant FT ages from different altitudes (or structural horizons) did not indicate a rapid cooling of this area because the age difference between zircon and apatite cannot be explained in that case.

In the central zone, we have investigated the origin and tectonothermal history of the Kuncha nappe and overlying Higher Himalayan Crystalline (HHC) nappe in the Taplejung window in eastern Nepal Lesser Himalaya⁷. It was confirmed that FT ages of zircon and apatite of eight samples from different tectonostratigraphic horizons concentrate within a small range from 6.2 to 4.6 Ma and 2.9 to 2.1 Ma, respectively, although the total thickness of the sequence is more than 10 km. Altitudes of these sampling horizons are from the lowest 580 m to 1440 m. There was no tendency that the FT ages become younger from site at higher altitude to lower altitude. This means that the FT ages are controlled neither by the altitude nor by the structural distance from the MCT as shown in the root zone. Of the eight samples, however, the zircon FT ages of three granite bodies seem to become younger from south to north: 6.2 Ma from Amarpur granite, 5.2 Ma from Kabeli Khola granite, and 4.8 Ma from Tamor River granite from the south to the north. Similarly, apatite FT ages become younger toward north from 2.9 Ma, 2.3 Ma, to 2.1 Ma.

Preliminary zircon FT ages for the Tribeni Quartzite overlying the Kuncha schist and mylonitic granite in Dhankuta area⁸, which is located on the nappe front at 52 km to the south-west of Taplejung indicated that their zircon FT ages were 9.9 Ma, 10.1 Ma, respectively. The zircon FT ages of gneiss on the MCT were

determined to be about 12 Ma. Furthermore, the FT age of zircon from garnetiferous gneiss from the base of the HHC at Dhankuta is dated as 11.4 Ma. These age data suggest that the frontal zone of both HHC and Kuncha nappe cooled to 240 centigrade degree by 12-10 Ma. It indicates that rocks of the nappe front cooled 7-5 myr earlier than the central part in the Taplejung area and that 9-7 myr earlier than the root zone.

Above these FT data in three different zones in eastern Nepal evidently indicate that metamorphic nappe rapidly cooled down from the surface and frontal zone, and inner part gradually cooled down from the front to the root zone. In other word, both the Kuncha nappe and overlying HHC nappe seem to have cooled laterally. A difference between FT ages of gneiss on the MCT at the nappe front and its root is about 9 myr. If we calculate the northward lateral cooling rate of the nappe by dividing the 90-km distance between both sampling sites by the age difference of 9 myr, we get approximately 10 km/myr as the cooling rate. Our northward and lateral cooling model for Himalayan nappe (Figure 1) can also explain FT data from Jumla-Surkhet region, western Nepal Himalaya⁹.

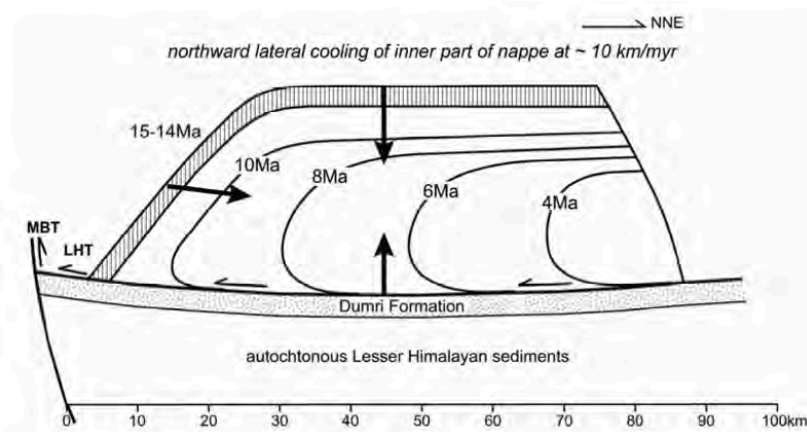


Figure 1. Conceptual cooling model of the Himalayan metamorphic nappe⁹. Isotherm lines are based on fission-track ages of zircon. Thick arrows indicate cooling directions.

References

1. Zeitler, P. K., Johnson, N. M., Naeser, C. W. & Tahirkheli, R. A. K. Fission-track evidence for Quaternary uplift of the Nanga Parbat region, Pakistan *Nature* **298**, 255-257 (1990).
2. Sorkhabi, R. B., Stump, E., Foland, K. A. & Jain, A. K. Fission-track and ⁴⁰Ar/³⁹Ar evidence for episodic denudation of the Gangotri granites in the Garhwal Higher Himalaya, India *Tectonophysics* **260**, 187-199 (1996).
3. Arita, K. & Ganzawa, Y. Thrust tectonics and uplift of the Nepal Himalaya revealed from fission-track ages *Journal of Geography (Chigaku Zasshi)* **106**, 156-167 (1997) (in Japanese with English abstract).
4. Jain, A. K., Kumar, D., Singh, S., Kumar, A. & Lal, N. Timing, quantification and tectonic modeling of Pliocene- Quaternary movements in the NW Himalaya: evidence from fission track dating *Earth and Planetary Science Letters* **179**, 437-451 (2000).
5. Blythe, A. E., Burbank, D. W., Carter, A., Schmidt, K. & Putkonen, J. Plio-Quaternary exhumation history of the central Nepalese Himalaya: 1. Apatite and zircon fission track and apatite [U-Th]/He analyses *Tectonics* **26**, doi: 10.1029/2006TC001990 (2007).
6. Sakai, H., Sawada, M., Takigami, Y., Orihashi, Y., Danhara, T., Iwano, H., Kuwahara, Y., Dong, Q., Cai, H. & Li, J. Geology of the summit limestone of Mount Qomolangma (Everest) and cooling history of the Yellow Band under the Qomolangma detachment *Island Arc* **14**, 297-310 (2005).
7. Sakai, H., Iwano, H., Danhara, T., Takigami, Y., Rai, S. M., Upreti, B. N. & Hirata, T. Rift-related origin of the Paleoproterozoic Kuncha Formation, and cooling history of the Kuncha nappe and Taplejung granites, eastern Nepal Lesser Himalaya: a multichronological approach *Island Arc* **22**, 338-360 (2013).
8. Sakai, H. Uplift of the Himalayan range and Tibetan plateau – From a viewpoint of birth of monsoon system and its changes *Journal of Geological Society of Japan* **111**, 701-716 (2005) (in Japanese with English abstract).
9. Sakai, H., Iwano, H., Danhara, T., Hirata, T. & Takigami, Y. Emplacement of hot Lesser Himalayan nappes from 15 to 10 Ma in the Jumla-Surkhet, western Nepal, and their thermal imprint on the underlying Early Miocene fluvial Dumri Formation *Island Arc* **22**, 361-381 (2013).

Late Miocene-present exhumation kinematics of the Sikkim Himalaya derived from inversion of zircon (U-Th)/He and apatite fission-track ages using 3-D thermokinematic modelling

Kyle Landry¹, Isabelle Coutand¹, David M. Whipp Jr.², Djordje Grujic¹

1 Dalhousie University, Canada

2 University of Helsinki, Finland

Erosion and exhumation of upper crustal material in the Himalayas results from a combination of tectonic and surface processes¹⁻³. Although recent studies have well defined the Miocene-Pliocene exhumation history and deformation kinematics along much of the Himalayan arc^{2,4-6}, the exhumation history of the Sikkim Himalaya is unknown despite being intriguing. The Sikkim Himalaya (Figure 1) is located in a transition zone between two regions of the Himalaya with substantial structural and geomorphological differences, the Nepal Himalaya to the west^{7,8} and the Bhutan Himalaya to the east^{3,9}. Late Miocene-present deformation of the Sikkim Himalaya is driven by slip along the Himalayan basal décollement (Main Himalayan thrust; MHT) and duplex development in the Lesser Himalaya. In addition, coupling and feedbacks between duplexing and efficient fluvial erosion have exposed meta-sedimentary rocks of the Lesser Himalayan Sequence (LHS) in a large, double tectonic window¹⁰ from beneath the structurally overlying Greater Himalayan Sequence (GHS; Figure 1). The comparative contribution of the two processes is relatively poorly understood in general and in particular in the study area.

This study adopts a multi-disciplinary approach coupling zircon (U-Th)/He (ZHe), and apatite fission-track (AFT) thermochronology with 3D thermokinematic modelling, to define the Neogene-present deformation and exhumation history of the Sikkim Himalaya. 44 rock samples were collected along two N-S-trending profiles across the windows (Figure 1). 15 samples were processed for ZHe and 34 for AFT dating. Published AFT data (Figure 1), collected in the footwall of the South Tibetan Detachment Zone¹¹ (STDZ; Figure 1), were used to augment our dataset. The ZHe cooling ages range from 11.87 ± 0.49 Ma to 1.30 ± 0.07 Ma. Approximately 20-30 km north of the Main Boundary Thrust (MBT; Figure 1), ZHe cooling ages show a marked age decrease; south of this break cooling ages range from 12 to 6 Ma, and north of the break, within the double window and beyond, ages are younger than ~ 4 Ma. This break corresponds roughly to the southern exposure of the LHS units within the windows. Analysis of AFT samples is ongoing.

The age dataset is inverted using the thermo-kinematic modelling software Pecube¹² to define the Late Miocene-present deformation and exhumation kinematics of the Sikkim Himalaya. We combine our dataset with published AFT¹¹, structural¹⁰ and geophysical data¹³ to define the model input parameters and their ranges. Rock exhumation results from rock uplift determined by the underlying fault kinematics and geometry, and surface erosion, which maintains modern steady-state topography. Late Miocene-present deformation of the Sikkim Himalaya is driven by slip along the Himalayan basal décollement (Main Himalayan thrust; MHT) and duplex development in the Lesser Himalaya. Duplexing is simulated by a zone of enhanced rock uplift focussed within the bounds of the double window. Free parameters in the inversions include: basal temperature, radiogenic heat production, convergence rate, the ratio of under-thrusting to over-thrusting, the position of ramp and flat portions of the MHT as well as the location, timing and rate of duplex driven rock uplift. Our numerical models focus on defining the exhumation kinematics (fault geometry, slip rate) over the last 12 Ma that are most consistent with the observed age data for tectonic scenarios with and without upper-crustal duplexing.

We find that duplex-driven rock uplift in the LHS is required to produce the young ages observed in the core of the double tectonic window in the Sikkim region. The tectonic scenario involving slip only on the basal décollement and no duplexing does not provide a satisfactory fit to the age data. Specifically, modelled cooling ages from samples in and around the tectonic windows tend to be too old while the

samples north of the windows (≥ 70 km north of the MBT) tend to be too young. Additional uplift as a result of simulated duplexing in the model provides a much better fit to the age data, with many of the predicted cooling ages within the uncertainty of the observed ages. Combined, these results suggest that duplexing is a dominant process in the tectonic evolution of Sikkim during the late-Miocene.

References

1. Beaumont, C., Jamieson, R. A., Nguyen, M. H. & Lee, B. Himalayan tectonics explained by extrusion of a low- viscosity crustal channel coupled to focused surface denudation. *Nature* **414**, 738-742 (2001).
2. Hodges, K. V., Wobus, C., Ruhl, K., Schildgen, T. & Whipple, K. Quaternary deformation, river steepening, and heavy precipitation at the front of the Higher Himalayan ranges. *Earth and Planetary science letters* **220**, 379- 389 (2004).
3. Grujic, D. et al. Climatic forcing of erosion, landscape, and tectonics in the Bhutan Himalayas. *Geology* **34**, 801-804 (2006).
5. Wobus, C., Heimsath, A., Whipple, K. & Hodges, K. Active out-of-sequence thrust faulting in the central Nepalese Himalaya. *Nature* **434**, 1008-1011 (2005).
6. Herman, F. et al. Exhumation, crustal deformation, and thermal structure of the Nepal Himalaya derived from the inversion of thermochronological and thermobarometric data and modeling of the topography. *Journal of Geophysical Research: Solid Earth* **115**, B6 (2010).
7. Robert, X., Van Der Beek, P., Braun, J., Perry, C. & Mugnier, J. L. Control of detachment geometry on lateral variations in exhumation rates in the Himalaya: Insights from low-temperature thermochronology and numerical modeling. *Journal of Geophysical Research: Solid Earth* **116**, B5 (2011).
8. Whipp, D. M., Ehlers, T. A., Blythe, A. E., Huntington, K. W., Hodges, K. V. & Burbank, D. W. Plio-Quaternary exhumation history of the central Nepalese Himalaya: 2. Thermokinematic and thermochronometer age prediction model. *Tectonics* **26** (2007).
9. Coutand, I. et al. Geometry and kinematics of the Main Himalayan Thrust and Neogene crustal exhumation in the Bhutanese Himalaya derived from inversion of multithermochronologic data. *Journal of Geophysical Research: Solid Earth* (2014).
10. Bhattacharyya, K. & Mitra, G. A new kinematic evolutionary model for the growth of a duplex - an example from the Rangit duplex, Sikkim Himalaya, India. *Gondwana Research* **16**, 697-715 (2009).
11. Kellett, D. A., Grujic, D., Coutand, I., Cottle, J. & Mukul, M. The South Tibetan detachment system facilitates ultra-rapid cooling of granulite-facies rocks in Sikkim Himalaya. *Tectonics* **32**, 252-270 (2013).
12. Braun, J. Pecube: a new finite-element code to solve the 3D heat transport equation including the effects of a time- varying, finite amplitude surface topography. *Computers & Geosciences* **29**, 787-794 (2003).
13. Acton, C. E., Priestley, K., Mitra, S. & Gaur, V. K. Crustal structure of the Darjeeling–Sikkim Himalaya and southern Tibet. *Geophysical Journal International* **184**, 829-852 (2011).

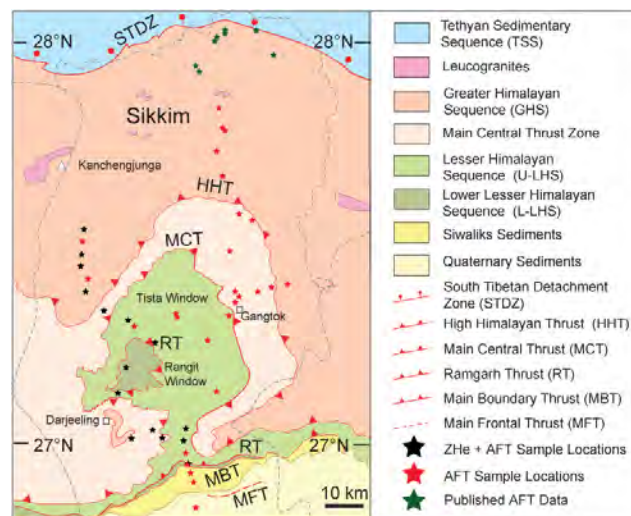


Figure 1. Geologic Map of the Sikkim Himalaya. The Tista and Rangit windows are shown in the centre of the map, bounded by the Main Central Thrust and Ramgarh Thrust respectively. Samples dated by AFT are denoted in by red stars, samples dated using both ZHe and AFT are denoted by black stars. Green stars show previously published AFT data¹¹. After Kellett et al., 2013¹¹.

Neogene exhumation history of the Bhutan Himalaya quantified using multiple detrital proxies

Isabelle Coutand¹, David M. Whipp Jr.², Bodo Bookhagen³, Matthias Bernet⁴, Eduardo Garzanti⁵ and Djordje Grujic¹

1 Department of Earth Sciences, Dalhousie University, Halifax, NS, Canada

2 Institute of Seismology, Department of Geosciences and Geography, University of Helsinki, Helsinki, Finland

3 Department of Geography, University of California, Santa Barbara, California, USA

4 Institut des Sciences de la Terre, Université Joseph Fourier, Grenoble, France

5 Department of Earth and Environmental Sciences, Università di Milano-Bicocca, Milano, Italy

Proper sampling to constrain the evolution of fault geometries and kinematics, and quantify erosion rates in active orogens using *in situ* bedrock thermochronological data is often difficult, due to logistical and infrastructural challenges in high-elevation areas. Detrital thermochronology of modern river sands is an appealing alternative that has been used successfully in many instances, but typical assumptions that underlie the interpretation of detrital data, such as uniform catchment-wide erosion rates, can introduce bias in detrital data interpretation. Numerical tools able to predict detrital cooling ages subject to differential exhumation rates across individual catchments are now available (e.g. ^{1,2}) to overcome some of these limitations. The aim of this paper is to quantitatively test whether the detrital thermochronometer record from modern river sands supports the tectonomorphic scenario extracted from *in situ* thermochronometer data along the Bhutanese range front³. In a second step, we use various topographic indices (e.g., channel steepness, relief, specific stream power) to test how topographic expression correlates with predicted exhumation patterns.

Our study focuses on the Bhutanese Himalaya, where the spatial and temporal evolution of Neogene exhumation was recently constrained by inverting a large dataset of strategically located *in situ* multi-thermochronological ages using a modified version of the 3-D thermokinematic model Pecube³. We have collected 18 sand samples from the modern channels of the main rivers draining the Bhutan Himalaya and processed them for apatite and zircon fission-track thermochronology (AFT and ZFT, respectively), cosmogenic radionuclide dating (CRN) and sandstone petrography. Measured thermochronometer age distributions are first compared to predicted age distributions generated using the preferred fault kinematics and thermal parameters from Coutand et al.³ using the approach of Whipp et al.¹. Preliminary results suggest the measured age distributions are statistically equal to $\geq 99\%$ predicted age distributions from Monte Carlo sampling of predicted basin ages for 12 of 14 basins dated thus far. Predicted age distributions from the other 2 basins show a poor fit to the measured ages; $< 2\%$ of the predicted age distributions are statistically equal to the measured ages. The source of the poor fit in these basins is currently unclear.

It is important to note that our predicted detrital ages are from a thermokinematic model that is not coupled to a surface process or landscape-evolution model; as a consequence, the model topography does not evolve through time and exhumation is exclusively controlled by a combination of modern steady-state topography and the underlying fault

kinematics/geometry (i.e., tectonic processes)³. To identify and quantify the contribution of surface processes to exhumation in each catchment, we compare the measured detrital thermochronologic ages and CRN records to a number of geomorphic indices including channel steepness, relief, and specific stream power⁴. Ultimately, this research will help to understand how transient landscape evolution in active orogens affects erosion rates measured at different temporal and spatial scales.

References

1. Whipp, D. M., Ehlers, T. A., Braun, J. & Spath, C. D. Effects of exhumation kinematics and topographic evolution on detrital thermochronometer data. *Journal of Geophysical Research* **114**, F04021 (2009).
2. Braun, J. *et al.* Quantifying rates of landscape evolution and tectonic processes by thermochronology and numerical modeling of crustal heat transport using PECUBE. *Tectonophysics* **524-525**, 1-28 (2011).
3. Coutand, I. *et al.* Geometry and kinematics of the Main Himalayan Thrust and Neogene crustal exhumation in the Bhutanese Himalaya derived from the inversion of multithermochronologic data. *Journal of Geophysical Research: Solid Earth* (2014).
4. Bookhagen, B. & Strecker, M. R. Spatiotemporal trends in erosion rates across a pronounced rainfall gradient; examples from the southern Central Andes. *Earth and Planetary Science Letters* **327-328**, 97-110 (2012).

Thermochronological investigation of Higher and Lesser Himalayan Crystallines of West Siang, NE India: constraints from apatite fission track dating and three-dimensional modelling

Dnyanada Salvi¹, George Mathew¹

¹ Indian Institute of Technology, Bombay, Mumbai, India

Dominant dip-slip faulting along the Himalayan orogen changes to strike-slip tectonics in the vicinity of the eastern syntaxial zone^{1,2}. The study area lies within this transition zone, to the southwest of the Namche Barwa antiform. Rapid exhumation and erosion in the syntaxial region²⁻⁵ to the north and a disparately slow exhuming Siang window⁵ to the east has created a unique structural setting for this area.

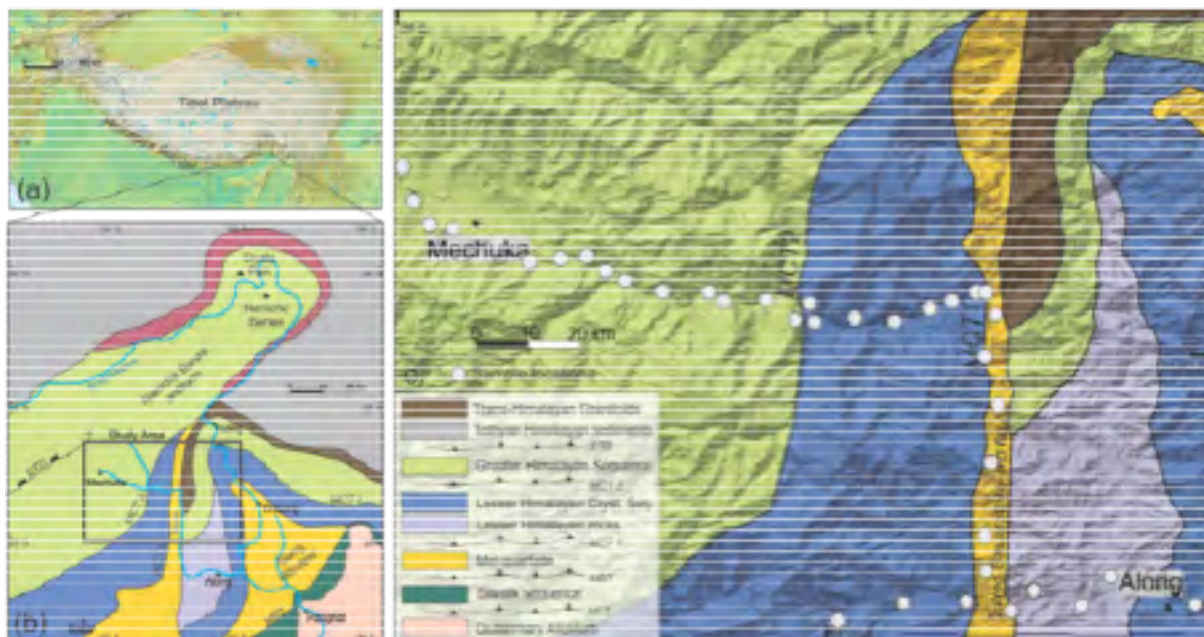


Figure 1. Location of the study area with respect to the (a) Himalayas, (b) Namche Barwa and the Siang Window; (c) is the geological map of the study area marking the sample locations.

We report new apatite fission track (AFT) ages from the Greater Himalayan Sequence and the Lesser Himalayan Crystalline Sequence from north-eastern Arunachal Himalayas. Derived ages are reasonably young (<5 Ma) and compare well with similar studies in the central and eastern Himalayas^{6,7}. Exceptionally young ages (<1 Ma) have been obtained close to fault zones of Main Central Thrust (MCT) indicating high exhumation rates presumably associated with climate induced rapid erosion⁷⁻⁹.

A modified version of the finite element code Pecube¹⁰ was used to predict the ages for various scenarios in which the fault geometries were varied^{11,12}. Both forward and inverse modeling approaches were used to constrain the geometry of the two major faults (MCT1 and MCT2) that branch out from the main crustal decollement, the Main Himalayan Thrust (MHT) whose geometries are virtually unknown. The best-fit models obtained require presence of an out- of-

sequence thrust along MCT1 and a shallow dipping MHT. Presence of a steep ramp (~18°) along MCT2 recreates the age distribution in the Higher Himalayas.

References

1. Ding, L. et al. Cenozoic structural and metamorphic evolution of the eastern Himalayan syntaxis (Namche Barwa). *Earth and Planet. Sci. Lett.* **192**, 423-438 (2001).
2. Burg, J. P. et al. Exhumation during crustal folding in the Namche-Barwa syntaxis. *Terra Nova*. 9, 53-56 (1997).
3. Burg, J. P. et al. The Namche Barwa syntaxis: evidence for exhumation related to compressional crustal folding. *J. Asian Earth Sci.* **16**, 239-252 (1998).
4. Seward, D. & Burg, J. P. Growth of the Namche Barwa Syntaxis and associated evolution of the Tsangpo Gorge: Constraints from structural and thermochemical data. *Tectonophysics*, **451**, 282-289 (2008).
5. Enkelmann, E. et al. Denudation of the Namche Barwa antiform, eastern Himalaya. *Earth and Planet. Sci. Lett.* **307**, 323-333 (2011).
6. De Sarkar, S. et al. Rapid denudation of Higher Himalaya during Late Pliocene, Evidence from OSL, Thermochronology of quartz. *Geochronometria* **40**, 304-310 (2013).
7. Adlakha, V. et al. Rapid long-term erosion in the rain shadow of the Shillong Plateau, Eastern Himalaya. *Tectonophysics* **582**, 76-83.
8. Hodges, K. V. et al. Quaternary deformation, river steepening, and heavy precipitation at the front of the Higher Himalayan ranges. *Earth Planet. Sci. Lett.* **220**, 379-389 (2004).
9. Wobus, C. W. et al. Has focused denudation sustained active thrusting at the Himalayan topographic front? *Geology* **30**, 861-864 (2003).
10. Braun, J., Pecube: A new finite element code to solve the heat transport equation in three dimensions in the Earth's crust including the effects of a time-varying, finite amplitude surface topography, *Comput. Geosci.*, **29**, 787 – 794 (2003).
11. Herman, F. et al. Exhumation, crustal deformation, and thermal structure of the Nepal Himalaya derived from the inversion of thermochronological and thermobarometric data and modeling of the topography. *J. Geophys. Res.* **115**, B06407 (2010).
12. Robert, X. et al. Control of detachment geometry on lateral variations in exhumation rates in the Himalaya: Insights from low-temperature thermochronology and numerical modeling. *J. Geophys. Res.* **116**, B05202 (2011).

Post-collisional cooling history of the Northern Tethyan Himalaya, SE Tibet

Guangwei Li¹, Yuntao Tian², Mike Sandiford¹, Barry P. Kohn¹

¹ School of Earth Sciences, University of Melbourne, Victoria 3010, Australia

² Department of Earth Sciences, University College London, London, United Kingdom

Major structures developed in south Tibet during the Miocene played an especially important role in shaping the giant Tibetan Plateau, whose formation was triggered by the Early Cenozoic India-Asia collision¹. In this work, we report a low-temperature thermochronology data set from the northern Tethyan Himalaya and Indus-Yarlung suture zone in the Zedang area, where structures are defined by two parallel thrusts (the Zhongba-Gyantse Thrust to the south and Great Counter Thrust to the north)². Seventeen samples were collected from the hanging and foot walls of the two thrusts, to constrain their cooling and exhumation histories and further elucidate the post-collisional evolution of the southern Tibetan Plateau. Thermal history modelling reveals a strong cooling episode since Middle Miocene with high peak onsets at ca.11-9 Ma and at ca. 6-5 Ma, and an Eocene-Oligocene cooling episode as well. Based on the temporal and spatial pattern, the Eocene-Oligocene fast cooling can be directly linked to the activity of Zhongba-Gyantse thrust and the eminent cooling commencing at Middle Miocene was probably caused by the exhumation of the Yardoï dome³, slip of the Great Counter Thrust⁴ and Cona extension in the study area, respectively. These results imply that regionally different exhumation histories result from different periods of transpression and extension created by the ongoing convergence of the India and Asia plates.

References

1. Yin, A. Cenozoic tectonic evolution of the Himalayan orogen as constrained by along-strike variation of structural geometry, exhumation history, and foreland sedimentation. *Earth-Science Reviews* **76**, 1-131 (2006).
2. Ding, L., Kapp, P. & Wan, X. Paleocene-Eocene record of ophiolite obduction and initial India-Asian collision, south central Tibet. *Tectonics* **24**, TC3001 (2005).
3. Zhang, J., Santosh, M., Wang, X., Guo, L., Yang, X. & Zhang, B. Tectonics of the northern Himalaya since the India-Asia collision. *Gondwana Research* **21**, 939-960 (2012).
4. Quidelleur, X., Grove, M., Lovera, O. M., Harrison, T. M., Yin, A. & Ryerson, F. J. Thermal evolution and slip history of the Renbu Zedong Thrust, southeastern Tibet. *Journal of Geophysical Research* **102**, 2659-2679 (1997).

Crustal flow along India's eastern margin, western Yunnan, China

Benita-Lisette Sonntag¹, Myo Min¹, Eva Enkelmann², Daniela Kornfeld³, Lothar Ratschbacher¹, Jörg Pfänder¹, Raymond Jonkhoeere¹, István Dunkl⁴

1 Geologie, TU Bergakademie Freiberg, Freiberg, Germany

2 Department of Geology, University of Cincinnati, Cincinnati, Ohio, USA

3 Department of Geosciences, University of Tübingen, Tübingen, Germany

4 Geoscience Center, University of Göttingen, Göttingen, Germany

The mode of Cenozoic deformation around and south of the Eastern Himalayan Syntaxis (EHS) during the Cenozoic is described among others by (I) southward lateral escape of at least two crustal blocks between the right-lateral, S-striking Gaoligong Shan shear zone (GSSZ), the NW-trending, left-lateral Chong Shan shear zone (CSSZ), and the left-lateral Ailao-Shan shear zone (ASSZ) in Yunnan, or (II) southward lateral escape of a single crustal block bounded by the right-lateral Sagaing fault zone in Myanmar and the ASSZ.

New structural and low-temperature thermochronologic data lead to a different model: the GSSZ and CSSZ form a folded, initially sub-horizontal detachment separating the brittle upper crust from the middle-lower crust represented by the Mogok igneous and metamorphic belt. The kinematics of flow along the detachment was mostly top-to-S. Folding of the detachment was mostly coeval with and locally followed top-to-S flow. In the brittle crust, ~E-W shortening is expressed by a fold-thrust belt, and in the ductile crust by L>S tectonites. The deformation pattern is preliminary interpreted as reflecting gravitationally driven flow of upper crustal material from Tibet towards SE-Asia, reminiscent to what is observed by GPS geodesy today.

New Mogok-belt granitoid U-Pb zircon data span the Early to Late Cretaceous (peaks at ~125; 115; 90; 65 Ma) and show, in contrast to the Gangdese-arc magmatism, a negative ϵ_{Hf} signature; this ties the Mogok belt in Yunnan to the northern magmatic belt of the Lhasa block in southern Tibet. New Tertiary magmatic and metamorphic U-Pb zircon data yield 40-30 Ma, similar to magmatism observed across SE-Asia and the CSSZ monazites in undeformed leucogranitic dike ages¹ that we interpret as pre-tectonic. Published and new ⁴⁰Ar/³⁹Ar data show that rapid cooling, which we relate to onset of high-strain deformation along the shear zones, started at 20-15 Ma^{2,3}. Apatite and Zircon fission-track and (U-Th)/He thermochronology indicates that this movement lasted at least until 6-3 Ma.

References

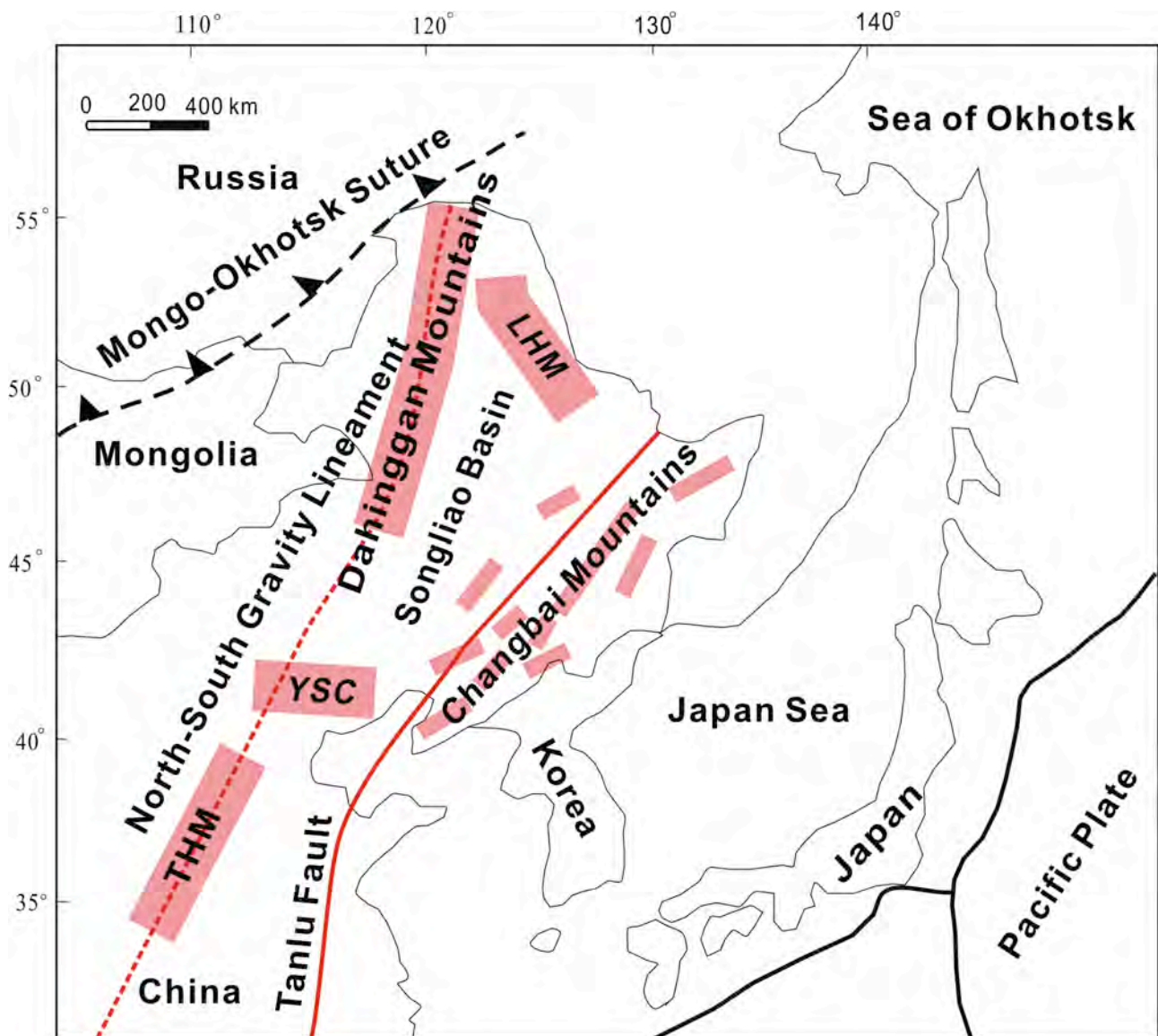
1. Akciz, B., Burchfiel, C., Crowley, J. L., Jiyun, Y. & Liangzhong, C. Geometry, kinematics, and regional significance of the Chong Shan shear zone, Eastern Himalayan Syntaxis, Yunnan, China. *Geosphere* **4**, 292-314 (2008).
2. T. H. Lin, S. L. Lo, F. J. Hsu, M. W. Yeh, T. Y. Lee, J. Q. Ji, Y. Z. Wang & D. Liu. ⁴⁰Ar/³⁹Ar dating of the Jiali and Gaoligong shear zones: Implications for crustal deformation around the Eastern Himalayan Syntaxis. *Journal of Asian Earth Science* **34**, 674-685 (2009).
3. B. Zhang, J. Zhang, D. Zhong, L. Yang, Y. Yue & S. Yan. Polystage deformation of the Gaoligong metamorphic zone: Structures, ⁴⁰Ar/³⁹Ar mica ages, and tectonic implications. *Journal of Structural Geology* **37**, 1-18 (2012).

Comparative study on the Late Mesozoic-Cenozoic exhumation of the Changbai Mountains and the Dahinggan Mountains, NE China

Xiaoming Li¹

¹ Key Laboratory of Mineralogy and Metallogeny, Guangzhou Institute of Geochemistry, Chinese Academy of Sciences, Guangzhou 510640, China

The Changbai Mountains and the Dahinggan Mountains are the most important and northeast to north-northeast-trending orogens in Northeastern (NE) China, which are roughly parallel to each other (Fig. 1). The widely exposed Jurassic and Early Cretaceous granitoids in the Changbai Mountains and the Dahinggan Mountains suggest that the overlying rocks of these granitoids have largely been unroofed or denuded. The total exhumation since the Late Mesozoic is on kilometer scale. New and mostly published thermochronological data^{1,2} are compiled to reveal the similarity and difference of the exhumation mechanism and the exhumation processes between the Changbai Mountains and the Dahinggan Mountains since the Late Mesozoic.



Note: THM is the Taihangshan Mountains; YSC is the Yanshan Chain; and LHM is the Lesser Hinggan Mountains.

Figure 1. Geotectonic sketch of Northeastern China.

Three cooling stages from the Late Mesozoic to the Cenozoic have been identified in the studied region based on fission-track results and modeling. Also, the steady-state geothermal gradient can be 35 °C/km, inferred from the average geothermal gradient of 37 °C/km in the present-day, decreasing gradually outward to ~30 °C/km, all less than the paleogeothermal gradient in the Songliao Basin³. Thus, they have probably experienced an episodic cooling, and inferred exhumation in the Dahinggan Mountains and the Changbai Mountains since the Late Mesozoic.

The exhumation processes of the Changbai Mountains can be depicted in the following three stages. The first rapid exhumation process and contemporary magmatic activities in the late Cretaceous, led by the subduction of the Farallon-Izanagi and Kula- Pacific ridges toward the NE Asian continental margin. The weak exhumation occurred during 80–15 Ma, possibly owing to the extensional process. The compression, mainly by the subduction of the Pacific Plate beneath the Eurasian Plate, led to the second rapid exhumation process during 15–0 Ma.

The three-stage exhumation in the Dahinggan Mountains can be described below. The first rapid exhumation and contemporary magmatic activity during the Late Cretaceous were caused by the intracontinental orogeny associated with asthenospheric upwelling, as a result of the subduction of the Farallon-Izanagi and Kula- Pacific ridges toward the NE Asian continental margin. Subsequent slow exhumation during the Paleogene was the postorogenic uplift and denudation process, mainly caused by the post-subduction extension. The second rapid exhumation under the compression regime during the Neogene and Quaternary was predominantly controlled by the subduction of the Pacific plate beneath the Eurasia Plate.

Obviously, the Late Mesozoic-Cenozoic exhumation of the Dahinggan Mountains is markedly distinct from that of the Changbai Mountains in the east of Songliao Basin, mainly led by the subduction of the Pacific plate beneath the Eurasian Plate, and slightly different from that of the Lesser Hinggan Mountains in the northeast of Songliao Basin⁴, resulted from the Pacific plate subduction combined with intracontinental orogeny associated with asthenospheric upwelling. This implies the varied exhumation history of different regions in NE China together with neighbouring regions^{1-3,5,6}.

This work was financially supported by the National Natural Science Foundation of China (Grant Nos. 41372227 and 41072158).

References

1. Li, X. M., Gong, G. L., Yang, X. Y. & Zeng, Q. S. Late Cretaceous-Cenozoic exhumation of the Yanji area, NE China: Constraints from fission track thermochronology. *Island Arc* **19**, 120-133 (2010).
2. Li, X. M., Yang, X. Y., Xia, B., Gong, G. L., Shan, Y. H., Zeng, Q. S., Li, W. & Sun, W.D. Exhumation of the Dahinggan Mountains, NE China from the Late Mesozoic to the Cenozoic: New evidence from fission-track thermochronology. *Journal of Asian Earth Sciences* **42**, 123-133 (2011).
3. Ren, Z. L. Study on tectono-thermal histories of sedimentary basins in the north China (Petroleum Industry Press, Beijing, 1999) (in Chinese).
4. Li, X. M. & Gong, G. L. Late Mesozoic-Cenozoic exhumation history of the Lesser Hinggan Mountains, NE China, revealed by fission track thermochronology. *Geological Journal* **46**, 277-287 (2011).
5. Xiang, C. F., Feng, Z. Q., Pang, X. Q., Wu, H. Y. & Li, J. H. Late stage thermal history of the Songliao Basin and its tectonic implications: Evidence from apatite fission track (AFT) analyses. *Science in China Series D* **50**, 1479-1487 (2007).
6. Choi, T. & Il Lee, Y. Thermal histories of Cretaceous basins in Korea: Implications for response of the East Asian continental margin to subduction of the Paleo-Pacific Plate. *Island Arc* **20**, 371-385 (2011).

Late stage evolution of the Yanshanian Orogeny in Southeast China : Insights using detailed Thermochronological Studies from Hong Kong

D.L.K. Tang^{1,4}, D. Seward¹, C.J.N. Wilson¹, B.T. Paul³, A. Carter², R.J. Sewell⁴

1 SGEES, Victoria University, PO Box 600, Wellington, New Zealand

*2 University College London and Birkbeck College, Gower Street, London WC1E 6BT,
UK*

*3 Department of Earth Sciences, University of Melbourne, McCoy Building, Parkville,
Victoria, Australia 3010*

4 Hong Kong Geological Survey, CEDD, 101 Princess Margaret Road, Hong Kong

During the late Mesozoic, widespread arc magmatism occurred along the margin of southeast China, now represented by the 1,300-km long and 400-km wide Southeast China Magmatic Belt (SCMB). A transition from active continental margin to a passive tectonic setting took place through multiple phases of crustal extension after the late Mesozoic¹. The timing of the shutdown of magmatism and the post-magmatic evolution have never been well constrained. Hong Kong, located on the coastal margin of southeast China, represents a microcosm of the southern SCMB. The geology of Hong Kong is dominated by late-Mesozoic subduction-related silicic volcanic and sub-volcanic plutonic rocks, exposed today as a result of crustal uplift and erosion². These suites are unconformably overlain by continental sedimentary sequences of (?)Late Cretaceous age. Minor outcrops of Eocene sediments also occur. To investigate the post-volcanic events, we have employed low-temperature thermochronology on the Middle Jurassic to Early Cretaceous volcanic and plutonic suites of Hong Kong as well as the sedimentary sequences.

The combined results from the Mesozoic igneous suites and the sediments show that both the zircon and apatite fission-track (ZFT and AFT) systems have been reset. All Mesozoic rock bodies, igneous or sedimentary, have ZFT ages younger than their igneous/depositional ages, all overlapping statistically between 75 and 89 Ma at 2s level. They all pass the χ^2 test suggesting total removal of the initial signatures and indicating that the sequences have experienced post-emplacement/post-depositional heating to temperatures of possibly up to 250 °C. Inverse modelling of FT data³ from the igneous suites all yield comparable temperature-time paths, suggesting that they shared a similar thermal history and behaved as a package. We interpret the thermal effect to be a joint result of heating due to burial and an elevated geothermal gradient driven by intrusion-related hydrothermal activity associated with the ongoing Yanshanian magmatism in the region. This conclusion is supported by abundant petrological evidence for hydrothermal activity and some Ar-Ar age data in the same range for igneous rocks in Hong Kong and elsewhere in the SCMB.

Double dating of the ZFT detrital grains in the overlying sedimentary sequences was undertaken using the LA-ICP-MS techniques to determine potential source/provenance areas and to constrain maximum depositional ages. The oldest stratigraphic unit contains the youngest detrital zircon component of ~120 Ma. There is no equivalent-aged rock exposed today in Hong Kong and we conclude that this unit has been eroded away, either from the local Hong Kong region or nearby mainland China. The unit was exposed at the time the sediments were being deposited and hence the sediments are younger than 120 Ma. Apart from the ~120 Ma population, the unit contains other age populations at ~142 Ma and ~162 Ma, which coincide identically with the major

magmatic episodes identified and exposed today in Hong Kong⁴⁻⁶. The younger Cretaceous sediments contain no detrital zircons younger than ~143 Ma, reflecting slightly different detrital age components. In contrast, the Eocene unit, containing mixed rounded and euhedral detrital zircon grains yielded ZFT grain ages between 70 and 110 Ma, i.e. older than its stratigraphic age and in the same range as the reset ZFT ages of the Mesozoic rocks. This result implies that the ZFT system had not been reset in the Eocene sediments, which were partially sourced from the exhuming Mesozoic sequences. The detrital U-Pb age populations of ~152 Ma and 164 Ma plus some Palaeozoic to Palaeoproterozoic grains imply a more extensive provenance possibly including reworked detrital grains from Palaeozoic formations which outcrop presently in Hong Kong and neighbouring mainland China.

Our results suggest that late-Mesozoic Yanshanian magmatism probably lasted longer than previously estimated - until at least 120-85 Ma in this part of southeast China. The cessation of magmatism probably induced the onset of continental arc collapse that caused the large-scale crustal extension in the region. The focus of this crustal extension is inferred to have shifted elsewhere in the region during the early Eocene, prior to the opening of South China Sea. By then, a passive continental margin had developed.

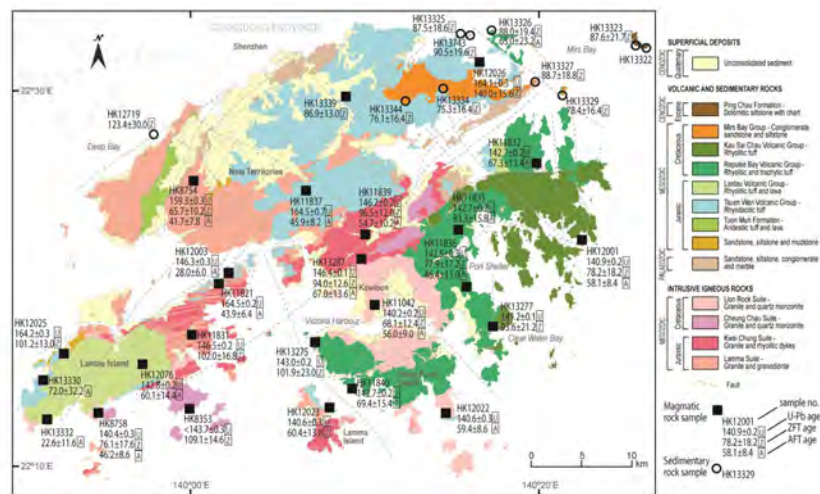


Figure 1. Geological map of Hong Kong, sample locations and fission-track ages.

References

1. Chan, L. S., Shen, W. & Pubellier, M. Polyphase rifting of greater Pearl River Delta region (South China): evidence for possible rapid changes in regional stress configuration. *J. Struct. Geol.* 32, 746-754 (2010).
2. Sewell, R. J., Tang, D. L. K. & Campbell, S. D. G. Volcanic-plutonic connections in a tilted nested caldera complex in Hong Kong. *Geochem. Geophys. Geosy.* 13, Q01006 (2012).
3. Ketchum, R. A. Forward and inverse modeling of low-temperature thermochronometry data. *Rev. Mineral. Geochem.* 58, 275-314 (2005).
4. Davis, D.W., Sewell, R. J. & Campbell, S. D. G. U-Pb dating of Mesozoic igneous rocks from Hong Kong. *J. Geol. Soc. London* 154, 1067-1076 (1997).
5. Campbell, S. D. G., Sewell, R. J., Davis, D. W. & So, A. C. T. New U-Pb age and geochemical constraints on the stratigraphy and distribution of the Lantau Volcanic Group, Hong Kong. *J. Asian Earth Sci.* 31, 139-152 (2007).
6. Sewell, R. J., Davis, D.W. & Campbell, S. D. G. High precision U-Pb zircon ages for Mesozoic igneous rocks from Hong Kong. *J. Asian Earth Sci.* 43, 164-175 (2012).

Compilation of thermochronological data from central Japan Arc and its neotectonic implications

Shigeru Sueoka¹, Takahiro Tagami²

1 Japan Atomic Energy Agency, Tsuruga 919-1279, Japan

2 Kyoto University, Kyoto 606-8502, Japan

We compiled thermochronological data along the Niigata-Kobe Tectonic Zone, a high-strain rate zone located in central Japan, and its vicinity areas to illustrate its vertical deformation over geological time scale. We discuss uplift/denudation histories in the five subareas below. (1) The Pacific coast region of the NE Japan: apatite fission-track (AFT) ages were reported at 100-82.4 Ma in Mts. Kitakami and at 78.6-46.0 Ma in Mts. Abukuma for the middle-late Cretaceous granitoids¹, indicating stable tectonic settings since the late Cretaceous. (2) The Japanese Sea coast region of the NE Japan: AFT ages of 4.7 Ma and 6.1 Ma were reported in the Mts. Iide (Sueoka, unpublished data) and Mt. Gozu¹, respectively, for the late Cretaceous granitic rocks. These ages are interpreted as reflections of uplift/denudation of the mountains since the end of the Miocene or early Pliocene. (3) The northern Japanese Alps region: AFT ages of ~0 Ma, zircon fission-track (ZFT) ages of 85- 1.0 Ma, and biotite/hornblende K-Ar ages of 7.1-3.6 were obtained²⁻⁵. These young ages may reflect not only high-denudation rates caused by rapid uplifting of the range but also young formation ages of the bodies, taking the zircon U-Pb ages of 251-0.67 Ma⁵ into account. (4) The Japanese Sea coast region of the western Chubu district: For the late Cretaceous Nohi rhyolite and Jurassic tonalitic masses in the Hida Plateau, younger AFT ages of 15.6-4.5 Ma were reported near the Japanese Sea coast, while older AFT ages of 51.5-39.2 Ma were obtained in the sites inland^{1,6}. Also, AFT ages of 33.8-13.7 Ma and ZFT ages of 142.3-80.0 Ma were reported for the Jurassic Mino-Tanba accretionary complex in the Yanagase area⁷, implying differential uplift/denudation histories in this region. (5) The Japanese Sea coast region of the Kinki district: AFT age of 50.8 Ma and ZFT age of 71.6 Ma were obtained for the late Cretaceous Kojyaku granite in the Tsuruga Peninsula⁸. The old AFT age is attributable to slow denudation derived from peneplanation during the Tertiary.

References

1. Goto, A. Formation ages of elevated peneplains of the Japanese Islands — An approach from the fission-track dating. *Grants-in Aid for Scientific Research Paper* **10440144** (2001).
2. Ito, H. & Tanaka, K. Radiometric age determination on some granitic rocks in the Hida Range, central Japan — Remarkable age difference across a fault. *Journal of the Geological Society of Japan* **105**, 241-246 (1999).
3. Yamada, R. Cooling history analysis of granitic rock in the Northern Alps, central Japan. *The Earth Monthly (Gekkan Chikyu)* **21**, 803-810 (1999).
4. Yamada, R. & Harayama, S. Fission track and K-Ar dating on some granitic rocks of the Hida Mountain Range. *Geochemical Journal* **33**, 59-66 (1999).
5. Ito, H., Yamada, R., Tamura, A., Arai, S., Horie, K. & Hokada, T. Earth's youngest exposed granite and its tectonic implications: the 10–0.8 Ma Kurobegawa Granite. *Scientific Report* **3**, 1306 (2013).
6. Matsuda, T. Apatite Fission track ages and track length of the Jurassic Granitoid in the Hida Mountain Region, Southwest Japan. *Fission-Track News Letter* **13**, 57 (2000).
7. Ito, H. Evaluation of thermal and tectonic history of shallow crust by dating methods with low closure temperature — Examples of Nojima and Yanagase faults. *CRIEPI Research Reports* **N05060** (2006).
8. Sueoka, S., Yasue, K., Niwa, M., Hanamuro, T., Shimada, K., Ishimaru, T., Umeda, K., Danhara, T., Iwano, H. & Gouzu, C. Cooling history of the Koujaku granite pluton constrained from multi-system thermochronology and its geologic implications. *Abstracts of the 120th Annual meeting of the Geological Society of Japan*, R1-P-5 (2013).

Low-temperature constraints for cooling and exhumation trends in the westward propagating Late Miocene-Recent Woodlark rift system of eastern Papua New Guinea: Implications for active (UHP) exhumation

Paul G. Fitzgerald¹, Suzanne L. Baldwin¹, Mauricio A. Bermúdez^{1,2}, Scott R. Miller¹,
Laura E. Webb³, Robert Moucha¹, Timothy A. Little⁴, Diane Seward⁴

1 Department of Earth Sciences, Syracuse University, Syracuse, NY, USA

2 Departamento de Geología, Universidad Central de Venezuela, Caracas, Venezuela

3 Department of Geology, University of Vermont, Burlington, VT, USA

4 School of Geography, Environment & Earth Sciences, Victoria University of Wellington, New Zealand

The Woodlark Basin of eastern Papua New Guinea has formed due to seafloor spreading between the Australian plate and the Woodlark microplate¹. Seafloor spreading there has been propagating westward since at least ~6 Ma into heterogeneous crust of the Woodlark Rift. The Woodlark Rise defines the northern margin and the Pocklington Rise the southern conjugate margin of the Woodlark Basin. Lying west of the active seafloor spreading rift tip are the metamorphic core complexes and gneiss domes of the D'Entrecasteaux Islands (DEI). Comprised of cores of amphibolite and eclogite-facies gneisses as well as Pleistocene granitoid intrusions the islands are flanked by mylonitic shear zone carapaces that are cut by younger (still active) normal faults². The high-grade interiors of the domes are juxtaposed against an upper plate that includes ultramafic rocks and gabbro that are correlated with the Papuan ultramafic belt. The world's youngest (U)HP rock is located in the DEI and has been exhumed from depths of ~90 km since ~8 Ma³. Tomographic images of the mantle and the high geoid over the New Guinea region suggest other subducted continental material remains at mantle depths, a result of Cenozoic slab accumulation at the leading edge of the Australian plate.

Thermochronology is being applied to understand the thermal and late-stage exhumation histories in the DEI and conjugate rift margins of the Woodlark Basin, and hence help constrain mechanisms of (U)HP exhumation. We present apatite and zircon fission track (AFT and ZFT), and apatite and zircon (U-Th)/He (ZHe and AHe) data from the conjugate margins and the gneiss domes of the DEI. AFT ages generally decrease from ~8 Ma at Misima Island in the east, to between ~1.5 and 0.5 Ma in the DEI. AHe minimum ages similarly decrease to the west, from ~6 Ma at Misima Island to between 2.0 and 0.3 Ma within the DEI. Ages are youngest on Goodenough Island, the western-most and highest-standing DEI. Within the general westward-younging trend there is some local variation indicating younger more-local events follow the dominant westward propagating rift control. ZHe ages from Normanby and Fergusson Islands range from 1.7 to 1.3 Ma. ZFT ages are all from Goodenough Island and range from 1.6 to 1 Ma.

Higher temperature thermochronometers and exposure at the Earth's surface provide boundary constraints within which to interpret this data. Care is needed when interpreting data and age trends due to young ages and low [U] resulting in few fission tracks (AFT). Measured radiogenic ⁴He is often near background levels thus AHe ages may not be accurate and there is significant single grain age variation. Single grain AHe age variation is relatively large with no apparent variation with [eU], therefore the RDAMM model is not applicable. Lithology can also play a role in the relative signal size of ⁴He in apatite. For example, higher [eU] from pegmatitic apatites give reliable ages whereas lower [eU] apatites from a muscovite granite yield unreliable ages. In the absence of a correlation of single grain ages with [eU] or grain size, we use the trends of minimum single grain AHe ages. Minimum AHe age trends are the same as the westward-younging pattern revealed by data from other thermochronologic methods.

Confined track-length distributions (CTLD) were obtained for some samples using ²⁵²Cf implantation. CTLD's generally indicate rapid cooling (means \geq ~14 microns), except on Goodenough Island. There,

core zone and upper elevation samples (>800 m) have AFT ages up to ~1.5 Ma with track length distributions (means 10-13 μm) indicative of residence within a PAZ, or reheating before final cooling/exhumation at ca. 0.75 Ma. Inverse thermal models do not constrain well the timing of initial cooling into the PAZ – there we rely on higher temperature data (e.g., ZFT). Carapace zone and lower elevation, including coastal samples, on Goodenough Island tend to be younger (<1 Ma) and where available, have longer mean lengths (~13 μm). Inverse models usually indicate a simple rapid cooling history for these samples, yet some inverse models also suggest some minor partial annealing is permissible for some. For all samples on Goodenough Island the final phase of rapid cooling, with or without partial annealing is <1 Ma, typically ≤ 0.75 Ma.

Overall, the systematic westward-younging of thermochronologic ages can be correlated with westward propagation of rifting ahead of the seafloor spreading rift tip. As samples from the DEI lie on this trend, core complex and dome formation in the DEI are most likely also controlled by rifting. Thermochronologic data from Goodenough Island is being used to constrain thermokinematic models (PeCube) in order to test the relative roles of buoyancy and normal faulting associated with rifting during exhumation to form the eclogite-bearing domes⁴.

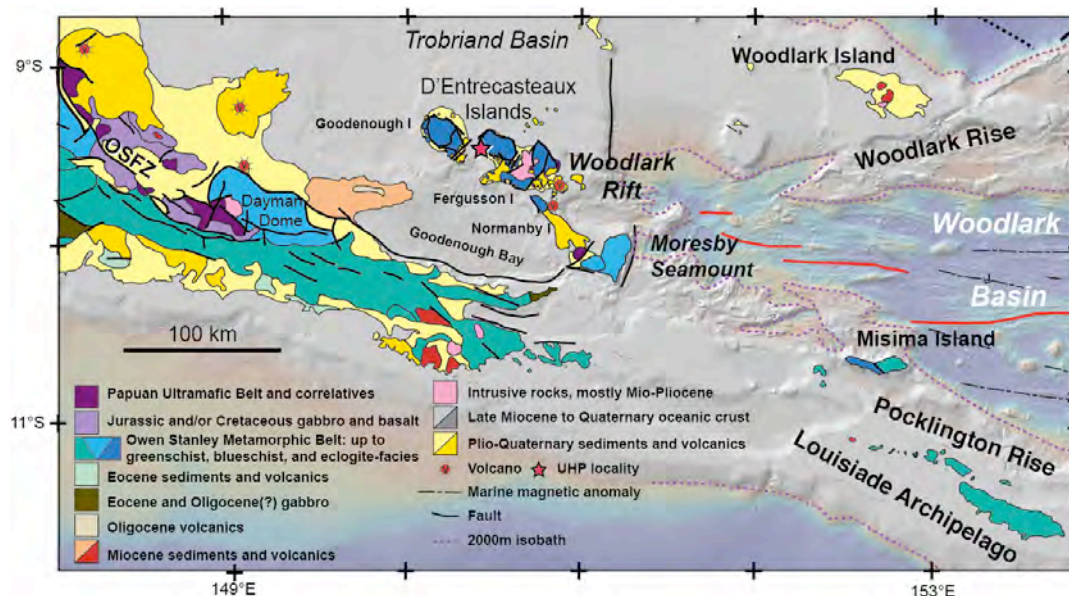


Figure 1. (A) Regional geologic map of eastern Papua New Guinea after Baldwin et al. (2012)¹.

References

1. Baldwin, S. L., Fitzgerald, P. G. & Webb, L. E. Tectonics of the New Guinea Region. *Annual Review of Earth and Planetary Sciences* **40**, 495-520 (2012).
2. Baldwin, S. L., Monteleone, B. D., Webb, L. E., Fitzgerald, P. G., Grove, M. & Hill, J. E. Pliocene eclogite exhumation at plate tectonic rates in eastern Papua New Guinea. *Nature* **431**, 263-267 (2004).
3. Little, T. A., Hacker, B. R., Gordon, S. M., Baldwin, S. L., Fitzgerald, P. G., Ellis, S. & Korchinski, M. Diapiric exhumation of Earth's youngest (UHP) eclogites in the gneiss domes of the D'Entrecasteaux Islands, Papua New Guinea. *Tectonophysics* **510**, 39-68 (2011).
4. Bermúdez, M. A., Baldwin, S. L., Fitzgerald, P. G. & Braun, J. The exhumation of gneiss domes in the D'Entrecasteaux Islands, eastern Papua New Guinea, the role of complex inherited structures, thermal overprint and fault reactivations in an extensional context: Insights from thermochronology and 3D thermo-kinematic modeling. *This conference*, (2014).

The role of inherited structures, thermal overprint and fault reactivations in rifts: Insights from thermochronology and 3D thermokinematic modeling

Mauricio A. Bermúdez¹, Suzanne L. Baldwin², Paul G. Fitzgerald², Jean Braun³
1 Escuela de Geología, Minas y Geofísica, Universidad Central de Venezuela,
Venezuela

2 Department of Earth Sciences, Syracuse University, Syracuse, New York 13244, USA

3 Institut des Sciences de la Terre, Université Joseph Fourier, CNRS, Grenoble, France

The active Woodlark rift of southeastern Papua New Guinea has been propagating westwards since at least 6 Ma into a regionally extensive subduction complex formed within the Australian-Pacific obliquely converging plate boundary zone¹. At the westernmost part of this propagating rift lie the extensional gneiss domes of the D'Entrecasteaux Islands (DEI). Domes comprise amphibolite and eclogite-facies gneisses, coesite-bearing (U)HP rocks and Pleistocene granitoid intrusions indicating that rocks have been exhumed from depths of ca. 90 km since the onset of rifting¹⁻³. Several (U)HP exhumation mechanisms have been proposed including diapiric rise of buoyant crust from mantle to crustal depths, assisted by propagating extension, with feedback between both mechanisms⁴⁻⁵. The possible interaction between different exhumation mechanisms, the role of inherited structures and successive thermal or partial thermal overprints on various minerals in different thermochronologic systems potentially make deciphering the thermal and exhumation history of these gneiss domes difficult. In order to understand the influence of such processes and the different mechanisms we use thermochronologic data from Goodenough Island, the western-most and highest standing island. Data from a number of different methods (apatite fission-track, including track lengths, apatite (UTh)/ He ages and ⁴⁰Ar/³⁹Ar ages) are used to constrain 3D thermokinematic models (PeCube⁷⁻⁸) to explore different tectonic scenarios, the number, timing and rate of exhumation pulses, as well as the starting depth for these rocks. The main conclusions of our study are: (1) Integrated high and low-temperature thermochronologic data constrain T-t paths for Goodenough Island in a continuous temperature window between 600 and 60 °C. The models suggest rapid cooling (~8 Ma initiation), deceleration (~4-2 Ma), followed by a rapid Pliocene cooling and exhumation. (2) 3D thermo-kinematic forward and inverse modeling of thermochronology data allows more rigorous constraints to be placed on the onset of extensional exhumation in the Goodenough dome at ~8 Ma. Initiation of buoyancy-assisted exhumation of (U)HP rocks and as well as extension-assisted exhumation may be synchronous. These observations favor a model of extension driven by east to west rift-propagation into a regionally-extensive subduction complex. (3) Additionally, our results demonstrate that across the entire Goodenough dome, the contrasting exhumation patterns between shear and core zones show the presence of different phenomena such as: isothermal decompression, fluid flow, shear heating and episodic local volcanism whose convergence and preservation may depend on inherited structural elements.

References

1. Baldwin, S.L., Fitzgerald, P.G., & Webb, L.E., Tectonics of the New Guinea Region. *Annual Review of Earth and Planetary Sciences* **40**, 495-520 (2012).
2. Baldwin, S.L., Monteleone, B.D., Webb, L.E., Fitzgerald, P.G., Grove, M., & June Hill, E. Pliocene eclogite exhumation at plate tectonic rates in eastern Papua New Guinea. *Nature* **431**, 263-267 (2004).

3. Baldwin, S.L., Webb, L.E., & Monteleone, B.D. Late Miocene coesite-eclogite exhumed in the Woodlark Rift. *Geology* **36**, 735-738 (2008).
4. Ellis, S.M., Little, T.A., Wallace, L.M., Hacker, B.R., & Buitter, S.J.H. Feedback between rifting and diapirism can exhume ultrahigh-pressure rocks. *Earth and Planetary Science Letters* **311**, 427-438 (2011).
5. Little, T.A., Hacker, B.R., Gordon, S.M., Baldwin, S.L., Fitzgerald, P.G., Ellis, S., & Korchinski, M. Diapiric exhumation of Earth's youngest (UHP) eclogites in the gneiss domes of the D'Entrecasteaux Islands, Papua New Guinea. *Tectonophysics* **510**, 39-68 (2011).
6. Ketchum, R.A.. Thermal models of core-complex evolution in Arizona and New Guinea: Implications for ancient cooling paths and present-day heat flow. *Tectonics* **15**, 933-951 (1996).
7. Braun, J. Pecube: a new finite element code to solve the heat transport equation in three dimensions in the Earth's crust including the effects of a time-varying, finite amplitude surface topography. *Computational Geosciences* **29**, 787-794 (2003).
8. Braun, J., van der Beek, P., Valla, P., Robert, X., Herman, F., Glotzbach, C., Pedersen, V., Perry, C., Simon-Labric, T., & Prigent, C., Quantifying rates of landscape evolution and tectonic processes by thermochronology and numerical modeling of crustal heat transport using PECUBE. *Tectonophysics* **524-525**, 1-28 (2012).

Exhumation on the hanging wall of the Hikurangi subduction margin, central North Island, New Zealand

Ruohong Jiao^{1*}, Diane Seward¹, Barry P. Kohn², Tim A. Little¹

1 School of Geography, Environment and Earth Sciences, Victoria University of Wellington, New Zealand

2 School of Earth Sciences, the University of Melbourne, Australia

[*ruohong.jiao@vuw.ac.nz](mailto:ruohong.jiao@vuw.ac.nz)

We represent new zircon fission-track (ZFT), apatite fission-track (AFT) and apatite (U-Th-Sm)/He (AHe) data of samples from the Mesozoic terranes of North Island, New Zealand. The data and interpretation contribute to resolve the timing and rates of vertical movement and exhumation associated with extensional break-up of New Zealand from Gondwana since the Late Jurassic, followed later by the initiation of subduction between the Australian and Pacific plates along the Hikurangi Margin in the Neogene. Samples were collected across the upper plate of the Hikurangi Margin in central North Island along a transect oriented normal to the subduction trench. The transect includes an uplifted forearc high in the east (the North Island Axial Ranges) and the extending back-arc region farther to the west (the Taupo Volcanic Zone, TVZ). In most of the greywacke-dominant basement, ZFT ages of 121-264 Ma are interpreted to be detrital or partially reset ages that indicate less than ~8 km of burial depth since sedimentation in the Jurassic. ZFT ages that are younger than the stratigraphic age and that indicate structurally deeper exhumation levels occur only in the western part of the central Axial Ranges, where the exposed terrane has experienced pumpellyite-actinolite facies metamorphism¹. AFT ages are between 19.8 and 122 Ma, and the AHe are between 10.3 and 95.3 Ma. All indicate thermal resetting during a history of post-depositional burial and low-grade metamorphism. Thermal history modelling² of individual and stacked samples reveals that: (1) the accretionary terrane of the Jurassic subduction margin was exhumed to the near surface (0-2 km) at ~150 Ma (Fig. 1), followed by an episode of reheating until ~100 Ma (Fig. 1), which is interpreted as the result of burial by sedimentation during extensional deformation and thinning; (2) after break-up of the eastern margin of Gondwana in the latest Early Cretaceous³, the basement of central North Island was in a passive margin setting – this thermal tectonic quiescence remained throughout the Late Cretaceous and Palaeogene (Fig. 1); (3) in the forearc of the Neogene subduction margin, rapid cooling and exhumation started between 27-20 Ma in the eastern part of central North Island, while the back-arc region to the west of present TVZ, experienced subsidence from about 30 Ma, returning to cooling/exhumation conditions in the Pliocene; (4) the rapid exhumation in the forearc ranges slowed down at the end of the Miocene (Fig. 1) when local relief decreased and the erosion-resistant basement rocks became extensively exposed.

References

1. Adams, C. J., Mortimer, N., Campbell, H. J. & Griffin, W. L. Age and isotopic characterisation of metasedimentary rocks from the Torlesse Supergroup and Waipapa Group in the central North Island, New Zealand. *N. Z. J. Geol. Geophys.* **52**, 149-170 (2009).
2. Gallagher, K. Transdimensional inverse thermal history modeling for quantitative thermochronology. *J. Geophys. Res.* **117**, B02408 (2012).
3. Laird, M. G. & Bradshaw, J. D. The Break-up of a Long-term Relationship: the Cretaceous Separation of New Zealand from Gondwana. *Gondwana Res.* **7**, 273-286 (2004).

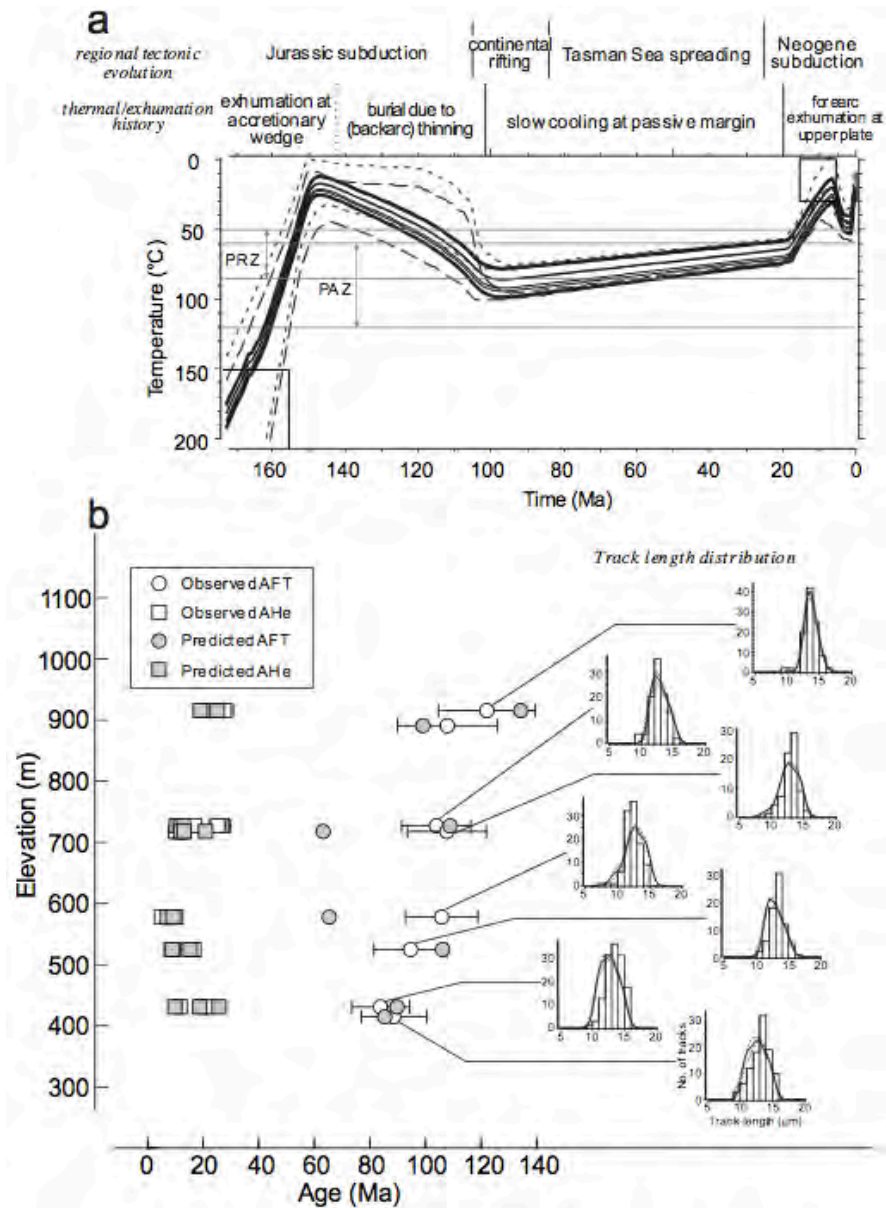


Figure 1. (a) The expected thermal history of the Ahimanawa Range, North Island, New Zealand. Models were simulated using AFT and AHe data of 8 samples on a vertical profile. Heavy lines show the uppermost and lowermost sample histories, and the dashed lines define the 95% credible intervals (top sample in short dash and bottom long). Boxes represent input constraints from low-grade metamorphic ages (175-155 Ma)¹ and the age of Neogene cover sediments (15-5 Ma). (b) The model predictions versus observations. The observed ages are shown as central ages for AFT (2σ errors) and uncorrected single-grain ages for AHe. The predicted track-length distributions (solid lines) are plotted with 95% credible intervals (dashed lines) in comparison with observed data (histograms).

Re-interpretation of the Exhumation Profile of the Southern Lakes Region, New Zealand, from Apatite and Zircon Fission-Track Ages.

Emily Warren-Smith¹, Diane Seward¹, Simon Lamb¹

¹ School of Geography, Environment and Earth Sciences, Victoria University of Wellington, New Zealand

Apatite and zircon fission-track (FT) ages have been extensively used throughout New Zealand's South Island to constrain the Cenozoic vertical kinematics of the Pacific plate¹. These studies show that displacement on the Alpine Fault largely controls rock uplift in the Southern Alps². Based on previous data¹ and later re-analysis³ a zone of young reset apatite ages consistently extends ~25 km southeast of the Alpine Fault (~10 km for zircons) in the northeast of the orogen. However, in the southwest of the orogen the width of this zone of fully reset ages increases to ~60 km for apatite and ~25 km for zircon, implying recent exhumation has been dissipated over a wider area in the southwest of the orogen (Figure 1).

Many other geological observations from the Southern Alps also show along-strike variation (e.g. a southwest increase in the width of the gravity anomaly and crustal thickness⁴). However, the significant increase in width of the high exhumation zone around the Southern Lakes, as implied by the previous thermochronology, is inconsistent with unroofing estimates from geological markers⁵ (e.g. schistosity and erosion surfaces) and requires further investigation.

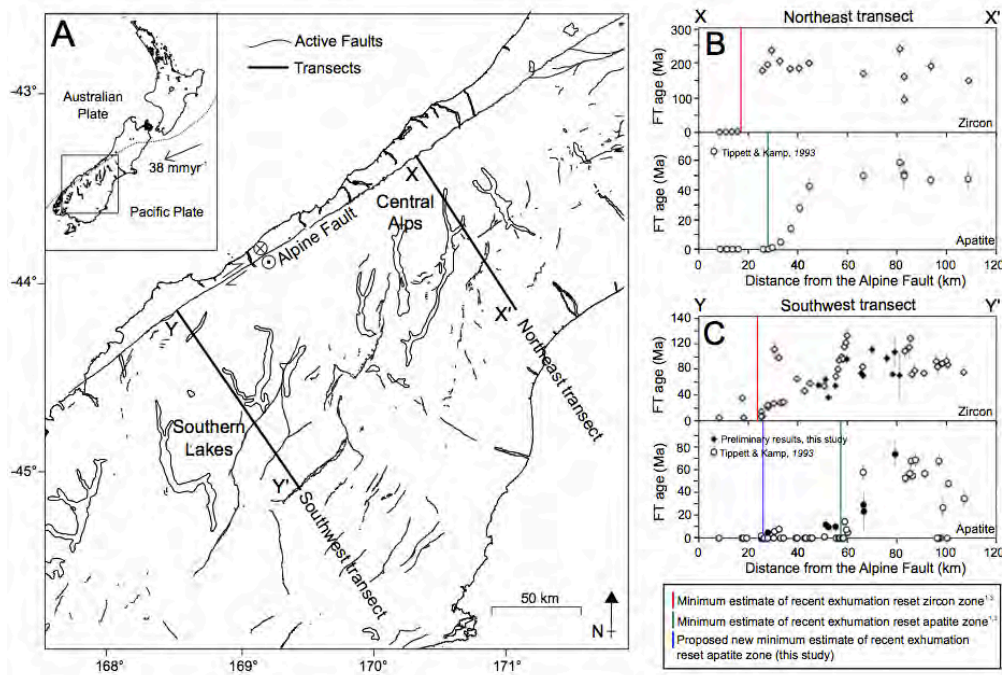


Figure 1. A) Location map of study area showing transects perpendicular to the Alpine Fault and active faults in central South Island. B) Zircon and apatite FT age transects¹ in the central Alps. C) Zircon and apatite FT age transects for the Southern Lakes showing previously published ages¹ and preliminary results from this study.

Here we present new apatite and zircon fission-track ages for samples from the Haast schist around the Southern Lakes where this apparent recent exhumation zone is widest. Sampling has been designed to improve the resolution of the apatite partial annealing zone as well as include high altitude samples (>1500 m) and re-sample sites from previous studies¹ for control purposes. We prepare samples using the external detector method⁶ and calculate central ages⁷ based on at least 20 individual grain ages per sample, usually many more.

Preliminary results support an increased width of the zone of the youngest zircon ages (<10 Ma) at ~ 25 km in the southwest of the Southern Alps. On the other hand, the extremely low ²³⁸U concentration (<1 ppm) of apatite complicates an estimation of the width of the lower temperature high exhumation zone. For many samples, this low ²³⁸U content means the external detector method is no longer appropriate for calculating accurate apatite FT ages, as it forces artificially low ages when an insufficient surface area is counted (number of grains). We believe this may be the explanation for the large number of zero Ma apatite FT ages previously produced¹ around the Southern Lakes that do not match geological observations.

We propose therefore that the width of the high exhumation zone around the Southern Lakes, based on previously calculated apatite FT ages, has been over-estimated. We infer that the width of the plateau of fully reset apatite ages in the southwest of the orogen is most likely less than 30 km, a value more consistent with geological estimates of unroofing⁵. We believe however, that the high exhumation zone in this area may be complicated by a significant overprint of glacial erosion superimposed on the background tectonic uplift pattern.

Future work will include landscape evolution modeling using Pecube⁸ to examine the effect of this possible glacial overprint. LA-ICP-MS will be used to re-calculate accurate ages for low ²³⁸U apatites to more accurately define the apatite partial annealing zone.

References

1. Tippett, J. M. & Kamp, P. J. Fission track analysis of the late Cenozoic vertical kinematics of continental Pacific crust, South Island, New Zealand. *Journal of Geophysical Research: Solid Earth* **98**, 16119-16148 (1993).
2. Tippett, J. M. & Kamp, P. J. The role of faulting in rock uplift in the Southern Alps, New Zealand. *New Zealand Journal of Geology and Geophysics* **36**, 497-504 (1995).
3. Waschbusch, P., Batt, G. & Beaumont, C. Subduction zone retreat and recent tectonics of the South Island of New Zealand. *Tectonics* **17**, 267-284 (1998).
4. Stern, T. A. Gravity anomalies and crustal loading at and adjacent to the Alpine Fault, New Zealand. *New Zealand Journal of Geology and Geophysics* **38**, 593-600 (1995).
5. Craw, D. Reinterpretation of the erosion profile across the southern portion of the Southern Alps, Mt Aspiring area, Otago, New Zealand. *New Zealand Journal of Geology and Geophysics* **38**, 501-507 (1995)
6. Tagami, T. & O'Sullivan, P. B. Fundamentals of fission-track thermochronology. *Reviews in Mineralogy and Geochemistry* **58**, 19-47 (2005).
7. Galbraith, R. F. *Statistics for fission track analysis* (CRC Press., 2005).
8. Braun, J. Pecube: A new finite-element code to solve the 3D heat transport equation including the effects of a time- varying, finite amplitude surface topography. *Computers & Geosciences* **29**, 787-794 (2003).

Session 5:

Thermochronology applied to georesources

An overview of thermochronological studies at Petrobras - research activities and upstream exploration in Brazil

Adriano Roessler Viana¹, Isabela de Oliveira Carmo¹, João Marinho de Morais Neto¹,
Gilvan Pio Hamsi Jr.¹

1 Petrobras, Rio de Janeiro, Brazil

Thermochronological studies at Petrobras S.A. comprise various applications and techniques (fission track, (U-Th)/He, $^4\text{He}/^3\text{He}$, and $^{40}\text{Ar}/^{39}\text{Ar}$) to accomplish a better understanding of source-to-sink connection. A large dataset with ca. 900 results have been obtained since the late 80's and is available to all the company's geoscientists through reports and an extensive data bank. Most of these data are apatite fission track analysis from the onshore crystalline basement cropping out along the margin, and the remaining amount, not less important, come from both offshore and onshore basins. These studies have been carried out through service contracts with commercial laboratories, partnership with other oil companies, and collaboration projects with universities (Brazilian and foreigners).

The Brazilian territory comprises Precambrian, Paleozoic, Cretaceous, and Cenozoic sedimentary basins. Its rifted margins were mostly formed during the Early Cretaceous Gondwana break-up and most of them record the rift-to-drift phases. Along the eastern coast, some of these basins are bordered by an elevated topography, as many other passive margins, has been interpreted as a rift-related feature. Nevertheless, stratigraphic, sedimentologic, and structural analysis in the offshore basins has indicated that the East Brazilian Rifted margin has remained tectonically active since continental break-up¹⁻⁹. As a proxy, regional thermochronological studies (mostly AFT and (U-Th)/He) have indicated that most of the outcropping basement rocks underwent Late Cretaceous/Early Tertiary significant cooling, long after rifting.

One of the most comprehensive thermochronological studies was carried out in the Borborema Province, northeastern Brazil⁷⁻⁹, where distinct thermochronometers were used to infer a complete thermochronological history of the different tectonic domains of this geological province, as well as to test whether the current topography is rift-related or younger⁹.

The burial history and episodes of basin inversion have also been investigated with thermochronological data. AFT thermal histories models combined with vitrinite reflectance information also have been locally applied to analyze erosion episodes interpreted from well data, sonic logs and vitrinite reflectance profiles, integrated with basin modeling.

More recently, numerical modeling of tectonic and erosional processes have been used to test different scenarios by comparing the topographic evolution, erosion rates estimates, and distinct patterns of thermal histories provided by the numerical models with the "observed" basin data (e.g., isopachs, sedimentation rates) and modeled thermal histories from thermochronological data.

References

1. Macedo, J. M., Bacoccoli, G. & Gamboa, L. A. P. in 2° Simpósio de Geologia do Sudeste, 429-437 (SBG/Núcleo São Paulo, 1991).

2. Bacocoli, G. & Aranha, L. G. F. Evolução estrutural fanerozóica do Brasil Meridional. PETROBRAS, Internal Report, Rio de Janeiro (1984).
3. Riccomini, C. O. Rift Continental do Sudeste do Brasil. Ph.D. thesis, IG/USP (1989).
4. Riccomini, C. Arcabouço estrutural e aspectos do tectonismo gerador e deformador da bacia Bauru no estado de São Paulo. *Revista Brasileira de Geociências* **27**, 153-162 (1997)
5. Fetter, M. The role of basement tectonic reactivation on the structural evolution of Campos Basin, offshore Brazil: Evidence from 3D seismic analysis and section restoration. *Marine and Petroleum Geology* **26**, 873-886 (2009).
6. Fetter, M., De Ros, L. F. & Bruhn, C. H. L. Petrographic and seismic evidence for the depositional setting of giant turbidite reservoirs and the paleogeographic evolution of Campos Basin, offshore Brazil. *Marine and Petroleum Geology* **26**, 824-853 (2009).
7. Morais Neto, J. M., Green, P. F., Karner, G. D. & Alkmim, F. F. Age of the Serra do Martins Formation, Borborema Province, northeastern Brazil: constraints from apatite and zircon fission track analysis. *Boletim de Geociências da Petrobras* **16**, 23-52 (2008).
8. Morais Neto, J. M., Hegarty, K. A., Karner, G. D. & Alkmim, F. F. Timing and mechanisms for the generation and modification of the anomalous topography of the Borborema Province, northeastern Brazil. *Marine and Petroleum Geology* **26**, 1070-1086 (2009).
9. Morais Neto, J. M. Thermochronology, landscape evolution and denudation history of the eastern Borborema Province, northeast Brazil. Ph.D. thesis, The University of Queensland (2009).

Assessing economic resource potential in the northern Canadian Cordillera: deciphering gaps in the rock record from zircon (U-Th)/He thermochronology

D. A. Schneider¹, J. Powell¹

1 Department of Earth Sciences, University of Ottawa, Canada

Rocks, whether they originate as sediments laid in basins or granites formed at depth, usually undergo a unique evolution that involves heating and then cooling until they arrive where they are found today. Of particular importance is the final part of that path, where rocks cool below 250 °C as this is the temperature range in which many ore deposits form and hydrocarbons mature into oil and gas. Due to its high radiogenic concentration and refractory nature, the zircon (U-Th)/He thermochronometer is commonly used to assess the temperature-time history of sedimentary basins. In the case of sedimentary strata that have been cooled through the mineral's closure temperature, the (U-Th)/He ages are useful in discerning the timing of deformation and exhumation. However, interpretation of these ages is complicated by the natural variation in helium diffusion between detrital grains, which creates a wide range of single crystal closure temperatures within a single rock, and consequently a large spread in cooling ages within a sample. The strong kinetic control that radiation damage in zircon has on helium diffusion suggest the intra-sample scatter in zircon cooling ages may reflect, not only cooling rate and grain size, but also multiple kinetic populations within a single sample. The siliciclastic Neoproterozoic strata of the Mackenzie Mountains, the northern-most extension of the Canadian Cordillera, are an appropriate field-based experiment to evaluate these relationships; the rocks possess a Neoproterozoic to Mesoproterozoic provenance and have experienced repeated episodes of burial and exhumation through the Phanerozoic. Adjacent to the Mackenzie Mountains, these units serve as the basement to a hydrocarbon-bearing sedimentary basin that is complicated by a regional Devonian-Cretaceous unconformity. Understanding the tectonothermal history of the Neoproterozoic strata may be the key to understanding the evolution of the basin.

For this study, samples were collected at regular intervals along a strike-perpendicular 130 km traverse through the Mackenzie Mountain fold-thrust belt. Our study stratigraphically targeted the siliciclastic units within the Neoproterozoic Mackenzie Mountains Supergroup, and the younger Neoproterozoic Windermere Supergroup. To assess grain-age relationships, single grain (U-Th)/He analysis was performed on 12 zircon grains/sample of varying size and morphology using the facilities at the Jackson School of Geoscience, University of Texas at Austin. Effective uranium concentration (eU) was used as a proxy for zircon-specific radiation damage. Although our results show as many as 300 m.y. of age scatter within individual samples, we believe that these data can be explained by the variability in grain size and radiation damage in the detrital population. In all samples, grains with the highest eU concentrations yield the youngest ages, and grains with low eU values have older ages, potentially reflecting partial retention of relict thermal histories. Thermal modeling was used to quantify these relationships and their implications for regional tectonothermal history.

A combination of forward and inverse models allows us to better understand >300 m.y. of basin growth and inversion. ZHe ages from our oldest stratigraphic samples suggest that these strata were buried below the ZHe closure temperature. Consequently, the thermal models show tightly constrained Paleocene-Eocene cooling histories, with cooling rates of 10 °C/m.y. initiating at 60 Ma. Ages from our younger Neoproterozoic strata possess a significantly wider spread, indicating that the material likely resided in a ZHe partial retention zone. Thermal models of these samples monopolize on the relationship between this scatter and grain-specific variables to quantify the Phanerozoic temperature-time history. Specifically, our models suggest that the basin continued to undergo heating following the Devonian, reaching temperatures of 140-190 °C in Permian times.

Regional cooling began in the Triassic, with renewed heating in the Cretaceous. Models from our dataset suggest that the onset of cooling and likely exhumation in the hinterlands of the Mackenzie Mountains is coincident with a Late Albian-Early Cenomanian erosional event modeled through borehole AFT data in the adjacent basin¹. In the Mackenzie Mountains foreland, maximum Mesozoic temperatures (160-180 °C) occurred in the Campanian to Maastrichtian.

Hundreds of kilometers to the west, 30 Paleozoic and Mesozoic granitoids from the Cordilleran hinterland, proximal to Klondike gold mineralization, yield robust and reliable ZHe ages that broadly mirror the thermal history recorded in our foreland dataset. This new ZHe dataset across the northern Canadian Cordillera demonstrate a strong coupling between hinterland and foreland Late Cretaceous-Paleocene tectonism. Despite missing 200 m.y. of the rock record, and >300 m.y. of age scatter in the single crystal ages, we are able to resolve a basin's burial-inversion history that is consistent across the foreland. The ages also provide temporal resolution of important economic resource potential in northern Canada, and will be used to assist exploration efforts in the Arctic frontier.

References

1. Issler, D., Grist, A. M. & Stasiuk, L. D. Post-Early Devonian thermal constraints on hydrocarbon source rock maturation in the Keele Tectonic Zone, Tulita area, NWT, Canada, from multi-kinetic apatite fission track thermochronology, vitrinite reflectance and shale compaction. *Bulletin of Canadian Petroleum Geology* **53**, 405-431 (2005).

Detecting Andean deformation in Peruvian Subandean zone (Madre de Dios) using Low-temperature thermochronology

M. Louterbach^{1,2,3,*}, S. Brichau¹, M. Roddaz¹, P. Baby¹, S. Brusset¹, J. Bailleul², W. Gil⁴, Y. Calderon⁵

1 Université Paul Sabatier, OMP/ IRD/ CNRS, GET, 14 Av. E. Belin, F-31400 Toulouse, France

2 Institut Polytechnique Lasalle Beauvais, Dept. Géosciences, 19 rue P. Waguet, 60026 Beauvais Cedex, France

3 REPSOL Exploración, Méndez Álvaro, 44. 28045, Madrid (España)

4 REPSOL Lima, Av. Victor Andrés Belaunde, 147 Vía Principal, 110 Torre Real 5, San Isidro, LIMA27, Peru

5 PERUPETRO S.A., Av. Luis Aldana 320, San Boja, Lima 41, Peru

*Corresponding Author: melanie.louterbach@repsol.com

The discovery of new hydrocarbon reservoirs is closely related to new concept development regarding sedimentary basin analyses and characterization of their petroleum systems. Becoming more often “unconventional”, oilfields are more difficult to spot due to their location in hidden traps, particularly in trust belt.

In such complex area, it is of primary importance to decipher tectonic structures and thermal history. Low-temperature thermochronology (Fission tracks and (U- Th)/He on apatite: AFT and AHe) associated with measurement of vitrinite reflectance, allow constraining thermal history through time, including hydrocarbon production periods, exhumation and structural trap related to thrust systems¹. Understanding these processes can significantly help hydrocarbon prospection.

In this study, we focused on the Madre de Dios Sub Andean zone (SAZ) in Peruvian Andes. Timing of deformation in this region of central Andes, as well as the Cenozoic paleoenvironmental and paleogeographical history of associated foreland basins in the SAZ, are still matter of intense debate. Most of the recent studies suggest that the SAZ experienced high subsidence and sedimentation rates during Oligocene-early Miocene times, prior to shortening resulting from thrust system development¹⁻³. However, in southern Peru (13-15° S) the timing of Andean shortening transfer into the SAZ still needs to be addressed.

New low-temperature thermochronometric results, associated with balanced cross sections based on interpreted seismic profiles and subsurface data reveal differences in exhumation ages from the north to the south of Madre de Dios SAZ and the adjacent Eastern Cordillera.

In the northern part of the studied area, AFT data from Devonian formation give an age of 23.3 ± 6.4 Ma⁴ while for Carboniferous terrains we obtained an age of 25.8 ± 2.5 Ma in the lower part of the formation while the upper level display an age of 90.4 ± 15.5 Ma. This variation in the same Carboniferous unit seems to indicate the transition from structural depths corresponding to full thermal resetting of the AFT system before Cenozoic exhumation to the exhumed partial annealing zone. These results also show that the thrusting related exhumation onset occurred prior to ~25-30 Ma.

In the southern part of the studied area, AFT from Eastern Cordillera display ages around 3 Ma. In the adjacent Subandean zone, three formations of Cretaceous and Paleogene ages have been sampled above the duplex and in the eastern flank of Punquiri syncline. All AFT ages are between 2.6 and 5.5 Ma. According to age uncertainties, we can estimate that the exhumation in southern Madre de Dios (in Eastern cordillera and SAZ) occurred before ~4 Ma. In both part of the SAZ, growth strata identified in 2D seismic lines and dated by biostratigraphy are associated with these two periods of erosion suggesting that the erosion recorded by thermochronometers is related to SAZ thrust motion.

References

1. Espurt, N., Barbarand, J., Roddaz, M., Brusset, S., Baby, P., Saillard, M. & Hermoza, W. A scenario for late Neogene Andean shortening transfer in the Camisea Subandean zone (Peru, 12°S): Implications for growth of the northern Andean Plateau. *GSA Bulletin* **123**, 2050-2068 (2011).
2. Hermoza, W., Brusset, S., Baby, P., Gil, W., Roddaz, M., Guerrero, N. & Bolaños, M. The Huallaga foreland basin evolution: Thrust propagation in a deltaic environment, northern Peruvian Andes. *Journal of South American Earth Sciences* **19**, 21-34 (2005).
3. Roddaz, M., Hermoza, W., Mora, A., Baby, P., Parra, M., Christophoul, F., Brusset, S. & Espurt, N. in Amazonia, Landscape and Species Evolution (eds. Hoorn, C. & Wesselingh, F. P.) 61-88 (Blackwell Publishing, 2010).
4. Ruiz G., Andriessen, P. & van Heiningen, P. From steady-state to climatically-driven denudation across the Central Andes, SE Peru. *Abstract for the 33rd International Geological Congress in Oslo* (2008).

Tectono-thermal history of Pilgrim Hot Springs, Alaska

Jeff Benowitz¹, Christian Haselwimmer¹, Jim Metcalf², Paul B. O'Sullivan³, Rebecca Flowers², Gwen Holdmann⁴ Joshua Miller¹

1 jbenowitz@alaska.edu Geophysical Institute University of Alaska Fairbanks, Alaska, USA

2 University of Colorado Boulder, Colorado, USA

3 Apatite to Zircon, Idaho, USA

4 Alaska Center for Energy and Power University of Alaska Fairbanks, Alaska, USA

Energy security and energy access in remote communities is a priority for the state of Alaska. Consistent with an emphasis on local renewable resource development to support community-based energy needs, geothermal resources are under renewed consideration as a potential energy source. One of the fundamentals of evaluating a geothermal resource is understanding both the tectonic regime and spatio-temporal evolution of the thermal anomaly. This project served as a pilot study to a) use thermochronology modeling to constrain the tectonic regime responsible for the Pilgrim Hot Springs thermal anomaly of the Seward Peninsula and b) integrate geological time scale thermal modeling with remote sensing imagery, cation geothermometry, and modern temperature drill logs to investigate the thermal anomaly's evolution.

Pilgrim Hot Springs was selected as the subject of this analysis because it is undergoing serious evaluation for development of a 2 MW geothermal power plant to serve the nearby population of Nome. This site is located ~5 km north of the Kigluiak Range Front Fault, a normal fault with geomorphological evidence of Quaternary slip. Rock and sediment samples were collected from regional surface gneiss and granitic bedrock outcrops, mica-schist, felsic and mafic dikes, and indurated muscovite-rich sediment cores that were obtained from coring of the modern expression of the thermal anomaly (i.e. the hot springs site). These samples were analyzed using multiple thermochronology methods with a range of closure temperatures from ~400 °C to ~70 °C.

Preliminary ⁴⁰Ar/³⁹Ar analysis of chlorite on a felsic dike sampled during coring of the modern expression of the thermal anomaly produced an age (~82 Ma) similar to a known regional magmatic event (~85 Ma). Apatite fission track ages from both bedrock and detrital samples (indurated sediments) from the Pilgrim Hot Springs thermal anomaly region were all approximately ~65 Ma. HeFTy thermal modeling of these samples indicate that the samples cooled very quickly to below ~20 °C. This ~65 Ma timing coincides with the timing of the final docking of the Wrangellia Terrane and the initiation of major strike-slip fault movement on the Denali Fault System. Further work is planned to better understand the tectonic significance of this ~65 Ma rock cooling event of the Seward Peninsula. Additionally, HeFTy thermal models of apatite fission track data from bedrock and sediment core samples collected in the immediate vicinity of the present day thermal springs demonstrate evidence of subsequent reheating in the last 0.1 Ma.

(U-Th)/He single grain apatite ages from both bedrock and detrital samples (indurated sediments) from the Pilgrim Hot Springs thermal anomaly region ranged from ~62 Ma to ~0.5 Ma. The youngest (U-Th)/He single grain age was produced from a sediment core sample apatite collected at the modern expression of the thermal anomaly. The He dates are therefore recording a younger thermal history than the corresponding fission track dates, but fission track length shortening to a

lesser degree also reflects this young thermal event. The data are qualitatively consistent with more recent thermal events with temperatures sufficient to primarily affect the He data. Thermal modeling of multiple data sets from the same sample will allow for exploration of possible thermal histories consistent with the data and provide insight into the behavior of these systems during short duration reheating events. Overall the combination of a full range of thermochronometers allowed for a more complete reconstruction of the Pilgrim Hot Springs region tectono-thermal history.

The maximum well log temperature measured at Pilgrim Hot springs to date (summer 2013) was 91 °C. Na-K-Ca geothermometry predict subsurface temperatures of 145 °C¹. Combined HeFTy thermal modeling indicated the Pilgrim thermal anomaly is young (< 10,000 years) and the hot springs region core has likely reached a temperature of ~150 °C in the recent past (<1,000 years). This is consistent with the range of temperatures estimated using a variety of common geothermometers.

We infer based on the overall thermochronology data set that the thermal anomaly at Pilgrim Hot Springs is related to the youthful extensional setting of the Kigluiak Range Front Fault and is not thermally equilibrated. It is quite likely that the hottest thermal fluids have not been accessed to date. We suggest that stressing the resource by artificially increasing the total discharge from the system through pumping could draw up hotter fluids which could improve the efficiency of a hypothetical power plant.

References

1. Liss, S. A., & Motyka, R. J. Pilgrim Springs KGRA, Seward Peninsula, Alaska: Assessment of fluid geochemistry. *Transactions-Geothermal Resources Council* **213-213** (1994).

Low temperature Paleogene thermal evolution of the British Mountains using U-Th(He), Northern Yukon, Canada

Julia Pickering¹, Bernard Guest¹, David Schnieder², Larry Lane³

1 University of Calgary, Department of Geoscience, Canada

2 University of Ottawa, Department of Earth Science, Canada

3 Geological Survey of Canada, Calgary, Canada

The age and rate of exhumation of the British Mountains is tied to the timing of deformation in the Beaufort Sea, an active site for hydrocarbon exploration. This region contains a large portion of North America's oil and gas reserves. The British Mountains, the eastern extent of the Brooks Range in Alaska, include Paleogene structures that are the onshore portion of the Beaufort fold belt. In the Beaufort Sea, deformation is dominated by thin-skinned folding and thrusting of Paleocene to Oligocene sediments⁴ that is sourced from the British Mountains. Onshore, Paleogene deformation overprints multiple older structural events. The low temperature time history of the onshore Paleogene structures will be determined through U-Th/He dating of apatites (AHe). The results will contribute to better understanding of the timing of the maturation and migration of hydrocarbons in the Beaufort Sea. Previous work on the thermal history of northern Yukon and the North Slope of Alaska¹⁻³ provides a regional framework for the region's low temperature-time history. These regional studies of the northern Yukon and Alaska yielded Paleocene to early Eocene apatite fission track (AFT) cooling ages that progressively young to the north, consistent with geological evidence for northward propagating deformation¹. The British Mountains consist of Neoproterozoic to early Paleozoic marine sediments that are intruded by scattered Devonian plutons; both rock types will be included in the study

This study aims to improve the understanding of the Paleogene tectonic activity of the British Mountains and the deformation history of the Beaufort fold belt. AHe will be used to better constrain the exhumation and deformation rates at low temperatures (~60-90°C closure temperatures). A sampled transect through the British mountains, along the Firth River valley (Figure 1) will provide better resolution on the rates of the deformation. The results will be used to relate the onshore time-temperature history with the development of offshore structures. This study is part of the TAFTEE project in the Arctic Canadian Cordillera.

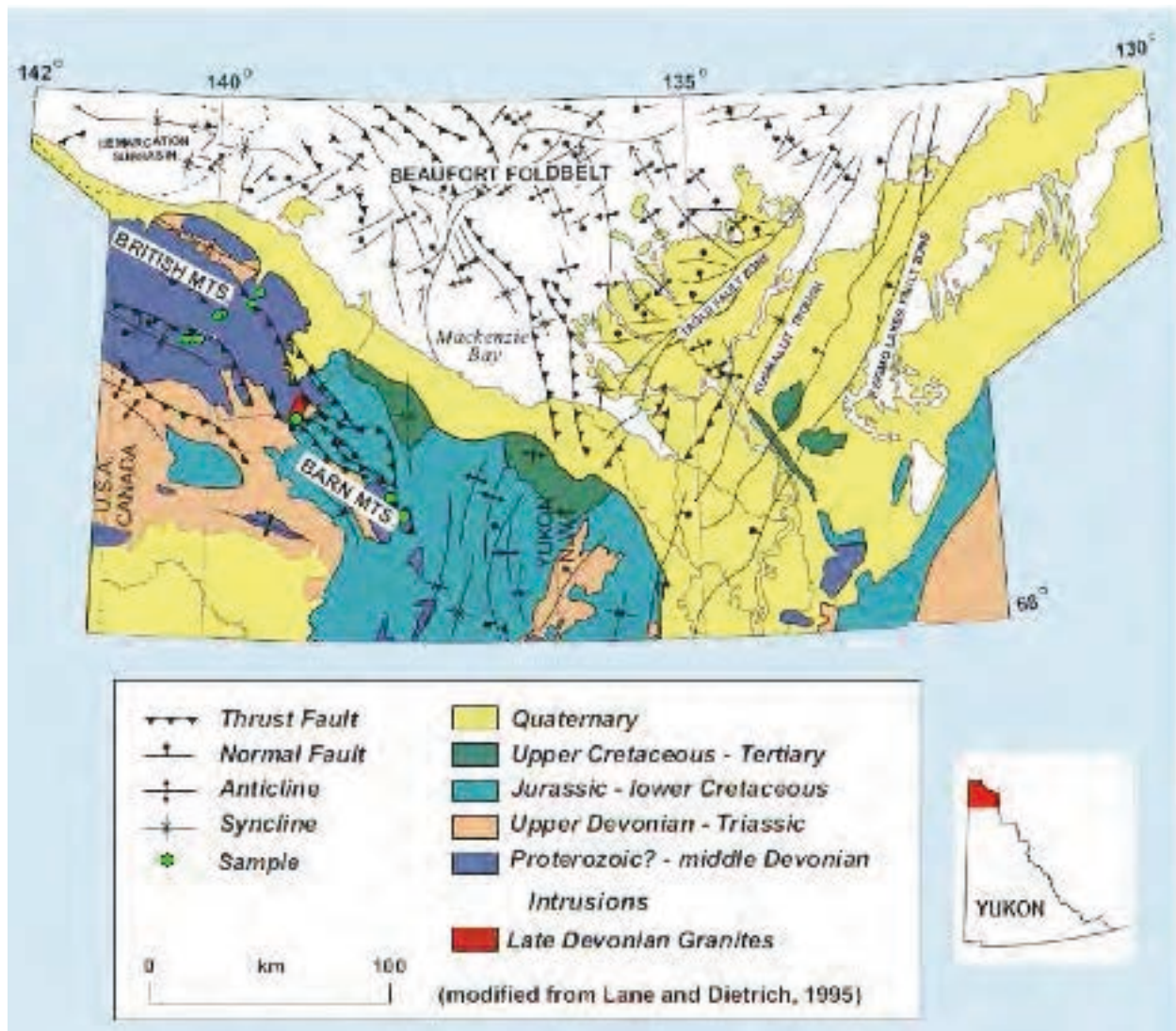


Figure 1. AHe samples (green) in the British and Barn Mountains. Base map modified from Lane and Dietrich 1995.

References

1. Lane, L. S., & Issler, D. R. Overview of the Tertiary Cooling-uplift History of Northernmost Yukon Adjacent to the Beaufort Basin, Based on Apatite Fission Track Studies. In Recovery-2011 CSPG CWLS Convention abstract (2011).
2. O'Sullivan, P. B., & Lane, L. S. Early Tertiary thermotectonic history of the northern Yukon and adjacent Northwest Territories, Arctic Canada. *Canadian Journal of Earth Sciences* **34**, 1366-1378 (1997).
3. O'Sullivan, P. B., Hanks, C. L., Wallace, W. K., & Green, P. F. Multiple episodes of Cenozoic denudation in the northeastern Brooks Range: fission-track data from the Okpilak batholith, Alaska. *Canadian Journal of Earth Sciences* **32**, 1106-1118 (1995).
4. Lane, L. S. & Dietrich, J. R. Tertiary structural evolution of the Beaufort Sea - Mackenzie Delta region, Arctic Canada. *Bulletin of Canadian Petroleum Geology* **43**, 293-314 (1995).

Low temperature thermochronology and porphyry-Cu ore deposits: a clue to understand relationships between pediment development and supergene enrichment of mineralized systems

Caroline Sanchez^{1,2}, Stéphanie Brichau², Sébastien Carretier^{2,3}, Rodrigo Riquelme¹, Vincent Regard², Mickael Bonno⁴, Patrick Monié⁴

1 Universidad Catolica del Norte, Antofagasta, Chile

2 Laboratoire GET/IRD, 14 Avenue de Belin, Toulouse, France

3 Universidad de Chile, Santiago, Chile

4 Geosciences Montpellier, Montpellier, France

In mountain belts, exhumation of bedrock results from interactions between rock uplift, erosion and climate^{1,2}. In metallogenic contexts as the Andean mountains, Cu-supergene enrichment (consequently economic viability of Cu-ore deposits) results from oxidation of porphyry- Cu deposits during surface exhumation³ and eventually deposition of an exotic deposit by lateral copper transport.

The rate and mode of landscape development processes exerts a first order control on the supergene Cu-enrichment. The conditions for efficient copper enrichment within the mineralized porphyry depend on the balance between supergene leaching of Cu and erosion of the oxidized portions of the porphyry. Understanding the role and importance of sediment distribution relative to uplift and climate variation is fundamental and only few studies have addressed this question⁴.

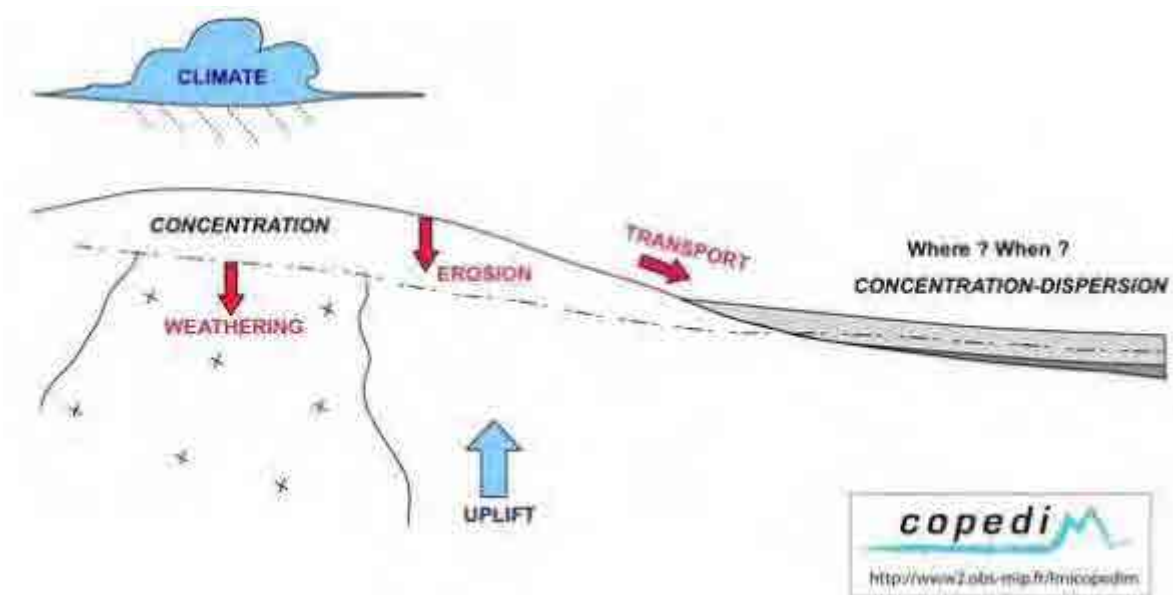


Figure 1. Schematic representation of processes and factors involved in supergene enrichment of Cu-porphyry Cu systems during pediment evolution (after ¹, COPEDIM project)

In the Atacama Desert, pediment systems (a low slope erosive structure developed on bedrock; Cooke, 1970) are evolving by erosion since at least the last 30 Ma^{5,6}. Previous field observations suggest that the most important part of the exhumation took place before Oligocene while actual

pediments seem to be the result of a slow million-year scale evolution.

This area is particularly interesting because it offers the opportunity to combine different fields of study to constrain the evolution of this system since the offset of erosion. First, denudation will be quantified using low temperature thermochronology (fission track and (U-Th)/He on apatite) applied on porphyries located along the pediment system (~20 samples, the youngest dated at about 42Ma). In a second time, erosion and burial rates related to the denudation onset will be measured using a combination of in-situ produced cosmogenic nuclides such as ^{10}Be , ^{26}Al and ^{21}Ne ⁷.

This study should shed new light on long-term evolution of the geomorphologic conditions required for supergene and exotic copper deposits.

References

1. England, P., & Molnar, P. Surface uplift, uplift of rocks, and exhumation of rocks. *Geology* **18**, 1173-1177 (1990).
2. Whipple, K. X. The influence of climate on the tectonic evolution of mountain belts. *Nature Geoscience* **2**, 97-104 (2009).
3. Sillitoe R. Supergene Oxidized and Enriched Porphyry Copper and related Deposits. *Economic Geology* **100th Anniversary Volume**, 723-768 (2005).
4. Bissig, T., & Riquelme, R. Andean uplift and climate evolution in the southern Atacama Desert deduced from geomorphology and supergene alunite-group minerals. *Earth and Planetary Science Letters* **299**, 447-457. (2010).
5. Tapia, M., Riquelme, R., Marquardt, C., Mpodozis, C. & Mora, R. Estratigrafía y sedimentología de la Cuenca El Tesoro, Distrito Centinela (región de Antofagasta) y su relación con la mineralización exótica de cobre. En XIII Congreso Geológico Chileno, Antofagasta (2012).
6. Riquelme, R., Héral G., Martinod, J., Charrier, C. & Darrozes, J. Late Cenozoic geomorphologic signal of forerarc deformation and tilting associated with the uplift and climate of the Andes, Southern Atacama Desert (26o-28oS). *Geomorphology* **86**, 283-306 (2007).
7. Gosse, J. C., & Phillips, F. M. Terrestrial in situ cosmogenic nuclides: theory and application. *Quaternary ScienceReviews* **20**,1475-1560 (2001).

Insights into evolution and ore mineralisation of the Murchison Greenstone Belt (South Africa) from $^{40}\text{Ar}/^{39}\text{Ar}$ dating

Blanka Sperner¹, Jörg A. Pfänder¹

1 Geological Institute, TU Bergakademie Freiberg, Bernhard-von-Cotta-Str. 2, 09599 Freiberg, Germany

$^{40}\text{Ar}/^{39}\text{Ar}$ dating of secondary minerals in the originally mafic to ultramafic volcano-sedimentary sequences of the Archean Murchison greenstone belt (MGB) in South Africa reveals new insights into its geological evolution and the timing of ore mineralisation. Sb-Au ores are concentrated along the Antimony line in the central part of the Murchison schists which show U-Pb zircon ages of 3.07-2.97 Ga¹. Today, they have a subvertical orientation and primary features were overprinted by a pervasive ENE-trending foliation, obtained under greenschist facies conditions during the collision of Kaapvaal craton and Pietersburg block. Syn- and post-collisional intrusions as well as subsequent alteration processes repeatedly initiated hydrothermal fluid circulations which were, amongst others, accompanied by foliation-parallel growth of mica, mainly fuchsite, a Cr-rich muscovite, and, more scarce, biotite. Hydrothermal fluids were also responsible for mobilisation, concentration, and structurally-controlled precipitation of various sulphides leading to the Sb-Au deposits along the Antimony line². Deformation along the Antimony line (contractional and/or shear movements) affected both, mica and ore mineralisation, so that dating of the mica reveals information about the timing of ore mineralisation.

We analysed fuchsite samples from ore mines, quarries, and natural outcrops along the trend of the Antimony line covering a vertical extent of c. 1000m. Additionally, several biotite separates were investigated, if possible taken from localities close to the fuchsite occurrences. Minerals were liberated using electrical fragmentation, so that original grain sizes are preserved³. For some samples, different grain sizes were analysed to test whether small grains are younger compared to potentially longer-grown large grains. Analyses were done at the Argon Lab Freiberg (ALF)⁴. All $^{40}\text{Ar}/^{39}\text{Ar}$ fuchsite ages are in the range 2000-2040 Ma; in cases where different grain sizes were analysed, no significant variations are found. Biotite samples are consistently older, ranging from 2077 to 2133 Ma. An undeformed granitic dyke revealed a biotite age of 2050 Ma. All these ages are several hundred Ma younger than the currently known U-Pb zircon ages of the granitoids intruding and neighboring the MGB (2670-3330 Ma⁵).

Several interpretations are under discussion: (a) The fuchsite ages reflect cooling instead of crystallisation. This conflicts with the biotite ages, which are older than the fuchsite ages. Due to the fact that the closure temperature of fuchsite/ muscovite is higher than the one for biotite (350°C vs. 300°C⁶), the biotite age should be younger in the case of cooling ages. (b) There are younger intrusions at depth. This interpretation is supported by the 2050 Ma biotite age of an undeformed granitic dyke. (c) The growth of fuchsite is related to other, non-intrusive processes. Deformation and alteration of igneous bodies (now altered to albitites) might have mobilised the elements necessary for mica growth in the surrounding schists. In most cases, albitites are accompanied by fuchsite-rich schists, but not for all fuchsite-rich schists the neighborhood of an altered igneous body could be proven.

Despite of these open questions, our $^{40}\text{Ar}/^{39}\text{Ar}$ fuchsite ages show that hydrothermal processes

had been active for a much longer time than previously assumed. The undeformed granitic dyke with the 2050 Ma biotite age post-dates the first deformation event (D1) responsible for the pervasive ENE-trending foliation. However, it pre-dates the event which induced the fuchsite mineralisation (2000-2040 Ma) and which probably is related to the second deformation (D2), characterised by a sinistral reactivation of the D1-foliation. D2 is restricted to localised zones and shows a transition from ductile to brittle. Ore mineralisation is partly also related to brittle structures (tension gashes, normal faults), which consequently must be younger or at the same age as the 2000-2040 Ma fuchsite mineralisation event.

Acknowledgement: This study was financed by the Federal Institute for Geosciences and Natural Resources (BGR, Bundesanstalt für Geowissenschaften und Rohstoffe) in Hannover, Germany.

References

1. Poujol, M., Robb, L. J., Respaut, J.-P. & Anhaeusser, C. R. 3.07-2.97 Ga greenstone belt formation in the northwestern Kaapvaal craton: implications for the origin of the Witwatersrand basin. *Economic Geology* **91**, 1455-1461 (1996).
2. Vearncombe, J. R. et al. Geology, geophysics and mineralisation of the Murchison schist belt, Rooiwater complex and surrounding granitoids. *Memoirs Geological Survey of South Africa* **81**, 139 pp. (1992).
3. Sperner, B., Jonckheere, R. & Pfänder, J. A. Testing the influence of high-voltage mineral liberation on grain size, shape and yield, and on fission track and $^{40}\text{Ar}/^{39}\text{Ar}$ dating. *Chemical Geology* **371**, 83-95 (2014).
4. Pfänder, J. A., Sperner, B. & Ratschbacher, L. The new Ar-Ar geochronology facility at Freiberg, Germany: Instrumentation, applications, and current limitations. *Geophysical Research Abstracts* **12**, EGU2010-5496 (2010).
5. Poujol, M., Robb, L. J., Anhaeusser, C. R. & Gericke, B. A review of the geochronological constraints on the evolution of the Kaapvaal Craton, South Africa. *Precambrian Research* **127**, 181-213 (2003).
6. McDougall, I. & Harrison, T. M. *Geochronology and thermochronology by the $^{40}\text{Ar}/^{39}\text{Ar}$ method* (Oxford University Press, 1999).

Session 6:

Thermochronology of Sedimentary Basins

Radiation-damage and cooling ages of Precambrian detrital zircon

John I. Garver

Geology Department, Union College Schenectady NY, United States of America

Zircon ($ZrSiO_4$) is a common accessory mineral in siliciclastic sedimentary rocks and because it can be dated by several radiometric techniques it is widely used in provenance studies. These studies are aimed at understanding the age, thermal history, and composition of the source rocks that supplied sediment to the basin. Crystallization ages (U/Pb) can provide critical information about the range of ages of rock units in an orogenic belt, but the signal can get complicated when there is a significant fraction recycled zircon from sedimentary or metasedimentary rocks. Cooling ages of detrital zircon (ZFT and ZHe) provide information about the integrated cooling history of the source terrain, which in most cases is directly related to tectonic processes that drove source rock exhumation and subsequent accumulation in flanking sedimentary basins. In the last decade or so, we've seen that the analyses of detrital suites of zircon has become more or less routine (U/Pb, ZFT, and ZHe). Very old zircon grains, and zircon with significant radiation damage provide analytical challenges, but they also present us with important opportunities that we can use to refine our understanding of zircon provenance.

Most radiation damage in zircon accumulates from alpha-recoil primarily from the decay of ^{238}U . The accumulated damage results in many changes in a zircon including the progressive loss of crystallinity (disorder), the activation of color centers in the pink series, reduction in density, and susceptibility to chemical dissolution. For a zircon with 300-400 ppm uranium and a U:Th of 2, significant change in color and crystallinity typically occurs over 100 to 1000 Myr. When strata have been heated after deposition, the differential annealing of fission tracks in zircon is governed by radiation damage and composition, and this annealing occurs in rocks of prehnite-pumpellyite grade, or higher. Annealing of wide-spectrum radiation damage requires higher temperatures, and occurs over a much broader range of temperatures, and in typical geological setting it requires greenschist facies or higher. Here we present three cases where we can evaluate old, high-damage zircon in sedimentary basins.

1. Detrital zircon with Precambrian fission track ages. In some suites of detrital zircon, some grains have considerable radiation damage, but also very old fission-track ages. In these cases, fission-track ages can only be determined with great difficulty, and data sets tend to rely on relatively low-uranium grains because other grains are too damaged for analysis. High Density Fission Track (HDFT) dating can provide unique insight into exhumation and cooling in Precambrian settings provided the strata have not been significantly heated since deposition¹. Stratigraphic units are from the Powder River Basin record Laramide tectonism and unroofing of the Precambrian-cored Big Horn Mountains in Wyoming. Analysis of these detrital suites is difficult because they retain such a wide range of cooling ages, and many of the cooling ages are Precambrian. U/Pb ages of detrital zircon from the Eocene Wasatch Formation are almost exclusively Precambrian (93%) with most at ~ 1800 Ma³. HDFT dating of zircon in the Eocene Wasatch Formation show that the majority of grains (80%) having cooling ages of ~ 950 Ma, but with wide a range and a few grains with Paleoproterozoic cooling ages. The HDFT cooling ages in stratigraphically lower Cambrian Flathead are also almost exclusively Neoproterozoic (c. 790 Ma). For both the Flathead and the Wasatch formations, two populations show dramatic discordance in the U/Pb system with lower intercept of 0 ± 35 Ma, and we conclude that discordance of high-damage grains has occurred since deposition. The Wasatch Formation is unique because it has an abundance of Paleoproterozoic and Archean grains with cooling ages that are mainly Neoproterozoic, but most are undatable because the FT density is too high. Collectively these grains have extremely high radiation damage, which dramatically affects the internal isotopic systems and resistance to in situ weathering and alteration.

2. Annealing of damaged-induced color in detrital zircon. In typical detrital zircon a significant fraction have an internal geochemistry amenable to the accumulation of radiation-damage-induced color in the pink series². The pink color accumulates in intensity with time as a function of increasing disorder and activation of color centers. Field settings and laboratory studies show that annealing occurs at temperatures of about 350-400°C, and this has been well documented in the exhumed crustal section of the Mesozoic Torlesse terrane in the Southern Alps of New Zealand. In this unique setting, graywackes of the Torlesse show a spectrum of metamorphic grade due to differential exhumation. Rocks of prehnite–pumpellyite-grade (and lower) greywacke show no color-annealing and are dominated by pink, radiation-damaged grains (up to 60%). All color appears to be annealed in a rocks originally with temperatures of 350-400°C or higher, and in this case greenschist to amphibolite facies of the Alpine Schist. Annealing of this damage-induced color corresponds to an effect of radiation damage, but the amount of radiation-damage annealing (reordering of the crystalline structure) in this zone is not well known. In suites of detrital zircon with old grains, the absence of color in the pink series may indicate a source with old zircon, but relatively young high-temperature thermal history.

3. Radiation damage ages of Precambrian Detrital zircon. The progressive accumulation of the full spectrum of radiation damage in zircon can be used to understand the high-temperature thermal history of a zircon grain, and this information can complement U/Pb and ZFT dating. The most widely used proxy for measuring disorder in zircon relies on using μ -Raman spectroscopy, which is routine for single grains⁵. Part of the basement of the volcano-plutonic source terrain that supplied clastic sediment to the flysch of the Chugach-Prince William terrane (CPW) in Alaska delivered a small but significant fraction of Precambrian zircon. Using a combined approach of U/Pb dating, Fission-track, and μ -Raman analysis, we discovered⁴ the source rocks for the Precambrian grains have two distinct high-temperature thermal histories: (1) western units of the CPW have a wide range of grain ages characteristic of a northern Laurentian source, and these grains have considerable disorder and have likely accumulated radiation damage for 500 to 1000 Myr; (2) zircon from the eastern units of the CPW are similar to southwestern Laurentia, but they have very little disorder and have likely only accumulated significant radiation damage since the late Mesozoic (c. 100 Ma). Thus the low levels of disorder as revealed from μ -Raman analysis of this latter suite of detrital Precambrian zircon indicate derivation from an exhumed metamorphic source where the accumulated radiation damage was reset (annealed) in the Cretaceous. Our laboratory experiments and empirical data from samples in thermal aureoles of plutons indicate: 1) that amphibolite grade metamorphism is required to fully anneal disorder caused by radiation damage; 2) the full spectrum of radiation damage is progressively annealed at temperatures well above that required for the annealing of fission tracks (and helium loss).

References

1. Montario, M.J., Garver, J.I., 2009, The thermal evolution of the Grenville terrane revealed through U-Pb and Fission-Track analysis of detrital Zircon from Cambro-Ordovician quartz arenites of the Potsdam and Galway Formations; *J. of Geol.*, 117, 6, p. 595-614.
2. Garver, J.I., and Kamp, P.J.J., 2002, Integration of zircon color and zircon fission track zonation patterns in Orogenic belts: Application of the Southern Alps, New Zealand; *Tectonophysics*. v. 349, n. 1-4, p. 203-219.
3. Garver, J.I., and Wold, J.S., 2011, Discordance and dissolution of radiation-damaged detrital zircon in the Wasatch Formation and adjacent units in the Powder River basin, Wyoming, *Geol. Soc. of Am. Abs. with Prog.*, 43, 4, p. 50.
4. Garver, J.I., Davidson, C., Kaminski, K., Riehl, M., Suarez, K., 2013, Thermal evolution of source rocks of detrital Precambrian zircon revealed through integrated radiation damage, Chugach-Prince William terrane, Alaska, *Geol. Soc. of Am. Abs. with Prog.*, 45, 7, p. 221.
5. Marsellos, A.E., Garver, J.I., 2010, Radiation damage and uranium concentration in zircon as assessed by Raman spectroscopy and neutron irradiation; *Am. Mineralogist*, 95, p.1192–1201.

Exploring uncertainty and bias in the inversion and interpretation of detrital fission track data

Mark Naylor¹, Hugh Sinclair¹, Matthias Bernet², Peter Van der Beek², Linda Kirstein¹

1 University of Edinburgh, UK

2 Université Joseph Fourier, France

The utility of detrital fission track measurements is contingent on both (i) our ability to invert for meaningful closure age distribution and (ii) the methods we use to interpret resulting age distribution in terms of geological history. These problems are particularly acute in young detrital samples, such as those from the Alps, where the best fit age distribution is commonly modeled as a parsimonious set of discrete closure ages which produces overlapping distributions of grain ages. Where there is significant overlap in the grain age distributions we should expect a degree of non-uniqueness in the inversion and interpretation process – but how significant is this problem?

In this presentation we use computational sampling to explore potential pitfalls in the inversion process. By using a range of synthetic grain data generated from known closure age distributions we systematically explore the roles of uncertainty and consequent bias. Further, we present a new MCMC modeling framework for testing more general age distributions. Lessons learned from this analysis will be motivated using Alpine samples.

This analysis has resulted in me recoding BINOMFIT into R to make it easier to bootstrap uncertainties and link with OpenBUGS¹, an open source Bayesian sampler; for the MCMC analysis. All code is freely available for research purposes.

References

1. Lunn, D., Spiegelhalter, D., Thomas, A. and Best, N. (2009) The BUGS project: Evolution, critique and future directions (with discussion), *Statistics in Medicine* **28**: 3049--3082.

Using detrital thermochronology to quantify glacial catchment denudation and sediment mixing

Eva Enkelmann¹, Todd A. Ehlers², Sarah Falkowski²,
1 University of Cincinnati, OH, USA
2 Universität Tübingen, Germany

The fission track (FT) and (U-Th)/He dating methods have been applied successfully on bedrock samples as well as detrital material to quantify rock exhumation in orogens. Bedrock dating has the advantage to record the cooling of rocks at a specific location in the orogen. Additionally, it allows the application of several thermochronometric systems on the same sample, providing an entire cooling history over a large temperature range for a specific rock sample. However, in some areas it is difficult or impossible to access bedrock due to coverage by soil, vegetation, or ice, or due to extreme remoteness or political reasons. The analysis of detrital material yields integrated cooling signals of entire catchments and can possibly provide access to conventionally unreachable locations such as ice-filled valleys.

In this study we investigate how well the detrital thermochronometric record of glacial detritus represents erosion of the entire catchment. We present thermochronometric data from two locations; (1) detrital apatite FT and (U-Th)/He ages from the Tiedemann Glacier covering the eastern flanks of Mt. Waddington (BC, Canada), and (2) the detrital zircon FT and (U-Th)/He ages from sand and cobble-size material, respectively, of the Seward-Malaspina Glacier (southeast Alaska).

The Tiedemann Glacier catchment is entirely composed of one batholith and is not affected by faulting. Thus this area is a perfect natural laboratory to study the use of detrital thermochronology to quantify catchment-wide rock exhumation by excluding any bias due to variability in apatite content in the underlying bedrock or structurally related variations in rock exhumation. We analyzed detrital apatites from sand-size material collected from various locations on the glacier terminus. The samples were collected along a profile crossing the debris covered glacier terminus and two ice-cored terminal moraines, from 1600 A.D. and 2900 B.C., and from modern deposits of the pro-glacial river. We compare the grain-age distributions of the individual samples to understand sediment mixing and identify sampling strategies that result in a well-mixed sample representing material from the entire catchment. The detrital apatite FT and (U-Th)/He ages are compared with bedrock ages from the Tiedemann Glacier catchment. We show that detrital apatite thermochronology is a viable and powerful tool to obtain a robust cooling age distribution of a catchment that can elucidate age populations originating from those parts of the catchment that are covered by ice and therefore remain undetected by bedrock studies. We also show that sampling the ice-cored terminal moraines is an alternative sampling approach to the often sampled pro-glacial river sediments to obtain cooling age distributions representative of erosion in the entire catchment including sub-glacially eroded material.

These findings are in agreement with the result of our second study area. The ~5000 km² large catchment area of the Seward-Malaspina Glacier is composed of a variety of lithologies and different terranes comprising rocks with various concentrations of zircon and apatite. However, due to the thick ice cover of the region, bedrock dating is limited to the ice-free mountain ridges that surround the high-elevated Seward Ice field. Due to the fact that the large Malaspina Glacier lobe extends into the Pacific Ocean, sampling of glacial detritus is only possible on top of the debris-covered glacier terminus. We present detrital zircon FT data from sand-size material that reveals

cooling ages¹ that are much younger than any bedrock dated in the region²⁻⁴. Similar results have been found in the zircon FT age populations in neighboring glacial catchments resulting in the discovery of a region of high exhumation rates centered at the orogenic syntaxis^{1,5}. Zircon FT ages are combined with U-Pb dating on the same grains, providing sediment provenance¹. Another detrital sampling approach uses cobble-size material (30–80 cm large) from the debris covered Malaspina Glacier lobe allowing the use of multiple thermochronometric methods on individual samples and combine it with lithologic information⁶. The use of double-dating techniques or the combination of multiple methods and lithology allows identifying the provenance of the cooling signal within the catchment.

Both studies show that detrital thermochronology is a powerful tool to reveal cooling age signals undetected in high-elevation bedrock samples of glacial catchments. The results also show that the sediments are mixed and even cobble-size material originating from glacier beds is transported to the top of debris-covered glacier terminus allowing access to this material.

References

1. Enkelmann, E., Zeitler, P. K., Pavlis, T. L., Garver, J. I. & Ridgway, K. D. Intense localized rock uplift and erosion in the St. Elias orogen of Alaska. *Nat. Geosci.* **2**, 360–363 (2009).
2. O'Sullivan, P. B. & Currie, L. D. Thermotectonic history of Mt. Logan, Yukon Territory, Canada: Implications of multiple episodes of Middle to Late Cenozoic denudation. *Earth Planet. Sci. Lett.* **144**, 251–261 (1996).
3. McAleer, R. J., Spotila J. A., Enkelmann, E. & Berger, A. L. Exhumation along the Fairweather Fault, southeastern Alaska, based on low-temperature thermochronometry. *Tectonics* **28**, TC1007 (2009).
4. Spotila, J. A. & Berger, A. L. Exhumation at orogenic indentor corners under long-term glacial conditions: Example of the St. Elias orogen, southern Alaska. *Tectonophysics* **490**, 241–256 (2010).
5. Falkowski, S., Enkelmann, E. & Ehlers, T. A. Constraining the area of rapid and deep-seated exhumation at the St. Elias syntaxis, Southeast Alaska, with detrital zircon fission-track analysis. *Tectonics* (2014).
6. Grabowski, D. M., Enkelmann, E. & Ehlers, T. A. Spatial extent of rapid denudation in the glaciated St. Elias syntaxis region, SE Alaska. *J. Geophys. Res. Earth Surf.* **118**, 1921–1938 (2013).

Thermal and exhumation histories from borehole thermochronometer samples in the Swiss Molasse Basin

C.Fillon^{1,2}, T. Ehlers¹, E. Enkelmann³, J.K. Becker⁴ and M. Schnellmann⁴

*1 Department of Geosciences, University of Tübingen, Wilhelmstr.56, 72074
Tübingen, Germany*

*2 now at: Instituto de Ciencias de la Tierra Jaume Almera (ICTJA-CSIC), Solé i
Sabarís s/n, 08028 Barcelona, Spain*

*3 Department of Geology, University of Cincinnati, 500 Geology Physics Building
Cincinnati, OH 45221-0013, US*

4 Nagra, Hardstrasse 73, CH-5430 Wettingen, Switzerland

In the last decade, significant interest has emerged to better understand the links between the foreland basin evolution and the erosion history of the Alps. For this, the European Alps are indeed a well-suited study region since the hinterland and the Swiss Molasse basin erosion rates and timing were extensively studied using basin analysis, and low-temperature thermochronology^{1-4,5,6}. However, the driving mechanisms for the post-Miocene erosion of the Swiss Molasse basin remains controversial, and several papers discuss whether global climatic changes¹ or local variations of base level^{7,8,9} have controlled the erosion of the basin.

With this study, we add quantitative constraints on the late-stage history of the basin by presenting new AFT and AHe dataset (respectively 16 and 19 samples) from two boreholes located ~30 km apart from each other, one located close to the center (Sonnengarten, depth of 3500 m) and one located to the North (Benken, depth of 100 m) of the basin. The data are derived from Triassic to Pliocene sand deposits as well as the underlying gneissic basement rocks and both AFT and AHe results are ranging from Pliocene to Triassic ages.

The two dataset present very different age patterns which make the direct interpretation difficult. Therefore, thermal models using the *QTQt* software^{10,11} have been performed. This software is capable to evaluate cooling rates and timing using multiple samples from a single borehole. To test the robustness of the simulations, several runs for each borehole based on different data sets were performed, and showed some discrepancies between the resulting thermal histories. We provide, based on the simulations results, the most probable erosion estimates which are in the same range as the ones proposed in previous studies in the basin. For the borehole Benken, we reproduce a long and slow erosion phase starting at 23 Ma, with an overall estimate of the amount of eroded sediments ranging between 1.2 to 2 km. For the central borehole (Sonnengarten), the thermal modeling suggests compatible amounts of total erosion, with estimates of ~2 km, but with also a higher erosion rate from 3 Ma to present. We conclude that these values support much lower erosion rates in the Northern part than in the central or Southern parts of the basin as the samples from the borehole Benken were clearly less affected by the Pliocene erosion phases. These erosion estimates are also discussed, considering some inconsistencies with preserved thicknesses of Pliocene sediments still outcropping in the basin. Finally, this study also points out the limitations of the modeling technique on a complete dataset that incorporates a large number of bedrock and detrital samples on large (>2km) vertical profiles.

References

- 1 Cederbom, C. E., Sinclair, H. D., Schlunegger, F. & Rahn, M. K. Climate-induced rebound and exhumation of the European Alps. *Geology* **32**, 709-712, doi:10.1130/g20491.1 (2004).

- 2 Cederbom, C. E., van der Beek, P., Schlunegger, F., Sinclair, H. D. & Oncken, O. Rapid extensive
erosion of the North Alpine foreland basin at 5–4 Ma. *Basin Research* **23**, 528-550, doi:10.1111/j.1365-
2117.2011.00501.x (2011).
- 3 von Hagke, C. *et al.* Linking the northern Alps with their foreland: The latest exhumation history
resolved by low-temperature thermochronology. *Tectonics* **31**, TC5010, doi:10.1029/2011tc003078
(2012).
- 4 Mazurek, M., Hurford, A. J. & Leu, W. Unravelling the multi-stage burial history of the Swiss Molasse
Basin: integration of apatite fission track, vitrinite reflectance and biomarker isomerisation analysis.
Basin Research **18**, 27-50, doi:10.1111/j.1365-2117.2006.00286.x (2006).
- 5 Reiter, W., Elfert, S., Glotzbach, C., Bernet, M. & Spiegel, C. Relations between denudation, glaciation,
and sediment deposition: implications from the Plio-Pleistocene Central Alps. *Basin Research* **25**, 659-
674, doi:10.1111/bre.12023 (2013).
- 6 Kuhlemann, J. & Rahn, M. Plio-Pleistocene landscape evolution in Northern Switzerland. *Swiss j
geosci* **106**, 451-467, doi:10.1007/s00015-013-0152-6 (2013).
- 7 Willett, S. D., Schlunegger, F. & Picotti, V. Messinian climate change and erosional destruction of the
central European Alps. *Geology* **34**, 613-616, doi:10.1130/g22280.1 (2006).
- 8 Schlunegger, F. & Mosar, J. The last erosional stage of the Molasse Basin and the Alps. *International
Journal of Earth Sciences* **100**, 1147-1162, doi:10.1007/s00531-010-0607-1 (2011).
- 9 Yanites, B. J., Ehlers, T. A., Becker, J. K., Schnellmann, M. & Heuberger, S. High magnitude and rapid
incision from river capture: Rhine River, Switzerland. *Journal of Geophysical Research: Earth Surface*
118, 1060-1084, doi:10.1002/jgrf.20056 (2013).
- 10 Gallagher, K. Transdimensional inverse thermal history modeling for quantitative thermochronology.
Journal of Geophysical Research **117**, B02408, doi:10.1029/2011jb008825 (2012).
- 11 Gallagher, K., Charvin, K., Nielsen, S., Sambridge, M. & Stephenson, J. Markov chain Monte Carlo
(MCMC) sampling methods to determine optimal models, model resolution and model choice for Earth
Science problems. *Marine and Petroleum Geology* **26**, 525-535 (2009).

Linking Oligo-Miocene drainage divide migration to orogenic wedge state in the European Alps: a multi-proxy provenance approach.

Chris Mark, David Chew, Nathan Cogne

Department of Geology, Museum Building, Trinity College Dublin, Dublin 2, Ireland.

Two competing hypotheses describe Oligo-Miocene exhumation of the European Alps. The first¹⁻³ argues that exhumation rates on scales of 10^6 - 10^7 years were relatively constant during this time; an alternative model⁴⁻⁷ proposes variable exhumation rates, which are linked to predictions made by the Coulomb orogenic wedge model. This model predicts that orogen deformation behaviour is governed by wedge taper angle: when in a subcritical state the orogenic wedge should deform internally, promoting hinterland exhumation, and when supercritical the wedge should propagate by foreland thrusting, leading to decreasing exhumation. Crucially, as wedge-toe thrust propagation will tend to build foreland topography, periods of supercritical wedge state will tend to promote foreland migration of the orogenic drainage divide. Conversely, internal deformation of a subcritical wedge should promote retention of the drainage divide in the internal Alps. Constraining past locations of the Alpine drainage divide is therefore key to understanding the exhumation history and geodynamic evolution of the orogen.

In geological settings too active to permit preservation of palaeo-landscapes, thermochronologic detrital provenance analysis is a tool commonly applied to study palaeo-drainage development and divide migration. This has proved challenging in Alpine basins because the low-temperature chronometers typically employed are highly sensitive, have often been widely reset across the orogen, and thus cannot easily distinguish candidate source terrains⁶. Instead, the presence of thermochronologically distinctive source units of high metamorphic grade, mostly in the internal Alps, demands the use of a chronometer sensitive to higher temperatures⁸. In the western Alps, these comprise the upper-blueschist Schistes Lustrés and eclogitic Viso and Dora Maira units; and in the central Alps, the amphibolite-granulite Lepontine dome, eclogitic Monte Rosa, and the external upper-greenschist southern Aar massif⁹ (see Fig. 1). The maximum Alpine palaeotemperatures experienced by these units are typically in excess of ~ 350 °C, were attained diachronously, and increase toward the retro-basin.

Today, the Alpine drainage divide runs largely through the external Alps, and the high-grade units drain almost exclusively east and south to the retro-basin. However, past retention of the drainage divide in a more retro position, within the internal Alps, should be recorded in foreland basin sediments by the presence of distinctive high-grade detritus. Thus, thermochronometers are required which are both sensitive to the temperatures associated with high-grade Alpine metamorphism, and easily applied to detrital provenance study.

Here, we utilise the apatite and rutile U-Pb thermochronometers, sensitive to temperatures of ~ 375 - 550 °C and ~ 490 - 640 °C respectively¹⁰⁻¹³, in addition to the zircon U-Pb geochronometer. We present preliminary detrital apatite, rutile, and zircon U-Pb spectra, and rutile trace element chemistry, from the Barrême and Digne-Valensole basins in the foreland of the western Alps and also from the Swiss Molasse basin of the Central Alps. We use these to test the hypothesis that *proposed periods of wedge subcriticality in the Oligo-Miocene⁷ are accompanied by a shut-off of the high-grade sedimentary detritus supply to the foreland as the drainage divide shifts west and north.*

References:

1. Bernet, M., Zattin, M., Garver, J. I., Brandon, M. T. & Vance, J. A. Steady-state exhumation of the European Alps. *Geology* **29**, 35–38 (2001).
2. Bernet, M. *et al.* Exhuming the Alps through time: clues from detrital zircon fission-track thermochronology. *Basin Res.* **21**, 781–798 (2009).
3. Garzanti, E. & Malusà, M. G. The Oligocene Alps: Domal unroofing and drainage development during early orogenic growth. *Earth Planet. Sci. Lett.* **268**, 487–500 (2008).
4. Spiegel, C., Kuhlemann, J., Dunkl, I. & Frisch, W. Paleogeography and catchment evolution in a mobile orogenic belt: the Central Alps in Oligo–Miocene times. *Tectonophysics* **341**, 33–47 (2001).
5. Carrapa, B., Wijbrans, J. & Bertotti, G. Episodic exhumation in the Western Alps. *Geology* **31**, 601 (2003).
6. Spiegel, C., Siebel, W., Kuhlemann, J. & Frisch, W. in *Detrital thermochronology—Provenance Anal. Exhum. Landsc. Evol. Mt. belts* (Bernet, M. & Spiegel, C.) **378**, 37–50 (Geological Society of America Special Paper 378, 2004).

7. Carrapa, B. Tracing exhumation and orogenic wedge dynamics in the European Alps with detrital thermochronology. *Geology* **37**, 1127–1130 (2009).
8. Von Eynatten, H. & Wijbrans, J. R. Precise tracing of exhumation and provenance using $^{40}\text{Ar}/^{39}\text{Ar}$ geochronology of detrital white mica: the example of the Central Alps. *Geol. Soc. London, Spec. Publ.* **208**, 289–305 (2003).
9. Bousquet, R. *et al.* Metamorphic framework of the Alps. *CCGM/CGMW* (2012). at <<http://www.geodynamalps.org>>
10. Mezger, K., Hanson, G. N. & Bohlen, S. R. High-precision U-Pb ages of metamorphic rutile: application to the cooling history of high-grade terranes. *Earth Planet. Sci. Lett.* **96**, 106–118 (1989).
11. Chamberlain, K. R. & Bowring, S. A. Apatite-feldspar U-Pb thermochronometer: a reliable, mid-range (~450 °C), diffusion-controlled system. *Chem. Geol.* **172**, 173–200 (2000).
12. Kooijman, E., Mezger, K. & Berndt, J. Constraints on the U–Pb systematics of metamorphic rutile from in situ LA-ICP-MS analysis. *Earth Planet. Sci. Lett.* **293**, 321–330 (2010).
13. Cochrane, R. *et al.* High temperature (>350°C) thermochronology and mechanisms of Pb loss in apatite. *Geochim. Cosmochim. Acta* **127**, 39–56 (2014).

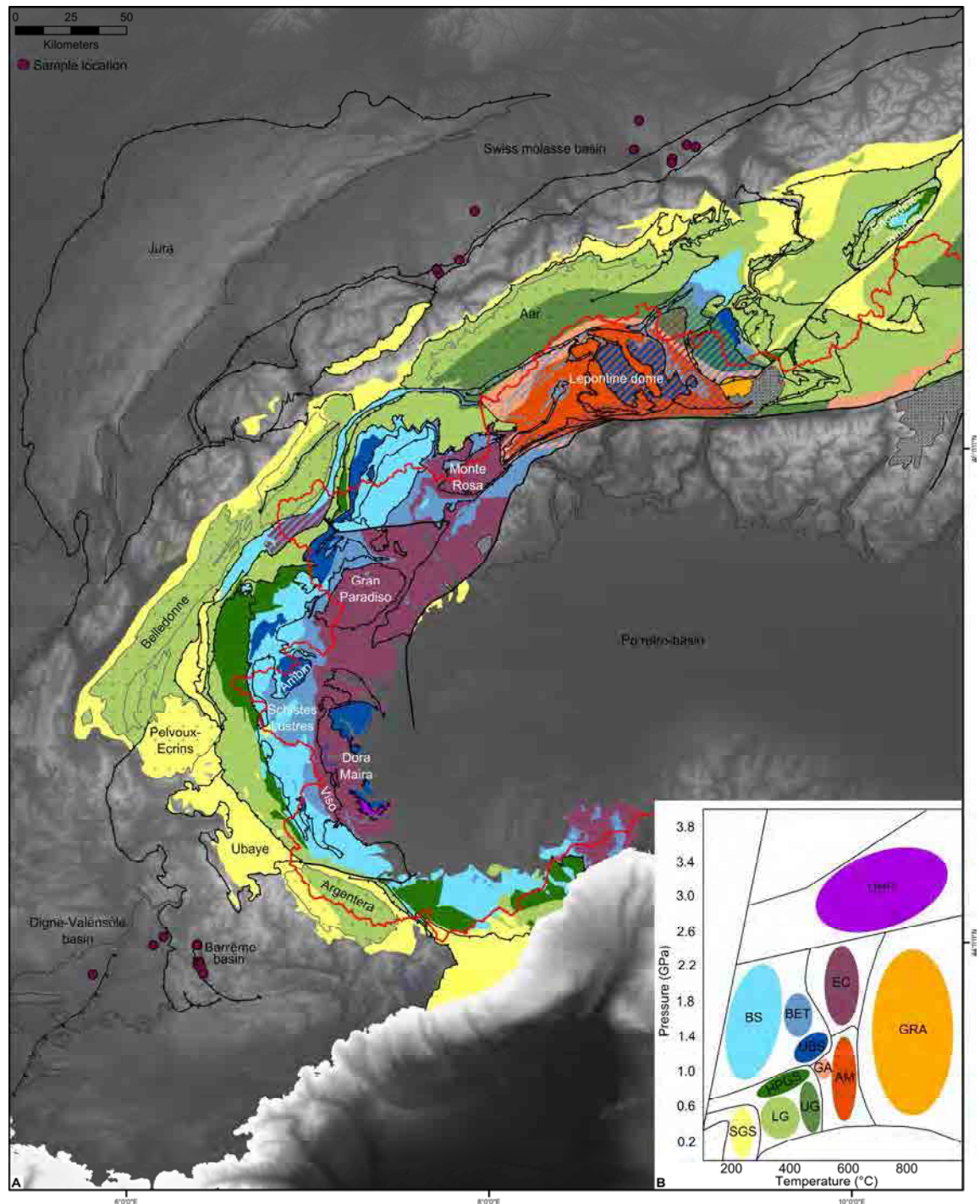


Figure 1. A: Metamorphic facies of the Alps⁹; red line denotes modern drainage divide. **B:** Metamorphic facies boundaries; SGS – sub-greenschist; LG – lower greenschist; UG – upper greenschist; HPGS – high-pressure greenschist; BS – blueschist; UBS – ultra-blueschist; BET – blueschist-eclogite transition; GA – greenschist-amphibolite transition; AM – amphibolite; EC – eclogite; GRA – granulite; UHP – ultra-high pressure facies.

Provenance of Pleistocene fluvial and glacial sediments deduced from fission track data

Christoph Glotzbach¹, Johanna Hertel¹, Freek Busschers², Jutta Winsemann¹
1 Institute of Geology Leibniz Universität Hannover, Germany
2 TNO – Geological Survey of the Netherlands, Utrecht, Netherland

Pleistocene sediments blanket a large portion of the Earth's Surface. The provenance of these sediments is traditionally deciphered by heavy mineral and geochronological (e.g. U-Pb dating) analyses, but as with most provenance methods, similarities in the source signal and repeated recycling of older sediments often complicate or even prevent a robust interpretation. In this study we investigate the potential of apatite and zircon fission track (AFT and ZFT, respectively) analyses to unravel the provenance of fluvial and glacial Pleistocene sediments in the Lower Rhine Embayment and the northeastern Netherlands. Measured detrital AFT and ZFT age distributions are compared to in situ AFT and ZFT ages of potential source areas in central and northern Europe (Fig. 1).

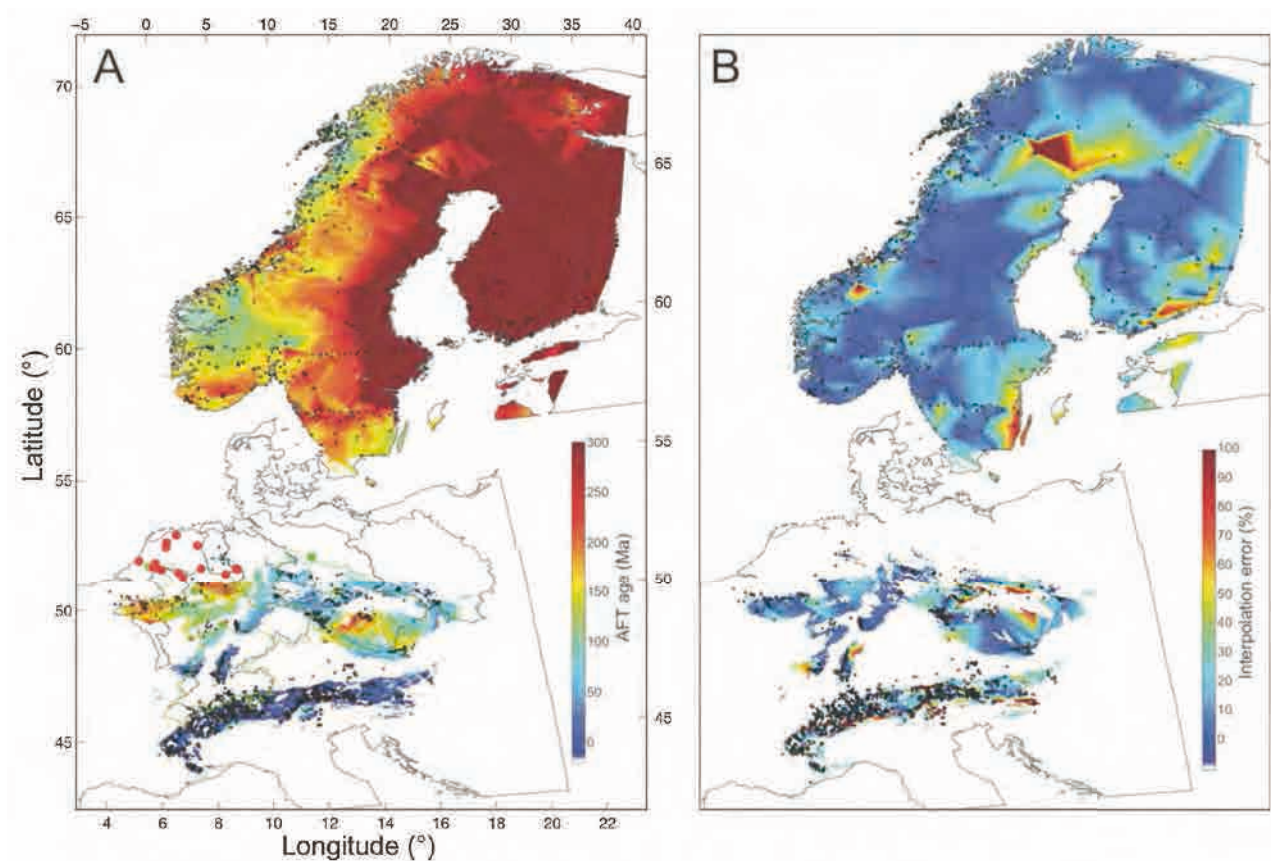


Figure 1. Interpolated in-situ/bedrock apatite fission track ages and interpolation errors of apatite bearing rocks (e.g. granite, gneiss, sandstone) in central and northern Europe. Interpolation is based on ~2000 single ages¹⁻² (small black dots). Location of sampled Pleistocene deposits is marked as red dots.

Due to differing cooling histories of these regions, it should be possible to distinguish five source regions (from young to old): the Alps, the Black Forest and Vosges Mountains, regions inverted during Late Cretaceous times (e.g. Harz Mountains, Bohemian Massif), the Rhenish Massif and the Fenno-Scandinavian region. Analogous to accompanied heavy mineral analyses the observed AFT and ZFT age distributions reveal a more or less pre-dominant provenance from the Alps, suggesting that the majority of sand was originally deposited by the River Rhine. The drainage basin of the

River Rhine also comprises the Black Forest and Vosges Mountains and the Rhenish Massif, which according to our AFT and ZFT results make up only a minor source in the majority of analyzed sediments. Some samples, especially in the Münsterland Embayment and northeastern Netherland also contain grains from Fenno-Scandinavian source regions. Based on these results, we suggest that detrital thermochronology, such as AFT and ZFT methods, are capable to unravel the provenance of Pleistocene deposits. Advantages compared to alternative methods such as heavy mineral analyses are: i) the provenance signal (age distribution) is less influenced by the grain size of sampled sediments, and (ii) although source regions are composed of similar lithologies and/or crystallization ages (e.g. widespread Variscan basement rocks in Central Europe), variable cooling histories result in distinguishable cooling ages. A major uncertainty of the applied detrital thermochronological analyses arises from the unknown amount of recycled sediments, which can perturb detrital age distributions and corresponding provenance analyses. The combination of heavy mineral and thermochronological analyses, however, yield valuable information about the previously unresolved or poorly defined provenance of Middle Pleistocene fluvial sediments in the Lower Rhine Embayment and the northeastern Netherlands. In addition, our results challenge the straightforward usage of augite as an index mineral for Rhine provenance in the northern Netherlands.

References

1. Hendriks, B., Andriessen, P., Huigen, Y., Leighton, C., T. Redfield, G. Murrell, K. Gallagher and S. Bom Nielsen (2004), A fission track data compilation for Fennoscandia. *Norw. J. Geol.* 87, 143-155.
2. Vernon A., P.A. van der Beek, H.D. Sinclair and M.K. Rahn (2008), Increase in late Neogene denudation of the European Alps confirmed by analysis of a fission-track thermochronology database. *Earth Planet. Sci. Lett.* 270, 316-329.

Thermochronology of the Uncompahgre Plateau and La Sal Mountains: new apatite fission track, (U-Th)/He and zircon U/Pb data

Christian Rønnevik¹, Anna K. Ksienzyk¹, Haakon Fossen¹, Joachim Jacobs¹, István Dunkl², Fernando Bea³

¹ Department of Earth Science, University of Bergen, P.O. Box 7803, 5007 Bergen, Norway

² Geoscience Centre, University of Göttingen, Goldschmidtstraße 3, 37077 Göttingen, Germany

³ Department of Mineralogy and Petrology, University of Granada, 18002 Granada, Spain

The Cenozoic uplift history of the Colorado Plateau is poorly understood. A major problem for reconstructions of the thermo-tectonic history is the lack of Cenozoic sediments on top of the plateau. The story is further complicated by locally intense magmatism associated with elevated thermal gradients that are subject to both spatial and temporal changes. While vertical movements within the upper crust can be constrained by low-temperature thermochronological techniques, care must be taken to understand and consider the effect of Cenozoic magmatism on cooling histories derived from thermochronological data. In the present study, we combine apatite fission track and (U-Th)/He analyses with high-precision U/Pb zircon dating to investigate the effect of the Oligocene La Sal Mountains intrusion on the Cenozoic thermal history of the Uncompahgre Plateau, located in the northeastern part of the larger Colorado Plateau (Fig. 1).

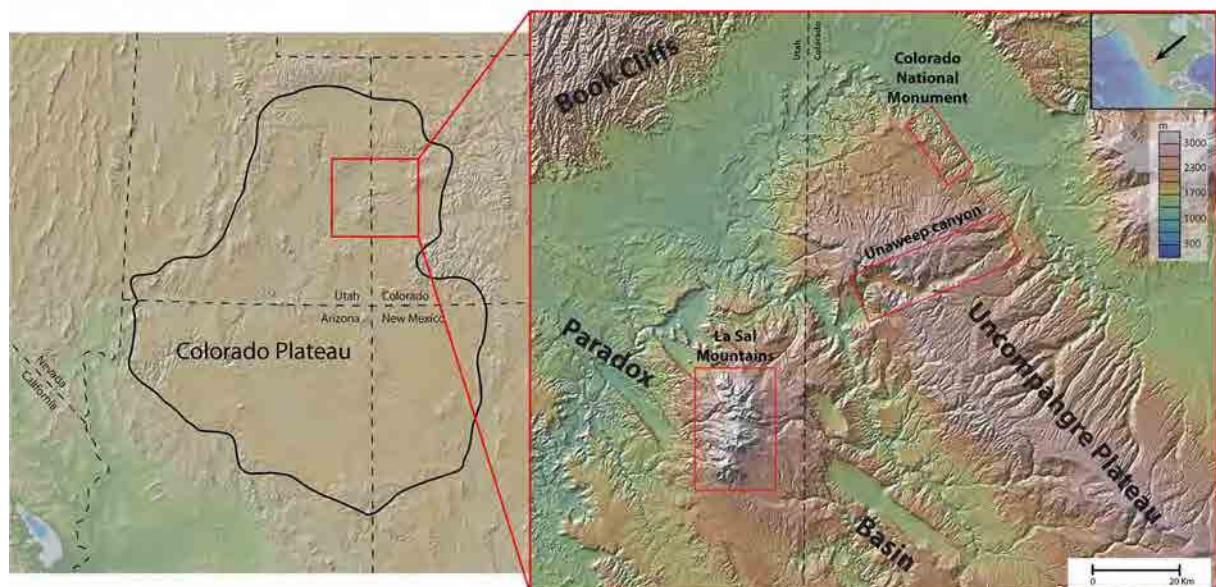


Figure 1. Location of the La Sal Mountains, Uncompahgre Plateau, and Unaweep Canyon.

U/Pb SHRIMP zircon dating was performed on one sample from the La Sal Mountains laccolith in order to establish a precise crystallization age for this intrusion. Zircons exhibit clear core-rim structures with rounded and resorbed cores surrounded by oscillatory zoned rims. The rims gave an Oligocene age of 29.2 ± 0.3 Ma, which is interpreted as the crystallization age and is in general agreement with previously published data¹⁻⁴. Apatite fission track ages from the La Sal Mountains laccolith range from 27 to 33 Ma with no discernible correlation of age with elevation. This is indicative of rapid cooling and the mean

apatite fission track age of 29.7 ± 2.1 Ma is, within the uncertainties, identical to the U/Pb crystallization age.

Six samples collected along the Unaweep Canyon yielded apatite fission track ages between 27 and 35 Ma. Even though they were sampled up to 60 km away from the La Sal Mountains, these ages still overlap, within their uncertainties, with the crystallization age of the La Sal Mountains intrusion, indicating extensive thermal resetting during Oligocene magmatism. Three samples collected from the top of the Uncompahgre Plateau, however, gave older apatite fission track ages of 63 to 65 Ma. Apatite (U-Th)/He analyses were performed on two of these samples, in order to investigate the presence of an Oligocene thermal overprint on top of the plateau. One sample gave single grain (U-Th)/He ages between 28 and 34 Ma, with a mean age of 30.6 ± 1.0 Ma, while the second sample gave somewhat older ages from 36 to 40 Ma (mean age 38.3 ± 1.3 Ma). Thus a thermal overprint is clearly present even on top of the plateau, but temperatures were not high enough to reset the apatite fission track system. These findings are in agreement with previously presented data suggesting complete thermal resetting in the western Unaweep Canyon during La Sal Mountains magmatism⁵.

Thermal history modelling reveals some significant differences between samples from within the Unaweep Canyon and the top of the Uncompahgre Plateau: Plateau samples record Late Cretaceous burial and heating to temperatures in excess of 90 °C, followed by cooling throughout the latest Cretaceous to Eocene. They experienced mild reheating to temperatures between 40 and 80 °C during the Oligocene and have been steadily cooling ever since. Canyon samples experienced complete thermal resetting during the Oligocene, erasing all previous history. Temperatures during the thermal event were at least 90 °C but probably significantly higher. Since the Oligocene, canyon samples also experienced cooling, however, with a significant increase in cooling rates in the last 5 to 10 Ma. Thomson et al.⁵ found increased cooling rates in the last 6 Ma for canyon samples and interpreted them as an effect of rapid canyon incision. The youngest apatite fission track ages (17-20 Ma) were encountered in the northeastern part of the Uncompahgre Plateau, within the Colorado National Monument. These samples were collected close to the Monument and Fruita Canyon fault systems, and the young ages might be attributed to advective heating related to fluid flow along these faults, which is partially resetting the apatite fission track ages.

Summarizing, the thermal effect of Oligocene magmatism is extensive on the Uncompahgre Plateau and the thermal gradient appears to decrease upwards. However, if the La Sal Mountains intrusion was the source of the thermal overprint, a decrease of maximum temperatures horizontally away from the La Sal Mountains would be expected. Whether the vertical thermal gradient on the Uncompahgre Plateau is due to regionally elevated temperatures in the Oligocene or an additional intrusive body under the plateau can at this point only be speculated about.

References

1. Chew, D. & Donelick, R. Combined apatite fission track and U-Pb dating by LA-ICP-MS and its application in apatite provenance analysis. *Mineralogical Association of Canada Short Course* **42**, 219-247 (2012).
2. Nelson, S., Davidson, J., & Sullivan, K. New age determinations of central Colorado Plateau laccoliths, Utah: Recognizing disturbed K-Ar systematics and re-evaluating tectonomagmatic relationships. *Geological Society of America Bulletin* **104**, 1547-1560 (1992).
3. Stern, T., Newell, M., Kistler, R. & Shawe, D. Zircon uranium-lead and thorium-lead ages and mineral potassium-argon ages of La Sal Mountains rocks, Utah. *Journal of Geophysical Research* **70**, 1503-1507 (1965).
4. Sullivan, K., Kowallis, B. & Mehnert, H. Isotopic Ages of Igneous Intrusions in Southeastern Utah: Evidence for a Mid-Cenozoic Reno – San Juan Magmatic Zone. *Brigham Young University Geology Studies* **37**, 139-144 (1991).

5. Thomson, S., Soreghan, G. & Eccles, T. Elevated Cenozoic geothermal gradients and later post-6 Ma incision of the Uncompahgre Plateau and Unaweep Canyon (western Colorado) revealed by low-temperature thermochronology. *Geological Society of America Abstracts with Programs* **44**, 18 (2012).

Bentonite Zircon U/Pb Geochronology, Cenomanian-Turonian Boquillas Formation, Texas, USA

Bergman, S.C.¹, Eldrett, J.S.¹, Ma, C.², Minisini, D.¹, Macaulay, C.I.¹, Ozkan, A.¹, & Kelly, A. E.¹

1Shell International Exploration and Production Inc., Houston, Texas 77082, USA,

2 Univ. Wisconsin, Dept. Geosciences, Madison, WI USA.

The Boquillas (equivalent to the Eagle Ford) Formation is a prolific source rock and a gas and liquid-rich unconventional play in West Texas. It was deposited at the junction of the southern end of the Cretaceous Western Interior Seaway and the northwestern margin of the Gulf of Mexico Carbonate Shelf (passive margin) in a retroarc foreland basin, behind the North American Cordilleran orogen, and encompasses the Cenomanian-Turonian (C-T) Oceanic Anoxic Event-2 and global Carbon Isotope Excursion (CIE). Here we provide a robust zircon U/Pb geochronologic framework used to accurately interpret and predict variability in facies distribution within the Boquillas Formation. The Boquillas Formation consists of a succession of cyclic marlstone and limestone beds and over 300 bentonites deposited in a distal, restricted, suboxic setting mostly below the base of the storm waves. Bentonites are generally homogenous clay-rich layers 1-10 cm thick (average 5 cm, up to 60 cm) showing sharp contacts and strong yellow-orange mineral fluorescence under UV light. Shell has been conducting research on road cuts and natural outcrops in the vicinity of Del Rio, Austin, San Antonio and Big Bend National Park (Texas) that provide excellent exposures of the formations, bottom-up: Buda Limestone, Boquillas Formation and Austin Chalk. In addition, Shell has drilled two research wells behind two outcrops, Shell IONA-1 and Shell INNES-1, recovering >330 m of continuous core from the Austin Chalk through the Eagle Ford and Buda Limestone formations (Figure 1). The bentonites form ~5% of the 60-111 m thick Boquillas Formation and are interpreted as distal pyroclastic fall deposits from large volume (>10-100 km³) Plinian eruptions from calderas associated with the Western North American Cordilleran magmatic arc. Some of the Boquillas bentonites can be correlated using petrophysical logs, geochemistry, and biostratigraphy for more than 1000 km to the north within the Western Interior Seaway at the C-T global stratotype (GSSP) section at Pueblo, CO.

This contribution reports new high-precision zircon U/Pb TIMs age data (2σ as low as 0.05 Myr) from both core and outcrop samples and integrates the dates with independent proxies derived from sedimentology, biostratigraphy, cyclostratigraphy, isotopic stratigraphy and geochemistry. We present a robust chronostratigraphic framework for the C-T formations, key to interpret sediment accumulation rates (compacted rates=1.4-6.5 cm/kyr, lowest in the Boquillas and highest in the Buda and Austin Chalk), lateral variability and character of depositional environments, diagenetic effects, and sequence stratigraphy in the Cenomanian, Turonian and lowermost Coniacian (88-99 Ma) rocks of West Texas.

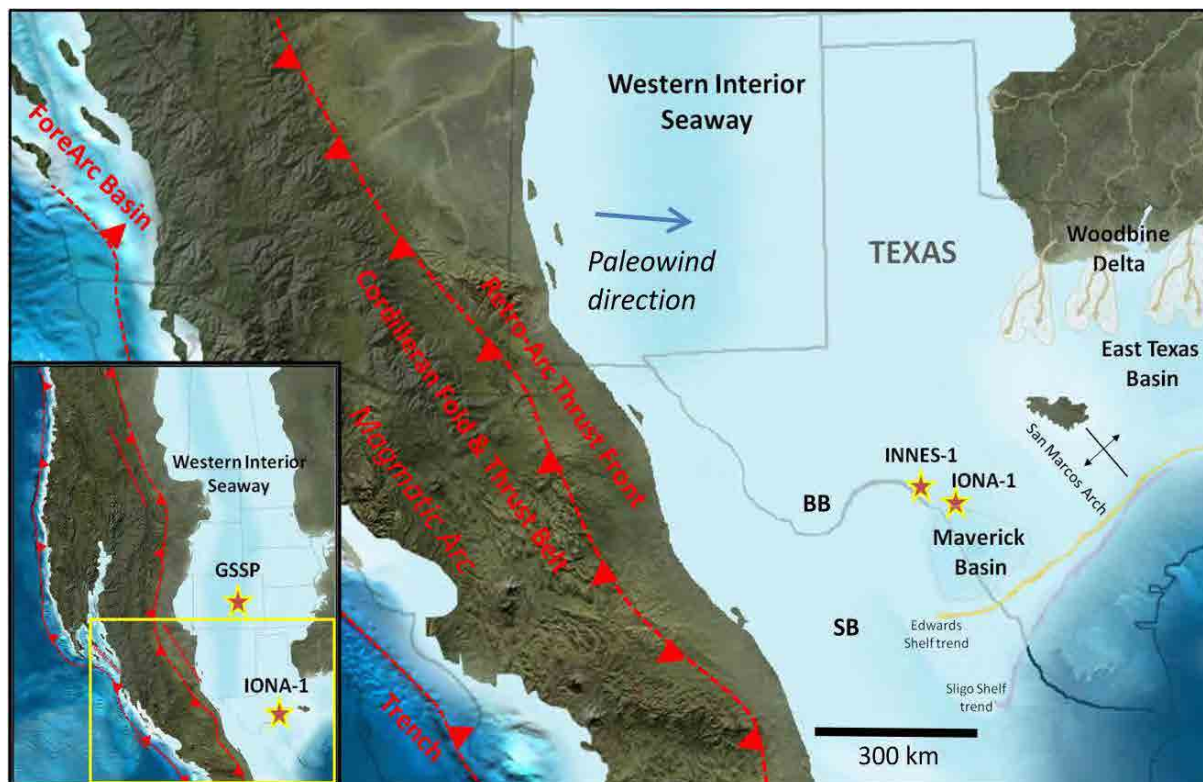


Figure 1. Middle Cenomanian (~96 Ma) palaeogeographic map showing the location of Iona-1, Innes-1, and USGS Portland-1 cores (GSSP) in the regional tectonic context; modified from Ron Blakey and the Colorado Plateau Geosystems Inc.
 SB: Sabinas Basin, Mexico; BB: Big Bend National Park.

Thermochronology of the Northern border of Paraná Basin, Brazil

Carlos Alberto Tello Sáenz¹, Rosana Silveira Resende¹, Wagner Massayuki Nakasuga¹, Caio Augusto Marques dos Santos¹, Luiz Rodrigo Hamada¹, João Victor Andrade¹, Nathalia Gomes¹

1 Univ Estadual Paulista, Rua Roberto Simonsen, 305, 19060-900 Presidente Prudente, Brazil

Studies using the Zircon Fission-Track Method, ZFTM, showed that there is a strong etching variation from grain to grain of the same sample. There is also variation on different areas of the same zircon grain surface, resulting in some small areas where the fission track density is uniform.

These zircon grains have been characterized through Optical Microscopy, micro-Raman Spectroscopy, Cathodoluminescence (SEM-CL), Electron microprobe analysis, and Scanning Electron Microscopy to analyze the possibility of using these grains to determine the fission-track and LA-ICPMS U-Pb ages. This methodology has been used to determine the thermochronology of Bauru Group located in the north of Paraná Basin, Brazil.

The preliminary zircon fission-track age results varied from 200 to 900 Ma and the U-Pb data show clearly two source areas: i) the Early Paleozoic to Neoproterozoic zircons, ranging from 445 to 708 Ma, and ii) the Paleoproterozoic zircons, ranging from 1879 to 2085 Ma. The combined information allows us to characterize Early Brazilian, Brazilian and Rhyacian materials as the main source for the zircons, which are areas situated at the west of the Bauru Basin (e.g., Goiás Massif) that have been incorporated into the sedimentary cycles in the Phanerozoic (mainly in the Paraná Basin).

Strengths and challenges of detrital apatite fission track thermochronology: a case study from the Andes

Andrea Stevens¹ and Barabara Carrapa¹

1 Department of Geosciences, University of Arizona, Tucson, AZ, United States

The use of detrital fission track thermochronology, in particular on apatites (AFT), has proven a valuable tool to interpret the thermal history of the sediment sources and basins. AFT is particularly useful in orogenic settings to determine the timing of exhumation. Here, synorogenic detrital samples that contain apatite can potentially preserve multiple pulses of paleo-exhumation; however, the interpretation of detrital AFT data contains unique challenges that need to be considered. These challenges include: 1) High error associated with a single grain age renders this individual data inconsequential. A robust age requires the combination of multiple grains' ages which can be difficult in a detrital sample. 2) Extraction of populations in AFT analysis requires unmixing of data by grouping grain ages with high errors into these meaningfully populated groups. 3) Data generation of an AFT sample, using the external detector method, requires ~20 man hours to count 100 grains; consequently, production of large sample sizes is limited from a practical perspective.

This study used four synthetic basement samples and three real detrital samples to test the limitations of standard AFT unmixing models. When combining the discrete synthetic basement samples to simulate detrital samples we identify two key exponential relationships that govern the number of grains necessary to accurately resolve detrital AFT populations:

- 1) An exponential relationship exists between the difference in age of the populations being decomposed, where small age differences require exponentially more grains to accurately resolve decomposition than large age differences.
- 2) An exponential relationship exists between the number of populations being decomposed and the number of grains, where additional populations require exponentially more grains for an accurate decomposition.

This shows that, when dealing with more than two distinct and independent populations accurate resolution of populations from detrital AFT samples requires large AFT data sets for all unmixing models. The time-consuming acquisition of these data sets limits the utility of identifying discrete pulses of exhumation. When not enough grains are available to reliably decompose a detrital AFT sample into populations, interpretations should be adjusted to ensure the integrity of the data being presented.

These experiments on synthetic samples serve as a cautionary tale of the risks of the improper use of detrital AFT; however, with appropriate research questions, detrital AFT data may represent an accurate regional exhumation signal. In the northern Argentina three modern river samples collected from basement ranges demonstrate the utility of detrital AFT data while respecting the conservative interpretations the previous experiments support. These samples do identify the broad distribution of grain ages recorded in the sediment source. These results suggest that where regional exhumation affected different sources in a similar way and or in case of rapid exhumation of well-defined sources, detrital AFT can appropriately capture the source exhumation signal.

Exhumation and magma history of the West Kunlun Mountains, northern Tibetan Plateau: evidence for a long-lived, rejuvenated orogen

Kai Cao^{1, 2, 3*}, Guo-Can Wang^{1, 2, 3}, Matthias Bernet⁴,
Peter van der Beek⁴, Ke-Xin Zhang⁵, Lothar Ratschbacher⁶

1 State Key Laboratory of Geological Processes and Mineral Resources, China University of Geosciences, Wuhan 430074, China

2 School of Earth Sciences, China University of Geosciences, Wuhan 430074, China

3 Center for Global Tectonics, China University of Geosciences, Wuhan 430074, China

4 Institut des Sciences de la Terre, Université Joseph Fourier, BP 53, Grenoble 38041, France

5 State Key Laboratory of Biogeology and Environmental Geology, China University of Geosciences, Wuhan 430074, China

6 Geowissenschaften, Technische Universität Bergakademie Freiberg, 09599 Freiberg, Germany

*Corresponding: kai.cao@cug.edu.cn

Robust constraint on orogenic history of the northern Tibetan Plateau is critical for understanding the pattern of plateau growth and relevant geodynamics. An integrated analysis of paleocurrent, detrital zircon U-Pb and fission-track double dating was applied to late Cenozoic synorogenic sediments in the southern Tarim Basin, with the aim to locate their sources, and reveal orogenesis of the least-explored West Kunlun Mountains. Paleocurrent results indicate these deposits were constantly transported from the West Kunlun range since at least 7 Ma. Further, zircon U-Pb and fission-track datasets suggest that the majority of pre-Jurassic zircons were likely recycled from Triassic meta-sediments in the Songpan-Ganzi terranes with some from the Kunlun terrane, while Cenozoic igneous zircons were derived from volcanic and magmatic rocks in the Tianshuihai and Karakoram terranes.

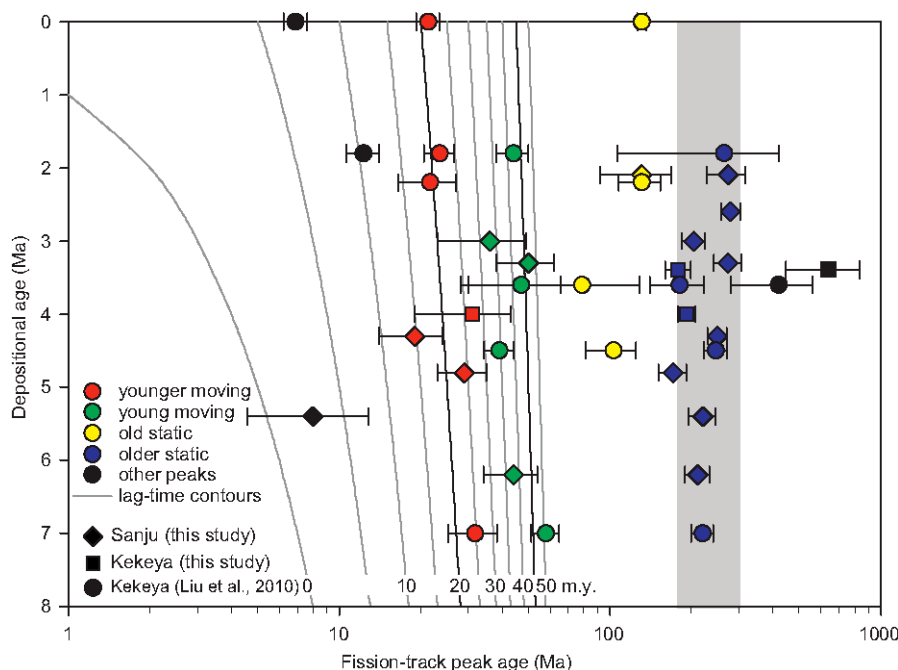


Figure 1. Zircon fission track peak ages plotted against depositional ages of late Cenozoic sediments at Kekeya and Sanju, southern Tarim Basin. Contour lines indicate lag time. Gray band designates the oldest static peak spanning from Triassic to Early Jurassic. The majority of samples show relatively constant trends (moving peaks marked by red and green symbols), suggesting constantly steady-state exhumation of the source terrain during early Eocene and Oligocene-Miocene times. Note half-logarithmic axes.

Zircon fission-track data along depositional successions presents prominent Triassic-early Jurassic (250-180 Ma) static peak, and early Eocene (58-40 Ma) and Oligocene-Miocene (30-20 Ma) moving peaks (Figure 1), coeval with magmatic episodes. The oldest peak ages record strong exhumation and unroofing of paleo-Kunlun terrane during subduction and closure of the Paleotethys Ocean¹⁻⁵, supported by provenance analysis in the accretionary complex to the south². Early Eocene exhumation records initial motion of the Oyttag-Tam Karaul fault⁶ simultaneous with transpression or thrusting of the Altyn Tagh, southern Qaidam and West Qinling faults⁷⁻⁹, suggesting the establishment of a first-order tectonic regime on the northern plateau margin in response to India-Asia collision. Oligocene-Miocene exhumation covering the whole West Kunlun Mountains reflects rise of the orogen upward and northward related to widespread crustal shortening, collaborated by seismic reflected analysis¹⁰. This process of plateau formation may continue thereafter. We propose that nascent topography of the West Kunlun Mountains has emerged as early as Triassic times, but modern plateau configuration has only attained during the Cenozoic in an episodic manner. This could be a paradigm for the orogenesis of the Tibetan Plateau.

References

1. Matte, P., et al.. Tectonics of western Tibet, between the Tarim and the Indus. *Earth Planet. Sc. Lett.* **142**, 311 (1996).
2. Robinson, A. C., Ducea, M. and Lapen, T. J.. Detrital zircon and isotopic constraints on the crustal architecture and tectonic evolution of the northeastern Pamir. *Tectonics* **31**, C2016 (2012).
3. Xiao, W. J., et al.. Carboniferous-Triassic subduction and accretion in the western Kunlun, China: Implications for the collisional and accretionary tectonics of the northern Tibetan Plateau. *Geology* **30**, 295 (2002).
4. Yao, Y. J. and Hsü, K. J., Origin of the Kunlun Mountains by arc-arc and arc-continent collisions. *Isl. Arc* **3**, 75 (1994).
5. Cowgill, E., et al., Reconstruction of the Altyn Tagh fault based on U-Pb geochronology: Role of back thrusts, mantle sutures, and heterogeneous crustal strength in forming the Tibetan Plateau. *J. Geophys. Res.* **108** (B7), 2346 (2003).
6. Cao, K., et al., Cenozoic thermo-tectonic evolution of the northeastern Pamir revealed by zircon and apatite fission-track thermochronology. *Tectonophysics* **589**, 17 (2013).
7. Clark, M. K., et al., Early Cenozoic faulting of the northern Tibetan Plateau margin from apatite (U-Th)/He ages. *Earth Planet. Sc. Lett.* **296**, 78 (2010).
8. Yin, A., et al., Tectonic history of the Altyn Tagh fault system in northern Tibet inferred from Cenozoic sedimentation. *Geol. Soc. Am. Bull.* **114** (10), 1257 (2002).
9. Zhuang, G. S., et al., Cenozoic multiple-phase tectonic evolution of the northern Tibetan Plateau: Constraints from sedimentary records from Qaidam basin, Hexi Corridor, and Subei basin, northwest China. *Am. J. Sci.* **311**, 116 (2011).
10. Jiang, X. D., Li, Z.X. and Li, H.B., Uplift of the West Kunlun Range, northern Tibetan Plateau, dominated by brittle thickening of the upper crust. *Geology* **41**, 439 (2013).

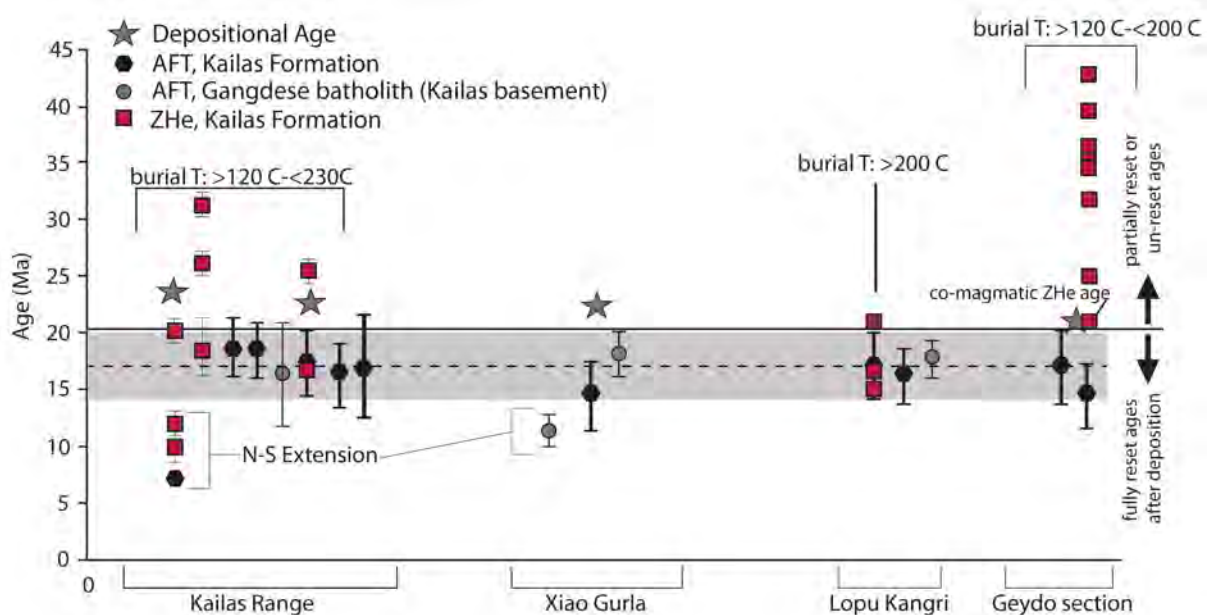
Rapid Miocene exhumation of the Indus-Yarlung Suture Zone, Tibet: Evidence from the Xigaze Forearc and Kailas Formation

Devon A. Orme¹ and Barbara Carrapa¹

¹ Department of Geosciences, University of Arizona, Tucson, AZ, United States

The Indus-Yarlung Suture Zone (IYSZ), which forms the boundary between Indian passive margin rocks to the south and the Lhasa terrane (Asia) to the north, extends across southern Tibet for over 2,000 km at an average elevation of 5,000 m. Along the IYSZ, a record of pre- and post-collisional processes are preserved in sedimentary basins of the southern Lhasa terrane, namely the Cretaceous-Eocene Xigaze forearc and Oligocene-Miocene Kailas basins. The post-depositional history of these basins is poorly constrained owing to the limited spatial extent of thermochronologic data from the Lhasa terrane. This study's overall objective is to decipher the burial and exhumation history of the IYSZ from detrital geo-thermochronology. Our results provide the first robust estimates on when and how much material was removed from across the IYSZ in Tibet.

We utilize apatite fission track (AFT) and zircon (U-Th)/He (ZHe) thermochronology coupled with U-Pb geochronology to determine the timing of exhumation of the Xigaze forearc and Kailas basins. AFT and ZHe data from twelve samples of the Kailas Formation, between Mt. Kailas to the west to the Xigaze area to the east, show Miocene cooling ($\sim 17 \pm 3$ Ma) overall younger than the depositional ages of the Kailas deposits¹ (Figure 1). ZHe data show partial resetting with the young age components being consistent with AFT ages, supporting rapid Miocene cooling¹. Preliminary double-dated (ZHe and U-Pb) zircon crystals from late Cretaceous age deposits in the Xigaze forearc also show partial resetting, but older forearc strata indicate burial to $>200^\circ\text{C}$ and cooling at $\sim 19 \pm 4$ Ma. In addition, preliminary Zircon Fission Track (ZFT) analyses suggest that burial of Xigaze forearc strata was less than 240°C .



Our results, along with previous geologic mapping, suggest that following collision in the early Cenozoic, the Xigaze forearc basin was buried by movement along the Gangdese and Great Counter Thrust systems, as well as deposition of the Kailas Formation from 26-23 Ma. Subsequent burial of the Kailas Formation from 23-17 Ma likely reflects fast subsidence and sediment accumulation related to roll back of the Indian slab. In turn, rapid cooling of both basins between 19-17 Ma is consistent with uplift associated with the return of hard collision. The rapid removal of ~4-8 km of sediment from the suture zone can be explained by efficient river incision of the paleo-Tsangpo in response to Miocene uplift¹.

References

1. Carrapa, B., Orme, D.A. , DeCelles, P.G., Kapp, P., Cosca, M. , Waldrup, R., Miocene burial and exhumation of the India-Asia collision zone in southern Tibet: response to slab dynamics and erosion, *Geology*, in press.

Cenozoic exhumation processes of the Tethyan Himalaya , revealed by sedimentology, detrital zircon U-Pb geochronology and the fission track thermochronology in the Gyirong area, southern Tibet

Shen Tianyi¹²³, Wang Guocan^{123*}, Wang An¹²³, John I. Garver⁴, Kai Cao¹²³, Chao Liu⁵,
Yanning Meng⁶

*1 State Key Laboratory of geological Process and Mineral Resources (GPMR), China
University of Geosciences, Wuhan 430074, China*

2 Center for Global Tectonics, China University of Geosciences, Wuhan 430074, China

3 School of Earth Sciences, China University of Geosciences, Wuhan 430074, China

4 Geology Department, Union College, Schenectady, NY 12308-2311, USA

*5 Liaoning Nonferrous Geological Exploration Research Institute, Shenyang 110013,
China*

6 Beijing Research Institute of Uranium Geology, Beijing 100029, China

A knowledge of Himalayan exhumation and erosion history is important to understanding the tectonic processes. The most commonly quoted time of India-Asia collision is Paleocene to Early Eocene. Until recently, most of previously thermochronological data have revealed to tectonic evolution since Miocene, possibly less than half of the orogen's history. Detrital fission track analysis from synorogenic sediments is a useful tool to find out the long-term cooling and exhumation history of convergent mountain belts. In this paper, we present a comprehensive detrital FT analysis of zircons and apatite from 9 samples from Late Miocene to Pliocene sediments in Gyirong basin, and modern rivers, and bedrock zircon FT analysis from 6 samples collected from the section across the N-S Gyirong Fault. The detrital zircon U-Pb geochronology analysis indicates that these sediments of the Gyirong basin filling mainly derived from the Tethyan Himalaya sequence and the Neogene granites around the basin. Based on the provenance analysis, our fission track results show that (a) 43-36Ma zircon grains are evidence for Eohimalayan crustal thickening and metamorphism after the collision between the Indian and Asian plate; (b) ~17Ma ZFT peak age represents the granite intrusion in Miocene; the AFT moving peak from 17 to 13Ma reflects the doming along the northern Himalaya which is associated to the detachment of STDS; (c) a slower cooling of the source zone since ~12 Ma which may be related to the ceasing of the STDS. Our data reveals the differential exhumation history between the Greater Himalaya and Tethyan Himalaya after ~17Ma, and proposes a geological evolution model of the Tethyan Himalaya during the Cenozoic.

Constraining the timing of exhumation of the Eastern Himalayan syntaxis, from a study of the palaeo-Brahmaputra deposits, Siwalik Group, Arunachal Pradesh, India

Gwladys Govin¹, Yani Najman¹, Peter van der Beek², Ian Millar³, Matthias Bernet²,
Guillaume Dupont-Nivet⁴, Jan Wijbrans⁵, Lorenzo Gemignani⁵, Natalie Vögeli²,
Pascale Huyghe²

1 Lancaster Environment Centre, Lancaster University, UK

2 Institut des Sciences de la Terre, Université Joseph Fourier, Grenoble, France

3 NERC Isotope Geosciences Laboratory, Keyworth, UK

4 Géosciences Rennes UMR-CNRS, France

5 VU University Amsterdam, Faculty of Earth and Life Sciences, Netherlands

The evolution of Himalayan syntaxes is debated: they have been subjected to anomalously young (<10 Ma) high grade metamorphism, melting and unusually high rates of exhumation (~10mm/yr), compared to the main arc of the range where peak metamorphism / melting occurred in the Early Miocene and exhumation rates of ca 2mm/yr are more common¹. The history of the young metamorphism and rapid exhumation of the eastern syntaxis is debated. Bedrock studies have been interpreted to imply rapid exhumation since either 3-4 Ma² or 8-10 Ma³. However, the earlier history of the sampled region is removed by erosion and should be preserved in the sedimentary record. Bracciali et al⁴ focused on distal detrital deposits and suggested a much more recent onset, during the Quaternary.

A number of models have been proposed to explain the syntaxial evolution, supporting different controlling influences, from lithospheric channel flow, to tectonic-surface process interactions.

Ductile extrusion of weak lower crust from beneath Tibet by “channel flow”⁵ is a process that has been proposed to account for the outward growth of the plateau to the east⁶, exhumation of the Higher Himalaya in the Miocene when coupled with high erosion rates, and could be responsible for rapid exhumation of the syntaxis⁷. Ehlers and Bendick⁸ propose that initiation of rapid and localised exhumation at subduction arc terminations may result from the 3D geometry imposed by subducting curved shells at such locations. Clark and Bilham⁹ evoke a change in regional stress along the India-Asia-Burma plate boundary, perhaps due to the introduction of denser (oceanic and transitional crust) material into the eastern part of the boundary late in the orogen’s history. Zeitler et al¹⁰ consider that exhumation of the syntaxis is driven by surface processes.

In order to understand how and why the syntaxis formed, this project aims to better constrain the onset of exhumation of the Namche Barwa using the proximal detrital record of material eroded from the syntaxis by the paleo-Brahmaputra. We analyse the sedimentary record to have access to earlier erosion products than preserved in the bedrock itself, in a proximal location. The Remi River section, in the Siwalik Group, is located directly downstream of the syntaxis and therefore is the most likely location to contain these sediments. Sediment provenance is characterized by U-Pb dating on detrital zircons, which allows specifically documenting an Indus-Yarlung suture-zone (and therefore paleo-Brahmaputra) provenance. Detrital U-Pb rutile, zircon fission track and Ar/Ar mica dating is used to document rapid exhumation. When ages of the youngest population for all analysis types are essentially the same (stacked thermochronological ages), a period of very rapid exhumation at this time is indicated.

Depositional ages are determined through magnetostratigraphic dating of the Upper and Middle Siwaliks in the Remi section. Comparison of the detrital mineral cooling ages with their host sediment depositional age will allow us to determine the lag time and then exhumation rates.

Preliminary results will be discussed; they better constrain the period of rapid exhumation history of the syntaxis and will better inform the crustal deformation models presented above.

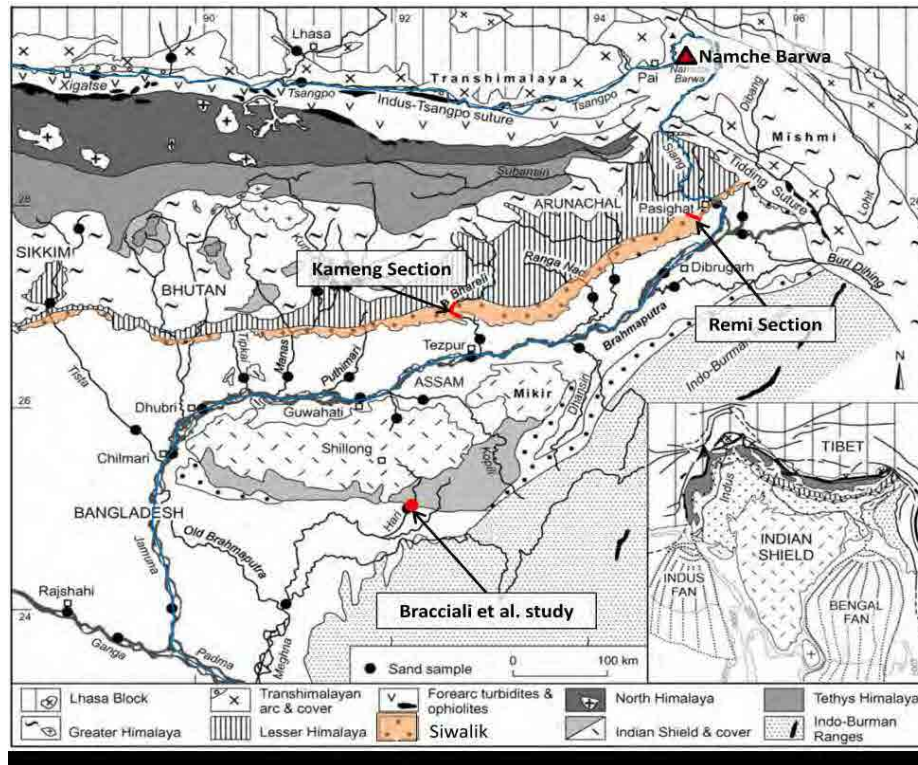


Figure 1. Geological map of the eastern syntaxis, Kameng¹¹ and Bracciali et al.⁴ study locations, after Garzanti et al. 2004¹².

References

1. Rasmus, C., Thiede, R.C., Bookhagen, B., et al. Climatic control on rapid exhumation along the Southern Himalayan Front. *Earth and Planetary Science Letters* **222** 791-806 (2004).
2. Seward, D. & Burg, J.-P. Growth of the Namche Barwa Syntaxis and associated evolution of the Tsangpo Gorge: Constraints from structural and thermochronological data. *Tectonophysics* **451**(1-4): 282-289 (2008).
3. Zeitler, P.K., Meltzer, A.S. & Brown, L. Tectonics and topographic evolution of Namche Barwa and the easternmost Lhasa Block. Towards and improved understanding of uplift mechanisms and elevation history of the Tibetan Plateau. *GSA Special Paper* (in press).
4. Bracciali, L., Parish, R., Najman, Y. et al. Using Detrital Zircon, Rutile and White Mica Chronometry to Constrain Exhumation and Provenance of the Brahmaputra River in the Eastern Himalaya. Abstract T33C-2671 *AGU Fall Meeting* (2012). (Note that Plio-Pleistocene was incorrectly written in the text and has been corrected to read "Quaternary" post publication).
5. Beaumont, C., Jamieson, R.A., Nguyen, M.H., et al. Himalayan tectonics explained by extrusion of a low-viscosity crustal channel coupled to focused surface denudation. *Nature* **414**(6865) 738-742 (2001).
6. Clark, M.K. & Royden, L.H. Topographic ooze: Building the eastern margin of Tibet by lower crustal flow. *Geology* **28**(8) 703-706 (2000).
7. Booth, A.L., Chamberlain C.P., Kidd, W.S.F., et al. Constraints on the metamorphic evolution of the eastern Himalayan syntaxis from geochronologic and petrologic studies of Namche Barwa. *Geological Society of America Bulletin* **121**(3-4) 385-407 (2009).
8. Ehlers, T.A. & Bendick R. "Bottom up" subduction geometry initiation of extreme localised exhumation at orogeny syntaxes. *GSA Abstracts with Programs* **45**(7) 222 (2013).
9. Clark, M.K. & Bilham, R. Miocene rise of the Shillong Plateau and the beginning of the end for the Eastern Himalaya. *Earth and Planetary Science Letters* **269**(3-4) 336-350 (2008).
10. Zeitler, P.K., Meltzer, A.S., Koons, et al. Erosion, Himalayan Geodynamics and the geomorphology of metamorphism. *GSA Today* **January** 4-9 (2001).
11. Chirouze, F., Dupont-Nivet, G., Huyghe, P., et al. Magnetostratigraphy of the Neogene Siwalik Group in the far eastern Himalaya: Kameng section, Arunachal Pradesh, India. *Journal of Asian Earth Sciences* **44** 117-135 (2012).
12. Garzanti, E., Vezzoli, G., Andó, S., et al. "Sediment composition and focused erosion in collision orogens: the brahmaputra case". *Earth Planet. Sci. Lett* **220** 157-174 (2004).

Isotope provenance of Eastern Himalayan rivers draining to the south into India, Nepal and Bhutan.

L. Gemignani¹, J.R. Wijbrans¹, Y. Najman², P. van der Beek³, G Govin²

1 Department of Earth Sciences, Faculty of Earth and Life Sciences VU University, Amsterdam.

2 University of Lancaster, Lancaster Environmental Centre, Lancaster LA1 4YQ.

3 ISTerre, University Joseph Fourier, Grenoble, France.

The Himalayas represent a unique natural laboratory where the interactions between tectonics, erosion, climate and drainage evolution can be investigated. The purpose of this work is to understand, in collaboration with other PhD students and researchers collaborating in the iTECC Marie Curie Initial Training Network, the importance of processes involving the complex links and feedbacks between climate, tectonics and erosion.

The two syntaxes of the Himalaya (eastern and western) show anomalously fast recent exhumation compared to the rest of the Himalaya, as typified by mineral ages <10 Ma¹. Various hypotheses and models have been proposed to explain this anomaly, for example those include coupling between tectonics and erosion, such as the Tectonic Aneurism model²⁻³, which calls on ductile upwelling of weak lower crust⁴.

Understanding the timing of onset of this rapid exhumation is critical to informing these models. Bedrock studies suggest rapid exhumation since 4 Ma⁵ or maybe 10 Ma. However, detrital studies (Ar-Ar micas, ZFT), using the record of material eroded from the syntaxis and preserved in the foreland basin, show no evidence of anomalously young grains and thus rapid exhumation throughout the duration of the sedimentary succession studied⁶⁻⁷. However, both these detrital studies were conducted in regions distal to the syntaxes, and it is possible that downstream dilution may have affected the signal.

The purpose of this research is to investigate the potential effect of dilution on the detrital signal by 1) looking at how the detrital signal evolves downstream i.e. the degree to which the “young” grain signal is diluted at increasing distance from the source and 2) a comparison of ZFT and Ar-Ar mica ages from the same samples, to investigate whether there is any distinction in the dilution effect depending on mineral type. Building on the existing database, eleven samples from the Yarlung-Brahmaputra River system and from tributaries draining the Himalaya, the Arakan belt and the Shillong plateau have been collected in the Arunachal Pradesh and Assam regions of the North-east India (Figure 1). We will analyze this potentially important aspect in detail, using high-resolution dating of micas of different grain sizes. To analyze smaller and younger grains, newly developed high-sensitivity multi-collection noble-gas mass spectrometry will be used. In this way, we will determine the extent to which dilution should be taken in to account when interpreting detrital signals, and also contribute further to our knowledge of exhumation ages in the source regions.

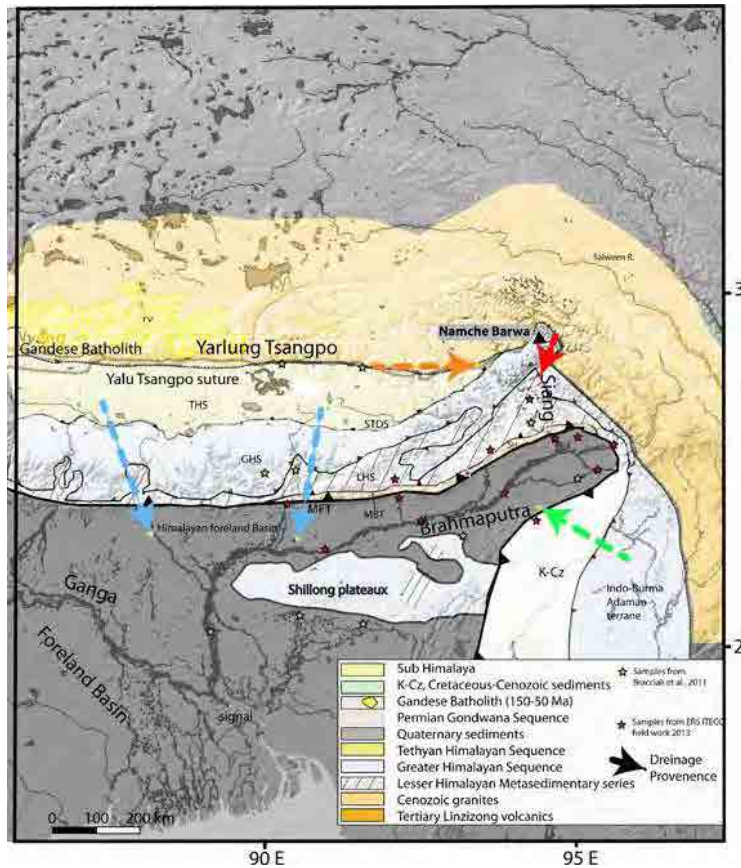


Figure 1. Geological maps Regional tectonic map showing sampled geology and location of major rivers. The red stars indicates the location of the samples collected during the fieldwork. The arrows indicates the main provenance sediments into the Yarlung Tsangpo-Bramaputra River system. (modified after Yin et al., 2010)⁵⁻⁶.

References

1. Zeitler, P.K., et al. Tectonics and topographic evolution of Namche Barwa and the easternmost Lhasa Block. Towards and improved understanding of uplift mechanisms and elevation history of the Tibetan Plateau. *GSA Special Paper* (in press).
2. Zeitler, P. K., et al. Erosion, Himalayan geodynamics, and the geology of metamorphism. *GSA Today*, **11**, 4-8. (2001).
3. Zeitler, P.K., et al. Tectonics and topographic evolution of Namche Barwa and the easternmost Lhasa Block. Towards and improved understanding of uplift mechanisms and elevation history of the Tibetan Plateau. *GSA Special Paper*. (in press).
4. Beaumont, C et al. Himalayan tectonics explained by extrusion of a low-viscosity crustal channel coupled to focused surface denudation. *Nature* **414**(6865) 738-742. (2001).
5. Seward, D. & Burg, J.-P. Growth of the Namche Barwa Syntaxis and associated evolution of the Tsangpo Gorge: Constraints from structural and thermochronological data. *Tectonophysics* **451**(1-4): 282-289 (2008).
6. Bracciali et al. Using Detrital Zircon, Rutile and White Mica Chronometry to Constrain Exhumation and Provenance of the Brahmaputra River in the Eastern Himalaya. Abstract T33C-2671 AGU fall meeting (2012) (Note that Plio-Pleistocene was incorrectly written in the text and has been corrected to read "Quaternary" post publication)
7. Chirouze, F., et al. Magnetostratigraphy of the Neogene Siwalik Group in the far eastern Himalaya: Kameng section, Arunachal Pradesh, India. *Journal of Asian Earth Sciences* **44** 117-135 (2013).

$^{40}\text{Ar}/^{39}\text{Ar}$ muscovite dating as a constraint on erosion patterns and evolution of the Yangtze River

X. Sun^{1,2}, J.R. Wijbrans¹, Changán.Li², Klaudia F. Kuiper¹,

1 Department of Earth Sciences, VU University Amsterdam, De Boelelaan 1085, 1081 HV Amsterdam, The Netherlands

2 Faculty of Earth Sciences, China University of Geosciences, Wuhan, 430074, China

The intense erosion and complex river systems in the eastern Tibetan Plateau have attracted considerable attention. However, the large-scale picture of the erosion pattern in this area is not yet resolved. Moreover, the evolution of the river systems in the eastern Tibetan Plateau should be taken into account when researching the Myr-scale long-term erosion, because the configuration of the drainage network affects the distribution of erosion.

Here, we report $^{40}\text{Ar}/^{39}\text{Ar}$ results of detrital muscovite grains from river sediments of the major tributaries of the Yangtze River and older samples from a core (the depth up to 300m, spanning at least 3Ma) in the Jiangnan Basin, middle reaches of the Yangtze River. Mica age distribution patterns in the Three Gorges and the Yangtze Delta¹ match well with that of the Min River (6-142Ma) which originates from the Longmen Shan orogenic belt. This indicates that the sediment reaching the Yangtze Delta is dominated by sources derived from the Longmen Shan and that this region is experiencing rapid erosion. The ages of the top and bottom of the core show different age populations, suggesting these sediments have different source areas. This is strengthened by the fact that muscovite from the bottom and top of the core have different chemical compositions. This change in provenance could be caused by the extension of the Yangtze River from the lower Yangtze River basin into the Sichuan Basin. From the magnetostratigraphic framework of the core, we suggest the capture event that the lower Yangtze River extended to the Sichuan Basin happened around ca 2- 3Ma.

References

1. van Hoang, L., Clift, P.D., Mark, D., Zheng, H.B., Mai, T.T. Ar–Ar muscovite dating as a constraint on sediment provenance and erosion processes in the Red and Yangtze River systems, SE Asia. *Earth and Planetary Science Letters* 295, 379–389 (2010).

Constraining the vertical tectonic movements in southern South China by multi-system geo-/thermochronology

Ni Tao¹, Zheng-Xiang Li¹, Martin Danišik², Noreen J. Evans³, Geoffrey E. Batt⁴, Wu-Xian Li⁵, Chong-Jin Pang¹, Fred Jourdan⁶, Yi-Gang Xu⁵,

1 ARC Centre of Excellence for Core to Crust Fluid Systems (CCFS) and the Institute for Geoscience Research (TIGeR), Department of Applied Geology, Curtin University, GPO Box U1987, Perth, WA 6845, Australia

2 Department of Earth and Ocean Sciences, Faculty of Science and Engineering, The University of Waikato, Private Bag 3105, Hamilton 3240, New Zealand

3 John de Laeter Centre for Isotope Research, Department of Applied Geology, Curtin University of Technology, GPO Box U1987, Perth, WA 6845, Australia

4 Centre for Exploration Targeting and School of Earth and Environment, The University of Western Australia, Perth, WA 6009, Australia

5 State Key Laboratory of Isotope Geochemistry, Guangzhou Institute of Geochemistry, Chinese Academy of Sciences, Guangzhou 510640, China

6 Western Australian Argon Isotope Facility, John de Laeter Centre for Isotope Research and Department of Applied Geology, Curtin University, GPO Box U1987, Perth, WA 6845, Australia

The thermal history of the Daxi region in southern South China records a complicated tectonic evolution of the paleo-Pacific plate margin since the Mesozoic. In this study, we applied a combination of zircon U-Pb, mica ⁴⁰Ar/³⁹Ar, zircon and apatite fission track and (U-Th-Sm)/He dating methods to basement and sedimentary cover rocks in order to constrain timing and rate of the major cooling events. This allows us to address the questions related to geodynamic processes of the flat-slab subduction¹, delamination of the subducting slab and rebound of the overriding slab.

The ⁴⁰Ar/³⁹Ar age of ca. 193 Ma measured on biotite from a granite records the reinitiation of magmatic activity after the Late Triassic – Early Jurassic period of magmatic quiescence. We measured middle Jurassic muscovite ⁴⁰Ar/³⁹Ar age (ca. 167 Ma) in an Upper Triassic granite. This age is interpreted as to reflect a heating event related to the emplacement of Middle Jurassic intrusions generated in an extensional setting. The biotite ⁴⁰Ar/³⁹Ar age of ca. 160 Ma revealed by a Upper Jurassic granite records a rapid cooling following the intrusion, implying ongoing extension.

Zircon fission track and zircon (U-Th-Sm)/He data from all dated samples range from ca. 150 to ca. 75 Ma. This age range records protracted cooling through the 270–160 °C temperature range during Late Jurassic to Cretaceous times. This late Mesozoic cooling, which is supported by inverse modelling results, is likely linked to exhumation caused by lithospheric rebound during slab break-off and associated uplift and erosion. A final cooling episode during the Eocene, recorded by apatite fission track and apatite (U-Th-Sm)/He ages of ca. 53–42 Ma, is related to Cenozoic rifting across southern South China induced by the roll-back of the Paleo-Pacific plate.

References

1. Li, Z. X. & Li, X. H. Formation of the 1300-km-wide intracontinental orogen and postorogenic magmatic province in Mesozoic South China: A flat-slab subduction model. *Geology* **35**, 179-182, (2007).

Tectonic evolution of the Unegt-Zuunbayan basin (SE Mongolia) constrained by apatite fission track and (U-Th)/He thermochronology

Anna Giné¹, Bertrand Saint-Bézar¹, Antonio Benedicto², Jocelyn Barbarand¹, Cécile Gautheron¹, Remi Leprêtre¹, Rosella Pinna¹

1 Geosciences Paris Sud (GEOPS, UMR 8148), Université Paris Sud XI- Orsay, France

2 AREVA Mines, France

The Unegt-Zuunbayan basin, East Gobi Basin (SE Mongolia), recorded complex tectonic history since the Paleozoic to the present^{1, 2, 3}. After Paleozoic accretionary tectonics, the East Gobi Basin followed a large scale intracontinental rifting event during the Mesozoic. A post rift basin inversion led to erosion and regional-scale unconformity development during the late Early Cretaceous. A second basin inversion related to the Indo-Asian collision deformed the Upper Cretaceous post rift detrital infill during Tertiary. Actually, the area is composed by two sub basins, the northern Unegt and the southern Zuunbayan, separated by the crustal scale Zuunbayan fault. We present the recent results from an ongoing study focused on constraining the tectonic evolution of the Unegt-Zuunbayan basins. Timing and significance of tectonic events allow a better understanding of the development of hydrocarbon and sandstone-type uranium deposits present in these basins. Apatite fission track (AFT) and (U-Th)/He (AHe) analysis were carried out on the basement and the post-rift detrital infill samples. We collected four basement samples from the northern and the southern basin boundary outcrops, and from the basement cropping out along the Zuunbayan fault. The six sand samples of the Upper Cretaceous Sainshand Formation came from drill-cores of both sub basins.

Basement samples gave AHe ages ranging from 73±7 to 120±11 Ma and AFT ages ranging from 128±8 Ma to 255±17 Ma; the mean track lengths varies from 11.92±1.89 to 12.26±1.78 μm. Thermal modelling of AHe and AFT data using QTQt software⁴ reveal the existence of a Lower Cretaceous heating coeval with the rifting for the central basin outcrop, followed by a general and rapid cooling at the end of the Lower Cretaceous. These results reveal a denudation event of ~1km related to the first basin inversion and a minor impact of the Tertiary inversion. A fourth basement sample collected in the southern border shows Lower Cretaceous AHe and AFT ages coeval to the measured U/Pb zircon age, suggesting a syntectonic origin of this intrusion during the early rift stage, and thus involving a high strain deformation along the southern boundary faults. The sedimentary samples gave distinct AFT age populations showing that the Upper Cretaceous basin fill did not reach the temperature needed to affect significantly the AFT system. It can be then assumed that the AFT ages correspond to the inherited source age. The younger AFT, very close to the stratigraphic age, implies rapid uplift and denudation of the first inversion reliefs.

This study evidences a rift related thermal event and a late Lower Cretaceous uplift and denudation during the first basin inversion. There is no evidence of tertiary thermal anomaly which suggest that the second basin inversion did not imply important uplift and erosion.

References

1. Sengör A.M.C., Natal'in B.A., 1996. Paleotectonic of Asia: fragments of a synthesis. In: Yin A, Harrison TM (eds) *The Tectonic Evolution of Asia*. Camb Univ Press, Camb, pp 486-640
2. Graham, S.A., Hendrix, M.S., Johnson, C.L., Badamgarav, D., Badarch, G., Amory, J., Porter, M., Barsbold, R., Webb, L.E., and Hacker, B.R., 2001. Sedimentary record and tectonic implications of Mesozoic rifting in southeast Mongolia. *Geological Society of America Bulletin*, v. 113, p. 1560-1579
3. Johnson, C.L., 2004. Polyphase evolution of the East Gobi basin: Sedimentary and structural records of Mesozoic-Cenozoic intraplate deformation in Mongolia. In: *Basin Research* 16, 79-99
4. Gallagher, K (2012) Transdimensional inverse thermal history modeling for quantitative thermochronology, *J. Geophys. Res.*, 117

Transient thermal events in response to the central Asia mantle plume in the Tarim Basin, Northwest China: Evidence from zircon (U-Th)/He thermochronology

Caifu Xiang^{1,2}, Brent I.A. McInnes^{3,4}, Noreen J. Evans³, and Martin Danišik^{3,4,5}

1 State Key Laboratory for Petroleum Resource and Prospecting, China University of Petroleum, Beijing 102249, China

2 College of Geosciences, China University of Petroleum, Beijing 102249, China

3 John de Laeter Center for Mass Spectrometry, Applied Geology, Curtin University, Perth 6152, Australia

4 CSIRO Earth Science and Resource Engineering, ARRC, Kensington 6151, Australia

5 Department of Earth and Ocean Sciences, The University of Waikato, Private Bag 3105, Hamilton 3240, New Zealand

Transient thermal events in response to Permian volcanism and Triassic fluid flow have been recognized by apatite and zircon fission track thermochronology in the central uplift zone of the Tarim Basin, Northwest China¹. Whether the events happened in a local or a basin wide scale need to be answered. Samples from the Jurassic formation (five samples) and the underlying Silurian to Triassic formation (eight samples) were selected from the hydrocarbon exploration wells that lined along an EW striking profile. Taking the present day thermal gradient (2.5 °C/100 m) and the burial depth (deepest burial depth of 4300 m) into consideration, the present burial temperature of the samples (<120 °C) is much lower than the helium closure temperature of zircon. Thus, basin scale transient thermal events during Permian to early Triassic period can only be recorded by samples that are underlying Jurassic formation. Zircon (U-Th)/He (ZHe) Ages of the Jurassic samples fall within late Triassic (218.6±8.1 Ma) to early Silurian (398.3±8.1 Ma), and thus are older than their depositional ages. However, ZHe ages of the underlying formation are changing laterally with increasing distance to the centre of the Permian volcanism and can be divided into three circles. ZHe ages of the samples from within the range of Permian volcanism fall between middle Triassic (oldest age of 243.7±11.0 Ma from a Carboniferous sample) and early Jurassic (youngest age of 172.7±6.4 Ma from a Silurian sample). Early Permian (oldest age of 288.6±10.4 Ma from a Devonian sample) to early Triassic (youngest age of 197.9±7.0 Ma from a Devonian sample) were found in the middle circle that lies within the radius of 150 km to the border of Permian volcanism. ZHe ages that are both older and younger than their depositional ages were found in the outer circle. All the samples from the inner and middle circles show ZHe ages that are younger than their depositional ages, indicating post depositional total resetting of the ZHe system. Histogram of the ZHe age data suggests two main populations of 240-280 Ma (middle - late Permian) and 180-220 Ma (late Triassic - early Jurassic). The former correlates with the plume-related basalt eruption dated at 260- 290 Ma. The early Triassic age is interpreted to record the transient thermal effect of localized hydrothermal fluid flow in the Tarim Basin.

This work was supported by the National Natural Science Foundation of China (Grant No.: 40872097; 41272161) and the Major National Science & Technology Program (Grant No.: 2011ZX05007-002).

References

1. Xiang, C.F., Pang, X.Q., Danišik, M. Post-Triassic thermal history of the Tazhong Uplift Zone in the Tarim Basin, Northwest China: Evidence from apatite fission-track thermochronology. *Geoscience Frontiers*, **4(6): 743-754** (2013).

The interior of Gondwana: A Mesozoic Antarctic Basin System

Frank Lisker¹, Andreas L. Läufer²

1 Department of Geosciences, University of Bremen, Germany

2 Federal Institute for Geosciences and Natural Resources, Germany

The Mesozoic geological evolution of Gondwana is characterised by the formation of enormous sedimentary basins that are still preserved in Africa, India, Australia, and South America. Only the heart of Gondwana, Antarctica, yields little evidence of sediment deposition at this time. Triassic/Jurassic terrestrial strata of very limited extent are known merely from some locations in the Ross and Weddell Sea regions and Prydz Bay, whereas Cretaceous and Paleogene sediments are restricted to the Antarctic Peninsula.

The geological history of the Gondwana interior can only be assessed by combining thermochronological and geophysical data, and kinematic, thermal and geomorphological indicators. Numerous studies conducted during the last two decades, mainly from the Transantarctic Mountains, produced a comprehensive data set of >500 apatite fission track and (U-Th-Sm)/He ages between ~20 and ~350 Ma, with the bulk of ages being younger than 100 Ma¹. These data were traditionally interpreted in terms of monotonous cooling and referred to stepwise exhumation and uplift of the Antarctic rift structures and passive margins since Jurassic times. However, many of the thermochronological data were obtained from basement rocks that are covered by volcanic rocks extruded at ~180 Ma². Such a crossover relationship between stratigraphic information and thermochronological age data implies heating of the Jurassic surfaces to temperatures in excess of 100°C. Supplementary petrographic and geochronological analyses also indicate elevated post-Jurassic paleotemperatures, with diachronous thermal peaks³.

Thermal history modelling of the thermochronological data requires substantial burial of the now exposed rocks, and refers to heterogeneous heat flow. Our approach allowed us to identify a whole system of Jurassic–Paleogene sedimentary basins throughout the Transantarctic Mountains, in Dronning Maud Land, Marie Byrd Land, Mac.Robertson Land, and the Shackleton Range. Other basins, such as the Wilkes Subglacial Basin and the Aurora Through, have been recognized from geophysical data. The development of the Mesozoic – early Cenozoic Antarctic depocentres is obviously related to intracontinental extension within Gondwana that eventually led to the dispersal of the supercontinent. These Antarctic basins all correlate with counterparts of the once juxtaposed Gondwana fragments, and represent a crucial tool for reconstructing continental breakup processes and the long-term climate evolution.

References

1. Lisker, F. Review of fission track studies in northern Victoria Land – Passive margin evolution versus uplift of the Transantarctic Mountains. *Tectonophysics* **349**, 57-73 (2002).
2. Lisker, F. & Läufer, A. L. The Cretaceous Victoria Basin between Australia and Antarctica. *Geology* **41**, 1044–1046 (2013).
3. [1] Prenzel, J., Lisker, F., Elsner, M., Schöner, R., Balestrieri, M.L., Läufer, A., Berner, U. & Spiegel, C. Burial and exhumation of the Eisenhower Range, Transantarctic Mountains, based on thermochronological, maturity and sediment petrographic constraints. *Tectonophysics* TECTO-S-13-00913 (accepted).

Session 7:

New quantitative tools and approaches in geomorphology

Production and diffusion of cosmogenic noble gases: Using open-system behavior to study surface processes

David L. Shuster^{1,2}, Marissa M. Tremblay^{1,2}, Greg Balco²

1 *Department of Earth and Planetary Science, University of California, Berkeley, USA*

2 *Berkeley Geochronology Center, USA*

We present a new geochemical technique to quantify past temperatures and surface exposure histories on Earth and, in principle, other planetary surfaces over timescales of $\sim 10^3$ to $>10^6$ years. The technique is based on the simultaneous production and diffusion of cosmogenic noble gases, which are produced in rocks and sediments exposed near Earth's surface by nuclear reactions induced ultimately by cosmic rays. This method takes advantage of "open-system" behavior that has previously been viewed only as an undesirable obstacle to surface exposure dating. However, if properly understood, such behavior also contains potentially rich information on near surface temperatures and exposure histories that have yet to be exploited. Given knowledge of diffusion kinetics, the relative abundance of cosmogenic ^3He , ^{21}Ne and other cosmogenic nuclides in mineral samples provides a record of their integrated temperature histories during residence near Earth's surface. This technique should quantify past temperatures and exposure histories of surface materials that can inform a broad range of scientific research. First, measuring exposure durations of surface rocks is important for understanding geologic processes that modify Earth's surface, including surface erosion, sediment transport, and earthquake-related surface deformation. Second, measuring past temperatures is important for understanding Earth's natural climate variability during the last few million years. For example, such information is important to establish how past changes in environmental conditions influenced biota at various regions across the globe, and how past climate changes were potentially controlled by natural phenomena such as the gradual development of mountain ranges. However, our ability to quantify past temperatures is currently limited to a small number of geochemical techniques. This new method could provide an independent test of existing methods, and potentially benefit a broad range of research sub disciplines, including quantitative geomorphology, landscape evolution studies, late Cenozoic climate change, glacier and ice sheet change, and potentially paleo-elevation of actively uplifting landscapes. In principle, the theory and mathematics of production and diffusion that have been successfully applied to radiogenic noble gases in minerals^{1,2} and references therein can also be applied to cosmogenic noble gases. Important differences are in (i) the depth over which cosmogenic nuclides are produced (i.e., mostly within meters of the surface), (ii) the different nuclide-mineral pairs involved, and (iii) the potential for production rate changes (i.e., in contrast to steady parent nuclide decay rates). When interpreted with a simple theoretical framework, our preliminary experimental results³⁻⁵ indicate several pairs of common minerals and easily measureable cosmogenic noble gases that display open-system behavior at Earth surface temperatures [Figure 1; i.e., between -40 °C to $+40$ °C depending on the mineral and grain size]. Importantly, both axes in Figure 1 are observable, such that the mean temperature during a sample's surface exposure is constrained by the observables. These potentially provide a set of nuclide-mineral systems that can be selected and optimized for a broad range of research questions, climate settings, and lithologies. An attractive aspect of this method is that different isotope and mineral pairs, along with different crystal/grain sizes, can be selected to optimize temperature sensitivity for a particular problem. In addition, multiple mineral systems, and likewise multiple combinations of mineral system and diffusion domain size, can provide tests for internal consistency and validation of assumptions.

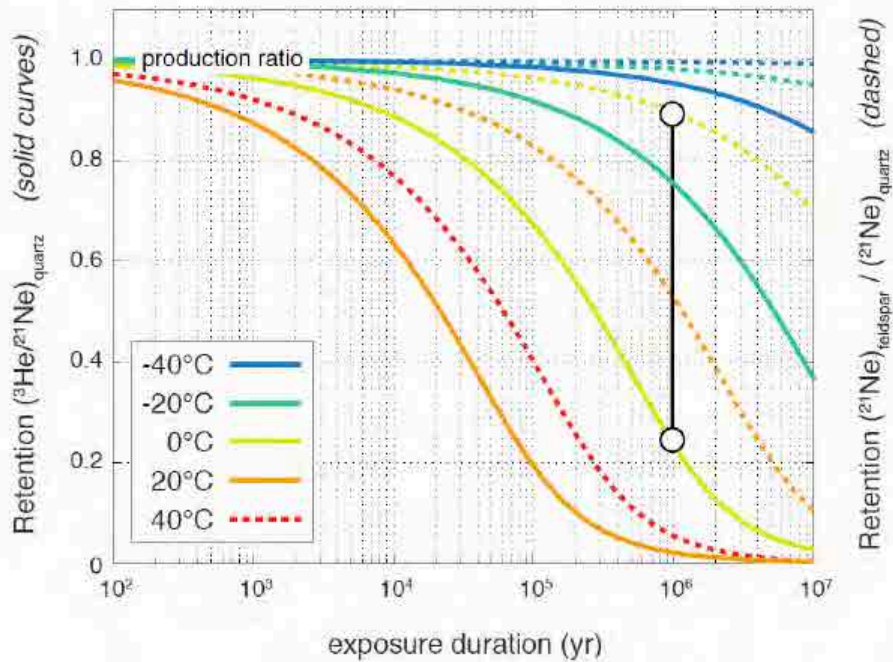


Figure 1. Retention of cosmogenic ^3He and ^{21}Ne expressed as a function of exposure duration and temperature. Calculated ratios of $^3\text{He}/^{21}\text{Ne}$ in quartz (solid curves; $a=5\text{mm}$) and $^{21}\text{Ne}_{\text{feldspar}}/^{21}\text{Ne}_{\text{quartz}}$ (dashed curves; $a=0.1\text{mm}$) are normalized to the production ratio (i.e., quantitative retention =1) using diffusion kinetics of He and Ne in gem quality quartz (Shuster and Farley, 2005), and Ne in plagioclase feldspar (Gourbet et al., 2012). The two white points show predictions for a sample exposed for 1 Ma at 0 °C. Because all axes are observable, the mean temperature during exposure can be determined; co-existing phases provide tests for internal consistency.

As a test of this method's validity, we present results from quartz-bearing Antarctic sandstones and a rhyolitic ignimbrite from Peru, each with simple Holocene exposure histories. For the Antarctica samples, if we assume that ^3He diffusion kinetics in quartz⁴ applies and normalize to the local production rate, exposure duration and grain size, the observed ^3He concentrations correspond to an effective diffusion temperature of approximately -15 °C over 5-10 ka of surface exposure, as determined by cosmogenic ^{10}Be concentrations measured in the same samples. For the sample from Peru, a production and diffusion model incorporating sample-specific diffusion parameters and the measured ^3He abundance predicts an effective exposure temperature consistent with the mean modern temperature at the sample location. This internal consistency demonstrates that the empirically-determined, sample-specific diffusion kinetics apply to cosmogenic ^3He and ^{21}Ne in quartz in natural settings over geologic timescales. Quantitative applications of this method may require quantification of diffusion kinetics for individual samples of interest.

References

1. McDougall, I. & Harrison, T. M. Geochronology and Thermochronology by the $^{40}\text{Ar}/^{39}\text{Ar}$ Method. (Oxford University Press, USA, 1999).
2. Reiners, P. W., Ehlers, T. A. & Zeitler, P. K. Past, present, and future of thermochronology. *Reviews in Mineralogy and Geochemistry* 58, 1-18 (2005).
3. Gourbet, L. et al. Neon diffusion kinetics in olivine, pyroxene and feldspar: Retentivity of cosmogenic and nucleogenic neon. *Geochimica et Cosmochimica Acta* 86, 21-36 (2012).
4. Shuster, D. L. & Farley, K. A. Diffusion kinetics of proton-induced ^{21}Ne , ^3He , and ^4He in quartz. *Geochimica et cosmochimica acta* 69, 2349-2359 (2005).
5. Tremblay, M. M., Shuster D. L., Balco, G.. Diffusion kinetics of ^3He and ^{21}Ne in quartz and implications for cosmogenic noble gas paleothermometry. *Geochimica et Cosmochimica Acta* In Review (2014).

Paleo-denudation rates at the Plio-pleistocene transition: a cosmogenic nuclides perspective from Asia

Pierre-Henri Blard¹, Julien Charreau¹, Nicolas Puchol¹, Raphaël Pik¹, Jérôme Lavé¹, Didier Bourlès², Régis Braucher²

1 - CRPG-CNRS, Université de Lorraine, Vandoeuvre-lès-Nancy, France

2 - CEREGE-CNRS, Aix Marseille Université, Aix-en-Provence, France

Denudation is a key factor for the evolution of the Earth's surface since this process may induce several feedbacks between tectonics and climate. Notably, denudation is supposed to impact climate, by increasing the sequestration of atmospheric CO₂ into the ocean¹. However, the long-term evolution of denudation rates still remains a matter of debate. Indeed, several authors² proposed that the onset of Quaternary glaciations was associated with a climatic change that led to a significant increase of worldwide denudation, about ~3 Ma. This increase is nevertheless established from sediment budgeting from various basins, a method which can suffer from severe flaws. Moreover a recent study based on the long-term oceanic record of the ⁹Be/¹⁰Be ratio on the contrary suggested that the global weathering rates remained stable over the last 10 Ma³.

There is thus crucial need for unequivocal records of the long-term evolution of continental denudation, particularly at the onset of Quaternary glaciation.

We present here an innovative approach based on the analyses of in situ produced cosmogenic ¹⁰Be in independently dated ancient sediments. A pioneer study carried out in the Northern Tianshan (Central Asia) suggested that a transient increase in denudation rate occurred in this watershed between 4 and 2 Ma⁴. To go further these preliminary results, we present here new cosmogenic paleo-denudation records from four different locations: three new records from both sides of the Tianshan range and one record from the Surai river, in the southern Siwalik piedmont of the Himalayas. All these records display local and sometimes significant variations of denudation rates since ~10 Ma. Although some of these variations may result from local tectonic forcing or changes in the watershed geometry, the synthetic record indicates a long term and progressive increase in denudation rates between 10 and 3 Ma. Between 3 Ma and present, the denudation rates have remained constant. These results suggest that the onset of Quaternary glaciations had only a limited impact on the denudation rates in the Northern Hemisphere, the erosion increase being lower than to a factor of two at the Cenozoic-Quaternary transition, 3 Ma.

The method uncertainty can be significantly reduced combining independent constraints, notably by estimating the accumulation rate from magnetostratigraphy and paleoelevation from oxygen and carbon isotopic records.

References

1. M. E. Raymo and W. F. Ruddiman, *Nature* 359 (6391), 117 (1992).
2. P. Z. Zhang, P. Molnar, and W. R. Downs, *Nature* 410 (6831), 891 (2001); W. W. Hay, J. L. Sloan, and C. N. Wold, *Journal of Geophysical Research - Solid Earth And Planets* 93 (B12), 14933 (1988).
3. J. K. Willenbring and F. von Blanckenburg, *Nature* 465 (7295), 211 (2010).
4. J. Charreau, P.-H. Blard, N. Puchol et al., *Earth and Planetary Science Letters* 304 (1-2), 85 (2011).

OSL-Thermochronometry: observations, theory, and applications

Benny Guralnik¹, Pierre G. Valla^{1,2}, Frédéric Herman²

1 Department of Earth Sciences - ETH Zurich, Switzerland

2 Institute of Earth Surface Dynamics - University of Lausanne, Switzerland

Optically stimulated luminescence (OSL) is a Quaternary dating method used to estimate the last exposure of target minerals to sunlight, commonly quartz and feldspar grains^{6,8}. OSL ages are typically interpreted as deposition ages of the corresponding sedimentary units. However, the typically low thermal stability of various luminescence signals can also be utilized to interpret bedrock OSL ages as cooling ages¹. A recent introduction of OSL⁵ proposed that this method would allow studying the very last stages of rock exhumation on previously unexplored temporal and thermal scales (i.e. focusing on the late Quaternary period). Here, we report recent results on the characterization and calibration of feldspar OSL as a low-temperature thermochronometer:

1. In a tectonic setting where the crustal thermal regime has been stable on a timescale of >10 Ma (KTB borehole, Germany), a strong dependence of feldspar infrared stimulated luminescence (IRSL₅₀) with depth (12 depth samples uniformly covering the 10-70 °C range) has been both observed and successfully modeled using laboratory-derived kinetic parameters⁴. Specifically, the proposed kinetic model (whose parameters have been calibrated on a sample-to-sample basis using standard laboratory protocols), has been used to predict the observed IRSL₅₀ intensities for a given set of storage borehole temperatures, and to successfully invert observed intensities into an effective paleo-geotherm (with a goodness of fit of $R^2 > 0.97$ for both forward and inverse models). Falling within the errors of its present-day estimates, such paleo-geotherm (averaged over 10-100 ka timescales) highlights the potential of feldspar IRSL₅₀ in geothermal prospecting, and in other potential fields where recent thermal perturbations of the shallow crust play an important role.

2. We have generalized Dodson's closure theory² to account for arbitrary thermal boundary conditions³. The resulting generalized formula for closure temperature (equally applicable to standard and luminescence thermochronometers) is particularly crucial for OSL systems, where the storage space for the radiogenic product is physically limited. Our formulation allows to interpret any thermochronometric system which is prone to attain an apparent steady-state during its final stages of cooling. Analysis of the thermal stability of feldspar IRSL₅₀ reveals that its application is restricted to only extremely high cooling rates (>300 °C Ma⁻¹), below which IRSL₅₀ can be expected to be found in field steady-state.

3. Targeting an exhumation/cooling rates range across ~2 orders of magnitude, surface bedrock samples from various mountain ranges (Alaska, Norway, Pamir and Himalaya) have been collected and processed in a similar manner to the borehole calibration study. Most feldspar IRSL₅₀ signals appear to be in field steady-state and dominated by athermal loss⁷, reflecting this particular signal's insensitivity to typical bedrock cooling rates. Thermally-reset outliers correlate with a major fault shear zone, and could suggest resetting due to fault shear-heating or hydrothermal activity⁹. We are currently investigating other mineral-signal pairs, where the combination of lower thermal stability and later saturation characteristics could suggest radiometric closure at very low temperatures.

References

1. Daniels, F., Boyd, C. A. & Saunders, D. F. Thermoluminescence as a research tool. *Science*, **117**, 343-349 (1953).
2. Dodson, M.H. Closure temperatures in cooling geochronological and petrological systems. *Contributions to Mineralogy and Petrology*, **40**, 259-274 (1973).
3. Guralnik, B., Jain, M., Herman, F., Paris, R.B., Harrison, T.M., Murray, A.S., Valla, P.G. & Rhodes, E.J. Effective closure temperature in leaky and/or saturating thermochronometers. *Earth and Planetary Science Letters*, **384**, 209-218 (2013).
4. Guralnik, B., Jain, M., Murray, A. S., Valla, P. G., Ankjærgaard, C., Lowick, S. E., Preusser, F., Chen, R., Kook, M. H., Rhodes, E. J., Herman, F. A novel luminescence thermochronometer for reconstructing near-surface thermal

histories (in revision).

5. Herman, F., Rhodes, E.J., Braun, J. & Heiniger, L. Uniform erosion rates and relief amplitude during glacial cycles in the Southern Alps of New Zealand, as revealed from OSL-thermochronology. *Earth and Planetary Science Letters*, **297**, 183-189 (2010).
6. Huntley, D. J., Godfrey-Smith, D. I., Thewalt, M. L. Optical dating of sediments. *Nature*, **313**, 105-107 (1985).
7. Huntley, D.J. & Lamothe, M. Ubiquity of anomalous fading in K-feldspars and the measurement and correction for it in optical dating. *Canadian Journal of Earth Sciences*, **38**, 1039-1106 (2001).
8. Hütt, G., Jaek, I. & Tchonka, J. Optical dating: K-feldspars optical response stimulation spectra. *Quaternary Science Reviews*, **7**, 381-385 (1988).
9. Ikeya, M., Miki, T., & Tanaka, K., Dating of a fault by electron spin resonance on intrafault materials. *Science*, **215**, 1392-1393 (1981).

Quantifying global erosion from thermochronometric data

Frédéric Herman

Institute of Earth Surface Dynamics, University of Lausanne

There is an on-going debate on the effect of climate on erosion efficiency and, in particular, whether the cooling of the Earth's climate during the Late Cenozoic has led to enhanced erosion of mountain belts, as suggested (or not) by conflicting evidence from the sedimentary record^{1,2}. Unlike sediment accumulation budgets, which are subject to many assumptions on transport and deposition, thermochronometry provides a first order unbiased estimate of erosion in the bedrock source regions.

I will present how erosion rates from the source areas that produce the sediment record at a Myr timescale were recently quantified using low-temperature thermochronometry³. We have compiled about 18,000 bedrock fission and (U-Th)/He data from around the world and used a formal inversion procedure⁴ to quantify temporal and spatial variations in erosion rates. Results identify a robust increase in erosion rates in mountain ranges since ca. 6 Myr ago and most rapidly since 2 Ma. The effect is most pronounced in glaciated mountain ranges, indicating that glacial processes played a significant role. Because the production of sediments is largely dominated by mountains compared to lowland continental areas, our results imply an increase of sediment fluxes at a global scale that tightly coincides with enhanced cooling during the Plio-Pleistocene.

The observed increase in erosion rates also appears to reach a maximum at mid-latitudes^{3,5}. Although it seems clear that such latitudinal variations were related to climate, the processes responsible for adjustments in glacial erosion remain uncertain. I will present more detailed results on the Patagonian Andes (Herman and Brandon, submitted). The nearly 2000 km meridional extent of the Patagonian Andes provides a unique opportunity to establish the long-term relationship between climate and erosion. By exploiting its latitudinal distribution one can investigate the role climate played on modulating glacial erosion rates through time. From the inversion of compiled thermochronometric data, erosion rates appear to have been higher in the northern regions, peaking about 44°S during the last 2 Myr. The position of this maximum coincides with the location of maximum precipitation that follows the southern hemisphere Westerlies during glacial maxima. I will show that such increased precipitation rates about 44°S lead to enhanced ice flux, ice sliding velocity and, in turn, higher glacial erosion rates. These results suggest that the migration of westerly winds belts toward the equator since 2 to 3 Myr ago played an important role on setting the distribution of mountain erosion on Earth.

These studies reveal that the increasing amount of thermochronological data allowed us to move from local, to regional and global studies. More importantly, they seem to help image the effect of climate on erosion, to extent that could not be reached with other proxies, such sedimentation accumulation curves.

References

1. Zhang, P., Molnar, P., & Downs, W. R. Increased sedimentation rates and grain sizes 2-4 Myr ago due to the influence of climate change on erosion rates. *Nature*, **410**, 891–897 (2001).
2. Willenbring, J. K., & von Blanckenburg, F. Long-term stability of global erosion rates and weathering during late-Cenozoic cooling. *Nature*, **465**, 211–214 (2010).
3. Herman, F., Seward, D., Valla, P. G., Carter, A., Kohn, B., Willett, S. D., & Ehlers, T. A. Worldwide acceleration of mountain erosion under a cooling climate. *Nature*, **504**, 423–426 (2013).

4. Fox, M., Herman, F., Willett, S. D., & May, D. A. A linear inversion method to infer exhumation rates in space and time from thermochronometric data. *Earth Surface Dynamics*, **2**, 47–65 (2014).
5. Champagnac, J.-D., Valla, P. G., & Herman, F. Late-Cenozoic relief evolution under evolving climate: A review. *Tectonophysics*, **614**, 44–65, doi:10.1016/j.tecto.2013.11.037 (2014).

Numerical modeling and quantification of surface and tectonic processes combined with low-temperature thermochronological data in southeastern Brazil

Victor Sacek¹, Isabela O. Carmo², Barry P. Kohn³, Paulo M. Vasconcelos⁴

1 IAG - Universidade de São Paulo, Brazil

2 CENPES - Petrobras, Brazil

3 University of Melbourne - School of Earth Sciences, Australia

4 University of Queensland - School of *Earth Sciences*, Australia

Over the last few decades different mechanisms have been proposed to explain the elevated present day topography of southeastern Brazil¹⁻⁴, which locally attains elevations >2 km. To evaluate some of these mechanisms, we numerically simulated the post-rift evolution of the margin coupling surface and tectonic processes. This model takes into account the flexural behavior of the lithosphere, the thermal evolution of the mantle and the surface processes of erosion and deposition⁵.

The landscape evolution and the exhumation history obtained from the numerical simulations are used to retrieve the thermal history of particles at the top of the basement, using a numerical model based on the software Pecube⁶. We compared the thermal histories retrieved by the numerical models with those obtained from apatite fission track (AFT) and (U-Th)/He data along transects orthogonal to the coast in different parts of the southeastern Brazilian rifted continental margin, from Vitória to São Paulo (Carmo et al., in preparation and ref. 3). These datasets show a systematic increase of AFT age from ~49 Ma (coast) up to ~178 Ma (inland).

To quantify the influence of each process in the exhumation history of the margin we tested different geotectonic scenarios, taking into account flexural rebound of the lithosphere due to rifting, magmatic underplating, post-rift reactivation of pre-existing faults, thermal anomalies at the base of the lithosphere and variable climatic conditions. We demonstrate that the present day topography and the exhumation history predicted by thermochronological data can be explained without invoking pronounced regional post-rift uplift of the margin. We observed that periods of generalized fast cooling rate retrieved from the thermochronological data could be related to climate variability. Furthermore, we conclude that the reactivation of pre-existing faults resulted in local increase of the observed cooling rate and, therefore, cannot explain the regional cooling pattern observed from thermochronological data in southeastern Brazil.

References

1. Gallagher, K., Hawkesworth, C. J., & Mantovani, M. S. M. The denudation history of the onshore continental margin of SE Brazil inferred from apatite fission track data. *Journal of Geophysical Research*, **99**, 18117-18145 (1994).
2. Zalán, P., & Oliveira, J. Origem e evolução estrutural do Sistema de Riftes Cenozóicos do Sudeste do Brasil. *Boletim de Geociências da PETROBRÁS*, **13**, 269-300 (2005).
3. Cogné, N., Gallagher, K., Cobbold, P. R., Riccomini, C., & Gautheron, C. Post-breakup tectonics in southeast Brazil from thermochronological data and combined inverse-forward thermal history modeling. *Journal of Geophysical Research*, **117**, B11413, (2012).
4. Japsen, P., Chalmers, J. A., Green, P. F., & Bonow, J. M. Elevated, passive continental margins: Not rift shoulders, but expressions of episodic, post-rift burial and exhumation. *Global and Planetary Change* **90**, 73-86, (2012).
5. Sacek, V., Braun, J., & Beek, P. The influence of rifting on escarpment migration on high elevation passive continental margins. *Journal of Geophysical Research* **117**(B4) (2012).
6. Braun, J. Pecube: A new finite-element code to solve the 3D heat transport equation including the effects of a time-varying, finite amplitude surface topography. *Computers & Geosciences* **29**, 787-794 (2003).

Unravelling the links between brittle faulting, weathering and landscape evolution: the new clay geochronology facility of the Geological Survey of Norway

Roelant van der Lelij¹, Giulio Viola^{1,2}, Jochen Knies¹, Ola Fredin^{1,3}, Morgan Ganerød¹, Ana Banica¹

1 Geological Survey of Norway, PO Box 6315 Sluppen, Trondheim, Norway

2 Department of Geology and Mineral Resources, Norwegian University of Science and Technology, 7491, Trondheim, Norway

3 Department of Geography, Norwegian University of Science and Technology, 7491, Trondheim, Norway

The excellent exposure of basement rocks onshore Norway and the well explored offshore continental shelf provide an ideal natural laboratory to investigate landscape evolution by studying the interactions between brittle tectonics, weathering and basin formation. An accurate and comprehensive geochronological framework is required to investigate the links between these processes. The common association of fault gouges and saprolite weathering horizons with K-bearing clays such as illite and sericite provides a possible approach to the direct dating of these features.

There are several major technical challenges in dating clays: 1) Authigenic clays are frequently mixed with detrital minerals from the host rock; 2) Previous studies have shown that the finest grained material (<0.1 μm and below) provides the most reliable geochronological results, yet this material is difficult to isolate and manipulate; and 3) Fine grained material is difficult to date using the $^{40}\text{Ar}/^{39}\text{Ar}$ technique because the ^{39}Ar parent proxy is lost by recoil during irradiation, resulting in excessively old ages. Consequently, extra care and specialised equipment are required for sample preparation and characterisation prior to analysis, and fine grained material is routinely and more conveniently dated by the conventional isotope dilution K/Ar technique.

Several pioneering studies show that the K/Ar technique yields sensible ages for Late Mesoproterozoic to Cretaceous¹⁻³ fault gouges and saprolites from Scandinavia. The possibility of generating a comprehensive framework for Norway, combined with the reservoir potential of highly weathered and fractured basement rocks with enhanced secondary porosity has resulted in the industry-funded "BASE" project, which aims to establish a temporal and conceptual framework for brittle tectonics, weathering patterns and landscape evolution affecting the basement onshore and offshore southwestern Norway.

Within the framework of this joint industry project, the Geological Survey of Norway is establishing a new K/Ar facility for the separation, full characterisation and dating of clay material. Clay samples are disintegrated by stimulated gelifraction in a cryostatic bath. Subsequently, fine grain samples are separated using Stokes' law. Grain size fractions down to <0.1 μm and below are isolated using high speed, combined fixed angle rotor and continuous flow centrifuges. A new laser particle size analyser with a detection limit down to 0.01 μm is used to check the separated size fractions. These fractions are subsequently examined with a SEM, and clay mineralogy and polytypes are determined using a Bruker D8 Advance X-Ray diffractometer which was specially acquired within the scope of the "BASE" project.

Our fully automated, low volume extraction line is specifically designed to handle the high water and impurity content of illite from fault gouges and saprolites. It is fitted with a dual pipette system to deliver calibrated molar quantities of a high purity ^{38}Ar spike for

quantitative determinations of $^{40}\text{Ar}^*$, as well as atmospheric Ar for mass discrimination. Samples are degassed using a double vacuum resistance furnace, and isotopes are measured using a high sensitivity IsotopX NGX multicollector mass spectrometer on seven detectors. Five (5) Faraday detectors with $10^{12} \Omega$ resistance can be used for routine simultaneous measurements of atomic masses 36 to 40. An additional ion counting multiplier at low mass, as well as one $10^{11} \Omega$ Faraday detector at the highest mass, provide a more versatile setup which allows the ion beams to be shifted to adapt the measurement conditions to vastly different Ar yields and facilitates the analysis of smaller or younger samples. Digested samples are analysed by ICP-OES for determinations of K concentration.

In addition to new technical developments in the K/Ar analysis of clays, we are interested in exploiting the technical capability of our mass spectrometer to analyse other cosmogenic or radiogenic noble gases such as neon or helium in the future.

References

1. Fredin, O., Zwingmann, H., Knies, J., Sørli, R., Grandal, E.M., Lie, J.-E., Müller, A., & Vogt, C. Saproclites on- and offshore Norway: New constraints on formation processes and age. *Goldschmidt Conference Abstracts*, 1108, Florence (2013).
2. Torgersen, E., Viola, G., & Zwingmann, H. How can K-Ar geochronology of clay-size mica/illite help constrain reactivation histories of brittle faults? An example from a Paleozoic thrust fault in Northern Norway. *EGU General Assembly*, TS3.4/ERE5.5. Vienna (2013).
3. Viola, G., Zwingmann, H., Mattila, J., & Käpyaho, A. K-Ar illite age constraints on the Proterozoic formation and reactivation history of a brittle fault in Fennoscandia. *Terra Nova*, 0, 1-9 (2013).

Session 8:

Landscape evolution on different timescales

Recent Advances in Quantifying Tectonic and Erosional Processes with Thermochronology and Numerical Models

Todd A. Ehlers

Department of Geosciences, University Tübingen, Germany

The background thermal state of the crust is controlled by the flux of heat into the base of the crust, surface temperature, and variations in thermophysical properties such as thermal diffusivity and radiogenic heat production. Variations to this background state occur in regions with large spatial and temporal gradients in erosion and sedimentation, deformation, magmatism, and fluid flow. In recent years significant advancements have been made in quantifying erosion/sedimentation and deformation processes with numerical models that predict cooling ages. Furthermore, increased sample throughput in laboratories has provided sufficiently detailed data sets to rigorously test model predictions and provide new constraints on the tectonic and surface process influences on cooling ages. However, despite some successes, in many cases model capabilities and predictions exceed the fidelity of data and a critical evaluation of how to best pair models of different complexity with observations is warranted.

This presentation presents a synthesis of how recent advances in thermochronometer data collection and numerical modeling have, or have not, improved the interpretation of tectonics and surface processes. Emphasis is placed on understanding: (a) the evolution of structural or topographically complex settings; and (b) quantification of topographic change and surface processes with model-data integration. Examples are provided from settings where bedrock and/or detrital thermochronometer data are interpreted using thermal kinematic and erosion models. Emphasis is placed on the sensitivity of different data sets to test model predictions of varying complexity. Time permitting, three different types of studies will be discussed. These include:

First, the interpretation of cooling ages is discussed for structurally complex settings such as a fold and thrust belt. Examples of regions with complex kinematic histories are shown whereby restored balanced cross sections are forward modeled and the resulting thermal field calculated. The cooling ages of samples exhumed to the surface are predicted and compared to observed cooling ages. This example highlights the sensitivity of cooling ages to different structural geometries and rates of shortening and how (and when) coupled model-data studies can be used to improve our understanding of the kinematic history of orogens.

Second, the influence of evolving topography on cooling ages is explored. Mountain topography evolves over the life cycle of orogen growth and decay. Over shorter time scales, rapid pulses of erosion and topographic change by river incision or glaciation have captured the attention of numerous studies. Examples of the limits to reconstructing topographic change in these settings are presented as well as the conditions required for the extraction of paleotopography from coupled model-data studies.

Finally, recent interest has emerged in quantifying surface processes from detrital thermochronometer samples collected from either modern river or glacial sediments. These types of studies exploit the fact that cooling ages (usually) increase with elevation such that the measurement of a distribution of ages in sediments can be used as a particle tracking tool to infer the elevation an individual grain age was derived from. This approach is intriguing because it

opens the door to use thermochronology as a tool for quantifying the spatial distribution of erosion from the geomorphic process(es) that produced the sampled sediment. Examples of these types of studies are discussed from grain-age distributions measured in fluvial and glacial sediments. The effects of landslides and glacial patterns of erosion on cooling ages are presented as well as how bedrock thermochronometer data can also be used to evaluate topographic change.

Constraining Dynamic Topography using low-Temperature Thermochronology

Jean Braun

ISTerre, Université Joseph Fourier, Grenoble, France

Low-temperature thermochronology is now routinely used to constrain the rate of landform evolution over geological time scales; modeling tools have been developed, such as Pecube, to invert the data to produce quantitatively and physically plausible surface evolution scenarios. This approach has been broadly embraced by the community and has led to some key discoveries in recent years, such as the timing of glacial valley incision in the European western Alps or the propagation of fjords in southern New Zealand.

More recently has emerged the concept that part of the Earth's surface topography may not be related to tectonically induced and isostatically supported crustal thickness variations, but caused by viscous flow in the underlying convecting mantle, the so-called dynamic topography. Estimates of dynamic topography vary greatly, both in amplitude and extent, in part due to our limited knowledge of the details of the viscosity and density structure in the mantle, in part due to our inability to compute with accuracy the non-isostatic component of surface topography, due to a lack of global coverage in crustal and lithospheric thickness. Efforts have also been deployed by many groups of geodynamicists to estimate the contribution of dynamic topography in the geological past, either using backward advected mantle flow models or forward calculations of the flow caused around subduction zones of which we hypothesize we can deduce the geometry and rate of subduction from the geological record.

Tests of these models are critical and should not only bring essential constraints on the physical parameters controlling mantle flow, but also help us better understand parts of the geological record that cannot be explained by plate tectonics alone. This requires better constraints on the height, extent and timing of this long wavelength, low amplitude dynamic topography that may have come and gone long ago. Thermochronology is one of the better tools that we have to achieve this goal. It relies however on whether dynamic topography creates sufficient relief to trigger enough surface erosion and rock cooling that can be recorded by thermochronology.

In this talk, I will try to explain these issues and describe under which conditions thermochronology is most likely to be useful to constrain past and dynamic topography, using a few examples from the Colorado Plateau, Patagonia and the south African craton.

Grand Canyon, models, and the interpretation of thermochronology data

Rebecca M. Flowers¹, Kenneth A. Farley²

1 Department of Geological Sciences, University of Colorado - Boulder, USA

2 Division of Geological and Planetary Sciences, California Institute of Technology, USA

Recently published apatite $^4\text{He}/^3\text{He}$ and (U-Th)/He (AHe) evidence for carving of portions of the Grand Canyon to within a few hundred meters of modern depths by ~ 70 Ma¹ has helped renew discussion about the antiquity of the Grand Canyon and how the data – especially thermochronology results^{2,3,4} – constrain the history of canyon incision. This controversial work and the ensuing interchange among several investigators illustrates both the power and the challenges of combining, interpreting, and concisely explaining rich thermochronologic data when applied in a complex geologic setting. Recent publication of a large new thermochronologic dataset⁵ from the region has increased the thermal history information available for understanding canyon evolution. In this talk we will provide an overview of models for Grand Canyon carving, a synthesis of the thermochronologic data and their simulations, and an assessment of how these data bear on the ancient canyon model.

Here we define the “eastern Grand Canyon” as the eastern segment also known as the Upper Granite Gorge, where Precambrian basement is exposed. The segment between the Hurricane fault and Lake Mead we refer to as the “westernmost Grand Canyon”, where Precambrian basement also crops out. AHe^{1,4,6}, $^4\text{He}/^3\text{He}$ ¹, and AFT^{4,5,7,8,9} data exist for canyon bottom samples from these segments. There are published AHe data for southwestern plateau surface samples⁶, for several vertical transects in the canyon (the most complete being for the South Kaibab transect in the eastern canyon)⁴, and for several boreholes on the plateau south of the canyon⁴. AFT data are also available for an eastern canyon vertical transect⁷. The combination of AHe and AFT data is an essential aspect of this dataset, not only because it provides access to two different closure temperatures, but also because He diffusion in apatite is thought to be controlled by radiation damage for which fission tracks provide a quantitative proxy.

Our interpretation of an eastern “proto”-Grand Canyon was based on the similarity of plateau surface and canyon bottom temperatures from 55-30 Ma derived from AHe data⁶. A criticism² of this interpretation was that our rim sample was collected north of the canyon on the Kaibab uplift and not optimally located to constrain the paleocanyon. Our analysis of the recently published AHe data⁴ shows that 1) rim samples from the South Kaibab transect yield thermal histories consistent with our previous results, 2) borehole samples from south of the canyon yield thermal histories consistent with the south rim sample indicating the regional nature of its tT signal, and 3) the new eastern canyon bottom AHe data overlap with our published results. We therefore conclude that the new data support the “proto”- Grand Canyon interpretation that was originally based on a more limited AHe dataset.

Second, our interpretation of an ancient westernmost Grand Canyon was based on apatite $^4\text{He}/^3\text{He}$ and AHe data that demanded cooling to temperatures <30 °C by 70 Ma. More recent western canyon AHe data^{4,5} support this interpretation³. The thermal history simulation on which our conclusion was based began at 100-80 Ma because available AFT

data from the area indicated complete annealing of fission tracks at peak temperature⁹; this observation provides a zero radiation damage, zero He age initial condition for modeling. However, it was suggested that if this assumption was flawed it would cause our apatites to be more He retentive and invalidate our conclusion². We showed previously that the AHe data require complete He loss at peak temperature because partial He loss predicts a strong date-eU correlation that is not observed³. However, we did not explicitly address the circumstance of complete He loss but only partial damage annealing. Our new analysis shows that simulations commencing at 540 Ma and allowing partial damage annealing do not change our key thermal history conclusion. Even an extreme endmember scenario starting at 1100 Ma and allowing 600 m.y. of damage accumulation prior to burial and partial annealing requires cooling to <30 °C by 64 Ma, leaving intact our ancient canyon interpretation.

Our conclusions for the westernmost Grand Canyon differ from those recently published by ref ⁵. However, in ref ⁵ the thermal histories shown for the western canyon: 1) are fully compatible with our interpretations, 2) are for samples that do not actually come from the western canyon, 3) use AHe or AFT data that are irreproducible and/or of questionable quality, or 4) are a consequence of *assumed* thermal history constraints that preclude paths that would allow an ancient canyon. Ref ⁵ also argues that western canyon AFT data are inconsistent with the AHe results. If true this is an important observation, but the above inconsistencies of the modeling do not allow this claim to be assessed.

The intense interest in Grand Canyon thermochronology data and their significance provides an opportunity to evaluate the fundamentals of the methods being applied and the limits of what we can understand from them. However, work thus far also highlights the compelling need for transparency and justification of time-temperature (tT) constraints in thermal history modeling, complete publication of all data on which interpretations depend so that they can be independently reproduced, presentation of the entire suite of statistically viable tT paths permitted by the data rather than selected tT paths, and the need to employ the same kinetic models when comparing results for multiple sample. Not adhering to these basic principles of thermochronology data reporting and interpretation makes it challenging to identify where discrepancies between datasets truly do or do not exist, and confuses rather than clarifies discussion about this problem.

References

1. Flowers, R.M. & Farley, K.A. Apatite ⁴He/³He and (U-Th)/He evidence for an ancient Grand Canyon *Science* **338**, 1616-1619 (2012).
2. Karlstrom, K.E., Lee, J., Kelley, S., Crow, R., Young, R.A., Lucchitta, I., Beard, L.S., Dorsey, R., Ricketts, J.W., Dickinson, W.R. & Crossey, L. Comment on: Apatite ⁴He/³He and (U-Th)/He evidence for an ancient Grand Canyon *Science* **340**, 143 (2013).
3. Flowers, R.M. & Farley, K.A. Response to comments on: Apatite ⁴He/³He and (U-Th)/He evidence for an ancient Grand Canyon *Science* **340**, 143 (2013).
4. Lee, J.P., Stockli, D.F., Kelley, S.A., Pederson, J.L., Karlstrom, K.E. & Ehlers, T.A. New thermochronometric constraints on the Tertiary landscape evolution of central and eastern Grand Canyon *Geosphere* **9**, 21-36 (2013).
5. Karlstrom, K.E., Lee, J.P., Kelley, S.A., Crow, R.S., Crossey, L., Young, R.A., Lazear, G., Beard, L.S., Ricketts, J.W., Fox, M. & Shuster, D.L. Formation of the Grand Canyon 5 to 6 million years ago through integration of older paleocanyons *Nature Geoscience* doi:10.1038/ngeo2065 (2014).
6. Flowers, R.M., Wernicke, B.P. & Farley, K.A. Unroofing, incision and uplift history of the southwestern Colorado Plateau from apatite (U-Th)/He thermochronometry *Geological Society of America Bulletin* **120**, 571-587 (2008).
7. Dumitru, T.A., Duddy, I.R., & Green, P.F. Mesozoic-Cenozoic burial, uplift, and erosion history of the west-central Colorado Plateau *Geology* **22**, 499-502 (1994).

8. Naeser, C.W., Duddy, I.R., Elston, D.P., Dumitru, T.A., & Green, P.F. in Colorado River Origin and Evolution (eds. Young, R.A. & Spamer, E.E.) 31-35 (Grand Canyon Association, 2001).
9. Kelley, S.A., Chapin, C.E., and Karlstrom, K.E. in Colorado River Origin and Evolution (eds. Young, R.A. & Spamer, E.E.) 37-42 (Grand Canyon Association, 2001).

$^{40}\text{Ar}/^{39}\text{Ar}$ geochronological constraints on long-term and continental-scale landscape evolution

Paulo M. Vasconcelos¹

¹ University of Queensland, School of Earth Sciences, Australia

Classic long-term landscape evolution models propose the existence of regional-scale erosion surfaces and raise hypotheses, currently abandoned but largely untested, about the cumulative effects of tectonics and climate on the evolution of continental landscapes. Weathering geochronology by $^{40}\text{Ar}/^{39}\text{Ar}$ analysis of supergene hollandite-group Mn-oxides provides a robust tool for testing these hypotheses. Laser incremental heating analysis of more than 1200 Mn-oxide grains from weathering profiles from four different regions in Brazil (Carajás¹, Urucum², Quadrilátero Ferrífero³⁻⁵, and Espinhaço⁶) provides a statistically robust database to assess whether weathering profiles and their underlying landsurfaces are correlative at regional and continental scales. The results reveal that deep and chemically stratified lateritic weathering profiles exposed at the surface today started to form at the end of the Cretaceous, and that their maximum ages – interpreted as the minimum ages of the hosting landsurfaces – can be correlated at continental scales. Geochronology of hollandite samples from vertical transects through these profiles also reveal an episodic history of evolution for each profile. This episodicity records changes in weathering conditions through time, but also reveal that the surfaces hosting the weathering profiles have been continuously exposed – and have not been buried and re-exhumed – for the entire Cenozoic. A positive correlation between the ages and the elevations of weathering profiles reveals a clear hierarchy of landsurfaces: the oldest weathering profiles sit at the highest elevation surfaces, and weathering profiles become progressively younger as topography decreases. This age vs. elevation correlation suggests that the long-term evolution of cratonic landscapes occurs by alternating periods of tectonic and climatic stability, when landsurfaces undergo deep weathering; and periods of active uplift, dissection, and erosion of previously formed weathering profiles and formation of a new, younger erosion surface. The maximum weathering ages reveal the minimum ages of these erosion surfaces. The denudation chronology history derived from weathering geochronology suggests that cratonic landscapes are not in dynamic equilibrium.

References

1. Vasconcelos, P. M., Renne, P. R., Brimhall, G. H. & Becker, T. A. Direct dating of weathering phenomena by $^{40}\text{Ar}/^{39}\text{Ar}$ and K-Ar analysis of supergene K-Mn oxides. *Geochimica et Cosmochimica Acta* **58**, 1635-1665 (1994).
2. Piacentini, T., Vasconcelos, P. M. & Farley, K. A. $^{40}\text{Ar}/^{39}\text{Ar}$ constraints on the age and thermal history of the Urucum Neoproterozoic banded iron-formation, Brazil. *Precambrian Research* **228**, 48-62 (2013).
3. Carmo, I. O. *Geocronologia do intemperismo Cenozóico no Sudeste do Brasil*, Universidade Federal do Rio de Janeiro, Ph.D. Thesis, unpublished, (2005).
4. Carmo, I. O. & Vasconcelos, P. M. $^{40}\text{Ar}/^{39}\text{Ar}$ Geochronology of weathering profiles in Southeastern Brazil. *IV South American Symposium on Isotope Geology Extended abstracts, CD-ROM*, 49-52 (2003).
5. Spier, C. A., Vasconcelos, P. M. & Oliveira, S. M. B. $^{40}\text{Ar}/^{39}\text{Ar}$ geochronological constraints on the evolution of lateritic iron deposits in the Quadrilátero Ferrífero, Minas Gerais, Brazil. *Chemical Geology* **234**, 79-104 (2006).
6. Carmo, I. O. & Vasconcelos, P. M. in *34th International Geological Congress*.

Incision of the Three Rivers Region, southeastern Tibetan Plateau, using low-temperature thermochronometry and river profile analysis

Rong Yang¹, Frédéric Herman^{1,2}, Maria Giuditta Fellin¹, Sean D. Willett¹, Pierre G. Valla^{1,2}, Wei Wang³

1 Department of Earth Sciences, Swiss Federal Institute of Technology, Zurich, Switzerland

2 Institute of Earth Sciences, University of Lausanne, Switzerland

3 School of Ocean and Earth Science, Tongji University, Shanghai, China

The geodynamic processes and timing at which the Tibetan Plateau was raised remains uncertain, despite decades of studies. The Three Rivers Region (TRR: (Yangtze, Mekong and Salween rivers), located at the southeastern margin of the Tibetan plateau in China, is characterized by spectacular gorges that incise low-relief landscape. Rapid fluvial incision by the three rivers and their tributaries has created deep and narrow gorges 2 to 3 km in depth along this portion of the plateau margin, promoting efficient hillslope response. However, timing, forcing magnitude and potential onset of the erosional response and landscape evolution are still debated and require precise quantification. Towards this goal, we present an integrated analysis of the regional exhumation history, based on thermochronometric data and a topological analysis of the river network.

In this study, we report new apatite (U-Th)/He (AHe) and apatite fission-track (AFT) ages from the TRR, collected mainly along the main trunk of the rivers. Our AHe data range from ~1 to >80 Ma, while our AFT ages are between ~3 and 50 Ma. In the Tibetan plateau thermochronometric ages are older than 20 Ma, while along the river valleys most of the ages are younger than 10-15 Ma. Zircons are currently being analyzed by (U-Th)/He dating to better time the onset of rapid erosion in the TRR. After compiling the new and existing low-temperature thermochronologic data, we used a nonlinear inversion method to investigate the exhumation history in both space and time. Our results show variable exhumation rates across the three rivers, with the lowest incision rates on the Yangtze for the last 4-6 Myr. The rates are faster in the Mekong and Salween, with a sharp increase up to 1 km/Ma in the last 2 Myr for the Mekong river. We infer that a spatial tectonic uplift gradient is the primary control on fluvial incision. Our data also reveal the propagation of the incision towards the plateau interior, clearly visible in the thermochronologic data along the Mekong river. The fluvial systems in the TRR are still in a transient state today and they will continue to erode towards the plateau interior.

Our analysis of the river network is based on the extraction and mapping of the χ metric as a proxy for the steady state elevation, which provides a measure of the state of basin geometry disequilibrium (Willett et al., 2014). Our χ map reveals no large contrast across the main divides of the three rivers, suggesting that they are nearly in lateral geometric equilibrium. This is also supported by the symmetric mountain ranges between the lower Salween and Mekong basins. However, locally high χ anomalies are present on the low-relief landscape situated between large basins. In contrast, neighboring streams show small χ values. The differences in χ indicate that channels are not in steady state and incision is currently driving water divides into the undissected regions. As a result, the low-relief surface will eventually disappear. This inference is consistent with our independent constraint from thermochronology that the region has experienced a recent acceleration in

uplift.

We also use a linear inversion method (Goren et al., 2013) to infer the tectonic uplift history from river channel profiles. We inverted the Salween and Mekong river channel profiles for uplift rate. Our results suggest these two rivers are in a transient state with uplift rate that varies in both time and space. For simplicity, we assume uplift only varies in a N-S direction. We further divide each basin into a number of tectonic sub-regions, treated as rigid blocks. Uplift rate is uniform within each block, but varies in time and between blocks. Our inversion suggests that the Salween can be fitted with two blocks with lower uplift rates in the lower block and higher rates in the upper block. For the lower block, the uplift rate has slowly increased from ~0.02 mm/yr to a maximum of 0.25 mm/yr during the past 37 Myr. For the upper block, tectonic activity has only recently accelerated with increasing uplift rate since ~6 Myr following a long quiescent tectonic period. The Mekong is fit better with three tectonic blocks. Tectonic activity is almost constant in the lower block since 32 Myr. Although the uplift rates in the middle and upper blocks are independent, a common increase in uplift rate occurred at ~6 Myr and continues to the present.

References

1. Willett, S.D., McCoy, S.W., Perron, J.T., Goren, L. & Chen, C.Y., Dynamic Reorganization of River Basins *Science*, **343** (6175), doi: 10.1126/science.1248765 (2014).
2. Goren, L., Fox, M. & Willett, S.D. Finding temporal variations of tectonic uplift rate through inversion of long profiles of rivers: Formulation, algorithm, and application to tilted blocks in the western Basin and Range (CA). *AGU Fall Meeting*, EP41C-0803 (2013).

Temporal and spatial variations in erosion rate in the Sikkim Himalaya as a function of climate and tectonics

Rachel Abrahami^{1,2}, Pascale Huyghe^{1,2}, Peter van der Beek^{1,2}, Julien Carcaillet^{1,2}

¹ *Univ. Grenoble Alpes, ISTERre, F-38041 Grenoble, France.*

² *CNRS, ISTERre, F-38041 Grenoble, France.*

The Tista River is a major tributary of the Brahmaputra drainage system (Eastern Himalaya). Its headwaters are located in the glaciated northernmost parts of the Sikkim and its catchment area amounts to more than 12,000 km² including a depositional megafan (extending mostly in Bangladesh and West Bengal-India). The Tista has recently incised its megafan at the topographic front of the mountain range by about 30 meters. Neither the timing of deposition/incision of the megafan sediments, nor the erosion rates of the source areas as well as their potential relationships, have been investigated in detail. Comparing these data is essential to distinguish between a climatic and/or tectonic control of the evolution of the Sikkim Himalaya and piedmont.

To constrain erosion rates in the hinterland at different temporal scales (respectively millennial and geological timescales), we report cosmogenic nuclide (¹⁰Be) and thermochronological (apatite fission-tracks) data on modern river sands. ¹⁰Be concentrations in river sands vary from 1,712.10³ to 43,173.10³ at/g. Detrital AFT samples from major rivers show 1 or 2 main age populations, with peak ages varying from 3,4-8,2 Ma in the MCT zone to 5,8-17,5 Ma in northern Sikkim (Higher Himalaya and transition to Tethyan Himalaya).

Results were mapped to evidence spatial variations of erosion/exhumation rates in the Tista catchment. Cosmogenic nuclides were also used to date the onset of incision of the megafan and relate it to potential changes in hinterland erosion.

In addition, isotope geochemistry (ϵ_{Nd} and ⁸⁷Sr/⁸⁶Sr) performed on modern river sands and Late-Quaternary megafan sediments allows characterizing the isotopic signature of the different source areas and constraining variations in provenance of the Tista megafan deposits through time in response to changing climatic conditions. Results show that the Tista fan deposits are mainly sourced from the High Himalayan Crystalline domain with excursions more influenced by the Lesser Himalaya domain.

These data provide a new comprehensive view on modern erosion and long-term exhumation of the Sikkim Himalaya. This study of a “closed system” will help our knowledge and understanding of erosional processes and sediment fluxes in mountainous environments as a function of climate and tectonics.

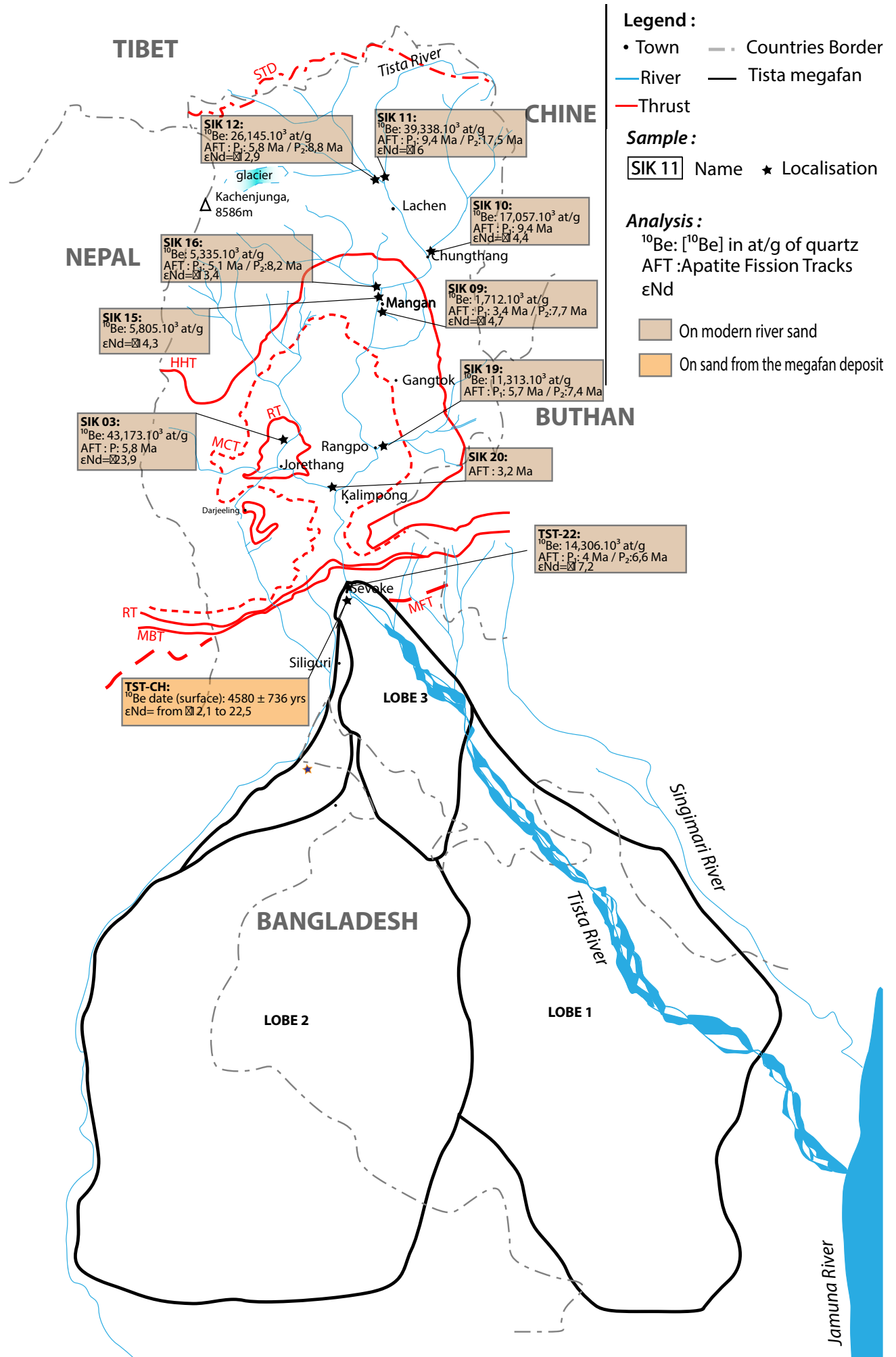


Figure 1: Localisation and results of Cosmogenic nuclide (^{10}Be), Detrital AFT, isotope geochemistry (ϵNd and $^{87}\text{Sr}/^{86}\text{Sr}$) analysis made on modern river sand and on Tista megafan deposits

Thermal history, exhumation, uplift, and long-term landscape evolution of the Eastern Great and Northern Lesser Caucasus, Azerbaijan

Tatiana Spilger¹, Ulrich A. Glasmacher¹, Jon Mosar²

¹ Institute of Earth Sciences, University of Heidelberg, Germany

² Department of Geosciences – Earth Sciences, University of Fribourg (Switzerland)

The Caucasus orogen (Great and Lesser Caucasus) is the highest mountain range between Asia and Europe, whose growth takes place since the beginning of the Cenozoic³. The orogen has evolved as a result of the active north directed convergence of the Arabian plate⁴. The Great Caucasus (GC) represents a doubly verging fold-and-thrust belt, with a per- and a retro wedge actively propagating into the foreland sedimentary basins to the south and to the north⁵.

Geomorphologic and thermochronological studies demonstrate a differentiated timing of exhumation and surface uplift as soon as differentiated exhumation and surface uplift rates of different tectonic zones of the GC. Studies on cooling history of recent granites in the western central Greater Caucasus show exhumation rates of 4 mm/a¹. The fastest and highest surface uplift rates (more than 12 mm/a) take place in the center of the mountain range². Some geomorphology studies also indicate fast and high uplift surface rates of 10 mm/a since late Pliocene in the Eastern GC, other introduce lower surface uplift rates of 0.33 to 1 mm/a^{2,6}.

Thermochronometric techniques (fission-track, (U-Th-Sm)/He, each on apatite and zircon) are used to reconstruct the thermal evolution of the upper crust, the subsidence, as well as the rock and surface uplift of the Eastern GC and Northern Lesser Caucasus and to connect them with the thrust kinematics of the GC.

Samples were taken along different transects in Eastern GC and Northern Lesser Caucasus in Azerbaijan. Most samples of Eastern GC are Lower Jurassic age sandstones (deep marine and slope facies). Several sedimentary rock samples of Cretaceous, Miocene, Pliocene and Quaternary age were taken from the outcrops in the Kura basin and along rivers in the Eastern GC. Samples of the Lesser Caucasus are igneous and sedimentary origin and have Lower Jurassic to Holocene age.

References

1. Hess, J.C., Lippolt, H.J., Gurbanov, A.G. & Michalski, I. The cooling history of the late Pliocene Eldzhurtinskiy granite (Caucasus Russia) and the thermochronological potential of grain-size/age relationships. *Earth and Planetary Science Letters* **117**, 393-406 (1993).
2. Mitchell, J. & Westaway, R. Chronology of Neogen and Quaternary uplift and magmatism in the Caucasus: constraints from K-Ar dating of volcanism in Armenia. *Tectonophysics* **304**, 157-186 (1999).
3. Mosar, J., Kangarli, T., Bochud, M., Glasmacher, U.A., Rast, A., Brunet, M.-F. & Sosson, M. Cenozoic-Recent tectonics and uplift in the Greater Caucasus: a perspective from Azerbaijan. *Geological Society, London, Special Publications* **340** 1, 261-280 (2010).
4. Nikishin, A.M., Ziegler, P., Panov, D.I., Nazarevich, B.P., Brunet, M.-F., Stephenson, R.A., Bolotov, S.N., Korataev, M.V. & Tiknomirov, P.L. Mesozoic and Cainozoic evolution of the Scythian Platform - Black Sea - Caucasus domain. In: Ziegler, P., Cavazza, W., Robertson, A.H.F. & Crasquin-Soleau, S. (éd.) *Peri-Tethys Memoir 6 - Peri-Tethyan rift/wrench basins and passive margins*. Mémoires du Muséum natn. Hist. nat., Paris **186**, 295-346 (2001).
5. Sholpo, V.N. Structure of inversion anticlinoria in the core of the Greater Caucasus: an advection hypothesis. *Geotectonics* **23**, 245-251 (1993).
6. Rastvorova, V.A. & Shcherbakova, E.M. The uplift of the Central Caucasus during late-glacial times. In: Gerasimov, I. P. (éd.) *Recent crustal movements*. Israel Program Sci. Transl., 318-326 (1967).

Late-Cenozoic exhumation and sediment budget of the central Pyrenees: a detrital thermochronology study of the Miocene Lannemezan megafan

Margaux Mouchen ¹, Peter van der Beek¹, Fr d ric Mouthereau²

1 Univ. Grenoble Alpes, ISTerre, F-38041 Grenoble, France

2 Sorbonne Universit s. UPMC Univ Paris 06, UMR 7193, Institut des Sciences de la Terre Paris (iSTeP), 4 Place Jussieu, F-75005 Paris, France

The landscape response to changes in external drivers such as tectonic activity and climate change can be deciphered from the study of exhumation and erosion patterns. To this end, carrying out a balance between eroded and depositional volumes is a powerful tool to understand the evolution of the sediment routing system. In addition, detrital thermochronological methods can provide meaningful constraints on the erosion rates averaged over the entire catchment area at geological time scales (10^6 years).

The Miocene Lannemezan megafan is the most striking geomorphic feature of the Northern Pyrenean foreland. It is exceptionally large (10^4 km²), especially when compared to the other fans of this foreland, and it exhibits an anomalous fan area/catchment area ratio. The fan was built from Early Miocene to Pliocene, while active deformation of the central Pyrenees (in particular its northern retro-wedge) had already ceased^{1,2} although the exact timing of the end of the deformation remains disputed³. The controls on the development and final abandonment of the fan thus remain elusive. However, its sedimentary record allows assessing the post-orogenic exhumation history of the central Pyrenees. To constrain this history, we investigate the temporal evolution of the sediment flux and erosion rates in the sediment routing system by calculating eroded and deposited volumes combined with detrital apatite fission-track thermochronology.

The Neste River, which most likely fed the megafan, was captured by the larger Garonne River in Quaternary times. Nevertheless, the delineation of its watershed on a digital elevation model (ASTER GDEM) provides an estimation of the eroded volume in the pre-Quaternary/Neogene paleocatchment of the megafan. Calculation of the depositional volumes for each stratigraphic level is done through comprehensive mapping of the Oligocene to Pliocene sediment series and interpolation of bounding surfaces between outcrops. The temporal evolution of the sediment supply, in terms of volumes and rates, can then be estimated by numerical calculation.

Each stratigraphic level of the fan (independently dated by pollen analysis – *JP Suc pers. comm.*) was sampled for detrital fission track analyses on apatites. The erosion rates estimated from these thermochronometric data is averaged over the time scale of the lag time immediately preceding the deposition to provide exhumation rates and can be directly compared to the independently determined sediment flux in order to estimate the efficiency of sediment trapping in the fan.

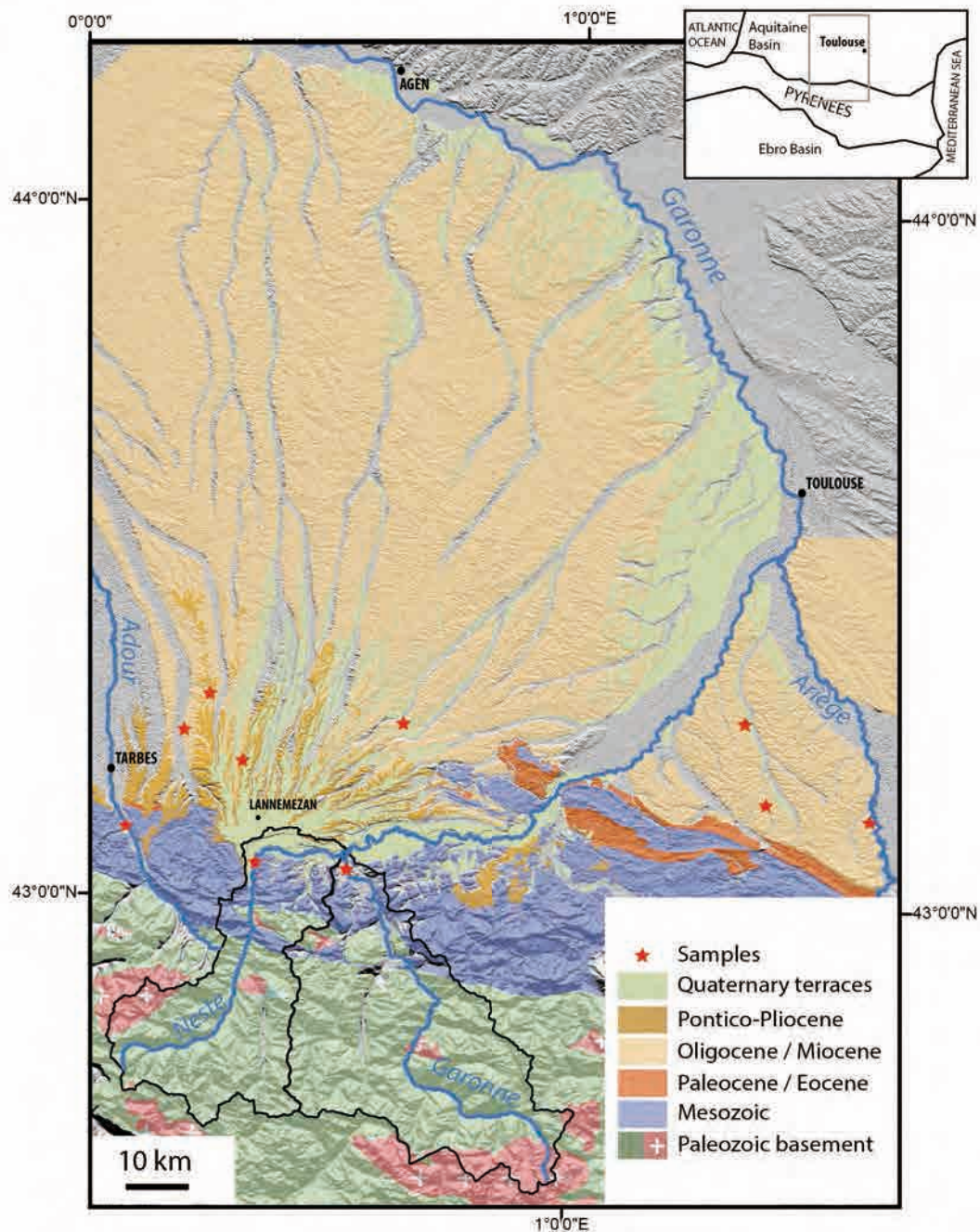


Figure 1. Geological map of the Northern Central Pyrenees and Lannemezan megafan. Location of the samples collected for apatite fission-track analysis is shown (red stars). Black solid lines delineate the basins drained by the Neste and Garonne rivers down to their confluence.

References

1. Muñoz, J. A. Evolution of a continental collision belt : ECORS-Pyrenees crustal balanced cross-section. *Thrust tectonics* 235–246 (1992).doi:10.1007/978-94-011-3066-0_21
2. Vergés, J., Fernández, M. & Martínez, A. The Pyrenean orogen: pre-, syn-, and post-collisional evolution. *Reconstruction of the evolution of the Alpine-Himalayan Orogen*. **8**, 57–74 (2002).
3. Jolivet, M. *et al.* Thermochronology constraints for the propagation sequence of the south Pyrenean basement thrust system (France-Spain). *Tectonics* **26**, TC5007 (2007).

Thermochronologic constraints in the Pyrenean belt evolution (western Axial Zone): Orogenic and post-orogenic processes

Gemma V. Bosch¹, Antonio Teixell², Marc Jolivet¹, Pierre Labaume³, Patrick Monié³, Daniel Stockli⁴, Kerry Gallagher¹

1 Géosciences Rennes, France

2 Universitat Autònoma de Barcelona, Spain

3 Géosciences Montpellier, France

4 Jackson School of Geosciences, Texas

The Pyrenees belt is a Late-Cretaceous-Miocene collision zone developed by inversion of rift structures created during Mesozoic times. Exceptional exposure along the chain, allow the study of how and when shortening occurred based on structural geology and tectonics-sedimentation relationship¹⁻⁴. Recently, low-temperature thermochronology studies (zircon fission tracks, apatite fission tracks, and apatite U-Th/He) were carried out in the Pyrenees to gain insight into relationships between the deformation (tectonics) and erosion (climate, base level) processes⁵⁻¹⁰. These have provided further constraints on the age of the main tectonic events involved in the mountain chain uplift, as well as the timing of erosion events during post-orogenic stages.

In this study, we combine three thermochronometers (apatite U-Th/He, apatite fission track analysis and zircon U-Th-Sm/He) and numerical modelling to unravel the exhumation history of west-central Pyrenees⁷, at the western Axial Zone¹¹ and the adjacent North Pyrenean Zone. A reconstruction of the whole exhumation history from all 3 thermochronometers, has been possible only in the Eaux-Chaudes, Balaitous et Panticosa granitic plutons of the Axial Zone. The lack of apatite in the Upper Cretaceous cover of the Axial Zone, and the poor quality of the apatite crystals in the North Pyrenean Zone, precluded such complete reconstructions. The combination of apatite fission track analysis and zircon U-Th-Sm/He ages in these plutons imply a very fast exhumation at ~20-25Ma during the activity of the Guarga thrust of the South Pyrenean thrust system. The structural geometry of this thrust ramp is consistent with large-scale uplift and exhumation of the Axial Zone^{1,11,12}. Zircon U-Th-Sm/He ages of 30-36Ma from the western Axial Zone termination (Lakora klippe -the southward thrust edge of the North Pyrenean Zone- and its footwall) record growth of the Axial Zone antiform and thus constrain the activity of the Gavarnie thrust. In the north, the zircon U-Th-Sm/He data imply no resetting in the footwall of the North Pyrenean frontal thrust (with Permian-Jurassic ages). In contrast the data imply resetting in the North Pyrenean Zone, which yield Alpine ages, between 35-50Ma in the Albian flysh and 30-40 in Permo-Triassic substrate.

Apatite U-Th/He data, obtained on both sides of the range, consistently allow us to recognize and date for the first time, a major erosional event at ~5-10Ma. We propose that this erosion event was driven by climatic/tectonic processes and not by the capture of the Ebro drainage system by the Mediterranean Sea, as previously proposed¹³.

References

1. Teixell, A. The Ansó transect of the southern Pyrenees: basement and cover thrust geometries. *J. Geol. Soc.* **153**, 301–310 (1996).
2. Muñoz, J. A. in *Thrust Tecton.* 235–246 (Mc Clay, K.R., 1992).
3. Vergés, J., Fernández, M. & Martínez, A. The Pyrenean orogen: pre-, syn-, and post-collisional evolution. *J Virtual Explor* **8**, 57–76 (2002).
4. Labaume, P., Séguret, M. & Seyve, C. Evolution of a turbiditic foreland basin and analogy with an accretionary prism: Example of the Eocene South-Pyrenean basin. *Tectonics* **4**, 661–685 (1985).
5. Sinclair, H. D., Gibson, M., Naylor, M. & Morris, G. Asymmetric growth of the Pyrenees revealed through measurement and modelling of orogenic fluxes. *Am. J. Sci.* **305**, 369–406 (2005).
6. Fitzgerald, P. G., Muñoz, J. A., Coney, P. J. & Baldwin, S. L. Asymmetric exhumation across the Pyrenean orogen: implications for the tectonic evolution of a collisional orogen. *Earth Planet. Sci. Lett.* **173**, 157–170 (1999).
7. Jolivet, M. *et al.* Thermochronology constraints for the propagation sequence of the south Pyrenean basement thrust system (France-Spain). *Tectonics* **26**, (2007).
8. Maurel, O. *et al.* The Meso-Cenozoic thermo-tectonic evolution of the Eastern Pyrenees: an 40Ar/39Ar fission track and (U-Th)/He thermochronological study of the Canigou and Mont-Louis massifs. *Int. J. Earth Sci.* **97**, 565–584

(2007).

9. Gibson, M., Sinclair, H. D., Lynn, G. J. & Stuart, F. M. Late- to post-orogenic exhumation of the Central Pyrenees revealed through combined thermochronological data and modelling. *Basin Res.* **19**, 323–334 (2007).
10. Metcalf, J. R., Fitzgerald, P. G., Baldwin, S. L. & Muñoz, J.-A. Thermochronology of a convergent orogen: Constraints on the timing of thrust faulting and subsequent exhumation of the Maladeta Pluton in the Central Pyrenean Axial Zone. *Earth Planet. Sci. Lett.* **287**, 488–503 (2009).
11. Meresse, F. Dynamique d'un prisme orogénique intracontinental: évolution thermochronologique (traces de fission sur apatite) et tectonique de la Zone Axiale et des piedmonts des Pyrénées centrooccidentales. (2010).
12. Teixell, A. Crustal structure and orogenic material budget in the west central Pyrenees. *Tectonics* **7**, 395–406 (1998).
13. Fillon, C. & Van Der Beek, P. Post-orogenic evolution of the southern Pyrenees: constraints from inverse thermo-kinematic modelling of low-temperature thermochronology data. *Basin Res.* **24**, 418–436 (2012).

Mechanical and morphological constraints on rates of Alpine valley evolution

Kerry Leith^{1,4}, Jeffrey R. Moore^{2,4}, Matt Fox^{3,4}, Florian Amann⁴, Julian Brosda¹,
Simon Loew⁴, Michael Krautblatter¹

1 Chair of Landslide Research, Technische Universität München, Munich, Germany

2 Geology and Geophysics, University of Utah, Salt Lake City, USA

3 Berkeley Geochronology Center, UC Berkeley, Berkeley, USA

4 Geological Institute, ETH Zurich, Zurich, Switzerland

Despite recent advances in optical and radiometric dating techniques, constraining rates of Alpine valley evolution between the onset of major glaciation (prior to the Mid Pleistocene Revolution at MIS 22) and the Last Glacial Maximum remains a challenge. Recent insights into the mechanics of sub-glacial bedrock fracture, however, provide a new appreciation of the process and likely timing of U-shaped valley formation within the European Alps^{1,2}. These are based on a model which suggests a one-off period of enhanced glacial incision can be driven by path-dependent development of bedrock stresses close to a valley axis, and modulated by the properties of sub-glacial bedrock and the rate of glacial transport. Today, the valley shoulder remains as a morphological marker reflecting the initial extent of critical landscape stresses, while exfoliation or sheeting fractures within the valleys bear testament to the proposed active fracturing process. Based on the required stress path, the most likely timing of this enhanced erosion can be constrained by dating evidence which suggests major valley incision and glacial sediment production was coincident with glaciation at MIS 12, 16, or 22³⁻⁵.

Capitalizing on these insights, we investigate morphological evidence supporting predominantly sub-aerial and fluvial geomorphological processes, which in combination with ongoing tectonic uplift, appear to overprint the signature of early glacial erosion since at least MIS 12. These observations are derived from comparison between stream power erosion models and knickpoint locations within the lower- to mid-reaches of major tributary valleys south of the Rhone River. The predicted timings are internally consistent with rates of mass wasting, tectonic uplift, and fluvial bedrock incision within the region.

References

- 1 Leith, K., Moore, J. R., Amann, F. & Loew, S. Sub-glacial extensional fracture development and implications for Alpine valley evolution. *J. Geophys. Res.* 119, 62-81, (2014).
- 2 Leith, K., Moore, J. R., Amann, F. & Loew, S. In situ stress control on micro-crack generation and macroscopic extensional fracture in exhuming bedrock. *J. Geophys. Res.* 119, 594–615 (2014).
- 3 Häuselmann, P., Granger, D. E., Jeannin, P.-Y. & Lauritzen, S.-E. Abrupt glacial valley incision at 0.8 Ma dated from cave deposits in Switzerland. *Geology* 35, 143-146, (2007).
- 4 Muttoni, G. et al. Magnetostratigraphic dating of an intensification of glacial activity in the southern Italian Alps during Marine Isotope Stage 22. *Quaternary Research* 67, 161-173, (2007).
- 5 Preusser, F., Reitner, J. & Schlüchter, C. Distribution, geometry, age and origin of overdeepened valleys and basins in the Alps and their foreland. *Swiss Journal of Geosciences* 103, 407-426. (2010).

Quantifying glacial erosion combining bedrock and detrital thermochronology in the Bernese Alps

Cornelia Wangenheim¹, Christoph Glotzbach¹, Peter W. Kubik²

¹ Institut für Geologie, Leibniz Universität Hannover, Callinstraße 30, D-30167 Hannover, Germany

² Laboratory of Ion Beam Physics, ETH Zurich, Schafmattstraße 20, 8093 Zurich, Switzerland

The topography of the European Alps is strongly influenced by Quaternary glaciations; the glacial erosion of several glacial cycles had a large impact on the landscape, as it formed characteristic features like overdeepened and hanging valleys. In this study I measured cosmogenic nuclide in stream sediments and applied apatite fission track dating (AFT) on both bedrock and sediments to quantify landscape evolution. The sample material derives from crystalline bedrock, stream sediments and glacial deposits from moraines and cave sediments.

The study area is located in the Central Alps of Switzerland (Fig.1), which is a high mountain area, strongly affected by glacial erosion during both the Quaternary and Holocene. At ~0.9 Ma glacial erosion has led to a considerable increase in valley incision rates in this area¹, and therefore the study area is ideally suited to investigate the glacial impact on landscape evolution.

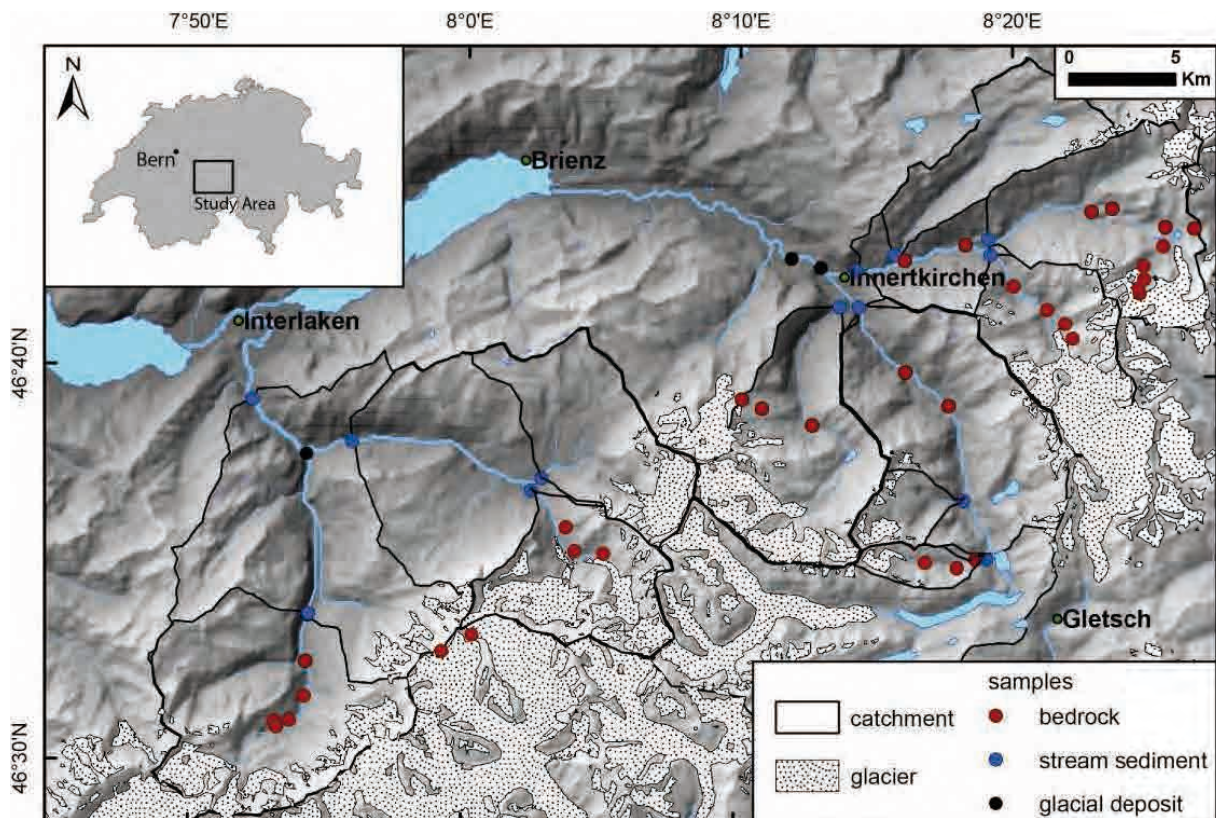


Figure 1. Shaded relief image of the study area based on 90 m SRTM data and sample locations of this study.

The bedrock samples are used to determine their thermochronological age, in order to obtain the long-term exhumation history. The relatively high spatial sample density derived from

published and new thermochronological data facilitates to figure out whether or not spatial differences and elevation dependencies exist. First apatite fission track ages vary between ~5 Ma and ~9 Ma, confirming previous studies². Ages do not only increase with elevation, but also show a distinct local trend along major valleys, which may be at least partly caused by focused valley incision during glaciations³.

The stream sediment samples were used for determination of catchment-wide denudation rates with in-situ produced Beryllium-10. The calculated denudation rates range from 100 to 1733 mm/ka, representing the last ~6000 years. Their potential comparability with the AFT results will be discussed. Additionally I will combine detrital thermochronology of the stream sediment samples, glacial deposits and cave sediments with bedrock ages to infer the lateral variations of Holocene erosion.

References

1. Haeuselmann, P. Granger, D. E. Jeannin, P.-Y. & Lauritzen, S.-E. Abrupt glacial valley incision at 0.8 Ma dated from cave deposits in Switzerland, *Geology* **35**, 143–146 (2007).
2. Vernon, A. J., van der Beek, P. A., Sinclair, H. D. & Rahn, M. K. Increase in late Neogene denudation of the European Alps confirmed by analysis of a fission-track thermochronology database, *Earth Planet. Sci. Lett.* **270**, 316-329 (2008).
3. Shuster, D. L., Cuffey, K. M., Sanders, J. W. & Balco, G. Thermochronometry reveals headward propagation of erosion in alpine landscape, *Science* **332**, 84-88 (2011).

Low temperature thermochronological constraints on the Cenozoic evolution of the Lake District and Southern Uplands Massifs (NW England, SW Scotland)

Katarzyna Łuszczak¹, Cristina Persano¹, Finlay Stuart²

1 School of Geographical & Earth Sciences, University of Glasgow, Glasgow, G12 8QQ, UK

2 Isotope Geosciences Unit, Scottish Universities Environmental Research Centre, East Kilbride G75 0QF, UK

The Lake District has the highest mountains in England, and is an iconic landscape that has been celebrated in art and literature for centuries. Apatite fission track (AFT) analyses from across the region, performed over the last 30 years, suggest that the last major rock exhumation event took place in Late Cretaceous-Early Palaeogene¹⁻³. The adjacent East Irish Sea Basin has experienced a complex thermal history that includes cooling episodes in the Early Cretaceous, Early Palaeogene and Neogene⁴. Recent AFT analyses of onshore NE England suggest that Neogene cooling has been more important than previously thought⁵. Although the Late Cretaceous - Early Palaeogene exhumation signal is evident elsewhere in the UK⁶, the Lake District and surrounding regions appear to have experienced the largest amount of exhumation at this time.

Despite the plethora of studies, several issues remained poorly resolved by the existing data. Firstly, the precise timing and rate of cooling of the Late Cretaceous-Early Palaeogene event are not well defined. Consequently the causes and mechanism/s of exhumation are not clear. There are two possible causes of uplift and exhumation in the Early Palaeogene. The eruption of huge thicknesses of picritic basalts related to the arrival of the proto-Iceland plume (62-58 Ma)⁷ require magmatic underplating that likely caused permanent uplift, and which is also supported by modeling of geophysical data⁸. The breakup of the North Atlantic at ~53 Ma⁹ may also have induced uplift and exhumation along the passive margin. Recent geophysical studies suggest that the maximum Cenozoic denudation occurred in northwest Scotland, not in the Lake District¹⁰. Resolving the cause of exhumation requires the precise determination of the time, amount and distribution of cooling and related denudation. The second main issue surrounds the amount of Neogene uplift and exhumation. That the British Isles have experienced an important Neogene denudation event is controversial and difficult to resolve by using AFT thermochronology alone.

We seek to refine the existing constraints on the regional exhumation history with the first complete thermochronometric study. We are using apatite and zircon (U-Th-Sm)/He data, combined with AFT, from igneous intrusives from the Lake District, Southern Uplands (SW Scotland) and North Wales. Initial AFT ages from the Shap granite in the Lake District and the Criffell granite in the Southern Uplands vary from 46 to 56 Ma, whereas apatite (U-Th-Sm)/He ages from 41 to 45 Ma. Preliminary thermal history modelling shows that these areas experienced rapid cooling from over 120°C at ~60 Ma to 40°C at 40 Ma. If cooling started at ~60 Ma, it suggests plume-related uplift, rather than North Atlantic break-up as the driver of exhumation. The cooling rate in excess of 4°C/Myr translates to denudation of 160-70 m/Myr, depending on the geothermal gradient (25-60°C/km); a 'normal' geothermal gradient of ~30°C/km implies that 2-3 km of denudation occurred during the Early Palaeogene. This exceeds the maximum amount of denudation measured in the surrounding sedimentary basins. This preliminary data and their modeling do not identify a resolvable Neogene cooling signature; however a Neogene compressional event has been identified in the surrounding basins.

The data imply that the mountainous landscape of the Lake District and Southern Uplands were developed in, and has persisted since, the Early Palaeogene. The Neogene compressional event identified in the basins, however, is unlikely to have affected only the offshore areas. Future work will be aimed at a precise determination of the timing and distribution of Early Palaeogene exhumation, and quantifying the amount of Neogene rock uplift.

References

1. Green P.F. 1986. On the thermo-tectonic evolution of northern England: evidence from fission track analysis. *Geological Magazine* 123, 493–506.
2. Lewis C.L.E., Green P.F., Carter A. & Hurford, A.J. 1992. Elevated K/T palaeotemperatures throughout northwest England: three kilometres of Tertiary erosion? *Earth and Planetary Science Letters* 112, 131–145.
3. Green P.F. 2002. Early Tertiary paleo-thermal effects in northern England: reconciling results from apatite fission track analysis with geological evidence. *Tectonophysics* 349, 131–144.
4. Holford S.E., Turner J.P. & Green P.F. 2005. Reconstructing the Mesozoic–Cenozoic exhumation history of the Irish Sea basin system using apatite fission track analysis and vitrinite reflectance. In: Doré, A.G., Vining, B.A. (Eds.), *Petroleum Geology of Northwest Europe: Proceedings of the 6th Conference*. Geological Society London, 1007–1030.
5. Green P. F., Westaway R., Manning D.A.C. & Younger P. L. 2012. Cenozoic cooling and denudation in the North Pennines (northern England, UK) constrained by apatite fission-track analysis of cuttings from the Eastgate Borehole. *Proceedings of the Geologists' Association*, 123: 450–463.
6. Persano, C., Barfod, D. N., Stuart, F. M., & Bishop, P. 2007. Constraints on early Cenozoic underplating-driven uplift and denudation of western Scotland from low temperature thermochronometry. *Earth and Planetary Science Letters*, 263(3-4), 404-419.
7. Fitton, J., Saunders, A., Norry, M., Hardarson, B., & Taylor, R. 1997. Thermal And Chemical Structure Of The Iceland Plume. *Earth and Planetary Science Letters*, 153(3-4), 197-208.
8. Tiley R., White N. & Al-Kindi S. 2004. Linking Paleogene denudation and magmatic underplating beneath the British Isles. *Geological Magazine* 141, 345–351.
9. Dore A.G., Lundin E.R., Jensen L.N., Birkeland Ø., Eliassen P.E. & Fichler C. 1999. Principal tectonic events in the evolution of the northwest European Atlantic margin. In: Fleet, A.J., Boldy, S.A.R. (Eds.), *Petroleum Geology of Northwest Europe: Proceedings of the 5th Conference*. Geological Society, London, 41–61.
10. Davis, M. W., White, N. J., Priestley, K. F., Baptie, B. J., & Tilmann, F. J. 2012. Crustal structure of the British Isles and its epeirogenic consequences. *Geophysical Journal International*, 190(2), 705-725.

Evolution of the elevated passive margin of Greenland

Cornelia Spiegel¹, Wolfgang Reiter¹, Frank Lisker¹, Volkmar Damm²

1 Department of Geosciences, University of Bremen, Germany

2 Federal Institute for Geosciences and Natural Resources, Hannover, Germany

The formation of elevated passive margins is controversially debated in the literature. This is particularly true for the high-standing margins of Greenland. They have alternatively been explained by resulting from prolonged very slow erosion following Paleozoic orogeny^{1,2}, resulting from rifting and opening of ocean basins adjacent to the Greenland continental margins³, or as young geomorphic features only formed during the Cenozoic⁴. This study focuses on the northwestern margin of Greenland, north of the Melville Bugt at the northern end of Baffin Bay. Opening and formation of oceanic crust of Baffin Bay took place during the Late Cretaceous. The study area is also situated at the southern termination of the postulated Wegener Fault, a controversially discussed large-scale strike-slip fault system supposedly active during the Paleogene, that has been described as one of the last problems of global plate tectonic reconstructions. Fission track data of the same region and towards the north did not yield evidence for Cenozoic accelerated cooling^{2,3}, whereas a complex history of Cenozoic cooling for the area further south around the Disko Bugt was proposed⁴.

AFT thermochronology yielded strongly scattering ages ranging from 403 to 91 Ma, associated with shortened mean track lengths between 9.8 and 12.2 μm . The sampled profiles cross several normal faults. These faults seem to have been active during or after the late Cretaceous, leading to jumps in the age patterns and to the juxtaposition of rocks from different crustal levels, thus explaining the strong age scatter. Normal faulting, however, was not associated with strongly increased erosion. Instead, as indicated by thermal history modeling, all samples experienced extremely slow cooling during the entire Mesozoic. We interpret these patterns in that (i) normal faulting was associated with extension during opening of the Baffin Bay in the Late Cretaceous, and (ii) that no significant relief was created in response to the opening of Baffin Bay, but that the area was rather characterized by subdued topography.

Our data are in agreement with accelerated cooling starting between 40 and 20 Ma and leading to 2 to 3 km of denudation. We interpret this accelerated denudation as indicating uplift and formation of topography along the continental margin of north-west Greenland. By contrast, thermal history modeling revealed that our data are not in agreement with slow and continuous cooling since the Paleozoic. The complex Cenozoic cooling history as proposed for the Disko Bugt area towards the south⁴ could be reconciled with some of our data, but not with all of them. However, our data clearly argue in favor for a young Cenozoic formation of the elevated margin of north-west Greenland, independent from earlier orogenic processes and independent from the opening of the Baffin Bay. The reason for this young uplift is still unclear. At that time, Greenland was moving north and had just collided with Arctic Canada / Ellesmere Island to the west and with Svalbard to the east. Although it was previously assumed that only northern Greenland was affected by collision and deformation, exhumation observed for the Baffin Bay margin may be related to this tectonic episode. Another explanation would be that Paleogene exhumation was associated with a vertical component of the postulated Wegener strike-slip fault. For verifying this, more data are required, particularly from the Canadian side of the Wegener fault.

References

1. Pedersen, V., Nielsen, S. & Gallagher, K. The post-orogenic evolution of the Northeast Greenland Caledonides constrained from apatite fission track analysis and inverse geodynamic modeling. *Tectonophysics* **530**, 318-330 (2012).
2. Hansen, K., Dawes, P., Frisch, T. & Jensen, P. A fission track transect across Nares Strait (Canada-Greenland): further evidence that the Wegener Fault is a myth. *Can. J. Earth Sci.* **48**, 819-840 (2011).
3. Grist, A. & Zentilli, M. The thermal history of the Nares Strait, Kane Basin, and Smith Sound region in Canada and Greenland: constraints from apatite fission track and (U-Th-Sm)/He dating. *Can. J. Earth Sci.* **42**, 1547-1569 (2005).

4. Japsen, P., Bonow, J., Green, P., Chalmers, J. & Lidmar-Bergström, K. Elevated passive continental margins: Long-term highs or Neogene uplifts? New evidence from West Greenland. *Earth Planet. Sci. Letters* **248**, 315-324 (2006).

(U-Th)/He thermochronology of Mont-Tremblant, Québec: Insight into an ancient landscape

R.A. Hardie¹, D.A. Schneider¹, J.R. Metcalf², R.M. Flowers²

¹*Department of Earth Sciences, University of Ottawa,, Canada*

²*Department of Geological Sciences, University of Colorado, USA*

Mont-Tremblant is one of the tallest (875 m) and steepest peaks within the southwestern Grenville Province of Canada. It is composed of 1.2 Ga Mesoproterozoic granulite facies orthogneiss and host to a 1.15 Ga AMCG suite. The region is situated at the transition from a thick to thin mantle root and is located off-axis to the Mesozoic Great Meteor hotspot track within the Western Quebec Seismic Zone. Advances in thermochronology make it possible to study the cooling and uplift history of the Mont-Tremblant region through crustal depths of <10 km with the application of zircon and apatite (U-Th)/He thermochronometry. Samples were collected along a ~650 m vertical traverse (~2400 m laterally) of Mont-Tremblant for an age-elevation profile, as well as from adjacent regions more distal from the peak to obtain the background thermal history signal. (U-Th)/He ages from the elevation transect were obtained for 20 individual prismatic to elongate subhedral zircon grains and 20 barrel shaped apatite grains. The zircon ages are notably scattered, exhibiting a strong correlation of younger ages with higher effective uranium concentrations (eU). The eU is a proxy for radiation damage within the zircon and can alter He diffusion kinetics. Samples with eU values <300 ppm yield (U-Th)/He ages of ca. 650 Ma at the highest elevation (875 m) and ca. 560 Ma at the base (235 m). Apatite ages from the same suite of rocks yield ca. 290 Ma at the highest elevation, and ca. 190 Ma from structurally low levels. By incorporating the (U-Th)/He data with regional geologic constraints into the thermal modeling program HeFTy, viable time-temperature paths for the area can be determined. Inverse and forward modelling of combined apatite and zircon data highlights three distinct episodes of moderate cooling through the zircon partial retention zone (PRZ) and slow continuous cooling through the apatite PRZ. Independent geological constraints from the region are limited, thus our initial inverse and forward models are coupled with published ⁴⁰Ar/³⁹Ar constraints¹ to resolve an inverse model with a more explicit thermal history. From this, the modeled and measured ages demonstrate a weak positive correlation between age and grain size for both zircon and apatite data. Resolvable thermal episodes as defined by our data correspond with post-Grenville cooling (Neoproterozoic) or cooling and exhumation of the orogen during rifting and passive margin formation associated with the Iapetus Ocean (Early Cambrian). Moreover, this indicates that the rocks from the area have not experienced sufficient heating (>200°C) to reset the zircon He systematics since the Proterozoic-Cambrian transition. Apatite (U-Th)/He ages of ca. 290-190 Ma suggest no significant post-Carboniferous burial and may reflect far-field tectonism related to ca. 320-250 Ma Alleghanian collision to the east. Surprisingly, neither the cooling ages nor topography were influenced by Mesozoic hot spot activity. By combining apatite and zircon (U-Th)/He thermochronometers in one model, we provide a unique look at the low-temperature history of the Mont-Tremblant region, as well as insight into ancient landscapes and cratonization processes.

References

1. Martignole, J. & Reynolds, P. ⁴⁰Ar/³⁹Ar thermochronology along a western Quebec transect of the Grenville Province, Canada. *Journal of Metamorphic Geology* **15**, 283-296 (1997).

Deep-time thermochronology: K-feldspar $^{40}\text{Ar}/^{39}\text{Ar}$ assessment of post-orogenic cooling within the North American craton – When did the Shield become a shield?

Kalin McDannell¹, Peter Zeitler¹, Bruce Idleman¹, David Schneider²,
Rebecca Flowers³

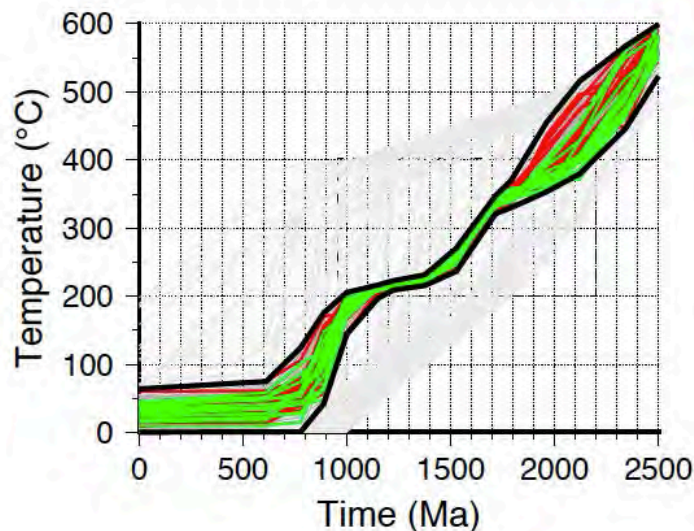
¹ Department of Earth and Environmental Sciences, *Lehigh University, Bethlehem, Pennsylvania, USA*

² *Department of Earth Sciences, University of Ottawa, Canada*

³ *Department of Geological Sciences, University of Colorado, Boulder, USA*

The low-relief topography commonly observed in cratons raises first-order questions about the ultimate fate of mountains with respect to the timing of lithospheric stabilization. In the North American craton, current low relief, as well as available stratigraphic and thermochronologic data¹ argue for up to billion-year time spans over which erosion rates have been extremely low. At many locations, how the stable cratonic thermal history connects to earlier orogenic episodes is unknown. We have used $^{40}\text{Ar}/^{39}\text{Ar}$ MDD analysis of K-feldspar to constrain thermal histories across an intermediate (~150-350°C) temperature range in an attempt to link constraints from orogenic geochronology with lower-temperature data. Our objective is to resolve the timescales for post-orogenic decay and thus learn something about how cratonic rocks in North America made the transition to stability (i.e. a lack of significant vertical motions due to crustal tectonics, isostasy, or dynamic topography).

$^{40}\text{Ar}/^{39}\text{Ar}$ age spectra from Precambrian rocks in Ontario (fig. 1) and Saskatchewan and the northern margin of the Canadian Shield (Baffin Island, Nunavut) exhibit slow cooling from ~1800-1000 Ma and ~1400-800 Ma, respectively. These rocks cooled at rates of <0.5°C/Ma following Paleoproterozoic orogenesis, seemingly characteristic of cratonic lithosphere. However, over these protracted intervals our samples experienced near-isothermal conditions at temperatures of ~200-300°C, roughly equivalent to mid-crustal depths of some 10 km (fig. 1). Only later, since ~1000 Ma, did the regions undergo further cooling such that they were at or near the surface (<< 60°C) since ~700 Ma¹. Our $^{40}\text{Ar}/^{39}\text{Ar}$ MDD models generate questions about the nature of the quiescent Proterozoic interval and what sort of lithospheric structure and evolution can support such a history of exhumation. Our ongoing work will include further modeling that assesses non-monotonic thermal histories, but even with reheating, our data still places samples at considerable depths in the Proterozoic.



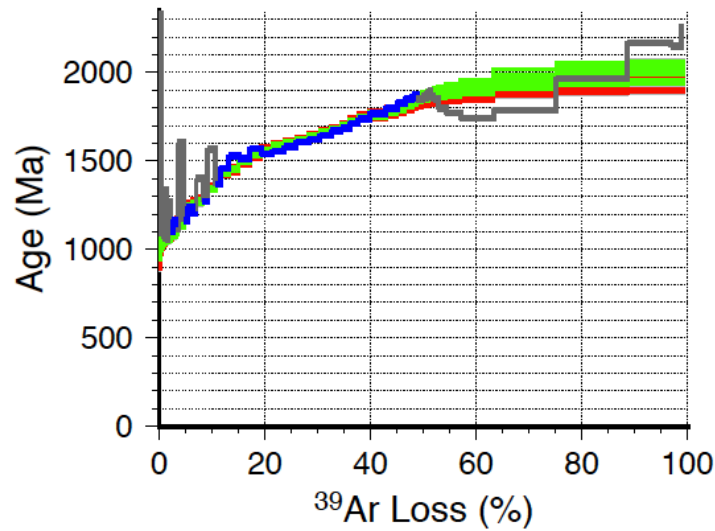


Figure 1: *MDD analysis of K-feldspar sample from the North Caribou Superterrane, northern Ontario, Canada. Monotonic-cooling, inverse time-temperature model (top) derived from measured age spectrum (bottom) and laboratory-determined diffusion-domain structure kinetics. Constrained portion (dashed box) of inverse model displays over 100°C of very slow cooling over the interval 1700 to 1000 Ma, especially in the later parts of that interval. Zircon and titanite U-Pb ages of 2700-2800 Ma provide a high-temperature context for the sample. Green and red paths and modeled spectra: 15 best and 15 worst model fits at end of run. Black lines show envelope around final inversion result but are not themselves solutions. Faint gray paths show initial Monte-Carlo time-temperature pool used to start the inversion. Blue lines show portion of age spectrum used to constrain inversion (omitting steps measured after incongruent melting, and also the earliest steps contaminated by excess Argon).*

References

1. Flowers, R.M., Bowring, S. A., and Reiners, P. W., Low Long-Term Erosion Rates and Extreme Continental Stability Documented by Ancient (U-Th)/He Dates. *Geology*. **34**, 925-928 (2006).

Exhumation in the southeast Caribbean plate corner

Jeanette C. Arkle¹, John C. Weber², Eva Enkelmann¹, Lewis A. Owen¹,

¹ Department of Geology, University of Cincinnati, Cincinnati, OH 45221, USA

² Department of Geology, Grand Valley State University, Allendale, MI 49401, USA

In the southeast Caribbean plate corner progressive east-directed tearing of subducting oceanic South American lithosphere from continental South America is associated with relative eastward motion of the Caribbean plate (Fig. 1). The Northern Range in Trinidad is located above the lithospheric tear zone and north of the transform Caribbean-South American plate boundary that transitions near Tobago to subduction in the Lesser Antilles region¹⁻³. Tertiary deformation in Trinidad has been attributed to Caribbean-South American oblique-collision plus a subsequent change ca. 10 Ma to the current dextral transform plate motion³. We constrain exhumation and basin-strata provenance in this region to explore the structural and orogenic evolution above the lithospheric detachment zone (Northern Range, Trinidad) and in the related forearc region (Tobago). Thermochronology and terrestrial cosmogenic nuclide (TCN) data are integrated to capture spatial patterns of exhumation and erosion through the late Tertiary period of plate motion change.

New thermochronology data in the forearc region are from onshore Tobago and from the Tobago Basin offshore. Published bedrock ZFT and AFT ages from Tobago show little variation in age across the mountain belt and average ~103 Ma and ~45 Ma, respectively⁴. New ZHe and AHe ages from three Tobago bedrock samples range from ~53–31 Ma and ~10–6 Ma, respectively. These ages suggest that following Mesozoic upper crustal emplacement, the Tobago igneous suites experienced slow to no exhumation through at least the Eocene. The relatively younger AHe ages imply a recent, about five-fold increase in cooling in the Late Tertiary. Offshore in the Tobago Basin, five detrital drill-core samples from a Pliocene clastic unit yield new ZHe and AHe ages that range from ~21–11 Ma and from ~6–3 Ma, respectively. These basin deposits record an intra-orogenic sediment source (Northern Range, ± Tobago) and may imply Plio-Miocene structural inversion in the Tobago foredeep.

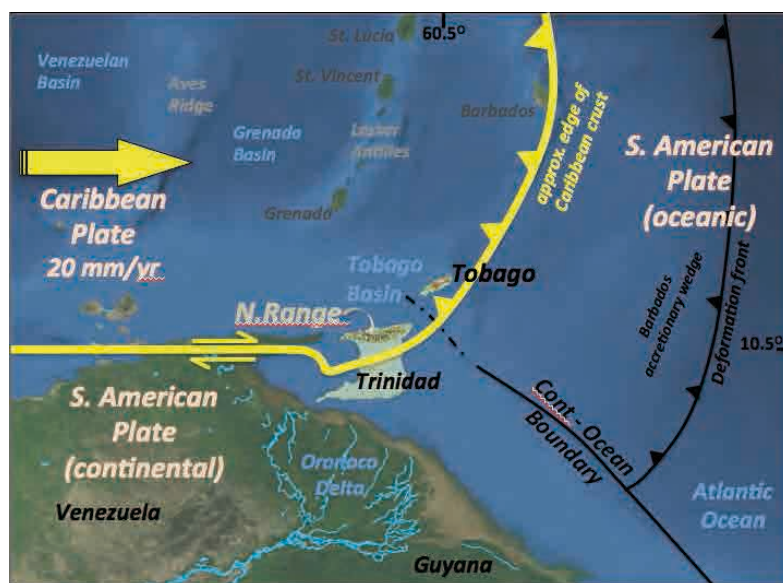


Figure 1. Map of the southeast Caribbean showing the current generalized plate boundary configuration and relative plate motion vector after Pindell et al. (1998) and Weber et al. (2001). The Northern Range in Trinidad, Tobago, and Tobago Basin study areas are located

in the apex of the Caribbean plate corner.

Exhumation and erosion above the tear in Trinidad was addressed with bedrock thermochronology and detrital TCN samples from the Northern Range. Published bedrock ZFT and AFT ages from the Northern Range young to the west from ~25–11 Ma⁵⁻⁷ and from ~15–4 Ma, respectively^{7,8}. We used seven of the same bedrock samples to determine ZHe ages, which also young to the west from ~18–5 Ma. Combined, these ages yield single-sample cooling histories that indicate asymmetric exhumation of the Northern Range⁸ at rates in west of ~1.1–0.8 mm/yr and in the east of ~0.6–0.4 mm/yr. Although asymmetric, these data suggest cooling of the west and east flanks of the Northern Range was fairly steady through the mid-Miocene to the Pliocene. Notably, these data clearly show that exhumation of the Northern Range has been persistent through the postulated late Miocene (ca. 10 Ma) transition of plate motion. Possible causes of exhumation after oblique-convergence are related to isostatic erosional unloading^{7,8}, exhumation related to extensional range-bounding faults^{5,6}, or exhumation related to the deep lithospheric tear.

Erosion of the Northern Range was investigated with TCN analysis to constrain millennial-scale surface processes. Detrital samples from 23 Northern Range catchments yield TCN basin-averaged erosion rates that range from ~0.01–0.15 mm/yr, over time periods of ~5–50 ka. There is no systematic difference in erosion rate across the range divide (north-south). However, erosion rates generally increase from west to east by about a factor of four, which is geographically reversed with respect to the thermochronology data. Taken as a whole, the recent (10⁴ yr) TCN erosion rates are at least an order of magnitude slower than long-term (10⁶ yr) thermochronology exhumation rates and may indicate a major change of Northern Range exhumation perhaps as recently as the late Pliocene. A transition in the nature of exhumation may be better constrained by forthcoming AHe ages from the Northern Range, which may provide key constraints on the timing of plate evolution and a potential southward structural narrowing associated with the complex lithospheric kinematics in the southeast Caribbean plate corner.

References

1. Weber, J., Dixon, T., DeMets, C., Ambeh, W., Jansma, P., Mattioli, G., Saleh, J., Sella, G., Bilham, R. & Perez, O. GPS estimate of relative motion between the Caribbean and South American plates, and geologic implications for Trinidad and Venezuela. *Geology* **29**, 75–78 (2001).
2. Govers, R. & Wortel, M. Lithosphere tearing at STEP faults: response to edges of subduction zones. *Earth and Planet. Sci. Lett.* **236**, 505–523 (2005).
3. Pindell, J.L., Higgs, R. & Dewey, J. Cenozoic palinspastic reconstruction, paleogeographic evolution, and hydrocarbon setting of the northern margin of South America, in Pindell, J.L. & Drake, C. *Paleogeo. Evol. & Non-Glac. Eust., N. So. Am., SEPM Sp. Pub.* **58**, 45–85 (1998).
4. Cervený, P.F. & Snoke, A.W. Thermochronologic data from Tobago, West Indies: Constraints on the cooling and accretion history of Mesozoic oceanic-arc rocks in the southern Caribbean. *Tectonics* **12**, 433–440 (1993).
5. Algar, S.T., Heady, E. C. & Pindell, J.L. Fission Track Dating in Trinidad: Implications for Provenance, Depositional Timing and Tectonic Uplift. in Pindell, J. L. and Drake, C. *Paleogeo. Evol. & Non-Glac. Eust., N. So. Am., SEPM Sp. Pub.* **58**, 111–128 (1998).
6. Weber, J.C., Ferrill, D. & Roden-Tice, M. Calcite And Quartz microstructural geothermometry of low-grade metasedimentary rocks, Northern Range, Trinidad. *J. Str. Geo.* **23**, 93–112 (2001).
7. Cruz, L., Fayon, A., Teyssier, C., & Weber, J. Exhumation and deformation processes in transpressional orogens: The Venezuelan Paria Peninsula, SE Caribbean-South American plate boundary. in Till, A.B., Roeske, S.M., Sample, J.C. & Foster, D.A., eds. *Exh. As. Cont. Strike-Slip Fault Sys., GSA Sp. Paper* **434**, 149–165 (2007).
8. Denison, C.W. [Undergraduate Thesis] Apatite Fission-Track Thermochronology, Northern Range, Trinidad and Paria Peninsula, Venezuela. *McNair Sch. J.* **12**, 25–39 (2008).

Age of topography in the highest coastal mountain range: What drives uplift of the Sierra Nevada de Santa Marta, Colombia

Mauricio Parra^{1,3}, Agustín Cardona^{2,3}

1 Institute of Energy and Environment (IEE), University of Sao Paulo, Brazil

2 Universidad Nacional de Colombia Sede Medellín, Colombia

3 Corporación Geológica Ares, Colombia

The Sierra Nevada de Santa Marta (SNSM) is a ~14500-km² triangular mountain range located adjacent to the Caribbean Sea in northern Colombia (Fig. 1A). With an average elevation of ~4 km and peaks up to ~5.8 km-high, the SNSM lie only 85 km to the south of an abyssal plain ~3.5 km deep, configuring the world's highest coastal mountain range, with a topographic relief in excess of 9 km. The tectonic development of the SNSM is related to dextral migration of the Caribbean Plate along northwestern South America and the associated episodes of collision, accretion and subduction that have shaped the continental margin since Late Cretaceous¹. Remarkably, a major positive gravity anomaly occurs beneath the SNSM (Fig 1B), which has led researchers to infer either support from a thick, buoyant oceanic lithosphere underthrusting the continent², or a very recent crustal stacking and uplift, so that the prominent topography has not yet been isostatically compensated at depth³. However, low-temperature cooling ages challenge this latter hypothesis inasmuch as thermochronometric data from the northwestern part of the range reveal apatite fission track (AFT) ages of 16-41 Ma¹ and (U-Th)/He ages ranging from ~19 to 27 Ma in zircon (ZHe), and from ~7 to 25 Ma in apatites (AHe)⁴. In order to reconcile relatively old bedrock ages and prominent topography, Villagomez et al¹, using only the AFT data, hypothesize that the SNSM must owe its actual topographic configuration to very recent rock uplift, so that insufficient erosion (<1.5 km) has failed to expose rocks that were hotter than ~60°C before this last pulse of exhumation. This is an unexpected finding, further emphasized by the lack of young AHe ages in the dataset by Cardona et al⁴, given the large erosive power that is inferred from rivers draining the range in a subtropical climate and that morphometric analysis suggest that local, 3-km-diameter relief exceeds 1.5 km in areas where cooling ages have been obtained (Fig 1B).

We are currently characterizing exhumation and denudation patterns in the SNSM by deriving catchment-wide erosion rates at different time scales using detrital thermochronology (AFT and AHe) and ¹⁰Be and ²⁶Al cosmogenic radionuclides (CRN) obtained from modern river sands in drainages from the SNSM. Through the understanding of the spatial and temporal evolution of erosion, the magnitude and timing of rock uplift can be deduced and therefore the potential driving mechanisms responsible for uplift of this exotic mountain range can be deconvolved. Preliminary estimations of expected erosion rates, using an empirical relationship between erosion and local slope⁵ (Fig 1E) suggest that recent surface uplift can have started as recently as ~2 My ago.

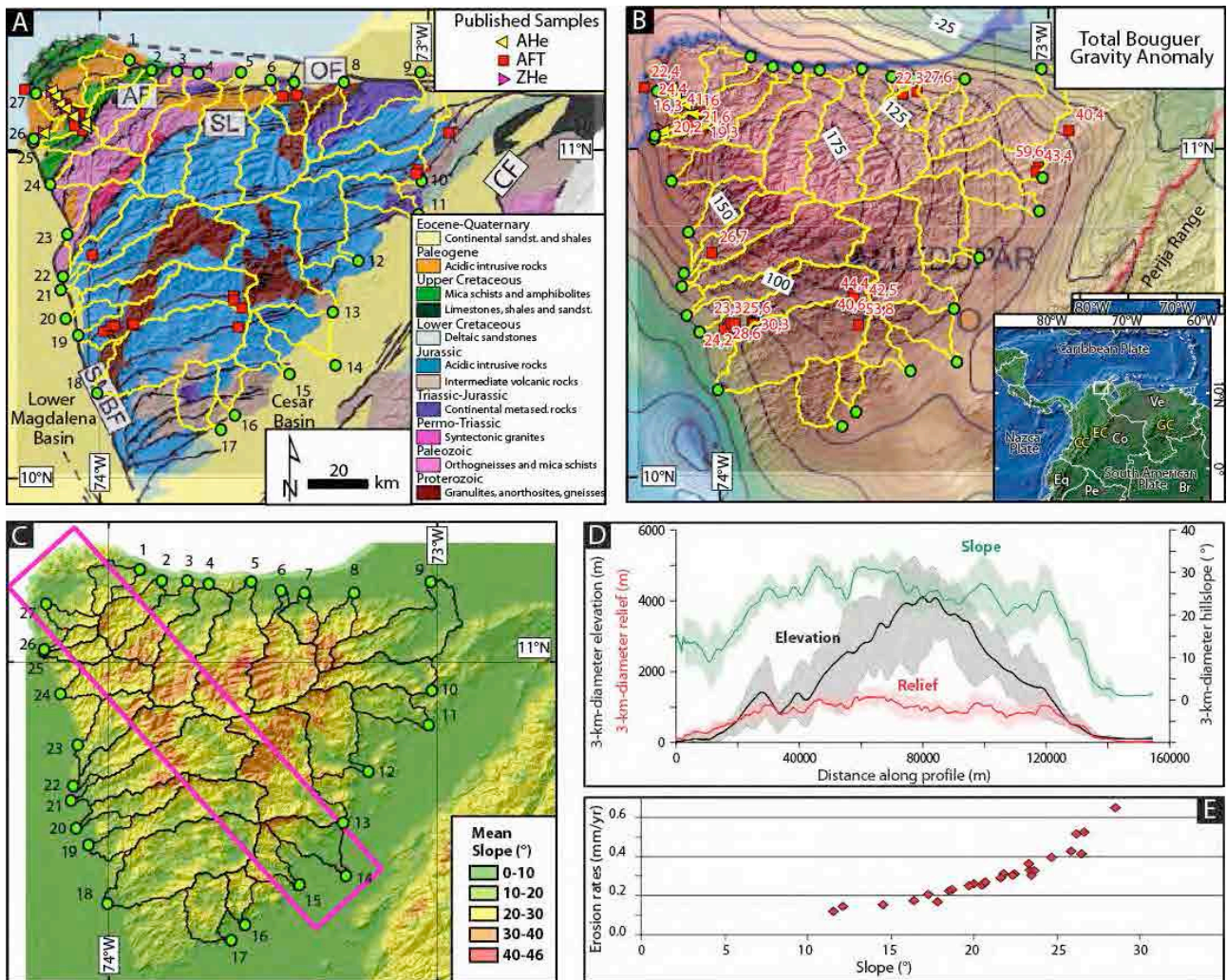


Figure 1. A. Geologic map¹ showing location of published bedrock thermochronometric samples and the 27 detrital samples of this work with their corresponding catchment areas. B. Total Bouguer Anomaly map and AFT ages (red). Inset map shows location of the SNSM. C. 3-km-diameter hillslope map and location of swath topographic profile. D. Swath profile showing 90-m SRTM topography, mean slope and local relief. Shaded envelopes are 1 Stdev. E. Estimated modern erosion rates for the 27 modeled catchments, based on an empirical relationship with local slope.

References

- Villagómez, D. *et al.* Vertical tectonics at a continental crust-oceanic plateau plate boundary zone: Fission track thermochronology of the Sierra Nevada de Santa Marta, Colombia. *Tectonics* **30**, TC4004, doi:10.1029/2010tc002835 (2011).
- Ceron, J. *Crustal structure of the Colombian Caribbean basin and margins* PhD thesis, University of South Carolina, (2008).
- Case, I. E. & MacDonald, W. D. Regional Gravity Anomalies and Crustal Structure in Northern Colombia. *Geological Society of America Bulletin* **84**, 2905-2916, doi:10.1130/0016-7606(1973)84<2905:rgaacs>2.0.co;2 (1973).
- Cardona, A. *et al.* Transient Cenozoic stages in the southern margin of the Caribbean plate: U-Th/He thermochronological constraints from Eocene plutonic rocks in the Santa Marta massif and Serrania de Jarará, northern Colombia. *Geologica Acta* **9**, 445-466, doi:10.1344/105.000001739 (2011).
- Montgomery, D. R. & Brandon, M. T. Topographic controls on erosion rates in tectonically active mountain ranges. *Earth and Planetary Science Letters* **201**, 481-489, doi:http://dx.doi.org/10.1016/S0012-821X(02)00725-2 (2002).

Long-term landscape evolution of the southeast Brazilian highlands: analysis of Poços de Caldas plateau

Carolina Doranti-Tiritan^{1,2}, Peter C. Hackspacher¹, Ulrich A. Glasmacher²

1 Institute of Earth Sciences, Heidelberg University, Im Neuenheimer Feld 234, 69120 Heidelberg, Germany

2 Instituto de Geociências e Ciências Exatas, UNESP, Av. 24A, 1515, 13506-000 Rio Claro, Brazil

The southeast Brazilian passive margin records a long history of tectonic magmatic events since the Late Jurassic. Those events were the consequence of the South Atlantic Ocean opening¹. The continental breakup preceded by intense tholeiitic magmatism in south and southeast of Brazil, with magmatic climax at 132 Ma². After the rifting process has ceased, an surface uplift of the continental crust has started in response to the drifting of the South American Platform over a Late Cretaceous thermal anomaly that accompanied an intense alkaline and basaltic magmatism³.

This alkaline volcanism generates a very particular structure on the Brazilian southeast named Poços de Caldas Alkaline Massif, (PCAM). The structure covers over 800 km². The formation ages for the predominant PCAM intermediate rocks were constrained as ~83 Ma. In addition, geologic observations indicates the phonolites, tinguaites and nepheline syenites were emplaced in a continuous and rapid sequence lasting between 1 to 2 Ma⁴.

The recent landscape of the PCAM is characterized by a dissected plateau of elevation between 1300 and 1700 m a.s.l. The landscape of the surrounding metamorphic basement is also characterized by a dissected plateau with irregular topographic ridges and peaks with elevations between 900 and 1300 m (a.s.l.), here called North Crystalline Zone (NCZ). Erosional surfaces were recognized in the area, nevertheless, there are different point of views about the age, origin and structure of the surface. The aim of the study is to understand how was the long-term landscape evolution of this region before and after the alkaline intrusion by quantifying the process responsible for generating and shaping the landforms. The thermochronological data-set shows three main groups of ages; two of them belong to the NCZ (Carboniferous-Permian; Triassic-Jurassic) and the third belongs to the PCAM region (Late Cretaceous-Eocene).

These patterns of ages are the same as in other areas of southeast Brazil and can be correlated to the “pre-rift” (older than 200 Ma), “rift” (200–100 Ma), and “post-rift” (100–50 Ma) periods (Cobbold et al 2001). The youngest ages can be interpreted as caused by exhumation processes in Paleocene and Eocene time. The age-elevation relationship shows that the ages decrease systematically with increasing elevation with a break-in-slope near the 250 Ma; 150 Ma and another in 80 Ma, which means three periods of exhumation. They are equal in time to the Late Paleozoic La Ventana Orogeny, the opening of the South Atlantic, and timing of alkaline intrusion, respectively.

In comparison to published thermochronological data from other southeast Brazilian highlands as Mantiqueira⁵⁻⁶ and Serra do Mar mountain ranges⁷⁻⁸⁻⁹, our data indicate that the landscape evolution is associated with several distinct exhumation events at the South American passive continental margin, which include the Gondwana break-up, the Late Cretaceous alkaline magmatism, and the Cenozoic evolution of a N-S trending continental graben system.

References

1. Almeida, F.F.M. Brito Neves, B.B. The origin and evolution of the South American Platform. *Earth-Science Reviews*, **50**, 77–111 (2000).
2. Marques, L.S. & Ernesto, M.O Magmatismo Toleítico da bacia do Paraná. (eds. Neto, V.M., Bartonelli, A., Carneiro, C.D., Brito-Neves. B.B.) 245-263 (Geologia do continente Sul-Americano: Evolução da obra de Fernando Flávio Marques Almeida, São Paulo, 2005).
3. Zalán P.V. & Oliveira, J.A.B. Origem e evolução estrutural do Sistema de Riftes Cenozóicos do Sudeste do Brasil. B. *Geociências Petrobras*, **13**, 2, 269-300, (2005).
4. Ulbrich, H. H. G. J., Vlach, S. R. F., Ulbrich, M. N. C., & Kawashita, K., Penecontemporaneous syenitic-phonolitic and basic-ultrabasic- carbonatitic rocks at the Poços de Caldas Alkaline massif , se brazil : geologic and geochronologic evidence. *Revista Brasileira de Geociências*, **32**, 1, 15–26 (2000).
5. Hackspacher, P.C; Ribeiro, L.F.B.; Ribeiro, M.C.S.; Fetter, A.H.; Hadler Neto,J.C.; S. Tello, C.E.; Dantas, E.L. Consolidation and break –up of the South American platform in southeastern Brazil: tectonothermal and denudation histories, *Gondwana Research* 1 91 -101 (2004)
6. Tello Saenz C.A, Hadler Neto J.C., Iunes P.J., Guedes S., Hackspacher P.C, Ribeiro L.F.B., Paulo S.R., Osorio A.M., Thermochronology of the SouthAmerican platform in the state of São Paulo, Brazil, through apatite fission tracks, *Radiation Measurements*, **39**, 635 – 640 (2005).
7. Hiruma, S. T. et al. Denudation history of the Bocaina Plateau, Serra do Mar, southeastern Brazil: Relationships to Gondwana breakup and passive margin development. *Gondwana Reearch*. **18**, 674–687 (2010).
8. Cogné, N., Gallagher, K. & Cobbold, P. R. Post-rift reactivation of the onshore margin of southeast Brazil: Evidence from apatite (U–Th)/He and fission-track data. *Earth Planet. Sci. Lett.* 309, 118–130 (2011).
9. Siqueira-Ribeiro, M. C., Hackspacher, P. C., Ribeiro, L. F. B., Hadler Neto, J. C. Evolução tectônica e denudacional da Serra do Mar (SE-Brasil) no limite entre o Cretáceo Superior e Paleoceno, Utilizando Análises de Traços de Fissão e U-Th/He em Apatitas, *Revista Brasileira de Geomorfologia* **3**, 3–14 (2011).

Timing and rates of long-term landscape evolution in Southern Argentina

Sebastian Kollenz¹, Ulrich Anton A Glasmacher¹, Rossello E.A.²

1 Institute for Earth Sciences, University of Heidelberg, Im Neuenheimer Feld 234, 69120 Heidelberg, Deutschland.

2 Depto de Ciencias Geológicas, Facultad de Ciencias Exactas y Naturales, Universidad de Buenos Aires, Ciudad Autónoma de Buenos Aires, Argentina.

The eastern Argentina South Atlantic passive continental margin is distinguished by a very flat topography. Out of the so called Pampean flat two mountain ranges are arising. These mountain ranges, the Sierras Australes and the Sierras Septentrionales, are located in the State of Buenos Aires south of the capital Buenos Aires. North of the Sierras Septentrionales the Salado basin is located. The Sierras Septentrionales and the Sierras Australes are also divided by a smaller intracratonic basin. Further in the South the Colorado basin is located. The Sierras Australes is a variscian fold belt originated by strong phases of metamorphosis, but till now it is unclear by how many tectonic phases the area was influenced (Tomezzoli & Vilas, 1999)¹. It consists of Proterozoic to Paleozoic rocks. The Sierras Septentrionales consists mainly of Precambrian crystalline rocks. The Precambrian sequences are overlain by younger Sediments (Cingolani, 2010)². The aim is to understand the long-term landscape evolution of the area by quantifying erosion- and exhumation-rates and by dating ancient rock-uplift-events. Another goal is to find out how the opening of the south atlantic took effect on this region. To fulfill this goal, thermochronological techniques, such as fission-track dating and (U-Th-Sm)/He dating has been applied to samples from the region. Because there was no low- temperature thermochronology done in this area, both techniques were applied on apatites and zircons. Furthermore, numerical modeling of the cooling history has provided the data base for the quantification of the exhumation rates. The data-set from the Sierras Australes shows clusters of different ages which can be linked to tectonic activities during late Paleozoic times. Also the thermokinematic modeling is leading to new insights of the evolution of both mountain ranges and shows patterns of ongoing tectonic processes in this region. Calculated exhumation rates show also varying cooling historys and the influence of tectonics throughout the research area. New thermochronological constraints from the Sierras Septentrionales draw a very homogeneous picture of the thermokinematic evolution of the mountain range and a big influence by late paleozoic tectonics.

References

1. Tomezzoli, R.N. and Vilas J.F., 1999. Palaeomagnetic constraints on the age of deformation of the Sierras Australes thrust and fold belt, Argentina. *Geophys. J. Int.*, 138: 857–870.
2. Cingolani, C.A., 2010. The Tandilia System of Argentina as a southern extension of the Rio de la Plata craton: an overview. *Int. J. Earth Sci. (Geol. Rundsch.)*, 100: 221–242.

Long-term landscape evolution of the South Atlantic "passive" continental margin in Eastern Argentina using apatite fission-track thermochronology

Sabrina Pfister¹, Ulrich A. Glasmacher¹, Sebastian Kollenz¹

¹ Institute of Earth Sciences, University Heidelberg, INF 234, 69120 Heidelberg, Germany

To understand the evolution of the "passive" continental margin in Argentina low temperature thermochronology is an appropriate method, which might lead to new insights in this area.

The Tandilia System, also called Sierras Septentrionales, is located south of the Río de la Plata Craton in eastern Argentina in the state of Buenos Aires. North of the hills the Salado basin is located whereas the Claromecó basin is situated south of the mountain range. In contrary to most basins along the South American "passive" continental margin, the Tandilia- System and the neighbouring basins trend perpendicular to the coast line. The topography is fairly flat with altitudes up to 350 m. The igneous-metamorphic basement is pre-Proterozoic in age and build up of mainly granitic-tonalitic gneisses, migmatites, amphibolites, some ultramafic rocks and granitoid plutons. It is overlain by a series of Neoproterozoic to early Paleozoic sedimentary rocks¹, like siliciclastic rocks, dolostones, shales and limestones².

The aim of the study is to quantify the long-term landscape evolution of the "passive" continental margin in eastern Argentina in terms of thermal, exhumation and tectonic evolution. For that purpose, samples were taken from the basement of the Sierra Septentrionales and analyzed with the apatite fission-track method. Further 2-D thermokinematic modeling was conducted with the computer code HeFTy^{3,4,5}. Because there are different hypotheses in literature regarding the geological evolution of this area two different models were generated, one after Demoulin et al.² and another after Zalba et al.⁶.

All samples were taken from the Neoproterozoic igneous-metamorphic basement. Apatite fission-track ages range from 101.6 (9.4) to 228.9 (22.3) Ma, and, therefore, are younger than their formation age, indicating all samples have been thermally reset. Six samples accomplished enough confined spontaneous fission-tracks and were used to test geological t-T models against the AFT data set. These models will lead to a more detailed insight on the cooling history and tectonic activities in the research area.

References

1. Cingolani, C. A. The Tandilia System of Argentina as a southern extension of the Río de la Plata craton: an overview. *International Journal of Earth Sciences* **100**, 221-242 (2011).
2. Demoulin, A., Zarate, M., Rabassa, J. Longterm landscape development: a perspective from the southern Buenos Aires ranges of east central Argentina. *Journal of South American Earth Sciences* **19**, 193–204 (2005).
3. Ketcham, R. A. Forward and inverse modeling of low-temperature thermochronometry data, in *Low-Temperature Thermochronology: Techniques, Interpretations, and Applications* (eds. by Reiners, P. W. & Ehlers, T. A.) 275-314 (Mineralogical Society of America/Geochemical Society Reviews in Mineralogy and Geochemistry, Chantilly, Virginia, 2005).
4. Ketcham, R. A., et al. Improved modeling of fission-track annealing in apatite. *American Mineralogist*, **92**, 789-798 (2007).
5. Ketcham, R. A., Donelick, R. A., Balestrieri, M. L., Zattin, M. Reproducibility of apatite fission-track length data and thermal history reconstruction, *Earth and Planetary Science Letters* **284**, 504–515 (2009).
6. Zalba, P. E., Manassero, M., La Verret, E., Beaufort, D., Meunier, A., Morosi, M., Segovia, L. Middle Permian telodiagenetic processes in Neoproterozoic sequences, Tandilia System, Argentina. *Int. J. of Sed. Res.* **77**, 525-538 (2007).

Rates, causes, and dynamic of long-term landscape evolution of the South Atlantic “passive continental margin”, Brazil and Namibia.

Glasmacher, U.A.¹; Hackspacher, P.C.²

1 Institute of Earth Sciences, University Heidelberg, Germany

2 IGCE/UNESP, Universidade Estadual Paulista “Julio de Mesquita Filho” Campus Rio Claro, Brazil

“Passive” continental margins are important geoarchives for processes like mantle and lithospheric dynamics, breakup of continents, and feedback mechanism between rock uplift and erosion, and therefore, also climate change. The onshore-offshore transition between São Paulo and Porto Alegre is a key area for the western margin of the South Atlantic; and the Namibia to Angola section for the eastern margin. Quantifying rates and timing of the long-term topography evolution provide insight into the causes. Analytical techniques applied are a combination of thermochronological dating techniques (fission track, (U-Th-Sm)/He), and numerical modeling of the time-temperature evolution. Special emphasis is given to the reactivation and activation of faults and fracture systems. The presentation will consider the influence of tectonic activities at major transform faults (also called: transfer zones, Fracture Zones), and discuss the influence of large intrusions on the reactivation of Pre-Intrusion structures. Comparison between onshore exhumation rates and offshore sedimentation rates will be used to quantify the surface uplift rates for both passive margins of the South Atlantic Ocean.

Long-term landscape evolution of the south Atlantic “passive continental margin”, Brazil and Namibia: rates, causes, and dynamic as revealed by thermo-kinematic numerical modeling

Christian Stippich¹, Ulrich A. Glasmacher¹, Peter C. Hackspacher²

1 Institute of Earth Sciences, Heidelberg University, Im Neuenheimer Feld 234, 69120 Heidelberg, Germany

2 Instituto de Geociências e Ciências Exatas da Universidade Estadual Paulista - IGCE/UNESP, Rio Claro, Brasil

The aim of the research is to quantify the long-term landscape evolution of the South Atlantic passive continental margin (SAPCM) in SE-Brazil and NW-Namibia. Excellent onshore outcrop conditions and complete rift to post-rift archives between Sao Paulo and Porto Alegre and in the transition from Namibia to Angola (onshore Walvis ridge) allow a high precision quantification of exhumation, and uplift rates, influencing physical parameters, long-term acting forces, and process-response systems. Research will integrate the published and partly published thermo-chronological data from Brazil and Namibia, and test lately published new concepts on causes of long-term landscape evolution at rifted margins.

The climate-continental margin-mantle coupled process-response system is caused by the interaction between endogenous and exogenous forces, which are related to the mantle-process driven rift – drift – passive continental margin evolution of the South Atlantic, and the climate change since the Early/Late Cretaceous climate maximum. Special emphasis will be given to the influence of long-living transform faults such as the Florianopolis Fracture Zone (FFZ) on the long-term topography evolution of the SAPCM's. A long-term landscape evolution model with process rates will be achieved by thermo-kinematic 3-D modeling (software code PECUBE^{1,2} and FastScape³). Testing model solutions obtained for a multidimensional parameter space against the real thermochronological and geomorphological data set, the most likely combinations of parameter rates, and values can be constrained. The data and models will allow separating the exogenous and endogenous forces and their process rates.

References

1. Braun, J., 2003. Pecube: A new finite element code to solve the 3D heat transport equation including the effects of a time-varying, finite amplitude surface topography. *Computers and Geosciences*, v.29, pp.787-794.
2. Braun, J., van der Beek, P., Valla, P., Robert, X., Herman, F., Goltzbaej, C., Pedersen, V., Perry, C., Simon-Labric, T., Prigent, C. 2012. Quantifying rates of landscape evolution and tectonic processes by thermochronology and numerical modeling of crustal heat transport using PECUBE. *Tectonophysics*, v.524-525, pp.1-28.
3. Braun, J. and Willett, S.D., 2013. A very efficient, O(n), implicit and parallel method to solve the basic stream power law equation governing fluvial incision and landscape evolution. *Geomorphology*, v.180-181, 170-179.

Long-term landscape evolution of the South Atlantic passive continental margin along the Kaoko- and Damara Belts, NW-Namibia

Daniel Peter Menges¹, Prof. Dr. Ulrich Anton Glasmacher¹, Prof. Dr. Peter Hackspacher², Dr. Gabriele Schneider³, Henning Zentner¹, Markus Karl¹

1. *University of Heidelberg, Heidelberg, Germany.*

2. *Universidade Estadual Paulista (UNESP), Campus Rio Claro, Brazil.*

3. *Geological Survey of Namibia, Windhoek, Namibia.*

The Kaoko Belt in northwestern Namibia originates in the collision of the Rio de la Plata and Kongo Craton during the Pan-African Orogeny in the Neoproterozoic¹ and represents the northern arm of the Damara Orogen. NW-Namibia's continental crust mainly consists of the NE-SW striking intracontinental branch of the Pan-African Damara mobile belt, which separates the Congo from the Kalahari craton. The Damara Orogen is divided into several tectonostratigraphic zones that are bounded by steeply dipping, ductile shear zones. These regional lineaments can be traced at least 150 km offshore². The lithostratigraphic units consist of Proterozoic and Cambrian metamorphosed rocks (534 (7) Ma – 481 (25) Ma³ as well as Mesozoic sedimentary and igneous rocks. From Permo-Carboniferous to Mid Jurassic northern Namibia was affected by deep erosion of the Damara Orogen, Permo-Triassic collisional processes along the southern margin of Gondwana and eastern margin of Africa⁴, and the deposition of the Nama Group sediments and the Karoo megasequence⁵. Between the Otjihorongo and the Omaruru Lineament-Waterberg Thrust early Mesozoic tectonic activity is recorded by coarse clastic sediments deposited within NE trending half-graben structures. The Early Jurassic Karoo flood basalt lavas erupted rapidly at 183 (1) Ma⁶. The Early Cretaceous Paraná-Etendeka flood basalts (132 (1) Ma) and mafic dike swarms mark the rift stage of the opening of the South Atlantic⁷. Early Cretaceous alkaline intrusions (137-124 Ma) occur preferentially along Mesozoic half-graben structures and are called the Damaraland Igneous Province⁸. Late Cretaceous alkaline intrusions and kimberlite pipes occur in northern Namibia. Post Early Paleocene siliciclastic sedimentation in Namibia was largely restricted to a 150 km wide zone⁹ and is represented by the Tsondab Sandstone Formation (~ 300 m thickness). The oldest part has an age of early Paleocene and the upper part spans from middle Miocene (~13 Ma) to Pliocene (~2 Ma)¹⁰. Cenozoic alkaline intrusions and kimberlite pipes are also known from the region.

The so-called "Great Escarpment" that reaches an elevation of up to 2350 m characterizes strongly the morphology of the passive continental margin in Namibia¹¹⁻¹². In contrast to Brazil, the escarpment is more than 150 km inland of Namibia. Interesting enough the Brandenburg intrusive complex of ~130 Ma age clearly indicates the post-intrusion denudation of more than 4,000m¹³. The Great Escarpment can be traced from central Angola to the eastern edge of South Africa. A considerable variation along its distribution reflects variations in tectonic history, in lithologies, and in the drainage system. In Namibia, the retreating model has dominated the genetic discussion¹⁴⁻¹⁶. However, surface process modeling has suggested other possibilities¹¹. In addition, apatite fission-track research, terrigenous cosmogenic nuclides (TCN) have been used on specific landscape elements to determine denudation rates. In the central Namib Desert, denudation rates calculated from ¹⁰Be and ²⁶Al are in the range of ±5 m Ma⁻¹ and might be representative for the last 10³ - 10⁶ a¹⁷. The persistence of arid climatic conditions throughout the Cenozoic might even lead to such low denudation rates for the past

10-12 Ma. A low retreat rate of $\sim 10 \text{ m Ma}^{-1}$ representative for the last 1 Ma was determined for the Great Escarpment in central and southern Namibia. Considering all currently, available thermochronological data for the Namibian margin¹⁸⁻²⁰, the validity of the scarp retreat model is highly problematic.

Apatite fission-track ages revealed so far range between 390.9 (17.9) Ma and 55.6 (6.7) Ma. The large spread in ages is partly related to significant changes of ages at the NW-SE trending Purros Lineament and at the Sesfontein thrust. In general, the AFT-ages are older northeast of the Purros Lineament. Furthermore, all basalt samples of Etendeka age display the same AFT-age range within error, between 103.5 (4.9) and 108.0 (5.6) Ma. The oldest ages are revealed from sandstones and glacial deposits of the Permo-Carboniferous Karoo series.

References

1. Goscombe, B. D., Gray, D. R., 2008. Structure and strain variation at mid-crustal levels in a transpressional orogen: A review of Kaoko Belt structure and the character of west Gondwana amalgamation and dispersal. *Gondwana Res.* **13**, 45–85.
2. Clemson, J., Cartwright, J., Booth, J., 1997. Structural segmentation and the influence of basement structure on the Namibian passive margin. *J. Geol. Soc. London* **154**, 477–482.
3. Miller, R.M., 1983. Evolution of the Damara Orogen, Vol. 11, Geol. Soc., South Africa Spec. Pub.
4. Coward, M.P., Daly, M.C., 1984. Crustal lineaments and shear zones in Africa: Their relationships to plate movements, *Precambrian Research* **24**: 27–45.
5. Stollhofen, H., 1999. Karoo Synrift-Sedimentation und ihre tektonische Kontrolle am entstehenden Kontinentalrand Namibias, *Z.dt.geol.Ges.* **149**: 519–632.
6. Duncan, R., Hooper, P., Rehacek, J., March, J., Duncan, A., 1997. The timing and duration of the Karoo igneous event, southern Gondwana, *J. Geophys. Res.* **102**: 18127–18138.
7. Renne, P.R., Glen, J.M., Milner, S.C., Duncan, A.R., 1996. Age of Etendeka flood volcanism and associated intrusions in southwestern Africa, *Geology* **24** (7): 659–662.
8. Watkins, R.T., McDougall, I., le Roex, A. P., 1994. K-Ar ages of the Brandberg and Okenyenya igneous complexes, north-western Namibia, *Geol. Rund.* **83**: 348–356.
9. Ward, J.D., 1988. Geology of the Tsondab Sandstone Formation, *Journal of Sedimentary Geology* **55**: 143–162.
10. Senut, B., Pickford, M., 1995. Fossil eggs and Cenozoic continental biostratigraphy of Namibia, *Pal. Afr.*, **32**: 33–37.
11. Gilchrist, A.R., Kooi, H., Beaumont, C., 1994. Post Gondwana geomorphic evolution of southwestern Africa: Implications for the controls on landscape development from observations and numerical experiments, *J. Geophys. Res.* **99**: 12211–12228.
12. Brown, R. W., Gallagher, K. and Gleadow, A. J. W., 2000. Morphotectonic evolution of the South Atlantic margins of Africa and South America, in M. A. Summerfield (ed.), *Geomorphology and Global Tectonics*, JohnWiley and Sons Ltd., Chichester, pp. 255–281.
13. Raab, M. J., Brown, R. W., Gallagher, K., Weber, K., Gleadow, A. J. W., 2005. Denudational and thermal history of the Early Cretaceous Brandberg and Okenyenya igneous complexes on Namibia's Atlantic passive margin *Tectonics* **24**: 1–15.
14. Guillocheau, F., Rouby, D., Robin, C. Helm, C., Rolland, N., Le Carlier de Veslud, C., Braun, J., 2012. Quantification and causes of the terrigenous sediment budget at the scale of a continent margin: a new method applied to the Namibia-South Africa Margin. *BasinRes.* **24**, 3–30.
15. Dauteuil, O., Rouby, D., Braun, J., Guillocheau, F., Deschamps, F., 2013. Post-breakup evolution of the margin of Namibia: constraints from numerical approach. *Tectonophysics* **604**, 122–138.
16. Rouby, D., Braun, J., Dauteuil, O., Deschamps, F., Robin, C., 2013. Long-term stratigraphic evolution of Atlantic-type passive margins: a numerical approach of interactions between surface processes, flexural isostasy and 3D thermal subsidence. *Tectonophysics* **604**, 83–103.
17. Cockburn, H. A. P., Brown, R. W., Summerfield, M. A. and Seidl, M. A., 2000. Quantifying passive margin denudation and landscape development using a combined fission-track thermochronology and cosmogenic isotope analysis approach, *EPSL* **179**: 429–435.
18. Brown, R. W., 1992. A fission track thermochronology study of the tectonic and geomorphic development of the sub-aerial continental margins of southern Africa., PhD thesis, La Trobe University, Bundoora, Australia.
19. Gallagher, K. and Brown, R. W., 1999. Denudation and uplift at passive margins: the record on the Atlantic Margin of southern Africa, *Philosophical Transactions Royal Society London A* **357**: 835–859.

20. Raab, M. J., Brown, R. W., Gallagher, K., Carter, A., Weber, K., 2002. Late Cretaceous reactivation of major crustal shear zones in northern Namibia: constraints from apatite fission track analysis. *Tectonophysics* **349**: 75-92.

Intracontinental deformation of the interior plateau and Atlantic continental margin of South Africa: Insights from combined AFT and AHe analysis

Mark Wildman¹, Roderick Brown¹, Cristina Persano¹, Fin Stuart², Romain Beucher^{1, 3}

1 School of Geographical and Earth Sciences, University of Glasgow, UK

2 Scottish Universities Environmental Research Centre, East Kilbride, UK

3 Department of Earth Science, University of Bergen, Norway

Passive continental margin evolution and dynamic topography are two major areas of discussion within the Earth Science community with ongoing work refining our understanding of plate tectonics and Earth surface processes. Indeed many studies have now provided evidence that questions the very nomenclature used to classify these processes with so called “passive” continental margins exhibiting significant post-rift fault reactivation¹ and the topographic influence of dynamic uplift being debated against regional plate stresses². Southern Africa is often used as a case study by those investigating these processes due to the well-developed continental margins and the presence of the well imaged zone of upward flow within the mantle beneath the African plate.

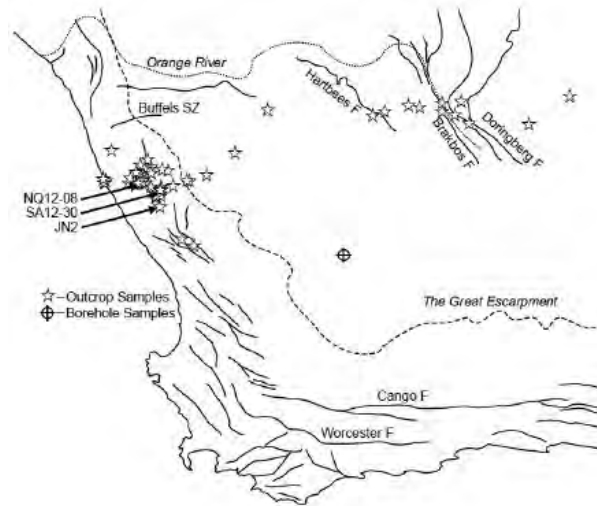
Much of our current understanding of continental margin evolution and dynamic topography has been provided by geodynamical models that attempt to link thermally driven convection within the upper and lower mantle with the lithospheric response to their associated stresses³,⁴. Despite the theoretical insights that these models provide, quantitative empirical information on the response of the surface to sub-crustal processes is required to constrain and further enhance our understanding. Apatite Fission Track thermochronology studies in South Africa have contributed significantly to constraining geodynamical models of landscape evolution by constraining the cooling of crustal rocks through 60 – 120°C as a response to kilometre scale erosion. However the AFT data set alone falls short in three ways: (i) it lacks validation through independent quantitative constraints on cooling through the upper km's of the Earth's crust, (ii) there remains gaps in the regional coverage of samples as well as detailed sampling over local areas to investigate structural deformation and (iii) fails to provide robust constraints for cooling below c. 60°C (i.e. upper c. 2 km of the crust).

In this study AFT analysis has been combined with the lower temperature Apatite (U-Th)/He (AHe) thermochronometer (c. 40 – 80°C) on samples from two transects: one through the structurally complex Namaqualand Highland terrain adjacent to the western continental margin and another across the interior plateau, crossing the Orange River Valley and major structural discontinuities of the Kheis Belt which marks the western boundary of the Kaapvaal Craton. These transects are combined with data from deep borehole samples located in the interior plateau in the southwestern Cape to constrain the post break-up thermal history of the crust. The approach for AHe analysis was to obtain multiple single grain age data (c. 15 – 20 grains) for selected samples in order to investigate the primary causes of natural dispersion commonly observed for AHe data (e.g. grain radius, radiation damage, fragment length) and their impact on the quality of thermal history modelling⁵. AFT and AHe data are jointly inverted using a Bayesian transdimensional approach⁶ incorporating the compositional influence on fission track annealing, radiation damage enhanced He retention and the effects of analysing broken apatite crystals.

Three distinct cooling episodes are identified from thermal history modelling. These cooling events occur at c. 150 – 130, 110 – 90 and 80 – 60 Ma. The cooling rate associated with these

episodes is not uniform, with certain samples cooling rapidly from elevated palaeotemperatures while others exhibit more protracted cooling. The two earliest cooling events can be observed regionally in both outcrop and borehole samples, whereas the third cooling event is only observed in certain samples but in both study areas. All of these cooling events are coeval with periods of enhanced deposition in the offshore Orange Basin⁷ and are therefore linked to periods of significant (> 3 – 5 km) erosion.

(A)



(B)

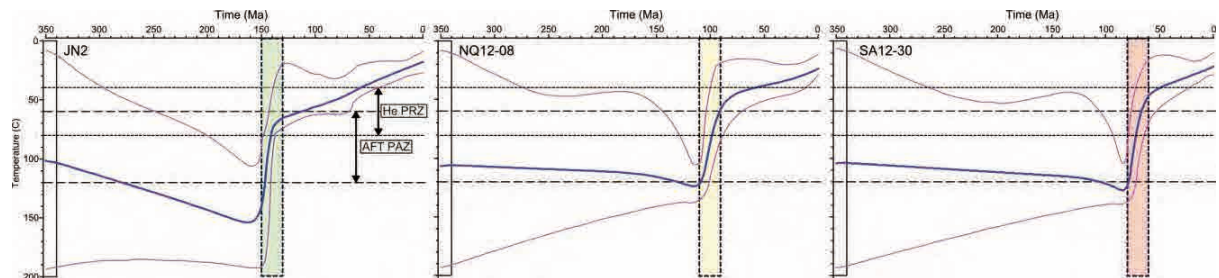


Figure 1. (A) Map of western South Africa showing sample locations, approximate location of The Great Escarpment and major structural lineaments. (B) Representative thermal histories obtained from AFT analysis (and AHe analysis for sample “JN2”) on samples across the Namaqualand Highland terrain along the western continental margin of South Africa. Three distinct cooling events are highlighted at 150 – 130 (green box), 110 – 90 Ma (yellow box) and 80 – 60 Ma (red box).

The driving processes behind this erosion remain speculative but are tentatively linked to the initial response of the landscape to continental rifting, regional tectonic inversion, and discrete local fault block uplift during structural reactivation of basement structures, respectively.

Through robust thermal history modelling, the data presented here enhances our knowledge of the crustal cooling history along the western South Atlantic continental margin and interior South African plateau. From a technical viewpoint, the large dataset provides a means to investigate AHe age dispersion and to assess their contribution to resolving thermal histories and the uncertainties that still remain a challenge to this approach.

References

1. Redfield, T. F., Osmundsen, P. T. & Hendriks, B. W. H., The role of fault reactivation and growth in the uplift of western Fennoscandia, *Journal of the Geological Society*, **162**, 1013-1030 (2005).
2. Braun, J., The many surface expressions of mantle dynamics, *Nature Geoscience*, **3**, 825 – 833, (2010).
3. Huismans, R. & Beaumont, C., Depth-dependent extension, two-stage breakup and cratonic underplating at rifted margins, *Nature*, **473**, 74 – 79, (2011).
4. Moucha, R. & Forte, A. M., Changes in African topography driven by mantle convection, *Nature Geoscience*, **4**, 707 – 712, (2011).
5. Brown, R. W., Beaucher, R., Roper, S., Persano, C., Stuart, F. & Fitzgerald, P., Natural age dispersion arising from the analysis of broken crystals. Part I: Theoretical basis and implications for the apatite (U-Th)/He thermochronometer, *Geochimica et Cosmochimica Acta*, **122**, 478 – 497, (2013).
6. Gallagher, K., Transdimensional inverse thermal history modeling for quantitative thermochronology, *Journal of Geophysical Research: Solid Earth (1978 – 2012)*, **117 (B2)**, (2012)
7. Guillocheau, F., Rouby, D., Robin, C., Helm, C., Rolland, N., Le Callier de Veslud, C., & Braun, J., Quantification and causes of the terrigenous sediment budget at the scale of a continental margin: a new method applied to the Namibia – South Africa margin, *Basin Research*, **24 (1)**, 3 – 30, (2012).

Low-temperature thermochronology in East Africa

Friederike U. Bauer¹, Joachim Jacobs¹, Bart W.H. Hendriks², Finlay M. Stuart³,
Matthijs C. van Soest⁴, Rajeev Kumar¹

1 Department of Earth Science, UiB, Allégaten 41, 5007 Bergen, Norway

2 Statoil ASA, Norway

3 Isotope Geosciences, SUERC, East Kilbride G75 0QF, UK

4 School of Earth and Space Exploration, ASU, Tempe, Arizona 85287, USA

In this contribution we will present a compilation of low-temperature thermochronology (LTT) data available in East Africa, comprising published data and new AHe and TiHe datasets from Mozambique. The area considered reaches from the western branch of the East African Rift System to the continental margins of East Africa.

The African continent, in particular the eastern part, was subjected to intense structural and geomorphic reorganization. Major geodynamic events in Africa's geological history trace back to the consolidation of Gondwana and subsequent break up, later followed by the formation of East Africa's superswell and the extension of the East African Rift System. As shown previously, the various phases of topographic growth, equilibrium and decay are stored in the thermal history of the rocks¹⁻⁴. It was also shown, that inherited fabrics play a major role in landscape evolution and margin formation: In the Albertine Rift of the western branch a broad LTT dataset is available, confirming that Precambrian thrust faults were reactivated, allowing for block movements in the Rwenzori Mountains³⁻⁵. Also from Madagascar and Mozambique a broad LTT dataset is available (Figure 1), demonstrating that "Pan-African" structures of the East African–Antarctic Orogen were decisive during Gondwana break-up and margin formation¹.

Compiling the LTT data available from East-Africa reveals a bigger picture, with cooling ages across East Africa showing a broad age-range. Apatite fission-track ages for example span the entire Phanerozoic, from Cambrian to Neogene times. Modelled cooling histories presented for some areas, indicate protracted cooling with a Mesozoic stagnant phase of low cooling rates. The compilation illustrates the distribution of LTT data and discloses different cooling patterns. It allows identifying similarities and differences, to compare various areas and to reveal a more general pattern of exhumation for East Africa.

Moreover, we aim to derive information on the implication of the LTT data with respect to the geotectonic framework: i) How can the LTT patten support our understanding of the structural and morphological evolution of the landscape of East Africa? ii) Do LTT data enable to derive information on the nature of East Africa's passive margin systems? Is there a distinctive LTT pattern for the various passive margin systems, allowing distinguishing strike-slip and oblique-slip tectonics?

Compiling all data available forms the basis to discuss the questions raised and allows deciphering areas of further research.

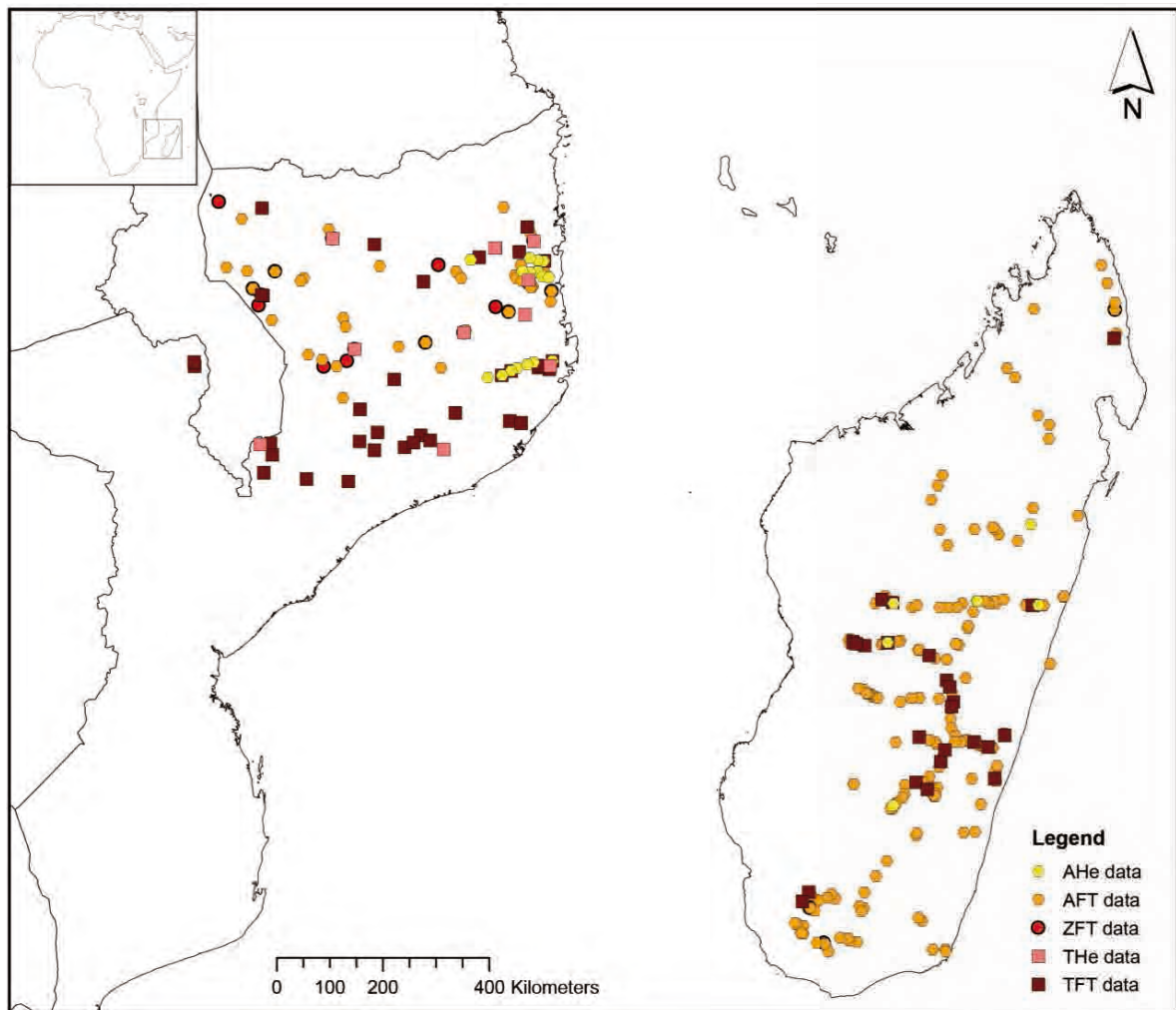


Figure 1. Detail map of compiled LTT data points available for East Africa. Map shows locations of new and published LTT data from northern Mozambique and Madagascar¹⁻² (and literature therein); AHe: Apatite (U-Th)/He, AFT: Apatite fission-track, ZFT: Zircon fission-track, THE: Titanite (U-Th)/He, TFT: Titanite fission-track.

References

1. Emmel, B. et al. Thermochronological history of an orogen-passive margin system — an example from N Mozambique. *Tectonics* **30**, TC2002 (2011).
2. Emmel et al. Maturity of central Madagascar's landscape — Low-temperature thermochronological constraints. *Gondwana Research* **21**, 704–713 (2012).
3. Bauer, F.U. et al. Thermal and exhumation history of the central Rwenzori Mountains, Western Rift of the East African Rift System, Uganda. *International Journal of Earth Sciences* **99**, 7, 1575-1597 (2010).
4. Bauer, F.U. et al. Tracing the exhumation history of the Rwenzori Mountains, Albertine Rift, Uganda, using low- temperature thermochronology, *Tectonophysics* **599**, 8-28 (2013).
5. Aanyu, K. & Koehn, D. Influence of pre-existing fabrics on fault kinematics and rift geometry of interacting segments: Analogue models based on the Albertine Rift (Uganda), Western Branch-East African Rift System. *Journal of African Earth Sciences* **59**, 2-3 (2011).

Long-term landscape evolution of the Basal Complexes of Fuerteventura and La Gomera Islands, Canary Archipelago

Sherif Mansour¹, Ulrich Anton Glasmacher¹, Marie Albinger¹, Daniel Fritz Stoeckli²
1 Institute of Geology and Palaeontology, Heidelberg University, Germany
2 Jackson school of Geosciences, University of Texas at Austin, USA

The Canarias archipelago consists from seven volcanic islands located at the northwestern African margin. Among them only Fuerteventura and La Gomera islands show distinctive wide exposures of the basal complex (BC) that is characteristic with complex geological history. The basal complex was exposed on the western part of Fuerteventura and northwestern sector of La Gomera because of giant landslide(s) which have removed most of the shield stage volcanic rocks¹⁻³. Generally, landslides are a common feature in the earlier constructive stages of the entire archipelago and many other volcanic islands⁴.

Integration of low temperature thermochronological data, and time-Temperature (t-T) numerical modelling have proven to be a powerful tool for reconstructing the thermal and tectonic history, defining and quantifying long-term landscape evolution in variety of geological settings. Therefore, zircon and apatite fission-track techniques and t-T paths modelling were applied to 36 samples representing the main rock units of the BC on both islands. Fuerteventura BC has experienced two very rapid cooling/exhumation events. While, La Gomera BC shows one longlived very fast cooling/exhumation event. Interestingly, these very rapid cooling/exhumation events are synchronous with these major landslides. There are many reasons for the major landslides on such a volcanic island⁴. The most recommended triggers for these huge mass wasting/landslides events on Fuerteventura and La Gomera are recommended to be the continuous igneous intrusions and dikes which have the potential to decrease the edifice stability, igneous extrusions which add new materials at the surface leading to over-steeping and overloading, and major climatic changes of the Middle Miocene Climatic Optimum which controls the sea level changes and the precipitation rate⁴⁻⁵.

References

1. Ancochea, E., Brändle, J.L., Cubas, C.R., Hernán, F., Huertas, M.J., 1996. Volcanic complexes in the eastern ridge of the Canary Islands: the Miocene activity of the Island of Fuerteventura. *Journal of Volcanology and Geothermal Research* **70**, 183–204.
2. Ancochea, E., Hernán, F., Huertas, M.J., Brändle, J.L., Herrera, R., 2006. A new chronostratigraphical and evolutionary model for La Gomera: implications for the overall evolution of the Canarian Archipelago. *Journal of Volcanology and Geothermal Research* **157**, 271–293.
3. Stillman, C.J., 1999. Giant Miocene landslides and the evolution of Fuerteventura, Canary Islands. *Journal of Volcanology and Geothermal Research* **94**, 89–104.
4. McGuire, W.J., 1996. Volcano instability: a review of contemporary themes. In: McGuire, W.J., Jones, A.P., Neuberger, J. (Eds.), *Volcano Instability on the Earth and Terrestrial Planets. Geological Society of London, Special Publication* **110**, 1–23.
5. Herold, N., Huber, M., Greenwood, D.R., Müller, R.D., Seton, M., 2011. Early to Middle Miocene monsoon climate in Australia. *Geology* **39**, 3–6.

Global Paleo Digital Elevation Mapping since the Ediacaran, implementing thermochronologic and geochronologic data

Fabian Kohlmann¹, Graham Baines¹, Ian Fletcher¹, James Etienne¹
1 Neftex, 97 Jubilee Avenue, Abingdon, OX14 4RW, United Kingdom

Paleo-Digital Elevation Models (PaleoDEMs) are the spatial reconstructions of past topography and bathymetry and have many important uses in understanding (for example) past climate, paleo- drainage, sediment provenance and sedimentation of organic-rich facies that may subsequently act as hydrocarbon source rocks. Here we illustrate how we use a globally integrated and geodynamically constrained plate-tectonic model coupled with an understanding of stratigraphy in sedimentary basins worldwide to generate a suite of PaleoDEMs with complete global coverage from the Ediacaran to Present Day. The plate tectonic model allows us to delineate zones of active tectonics through time, and account for the dynamic effects of uplift, subsidence, erosion and down- wearing. This inclusion of 'inherited topography' helps us to obtain better estimates of the evolving paleotopography rather than the use of static snapshots of data from a single time period. In addition, global maps of past depositional environments provide absolute constraints on paleo-elevation with respect to sea-level. Our automated process can be further improved by the incorporation of thermochronological data, such as fission track and (U-Th)/He ages, and geochronologic data to better constrain uplift and subsidence rates. The resulting PaleoDEMs provide important constraints for paleoclimate simulation and Earth System Science research in support of resource exploration.

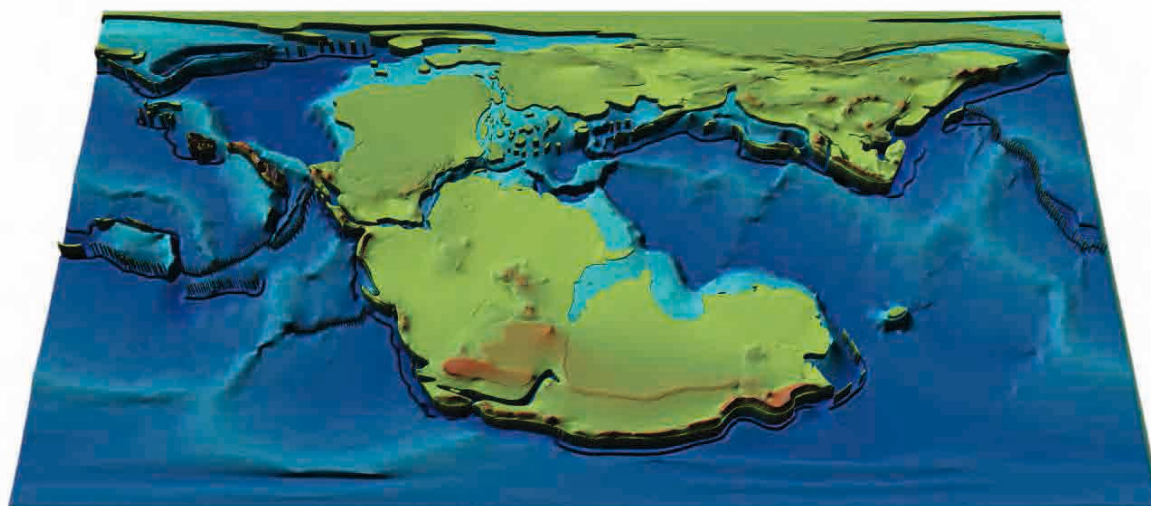


Figure 1. Global 3D reconstruction of the Early Toarci